

**Nd ISOTOPIC SIGNATURES AND STRATIGRAPHIC
CORRELATIONS: EXAMPLES FROM WESTERN PACIFIC
MARGINAL BASINS AND MIDDLE JURASSIC ROCKS OF THE
SOUTHERN CANADIAN CORDILLERA**

by

J. Brian Mahoney

B.S., University of Wisconsin-Madison, 1983

M.S., Idaho State University, 1987

**A THESIS SUBMITTED IN PARTIAL FULFILLMENT OF THE REQUIREMENTS
FOR THE DEGREE OF DOCTOR OF PHILOSOPHY**

in

**THE FACULTY OF GRADUATE STUDIES
DEPARTMENT OF GEOLOGICAL SCIENCES**

We accept this thesis as conforming to the required standard

THE UNIVERSITY OF BRITISH COLUMBIA

August, 1994

© J. Brian Mahoney, 1994

In presenting this thesis in partial fulfilment of the requirements for an advanced degree at the University of British Columbia, I agree that the Library shall make it freely available for reference and study. I further agree that permission for extensive copying of this thesis for scholarly purposes may be granted by the head of my department or by his or her representatives. It is understood that copying or publication of this thesis for financial gain shall not be allowed without my written permission.

(Signature

Department of GEOLOGICAL SCIENCES

The University of British Columbia
Vancouver, Canada

Date 16 DECEMBER 1994

ABSTRACT

The purpose of this investigation is twofold: 1) to evaluate the applicability of Nd and Sr isotopic analyses of fine grained clastic sediments to basin analysis and stratigraphic correlation; and 2) to document the lithostratigraphic, biostratigraphic, geochemical and isotopic characteristics of Lower to Middle Jurassic strata in tectonostratigraphic terranes of the southern Canadian Cordillera in order to evaluate potential terrane linkages.

Isotopic analyses of Neogene strata from three western Pacific marginal basins (Shikoku Basin, Sea of Japan, Sulu Sea) permit evaluation of isotopic analyses to basin discrimination and stratigraphic correlation. The isotopic signatures of the Sulu Sea and Sea of Japan demonstrate that modern marginal basins have an isotopic signature that varies within limits defined by the geology of its source regions. The highly evolved ($\epsilon_{Nd} < (-8)$) isotopic signature of the Shikoku Basin, however, strongly overlaps that of the Sea of Japan, and contrasts with the juvenile character of the crustal domains on the basin margins. This anomalous signature is interpreted to be the result of cratonal aeolian influx. Temporal isotopic fluctuations in the Shikoku Basin are roughly synchronous across 5600 km² of basin floor, and the pattern of isotopic fluctuations can therefore be used to correlate strata throughout the basin. Isotopic fluctuations are interpreted to result from changes in the relative contribution of each crustal domain within the source region to the basins' total sediment budget, which is a function of tectonism, volcanic episodicity, climatic factors, and basin hydrology. Isotopic fluctuations in a stratigraphic sequence may therefore prove to be important as both tools for stratigraphic correlation and as a monitor of basin evolution.

Lithostratigraphic data indicate that Lower to Middle Jurassic strata of the Harrison, Cadwallader, Bridge River, and Methow terranes each contain six strikingly similar, regionally consistent lithostratigraphic variations. Biostratigraphic data indicate that each terrane contains Aalenian to Bajocian strata with identical mixed fauna of Boreal, East Pacific and Tethyan faunal realms. Isotopic data indicate that the Harrison, Cadwallader, and Methow terranes contain coeval isotopic fluctuations of similar magnitude. Volcanic

geochemical data indicate that the Harrison and Methow terranes constitute separate volcanic arc systems flanking a basin containing back arc basin basalts. In addition, volcanic geochemistry and isotopic data suggest that the Harrison terrane represents the youngest eastern facies of the eastward migrating Bonanza-Harrison arc system, which provides an Early Jurassic link between Wrangellia and Harrison terranes. Results of this investigation strongly suggest that Lower to Middle Jurassic strata of the Wrangellia, Harrison, Cadwallader, Bridge River, and Methow terranes comprise a single marginal basin floored by trapped oceanic crust of the Bridge River terrane, and flanked by volcanic arc systems to the east and west. Wrangellia, Harrison, Cadwallader, Bridge River, and Methow terranes were amalgamated by the Early Jurassic, and have behaved as a coherent crustal block since that time.

TABLE OF CONTENTS

| | |
|---|----------|
| ABSTRACT | ii |
| TABLE OF CONTENTS | iv |
| LIST OF FIGURES | vii |
| LIST OF TABLES | x |
| LIST OF PLATES | xi |
| DEDICATION | xii |
| ACKNOWLEDGMENTS | xiii |
| <u>1. INTRODUCTION</u> | 1 |
| 1.1 OBJECTIVE AND METHODS | 6 |
| A. Lithostratigraphy | 6 |
| B. Biostratigraphy | 7 |
| C. Volcanic Geochemistry | 7 |
| D. Isotopic Characterization of Fine-Grained Sedimentary Rocks | 7 |
| E. U-Pb Zircon Analyses | 9 |
| 1.2 GOALS | 9 |
| 1.3 PRESENTATION | 10 |
| <u>2. ISOTOPIC FINGERPRINTING OF FINE-GRAINED CLASTIC SEDIMENTS: A CASE STUDY OF WESTERN PACIFIC MARGINAL BASINS</u> | |
| 2.1 INTRODUCTION | 13 |
| 2.2 BASIN DESCRIPTION | 15 |
| A. Sea of Japan | 17 |
| B. Shikoku Basin | 19 |
| C. Sulu Sea | 21 |
| 2.3 METHODS | 22 |
| A. Sample Selection | 22 |
| B. Age Control | 24 |
| C. Analytical Procedures | 24 |
| a. <i>Rb-Sr</i> | 25 |
| b. <i>Sm-Nd</i> | 25 |
| D. Data Presentation | 26 |
| 2.4 RESULTS | 27 |
| 2.5 DISCUSSION | 35 |
| A. Interbasinal Isotopic Signatures | 35 |
| B. Intrabasinal Isotopic Signatures | 39 |
| 2.6 CONCLUSIONS | 41 |
| <u>3. REGIONAL GEOLOGIC SETTING</u> | |
| 3.1 TERRANE DESCRIPTIONS | 46 |
| A. Wrangellia | 46 |
| B. Harrison | 48 |
| C. Bridge River | 49 |
| D. Cadwallader | 51 |
| E. Methow | 52 |

| | |
|---|-----|
| F Cache Creek | 54 |
| G. Quesnellia | 56 |
| 3.2 STRUCTURAL SETTING | 57 |
| 3.3 PLUTONIC SETTING | 60 |
| <u>4. EVOLUTION OF A MIDDLE JURASSIC VOLCANIC ARC: STRATIGRAPHIC, ISOTOPIC AND GEOCHEMICAL CHARACTERISTICS OF THE HARRISON LAKE FORMATION, SOUTHWESTERN BRITISH COLUMBIA</u> | |
| 4.1 INTRODUCTION | 64 |
| 4.2 GEOLOGIC SETTING | 64 |
| 4.3 PREVIOUS WORK | 67 |
| 4.4 STRATIGRAPHY | 67 |
| A. Celia Cove Member | 68 |
| B. Francis Lake Member | 70 |
| C. Weaver Lake Member | 72 |
| D. Echo Island Member | 75 |
| 4.5 AGE CONSTRAINTS | 77 |
| A. Biostratigraphic Data | 77 |
| B. U-Pb Geochronology | 78 |
| 4.6 STRUCTURAL DEFORMATION | 82 |
| 4.7 GEOCHEMISTRY | 83 |
| 4.8 Nd-Sr ISOTOPIC SYSTEMATICS | 93 |
| 4.9 ALTERATION | 98 |
| 4.10 MINERALIZATION | 98 |
| 4.11 EVOLUTION OF HARRISON LAKE FORMATION | 99 |
| 4.12 MODEL FOR VOLCANIC ARC DEVELOPMENT | 102 |
| 4.13 CONCLUSIONS | 103 |
| <u>5. EARLY TO MIDDLE JURASSIC VOLCANISM ON WRANGELLIA: EVOLUTION OF THE BONANZA-HARRISON ARC SYSTEM</u> | |
| 5.1 INTRODUCTION | 107 |
| 5.2 GEOLOGIC SETTING | 109 |
| 5.3 TERRANE STRATIGRAPHY | 111 |
| 5.4 LOWER TO MIDDLE JURASSIC STRATA | 114 |
| 5.5 AGE CONSTRAINTS | 116 |
| 5.6 GEOCHEMISTRY | 117 |
| A. Major and Trace Element Geochemistry | 124 |
| B. Rare Earth Elements | 131 |
| 5.7 ISOTOPIC SIGNATURE | 136 |
| 5.8 CONSTRAINTS ON ARC CORRELATION | 141 |
| A. Lithostratigraphic Considerations | 141 |
| B. Temporal Considerations | 143 |
| C. Geochemical Considerations | 144 |
| D. Isotopic Considerations | 145 |
| E. Structural Considerations | 145 |
| 5.9 CONCLUSIONS | 147 |
| <u>6. REGIONAL TECTONOSTRATIGRAPHIC CORRELATIONS IN THE SOUTHERN CANADIAN CORDILLERA: IMPLICATIONS FOR JURASSIC TERRANE LINKAGES AND BASIN EVOLUTION</u> | |
| 6.1 INTRODUCTION | 149 |
| 6.2 GEOLOGIC SETTING | 151 |
| A. Terrane Distribution | 152 |
| 6.3 STRATIGRAPHIC CHARACTERIZATION | 156 |
| A. Harrison Terrane | 156 |

| | |
|--|-----|
| <i>a. Terrane Description</i> | 156 |
| <i>b. Lithostratigraphy</i> | 157 |
| <i>c. Biostratigraphy</i> | 159 |
| <i>d. Volcanic Geochemistry</i> | 160 |
| <i>e. Isotopic signature</i> | 160 |
| <i>f. Depositional Environment</i> | 165 |
| B. Cadwallader Terrane | 166 |
| <i>a. Terrane Description</i> | 166 |
| <i>b. Lithostratigraphy</i> | 167 |
| <i>c. Biostratigraphy</i> | 170 |
| <i>d. Volcanic Geochemistry</i> | 171 |
| <i>e. Isotopic signature</i> | 172 |
| <i>f. Depositional Environment</i> | 172 |
| C. Bridge River Terrane | 175 |
| <i>a. Terrane Description</i> | 175 |
| <i>b. Lithostratigraphy</i> | 177 |
| <i>c. Biostratigraphy</i> | 181 |
| <i>d. Volcanic Geochemistry</i> | 183 |
| <i>e. Isotopic signature</i> | 186 |
| <i>f. Depositional Environment</i> | 189 |
| D. Methow Terrane | 191 |
| <i>a. Terrane Description</i> | 191 |
| <i>b. Lithostratigraphy</i> | 192 |
| 1. Boston Bar Formation | 192 |
| 2. Dewdney Creek Formation | 195 |
| <i>c. Biostratigraphy</i> | 198 |
| <i>d. Volcanic Geochemistry</i> | 199 |
| <i>e. Isotopic signature</i> | 201 |
| <i>f. Depositional Environment</i> | 203 |
| 6.4 STRATIGRAPHIC CORRELATIONS | 207 |
| A. Lithostratigraphic Correlations | 207 |
| B. Biostratigraphic Correlations | 212 |
| C. Volcanic Geochemistry Correlations | 213 |
| D. Isotopic Signatures | 216 |
| 6.5 BASIN EVOLUTION MODEL | 220 |
| <u>7. CONCLUSIONS</u> | 230 |
| a. Tectonic Implications | 234 |
| <u>8. REFERENCES</u> | 238 |
| <u>APPENDICES</u> | 254 |
| APPENDIX A - ANALYTICAL TECHNIQUES | 254 |
| APPENDIX B - ANALYTICAL PRECISION | 258 |
| APPENDIX C - SAMPLE LOCATIONS | 264 |
| APPENDIX D - THIN SECTION DESCRIPTIONS | 277 |
| APPENDIX E - CURRENT RESEARCH PUBLICATIONS | 291 |
| E1. Mahoney, 1991 | 292 |
| E2. Mahoney, 1992 | 298 |
| E3. Mahoney and Journeay, 1993 | 308 |
| E4. Journeay and Mahoney, 1994 | 318 |

LIST OF FIGURES

| | |
|--|-------------|
| Figure 1.1 - (a) - Morphogeologic map of the Canadian Cordillera; (b)- Schematic terrane map of the Canadian Cordillera | 2 |
| Figure 1.2 - Schematic terrane map of the southern Canadian Cordillera | 4 |
| Figure 2.1 - Geographic map of western Pacific marginal basins, with crustal isotopic domains | 16 |
| Figure 2.2 - Schematic stratigraphic sections of Neogene sediments in western Pacific marginal basins | 18 |
| Figure 2.3 - Schematic stratigraphic sections of Neogene Shikoku Basin sediments | 20 |
| Figure 2.4 - ϵ_{Nd} vs. $^{87}Sr/^{86}Sr$ isotopic diagram for three western Pacific marginal basins | 28 |
| Figure 2.5 - Depth vs. ϵ_{Nd} for drill holes in the Shikoku Basin | 32 |
| Figure 2.6 - Age vs. ϵ_{Nd} for drill holes in the Shikoku Basin | 33 |
| Figure 2.7 - Age vs $^{87}Sr/^{86}Sr$ for drill holes in the Shikoku Basin | 34 |
| Figure 2.8 - $f^{Sm/Nd}$ vs. ϵ_{Nd} for samples from the Shikoku Basin and Sea of Japan | 38 |
| Figure 3.1 - Geographic location map of the southwestern British Columbia | 45 |
| Figure 3.2 - Generalized geologic map of southwestern British Columbia | 47 |
| Figure 4.1 -Schematic terrane map of the southern Canadian Cordillera and generalized stratigraphic column of the Harrison terrane | 65 |
| Figure 4.2 - Geologic map of the southwestern 1/4 of Harrison Lake (92H/5) 1:50,000 map sheet | (in pocket) |
| Figure 4.3 - Schematic stratigraphic column of the Harrison Lake Formation | 69 |
| Figure 4.4 - Photomicrograph of altered crystal tuff of Francis Lake Member | 74 |
| Figure 4.5 - Photograph of columnar jointed dyke cutting altered lava flow in Weaver Lake Member | 74 |
| Figure 4.6 - Concordia plots of U-Pb dates discussed in text | 79 |
| Figure 4.7 - Major and trace element discrimination diagrams of Weaver Lake Member volcanic rocks | 86 |
| Figure 4.8 - Harker variation diagrams for the Weaver Lake Member | 88 |
| Figure 4.9 - Compatible-incompatible element diagrams for the Weaver Lake Member | 89 |
| Figure 4.10 - Ta-Hf/3-Th discriminate diagram for Weaver Lake Member | 91 |

| | |
|---|-----|
| Figure 4.11 - Incompatible element spider diagrams and REE diagrams for the Weaver Lake Member | 92 |
| Figure 4.12 - $^{87}\text{Sr}/^{86}\text{Sr}$ vs. ϵ_{Nd} diagram for Harrison Lake Formation | 94 |
| Figure 4.13 - estimated stratigraphic vs. ϵ_{Nd} position for Harrison Lake Formation | 97 |
| Figure 5.1 - Schematic terrane map of the southern Canadian Cordillera, highlighting Wrangellia and Harrison terranes | 108 |
| Figure 5.2 - Schematic geologic map of Bonanza Group, Bowen Island Group, and Harrison Lake Formation | 110 |
| Figure 5.3 - Time-stratigraphic column of the Bonanza Group, Bowen Island Group, and Harrison Lake Formation | 112 |
| Figure 5.4 - AFM and Zr/TiO_2 vs. SiO_2 for Bonanza Group, Bowen Island Group, and Harrison Lake Formation | 125 |
| Figure 5.5 - Harker variation diagrams for Bonanza Group, Bowen Island Group, and Harrison Lake Formation | 126 |
| Figure 5.6 - TiO_2 vs. Al_2O_3 and TiO_2 vs. SiO_2 diagrams for Bonanza Group, Bowen Island Group, and Harrison Lake Formation | 128 |
| Figure 5.7 - Incompatible element ratio diagrams for Bonanza Group, Bowen Island Group, and Harrison Lake Formation | 130 |
| Figure 5.8 - Rare earth element diagrams for Bonanza Group, Bowen Island Group, and Harrison Lake Formation | 132 |
| Figure 5.9 - Comparison of REE subgroups for each unit | 134 |
| Figure 5.10 - $^{87}\text{Sr}/^{86}\text{Sr}$ vs. ϵ_{Nd} diagram for Bonanza Group, Bowen Island Group, and Harrison Lake Formation | 137 |
| Figure 5.11 - ϵ_{Nd} vs. $f_{\text{Sm}/\text{Nd}}$ diagram for Bonanza Group, Bowen Island Group, and Harrison Lake Formation | 140 |
| Figure 6.1 - Schematic terrane map of the southern Canadian Cordillera | 150 |
| Figure 6.2 - Schematic geologic map of Lower to Middle Jurassic strata in the southern Canadian Cordillera. Modified from Wheeler and McFeely (1991) | 153 |
| Figure 6.3 - Schematic geologic cross-section across southern Canadian Cordillera. Modified from Monger and Journeay (1992) | 154 |
| Figure 6.4. - Time-stratigraphic column of terranes in the southern Canadian Cordillera | 155 |
| Figure 6.5 - Schematic stratigraphic section of the Harrison Lake Formation | 158 |

| | |
|--|-----|
| Figure 6.6 - Representative geochemical diagrams for the Weaver Lake Member of the Harrison Lake Formation | 161 |
| Figure 6.7 - $^{87}\text{Sr}/^{86}\text{Sr}$ vs. ϵ_{Nd} diagram for Harrison Lake Formation | 163 |
| Figure 6.8 - estimated stratigraphic position vs. ϵ_{Nd} for Harrison Lake Formation | 164 |
| Figure 6.9 - Schematic stratigraphic section of the Last Creek Formation | 168 |
| Figure 6.10 - $^{87}\text{Sr}/^{86}\text{Sr}$ vs. ϵ_{Nd} isotopic diagram for Last Creek Formation. | 173 |
| Figure 6.11 - stratigraphic position vs. ϵ_{Nd} for Last Creek Formation | 174 |
| Figure 6.12 - Schematic stratigraphic section of the Cayoosh Assemblage | 178 |
| Figure 6.13 - Photograph of pillow basalt from unit 2 of Cayoosh assemblage | 180 |
| Figure 6.14 - Photograph of thin-bedded quartz-rich clastic facies displaying chaotic bedding character | 180 |
| Figure 6.15 - Representative geochemical diagrams for volcanic rocks of unit 2 of the Cayoosh assemblage | 184 |
| Figure 6.16 - $^{87}\text{Sr}/^{86}\text{Sr}$ vs. ϵ_{Nd} isotopic diagram for Cayoosh assemblage | 187 |
| Figure 6.17 - stratigraphic position vs. ϵ_{Nd} for Cayoosh assemblage. | 188 |
| Figure 6.18 - Schematic stratigraphic section of the Ladner Group | 193 |
| Figure 6.19 - Representative geochemical diagrams for volcanic rocks of Dewdney Creek Formation | 200 |
| Figure 6.20 - $^{87}\text{Sr}/^{86}\text{Sr}$ vs. ϵ_{Nd} isotopic diagram for Dewdney Creek Formation | 202 |
| Figure 6.21 - stratigraphic position vs. ϵ_{Nd} for Dewdney Creek Formation. | 204 |
| Figure 6.22 - Lithostratigraphic correlation diagram for Lower to Middle Jurassic strata | 210 |
| Figure 6.23 - Hf/3-Th-Ta tectonic discrimination diagram for Middle Jurassic volcanic strata | 215 |
| Figure 6.24 - ϵ_{Nd} vs. $\int \text{Sm}/\text{Nd}$ diagram for all Lower to Middle Jurassic strata examined | 219 |
| Figure 6.25 - Schematic Lower to Middle Jurassic basin reconstruction | 222 |

LIST OF TABLES

| | |
|---|-----|
| Table 1.1 - Terrane description table | 5 |
| Table 2.1a- Isotopic data for western Pacific marginal basins | 29 |
| Table 2.1b - Isotopic data for western Pacific marginal basins | 30 |
| Table 4.1 - U-Pb analytical data for Harrison Lake Formation | 80 |
| Table 4.2a - Geochemical data for the Harrison Lake Formation | 84 |
| Table 4.2b - Geochemical data for the Harrison Lake Formation | 85 |
| Table 4.3 - Isotopic data for the Harrison Lake Formation | 95 |
| Table 5.1a - Geochemical data for the Bonanza Group in the Port Alberni area | 118 |
| Table 5.1b -Geochemical data for the Bonanza Group in the Nootka Sound area | 119 |
| Table 5.1c - Geochemical data for the Harrison Lake Formation | 121 |
| Table 5.1d - Geochemical data for the Bowen Island Group and Middle Jurassic plutons | 123 |
| Table 5.2 - Isotopic data for the Bonanza Group, Bowen Island Group, and the Harrison Lake Formation | 138 |
| Table 6.1 - Paleontologic data for the southern Canadian Cordillera | 224 |
| Table 6.2 - Middle Jurassic volcanic geochemical data | 226 |
| Table 6.3 - Lower to Middle Jurassic isotopic analysis data table | 227 |
| Table B.1 - Duplicate Analyses for Ocean Drilling Program sediments | 259 |
| Table B.2 - Duplicate Analyses for Jurassic rocks | 261 |
| Table B.3 - International Standards | 263 |

LIST OF PLATES

Plate 1 - Geologic map of the southwestern Canadian Cordillera (92G, H, I, J) with Nd and Sr isotopic sample locations and values. Scale 1:500,000. Geology compiled by J.M. Journeay and J.W.H. Monger; isotopic data compiled by J.B. Mahoney.

DEDICATION

I would first and foremost like to dedicate this thesis to Lori D. Snyder, the special woman in my life, without whom this thesis would not have been possible. I can never thank her enough for her help and encouragement through good times and bad. Thanks, Lori.

A special dedication to my sister, Chris, who was unable to see me finally graduate from college. Chris is sorely missed by all. Only the good die young.

ACKNOWLEDGMENTS

I would first like to thank the late R.L. Armstrong for introducing me to the geology of the Canadian Cordillera and for pointing out the problems and possibilities associated with Jurassic stratigraphy in the region. Dick and I discussed the potential application of radiogenic isotopes to stratigraphic studies endlessly as I was beginning this project, and the research herein is a test of those ideas. My thanks to Marc Bustin for becoming my thesis advisor following Dick's passing, and to John Ross for his interest in the project. Bill Barnes is especially thanked for helping to keep it all in perspective over the last few months.

This work would not have been possible without the generous support, encouragement, and scientific contributions of the Geological Survey of Canada. Cathie Hickson provided logistical support and field expenses, and was continually my sounding board for a vast array of ideas and problems, scientific and otherwise. My sincerest thanks are extended to Murray Journeay for his motivation, enthusiasm and expertise in Coast Belt geology; many of the ideas discussed in this thesis were developed while working with Murray in the eastern Coast Belt. Murray is also thanked for the use of his excellent digital map files that have been modified and used herein. I would like to thank Jim Monger for asking the thought-provoking questions about regional geology and the feasibility of my interpretations.

Rich Friedman kept me grounded in geologic reality over the past couple of years, and served as a filter for every wild idea that came up; I cannot thank him enough for his interest, enthusiasm and assistance. Jim Mortensen timed his arrival at UBC to direct the isotope lab perfectly, and has been a constant source of ideas and necessary critiques. His assistance is greatly appreciated.

This project involved an enormous amount of laboratory work, and I owe a debt to numerous people for their assistance. My thanks to Dita Runkle for helping with a myriad of lab activities, and to

Janet Gabites for keeping me from blowing up the mass spectrometer. Anne Pickering kept things lively and entertaining in the lab, and always kept a smile on my face.

Neodymium analyses were done at the isotopic lab of the Geological Survey of Canada, Ottawa. I would like to thank Reg Theriault, neodymium guru, for his help, advice, and isotopic expertise. My thanks to Randy Parrish for authorizing my use of the lab, and for just being a friend.

Sophie Weldon provided invaluable assistance in helping me organize megabytes of data. Lori Snyder was a constant source of computer expertise, geochemical assistance, and manuscript editing. Arnie Toma helped out with computer drafting when time was short. Finally, my thanks to other faculty and staff in the Department of Geological Sciences who provided the expertise needed to produce this tome.

1. INTRODUCTION

The Canadian Cordillera is a collage of fault-bounded terranes which have undergone varying degrees of deformation, metamorphism, and plutonism during Jurassic to Tertiary time (Wheeler and McFeely, 1991). Each terrane is defined on the basis of a characteristic internal stratigraphy that differs from that of its neighbor, in ways that are not easily explained by conventional facies changes or unconformable relations (Coney et al., 1980). The original temporal and spatial relationships among terranes, initial paleogeographic affinity, transport history and timing of accretion are poorly understood. Current theory holds that the Cordillera developed through the progressive accretion of numerous, unrelated, allochthonous terranes onto the western margin of ancestral North America during the Mesozoic (Coney et al., 1980; Monger et al., 1982, Silberling and Jones, 1987; Monger, 1989). These accreted terranes were subsequently variably deformed, intruded, and metamorphosed during a long and protracted geologic history that formed the complex orogen recognized today.

Current debate on the geology of the Canadian Cordillera centres on the tectonic setting, displacement history, and timing of accretion of the allochthonous terranes that comprise the Cordillera (Figs. 1.1a, b). Tectonic models for accretion fall into three categories: 1) late Early Cretaceous collision of Insular Superterrane (amalgamated Wrangellia, Alexander and Peninsular terranes or Terrane II of Monger, et al., 1982) with previously accreted terranes along the western edge of North America and closure of intervening ocean basins (Monger et al., 1982; Garver, 1992; Brandon and Garver, 1994); 2) Late Jurassic dextral translation and oblique transpression of Insular Superterrane along the North American margin with concomitant development of transtensional rift basins (Gehrels and Saleeby, 1985; Saleeby and Busby-Spera, 1992); and 3) Middle Jurassic accretion of Insular Superterrane and formation of an Andean-Sierran type continental arc, followed by Late Jurassic to late Early Cretaceous intra-arc rifting and basin formation (van der Heyden, 1992). Each of these models attempts to integrate substantial igneous, metamorphic, structural, and stratigraphic data sets into a comprehensive framework.

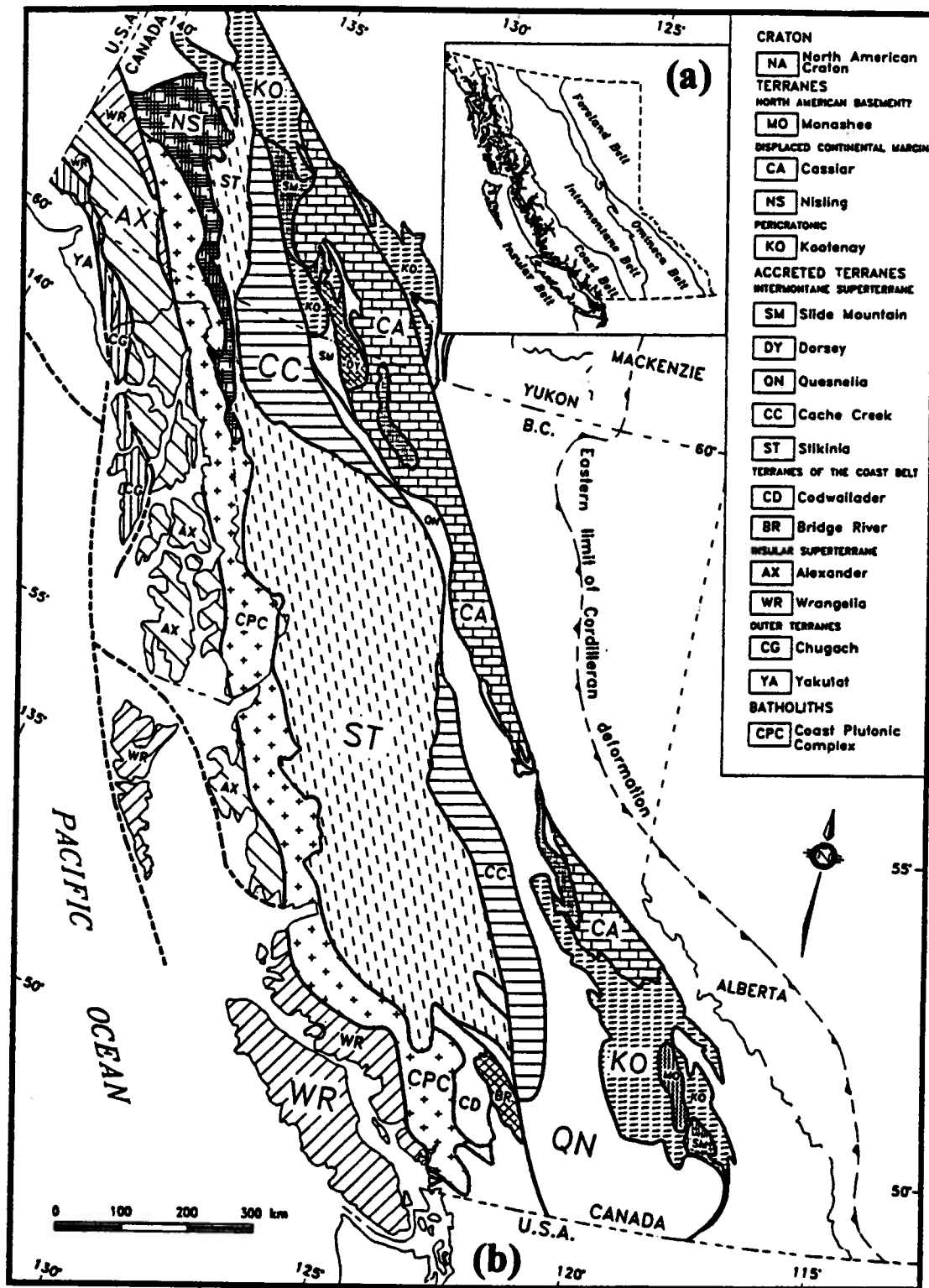


Figure 1.1(a) - Morphogeologic map of the Canadian Cordillera. Modified after Monger and Hutchinson (1971); (b) Schematic terrane map of the Canadian Cordillera. Modified after Wheeler and McFeely (1991).

Fundamental to any tectonic model of Cordilleran evolution is the establishment of linkages between terranes. Documentation of terrane linkages dates the earliest possible juxtaposition of disparate terranes, and thus provides constraints on the timing and mechanism of terrane accretion. Terrane linkages can be established by the documentation of stratigraphic overlap assemblages, identification of "stitching" igneous intrusions or metamorphic isograds, and provenance ties. Comprehensive tectonic models for the southern Canadian Cordillera have been contentious due to disagreements among workers regarding linkages among terranes (e.g. Umhoefer, 1989; Garver, 1992; Monger and Journeay, 1992).

The southern Canadian Cordillera provides an ideal setting within which to test the feasibility of current tectonic models. This portion of the Cordillera consists of a number of small, disparate terranes separated by regional fault systems or plutonic assemblages (Figs. 1.1 and 1.2, Plate I). These terranes include, from west to east, Wrangellia, Harrison, Cadwallader, Bridge River, Methow, and Quesnellia terranes (Table 1.1 Fig. 1.2). Each of the terranes contains Jurassic-Cretaceous basinal sequences overlying Triassic or older basement (Monger and Journeay, 1992). Stratigraphic linkages among these terranes are firmly established by the late Early Cretaceous (Albian; Garver, 1992), but proposed correlations of older strata are a matter of dispute (Mahoney, 1993; Mahoney and Journeay, 1993; Journeay and Mahoney, 1994, Garver and Brandon, 1994). Documentation of earlier terrane linkages would better constrain currently proposed tectonic models.

This investigation attempts to reconcile conflicting tectonic models by establishing the stratigraphic evolution and basin configuration of Middle Jurassic strata in a number of terranes in the southern Canadian Cordillera. These strata (and their terrane designations) include, from east to west, the Ashcroft Formation (Quesnellia), Ladner Group (Methow terrane), Lillooet Group (Methow terrane), Newby Group (Methow terrane), Cayoosh assemblage (Bridge River terrane), Last Creek Formation/Relay Mountain Group (Cadwallader terrane), and Harrison Lake Formation (Harrison terrane). Terrane descriptions are outlined in point form in Table 1.1. Documentation of Middle Jurassic stratigraphic ties between these formations would establish the earliest terrane linkages known in the southern Cordillera, and would therefore place important

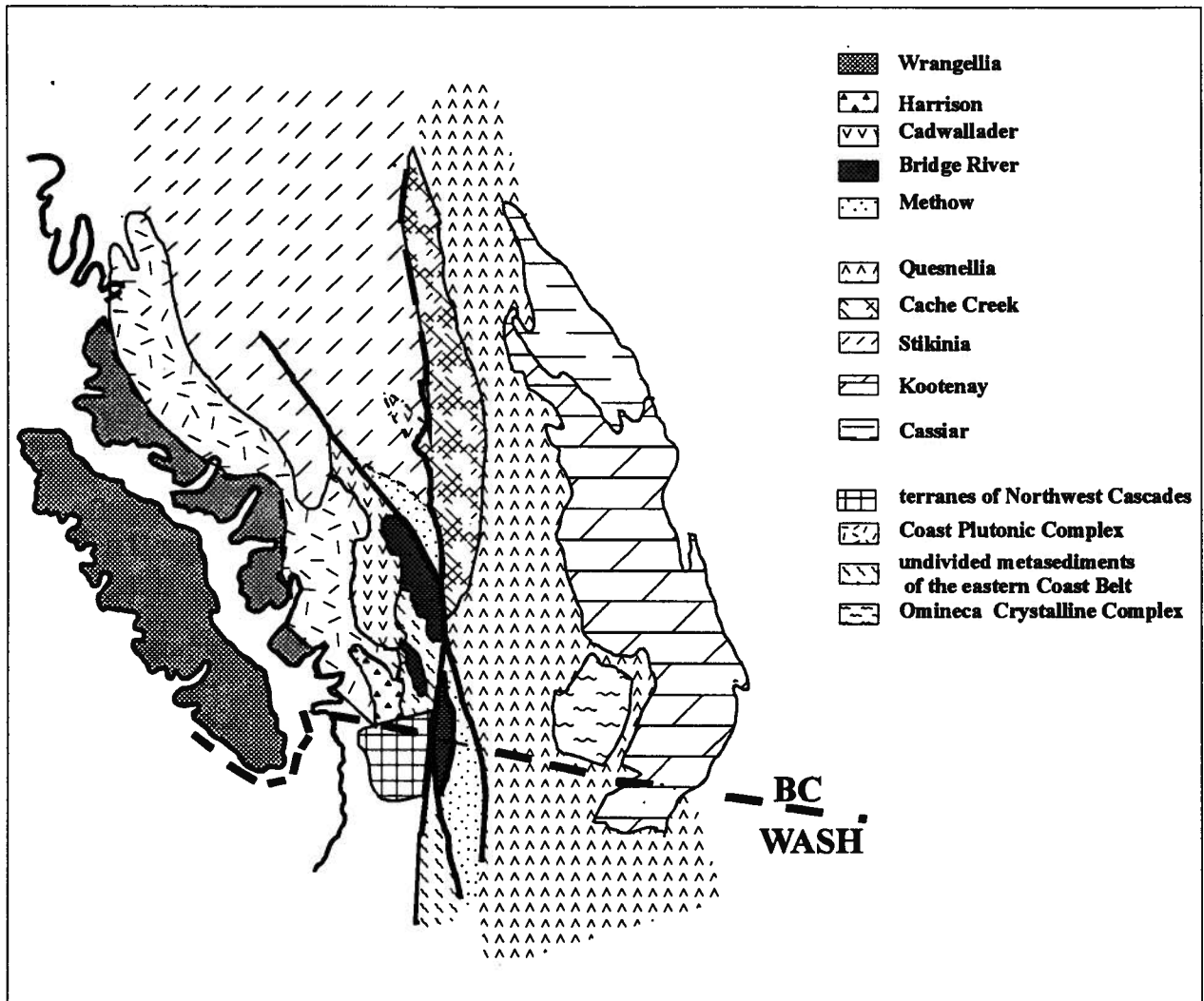


Figure 1.2 - Schematic terrane map of the southern Canadian Cordillera. Modified after Wheeler and McFeely (1991).

TABLE 1.1

TERRANE NOMENCLATURE

This investigation concentrates on the stratigraphic evolution and basin histories of Middle Jurassic strata contained in a number of disparate terranes in the southern Canadian Cordillera. These terranes include, from east to west, Quesnellia, Methow, Bridge River, Cadwallader, Harrison, and Wrangellia terranes. They are described in point form below; refer to figure 1.2 for terrane locations.

Quesnellia:

Fragmented record of Upper Paleozoic carbonate platform (?) and ocean floor rocks (Apex Mountain Group and Harper Ranch Group); overlain by Upper Triassic Nicola Group volcanic arc; unconformably overlain by Lower to Middle Jurassic fine-grained clastics of Ashcroft Formation; overlain by late Early Cretaceous Spences Bridge Group continental arc volcanics; capped by Eocene (Kamloops Group) and Miocene/Pleistocene (Chilcotin Group) plateau basalts. Intruded by Triassic/Early Jurassic through Eocene plutons (Monger, 1989, 1990).

Methow:

Upper Triassic ocean floor chert, limestone, greenstone (Spider Peak Formation; (Ray, 1986)) overlain by Lower Jurassic Boston Bar Formation fine-grained clastics, which grade upward into volcanoclastic rocks of the Dewdney Creek Formation (O'Brien, 1986; Mahoney, 1992); overlain by fluvial rocks of Upper Jurassic Thunder Lake assemblage; overlain by coarse clastics of the Lower to mid-Cretaceous Jackass Mountain Group; intruded by Cretaceous to Eocene plutons (Monger, 1989).

Bridge River:

Disrupted, variably metamorphosed argillite, greenstone, ultramafics, carbonate, and chert ranging in age from Mississippian to Middle Jurassic (Callovian; Cordey and Schriazza, 1993); overlain by Cretaceous clastic rocks of the Tyaughton Group (Schriazza et al., 1991; Journeay, 1993); intruded by Cretaceous and Eocene plutons.

Cadwallader:

Upper Triassic basaltic rocks of the Cadwallader Group (Rusmore, 1985, 1987) overlain by Lower Jurassic fine-grained clastics of the Last Creek Formation, Upper Jurassic volcanogenic clastics of the Relay Mountain Group (Umhoefer, 1990), and Lower to Upper Cretaceous coarse clastic rocks of the Taylor Creek Group and Silverquick Formation (Garver, 1992); capped by continental arc volcanics of the Upper Cretaceous Powell Creek Formation; intruded by Cretaceous to Eocene plutons (Journeay, 1993).

Harrison:

Upper Triassic greenstone, greywacke and chert (Camp Cove Formation; Arthur, 1993) unconformably overlain by Middle Jurassic volcanic rocks of the Harrison Lake Formation, fine-grained sedimentary rocks of the late Middle Jurassic Mysterious Creek and Billhook Creek Formations, Lower Cretaceous coarse clastic rocks of the Peninsula Formation, and Lower Cretaceous volcanic rocks of the Brokenback Hill Formation (Arthur, 1986, 1993); intruded by Middle Jurassic to Cretaceous plutons.

Wrangellia:

Devonian Sicker Group volcanic arc overlain by Upper Paleozoic carbonate platform; Paleozoic rocks unconformably overlain by Middle to Upper Triassic Karmutsen Formation tholeiitic basalt (oceanic plateau), in turn overlain by Lower Jurassic Bonanza Group volcanic arc and Upper Jurassic to Upper Cretaceous clastic sediments (Monger, 1980); intruded by Middle Jurassic to Eocene plutons.

constraints on models of tectonic evolution. Conversely, documentation of substantially different stratigraphic histories among these formations would preclude amalgamation of these terranes prior to the Late Jurassic.

1.1 OBJECTIVE AND METHODS

The primary objective of this investigation is to constrain the timing and sequence of terrane accretion in the southern Canadian Cordillera through stratigraphic correlations and facies analysis of Middle to Upper Jurassic volcanic arc and marginal basin assemblages. Jurassic strata in the region are contained in a number of terrane specific, unconformity-bounded sedimentary sequences separated by regional fault systems and plutonic assemblages. Original relationships between these sequences are uncertain. The basinal assemblages should contain evidence of terrane interaction in the form of unconformities, change in provenance, vertical facies variations, and the development of volcanogenic sequences as a result of the tectonic instability inherent in an accretionary tectonic setting. Documentation of geologically simultaneous lithologic, biostratigraphic, isotopic and geochemical changes in coeval sedimentary sequences that are currently tectonically separated would provide strong evidence for their original linkage. Evaluation of Middle to Late Jurassic basin configuration and evolution will therefore place constraints on terrane interactions and subsequent tectonic models for this time period.

Jurassic strata are examined and compared by a variety of stratigraphic techniques, including lithostratigraphy, biostratigraphy, isotopic characterization, geochemical analysis of primary volcanic rocks, and, to a lesser extent, U-Pb zircon analyses. Each of these techniques is described below:

A. Lithostratigraphy -

Physical stratigraphy and sedimentology forms an important component of this investigation. Most of the units under consideration have been examined in only a cursory manner by previous workers, and detailed stratigraphic descriptions are lacking. Multiple stratigraphic sections were examined and sampled in each unit (Appendix E), and lateral and vertical facies changes are documented throughout the area of exposure.

Thin section petrography was used to document compositional variations (Appendix D). Particular emphasis is placed on depositional environment interpretation and provenance determination for each unit.

B. Biostratigraphy -

Paleontologic data are used to refine the age range of each unit. New fossil dates are reported in the Ladner Group, Lillooet Group, Cayoosh assemblage, and the Harrison Lake Formation. These data add to existing biostratigraphy, and, in most cases, increase the age range of the unit concerned. Biostratigraphy also aids in ecological interpretation, and serves to limit the paleogeographic separation of the terranes.

C. Volcanic Geochemistry -

Major, minor, and trace element geochemistry of primary volcanic rocks, primarily lava flows, has been undertaken in an attempt to discriminate between coeval volcanic arc assemblages. The Harrison Lake Formation and the Ladner Group both contain thick volcanic sequences, and the original paleogeographic relations between these arc-related assemblages is unknown. Differences in volcanic arc geochemistry may be related to differences in source areas, particularly differences in assimilated contamination. Different geochemical signatures, in concert with isotopic data, suggest different basement compositions, and therefore different terrane affiliations. Conversely, similar geochemical signatures between arc assemblages suggest similar source areas, potentially within the same arc.

D. Isotopic characterization of fine-grained sedimentary rocks -

Delineation of isotopic signatures of sedimentary sequences is an integral part of this investigation. Radiogenic isotopic (Nd and Sr) data from fine-grained sedimentary sequences may aid in stratigraphic correlation and provenance determinations in Middle Jurassic strata. The viability of such isotopic correlations has been investigated in a pilot study of Neogene sediments in western Pacific marginal basins (Chapter 2). An introduction to the theory behind isotopic characterization of sedimentary strata is presented below.

Fine-grained sedimentary strata provide a unique challenge in stratigraphic studies due to the monotonous, non-distinctive character of the rocks, the paucity of sedimentary structures, and the absence of unique provenance indicators. This problem is compounded in geologically complex accreted terranes, where the original paleogeographic relationships among coeval strata are obscured by major crustal structures and igneous complexes. Radiogenic isotopic analysis of fine-grained sedimentary strata should provide a distinct isotopic signature that may be utilized as a stratigraphic correlation tool among coeval strata in geologically complex areas where traditional stratigraphic methods are of dubious value. A portion of this investigation examines the feasibility of using radiogenic isotopes (Sm/Nd, Sr) to "fingerprint" fine-grained sedimentary rocks for use as a tool in stratigraphic correlation, and therefore as an aid in basin analysis and tectonic reconstructions.

The applicability of radiogenic isotopic correlation of fine-grained sediments to unraveling the stratigraphic and tectonic history of the southern Canadian Cordillera is unknown, and requires a test study. Neogene sediments from modern marginal basins provide a well-constrained sample group with which to test the validity of radiogenic isotope characterization. Drill core retrieved by the Ocean Drilling Program provides well-dated, precisely located sediment samples from modern marginal basins in known tectonic settings with known provenance. Fine-grained Plio-Pleistocene sediments have been retrieved from three different basins (Sea of Japan, Philippine Basin, Sulu Sea). Whole-rock isotopic analyses provide data regarding the lateral and vertical variations in isotopic signatures within these sediments. Fine-grained sediments of limited stratigraphic range in any one basin should display approximately similar radiogenic isotope signatures, reflecting provenance, and this signature should differ from the signal of coeval sediments in other basins, due to differences in provenance crustal history. Data collected from this study of modern marginal basin sediments will determine the viability of isotopic correlations in older, less well-constrained strata of the southern Canadian Cordillera. The results of this pilot study are described in Chapter 2.

E. U-Pb zircon analyses -

Provenance studies are particularly important in the identification of any detritus of continental affinity (i.e. older) within the basinal assemblages. Isotopic signatures (Nd and Sr) will identify any extremely old (i.e. Precambrian) material., but the identification of Late Paleozoic or Mesozoic detritus requires zircon provenance studies. Both the Cayoosh assemblage and the Ladner Group contain sections of quartzo-feldspathic sandstone of unknown affinity. Detrital zircon studies may provide definitive provenance information. In addition, primary emplacement ages on volcanic sequences in the Harrison Lake Formation are determined by U-Pb (zircon) geochronology.

Taken alone, each of these techniques can provide only circumstantial evidence of stratigraphic correlation. However, utilization of a variety of techniques provides multiple lines of evidence that may be used in support (or refutation) of proposed stratigraphic correlations.

1.2 GOALS

This investigation specifically addresses the following questions:

1. Are radiogenic isotopes (Sr and Nd) useful in stratigraphic characterization and correlation of basinal sequences, and can they be used in paleogeographic reconstructions of allochthonous terranes?

2. What is the character of each Middle Jurassic stratigraphic sequence, and how does the stratigraphic evolution in each sequence compare to that of its neighbors?

3. Were these Middle Jurassic strata originally deposited in different basins that were sequentially added to the continental margin, or were these strata originally parts of a single Middle Jurassic basin that has been subsequently dismembered?

4. What is the earliest age at which continental detrital input, and therefore continental proximity, can be proven?

1.3 PRESENTATION

This thesis is divided into four interrelated segments, and the results of each are presented as an individual manuscript, in accordance with university guidelines. Preparation of each segment as an individual manuscript facilitates subsequent publication, but results in unavoidable overlap and repetition.

The first segment consists of a pilot study into the viability of radiogenic isotopic correlation of fine-grained sediments in modern marginal basins of the Western Pacific. This pilot study is undertaken to evaluate the applicability of Nd and Sr isotopic analyses to stratigraphic correlation and basin discrimination in a well constrained basinal setting. Successful application of isotopic correlations in modern basins will support the use of the technique in Jurassic strata of the southern Canadian Cordillera. The remainder of the thesis documents the geologic setting of terranes in the southern Canadian Cordillera and proposes correlations among them.

The second thesis section characterizes the geology and geochemistry of the Harrison terrane, which forms the eastern edge of the westernmost (modern geography) volcanic arc in Middle Jurassic time. The geology, geochemistry, and isotopic signature of the Middle Jurassic Harrison Lake Formation has not been previously documented in detail. These characteristics will be used for comparison with adjacent basinal sequences.

The third section attempts to link the Harrison terrane with slightly older arc assemblages on Wrangellia to the west. The geology, geochemistry, and isotopic signature of Middle Jurassic volcanic strata in Wrangellia is examined in detail and compared to Middle Jurassic volcanic strata in the Harrison terrane to evaluate potential correlations between the volcanic units. Links between Wrangellia and terranes to the east

have not been documented prior to this investigation. This link is important for documenting the original aerial extent of Wrangellia and the heterogeneity of its basement rocks.

The final, and most extensive, portion of this investigation describes Middle Jurassic stratigraphic evolution and proposes terrane linkages among Harrison, Cadwallader, Bridge River and Methow terranes, and develops a model of Middle Jurassic basin development in the southern Canadian Cordillera. The lithostratigraphy, biostratigraphy, volcanic geochemistry and isotopic signature of Lower to Middle Jurassic strata on each terrane are examined in detail, and correlations are proposed on the basis of similarities documented between the terranes. This investigation represents the first systematic regional examination of Lower to Middle Jurassic strata on terranes of the southern Canadian Cordillera.

CHAPTER 2

ISOTOPIC FINGERPRINTING OF FINE-GRAINED CLASTIC SEDIMENTS: A CASE STUDY OF WESTERN PACIFIC MARGINAL BASINS

2. ISOTOPIC FINGERPRINTING OF FINE-GRAINED CLASTIC SEDIMENTS: A CASE STUDY OF WESTERN PACIFIC MARGINAL BASINS

2.1 INTRODUCTION

Fine-grained sedimentary strata provide a unique challenge in stratigraphic studies due to their typically monotonous, non-distinctive character, lack of sedimentary structures, and absence of distinctive provenance indicators. Traditional sedimentologic techniques (stratigraphy, petrography) rely on coarser-grained materials, which bias the data toward local sediment sources, and ignore more distal sources of sediment that may be of equal or greater importance in basin evolution and paleogeographic reconstructions. Detailed analyses of fine-grained strata, which form the bulk (>60%) of the global sedimentary mass, should yield important data relevant to stratigraphic correlation and the evolutionary history of individual basins.

Fine-grained deep marine sediments are the product of pelagic and hemipelagic deposition within a sedimentary basin and comprise sediment primarily transported to the basin in suspension by fluvial or aeolian processes. These processes tend to uniformly sample a given source region, and the long transportation histories of fine-grained materials lead to a complete mixing of heterogeneous detrital components, producing sediment with a composition that approximates the average crustal composition of a lithologically heterogeneous source region (Taylor and McLennan, 1985). The original average crustal composition of the source region may be modified, however, as most major and minor elements undergo some degree of geochemical modification during the sedimentary cycle (Taylor and McLennan, 1985; McLennan and Taylor, 1991). Numerous studies have demonstrated that the rare earth element (REE) composition of fine-grained sedimentary rocks closely mirrors that of the source region, indicating that little or no REE fractionation occurs during the sedimentary cycle (Nance and Taylor, 1976; Goldstein et al., 1984; Taylor and McLennan, 1985; Miller et al., 1986; Andre et al., 1986; Grousset et al., 1988). Geochemical and isotopic variations in the REE composition of fine-grained strata through time therefore record temporal variations in the sediment flux within any given basin, and may be useful stratigraphic markers for deciphering basin evolution.

Neodymium isotopic analyses of fine-grained sediments have been successfully utilized in both provenance determination and modeling crustal growth and evolution (Allegre and Rousseau, 1984; Goldstein et al., 1984; Miller and O'Nions, 1984; Michard et al., 1985; Miller et al., 1986; Goldstein and Jacobsen, 1988; McLennan et al., 1990). The majority of previous studies have focused on Nd isotopes as geochemical indicators of crustal evolution or on long term isotopic variations applicable to tectonic reconstructions (Miller and O'Nions, 1984; Andre et al., 1986; Frost and Coombs, 1989). The isotopic character of sediments from a variety of tectonic settings was examined by McLennan et al. (1990) to test the relationship between tectonic setting and provenance. The use of variability of the Nd-Sr isotopic signatures within basinal strata as a tool in stratigraphic studies and basin evolution and reconstruction has never been rigorously tested.

The isotopic composition of fine-grained sediments should be controlled by the relative contribution of material from the various source terranes feeding the depositional basin. Temporal variation in isotopic composition in a stratigraphic sequence may record the response of a depositional basin to evolution of the source terranes. If variations in the isotopic signature of fine-grained strata record the evolution of the source terranes, analysis of this signature can potentially provide invaluable information regarding basin development and evolution.

The Nd isotopic signature of modern deep sea sediments fluctuates within relatively restricted limits, reflecting the domination of continentally derived fluvial influx (Goldstein and Jacobsen, 1987, 1988). However, Grousset et al. (1988) show that zonation of Nd values occurs throughout an ocean basin, reflecting variations in provenance. McLennan et al. (1990) demonstrate that the Nd-Sr signatures of modern turbidites vary considerably, and that this variation can be related to tectonic setting. The largest degree of variation has been found at active plate margins, and is the result of the lack of mixing between arc-derived marginal basin sediments and the ambient, continentally derived, oceanic sediment mass (Grousset et al., 1988; Frost and Coombs, 1989). Such variations suggest that Nd isotopic fluctuations within a marginal basin succession may uniquely fingerprint that succession, allowing it to be compared to, or discriminated from, strata in different, coeval basins. The inference is that coeval strata within a single basin should display similar and correlatable

isotopic variations, and these variations should differ from strata in other basins as a result of variations in provenance resulting from differences in tectonism, basement character, and magmatic episodicity within each basin's source area.

The purpose of this study is to assess the viability of utilizing sedimentary isotopic fluctuations as a stratigraphic tool in basin analysis and the reconstruction and discrimination of individual basinal sequences. This study focuses on the isotopic signatures of Plio-Pleistocene sediments from marginal basins in the western Pacific. It seeks to determine the lateral and vertical variability of the isotopic signature of fine-grained sediments within these basins. Assessment of the viability of utilizing isotopic fluctuations as a stratigraphic tool requires a rigorous test case that allows direct comparison between the sedimentary isotopic signature and the isotopic characteristics of the source terrane. Western Pacific marginal basins provide a test case wherein the evolution of each basin is relatively well understood, as is the geology, isotopic systematics, and volcanic and tectonic episodicity of the source regions. The isotopic variability within strata from these basins can therefore be interpreted within a well constrained geologic framework. The Nd and Sr isotopic signatures of fine-grained sediments spanning the Plio-Pleistocene boundary from the Shikoku Basin in Philippine Sea, Sea of Japan, and Sulu Sea are used as a test case. Specifically, this study aims to determine: 1) if coeval sediments from geographically and geologically separate basins are isotopically distinct; 2) if isotopic fluctuations within stratigraphic sequences can be used as a stratigraphic correlation tool; and 3) the utility of isotopic fluctuations in delineating basin evolution.

2.2 BASIN DESCRIPTION

Three basins were selected for evaluation based on the quality of constraints on basin evolution and sedimentary provenance, and on the presence of sufficient drill sites within the basin. Sediment samples were obtained from drill sites cored by the Deep Sea Drilling Project (DSDP) and the subsequent Ocean Drilling Program (ODP; Fig. 2.1).

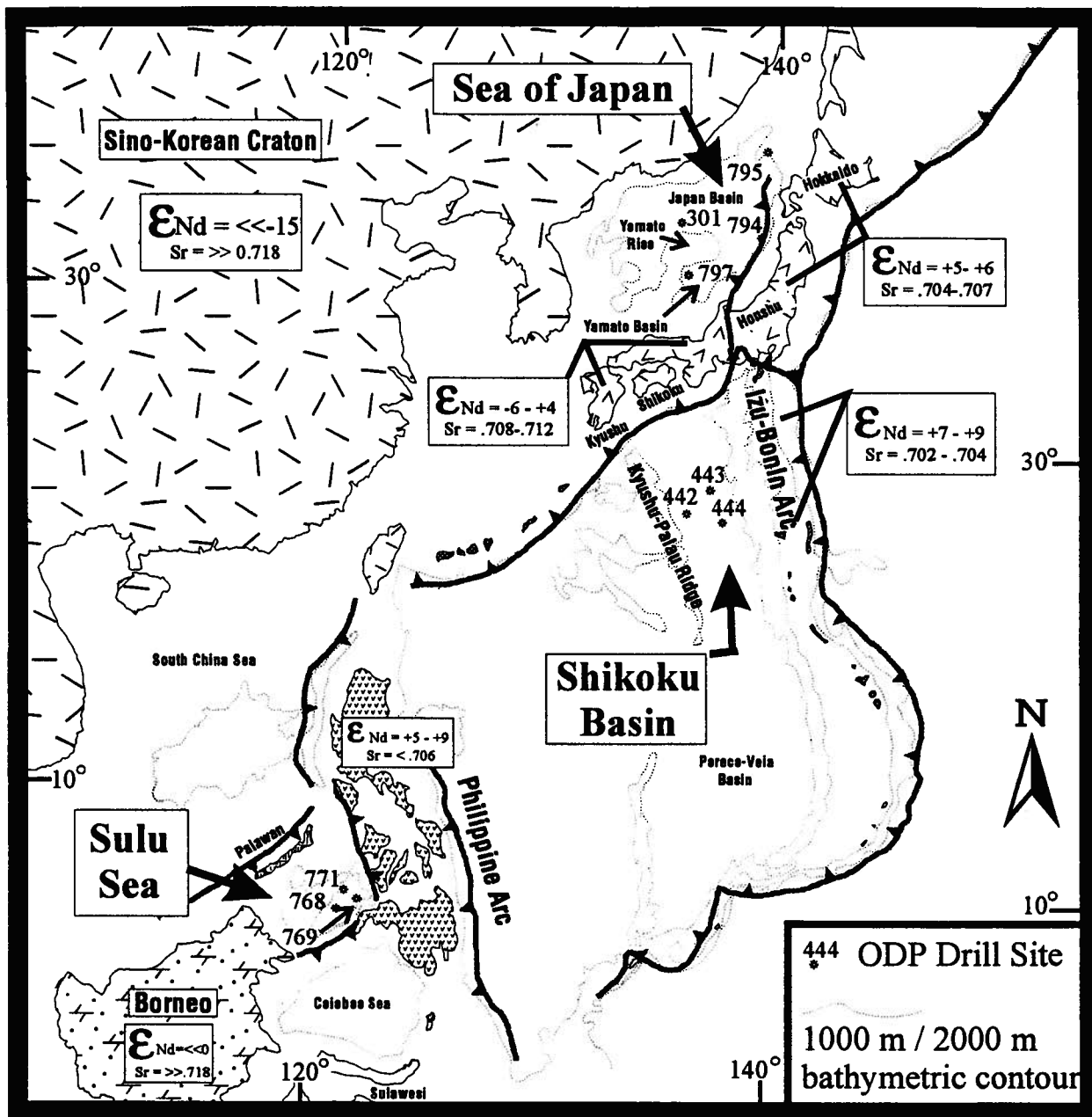


Figure 2.1 - Geographic map of western Pacific marginal basins, with location of ODP/DSDP drill sites examined in this study. Highly simplified crustal domains are shown, with average isotopic character of major source regions for marginal basin fine-grained sediments. Data sources listed in text.

Basins chosen for this study are the Shikoku Basin of Philippine Sea, Sea of Japan, and Sulu Sea (Fig. 2.1). These basins have been the subject of Ocean Drilling Program (ODP) investigations which have documented the basin morphology, physical sedimentology, biostratigraphy, sedimentation rates, and depositional setting of each basin (deVries Klein et al., 1980; Rangin et al., 1990; Tamaki, et al., 1990). A brief synopsis of each basin follows:

a. Sea of Japan

The Sea of Japan is a complex marginal basin that was initiated in early middle Miocene time by rifting of a continental arc. The Sea of Japan separates cratonal rocks of the Eurasian plate from the Japanese volcanic arc. It comprises two sub-basins, the Yamato Basin and the Japan Basin, which are separated by topographic highs interpreted as foundered and rifted continental blocks (Fig. 2.1; Tamaki, et al., 1990). The northern Sea of Japan contains the Japan Basin, which is a deep basin (3000-3700 m) underlain by oceanic crust capped by Miocene to Recent sediments. Ocean Drilling Program sites 794 and 795 are located along the eastern margin of the Japan Basin; site 301 is in the southern end (Fig. 2.1). The Yamato Basin is shallower (2000-2500 m) and smaller than the Japan Basin, and is separated from it by the Yamato Rise, a prominent topographic high composed of Mesozoic granitoids. Site 797 is located on the western margin of the Yamato Basin, immediately adjacent to the Yamato Rise (Fig. 2.1)

Sedimentation in the Sea of Japan was characterized by the deposition of diatomaceous hemipelagic sediment during the late Miocene and early Pliocene, and by an influx of terrigenous clastic debris during the late Pliocene and Quaternary. The increased clastic flux, accompanied by an increase in volcanic input, resulted from uplift of the northeast Honshu arc, which flooded both sub-basins with detritus during the late Pliocene and Quaternary.

Principal sediment sources to the Sea of Japan include: 1) northeast Japan "transitional" arc (Hokkaido and northern Honshu); 2) southwest Japan "continental" arc; and 3) Sino-Korean craton (Fig. 2.1).

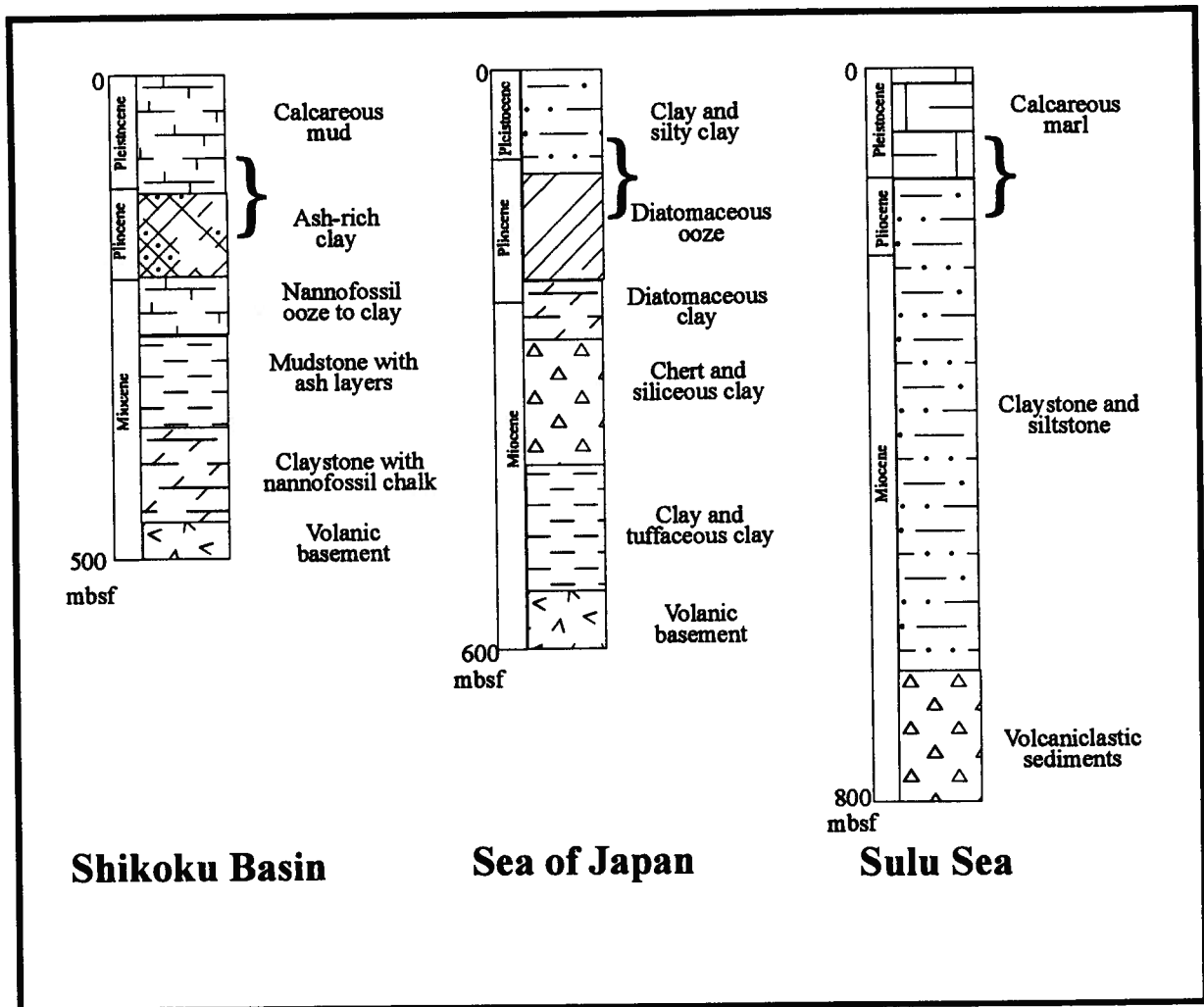


Figure 2.2 - Generalized stratigraphic columns of Shikoku Basin, Sea of Japan, and Sulu Sea ODP/DSDP drill holes. Data from deVries Klein et al. (1980), Rangin et al. (1990), and Tamaki et al. (1990). Brackets indicate stratigraphic interval examined; mbsf = metres below sea floor.

Northeast Japan contains extensive Cenozoic volcano-sedimentary cover, including the Miocene Green Tuff belt, overlying Mesozoic subduction-accretion complexes (Isozaki et al., 1990), and is characterized by transitional ϵ_{Nd} values ($\sim +5$ to $+6$; Nohda and Wasserburg, 1981). Southwest Japan is underlain by late Paleozoic to Tertiary subduction-accretion complexes and granitic intrusions. ϵ_{Nd} values vary from approximately -6 to $+4$, reflecting the influence of older continental basement (Morris and Kagami, 1989; Nakamura et al., 1990; Isozaki et al., 1990; Kagami et al., 1992). The Sino-Korean craton is primarily composed of Archean and Proterozoic igneous, metamorphic and metasedimentary rocks, minor Paleozoic sedimentary rocks and Mesozoic continental arc rocks (Xiong and Coney, 1985; Parfenov, and Natal'in, 1985). Isotopic values reflect the cratonic affinity of the region, with $^{87}Sr/^{86}Sr > 0.706$, and ϵ_{Nd} values < -15 (Xu, 1990).

b. Shikoku Basin

The Shikoku Basin of the Philippine Sea is an elongate, fan-shaped inactive backarc basin that opened in the early to middle Miocene (deVries Klein and Kobayashi, 1980; Park et al., 1990). The basin is located in the northeast portion of the Philippine Sea, and is flanked on the north by the Japanese Islands and on the east by the Izu Bonin arc. The Shikoku Basin merges to the south with the Parece Vela Basin, and both are isolated from the rest of the Philippine Sea by the Kyushu-Palau Ridge (Fig. 2.1). The Shikoku Basin is roughly divided into two subbasins by the Kinan Seamount Chain, with the eastern portion displaying a rougher and shallower topography than the western portion (Park et al., 1990). Water depth in both areas exceeds 4500 m (de Vries Klein et al., 1980). Deep Sea Drilling Project (DSDP) drill holes 297 and 442 are in the western subbasin; drill holes 443 and 444 are in the eastern subbasin (Fig. 2.1).

Seismic profiles demonstrate that the Shikoku Basin contains three coalescing clastic wedges, which prograded into the basin from the north, west, and east, reflecting clastic influx from Japan, the Kyushu-Palau Ridge, and the Izu-Bonin arc, respectively (Karig, 1975). Pliocene sedimentation was characterized by deposition of hemipelagic mudstone and volcanic ash (Figs. 2.2, 2.3) Abundant resedimented sandstones

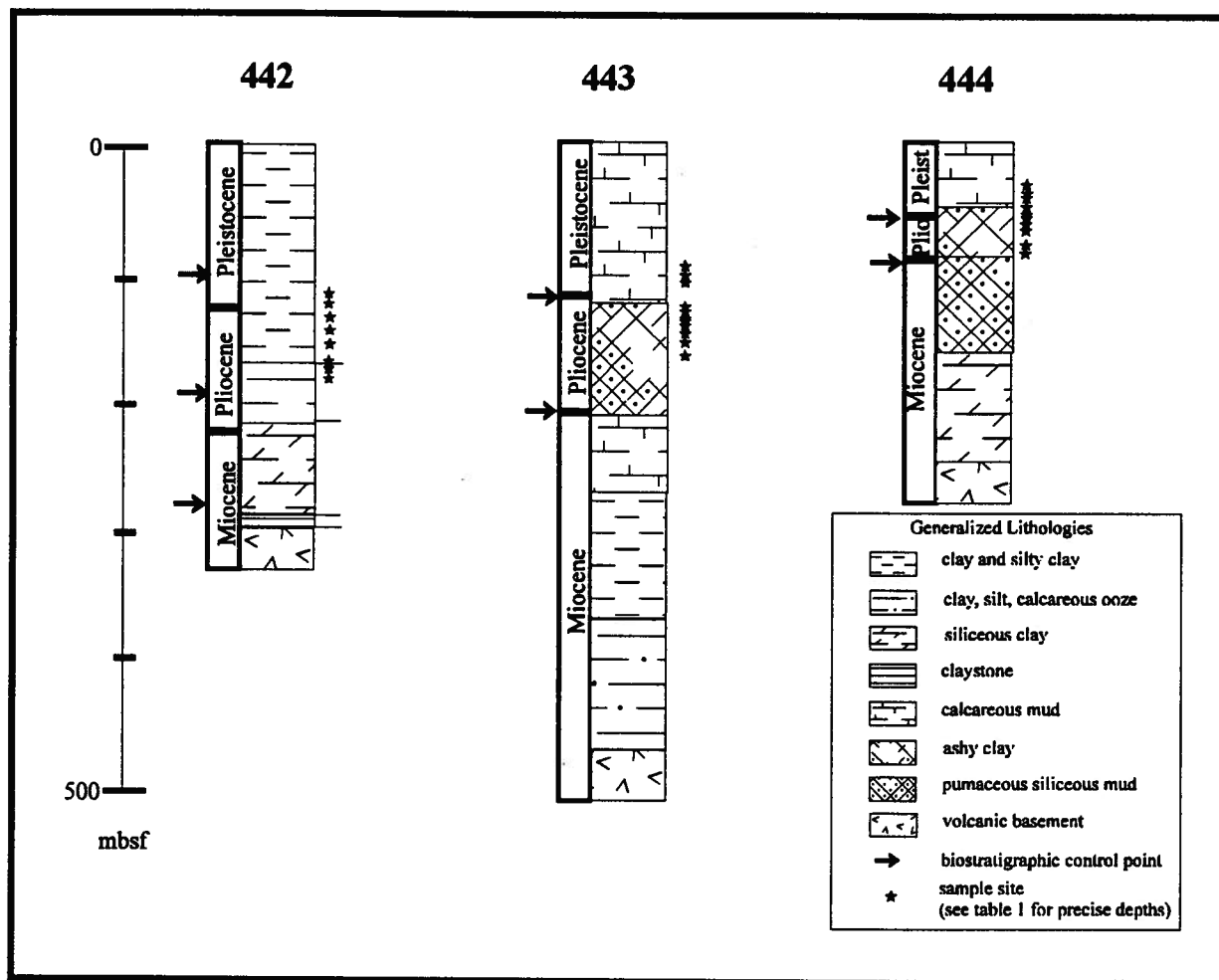


Figure 2.3 - Stratigraphic sections of DSDP drill holes in the Shikoku Basin. Arrows indicate biostratigraphic control points. Data from deVries Klein et al. (1980). Stars indicate sample sites; precise sample intervals are given in Table 2.1; mbsf = metres below sea floor.

occur in the northern portion of the basin (Curtis and Echols, 1980). Pleistocene sedimentation was dominated by the deposition of hemipelagic mudstone with a high percentage of calcareous biogenic sediments. The decrease in terrigenous clastic influx in the Pleistocene is the result of decreased volcanic activity in the Izu-Bonin arc, and the inception of the Nankai Trough at the northern end of the basin.

The Izu-Bonin arc on the east and southwest Japan to the north are the dominant sediment sources in the Shikoku Basin. The Kyushu-Palau Ridge to the west was intermittently emergent and supplied sediment to the basin during the Pliocene and Pleistocene. The Izu-Bonin arc is an oceanic arc that has supplied both volcanic ash and volcanic clastic debris to the Shikoku Basin since the Miocene (Curtis and Echols, 1980). The arc is typified by island arc tholeiitic basalt characterized by juvenile ϵ_{Nd} values (+8 - +9) (Nohda and Wasserburg, 1981). Southwest Japan, as previously described, displays ϵ_{Nd} values between approximately (-6) and (+4) (Morris and Kagami, 1989; Nakamura et al., 1989; Isozaki et al., 1990; Kagami et al., 1992). Isotopic data for the Kyushu-Palau Ridge are unavailable, but it is assumed to be juvenile in character.

c. Sulu Sea

The Sulu Sea is a deep (4000-5000 m), elongate, restricted basin situated west of the Philippine arc and northeast of Borneo (Fig. 2.1). It is one of the smallest marginal basins in the western Pacific. The Sulu Sea is divided into two subbasins by the northeast-trending Cagayan Ridge. The subbasins are flanked by prominent ridges that are parallel to the elongation of the basin. These ridges are alternately covered by reefs or emergent, exposing thrust faulted continental rocks on both the northwest and southeast side of the basin (Rangin and Silver, 1990).

Pliocene strata in the Sulu Sea consist of a thick sequence of turbidite sandstone, siltstone and clay overlain by hemipelagic claystone, which is in turn overlain by Pleistocene thin to thick-bedded pelagic foraminifer-nannofossil marls, carbonate turbidites, and volcanogenic clayey siltstone (Rangin et al., 1990). Volcanic ash beds occur throughout the sequence. The general fining-upward trend is interpreted to indicate a

decrease in the importance of terrigenous clastic input and an increasing importance of hemipelagic and pelagic sedimentation across the Plio-Pleistocene boundary.

The Sulu Sea is a back-arc basin formed within a Neogene collision zone involving Mesozoic accretionary prisms and the Philippine arc (Rangin, 1989). There are four principal sediment sources for the Sulu Sea: 1) Mesozoic metasediments, schist, olistostrome, and ophiolite of the Palawan accretionary prism and underlying continental basement exposed to the northwest; 2) Philippine arc volcanics to the east; 3) Sulu volcanic ridge and underlying Mesozoic accretionary prism to the southeast; and 4) eastern Borneo, which consists of a Mesozoic accretionary prism (Rangin, 1989; Rangin and Silver, 1990). Isotopic data are sparse for the Mesozoic accretionary complexes west of the Philippine arc, but tectonic models for the region indicate an affinity with cratonal materials from southern China, suggesting probable ϵ_{Nd} values < 0 (Faure et al., 1989). The Philippine arc is typified by ϵ_{Nd} values of (+5)-(+9), and $^{87}Sr/^{86}Sr$ of < 0.7060 (Defant et al., 1989).

2.3 METHODS

A. Sample Selection

Late Pliocene and Early Pleistocene fine-grained sediments were sampled in each basin (Fig. 2.2). Approximately the same chronostratigraphic interval was sampled in each basin in order to provide temporal constraints on isotopic fluctuations induced by changes in seawater chemistry, climatic conditions, and eustasy. Young sediments (< 4 Ma) were sampled because the modern geologic setting and basin configuration provide reasonably good constraints on basin morphology, sedimentologic patterns, and basin margin tectonism and volcanism during the time of deposition. The shallow burial depth of the sediments (< 250 m) limits diagenetic alterations to those imparted under shallow burial diagenesis, which should be limited to partial equilibration with seawater isotopic compositions and the deposition of authigenic cements (Singer and Muller, 1983; Hesse, 1990). The Plio-Pleistocene boundary in each basin is roughly coincident

with a significant change in sediment type, allowing the influence of provenance variations on the isotopic signature to be evaluated.

Multiple drill sites were sampled from each basin (Fig. 2.1). Drill cores were selected according to: 1) the density of drill sites in the basin; 2) the location of the drill site with respect to the basin margin; and 3) the percentage of core recovery through the stratigraphic interval of interest. Adequate spacing of drill sites was required to completely sample the basin and incorporate lateral sedimentologic variations throughout the basin. Drill sites in the interior of the basins were chosen where possible to avoid proximal sediment near the basin margin, thereby minimizing point source bias and maximizing the probability of complete hemipelagic sediment mixing. The percent core recovery was a deciding factor in selecting drill cores to be sampled; drill cores with poor recovery or excessive drilling disturbance were avoided.

Sediments within individual drill cores were sampled symmetrically about the Plio-Pleistocene boundary, which is biostratigraphically located in each drill hole, providing a control point for absolute age control (Fig. 2.2). Samples were taken at 0.4-0.5 Ma intervals, based on calculated sedimentation rates, and an interval of approximately 1-1.5 Ma was sampled on either side of the Plio-Pleistocene boundary. Higher sample frequency (0.1-0.3 Ma/sample) was utilized in the Shikoku Basin to test the viability of intrabasinal correlation. Samples were selected such that each lithologic unit within the sample interval was represented.

An assumption inherent in this sampling procedure was that fine-grained, homogeneous sedimentary intervals represent well-mixed hemipelagic and pelagic sediment, indicative of the ambient "background" sedimentation of the basin. Slightly coarser, graded beds, probably turbidite deposits, are considered to be of probable "point-source" origin, and thus were not sampled. Only relatively thick (> 20 cm), fine-grained, homogeneous clay and silty clay intervals were sampled, in order to avoid turbidity-current-related hemipelagic deposits. Laminated silt and fine sand intervals were avoided, as were volcanic ash layers. It is recognized that much of the fine-grained, homogenous sediment in any deep marine basin, even within thick sequences, may be of turbiditic origin. However, the majority of this fine-grained sediment was initially

transported in fluvial or aeolian suspension, and therefore has the highest probability of representing an integrated, "average" crustal composition of the source area.

B. Age Control

The age of sediment samples was determined by paleontologic studies of foraminifera, nannofossils, and radiolaria (de Vries Klein et al., 1980; Okada, 1980; Rangin et al., 1990). Paleontologic resolution varied considerably between drill holes, as a function of core recovery, faunal preservation, and paleontologic sampling interval. The Plio-Pleistocene boundary has been located as accurately as possible in all drill holes. (Okada, 1980; Tamaki et al. 1990). Sedimentation rates are established for each lithologic unit based on unit thickness and the estimated depositional time span; the accuracy of the calculated rate is dependent on the degree of paleontologic and magnetostratigraphic resolution (deVries Klien, 1980; Okada, 1980; Tamaki, 1990). This method of estimating sedimentation rate implies a steady sediment accumulation through time, which is obviously not the case in active marginal basins characterized by rapid episodic sediment accumulation. However, in the absence of reliable isotopic chronostratigraphy, sedimentation rates are the only method available for estimating the age of any particular sample interval. The absolute age of each sediment sample was estimated by extrapolating the sedimentation rate for each lithologic unit from the Plio-Pleistocene boundary to the sample depth in question. This method is the best available means of age estimation, although the confidence level of the age estimate is variable within each drill hole, and, in general, decreases with distance from the Plio-Pleistocene boundary.

C. Analytical Procedures

Sediment samples (n=70) were obtained from drill cores at the Ocean Drilling Program Gulf Coast and West Coast Repositories. Approximately 12 cm³ of sample were air dried and crushed to fine powder in a mechanical agate mortar. Sample splits of 200-300 mg each were processed separately for Sm/Nd concentration, and Sr and Nd isotopic composition.

a. Rb/Sr

Sample powders underwent warm (+100°C) dissolution in concentrated HF in Savillex beakers. No attempt was made to leach out the carbonate fraction prior to dissolution, with the exception of one test sample. Sr isotopic composition was measured on unspiked samples purified utilizing standard cation exchange techniques (Faure and Powell, 1972). Sr isotopic measurements were made on a VG-Isomass 54R mass spectrometer at The University of British Columbia. Measured isotopic ratios have been normalized to a $^{86}\text{Sr}/^{88}\text{Sr}$ ratio of 0.1194. Replicate analyses of National Bureau of Standards standard SrCO_3 (SRM987) during the course of this study give a value 0.000078 below the $^{87}\text{Sr}/^{86}\text{Sr}$ reference value of 0.710190 \pm 0.000020 (n=16).

Rb and Sr concentrations were determined by replicate X-Ray fluorescence analyses of pressed powder pellets, using U.S. Geological Survey rock standards for calibration. Rb/Sr ratios have a precision of 2% (1 s); concentrations have a precision of \pm 5%.

b. Sm/Nd

Isotopic dilution analysis was performed on spiked samples, whereas Nd isotopic concentration ($^{143}\text{Nd}/^{144}\text{Nd}$) analysis utilized unspiked samples. All samples underwent a 12-hour warm predissolution in concentrated HF in Krogh-style Teflon dissolution bombs (Krogh, 1973), followed by a 5-day dissolution in the same bombs in a HF-HNO₃ mixture at 190°C to ensure dissolution of all refractory phases.

For isotopic dilution analysis, a mixed ^{149}Sm - ^{150}Nd spike was added prior to initial dissolution (Andrew et al., 1991). Following 5-day dissolution, the "bomb" sample was fluxed repeatedly in 6N HCl to convert fluorides to chlorides. Rare Earth Elements (REE) were separated using standard cation exchange chromatography with 5N HCl as the elutant. The dried REE residue was loaded onto double Re filaments, and run on a modified VG-Isomass 54R mass spectrometer at The University of British Columbia. Replicate

analyses of international USGS standards (BCR, BHVO, BIR) and samples from the current study demonstrate a concentration reproducibility of < 5%, and ratio reproducibility of < 2%.

For isotopic composition analyses, the unspiked "bomb" sample was fluxed repeatedly in 6N HCl following 5-day dissolution and the group REE were purified by standard cation exchange chromatography, using 3N HCl followed by 6N HCl as the elutiant. Neodymium was separated from the group REE on Teflon columns containing Teflon powder treated with HDEHP (di-2-ethylhexyl orthophosphoric acid), using 0.25 N HCl as elutant. The concentrated Nd was loaded onto a double Re filament assembly, and analyzed on a Finnigan MAT 261 multicollector mass spectrometer in static collection mode at the Geochronology Laboratory of the Geological Survey of Canada (Theriault, 1990). Measured ratios are normalized to a $^{146}\text{Nd}/^{144}\text{Nd}$ ratio of 0.7219 (O'Nions, et al., 1979), and corrected to La Jolla Nd standard $^{143}\text{Nd}/^{144}\text{Nd}=0.511850$. Blanks for Sm and Nd are approximately 0.1 and 2 ng, respectively.

D. Data Presentation

Isotopic ratios are reported as initial ratios, calculated at the depositional age of the sediments. The young age of the sediments results in very minor corrections relative to present day values. The isotopic ratio of the sediments at the time of deposition is assumed to reflect the average isotopic composition of the entire drainage basin at that time; the drainage basin will in most cases comprise multiple sources of different isotopic signatures. The average isotopic composition will therefore vary with time as a function of the relative contribution of any individual source to the total sediment budget of the basin at any point in time. The depositional age of the sediments is younger than the actual age of the source areas; therefore, the initial ratios reported represent minimum initial isotopic values.

The possibility of strontium isotopic equilibration between seawater and terrigenous detritus makes it difficult to isolate either signal individually. Carbonate cement was leached from one sample using weak (1 N) hydrochloric acid in order to determine if isotopic equilibration had occurred. The leached fraction

displayed an $^{87}\text{Sr}/^{86}\text{Sr}$ ratio higher than that of coeval seawater values (Hodell et al., 1991), suggesting partial equilibration between seawater Sr from authigenic carbonate cement and detrital Sr. Therefore, strontium analyses are on whole rock sediment samples, and the measured $^{87}\text{Sr}/^{86}\text{Sr}$ ratios represent a mixture of seawater Sr and detrital Sr isotopic ratios. Seawater Sr isotopic values vary linearly from 0.7090 - 0.7092 (Hodell et al., 1991) during the time period being analyzed for this investigation; any Sr isotopic fluctuation outside this range is interpreted to be the result of changes in the detrital signature.

Neodymium analyses are expressed in initial ϵ_{Nd} notation (DePaolo and Wasserburg, 1977), using present-day values of CHUR $^{143}\text{Nd}/^{144}\text{Nd}=0.512638$ and $^{147}\text{Nd}/^{144}\text{Nd}=0.1967$ (Jacobson and Wasserburg, 1980).

2.4 RESULTS

Isotopic data for the Shikoku Basin, the Sea of Japan, and the Sulu Sea are graphically presented as initial $^{87}\text{Sr}/^{86}\text{Sr}$ versus initial ϵ_{Nd} on figure 2.4 and are tabulated in Table 1. The strontium values for all samples are between 0.7065-0.7160, and ϵ_{Nd} values are consistently negative [(-0.5) - (-9.3)].

The Sulu Sea isotopic signature is distinct from both the Sea of Japan and the Shikoku Basin, with lower initial Sr values and less evolved (= less "continental") ϵ_{Nd} values. There is a high degree of overlap between the Shikoku Basin and the Sea of Japan, with both displaying the same range in Sr values. The mean value for ϵ_{Nd} in Sea of Japan sediments, however, is slightly higher (less evolved) than coeval sediments in the Shikoku Basin. The more evolved values in the Shikoku Basin were unexpected, in that the Shikoku Basin is isolated from any obvious sources of evolved Nd. In both the Sea of Japan and the Shikoku Basin, there is a roughly inverse relationship between $^{87}\text{Sr}/^{86}\text{Sr}$ and ϵ_{Nd} . This relationship is not apparent in the Sulu Sea, but this is probably the result of the smaller sample set. There is no consistent linear relationship between either $^{87}\text{Sr}/^{86}\text{Sr}$ values or ϵ_{Nd} values and the age of the sediments in any of the basins.

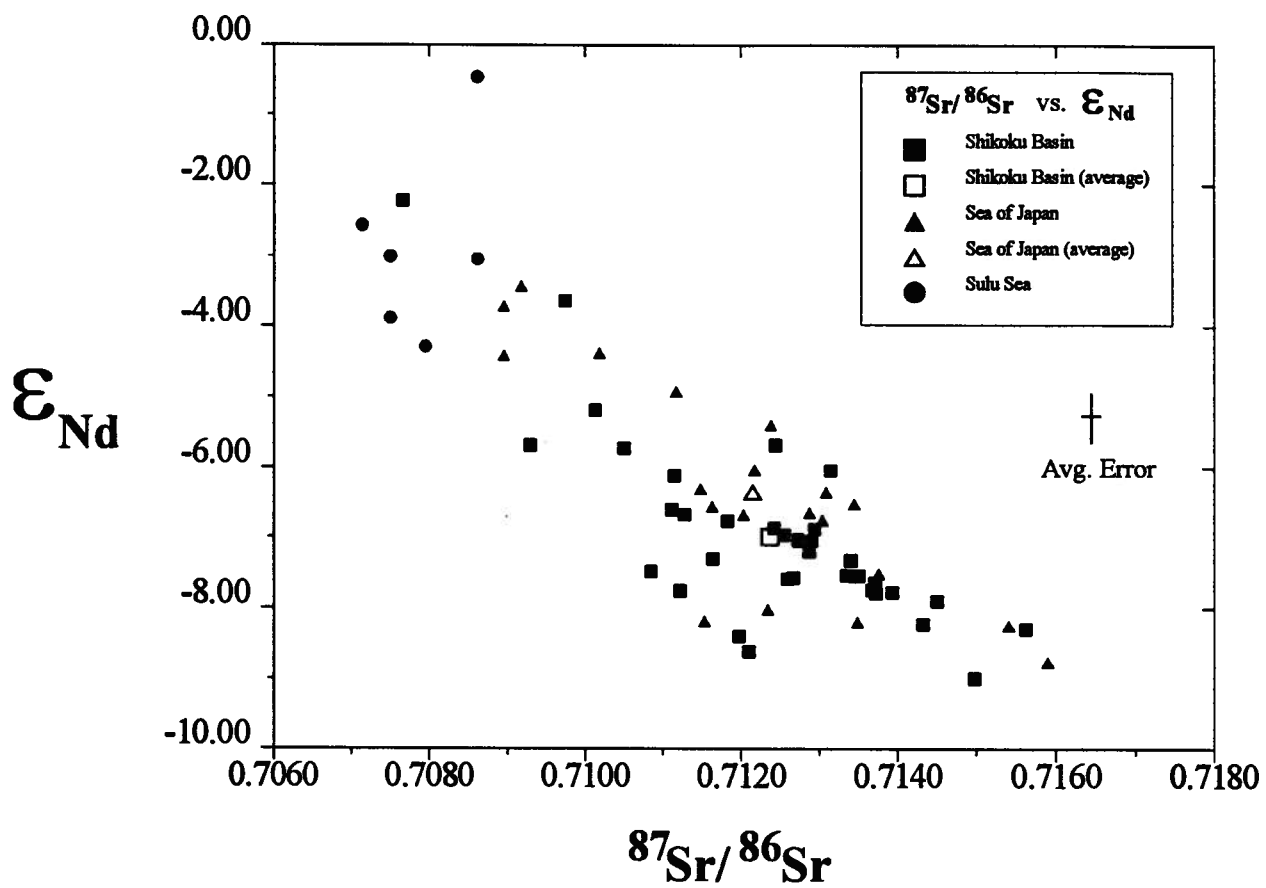


Figure 2.4 - $^{87}\text{Sr}/^{86}\text{Sr}$ versus ϵ_{Nd} values for all samples studied. Note strong degree of overlap between Shikoku Basin and Sea of Japan, contrasting with separation of Sulu Sea samples.

| SEA OF JAPAN | | | | | | | | | | 143/144 | | | | f | | Epsilon(E) | |
|---------------|---------|--------|---------|----|-----------|--------|--------|---------|-----------|---------|--------|----------|----|---------|-------|------------|-------|
| Depth (mbsef) | Age(Ma) | Sr (m) | Sr | Rb | 87Rb/86Sr | Sr (i) | Sm ppm | Nd ppm | mi47/ND14 | | | | | | | | |
| 301-4-5 | 161.28 | 1.39 | 0.71123 | 3 | 121.13 | 130.05 | 3.11 | 0.71117 | 6.02 | 29.60 | 0.1230 | 0.512385 | 5 | -0.3747 | -4.94 | -4.92 | |
| 301-5-6 | 182.20 | 1.64 | 0.71351 | 3 | 129.43 | 135.32 | 3.03 | 0.71344 | 6.10 | 31.00 | 0.1192 | 0.512303 | 5 | -0.3940 | -6.53 | -6.52 | |
| 301-7-1 | 213.45 | 2.00 | 0.71384 | 3 | 121.46 | 135.22 | 3.22 | 0.71375 | 5.91 | 30.40 | 0.1175 | 0.512252 | 5 | -0.4026 | -7.53 | -7.51 | |
| 301-8-1 | 240.59 | 2.32 | 0.71601 | 4 | 87.74 | 107.28 | 3.54 | 0.71590 | 4.67 | 23.28 | 0.1213 | 0.512188 | 5 | -0.3833 | -8.78 | -8.76 | |
| 794-5-5 | 42.74 | 1.21 | 0.71167 | 4 | 163.02 | 107.61 | 1.91 | 0.71163 | 7.16 | 33.86 | 0.1279 | 0.512301 | 7 | -0.3498 | -6.57 | -6.56 | |
| 794-7-1 | 55.54 | 1.64 | 0.71310 | 3 | 137.19 | 130.86 | 2.76 | 0.71303 | 6.37 | 31.00 | 0.1242 | 0.512291 | 5 | -0.3686 | -6.77 | -6.75 | |
| 794-8-6 | 72.71 | 2.32 | 0.71210 | 3 | 126.01 | 98.69 | 2.27 | 0.71203 | 4.52 | 22.45 | 0.1217 | 0.512295 | 8 | -0.3813 | -6.69 | -6.67 | |
| 794-10-4 | 88.38 | 2.79 | 0.71318 | 4 | 84.52 | 76.52 | 2.62 | 0.71308 | 3.99 | 19.33 | 0.1248 | 0.512311 | 8 | -0.3655 | -6.38 | -6.35 | |
| 794-11-2 | 94.05 | 2.96 | 0.71155 | 3 | 132.23 | 83.18 | 1.82 | 0.71148 | 4.81 | 22.49 | 0.1294 | 0.512313 | 5 | -0.3421 | -6.34 | -6.31 | |
| 794-11-6 | 101.20 | 3.14 | 0.71298 | 7 | 123.15 | 100.38 | 2.36 | 0.71287 | 5.71 | 27.27 | 0.1266 | 0.512296 | 4 | -0.3564 | -6.67 | -6.64 | |
| 795-7-5 | 63.48 | 1.05 | 0.70919 | 5 | 145.05 | 73.25 | 1.46 | 0.70917 | 4.65 | 20.87 | 0.1346 | 0.512462 | 14 | -0.3157 | -3.43 | -3.42 | |
| 795-9-1 | 76.26 | 1.28 | 0.71022 | 6 | 138.96 | 93.96 | 1.96 | 0.71019 | 5.67 | 25.35 | 0.1355 | 0.512413 | 4 | -0.3111 | -4.39 | -4.38 | |
| 795-10-1 | 86.31 | 1.45 | 0.70899 | 11 | 141.72 | 88.84 | 1.81 | 0.70895 | 4.84 | 21.89 | 0.1335 | 0.512447 | 8 | -0.3213 | -3.73 | -3.71 | |
| 795-11-7 | 104.11 | 1.64 | 0.71121 | 2 | 120.59 | 98.21 | 2.36 | 0.71092 | 4.96 | 23.21 | 0.1291 | 0.512361 | 2 | -0.3437 | -5.40 | -5.39 | |
| 795-14-5 | 129.71 | 1.97 | 0.70899 | 4 | 121.97 | 67.56 | 1.60 | 0.70895 | | 16.87 | 0.1317 | 0.512411 | 7 | -0.3305 | -4.43 | -4.41 | |
| 795-16-1 | 143.13 | 2.14 | 0.70964 | 6 | 82.91 | 72.01 | 2.16 | 0.70935 | 3.94 | 17.80 | 0.1337 | | | | | | |
| 797-7-4 | 58.59 | 1.13 | 0.71545 | 4 | 127.95 | 125.09 | 2.83 | 0.71540 | 6.92 | 34.60 | 0.1210 | 0.512215 | 6 | -0.3849 | -8.25 | -8.24 | |
| 797-9-5 | 79.29 | 1.58 | 0.71155 | 8 | 321.27 | 117.19 | 1.06 | 0.71153 | 5.54 | 26.59 | 0.1268 | 0.512218 | 6 | -0.3554 | -8.19 | -8.18 | |
| 797-11-6 | 100.24 | 2.01 | 0.71239 | 8 | 173.49 | 115.16 | 1.92 | 0.71234 | 5.65 | 26.94 | 0.1267 | 0.512226 | 6 | -0.3559 | -8.04 | -8.02 | |
| 797-13-5 | 117.77 | 2.36 | 0.71224 | 3 | 110.99 | 84.38 | 2.20 | 0.71217 | | | | 0.512328 | 4 | -0.3645 | -6.05 | -6.03 | |
| 797-15-6 | 137.81 | 2.76 | 0.71357 | 3 | 140.98 | 123.01 | 2.16 | 0.71348 | 4.24 | 19.49 | 0.1314 | 0.512217 | 4 | -0.3320 | -8.21 | -8.19 | |
| Average | | | | | | | | 0.71194 | | | | | | | | | -6.35 |
| SULU BASIN | | | | | | | | | | | | | | | | | |
| 768-11-2 | 91.23 | | | | 635.28 | 33.71 | 0.15 | 0.00000 | | | | | 0 | | | | |
| 768-13-4 | 113.04 | | | | 798.86 | 33.92 | 0.12 | 0.00000 | | | | | 0 | | | | |
| 768-14-1 | 119.17 | | | | 843.20 | 40.02 | 0.14 | 0.00000 | | | | | 0 | | | | |
| 768-14-5 | 124.17 | | | | 151.39 | 100.19 | 1.91 | 0.00000 | | | | | 0 | | | | |
| 768-15-6 | 135.48 | | | | 167.69 | 86.86 | 1.50 | 0.70749 | 4.16 | 19.51 | 0.1292 | 0.512439 | 6 | | -3.88 | | |
| 768-16-6 | 145.31 | | | | 111.94 | 102.91 | 2.66 | 0.70544 | | | | | 0 | | | | |
| 769-10-3 | 85.06 | | | | 644.54 | 34.26 | 0.15 | 0.70861 | 2.16 | 9.63 | 0.1358 | 0.512615 | 6 | | -0.45 | | |
| 769-11-2 | 93.07 | | | | 674.16 | 40.43 | 0.17 | 0.70861 | | | | 0.512482 | 24 | | -3.04 | | |
| 769-12-2 | 102.63 | | | | 206.41 | 71.85 | 1.01 | 0.70713 | 3.86 | 16.93 | 0.1384 | 0.512500 | 4 | | -2.56 | | |
| 769-13-5 | 116.81 | | | | 182.09 | 86.67 | 1.38 | 0.70795 | 4.71 | 20.65 | 0.1373 | 0.512418 | 8 | | -4.29 | | |
| 769-14-3 | 123.21 | | | | 1178.06 | 65.42 | 0.81 | 0.70750 | 4.07 | 18.66 | 0.1321 | 0.512484 | 7 | | -3.00 | | |
| 771-1R-1 | 100.81 | | | | 405.42 | 71.91 | 0.51 | 0.00000 | | | | | | | | | |

Table 2.1a - Isotopic data for western Pacific marginal basins.

| SHIKOKU BASIN | | | | | | | | | | | | | | | | |
|---------------|---------|--------|---------|----|-----------|--------|--------|---------|----------|---------|--------|----------|--------|---------|-------|-------|
| Depth (mbsef) | Age(Ma) | Sr (m) | Sr | Rb | 87Rb/86Sr | Sr (i) | Sm ppm | Nd ppm | ml47Nd14 | 143/144 | f | eNd(i) | eNd(o) | | | |
| 442-12-5 | 112.53 | 1.29 | 0.71277 | 3 | 118.42 | 114.70 | 2.80 | 0.71272 | 5.12 | 25.47 | 0.1217 | 0.512277 | 5 | -0.3813 | -7.04 | -7.03 |
| 442-13-2 | 119.00 | 1.52 | 0.71340 | 3 | 123.22 | 105.17 | 2.47 | 0.71335 | 5.54 | 28.03 | 0.1202 | 0.512251 | 6 | -0.3889 | -7.55 | -7.53 |
| 442-14-3 | 129.96 | 1.85 | 0.71346 | 11 | 125.97 | 61.78 | 2.57 | 0.71340 | 6.79 | 29.70 | 0.1382 | 0.512262 | 7 | -0.2974 | -7.33 | -7.32 |
| 442-15-2 | 137.40 | 2.09 | 0.71293 | 10 | 127.60 | 104.30 | 2.36 | 0.71286 | 5.73 | 27.35 | 0.1267 | 0.512268 | 9 | -0.3559 | -7.22 | -7.20 |
| 442-16-2 | 146.89 | 2.40 | 0.71572 | 3 | 115.96 | 122.99 | 3.07 | 0.71562 | 6.07 | 29.57 | 0.1242 | 0.512212 | 12 | -0.3686 | -8.31 | -8.29 |
| 442-18-1 | 164.58 | 2.97 | 0.71305 | 5 | 123.54 | 113.11 | 2.65 | 0.71294 | 5.89 | 29.31 | 0.1227 | 0.512284 | 8 | -0.3762 | -6.91 | -6.88 |
| 442-18-3 | 167.50 | 3.06 | 0.71022 | 18 | 139.61 | 99.27 | 2.06 | 0.71013 | 6.47 | 29.08 | 0.1345 | 0.512371 | 7 | -0.3162 | -5.21 | -5.18 |
| 442-19-2 | 175.60 | 3.33 | 0.71379 | 3 | 128.10 | 122.42 | 2.77 | 0.71366 | 7.36 | 33.35 | 0.1334 | 0.512240 | 6 | -0.3218 | -7.76 | -7.74 |
| 443-11-2 | 95.38 | 1.43 | 0.71125 | 5 | 253.72 | 116.63 | 1.33 | 0.71122 | 5.40 | 24.32 | 0.1341 | 0.512240 | 8 | -0.3183 | -7.76 | -7.75 |
| 443-11-6 | 100.20 | 1.49 | 0.71439 | 9 | 120.50 | 131.87 | 3.17 | 0.71432 | 6.11 | 28.82 | 0.1282 | 0.512216 | 4 | -0.3782 | -8.23 | -8.22 |
| 443-12-2 | 104.10 | 1.54 | 0.71201 | 3 | 165.78 | 114.77 | 2.00 | 0.71197 | 4.92 | 24.04 | 0.1238 | 0.512207 | 13 | -0.3706 | -8.41 | -8.39 |
| 443-14-2 | 123.84 | 1.90 | 0.71249 | 4 | 161.45 | 120.38 | 2.16 | 0.71243 | 5.27 | 25.49 | 0.1250 | 0.512346 | 16 | -0.3645 | -5.70 | -5.68 |
| 443-14-4 | 126.54 | 2.02 | 0.71123 | 4 | 121.20 | 118.98 | 2.84 | 0.71114 | 5.68 | 25.83 | 0.1329 | 0.512324 | 9 | -0.3244 | -6.13 | -6.11 |
| 443-15-2 | 133.19 | 2.33 | 0.71381 | 5 | 123.94 | 127.13 | 2.97 | 0.71371 | 5.84 | 29.44 | 0.1208 | 0.512245 | 9 | -0.3859 | -7.67 | -7.64 |
| 443-15-4 | 135.88 | 2.45 | 0.71508 | 4 | 128.48 | 127.05 | 2.86 | 0.71498 | 6.13 | 29.67 | 0.1250 | 0.512644 | 8 | -0.3965 | -9.01 | -8.99 |
| 443-15-6 | 139.02 | 2.59 | 0.71383 | 6 | 124.80 | 127.06 | 2.95 | 0.71372 | 5.82 | 29.40 | 0.1198 | 0.512238 | 7 | -0.3910 | -7.78 | -7.78 |
| 443-16-2 | 143.80 | 2.81 | 0.71324 | 4 | 138.30 | 121.62 | 2.54 | 0.71314 | 5.84 | 27.58 | 0.1283 | 0.512327 | 23 | -0.3477 | -6.07 | -6.04 |
| 443-17-1 | 151.85 | 3.18 | 0.71274 | 3 | 138.52 | 157.07 | 3.28 | 0.71259 | 5.43 | 27.34 | 0.1204 | 0.512248 | 9 | -0.3879 | -7.61 | -7.58 |
| 443-18-1 | 161.85 | 3.64 | 0.71196 | 4 | 132.72 | 115.87 | 2.54 | 0.71182 | 6.24 | 28.85 | 0.1306 | 0.512290 | 5 | -0.3360 | -6.79 | -6.76 |
| 444-4-5 | 31.23 | 0.45 | 0.70975 | 2 | 182.84 | 68.59 | 1.09 | 0.70974 | 4.71 | 20.41 | 0.1393 | 0.512452 | 5 | -0.2918 | -3.63 | -3.63 |
| 444-5-1 | 37.00 | 0.69 | 0.71244 | 4 | 146.22 | 116.60 | 2.31 | 0.71241 | 6.20 | 29.06 | 0.1281 | 0.512286 | 7 | -0.3488 | -6.87 | -6.86 |
| 444-5-4 | 41.60 | 0.88 | 0.71258 | 2 | 148.72 | 119.75 | 2.33 | 0.71255 | 5.54 | 28.15 | 0.1191 | 0.512281 | 8 | -0.3945 | -6.96 | -6.96 |
| 444-6-1 | 48.92 | 1.22 | 0.71114 | 3 | 209.89 | 110.73 | 1.53 | 0.71111 | 5.22 | 25.99 | 0.1216 | 0.512299 | 6 | -0.3818 | -6.61 | -6.60 |
| 444-7-1 | 54.74 | 1.75 | 0.71215 | 5 | 148.41 | 111.80 | 2.18 | 0.71210 | 6.21 | 29.86 | 0.1256 | 0.512196 | 10 | -0.3615 | -8.62 | -8.61 |
| 444-7-3 | 57.32 | 1.98 | 0.71056 | 4 | 144.54 | 106.93 | 2.14 | 0.71050 | 5.63 | 27.42 | 0.1227 | 0.512344 | 25 | -0.3762 | -5.74 | -5.72 |
| 444-7-6 | 61.23 | 2.33 | 0.71090 | 3 | 152.36 | 103.69 | 1.97 | 0.71084 | 6.23 | 29.14 | 0.1291 | 0.512254 | 9 | -0.3437 | -7.49 | -7.47 |
| 444-8-1 | 65.88 | 2.75 | 0.70769 | 2 | 220.36 | 73.12 | 0.96 | 0.70765 | 5.22 | 22.11 | 0.1430 | 0.512523 | 15 | -0.2730 | -2.24 | -2.22 |
| 444-9-1 | 77.15 | 3.77 | 0.70938 | 3 | 164.59 | 99.73 | 1.75 | 0.70929 | 5.40 | 29.01 | 0.1248 | 0.512345 | 10 | -0.3655 | -5.72 | -5.68 |
| 444-1-1A | 82.75 | 4.27 | 0.71140 | 2 | 141.25 | 106.14 | 2.17 | 0.71127 | 5.80 | 27.70 | 0.1268 | 0.512294 | 12 | -0.3554 | -6.71 | -6.67 |
| 297-6-5 | 83.49 | 0.85 | 0.71212 | 3 | 140.73 | 117.40 | 2.41 | 0.71184 | 5.40 | 27.37 | 0.1177 | 0.512236 | 13 | -0.4016 | -7.84 | -7.83 |
| 297-7-3 | 100.10 | 1.01 | 0.71397 | 3 | 144.45 | 128.10 | 2.57 | 0.71393 | 5.70 | 27.94 | 0.1248 | 0.512239 | 2 | -0.3655 | -7.78 | -7.77 |
| 297-8-4 | 110.10 | 1.12 | 0.71354 | 4 | 140.50 | 123.85 | 2.55 | 0.71350 | 5.50 | 27.36 | 0.1214 | 0.512251 | 6 | -0.3828 | -7.55 | -7.54 |
| 297-9-2 | 127.10 | 1.29 | 0.71456 | 5 | 117.22 | 133.73 | 3.30 | 0.71450 | 5.40 | 28.00 | 0.1167 | 0.512233 | 6 | -0.4067 | -7.9 | -7.89 |
| 297-10-2 | 154.70 | 1.56 | 0.71280 | 3 | 119.53 | 114.54 | 2.77 | 0.71274 | 5.29 | 27.31 | 0.1170 | 0.512276 | 7 | -0.4052 | -7.06 | -7.05 |
| 297-11-2 | 203.39 | 2.05 | 0.71298 | 3 | 125.29 | 118.33 | 2.73 | 0.71290 | 4.93 | 24.86 | 0.1200 | 0.512276 | | -0.3899 | -7.06 | -7.04 |
| 297-11-4 | 206.33 | 2.08 | 0.71169 | 3 | 176.86 | 62.68 | 1.84 | 0.71164 | 5.77 | 25.87 | 0.1349 | 0.512263 | 6 | -0.3142 | -7.32 | -7.30 |
| 297-12-2 | 249.95 | 2.52 | 0.71277 | 3 | 120.34 | 122.80 | 2.95 | 0.71266 | 5.52 | 27.26 | 0.1225 | 0.512249 | 8 | -0.3772 | -7.59 | -7.56 |
| Average | | | | | | | | 0.71235 | | | | | | | | -6.99 |

Table 2.1b- Isotopic data for western Pacific marginal basins.

The relationship between Sr and Nd isotopic values and stratigraphic position is detailed in Figs. 2.5-2.7. These figures portray isotopic fluctuations with depth and age for three drill holes in the Shikoku Basin (ODP site 442, 443, 444; Figs. 2.1, 2.3). Neodymium values fluctuate by up to 5 ϵ_{Nd} units in any one drill hole. Examination of depth versus ϵ_{Nd} indicates that similar isotopic patterns occur in every core, although at different depths (Fig. 2.5). Each graph in figure 2.5 shows two peaks characterized by shifts to more positive values, and two troughs, characterized by shifts to more negative values. Superimposing these graphs on one another suggests that similar isotopic variations occur at different depths in each drill hole; these differences in depth may be related to differences in sedimentation rates in different portions of the basin (deVries Klein et al., 1980). Plotting ϵ_{Nd} versus age (Fig. 2.6) for the same drill cores illustrates that the isotopic fluctuations appear to occur in all cores within a narrow time range. For example, the strongest positive shift in core 444 occurs between 2.35 and 2.75 Ma (65.88 metres below sea floor [mbsf]), and may be correlated with less dramatic shifts in core 443 at 2.81 Ma (143.8 mbsf) and core 442 at 3.06 Ma (167.5 mbsf).

Strontium values range from 0.7080-0.7160 in the Shikoku Basin, and the maximum range in $^{87}Sr/^{86}Sr$ ratios in any core within the stratigraphic interval studied is approximately 0.005 (Fig. 2.7). Strontium ratios are consistently higher (up to 0.006 higher) than ambient seawater values for this time period (Hoddel, 1991). Variations in $^{87}Sr/^{86}Sr$ ratios in the Shikoku Basin are roughly inversely correlated with variations in ϵ_{Nd} values (Figs. 2.6, 2.7). A strong increase in Sr initial ratios occurs between 3.0 and 2.5 Ma, followed by a significant decrease in Sr initial ratios between 2.50-2.00 Ma. This increase in Sr initial ratios corresponds to a decrease in ϵ_{Nd} during the same time period, and the subsequent decrease in Sr initial ratios corresponds to an increase in ϵ_{Nd} .

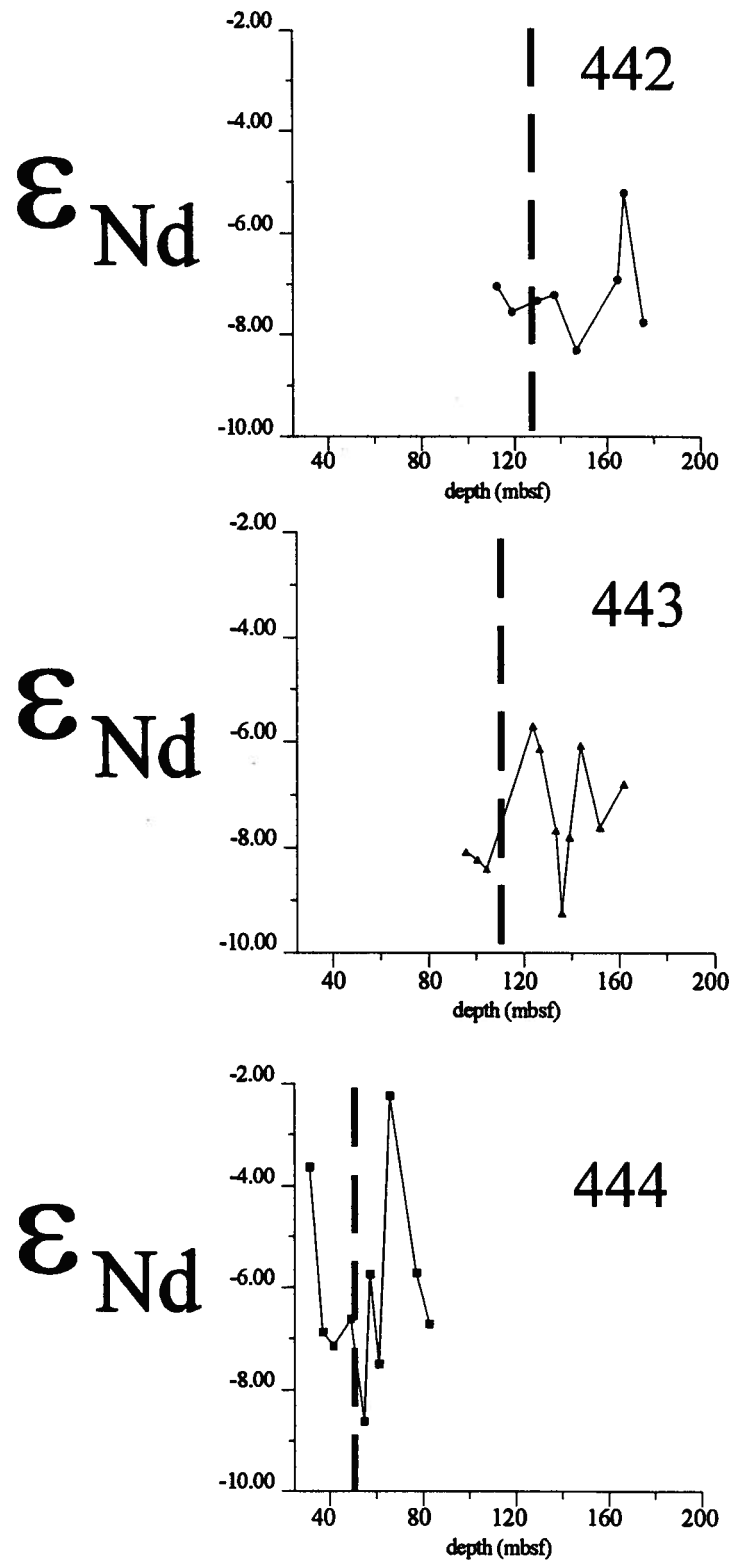


Figure 2.5 - Plots of depth (metres below sea floor) versus ϵ_{Nd} for Shikoku Basin drill cores. Heavy dotted line is Plio-Pleistocene boundary. Note boundary represents inflection point in isotopic values in all drill holes.

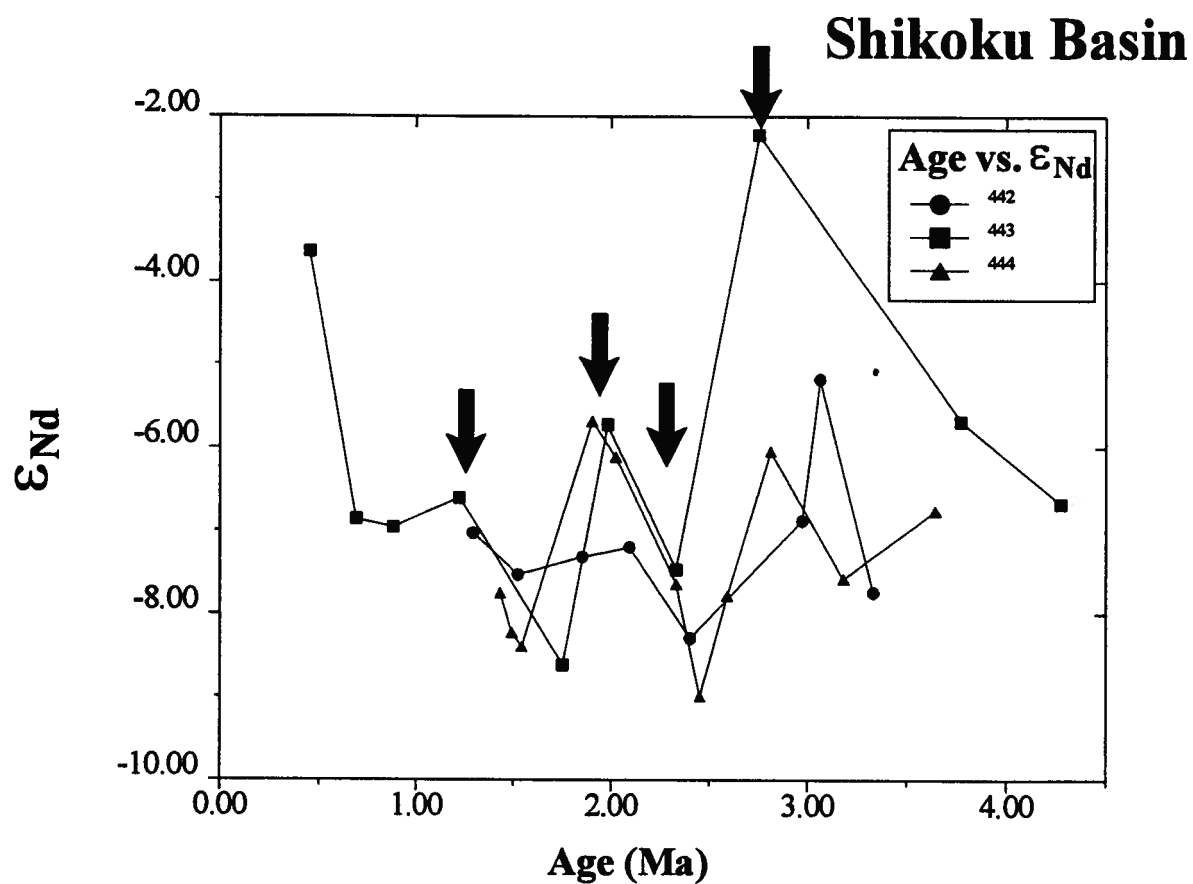


Figure 2.6 - Plot of age versus ϵ_{Nd} for Shikoku Basin samples. Note similarity of inflection points in all drill holes. Isotopic fluctuations are sharp, and occur in a relatively confined time span. Arrows indicate apparently correlative horizons between sections.

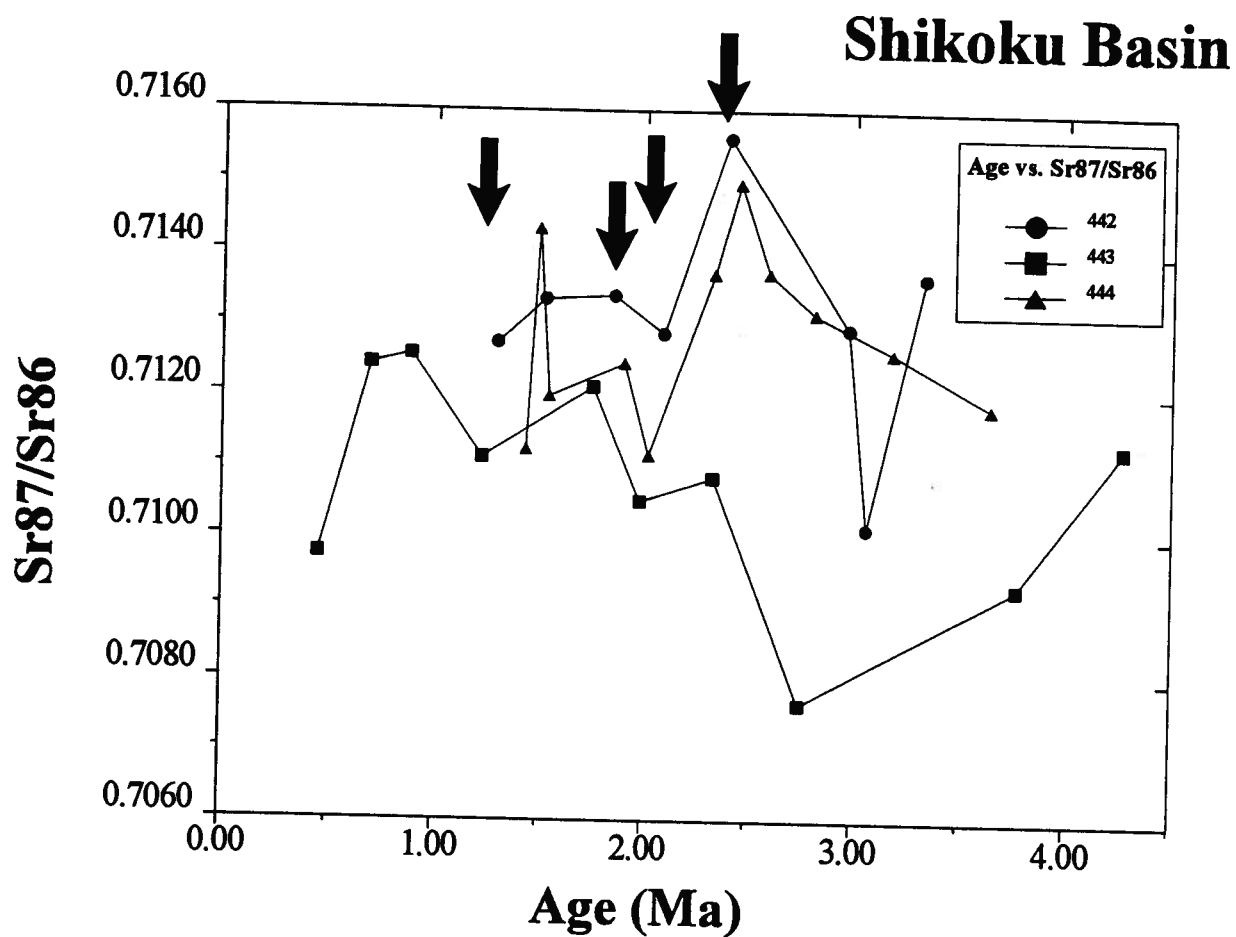


Figure 2.7 - Plot of age versus $^{87}\text{Sr}/^{86}\text{Sr}$ for Shikoku Basin samples. Note similarity of inflection points in all drill holes. Compare to figure 2.6, noting inverse relationship for Nd and Sr isotopic values in coeval samples.

2.5 DISCUSSION

A. Interbasinal Isotopic Signatures

The isotopic signatures of fine-grained sediments may be unique indicators useful in basin discrimination and stratigraphic correlation. The isotopic signature of fine-grained Plio-Pleistocene sediments in Western Pacific marginal basins varies substantially, but values within any individual basin are confined to a relatively limited range (Fig. 2.4). The range of values in any one basin is the result of the geology and geologic evolution of the source region. The geologic setting of each marginal basin is unique, and therefore the isotopic signature has potential for use in the discrimination of individual basins. McLennan et al. (1990) point out that back arc basin sediments vary petrographically, geochemically, and isotopically due to variability in provenance, particularly the availability of old continental crustal material. They differentiate between SW Pacific (Celebes and South China basins), Aleutian, and Japan basins based on variable petrographic and geochemical signatures.

Different crustal domains have different average isotopic values, and basins adjacent to these domains will have signatures characteristic of the domains on its margins. Crustal domains may be broadly grouped into: 1) old continental material ($\epsilon_{Nd} < -6$); 2) transitional crust (ϵ_{Nd} between -6 and +5); and 3) juvenile crust ($\epsilon_{Nd} > +5$; DePaolo et al., 1991; DePaolo, 1981). The isotopic signature of a basin represents variable degrees of mixing between basin margin domains and ambient seawater values, as reflected by intrabasinal carbonate. Fluctuations in mixing parameters through time will alter the isotopic signature, but within a relatively limited range defined by the isotopic range in the source regions.

In the present study, the absolute isotopic values vary between $\epsilon_{Nd} = (0) - (-9)$, and $^{87}Sr/^{86}Sr = (0.7060) - (0.7160)$. Samples with higher Sr values (> 0.7100) and lower ϵ_{Nd} values (< -7.00) indicate the increased importance of old continentally derived material; samples with lower Sr values

(<0.7100) and higher ϵ_{Nd} values (> ~ 6.00) indicate increased contamination by transitional and juvenile crustal material.

The isotopic values of each basin, with the exception of the Shikoku Basin, approximate anticipated values. The Sulu Basin has ϵ_{Nd} values between 0 and -4.25, suggesting a mixing of carbonate sediment (probable ϵ_{Nd} of -4 to -2 (Piepgras and Wasserburg, 1980)) with juvenile arc material (+5-+9) derived from the Philippine arc, together with very minor amounts of detritus from Mesozoic accretionary prisms and minor underlying continental basement (transitional to evolved ϵ_{Nd} values). This interpretation is consistent with the sedimentary petrology described by Rangin et al. (1990). The low $^{87}Sr/^{86}Sr$ values in the Sulu Basin also reflects the high influx of carbonate debris from flanking reef complexes (Rangin et al., 1990).

Sediments from the Sea of Japan are characterized by ϵ_{Nd} values between (-3) and (-9), and $^{87}Sr/^{86}Sr = (0.7090) - (0.7160)$. The ϵ_{Nd} values are strongly skewed to the more negative end of the range (Fig. 2.4), reflecting the contribution of cratonal detritus derived from the Sino-Korean craton to the north and west ($\epsilon_{Nd} = < -15$), and the rifted continental block of the Yamato Rise ($\epsilon_{Nd} = < -3$; Nakamura et al., 1990). This continental detritus is strongly diluted by volcanogenic material derived from both the southwest Japan "continental arc" ($\epsilon_{Nd} = (-6) - (+4)$; Morris and Kagami, 1989; Kagami et al., 1992) and the northwest Japan "transitional arc" ($\epsilon_{Nd} = (+5) - (+6)$; Nohda and Wasserburg, 1981). This dilution is supported by both sedimentary petrology of associated sandstones (Marsaglia et al., 1992), and by mixing models that indicate that only a minor amount of cratonally-derived sediment needs to mix with arc-derived detritus to significantly lower the ϵ_{Nd} value, due to low Nd abundance in juvenile crustal detritus and very negative ϵ_{Nd} values of older continental crust. The $^{87}Sr/^{86}Sr$ ratio is also skewed to the higher end of the range, supporting a mixing of cratonally-derived material and arc detritus.

The isotopic signature of Shikoku Basin sediments strongly overlaps with the signature of those from the Sea of Japan (Fig. 2.4). The ϵ_{Nd} values range from (-2) to (-9), but are skewed to the more negative end of the range, similar to the Sea of Japan values. However, ϵ_{Nd} values in the Shikoku Basin are generally

lower (more evolved) than those in the Sea of Japan, at the same value of $^{87}\text{Sr}/^{86}\text{Sr}$. Similarly, when any one ϵ_{Nd} value is considered, the $^{87}\text{Sr}/^{86}\text{Sr}$ ratio of the Shikoku Basin is generally lower than the corresponding ratio in the Sea of Japan. The lower Sr values were anticipated, due to the high influx of continentally derived material in the Sea of Japan, but the lower Nd values were not. These values are problematic, in that the Shikoku Basin is supplied with juvenile sediment from the Izu-Bonin arc ($\epsilon_{\text{Nd}} = (+8) - (+9)$; Nohda and Wasserburg, 1981) and with transitional sediment from southwest Japan ($\epsilon_{\text{Nd}} = (-6) - (+4)$; Morris and Kagami, 1989; Nakamura et al., 1990; Isozaki et al., 1990; Kagami et al., 1992). Carbonate detritus contributes ϵ_{Nd} values around $(-4) - (-2)$ (Piepgras and Wasserburg, 1980). Admixtures of these end members would be expected to produce sediment with ϵ_{Nd} values of approximately (-2) to $(+5)$, obviously dependent on the mixing ratio, yet the values in the Shikoku Basin ($\epsilon_{\text{Nd}} = (-2) - (-9)$) are considerably lower than expected. There is no old cratonic material adjacent to the Shikoku Basin, nor is any suggested at depth by isotopic systematics (Nohda and Wasserburg, 1981; Morris and Kagami, 1989; Nakamura et al., 1990; Isozaki et al., 1990).

A plot of $f^{\text{Sm/Nd}}$ vs. ϵ_{Nd} for samples from the Sea of Japan and the Shikoku Basin illustrates the strong degree of overlap in isotopic values between the two basins (Fig. 2.8). The value $f^{\text{Sm/Nd}}$ is a comparison of the $^{147}\text{Sm}/^{144}\text{Nd}$ of the sample against the $^{147}\text{Sm}/^{144}\text{Nd}$ of chondritic meteors ($f^{\text{Sm/Nd}} = (^{147}\text{Sm}/^{144}\text{Nd})_{\text{sample}} / ^{147}\text{Sm}/^{144}\text{Nd}_{\text{CHUR}} - 1$; Shirey and Hanson, 1986) that effectively measures the degree of light rare earth element enrichment of the sample. Samples from both basins show a very limited range of $f^{\text{Sm/Nd}}$ values, and plot within the range expected for modern marginal basins sediments (McLennan and Hemming, 1992). This restricted range indicates little or no REE fractionation has occurred during the sedimentary cycle. The samples form a well-defined mixing line between compositional and isotopic fields defined for arc rocks and Precambrian upper crust, highlighting the importance of continentally derived sediment throughout the Plio-Pleistocene evolution of the basins.

The most plausible explanation for the anomalous values in Shikoku Basin sediments is an aeolian sediment flux from cratonic materials on the Asian mainland. Studies have shown an order of magnitude

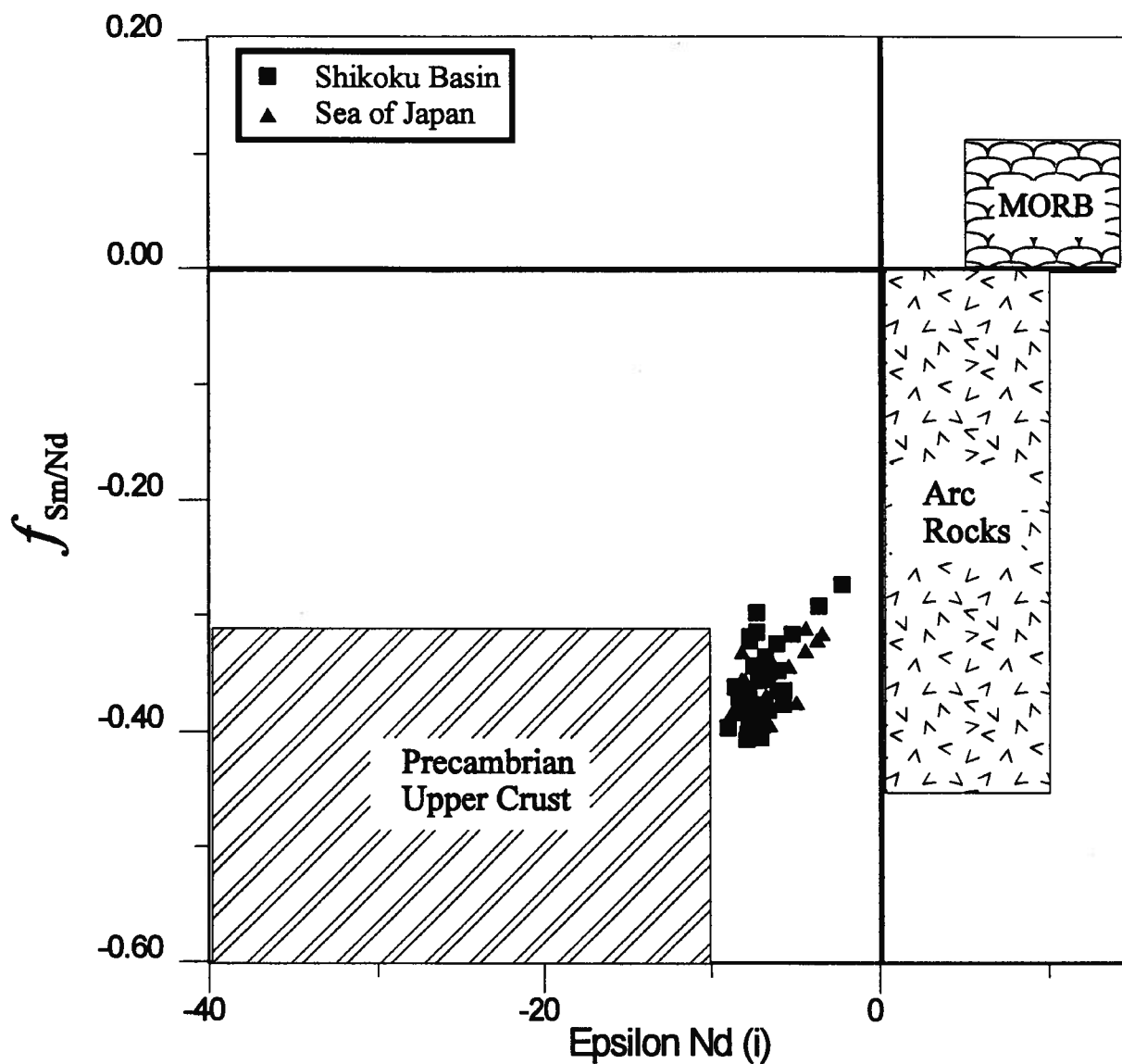


Figure 2.8 - Plot of $f_{\text{Sm/Nd}}$ vs. ϵ_{Nd} for samples from the Sea of Japan (triangles) and Shikoku Basin (squares). The data illustrate the strong degree of overlap between the two basins, and the limited range in isotopic values and $f_{\text{Sm/Nd}}$ for the samples. Note the well-defined mixing lines between Precambrian crust and arc rocks formed by the data array. MORB = mid-ocean ridge basalt.

increase in aeolian dust flux to the Pacific basin in Pliocene time due to increased intensity of atmospheric circulation associated with high-latitude cooling (Janecek and Rea, 1983; Rea et al., 1985). Much of this aeolian detritus was derived from the China-Gobi Desert aeolian source area (Janecek and Rea, 1983), and would be characterized by cratonic Nd values ($\epsilon_{Nd} < -15$; Rea, 1993). This material would have been transported by the prevailing westerlies over both the Sea of Japan and Shikoku Basin, but may have been preferentially deposited in the Shikoku Basin due to changes in atmospheric circulation associated with the horse latitudes at 30°N . The addition of cratonic affinity aeolian detritus would account for the low ϵ_{Nd} signature of the Shikoku Basin sediment, as well as accounting for the strong degree of overlap between it and the Sea of Japan. The influx of a moderate amount of cratonic dust would have strongly altered the Nd signal without substantially altering the Sr values in the Shikoku Basin, which are dominated by low $^{87}\text{Sr}/^{86}\text{Sr}$ ratios derived from juvenile volcanics and reef carbonates associated with the Izu-Bonin arc. In addition, sediments in the Plio-Pleistocene Shikoku Basin were deposited slightly above the carbonate compensation depth (CCD; deVries Klein et al., 1980), whereas sediments in the Sea of Japan were largely deposited below the CCD (with the exception of ODP site 797; Tamaki et al., 1990), which would preferentially elevate the $^{87}\text{Sr}/^{86}\text{Sr}$ ratio without affecting the ϵ_{Nd} value in the Sea of Japan.

B. Intrabasinal Isotopic Signatures

Neodymium and strontium isotopic signatures measured in the study display significant variations within vertical stratigraphic sections (Figs. 2.5-2.7). These fluctuations appear to be temporally controlled, basin-wide phenomena, and are potentially useful for correlations among stratigraphic sections throughout the basin (Figs. 2.5-2.7). Fluctuations in isotopic values reflect changes in the sediment flux in the basin, ultimately controlled by changes in the relative contribution from particular sediment sources. Isotopic fluctuations may therefore also prove useful in constraining basin evolution.

ϵ_{Nd} values span a range of more than five ϵ_{Nd} units in the Shikoku Basin, and $^{87}\text{Sr}/^{86}\text{Sr}$ ratios vary between 0.7075 and 0.7125. Fluctuations within this range are sharp, and appear to reflect major changes in

the isotopic character of the basin in limited periods of time. Fluctuations are roughly synchronous in all drill holes, generally occurring within 0.3-0.5 Ma of each other. Although the size of the sample set precludes rigorous statistical analysis, there appears to be good correlation in isotopic variation between drill holes, as major inflection points in ϵ_{Nd} values occur at about 1.5-1.6 Ma, 2.0 Ma, 2.5 Ma, and 2.6-2.8 Ma (Fig. 2.6). The strongest correlation occurs at inflection points at 1.5-1.6 Ma, 2.0 Ma, and 2.5 Ma; weaker correlations in older and younger strata may reflect age uncertainties, which increase with depth from the Plio-Pleistocene boundary, or poor biostratigraphic resolution, particularly in hole 444 (Fig. 2.3). However, the magnitude of these fluctuations is large enough, and the fluctuations are frequent enough to generate distinctive patterns in the isotopic record of each stratigraphic section, which appear to be correlative across the basin (Figs. 2.5-2.7). The generally synchronous variations in these stratigraphic sections occur over approximately 5,400 km² within a topographically complex basin, indicating that intrabasinal isotopic correlations are quite viable. Variations in ϵ_{Nd} values in these drill holes are inversely proportional to variations in Sr values, providing additional support to suggested correlations. These fluctuations may be distinct enough to allow biostratigraphically unconstrained stratigraphic sections to be correlated with sections with good biostratigraphic control by correlation of the isotopic patterns.

The potential applicability of isotopic fluctuations in a stratigraphic succession to provenance studies is extremely promising. For example, the strong decrease in ϵ_{Nd} values and increase in Sr values between 2.8 and 2.5 Ma in all drill holes likely reflects a cessation of volcanic activity during the late Pliocene, and an increasing importance of "continentally derived" material during this time. This trend ends abruptly at about 2.4 Ma, when there is a sharp increase in ϵ_{Nd} values, and a decrease in Sr values, which reflects the initiation of volcanism in the Izu-Bonin arc. Arc-derived hemipelagic sediment flooded the basin, and overwhelmed continentally derived input. This same line of reasoning can be used to suggest a volcanic event between about 3.5 and 2.8 Ma, cessation of volcanism at about 1.8 Ma, and renewed volcanism at about 1.5-1.6 Ma. This interpretation of volcanic episodicity vs. continental sediment influx is in general agreement with variations suggested by detailed studies of tephra and clay mineralogy within the basin (deVries Klein et

al., 1980). However, isotopic variability permits a higher resolution, is not subject to diagenetic modifications, and is not dependent on macroscopic characteristics such as grain size and colour (McLennan et al., 1991).

The range in isotopic values in any basinal sequence is a function of the dynamic evolution of the source region, and the absolute value of any stratigraphic level reflects a unique mixture of the different sources supplying the basin. Detailed analysis of the isotopic patterns in a basinal sequence should therefore provide constraints on the changes in provenance through time, allowing for detailed reconstructions of basin evolution.

2.6 CONCLUSIONS

The isotopic signature of fine-grained sediments from western Pacific marginal basins has been examined to test the applicability of isotopic fluctuations to basin discrimination, stratigraphic correlation, and provenance studies. The Sulu Sea, Shikoku Basin, and Sea of Japan display isotopic signatures that vary within limits defined by the geology of the source regions. The Sulu Sea contains a distinct signature, whereas the Sea of Japan and Shikoku Basin display strong overlap. The Shikoku Basin displays an isotopically evolved signature that could not have been derived from the crustal domains on its margins, and requires input from a previously unrecognized continental aeolian source. The influx of aeolian detritus in the Shikoku Basin coincides with an increase in aeolian flux to the northern Pacific associated with the onset of global glaciation (Rea et al., 1985).

Stratigraphic fluctuations in the isotopic signature of fine-grained sediment may potentially be useful for correlating strata basin-wide, and may provide constraints on the geologic history of a region. Stratigraphic sections in the Shikoku Basin display roughly synchronous fluctuation in ϵ_{Nd} and $^{87}Sr/^{86}Sr$ values, interpreted to reflect episodicity in basin margin volcanism. Isotopic variability within stratigraphic sections has been used to correlate drill holes from across 5400 km² of basin floor.

The combined $\epsilon_{\text{Nd}}\text{-}^{87}\text{Sr}/^{86}\text{Sr}$ signature of fine-grained sediments appears to be useful for fingerprinting geographically separated marginal basins. The isotopic signature of a basinal sequence is primarily a function of the average isotopic composition of all the crustal domains flanking a depositional basin. Thorough mixing of fine-grained sediments homogenizes the isotopic signal, and may provide a signature unique to an individual basin. Overlap of basinal signatures suggests similar provenance between basins, similar provenance's which may not be readily evident by traditional sedimentologic techniques. Although the isotopic composition of fine-grained sediments approximates the average crustal composition of the source region, this average crustal composition will vary within limits defined by the geology of the source region, reflecting changes in the sediment flux derived from different domains within the source region. These temporally controlled compositional fluctuations impart a temporally controlled isotopic variation that may be used as a stratigraphic marker to correlate strata basin-wide. In addition, these isotopic variations are controlled by geologic events in the source region, and may therefore be very useful in reconstructing basin evolution. The isotopic signature of fine-grained sedimentary rocks may be an extremely useful tool in discriminating ancient, structurally disrupted basinal sequences, and placing constraints on basin history.

CHAPTER 3

REGIONAL GEOLOGIC SETTING

3. REGIONAL GEOLOGIC SETTING

The southern Canadian Cordillera comprises a number of discrete, fault-bounded tectonostratigraphic assemblages, each with a distinct stratigraphy that differs from that of adjacent assemblages. These tectonostratigraphic assemblages are referred to as *terranes*, and include, from west to east, Wrangellia, Harrison, Cadwallader, Bridge River, Methow, Cache Creek and Quesnellia (Fig. 1.2; Table 1.1). Each terrane is defined by a stratigraphic suite that is lithologically distinct and regionally consistent, and is not easily correlated with the stratigraphy on adjacent terranes (Table 1.1). On a broad scale, each of these terranes consists of Paleozoic to Early Mesozoic oceanic or volcanic arc rocks, overlain by Jurassic and Cretaceous island-arc volcanic rocks and volcanoclastic sediments or ocean floor assemblages. Boundaries between the terranes are interpreted to be Cretaceous or Tertiary regional fault systems or Jurassic to Tertiary plutons (Wheeler and McFeeley, 1991; Monger and Journeay, 1992). In this chapter, the regional geologic setting of the southern Canadian Cordillera is reviewed to provide context for the stratigraphic analyses that follow. Terrane linkages are particularly important in this investigation, and currently established linkages are discussed for each terrane.

Intense Mesozoic and Cenozoic compressional, translational, and extensional deformation and widespread, multiphase plutonism imposed on tectonostratigraphic terranes of uncertain paleogeographic affinity has resulted in an extremely complex geologic setting for the southern Canadian Cordillera. Any interpretation of Middle Jurassic basin evolution and/or paleogeographic reconstruction in the region requires unraveling the structural, plutonic and metamorphic overprint prior to evaluating the original stratigraphic relationships among the terranes.

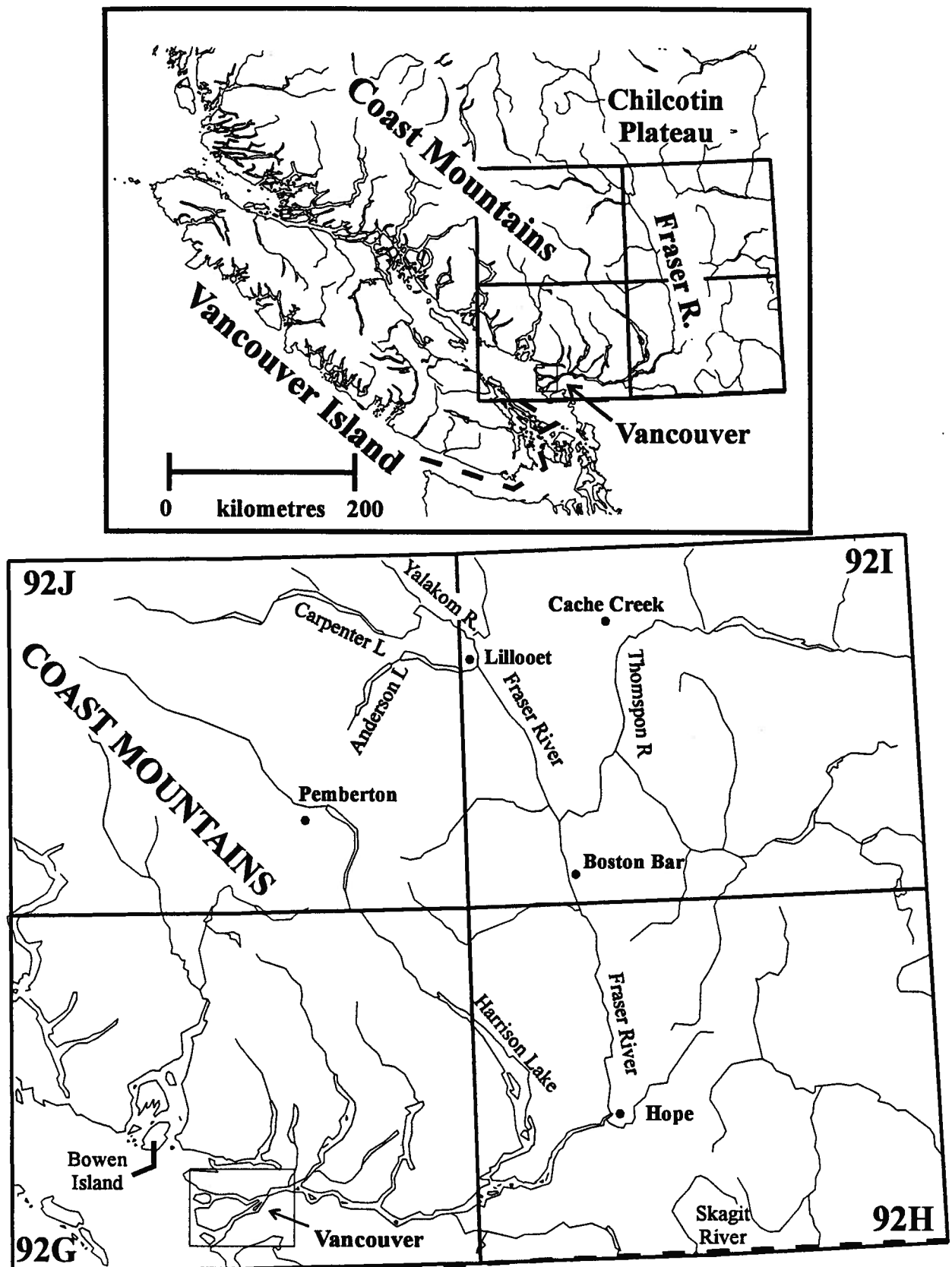


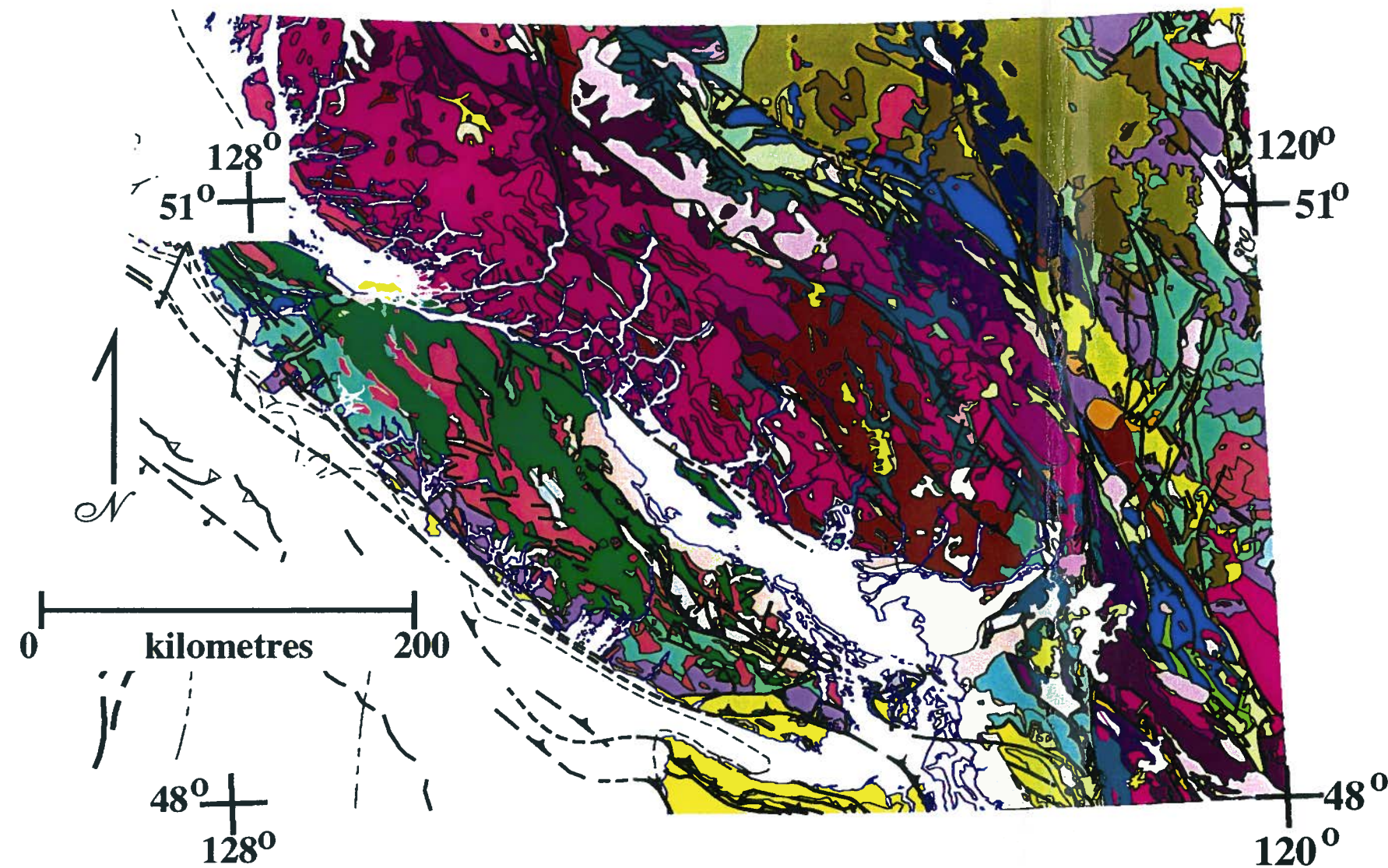
Figure 3.1 - Geographic map of southwestern British Columbia highlighting locations discussed in text.

3.1 TERRANE DESCRIPTIONS

A. Wrangellia

Wrangellia is the westernmost terrane in the southern Canadian Cordillera, and is contained within the morphogeologic Insular Belt. It underlies the majority of Vancouver Island, as well as portions of the Gulf Islands and coastal mainland British Columbia (Fig. 1.2). Wrangellia consists of Upper Paleozoic volcanic arc and carbonate platform rocks of the Sicker and Buttle Lake groups unconformably overlain by a thick succession (> 6 km) of Middle to Upper Triassic Karmutsen Formation tholeiitic basalt and associated sedimentary rocks (Muller, 1977, Jones et al., 1977). Lower to Middle Jurassic volcanic arc rocks of the Bonanza Group unconformably overlie the Karmutsen Formation, and are overlain by Upper Jurassic to Upper Cretaceous clastic sedimentary rocks of the Kyuquot Formation and Nanaimo Group (Monger and Journeay, 1994; Mustard, 1994). Early to Middle Jurassic Bowen Island Group volcanic rocks, correlated with the Bonanza Group, are overlain by Cretaceous clastic rocks along the eastern margin of Wrangellia (Friedman et al., 1990).

The eastern boundary of Wrangellia is interpreted as an intrusive contact with Middle Jurassic plutons of the Coast Plutonic Complex, and is exposed on Quadra Island, in the Strait of Georgia (Nelson, 1979; Monger and Journeay, 1994; Fig. 1.2, Plate 1). The eastern edge of Wrangellia and the western edge of the adjacent Harrison terrane are both intruded by Middle Jurassic (< 167 Ma) plutons of the southern Coast Plutonic Complex, suggesting that the two terranes formed a single crustal block since at least that time (Friedman et al., 1990; Monger and Journeay, 1994). The timing of accretion of this crustal entity with terranes to the east is uncertain (Monger et al., 1982; van der Heyden, 1992). The western edge of Wrangellia is the present-day accretionary wedge of the Cascadia subduction zone (Varsek et al., 1993).



PLUTONIC ROCKS

- Tertiary plutons
- late Cretaceous plutons
- mid-Cretaceous plutons
- JuraCretaceous plutons
- middle Jurassic plutons
- early Jurassic plutons
- undivided metamorphic rocks

STRATIFIED ROCKS

- Neogene volcanic rocks
- Kamloops Group (Eocene)
- Nanaimo Group (KT)
- Gambier Group (K)
- Spences Bridge Group (K)
- Jackass Mountain Group (K)
- Harrison Lake Fm. (ImJ)
- Ladner Group (ImJ)
- Bonanza Group (ImJ)
- Shuksan Group (J)
- Cadwallader Group (Tr)
- Nicola Group (Tr)
- Karmutsen Formation (Tr)
- Bridge River Complex (Pz-J)
- Cache Creek Group (Pz-J)
- Devonian sedimentary rocks

Figure 3.2 - Simplified geologic map of the southern Canadian Cordillera.
Modified from Wheeler and McFeely (1991). Legend refers to units discussed in text.

B. Harrison

The Harrison terrane is located in the southeastern Coast Belt, and is exposed primarily on the west side of Harrison Lake (Figs. 1.2, 2.1, Plate 1). The stratigraphic base of the Harrison terrane consists of Middle Triassic (Ladinian) greenstone, chert, greywacke, and minor limestone of the Camp Cove Formation. The Camp Cove Formation is unconformably overlain by Lower to Middle Jurassic (Toarcian(?) to Bajocian) arc volcanics, volcanoclastic rocks, clastic sedimentary rocks and minor conglomerate of the Harrison Lake Formation (Arthur, 1987; Arthur et al., 1993; Fig. 3.2). The Middle Jurassic arc sequence is disconformably overlain by fine-grained clastic rocks of the Upper Jurassic Mysterious Creek Formation (Callovian) and the overlying volcanoclastic Billhook Creek Formation (Lower Oxfordian). Upper Jurassic strata are unconformably overlain by Lower Cretaceous conglomerate of the Peninsula Formation (Lower Berriasian to Lower Valanginian) and overlying volcanic and volcanoclastic rocks of the Brokenback Hill Formation (Late Valanginian to Middle Albian; Arthur, 1987; Arthur et al., 1993).

The western boundary of the Harrison terrane is an intrusive contact with Middle Jurassic plutons of the Coast Plutonic Complex; the eastern boundary is the Harrison Lake shear zone, a Late Cretaceous to Tertiary dextral transcurrent fault system (Journeay and Csontos, 1989). The Harrison Lake shear zone separates weakly metamorphosed (subgreenschist grade) rocks of the Harrison terrane from penetratively deformed, highly metamorphosed (mostly amphibolite grade) imbricate thrust nappes of the Coast Belt Thrust System of the eastern Coast Belt (Journeay and Csontos, 1989; Journeay and Friedman, 1993; Plate 1).

Middle Jurassic plutonic rocks intrude both the western edge of Harrison terrane and the eastern edge of Wrangellia. Linkages between Harrison terrane and terranes to the east (Bridge River, Cadwallader, and Methow terranes) are uncertain, and are the focus of this study. Metasediments imbricated in the Late Cretaceous Coast Belt Thrust System, including the Sollicum Schist and Twin Island Group, are interpreted to be metamorphosed equivalents to the Harrison terrane (Journeay and Friedman, 1993). This suggests that

arc successions of the Harrison terrane formerly extended north and east of the Harrison Lake Shear Zone, but their original extent is unknown.

The Harrison terrane is in fault contact with the Chilliwack terrane to the south. The contact is inferred to be a high-angle fault in southern British Columbia, but Tabor (1994) documents a low-angle fault contact between the rocks of the Harrison terrane and the overlying Chilliwack terrane in Washington. The Chilliwack terrane consists of Devonian to Permian arc volcanics, limestone, and associated clastic sedimentary rocks of the Chilliwack Group and overlying Upper Triassic to Lower Jurassic fine-grained sedimentary rocks of the Cultus Formation (Monger, 1966; Monger and Journeay, 1994; Tabor, 1994). *Schwagerinid* fusulinid-bearing limestone clasts in the basal conglomerate of the Harrison Lake Formation have been interpreted to be derived from the Chilliwack Group, suggesting a stratigraphic link between the two in the Early Jurassic (Arthur, 1987; Arthur et al., 1993).

C. Bridge River

The Bridge River terrane is exposed in the southeastern Coast Belt, east of Harrison Lake and west of the Fraser River (Fig. 1.2, 3.1, Plate 1). The terrane includes rocks of the Bridge River Complex west of the Fraser fault, and rocks of the Hozameen Group east of the fault (Fig. 3.1, Plate 1). Thick successions of structurally disrupted greenstone, interbedded chert, fine-grained clastic rocks and minor limestone dominate the Bridge River terrane (Potter, 1983; Haugerud, 1985; Schriazza et al., 1990). The Bridge River Complex may be subdivided into two distinct melange belts with an intervening coherent sequence (Journeay, 1993). The easternmost melange belt, exposed directly west of the Yalakom Fault, contains abundant ultramafic rocks and serpentinite pods, including the Shulaps ultramafic complex (Calon et al., 1990). Rare blueschist yields Triassic $^{40}\text{Ar}/^{39}\text{Ar}$ ages, with no record of any younger thermal perturbation (Archibald et al., 1990). The western melange belt consists of ultramafic rocks and serpentinite of the Bridge River Complex. These rocks are interleaved with similar rocks of the Bralorne-East Liza complex along the west-vergent Bralorne Fault system, which records late Early Cretaceous deformation (Journeay et al., 1992). Between the two melange

zones, the Bridge River Complex is a coherent sequence of interlayered greenstone, chert and argillite, conformably overlain by fine-grained clastic rocks of the Cayoosh assemblage (Journey and Northcote, 1992; Mahoney and Journey, 1993).

Radiolarian biostratigraphy indicates an age range of Mississippian to late Middle Jurassic (Callovian) for the Bridge River Complex (Cordey and Schriazza, 1993). The Hozameen Group yields radiolaria of Permian to Middle Jurassic (Bajocian) age (Haugerud, 1985). Conodonts recovered from limestone pods within the Bridge River Complex are primarily Late Triassic in age. The age and depositional history of the Cayoosh assemblage is discussed in more detail in chapter 5. Jurassic and older strata are overlain by the Lower Cretaceous Taylor Creek Group, a coarse clastic succession of conglomerate, sandstone, and minor siltstone (Jeletzky and Tipper, 1968; Garver, 1992).

The Bridge River terrane is complexly imbricated along north and northwest-trending compressional, transcurrent and extensional fault systems of Late Early Cretaceous to Tertiary age (Schiarizza et al., 1990; Coleman and Parrish, 1992; Journey and Friedman, 1993). The westernmost boundary of structurally coherent Bridge River strata is the Central Coast Belt Detachment, although correlative high-grade metamorphic rocks (e.g. Cogburn Group) are contained in thrust slices within the imbricate zone of the Coast Belt Thrust System to the west (Journey and Friedman, 1993; Plate 1). The eastern boundary of the Bridge River terrane is the Yalakom/Hozameen fault system, a post-late Early Cretaceous dextral transpressional structure that has been offset by movement on the Fraser River-Straight Creek fault system.

Stratigraphic relationships between the Bridge River terrane and adjacent terranes are ambiguous; the terrane is everywhere fault bounded (Plate 1). The contact between the Bridge River terrane and the Harrison terrane to the west is an imbricate fault zone of the Late Cretaceous Coast Belt Thrust System (Journey and Friedman, 1993; Fig. 3.2, Plate 1). The boundary between the Bridge River terrane and the Methow terrane to the east are late Early Cretaceous to Tertiary transpressional structures associated with the Yalakom-Hozameen and Fraser River fault systems. The terrane pinches out to the northwest against the Coast Plutonic

Complex and Yalakom fault, and pinches out to the southeast against the Hozameen and Ross Lake faults. Rusmore et al. (1988) suggest that the Middle to Late Jurassic Relay Mountain Group provides a stratigraphic link between the Bridge River and Cadwallader terranes by late Middle Jurassic (Callovian) time. However, the Relay Mountain Group is everywhere fault-bounded, and the existence of a depositional contact between it and the Bridge River terrane has not been proven. The Lower Cretaceous Taylor Creek Group provides the oldest definitive tie between the Cadwallader and Bridge River terranes (Garver, 1992).

D. Cadwallader

The Cadwallader terrane is exposed in the eastern Coast Belt, along the eastern side of the Coast Mountains (Fig. 1.2). The base of the Cadwallader terrane is defined as the Cadwallader Group, which consists of Middle to Upper Triassic (Carnian to Norian) tholeiitic basalts of the Pioneer Formation and overlying siltstone, sandstone, and limestone-bearing conglomerate of the Hurley Formation (Rusmore, 1987). The Hurley Formation is conformable with Upper Triassic (middle to upper Norian) conglomerate, sandstone, bioclastic sandstone, limestone, and siltstone of the Tyaughton Group (Umhoefer, 1990). The Tyaughton Group is disconformably overlain by Lower to Middle Jurassic (Hettangian-Bajocian) fine-grained clastics of the Last Creek Formation (Umhoefer, 1990; Poulton and Tipper, 1991), these in turn are unconformably overlain by sandstone, siltstone, and shale of the late Middle Jurassic to Lower Cretaceous (Callovian to Barremian(?)) Relay Mountain Group. Conglomerate and sandstone of Lower Cretaceous (Aptian to Albian) Taylor Creek Group unconformably overlies the Relay Mountain Group, and the Cadwallader terrane is capped by the Upper Cretaceous (Cenomanian) Silverquick conglomerate and overlying Powell Creek volcanics (Garver, 1989, 1992).

The Cadwallader terrane occurs primarily in north to northwest-trending fault slices on the west side of the Bridge River terrane, and as isolated pendants along the eastern margin of the Coast Plutonic Complex (Wheeler and McFeely, 1991). The Cadwallader terrane occupies both hanging wall and footwall positions in

the west-vergent Coast Belt Thrust System. North to northwest trending contractional and strike-slip faults separate it from adjacent terranes (Journeay and Friedman, 1993)

The western margin of the Cadwallader terrane is dominantly an intrusive contact with late Early Cretaceous plutons of the Coast Plutonic Complex (Armstrong and Parrish, 1990; Friedman and Armstrong, 1994). The western margin of the Cadwallader terrane is also imbricated with Upper Cretaceous strata of Wrangellian and/or Harrison terrane affinity (Gambier Group) along the leading edge of the Coast Belt Thrust System (Journeay and Friedman, 1993). An apparent depositional contact between the Harrison and Cadwallader terranes has been described by Journeay and Mahoney (1994; Appendix E).

To the east, the Cadwallader terrane is everywhere in fault contact with the Bridge River terrane, and there is no known stratigraphic connection prior to Late Cretaceous time (Garver, 1992). The Cadwallader and Bridge River terranes are complexly imbricated along the western boundary of the Bridge River terrane by Cretaceous to Tertiary compressional and transpressional structures (Schriazza et al., 1990; Monger and Journeay, 1994; Plate 1). Along the eastern margin of the Bridge River terrane, thin slivers of Hurley Formation are imbricated with fault slices of Bridge River Complex along the Yalakom fault system (Schriazza et al., 1990). Near bedding parallel faults of the Yalakom fault system separate the Hurley Formation from Middle Jurassic and Lower Cretaceous strata of the Methow terrane to the east.

E. Methow

The Methow terrane is exposed along the boundary of the morphogeologic Coast and Intermontane belts, west of the Yalakom, Bridge and Fraser rivers, and east of the Thompson Plateau (Fig. 3.1). The Methow terrane comprises Jurassic and Cretaceous clastic strata overlying Middle Triassic oceanic basement (Fig. 3.2). The base of the Methow terrane is the Triassic Spider Peak Formation, a sequence of oceanic greenstone, chert, limestone and argillite (Ray, 1986, 1990). The Spider Peak Formation is unconformably overlain by clastic strata of the Ladner Group (Ray, 1990). The Ladner Group consists of fine-grained

sandstone, siltstone, and carbonaceous shale of the Early Jurassic (Pliensbachian(?) to Toarcian) Boston Bar Formation conformably overlain by volcanoclastic conglomerate, sandstone, siltstone, and minor volcanic rocks of the Lower to Middle Jurassic (Toarcian to Upper Bajocian) Dewdney Creek Formation (O'Brien, 1986, 1987; Mahoney, 1993). The Ladner Group is disconformably overlain by pebble conglomerate, sandstone, and siltstone of the Upper Jurassic (Oxfordian to Kimmeridgian) Thunder Lake sequence (O'Brien, 1986, 1987). Polymict, granitoid-bearing conglomerate and sandstone of the Lower Cretaceous (Hauterivian(?) to Albian) Jackass Mountain Group unconformably (disconformably(?)) overlie all older strata (Kleinspehn, 1982, 1985).

The western boundary of the Methow terrane is the Yalakom/Hozameen fault system; the eastern boundary is the Pasayten fault (Plate 1). The terrane is folded into northwest-trending asymmetric open folds, and locally cut by east-vergent thrust faults of moderate displacement (1-10 km; Coates, 1970, Monger, 1989). The Fraser fault system displaces the Methow terrane with approximately 100 km of dextral offset, from Boston Bar to north of Lillooet (Fig. 3.2; Coleman and Parrish, 1992; Mahoney, 1993; Appendix E).

The Yalakom-Hozameen fault system is a dextral transcurrent system (approximately 115 km offset; Riddell et al., 1993) that juxtaposes oceanic rocks of the Bridge River/Hozameen Complex (Bridge River terrane) with clastic strata of the Methow terrane. At the southern end of the Methow terrane, the Ross Lake fault zone separates Jurassic-Cretaceous clastic strata of the Methow terrane from amphibolite facies oceanic-type rocks of the Twisp Valley Schist, in the crystalline core of the North Cascades (Miller et al., 1993). Miller et al. (1993) correlate metamorphic rocks of the Twisp Valley Schist with oceanic rocks of the Bridge River-Hozameen Complex, and suggest that the Twisp Valley Schist is the product of thrust loading and pluton emplacement along a southern continuation of the Coast Belt Thrust System (Journeay and Friedman, 1993), or within slightly younger northeast- to east-directed thrust faults of the eastern Cascades foldbelt (McGroder, 1988). This interpretation is consistent with the present map pattern that shows the Bridge River terrane *sensu strictu* pinching out at the intersection of the Ross Lake and Hozameen faults (Fig. 3.2).

The eastern boundary of the Methow terrane is the Pasayten fault, which separates it from Upper Jurassic to Lower Cretaceous plutonic rocks of the Eagle Complex and the Okanogan Batholith (Grieg, 1992; Hurlow and Nelson, 1993). The earliest documented movement on the Pasayten fault is Early Cretaceous southwest-side-down dip-slip motion, followed by moderate (10's km) sinistral displacement (Hurlow, 1993). However, the Pasayten fault is parallel to and spatially associated with the Eagle Shear Zone, a Middle to Late Jurassic east-vergent contractional feature, and may be genetically related to this structure (Grieg, 1992; Hurlow, 1993).

The Methow terrane is lenticular in plan view, narrowing both to the north and to the south (Fig. 1.2, 3.2). To the south, the terrane is overlain by Miocene plateau basalts of the Columbia River Basalt Group (Stoffel et al., 1991). To the north, stratigraphic and structural relations within the Methow, Bridge River and Cadwallader terrane are ambiguous. Riddell et al. (1993) assigned Jurassic-Cretaceous strata on the *southwest* side of the Yalakom fault to the Methow terrane, and correlated these strata near Konni Lake with those of the Camelsfoot Range to the south. This correlation suggests about 115 km dextral offset along the Yalakom fault (Fig. 3.2). In the Konni Lake area, rocks assigned to the Methow, Bridge River and Cadwallader terranes are everywhere in fault contact, and stratigraphic relations are unclear. However, recognition of Methow strata *west* of the Yalakom fault precludes the fault from being a terrane boundary between the Methow and the Bridge River, as has been suggested to the south (Monger, 1985; Monger and Journeay, 1994).

F. Cache Creek

The Cache Creek terrane is exposed northeast of Lillooet, east of the Fraser River, along the southeastern margin of the Chilcotin Plateau (Fig. 3.1). Tectonic slivers of the Cache Creek terrane are exposed in the Chilcotin River drainage (Read, 1993), but the majority of the terrane trends northward along the southeastern and eastern margin of the Chilcotin Plateau from approximately 50°30'N. This investigation is concerned with primarily the southern terminus of the ~1500 km long terrane.

The Cache Creek terrane consists of chert, argillite, limestone, basalt and ultramafic rocks of Mississippian to Middle Jurassic age (Monger and McMillan, 1984). The terrane is divided into eastern, central, and western belts (Duffel and McTaggart, 1952; Monger and McMillan, 1989). The eastern belt comprises greenstone and melange, consisting of blocks of limestone, tuff, greenstone, bedded chert in a variably sheared matrix of carbonaceous argillite (Shannon, 1981). Microfauna from the eastern belt ranges from Middle Pennsylvanian to Late Triassic (Orchard, 1984; Cordey et al., 1986). The central belt consists of massive limestone of the Marble Canyon Formation with lesser amounts of argillite, tuff, and chert (Shannon, 1981; Monger and McMillan, 1984). Fusulinids and conodonts in the Marble Canyon Formation are Permian (Orchard, 1984); radiolaria in adjacent sedimentary rocks are Late Triassic (Cordey et al., 1986). The western belt consists of argillite, siliceous argillite, chert and volcanoclastic rocks, with subordinate limestone, conglomerate, and volcanic rocks (Trettin, 1980; Cordey et al., 1987). Volcanic lithic sandstone, siltstone, and siliceous volcanic rocks of the informally named "Pavilion beds" are included in the western belt (Trettin, 1980; Monger and McMillan, 1989). Middle to Late Permian fusulinids and Early and Late Triassic conodonts have been documented from the western belt; Cordey et al. (1987) report Middle to Late Triassic radiolaria derived from chert interbeds, and Early to Middle Jurassic (Pliensbachian to Bajocian) radiolaria derived from siliceous argillite of the "Pavilion beds".

The Cache Creek terrane is in fault contact with both the Methow terrane and Quesnellia. Internal structural complexities make relations between the three lithologic belts of the Cache Creek terrane itself difficult to assess (Trettin, 1980; Monger and McMillan, 1989). The Cache Creek terrane has long been considered a subduction complex genetically associated with the Late Triassic Nicola arc (Monger et al., 1982, 1991). However, the existence of Early to Middle Jurassic radiolaria in the "Pavilion beds" require sedimentation until at least that time (Cordey et al., 1987).

Numerous workers have speculated on correlations between the Cache Creek and Bridge River terranes (Potter, 1983; Haugerud, 1985; Cordey et al., 1987; van der Heyden, 1992). Arguments against correlation of the two terranes are based primarily on the absence of both massive limestone and Tethyan

fauna in the Bridge River terrane (Potter, 1983; Haugerud, 1985; Cordey et al., 1987; Monger and McMillan, 1989). Read and Cordey (1994) document an Early Jurassic(?) lithologic transition from pelagic oceanic rocks to clastic marine sedimentary rocks in the southern Cache Creek terrane, similar to that documented in the Bridge River terrane (Journeay and Northcote, 1992; Mahoney and Journeay, 1993). They argue that the southern Cache Creek terrane may actually be a thrust nappe of Bridge River terrane, an interpretation that requires the present map pattern to be the result of transcurrent motion on the Yalakom-Hozameen and Fraser-Straight Creek fault systems (Wheeler and McFeely, 1992; Figs. 1.2, 3.2).

G. Quesnellia

Quesnellia, the easternmost of the accreted terranes discussed in this investigation, comprises lower Mesozoic volcanic assemblages overlying Upper Paleozoic oceanic and arc sequences (Monger, 1989). The areally restricted Paleozoic basement of Quesnellia comprises argillite, sandstone, chert, limestone, and arc volcanic rocks of the Devonian to Permian Harper Ranch Group. The Paleozoic rocks are unconformably overlain by voluminous volcanic, volcanoclastic and sedimentary rocks of the Upper Triassic to Lower Jurassic Nicola Group that characterize Quesnellia (Mortimer, 1987). The Nicola Group is unconformably overlain by shale, siltstone, and sandstone of the Lower to Middle Jurassic (Sinemurian - Callovian) Ashcroft Formation, which overlies both Nicola Group volcanic rocks and comagmatic plutonic rocks (McMillan, 1974; Monger and McMillan, 1989). Along the western margin of Quesnellia upper Lower Cretaceous volcanic rocks of the Spences Bridge Group occupy a >200 km long structural depression, and unconformably overlie the Nicola Group and associated plutonic rocks, the Permian to Lower Mesozoic Mt. Lytton Complex, and the Cache Creek terrane. Hurlow and Nelson (1993) suggest comagmatic rocks to the Spences Bridge Group extend south into Washington, where they comprise the Cretaceous Okanagan Batholith.

In the southern Canadian Cordillera, the western boundary of Quesnellia is the Pasayten fault, which separates Jurassic-Cretaceous rocks of the Methow terrane from Mesozoic intrusive complexes and Triassic and Cretaceous arc volcanics of western Quesnellia (Wheeler and McFeely, 1991; Stoffel et al., 1991). North

of Lillooet, the western margin of Quesnellia is a fault contact with the Cache Creek terrane (Monger, 1989). The eastern boundary of Quesnellia is a series of extensional faults, such as the Okanagan fault, associated with Eocene uplift of the Omineca Crystalline Belt (Parrish et al., 1985). North of approximately 50.5°N, the eastern margin of Quesnellia stratigraphically and structurally overlies the pericratonic Kootenay terrane (Monger et al., 1991).

Quesnellia is interpreted to have been obducted onto the North American continental margin in late Early Jurassic time (~185 Ma; Monger, 1989; Monger et al., 1991; Ghosh and Armstrong, 1994). The eastern margin of Quesnellia is interpreted to be an Early Jurassic structural contact with pericratonic terranes to the east, overprinted by Jurassic to Tertiary intrusions, and modified by Eocene extensional faulting (Armstrong and Parrish, 1990; Ghosh and Armstrong, 1991; Monger et al., 1991). Quesnellia may therefore be viewed as the Middle Jurassic western edge of North America.

The earliest documented interaction between Quesnellia and the Methow terrane to the west was the deposition of the Lower Cretaceous Jackass Mountain Group on the Methow terrane, which received detritus from the Upper Jurassic-Lower Cretaceous Eagle Complex on the western edge of Quesnellia (Kleinsphen, 1982). The Eagle Complex displays evidence of Middle to Late Jurassic ductile deformation, but the relationship between this deformation and the Methow terrane is uncertain (Grieg, 1992).

3.2 STRUCTURAL SETTING

The present map pattern of the southern Canadian Cordillera is derived from Cretaceous to Tertiary compressional, transcurrent, and extensional structures generated during oblique convergence along the North American margin. Older (pre-Cretaceous) structures are strongly overprinted by younger structures or obliterated by plutons.

The oldest clearly identifiable structures in the southern Canadian Cordillera are early Mesozoic (Late Triassic-Early Jurassic) in age, and are associated with deformation in the Cache Creek terrane and Quesnellia. Monger (1985) reports Late Triassic to Early Jurassic deformation and metamorphism in the Mt Lytton Complex of western Quesnellia, and McMillan (1976) describes structures associated with emplacement of the Late Triassic-Early Jurassic Guichon Batholith. Numerous workers have described Early to Middle Jurassic deformation along the eastern margin of Quesnellia (Klepaki, 1985; Brown et al., 1986, Murphy et al., 1992). Late Triassic to Early Jurassic structures in the Cache Creek terrane, Quesnellia, and terranes to the east are interpreted to be associated with the obduction of Quesnellia onto North America (Monger et al., 1982).

Middle and Late Jurassic structures are documented in most terranes in the region. Friedman et al. (1990) and Monger (1991a) document Middle to Late Jurassic (post-185 Ma, pre-155 Ma) deformation of the Bowen Island Group in Wrangellia. Monger and McNichol (1994) document a post-Late Triassic deformed belt cut by a late Middle Jurassic (ca. 164 Ma) pluton on the eastern edge of Wrangellia. Rusmore et al. (1988) argue that folds and thrusts in Upper Triassic and Lower Jurassic strata of the Cadwallader terrane are not found in overlying Upper Jurassic strata, indicating a Middle Jurassic deformational episode. Middle and Late Jurassic structures have not been identified in Harrison, Bridge River, or Methow terranes. The Eagle shear zone on the west side of Quesnellia records ductile contractional deformation in the Middle to Late Jurassic (Grieg, 1992). Travers (1982) documents east-directed thrust faulting of Cache Creek terrane over Quesnellia in the Middle to Late Jurassic. This deformational event is supported by evidence of penetrative structural deformation and metamorphism in the Cache Creek terrane (Mortimer et al., 1990) and in the Mt. Lytton Complex of western Quesnellia (Grieg, 1992; Fig. 3.2, Plate 1).

Early Cretaceous deformation is cryptic in the southern Canadian Cordillera, and is primarily manifested by unconformities and thick synorogenic conglomerate sequences on all terranes (Kleinsphen, 1982; Arthur, 1987, Lynch, 1992; Garver, 1992; Mahoney and Journeay, 1993). Monger (1993) proposes Early Cretaceous extensional deformation in the western Coast Belt to account for exhumed Late Jurassic

plutons, oriented dike complexes, and sedimentologic and volcanic patterns in Lower Cretaceous strata. Definitive Early Cretaceous structures have not been identified in the Harrison, Bridge River, Cadwallader, or Methow terranes, although the presence of Lower Cretaceous granitoid-bearing conglomerates suggests substantial (>5 km) coeval uplift. Early Cretaceous structures in Quesnellia and the Cache Creek terrane are unknown.

Late Early Cretaceous (< 112 Ma; early Albian) to Late Cretaceous time heralded the beginning of a major deformational episode on all terranes. The most regionally significant structural feature formed during this period is the west-vergent Coast Belt Thrust System (Journey and Friedman, 1993), which is kinematically linked to the Northwest Cascade System to the south (Brown, 1987; Brandon et al., 1988; McGroder, 1991; Journey and Friedman, 1993). West-vergent deformation was preceded by local post-middle Albian south- to southeast-directed folds and thrust faults (Lynch, 1991, 1992). Shortening in the Coast Belt Thrust System consisted of southwest-directed thin-skinned thrust faulting followed by out-of-sequence thrusting and folding; deformation is bracketed by syn- and post-kinematic plutons at 91-97 Ma. Deformation in the Coast Belt Thrust System imbricates units of Harrison, Bridge River, Cadwallader, and Methow affinity (Journey and Friedman, 1993). Early Late Cretaceous (91-94 Ma) deformation in the western Coast Belt consists of discrete, west- to southwest-vergent contractional shear zones developed primarily in plutonic rocks (Monger, 1993; Monger and Journey, 1994). Journey and Friedman (1993) suggest that plutonic suites of the western Coast Belt acted as a rigid backstop during Late Cretaceous shortening. To the north, Rusmore and Woodsworth (1991) describe a system of east-vergent backthrusts antithetic to the main thrust system that was active from 87-84 Ma. To the south, west-directed thrust faulting in the Northwest Cascade System and metamorphism in the core of the Cascades is loosely constrained to be between 130-84 Ma, with most isotopic dates between 100-84 Ma (Brown, 1987; Brandon et al., 1988; McGroder, 1991). Antithetic, east-vergent thrust faults in the Methow terrane are coeval with this deformation (McGroder, 1991).

Ductile, sinistral displacement along the Pasayten fault between the Methow terrane and Quesnellia is constrained to be ca. 109-95 Ma, and is interpreted to be coeval with west-vergent contractional faulting along its southern extent (Greig, 1992; Hurlow, 1993). On Quesnellia, the northwest-trending Nicoamen syncline developed coeval to deposition of the upper Lower Cretaceous Spences Bridge Group (Monger et al., 1991). Additional regionally significant early Late and Late Cretaceous structures have not been identified east of the Pasayten fault.

Transcurrent displacement overlapped with, and continued after, cessation of contractional deformation throughout the region. Transcurrent, primarily dextral, movement on a complex system of north- to northwest-trending strike-slip faults in the region began in the early Late Cretaceous and continued into the Tertiary (Schriazza et al., 1990; Journeay et al., 1992; Parrish and Monger, 1992). The aggregate displacement on these fault systems is uncertain. Dextral transcurrent motion along the Yalakom fault system is interpreted to be kinematically linked with Eocene (55-47 Ma) extensional displacement (Coleman and Parrish, 1992). To the east, major extensional faulting in the southern Omineca Belt, along the eastern border of Quesnellia, occurred between 58 and 45 Ma and resulted in 60-80% extension (Parrish and Carr, 1986; Parrish et al., 1988).

Dextral transcurrent displacement of approximately 100 km occurred along the Fraser fault system between 46.5 and 34 Ma, offsetting both strata of the Bridge River, Methow and Cache Creek terranes, and high-grade metamorphic rocks of the Southern Coast Belt and Northwest Cascades (Coleman and Parrish, 1991; Mahoney, 1993; Monger and Journeay, 1994).

3.3 PLUTONIC SETTING

Plutonic rocks constitute a major proportion of the southern Canadian Cordillera; west of the Fraser River, plutons underlie between 60-80% of the region. The vast majority of plutons in the region are Jurassic to Tertiary in age. Plutonic rocks in the region may be broadly divided into two tracts: 1) an eastern tract,

east of the Pasayten fault, coincident with the Intermontane belt, including intrusions into Cache Creek, Quesnellia, and terranes to the east, and; 2) a western tract, west of the Pasayten fault, coincident with the Coast and Insular belts, including intrusions into Bridge River, Cadwallader, Harrison and Wrangellia terranes. The Methow terrane is largely amagmatic. The two tracts display differences in pluton age, distribution and geochemical and isotopic composition, although there is a strong degree of overlap between the two (Woodsworth et al., 1991)

The eastern tract is generally older, more randomly distributed, cuts across structural grain, and is more silicic than intrusions in the western tract (Woodsworth et al., 1991). The eastern tract generally displays more evolved strontium and neodymium isotopic values than the western tract (Ghosh, 1994; Friedman and Cui, 1994). The most voluminous plutonic suites in the eastern tract are Late Triassic/Early Jurassic and Middle to Late Jurassic, with areally less significant suites in the late Early to Late Cretaceous and Tertiary (Armstrong, 1988; Woodsworth et al., 1991; Hurlow and Nelson, 1993). Different age plutonic suites overlap each other without a consistent pattern (Wheeler and McFeely, 1991). Although early Late Cretaceous magmatic activity occurred throughout the eastern tract, the majority of this activity occurred in a >300 km north- to northwest-trending belt along the western margin of Quesnellia referred to as the Okanagan-Spences Bridge arc (Hurlow and Nelson, 1993). Tertiary intrusions are particularly widespread east of Quesnellia.

The Coast Plutonic Complex forms the vast majority of the western tract. Plutonic rocks are roughly aligned in northwest-trending belts of similar age, are intermediate in composition, and have juvenile isotopic values (Woodsworth et al., 1991; Friedman and Armstrong, 1994; Friedman and Cui, 1994; Cui and Russell, 1994). The oldest plutons are the Lower Jurassic Island intrusions, on the western side of Wrangellia, which are interpreted to be the intrusive equivalent of arc volcanics of the Bonanza Group (Andrew and Godwin, 1989a). Middle to Late Jurassic (167-145 Ma) plutons comprise the early Coast Plutonic Complex suite (ancestral Coast Belt of van der Heyden, 1992; Friedman and Armstrong, 1994). Plutons of this age extend across the western Coast Belt, and are contained in two parallel belts, separated by younger intrusions

(Friedman and Armstrong, 1994). Early Cretaceous (145-112 Ma) plutons are concentrated along the western margin of the Coast Belt (Fig. 3.2, Plate 1). Mid-Cretaceous (112-90 Ma) plutons are coeval with deformation in the Coast Belt Thrust System, and intrude all terranes west of the Pasayten fault. Late Cretaceous intrusions post-date the main phase of contractional deformation in the Coast Belt, and appear confined to the hanging wall of the Coast Belt Thrust System (Journeay and Friedman, 1993). These plutons are exposed east of the majority of older plutons, and represent a significant (85-115 km) eastward shift of magmatic activity. Tertiary intrusions occur as isolated plutons scattered throughout the western tract, but form an important component of the North Cascades region (Haugerud et al., 1991).

CHAPTER 4

EVOLUTION OF A MIDDLE JURASSIC VOLCANIC ARC: STRATIGRAPHIC, ISOTOPIC AND GEOCHEMICAL CHARACTERISTICS OF THE HARRISON LAKE FORMATION, SOUTHWESTERN BRITISH COLUMBIA

4. EVOLUTION OF A MIDDLE JURASSIC VOLCANIC ARC: STRATIGRAPHIC, ISOTOPIC AND GEOCHEMICAL CHARACTERISTICS OF THE HARRISON LAKE FORMATION, SOUTHWESTERN BRITISH COLUMBIA

4.1 INTRODUCTION

Early to Middle Jurassic arc sequences form an important component of many terranes in the Canadian Cordillera. The genetic relationships among these coeval sequences and the original paleogeographic configuration of the terranes they comprise are largely unknown. Documentation of the geologic and geochemical evolution of these Middle Jurassic arc sequences is required prior to any attempt at comparison between coeval sequences. The Harrison Lake Formation of the Harrison terrane is the most extensive Early to Middle Jurassic arc sequence preserved in the Coast Plutonic Complex in the southern Canadian Cordillera (Fig. 4.1). Adjacent terranes contain coeval volcano-sedimentary assemblages of uncertain affinity. Documentation of the geologic and geochemical characteristics of the Harrison Lake Formation thus provides a framework within which to evaluate potentially correlative strata on adjacent terranes. This chapter describes the stratigraphy, volcanic geochemistry, isotopic characteristics and U-Pb geochronology of the Harrison Lake Formation, discusses the geologic evolution of the formation, and briefly outlines intraformational mineral deposits. This study represents the first detailed geologic and geochemical description of the Harrison Lake Formation.

4.2 GEOLOGIC SETTING

The Harrison terrane, exposed west of Harrison Lake, contains the most intact and well preserved Mesozoic stratigraphic section in the southwestern Canadian Cordillera (Fig. 4.1; Monger, 1970). The terrane consists of Middle Triassic oceanic rocks of the Camp Cove Formation unconformably overlain by arc volcanic rocks of the Early to Middle Jurassic Harrison Lake Formation, that in turn are unconformably overlain by Middle to Upper Jurassic clastic rocks of the Mysterious Creek and Billhook Creek formations (Monger, 1985;

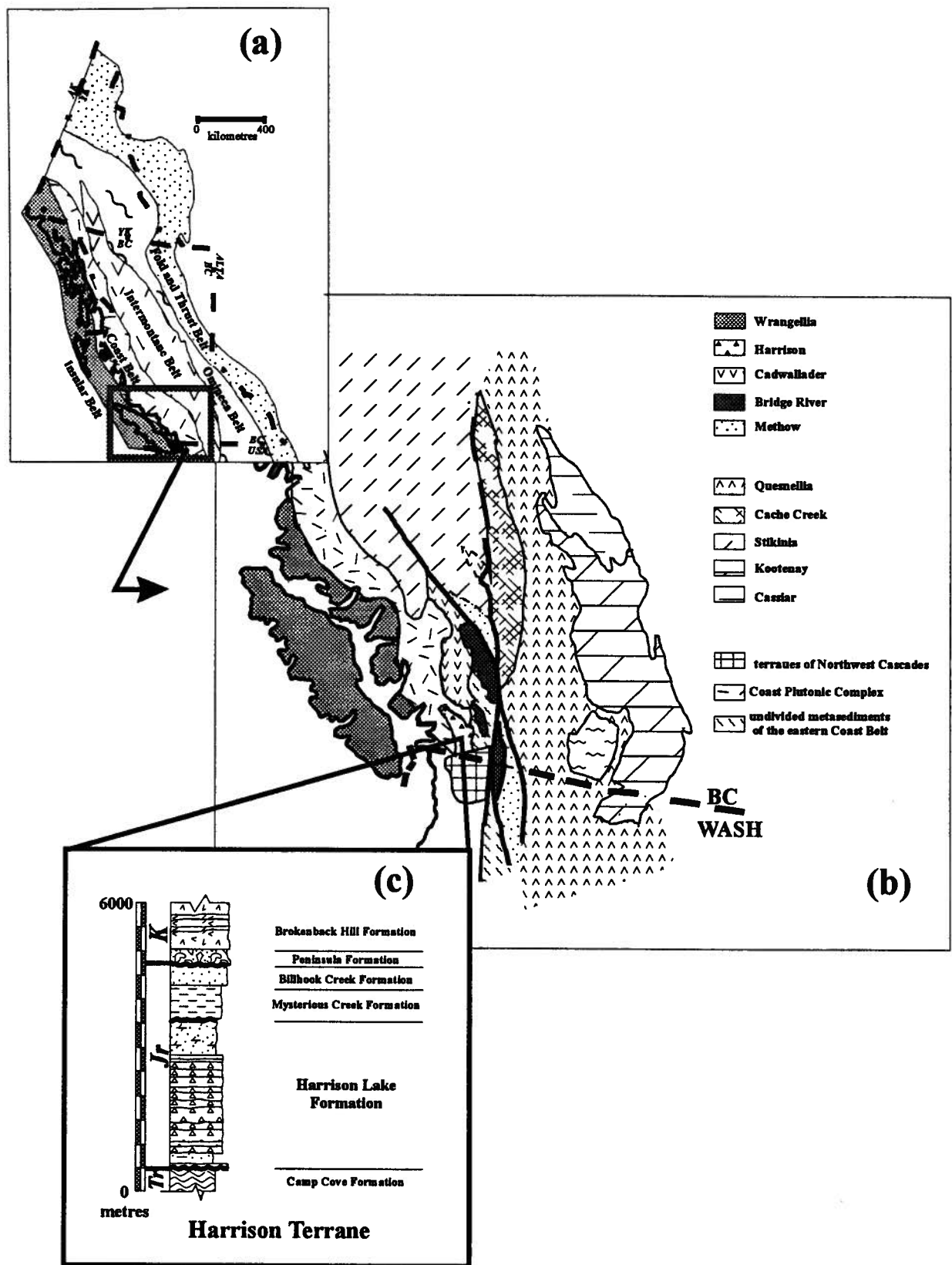


Figure 4.1 - a) morphogeologic belts of the Canadian Cordillera, with study area outlined. Modified from Monger and Hutchinson (1971); b) generalized terrane map of the southern Canadian Cordillera, illustrating terranes mentioned in text. Modified from Wheeler and McFeely (1991); c) schematic stratigraphic column of the Harrison Lake terrane. Modified from Arthur (1987).

Arthur, 1986, 1987; Arthur et al., 1993). Lower Cretaceous polymict conglomerate of the Peninsula Formation and volcanic strata of the Brokenback Hill Formations unconformably cap the sequence.

The Harrison terrane is intruded by Middle Jurassic and late Early Cretaceous plutons of the Coast Plutonic Complex to the west (Friedman and Armstrong, 1994; Fig. 4.1). The eastern boundary of the terrane is the Harrison Lake shear zone, a dextral transcurrent fault that separates subgreenschist facies rocks of the Harrison terrane from amphibolite facies metamorphic rocks within the Coast Belt Thrust System to the east (Journey and Csontos, 1989; Journey and Friedman, 1993). Rocks within the imbricate zone at the leading edge of the west-vergent Coast Belt Thrust System have been correlated with the Harrison terrane (Journey and Friedman, 1993; Journey and Mahoney, 1994), suggesting that rocks of the Harrison terrane extend farther east and north than previously recognized (Monger, 1985; Arthur et al., 1993)

The southern boundary of the terrane is the steeply dipping Vedder fault, which separates Late Paleozoic limestone and Jurassic-Cretaceous clastic rocks of the Chilliwack terrane from the Harrison terrane. The structural and stratigraphic relationship between the Harrison and Chilliwack terranes is enigmatic. Paleozoic limestone clasts found in the basal conglomerate of the Harrison Lake Formation are inferred to be derived from the Chilliwack terrane, thus suggesting an Early Jurassic stratigraphic linkage between the two (Arthur, 1987; Monger and Journey, 1992; Arthur et al., 1993). Structural relations in the Cascade range to the south suggest equivalents of the Chilliwack terrane structurally overlie rocks that have been correlated with the Harrison terrane (Misch, 1966; Tabor, 1994).

The Harrison Lake Formation comprises the southern two-thirds of the Harrison terrane. It is primarily exposed northeast of the Chehalis River, north of the Fraser River, south of Mystery Creek, and, with the exception of exposures on Echo Island, west of Harrison Lake (Figs. 4.1, 4.2 - in pocket). Strata of the Harrison Lake Formation are exposed in a poorly developed west-northwest trending, shallowly westerly plunging open anticline. The base of the formation is exposed in the core of the anticline approximately 2 km south of Camp Cove (Fig. 4.2). The northern limb of the anticline is truncated in part by a steeply dipping

northwest-trending structure near Camp Cove that juxtaposes the upper members of the formation with Triassic basement of the Camp Cove Formation (Fig. 4.2). The formation is cut by a myriad of smaller northwest and northeast-trending faults of modest (tens to hundreds of metres) offset.

4.3 PREVIOUS WORK

Crickmay (1925) described the volcanic rocks along the west side of Harrison Lake, subdividing them into the Harrison Lake, Echo Island, and Mysterious Creek formations, and established a Middle Jurassic biostratigraphic age for the main volcanic member. Thompson (1972) and Pearson (1973) mapped the southern portion of the outcrop belt to constrain the regional setting of Kuroko-style stratiform mineralization in the Seneca deposit (Fig. 4.2). Arthur (1986, 1987) and Arthur et al. (1993) described the formation, subdivided the Harrison Lake Formation into four formal members (Celia Cove, Francis Lake, Weaver Lake, and Echo Island members) and established a late Early Jurassic to Middle Jurassic (Middle Toarcian to mid-Aalenian) biostratigraphic age for the lower portion of the formation. McKinley et al. (1994) described the local stratigraphy and mineralization of the Seneca deposit in the southeastern portion of the study area.

Arthur (1987) mapped the west side of Harrison Lake at a scale of 1:50,000 during a biostratigraphic study of Jurassic and Cretaceous strata. Monger (1989) mapped the west side of Harrison Lake at a scale of 1:250,000. Thompson (1972) and Pearson (1973) mapped the area south of Mt. Klauadt at a scale of approximately 1:35,000, concentrating on economic mineralization. In this investigation, the outcrop area of the Harrison Lake Formation was mapped for the first time in its entirety at a scale of 1:50,000 (Fig. 4.2).

4.4 STRATIGRAPHY

The four-fold subdivision of the Harrison Lake Formation established by Arthur et al. (1993) is adapted herein (Fig. 4.3). The following descriptions are a significant modification and expansion of the

definitions of Arthur et al. (1993), and are based on extensive regional mapping, examination of lateral and vertical facies changes, drill hole data, and petrographic information.

Strata of the Harrison Lake Formation are predominantly volcanic lava flows and volcanoclastic sedimentary rocks. In this manuscript, volcanoclastic sedimentary rocks are distinguished according to their mode of deposition, and include: 1) *pyroclastic sediments*, which are direct products of pyroclastic eruptive processes, and display diagnostic features such as fiamme and glass shards; 2) *resedimented pyroclastic debris*, which consists of detritus initially formed by pyroclastic processes that has been redistributed prior to lithification by normal fluvial and marine processes; and 3) *epiclastic sediments*, which are clastic sediments formed by the normal weathering and erosion of pre-existing volcanic deposits (Fisher and Schminke, 1984; Cas and Wright, 1987; McPhie et al., 1994).

A. Celia Cove Member

The Celia Cove Member is a basal conglomerate unit unconformably overlying greenstone, chert, siltstone and sandstone of the Triassic Camp Cove Formation. The Celia Cove Member is only exposed in the core of the Camp Cove anticline (Fig. 4.2). The basal contact appears disconformable adjacent to massive greenstone, but an angular unconformity between the two is indicated by: 1) 1-2 m amplitude tight folds in chert and siltstone beds of the Camp Cove Formation along the lake shore south of Camp Cove that are absent in overlying rocks; 2) macroscopic folds suggested by structural orientation of bedded sediments in the Camp Cove Formation and not documented in immediately overlying strata; and 3) angular discordance between northeast dipping argillite of the Camp Cove Formation and west dipping conglomerate of the Celia Cove Member north of Francis Lake (Fig. 4.2).

The Celia Cove Member consists of volcanic and chert pebble to cobble conglomerate and medium to coarse-grained lithic sandstone. The base of the member is characterized by 1-2 m of granule to cobble-sized angular to subangular clasts of light grey to dark blue chert and lesser greenstone floating in a coarse lithic

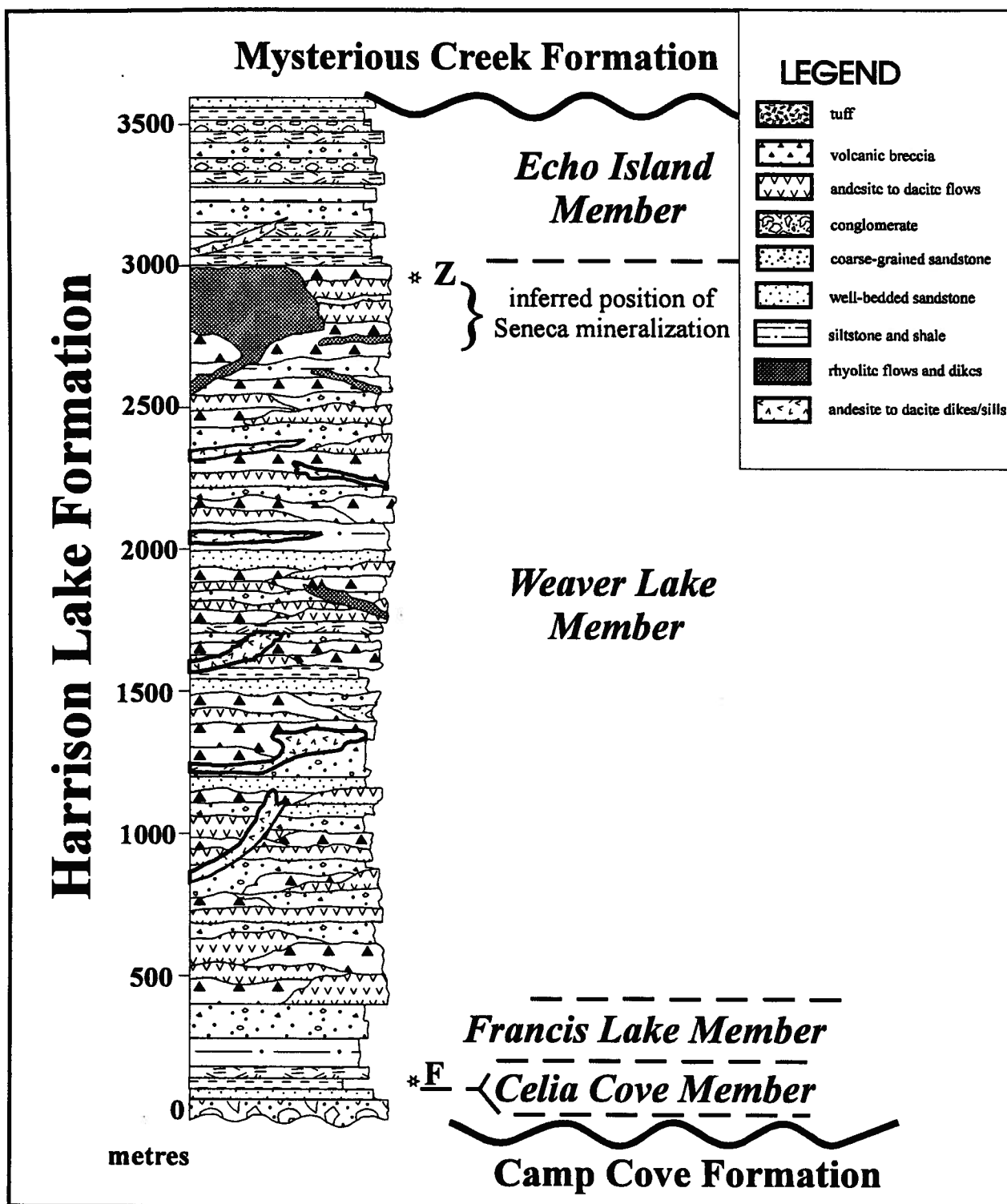


Figure 4.3 - Idealized stratigraphic column of the Harrison Lake Formation. Thicknesses estimated from outcrop patterns and cross-sections. Internal stratigraphic relations, particularly within the Weaver Lake Member, are idealized. Note location of new biostratigraphic data (☆F), U-Pb geochronology (☆Z), and inferred location of Seneca mineralization zone.

arenite matrix. Clasts become more well rounded, the sandstone content increases, and the conglomerate becomes more polymictic upsection, where it contains clasts of andesite porphyry, dacite porphyry, chert, volcanic lithic arenite, and rare well-rounded bioclastic limestone. Chert and limestone clast content decreases dramatically a few metres above the basal contact. Clast size reaches a maximum (cobble to boulder size) about 10 m above the base, then becomes progressively finer grained upsection. The conglomerate is thick bedded (1-2 m), locally clast supported, and intercalated with medium bedded matrix supported pebble to granule conglomerate and coarse-grained lithic sandstone. Contacts between beds are gradational; conglomerate beds become gradationally finer grained and thinner bedded upward, whereas the overlying sandstone and granule conglomerate beds coarsen and thicken as they grade into the next overlying conglomerate. Sandstone intercalated with the conglomerate is medium to coarse grained, moderately sorted, and is composed of sausseritized lithic volcanic fragments, plagioclase, and minor chert, quartz and sanidine. Thickness of the Celia Cove member varies from 10-60 m (Fig. 4.3).

The contact between the Celia Cove Member and the overlying Francis Lake Member is gradational, and is placed at the stratigraphically highest granule to pebble conglomerate bed. Conglomerate is gradationally overlain by thin to medium bedded, medium to coarse grained volcanic lithic wacke and siltstone of the lower Francis Lake Member. The transition from crudely stratified cobble conglomerates of the Celia Cove Member to sandstone and siltstone of the Francis Lake Member represents an overall fining upward stratigraphic succession.

B. Francis Lake Member

The Francis Lake Member gradationally overlies the Celia Cove Member. The unit weathers recessively, and is best exposed along Harrison Lake 1.5 km north of Celia Cove, and in roadcuts on the Harrison West Forest Service Road east of Francis Lake. It is conformable with the Celia Cove Member, and therefore mimics its arcuate outcrop pattern in the core of the Camp Cove anticline (Fig. 4.2). The Francis

Lake Member is estimated to be approximately 350–400 m thick, based on outcrop pattern and structural attitudes west of Celia Cove.

The Francis Lake Member is primarily thin bedded and fine grained, and comprises siliceous mudstone, calcareous siltstone, volcanic lithic wacke, crystal vitric tuff and lapilli tuff. Strata within the member initially fine upward from the underlying conglomerate, and then coarsen upward, incorporating increasingly larger proportions of crystal vitric tuff, lapilli tuff, and coarse grained tuffaceous feldspathic lithic wacke below the contact with the overlying volcanic Weaver Lake Member.

In the lower portion of the Francis Lake member, thin to medium bedded medium to coarse grained feldspathic lithic wacke above the Celia Cove Member grades upward over a 15–30 m interval into thin bedded, parallel laminated siltstone intercalated with minor thin bedded (3–5 cm) normally graded fine grained feldspathic wackes. Sedimentary structures include graded bedding, basal scour features, and parallel laminae. The fining upward sequence initiated in the Celia Cove Member is capped by a 15–20 m thick, ammonite-bearing, thin bedded shale and siltstone interval. The upper portion of the shale interval is interbedded with crystal tuff (Fig. 4.4). Grain size and bedding thickness increase upsection, where the member is dominated by thin to medium bedded medium to coarse grained tuffaceous lithic wackes and massive-appearing reddish and greenish black siliceous siltstone interbedded with thin to medium bedded crystal vitric tuffs and lapilli tuffs. Sedimentary structures are limited to parallel laminations, normally graded bedding, and minor scour features. Ammonite and pelecypod fragments are locally evident. Matrix-supported monomict vitric tuff breccia, consisting of a single layer of pebble to cobble sized angular clasts of light-colored siliceous vitric tuff floating in a dark grey siliceous siltstone locally forms a distinctive component of massive siltstone and mudstone intervals. The upper portion of the member is dominated by medium to thick bedded, medium to coarse grained tuffaceous lithic feldspathic wacke interbedded with thin crystal tuff.

Pyroclastic and epiclastic rocks of the upper Francis Lake Member are locally in sharp contact with overlying augite andesite porphyry of the basal Weaver Lake Member, but the presence of abundant

volcaniclastic rocks interbedded with massive flows in the lower portion of the Weaver Lake Member suggest the contact is gradational and conformable.

C. Weaver Lake Member

The Weaver Lake Member is the most areally extensive and volumetrically significant component of the Harrison Lake Formation. It is exposed over an area of over 150 km² between Weaver Lake and Mt. McRae (Fig. 4.2), and forms the prominent topographic highs between the Chehalis River and Harrison Lake. Laterally discontinuous units and the poor exposure of sedimentary interbeds makes structural interpretations difficult; the unit is cut by numerous small faults and mesoscale (1-10 m amplitude) open folds are locally evident.

The Weaver Lake Member comprises porphyritic andesite, dacite and locally rhyolite lava flows, associated flow breccia, hyaloclastite, volcanic breccia, tuff breccia, lapilli tuff, and minor intercalated epiclastic conglomerate, sandstone and siltstone. The member is dominated by lava flows, breccia, and tuff breccia that form prominent, resistant exposures. Individual units are lenticular and laterally discontinuous, and amalgamate into overlapping and interdigitating sequences with no stratigraphic continuity. Flows are generally massive, but locally display trachytic textures, amygdules, and brecciated flow tops. There is an overall transition from andesitic flows near the base of the member into flows of predominantly dacitic composition, followed by the rhyolitic units that characterize the upper portions of the member. The majority of the flows are dacitic in composition, characterized by plagioclase and lesser hornblende and quartz phenocrysts. Volcanic breccias and tuff breccias are most commonly matrix supported, vary from massive to crudely bedded (0.5-10 m thick), appear lensoidal, and locally contain porphyritic clasts with distinct alteration rinds. North of the outflow of Harrison Lake, a clast supported volcanic breccia containing large (> 30 cm) angular porphyritic clasts is interpreted as a vent-proximal agglomerate.

It is commonly difficult to distinguish between volcanic flows and synvolcanic dikes and sills in the Weaver Lake Member. This investigation suggests that there are a much higher percentage of synvolcanic dikes and sills within the Weaver Lake Member than earlier workers (Thompson, 1972; Pearson, 1973; Arthur, 1985, 1987; Arthur et al., 1993). Dikes are recognized by the presence of chilled margins, sharp contacts, lack of flow brecciation, cross-cutting relations with adjacent flows and sediments, blocky weathering character, relatively fresh appearance, and ubiquitous columnar jointing. Columnar jointing described by Arthur et al. (1993) as a characteristic flow feature actually occurs in cross-cutting dikes similar in composition to overlying volcanic flows (Fig. 4.5). There is very little textural, mineralogical, or bulk compositional difference between dikes and flows, and genetic classification must be based on field criteria.

A spectacular rhyolite dome complex forms the uppermost Weaver Lake Member on the east side of the study area. The complex is well exposed on the north and west side of Echo Island, where it forms cliffs over 160 m high. The rhyolite is light grey to pinkish red, ranges from aphanitic to porphyritic, and has a phenocryst assemblage variably dominated by plagioclase, chloritized hornblende, or quartz. The unit is locally massive, but commonly displays well-developed flow foliation and flow folds that lead to a bedded appearance in outcrop. Parallelism between flow foliation and overlying sediments, variation in phenocryst assemblages, lack of quench fragmentation/brecciation at the upper or lower surface, and the absence of a radial pattern in dip direction within the overlying sediments suggests the rhyolite may have been emplaced as a series of shallow hypabyssal intrusions rather than as a cryptodome or flow sequence.

Sedimentary sequences intercalated with primary volcanic rocks of the Weaver Lake Member include thin to thick bedded lapilli tuff, tuff, tuffaceous sandstone, siltstone, and epiclastic conglomerate. Thin to medium bedded immature tuffaceous lithic feldspathic wacke, tuffaceous siltstone and mudstone dominate sedimentary interbeds. Sedimentary structures include parallel and convolute laminae, trough cross laminae, flame structures, scour features, graded bedding, slump features, and small channels (approximately 1 m wide). Woody debris is locally abundant, and is found on bedding planes at the base of mass sediment gravity flow units. Sedimentary intervals tend to weather recessively, and locally may comprise 40-60% of the unit.

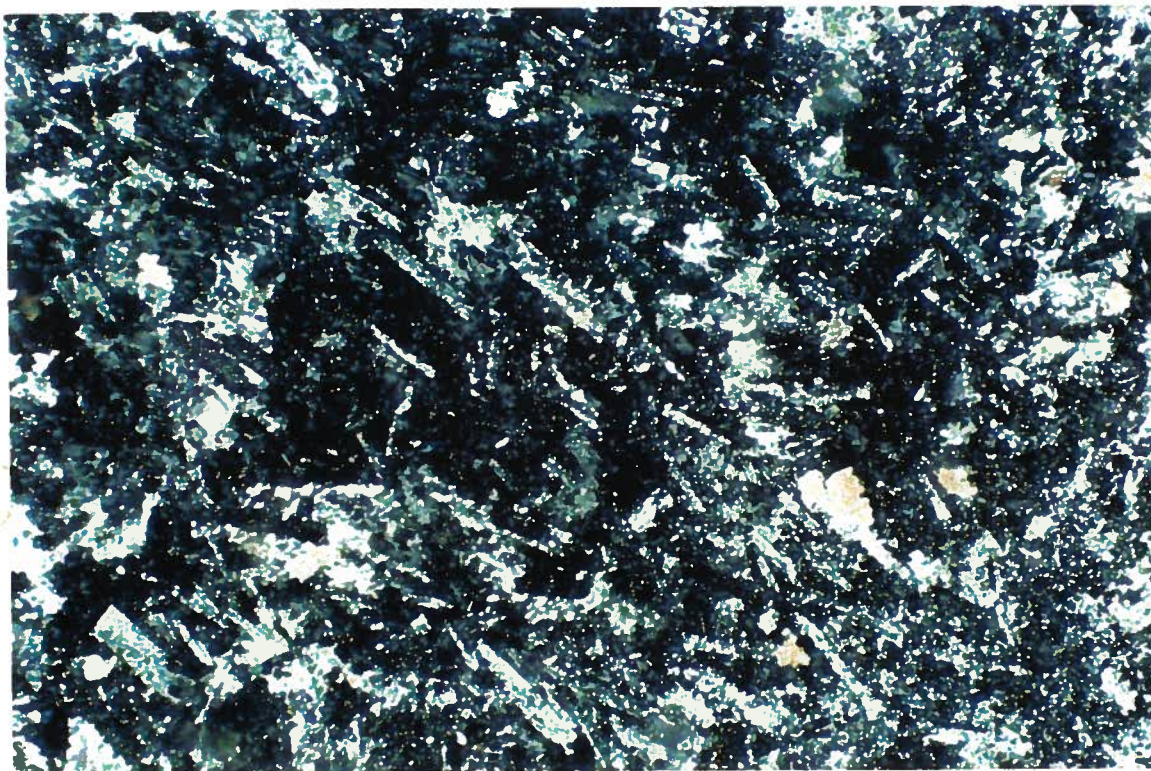


Figure 4.4 - Photomicrograph of trachytic crystal tuff of the Francis Lake Member.



Figure 4.5 - Photograph of dacite dike with well-developed columnar jointing cross-cutting altered dacite lava flow of the Weaver Lake Member.

The thickness of the Weaver Lake Member is difficult to ascertain because upper and lower contacts are not exposed within the same structural block, outcrop is discontinuous, marker beds are rare, and a paucity of younging indicators restrict assessment of structural and stratigraphic continuity. Crickmay (1925) measured 2800 m of volcanic strata north of Camp Cove in a section cut by faults and containing open folds of kilometre wavelength. Thompson (1972) estimated a minimum thickness based on topographic relief in the southern end of the outcrop area to be ~1400 m. In this investigation, the approximate thickness of the Weaver Lake Member, based on simplified fold geometry and structural cross sections, was determined to be about 2600 m. This value should be taken as a crude estimate at best.

The contact between the Weaver Lake Member and the overlying Echo Island Member is placed at the top of the uppermost lava flow or volcanic breccia in the Weaver Lake Member (Fig. 4.3). The nature of the contact varies across the study area due to the lateral variability of primary volcanic facies in the Weaver Lake Member. Thin to medium bedded sedimentary rocks of the Echo Island Member overlie a rhyolite dome complex on the south end of Echo Island, dacitic lava flows and breccia on the north slope of Mt. McRae, and dacitic breccia east of Morris Creek, north of the Harrison River (Fig. 4.2). The contact is easily located by a prominent break in topography and by the appearance of thick sequences of well-bedded volcanoclastic sedimentary rocks.

D. Echo Island Member

The Echo Island Member is the uppermost subdivision of the Harrison Lake Formation. The member is well exposed along the south shore of Echo Island, along both sides of the Harrison River east of Morris Creek, and on the north and east flanks of Mt. McRae (Fig. 4.2). The Echo Island Member conformably overlies the Weaver Lake Member; the contact is well exposed on Echo Island and the north flank of Mt. McRae (Fig. 4.2). The top of the member is an angular unconformity with the overlying Mysterious Creek Formation. The member is well-bedded, and generally forms gently dipping homoclines. However, metre-

scale open folds are locally evident, and overturned bedding is mapped on the north flank of Mt. McRae. The member is locally cut by dacitic dikes interpreted to be comagmatic with flows in the Weaver Lake Member.

The Echo Island Member comprises, in decreasing order of abundance, volcanoclastic sandstone, siltstone, mudstone, granule to cobble conglomerate, lapilli tuff, crystal to vitric tuff, and minor tuff breccia. Resedimented pyroclastic debris predominates, with subordinate epiclastic and pyroclastic deposits. The member is dominantly thin- to medium-bedded, medium- to coarse-grained lithic feldspathic wacke and tuffaceous siltstone. Thick-to very thickly-bedded lithic feldspathic wacke, granule conglomerate, and lapilli tuff are also present, and form prominent outcrops. Massive to crudely laminated sandstone beds locally amalgamate into units > 7 m thick. Cyclic sedimentation is evident in abundant fining and thinning upward and coarsening and thickening upward stratigraphic sequences (10-35 m). Sedimentary structures include parallel and convolute laminae, normal and inverse graded bedding, trough cross-bedding, channels, basal scour features, rip up clasts, load casts, soft sediment deformation, and rare complete Bouma (ABCDE) sequences. Thin bedded structureless siltstone and mudstone beds are commonly bioturbated.

Sedimentary rocks of the Echo Island Member are dominantly thin to medium bedded volcanic sandstone, siltstone, mudstone and lesser crystal tuff. This pattern is interrupted by thick-bedded to massive (2-15 m) lapilli tuff, tuff breccia, granule to pebble volcanic breccia or tuffaceous sandstone. These thick units are normally graded, although they may have a basal inversely graded segment (< 1 m), and are characterized by crude banding, bedding parallel clast alignment and relict fiamme. Normal grading is defined by a decrease in both grain size and the density and size of fiamme. In thin section, these units contain subangular to subrounded clasts of crystal tuff, vitric tuff, and lesser andesite and dacite porphyry floating in an altered matrix of clay and plagioclase microlites. These thick bedded intervals commonly overlie thin bedded fine sandstone, siltstone and mudstone, and are overlain by thin- to medium-bedded fine to coarse grained lithic feldspathic wacke containing abundant sedimentary structures. On the south end of Echo Island, clast-supported channelized and unchannelized pebble to cobble volcanic conglomerate occurs above one of the

massive intervals; the conglomerate fines and thins upward into thin to medium bedded parallel laminated volcaniclastic sandstone and siltstone.

The total thickness of the Echo Island Member is uncertain. The most complete section of the member occurs along the Harrison River, east of Morris Creek, where the thickness is estimated to be 600-650 m (Fig. 4.3). Arthur et al. (1993) suggest that the member thickens to the north, to about 1000 m north of Mt. McRae. However, this section is complicated by mesoscale folding, including overturned bedding, so this estimate must be treated with caution.

The top of the Echo Island Member is an unconformity with the overlying Mysterious Creek Formation. The contact is disconformable in exposures along Harrison River (Fig. 4.2). The contact is not exposed to the north, but on the north flank of Mt. McRae steeply south-dipping overturned beds and mesoscale folds of the Echo Island Member appear to be overlain by gently north-dipping beds of the Callovian Mysterious Creek Formation. This relationship suggests an angular unconformity separates the two.

4.5 AGE CONSTRAINTS

Age constraints in the Harrison Lake Formation are provided by ammonite biostratigraphy and U-Pb zircon geochronology.

A. Biostratigraphic Data

Fossils are rare in the Harrison Lake Formation. Crickmay (1925) reported probable Middle Jurassic brachiopods, pelecypods, and possible corals from sandstone of the Francis Lake or Weaver Lake Members. H. Frebold (in Monger, 1970) identified Toarcian ammonites from sedimentary beds apparently below volcanic rocks (Francis Lake Member of current usage) and Middle Bajocian ammonites from sedimentary beds intercalated with massive volcanics (Weaver Lake Member of current usage). Arthur (1986) and Arthur

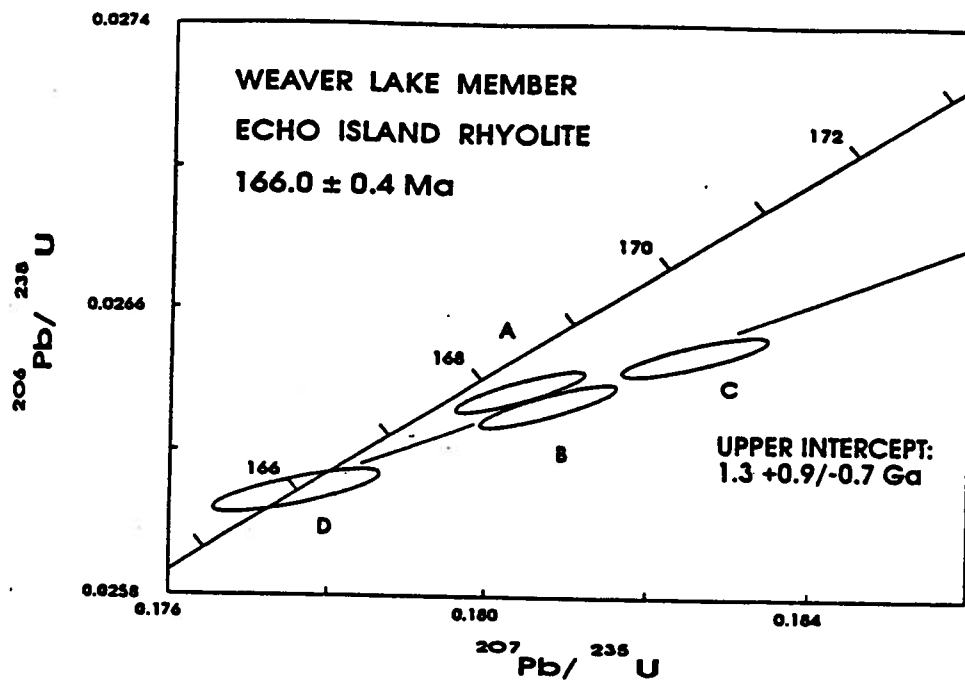
et al. (1993) present a comprehensive review of paleontology of the formation, and interpret the formation to range from Middle Toarcian(?) to Early Bajocian(?).

New biostratigraphic control is established by the discovery of well preserved *Dactyloceras* sp. ammonites in the Francis Lake Member, which establishes the age of the member as late Early Toarcian (G.K. Jakobs, written communication, 1992). The existence of crystal tuff intercalated with ammonite bearing argillite in the Francis Lake Member firmly establishes the initiation of volcanism in the Harrison Lake Formation to be late Early Toarcian (ca. 190 Ma).

B. U-Pb Geochronology

A sample of rhyolite from near the top of the Weaver Lake Member on Echo Island was collected for U-Pb zircon dating. Standard mineral separation techniques yielded abundant, high quality, clear, pale pink, moderately elongate to subequant zircon (length/width ratios of about 3.5 to 1.25). Mineral separation and analytical procedures are outlined in Friedman and Armstrong (1994). There were no visible cores observed in any zircons from this sample. All fractions were strongly abraded to eliminate or minimize the effects of Pb loss. Analyses of four zircon fractions (A-D) from the rhyolite form a quasi-linear array which indicates a Middle Jurassic magmatic age for the sample, and the presence of an old inherited component in fractions A, B, and C (Fig. 4.6a). Fraction D consisted of tips broken off of the most elongate zircon grains available, in order to eliminate any possible inherited core material. This fraction is concordant and provides the best estimate for the age of the sample of 166.0 ± 0.4 Ma (age and precision based on $^{206}\text{Pb}/^{238}\text{U}$ date for this fraction). The narrow error envelope assigned to this interpreted age is considered warranted because the high quality, strongly abraded, low uranium zircon tips from fraction D are unlikely to show the effects of Pb loss. However, if minor Pb loss has affected fraction D, a maximum possible age is given by its $^{207}\text{Pb}/^{206}\text{Pb}$ date and associated error (165.8 ± 9.9 Ma; Table 4.1). These results clearly indicate a Late Bajocian/Early Bathonian age for the rhyolite dome, and, together with biostratigraphic data, suggest that volcanism in the Harrison Lake Formation was active from Late Early Toarcian to Early Bathonian time. A regression line

A



B

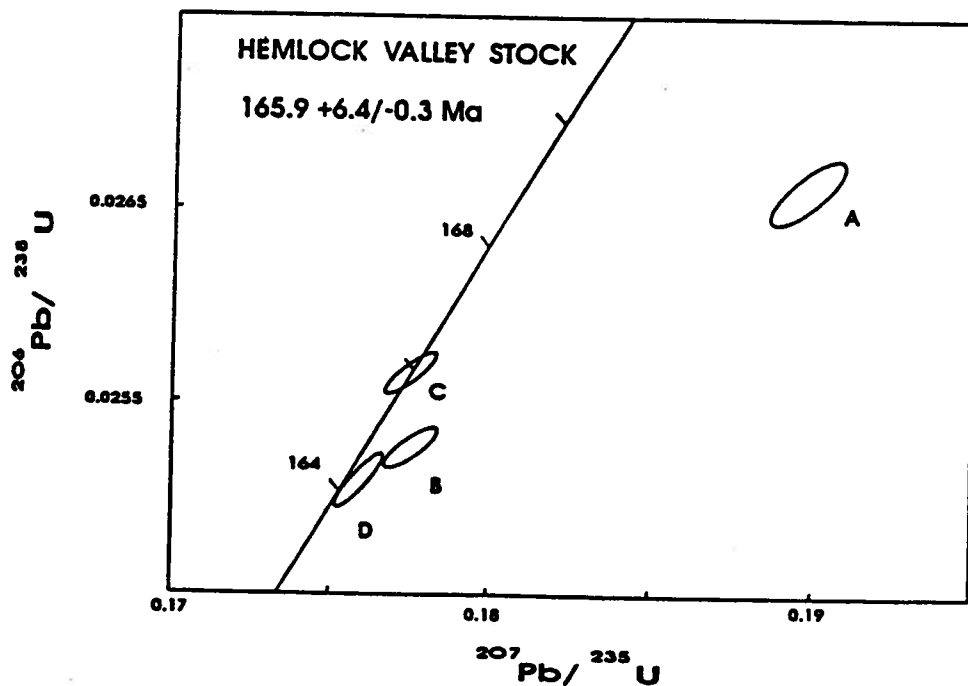


Figure 4.6 -a) Concordia diagram for rhyolite sample recovered from the upper Weaver Lake Member on Echo Island; b) Concordia diagram for the Hemlock Valley stock. See figure 4.2 for sample locations.

U-PB ZIRCON ANALYTICAL DATA FOR THE HARRISON LAKE FORMATION

| Fraction ¹ | Wt. mg | U ppm | Pb ² ppm | 206Pb ³ 204Pb | Pb ⁴ Pb | 208Pb ⁵ % | Isotopic ratios(±1σ,%) ⁶ | | | Isotopic dates(Ma,±2σ) ⁶ | | |
|---------------------------------|-----------|----------|------------------------|-----------------------------|-----------------------|-------------------------|-------------------------------------|-------------|--------------|-------------------------------------|------------|-------------|
| | | | | | | | 206Pb/238U | 207Pb/235U | 207Pb/206Pb | 204Pb/238U | 207Pb/235U | 207Pb/206Pb |
| Echo Island Rhyolite: 293JBM92 | | | | | | | | | | | | |
| A.c.N2.p | 0.246 | 149 | 3.9 | 2534 | 24 | 9.9 | 0.02637±0.11 | 0.1804±0.23 | 0.04962±0.14 | 167.8±0.4 | 168.4±0.7 | 177.2±6.4 |
| B.m.N2p | 0.110 | 178 | 4.8 | 2137 | 15 | 11.3 | 0.02633±0.12 | 0.1808±0.24 | 0.04979±0.14 | 167.5±0.4 | 168.7±0.7 | 185.2±6.7 |
| C.m.N2.p.eq | 0.071 | 170 | 4.6 | 1760 | 12 | 10.7 | 0.02648±0.11 | 0.1826±0.25 | 0.05002±0.17 | 168.4±0.4 | 170.3±0.8 | 195.9±7.8 |
| D.c.N2.p.ii | 0.057 | 158 | 4.2 | 1232 | 12 | 11.4 | 0.02609±0.12 | 0.1776±0.30 | 0.04938±0.21 | 166.0±0.4 | 166.0±0.9 | 165.8±9.9 |
| Hemlock Valley Stock: MV-85-HL1 | | | | | | | | | | | | |
| A.c.N1.p | 0.900 | 125 | 3.5 | 1245 | 149 | 13.4 | 0.02655±0.16 | 0.1898±0.31 | 0.05184±0.20 | 168.9±0.5 | 176.4±1.0 | 278.5±9.3 |
| B.f.N1.p | 1.500 | 132 | 3.6 | 4863 | 65 | 13.8 | 0.02580±0.14 | 0.1759±0.22 | 0.04946±0.11 | 164.2±0.4 | 164.5±0.7 | 169.6±5.1 |
| C.f.N2.p.e | 0.094 | 138 | 3.8 | 2499 | 9 | 13.7 | 0.02608±0.11 | 0.1775±0.23 | 0.04937±0.15 | 165.9±0.3 | 165.9±0.7 | 165.5±6.8 |
| D.m.N2.p | 0.147 | 133 | 3.6 | 2427 | 13 | 13.8 | 0.02588±0.10 | 0.1775±0.24 | 0.04975±0.16 | 164.7±0.3 | 165.9±0.7 | 183.2±7.4 |

¹All fractions are air abraded; Grain size, smallest dimension: c = >134µm, m = <134 and >74µm, f = <74µm; Magnetic codes: Franz magnetic separator sideslope at which grains are nonmagnetic; e.g., N1=nonmagnetic at 1°; Field strength for all fractions = 1.8A; Front slope for all fractions = 20°; Grain character codes: c=elongate, eq=equant, p=prismatic, ii=ilips;

²Radiogenic Pb

³Measured ratio corrected for spike and Pb fractionation of 0.0043/amu ±20% (Daly collector)

⁴Total common Pb in analysis based on blank isotopic composition determined from procedural blanks

⁵Radiogenic Pb

⁶Corrected for blank Pb (5-20pg), U (1-3pg) and common Pb (Stacey-Kramers model Pb composition at the 207Pb/206Pb date of fraction or age of sample); Note that fractions A and B for Hemlock Valley Stock were done in 1990 when procedural blanks were 50 and 10pg for Pb and U, respectively.

Table 4.1 - U-Pb zircon analytical data for Harrison Lake Formation and associated Hemlock Valley Stock.

through the four analyses yields a poorly constrained upper intercept of 1.3 Ga, indicating Late Proterozoic inheritance, and suggesting the incorporation of an older crustal component in Middle Jurassic magmatism (Friedman and Cui, 1994).

The age of the rhyolite dome complex is nearly identical to that of the Hemlock Valley stock, a quartz feldspar porphyry stock that intrudes the Weaver Lake Member north of Mt. Klautt (Fig. 4.2). A sample of the stock was originally collected for U-Pb dating in 1987 by J.W.H. Monger. At that time, two relatively imprecise analyses of unabraded zircon determined by P. van der Heyden indicated a crystallization age of about 165 Ma (R. Friedman, personal communication, 1994). Zircon fractions analyzed from this sample during the present investigation consist of moderate to good quality, clear to slightly cloudy grains with subequant to moderately elongate prismatic morphology (length/width ratios of about 1.5 to 3.0). No cores were visible. Four new analyses of abraded zircon fractions are shown on figure 4.6b. The data indicate the presence of varying amounts of inheritance in fractions A, B and D, with superimposed Pb loss on fractions B and D. Pb loss cannot be ruled out for fractions A and C. Fraction C, which consisted of abraded, relatively elongate prismatic grains, is concordant at 165.9 Ma and provides the basis for the interpreted age estimate of $165.9 \pm 6.4/-0.3$ Ma. The maximum age is based on the $^{207}\text{Pb}/^{206}\text{Pb}$ date and the minimum age on the $^{206}\text{Pb}/^{238}\text{U}$ date, both for fraction C. The larger upper error envelope takes into account the possibility of Pb loss that has not been completely eliminated through abrasion.

The similarity of magmatic age, inheritance characteristics, and Nd and Sr isotopic values (see following isotopic discussion) strongly argues the dome and stock are comagmatic. In addition, the western margin of the Harrison Lake Formation is intruded by the Mt. Jasper pluton, a massive tonalite/granodiorite intrusion. The Mt. Jasper pluton yields a 167 ± 4 Ma U-Pb zircon age (Friedman and Armstrong, 1994), which overlaps the age of both the rhyolite dome and the quartz feldspar intrusion, suggesting the granitoid rocks intruding the Harrison Lake Formation are simply the subvolcanic roots to the Middle Jurassic volcanic arc.

4.6 STRUCTURAL DEFORMATION

The Harrison Lake Formation is deformed into a broad, gentle west-northwest trending, shallowly westerly plunging anticline (Fig. 4.2). Limited continuous exposures suggest the formation forms gently dipping homoclines. The contact between the Harrison Lake Formation and the overlying Mysterious Creek Formation exposed on the south shore of the Harrison River appears disconformable. However, new mapping in the Harrison Lake Formation conducted during this investigation documents mesoscale folds in the Weaver Lake and Echo Island Members throughout the outcrop belt. Mesoscale folds are of 1-10 m amplitude, generally have near E-W fold axes, and are dominantly north vergent. Bedding on the north and northeast flanks of Mt. McRae is locally overturned to the south.

Poor exposure makes adequate documentation of the deformational history of the Harrison Lake Formation difficult. Folding about northwest-trending fold axes was documented by Pearson (1973). Arthur (1987) described close mesoscale folds with west-northwest-trending fold axes on the east side of Echo Island, together with EW-trending gentle folds and near-vertical bedding on the northwest flank of Mt. McRae. The chaotic distribution of structural attitudes throughout the outcrop belt, locally evident mesoscale folds, and overturned bedding in the Echo Island Formation contrast sharply with the unfolded, gentle, north to northeast dipping beds of the overlying Mysterious Creek Formation. The contrast in structural styles between the two formations strongly suggests the presence of an angular unconformity between the two, and indicates a post-Early Bathonian (ca. 165 Ma, pre-Early Callovian (ca. 160 Ma) compressional event in the region. The timing of this deformational event corresponds to the timing of isoclinal folding in the Bowen Island Group to the west, which is constrained to be post-185 Ma, pre-155 Ma (Friedman et al., 1990; Monger and Journeay, 1994).

4.7 GEOCHEMISTRY

Geochemical analyses are reported for a representative suite of primary volcanic rocks from throughout the entire stratigraphic range and lateral extent of the Weaver Lake Member. The suite comprises 13 extrusive volcanic rocks, 4 dikes, and one sample of a coeval quartz feldspar porphyry (Fig. 4.2). Sample selection was limited to relatively unaltered samples of andesitic to dacitic composition. Homogenized rock powders were prepared from 2-5 kg whole rock samples, with care taken to remove weathered surfaces and secondary veins. Major and minor element concentrations were determined by fused disc X-ray fluorescence; trace and rare earth elements were measured by inductively coupled mass spectrometry. Complete sample preparation and analytical techniques are given in Appendix A.

Geochemical results are also summarized from a detailed companion study of lithostratigraphy, geochemistry and mineralization of the Seneca area by Sean McKinley (Fig. 4.2). Data for 54 samples from the Seneca area indicate a bimodal volcanic suite characterized by a mafic suite ($\text{SiO}_2=45\text{-}53$ wt %, $n=14$) and a felsic suite ($\text{SiO}_2=66\text{-}74$ wt %, $n=40$; Fig. 4.2; Table 4.2).

Primary volcanic rocks in the Weaver Lake Member range from basaltic andesite to rhyolite (Table 4.2; Fig. 4.7). There is a general geochemical trend from mafic compositions near the bottom of the member to more felsic compositions near the top of the member. This trend is supported by field evidence that documents basaltic andesite to andesite near the base of the Weaver Lake Member, dacite comprising the majority of the member, and an increase in the proportion of rhyolite within the upper portions of the member. The increase in pyroclastic material evident in the Echo Island Member suggests an increase in explosive volcanism near the top of the formation, which is consistent with an increase in silica and probably volatile content of the system.

Major and trace element values indicate the rocks are of calc-alkaline magmatic affinity, and range from low- to high-K types (Fig. 4.7). However, elemental scatter on Harker variation diagrams suggests

| Sample | 4JBM92 | 116JBM92 | 122JBM92 | 123JBM92 | 142JBM92 | 150JBM92 | 151JBM92 | 287JBM92 | 291JBM92 | 292JBM92 |
|--------------------------------|--------|----------|----------|----------|----------|----------|----------|----------|----------|----------|
| SiO ₂ | 61.68 | 58.12 | 75.29 | 68.40 | 56.32 | 72.99 | 74.74 | 63.00 | 67.51 | 74.68 |
| TiO ₂ | 0.865 | 0.765 | 0.290 | 0.505 | 0.830 | 0.370 | 0.315 | 0.67 | 0.510 | 0.250 |
| Al ₂ O ₃ | 16.76 | 19.16 | 12.83 | 15.73 | 19.23 | 14.05 | 13.47 | 15.90 | 15.58 | 14.36 |
| FeO* | 7.30 | 6.98 | 1.50 | 4.18 | 9.56 | 2.49 | 2.96 | 5.13 | 4.19 | 2.15 |
| MnO | 0.15 | 0.20 | 0.05 | 0.09 | 0.18 | 0.11 | 0.10 | 0.10 | 0.09 | 0.05 |
| CaO | 5.03 | 2.37 | 1.51 | 1.61 | 3.16 | 2.07 | 0.63 | 2.45 | 1.20 | 5.12 |
| MgO | 2.54 | 4.62 | 0.45 | 2.46 | 5.82 | 1.05 | 1.03 | 2.22 | 2.54 | 0.80 |
| K ₂ O | 0.54 | 1.54 | 3.66 | 3.67 | 2.56 | 3.04 | 1.19 | 4.78 | 4.09 | 1.38 |
| Na ₂ O | 4.56 | 5.95 | 3.49 | 3.69 | 1.75 | 3.20 | 5.27 | 2.19 | 4.03 | 0.82 |
| P ₂ O ₅ | 0.25 | 0.21 | 0.07 | 0.17 | 0.22 | 0.10 | 0.07 | 0.21 | 0.15 | 0.05 |
| Total | 100.49 | 100.68 | 99.29 | 100.96 | 100.67 | 99.74 | 100.09 | 96.65 | 100.36 | 99.90 |
| LOI | | | | | | | | 2.75 | | |
| Trace Elements | | | | | | | | | | |
| Ni | - | 4 | - | - | 9 | - | - | - | 5 | - |
| Cr | 10 | 14 | 15 | 13 | 25 | 12 | 17 | 16 | 17 | 10 |
| Sc | - | - | - | - | - | - | - | - | - | - |
| V | 95 | 170 | 14 | 77 | 221 | 25 | 4 | 83 | 76 | 11 |
| Ba | 185 | 658 | 1438 | 1189 | 424 | 1488 | 395 | 838 | 1175 | 616 |
| Rb | 7.31 | 28.81 | 36.79 | 54.40 | 60.82 | 41.95 | 12.60 | 32.64 | 52.08 | 30.10 |
| Sr | 147 | 231 | 147 | 244 | 33 | 163 | 153 | 289 | 121 | 219 |
| Zr | 68 | 128 | 136 | 147 | 106 | 138 | 149 | 131 | 154 | 125 |
| Y | 30.40 | 23.60 | 19.14 | 23.26 | 21.72 | 22.16 | 56.20 | 33.57 | 24.85 | 19.01 |
| Nb | 2.67 | 4.98 | 5.40 | 6.02 | 4.48 | 5.68 | 5.32 | 6.62 | 6.49 | 5.44 |
| Ga | - | - | - | - | - | - | - | - | - | - |
| Cu | 19 | 7 | - | 8 | 34 | 3 | - | 9 | 26 | 2 |
| Zn | 88 | 108 | 46 | 53 | 117 | 52 | 62 | 68 | 88 | 45 |
| Pb | 2.32 | 3.40 | 1.37 | 4.18 | 1.92 | 3.59 | 1.58 | 3.91 | 17.55 | 7.73 |
| La | 7.37 | 14.33 | 9.03 | 17.85 | 12.60 | 15.42 | 15.32 | 15.66 | 16.47 | 14.16 |
| Ce | 15.73 | 27.75 | 18.72 | 28.71 | 24.31 | 25.04 | 29.73 | 30.56 | 27.24 | 24.98 |
| Pr | 2.34 | 3.36 | 2.30 | 3.40 | 3.02 | 3.12 | 4.66 | 3.95 | 3.28 | 2.80 |
| Nd | 11.81 | 14.92 | 9.99 | 13.86 | 13.34 | 12.70 | 21.95 | 17.82 | 13.66 | 10.93 |
| Sm | 3.83 | 3.90 | 2.49 | 3.20 | 3.59 | 3.05 | 6.63 | 4.91 | 3.38 | 2.63 |
| Eu | 1.43 | 1.15 | 0.69 | 0.98 | 1.02 | 0.80 | 1.69 | 1.35 | 0.93 | 0.65 |
| Gd | 4.26 | 3.85 | 2.57 | 2.98 | 3.56 | 2.97 | 7.21 | 5.01 | 3.38 | 2.41 |
| Tb | 0.82 | 0.67 | 0.48 | 0.56 | 0.63 | 0.54 | 1.42 | 0.90 | 0.59 | 0.46 |
| Dy | 5.45 | 4.21 | 2.96 | 3.64 | 4.04 | 3.43 | 9.27 | 5.87 | 3.92 | 3.01 |
| Ho | 1.18 | 0.88 | 0.67 | 0.80 | 0.83 | 0.77 | 1.98 | 1.25 | 0.84 | 0.65 |
| Er | 3.45 | 2.69 | 2.01 | 2.38 | 2.46 | 2.33 | 5.97 | 3.72 | 2.58 | 2.07 |
| Tm | 0.48 | 0.37 | 0.30 | 0.35 | 0.34 | 0.34 | 0.83 | 0.53 | 0.36 | 0.32 |
| Yb | 2.98 | 2.37 | 2.00 | 2.31 | 2.25 | 2.31 | 5.42 | 3.44 | 2.46 | 2.00 |
| Lu | 0.49 | 0.40 | 0.36 | 0.40 | 0.38 | 0.39 | 0.92 | 0.57 | 0.44 | 0.36 |
| Hf | 1.82 | 2.85 | 3.11 | 3.39 | 2.68 | 3.18 | 3.68 | 3.16 | 3.14 | 3.08 |
| Th | 0.71 | 3.23 | 2.61 | 3.98 | 2.97 | 2.45 | 1.12 | 1.94 | 3.39 | 2.57 |
| U | 0.25 | 0.98 | 0.83 | 1.31 | 0.96 | 0.79 | 0.44 | 0.66 | 1.10 | 1.00 |
| Ta | 0.20 | 0.43 | 0.42 | 0.49 | 0.39 | 0.48 | 0.38 | 0.43 | 0.52 | 0.54 |
| Cs | 0.36 | 0.18 | 0.48 | 0.38 | 0.94 | 2.38 | 0.10 | 1.21 | 0.15 | 2.50 |
| Ce/Yb | 5.3 | 11.7 | 9.4 | 12.4 | 10.8 | 10.8 | 5.5 | 8.9 | 11.1 | 12.5 |
| Ba/La | 25.1 | 45.9 | 159.2 | 66.6 | 33.7 | 96.5 | 25.8 | 53.5 | 71.3 | 43.5 |
| La/Th | 10.4 | 4.4 | 3.5 | 4.5 | 4.2 | 6.3 | 13.7 | 8.1 | 4.9 | 5.5 |
| La/Nb | 2.8 | 2.9 | 1.7 | 3.0 | 2.8 | 2.7 | 2.9 | 2.4 | 2.5 | 2.6 |
| Ba/Nb | 69.3 | 132.1 | 266.3 | 197.5 | 94.6 | 262.0 | 74.2 | 126.6 | 181.0 | 113.2 |
| Zr/Y | 2.2 | 5.4 | 7.1 | 6.3 | 4.9 | 6.2 | 2.7 | 3.9 | 6.2 | 6.6 |
| Normalized Values | | | | | | | | | | |
| La/Yb | 1.6 | 4.0 | 3.0 | 5.1 | 3.7 | 4.4 | 1.9 | 3.0 | 4.4 | 4.7 |
| La/Sm | 1.2 | 2.2 | 2.2 | 3.4 | 2.1 | 3.1 | 1.4 | 1.9 | 3.0 | 3.3 |

Table 4.2a- Geochemical data for the Harrison Lake Formation.

| Sample | 293JBM92 | 306JBM92 | 307JBM92 | 13JBM93 | 14JBM93 | 15JBM93 | 17JBM93 | 21JBM93 | 22JBM93 | 25JBM93 |
|--------------------------------|----------|----------|----------|---------|---------|---------|---------|---------|---------|---------|
| SiO ₂ | 73.44 | 79.57 | 68.11 | 75.52 | 77.39 | 67.44 | 70.40 | 68.11 | 77.88 | 74.53 |
| TiO ₂ | 0.250 | 0.200 | 0.610 | 0.248 | 0.228 | 0.592 | 0.512 | 0.541 | 0.164 | 0.299 |
| Al ₂ O ₃ | 15.08 | 11.35 | 15.60 | 13.38 | 13.37 | 15.53 | 14.73 | 14.81 | 12.55 | 13.53 |
| FeO* | 1.20 | 1.38 | 4.45 | 1.30 | 1.32 | 3.86 | 4.58 | 4.30 | 1.42 | 1.91 |
| MnO | 0.04 | 0.03 | 0.06 | 0.03 | 0.04 | 0.08 | 0.17 | 0.12 | 0.05 | 0.05 |
| CaO | 3.80 | 0.43 | 3.62 | 2.22 | 1.19 | 1.81 | 1.28 | 3.03 | 0.87 | 1.03 |
| MgO | 0.68 | 0.45 | 1.77 | 0.72 | 0.57 | 1.10 | 1.14 | 1.35 | 0.35 | 0.76 |
| K ₂ O | 3.27 | 2.91 | 1.62 | 0.24 | 0.25 | 3.89 | 0.07 | 1.49 | 1.63 | 3.33 |
| Na ₂ O | 1.55 | 3.36 | 4.12 | 5.11 | 6.67 | 5.62 | 7.41 | 4.56 | 5.65 | 4.57 |
| P ₂ O ₅ | 0.05 | 0.06 | 0.21 | 0.05 | 0.05 | 0.22 | 0.15 | 0.16 | 0.03 | 0.07 |
| Total | 99.49 | 99.88 | 100.65 | 98.82 | 101.08 | 100.14 | 100.43 | 98.48 | 100.59 | 100.08 |
| LOI | | | | | | | | | | |
| Trace Elements | | | | | | | | | | |
| Ni | - | - | - | 8 | 9 | 4 | 5 | 7 | 8 | 8 |
| Cr | 13 | 16 | 12 | 3 | 5 | 4 | 0 | 2 | 3 | 4 |
| Sc | - | - | - | 11 | 6 | 17 | 29 | 18 | 3 | 7 |
| V | 10 | 11 | 43 | 28 | 13 | 53 | 0 | 45 | 4 | 24 |
| Ba | 1190 | 1060 | 154 | 239 | 91 | 937 | 71 | 667 | 940 | 929 |
| Rb | 83.87 | 81.81 | 16.36 | 1.40 | 2.55 | 57.40 | 1.12 | 23.49 | 20.42 | 37.80 |
| Sr | 163 | 113 | 72 | 242 | 200 | 161 | 123 | 339 | 147 | 152 |
| Zr | 124 | 93 | 111 | 115 | 112 | 137 | 87 | 130 | 123 | 128 |
| Y | 19.40 | 13.98 | 31.08 | 21.01 | 13.94 | 36.08 | 36.85 | 31.61 | 23.22 | 21.24 |
| Nb | 5.44 | 6.31 | 3.38 | 2.95 | 3.47 | 7.22 | 3.87 | 7.00 | 5.36 | 4.77 |
| Ga | - | - | - | 12 | 9 | 14 | 15 | 13 | 9 | 13 |
| Cu | - | - | - | 6 | 6 | 13 | 4 | 5 | 8 | 8 |
| Zn | 38 | 35 | 75 | 8 | 11 | 64 | 92 | 69 | 30 | 32 |
| Pb | 8.07 | 1.55 | 2.53 | 0.84 | 0.69 | 6.50 | 1.42 | 4.51 | 2.32 | 2.27 |
| La | 12.65 | 16.50 | 11.55 | 11.10 | 10.66 | 18.38 | 7.38 | 12.46 | 14.24 | 14.42 |
| Ce | 24.62 | 28.13 | 22.86 | 22.24 | 19.99 | 31.50 | 17.06 | 24.93 | 26.51 | 23.89 |
| Pr | 2.84 | 3.01 | 3.31 | 2.81 | 2.32 | 4.45 | 2.53 | 3.25 | 3.07 | 3.07 |
| Nd | 11.59 | 11.15 | 15.41 | 11.77 | 9.01 | 19.59 | 12.52 | 15.16 | 12.74 | 12.27 |
| Sm | 2.72 | 2.11 | 4.59 | 3.02 | 2.16 | 5.19 | 4.06 | 4.53 | 3.11 | 2.99 |
| Eu | 0.62 | 0.57 | 1.46 | 0.68 | 0.57 | 1.37 | 1.39 | 1.25 | 0.69 | 0.77 |
| Gd | 2.76 | 1.89 | 4.67 | 2.82 | 1.83 | 5.16 | 4.96 | 4.50 | 2.88 | 2.90 |
| Tb | 0.51 | 0.32 | 0.84 | 0.51 | 0.32 | 0.95 | 0.97 | 0.84 | 0.53 | 0.54 |
| Dy | 3.25 | 2.07 | 5.48 | 3.30 | 2.14 | 5.98 | 6.43 | 5.35 | 3.68 | 3.25 |
| Ho | 0.68 | 0.42 | 1.17 | 0.72 | 0.46 | 1.25 | 1.44 | 1.15 | 0.81 | 0.65 |
| Er | 2.07 | 1.34 | 3.44 | 2.25 | 1.47 | 3.79 | 4.27 | 3.45 | 2.48 | 2.11 |
| Tm | 0.29 | 0.21 | 0.48 | 0.33 | 0.22 | 0.51 | 0.60 | 0.49 | 0.37 | 0.32 |
| Yb | 2.00 | 1.43 | 3.02 | 2.26 | 1.63 | 3.36 | 3.90 | 3.20 | 2.67 | 2.09 |
| Lu | 0.34 | 0.27 | 0.47 | 0.40 | 0.28 | 0.54 | 0.65 | 0.53 | 0.49 | 0.35 |
| Hf | 3.40 | 2.41 | 2.68 | 2.97 | 2.76 | 3.41 | 2.63 | 3.27 | 3.40 | 3.05 |
| Th | 3.08 | 5.30 | 1.25 | 1.87 | 1.56 | 2.59 | 0.70 | 1.76 | 2.39 | 2.43 |
| U | 1.13 | 1.77 | 0.43 | 0.70 | 0.52 | 0.96 | 0.26 | 0.60 | 0.91 | 0.83 |
| Ta | 0.58 | 0.63 | 0.21 | 0.20 | 0.22 | 0.43 | 0.21 | 0.39 | 0.37 | 0.30 |
| Cs | 1.73 | 0.34 | 1.18 | 0.07 | 0.05 | 0.12 | 0.01 | 0.83 | 0.64 | 0.25 |
| Ce/Yb | 12.3 | 19.7 | 7.6 | 9.8 | 12.3 | 9.4 | 4.4 | 7.8 | 9.9 | 11.4 |
| Ba/La | 94.1 | 64.2 | 13.3 | 21.5 | 8.5 | 51.0 | 9.6 | 53.5 | 66.0 | 64.4 |
| La/Th | 4.1 | 3.1 | 9.2 | 5.9 | 6.8 | 7.1 | 10.5 | 7.1 | 6.0 | 5.9 |
| La/Nb | 2.3 | 2.6 | 3.4 | 3.8 | 3.1 | 2.5 | 1.9 | 1.8 | 2.7 | 3.0 |
| Ba/Nb | 218.8 | 168.0 | 45.6 | 81.0 | 26.2 | 129.8 | 18.3 | 95.3 | 175.4 | 194.8 |
| Zr/Y | 6.4 | 6.7 | 3.6 | 5.5 | 8.0 | 3.8 | 2.4 | 4.1 | 5.3 | 6.0 |
| Normalized Values | | | | | | | | | | |
| La/Yb | 4.2 | 7.6 | 2.5 | 3.2 | 4.3 | 3.6 | 1.2 | 2.6 | 3.5 | 4.5 |
| La/Sm | 2.8 | 4.8 | 1.5 | 2.2 | 3.0 | 2.2 | 1.1 | 1.7 | 2.8 | 2.9 |

Table 4.2b - Geochemical data for the Harrison Lake Formation.

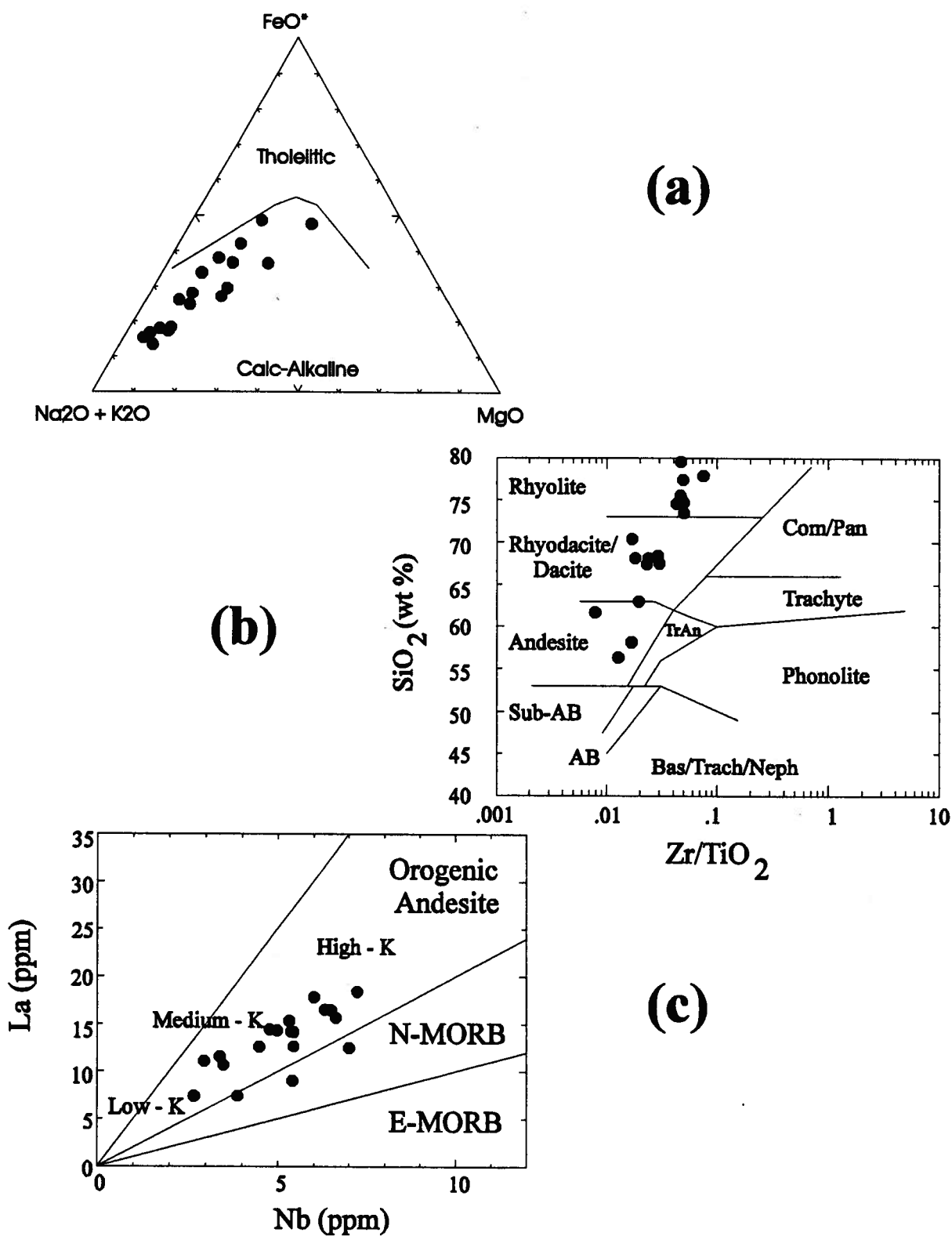


Figure 4.7 - a) AFM (FeO-Na₂O+K₂O-MgO) diagram illustrating strong calcalkaline affinity for Weaver Lake Member volcanic rocks. From Irvine and Baragar (1971); b) Zr/TiO₂ vs. SiO₂ compositional diagram for Weaver Lake Member volcanic rocks, showing a compositional range from basaltic andesite to rhyolite. From Winchester and Floyd (1977); c) Nb vs. La trace element diagram for Weaver Lake Member volcanic rocks, demonstrating medium- to high-K calcalkaline affinity of rocks. From Gill (1981).

post-depositional mobilization of K, Rb, and Ba (Fig. 4.8a); thus interpretations based on these elements should be used with caution. Although mobility of K, Rb, Ba, and to a lesser extent, Ca, Na, and Mn is indicated on Harker diagrams (Fig. 4.8a), linear to curvilinear trends in Al, Fe, Mg, Ti, V, and P_2O_5 against SiO_2 (Fig. 4.8b) suggest that at least part of the original volcanic fractionation trends has been preserved.

Evidence of elemental mobility casts doubt on analysis of any mobile constituent, including SiO_2 , and it is therefore necessary to examine relatively immobile components to assess fractionation trends. Investigations of hydrothermal alteration of volcanic rocks demonstrate that Al, Ti, the high field strength elements (HFSE; especially Zr, Y, Nb), and generally the REE are immobile, and are therefore useful in monitoring fractionation trends (MacLean and Barrett, 1993; Barrett and MacLean, 1993). However, examination of incompatible-compatible element pairs (Zr/SiO_2 , Zr/Al_2O_3 , Zr/TiO_2 , Y/SiO_2) in the Harrison Lake Formation indicate nonuniform behavior of some of HFSE (Zr, Y, Nb), suggesting that these elements behaved compatibly in the more felsic end of the compositional range. It is important to note that this compatible behavior is not a function of alteration, but is common in calcalkaline systems (MacLean and Barrett, 1993). It is therefore necessary to use immobile compatible elements (Al, Ti, Sc, V, and Cr) to monitor the evolution of the Harrison Lake Formation rock series. The immobile compatible element pair TiO_2/Al_2O_3 yields a well-defined linear trend consistent with a smooth fractionation sequence with minimal alteration effects (Fig. 4.9a). The two high Al data points are plagioclase-phyric samples. Three felsic samples plot off the fractionation trend along a linear trend through the origin, indicating alteration of these samples (292JBM93, 292JBM93, 306JBM93; MacLean and Barrett, 1993). The fractionation trend defined by the majority of the samples is supported by the linear relationship between TiO_2 and SiO_2 , a relationship that also suggests minimal mobility of SiO_2 (Fig. 4.9b). Significant gain or loss of silica would pull the data points away from their unaltered precursor composition on the fractionation trend, along lines oriented toward a point at 100 wt % SiO_2 and 0 wt % TiO_2 , reflecting enrichment or depletion of TiO_2 relative to SiO_2 . Note that the three samples displaying alteration on the TiO_2/Al_2O_3 diagram also show a similar deviation from the TiO_2/SiO_2 trend, that is consistent with silica mobility in these samples.

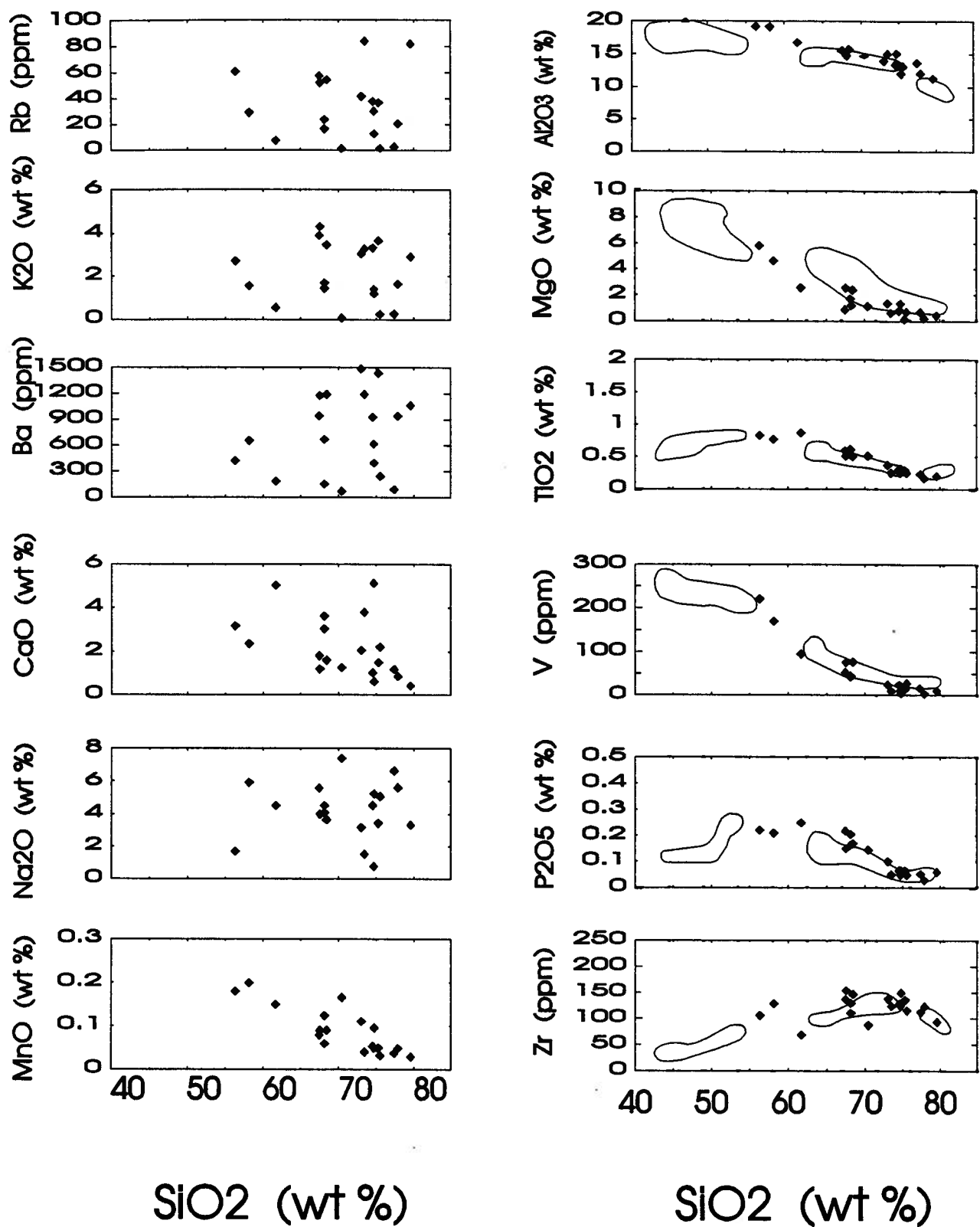


Figure 4.8 - a) Major and minor element Harker variation diagrams for Weaver Lake Member volcanic rocks, illustrating elemental scatter; b) Minor and trace element Harker variation diagrams for Weaver Lake Member volcanic rocks. Linear trends indicate a lack of elemental remobilization and suggest a genetic relationship between samples. Enclosed fields represent samples from the Seneca area.

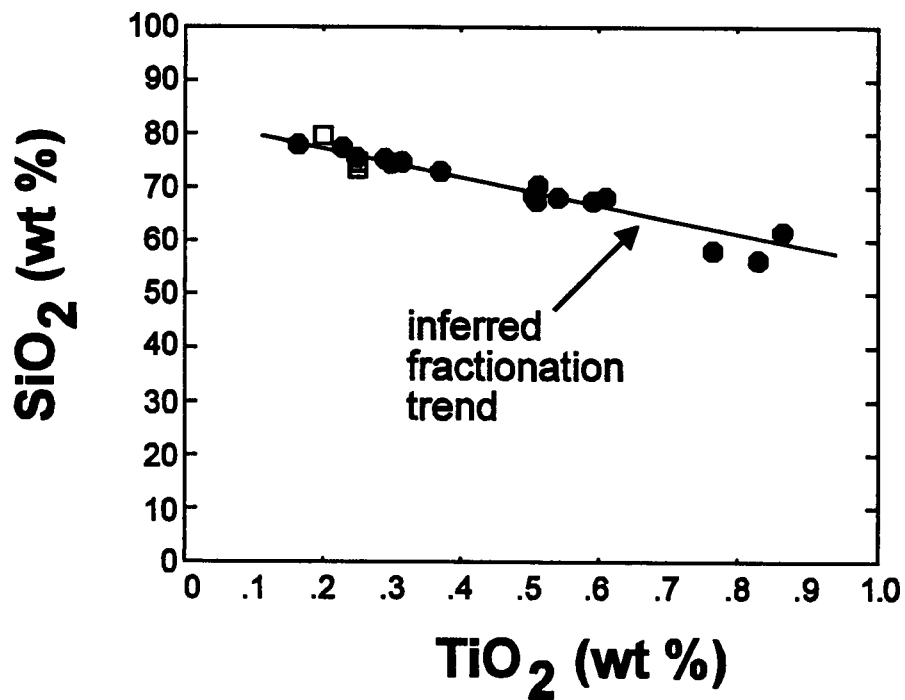
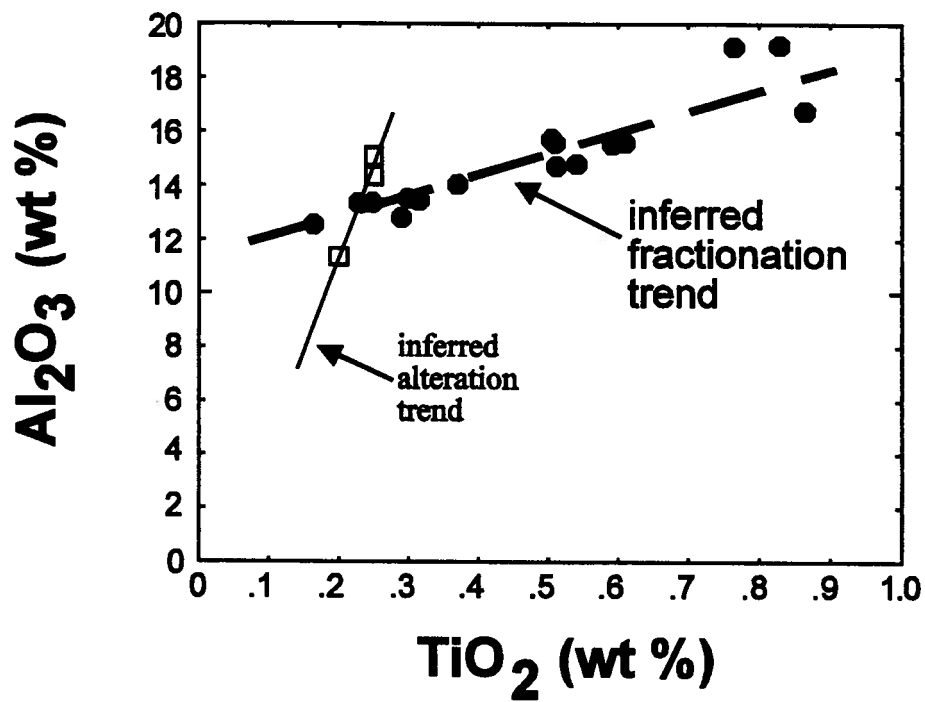


Figure 4.9 - a) TiO_2 vs. Al_2O_3 immobile compatible element diagram. Note well-defined linear fractionation trend. Altered samples (open boxes) plot on linear array trending toward origin; b) TiO_2 vs. SiO_2 diagram. Note linear fractionation trend, and slight displacement of altered samples.

Linear arrays of Al_2O_3 , MgO , TiO_2 , V and P_2O_5 on Harker diagrams are consistent with a simple fractionation trend within volcanic rocks of the Weaver Lake Member. Several of the patterns are characterized by an inflection point between 59-63 wt % SiO_2 , which is inferred to represent the cessation of crystallization of ferromagnesian phases, and the onset of felsic mineral crystallization. Data from the Seneca area partially overlap the fractionation trends suggested by the regional data set. The Seneca data appear to outline distinct mafic and felsic subgroups, with a compositional gap between 53-66 wt % SiO_2 . The compositional groupings in the Seneca area could be used to infer a bimodal distribution of the volcanic rocks of the Weaver Lake Member. However, the entire sample set in the Seneca area is derived from less than 400 m of strata within a 6 km² area, so caution is necessary in deriving regional implications from such an areally and stratigraphically limited data set. Further sampling is required to determine if these subgroups are regionally consistent.

Trace element values for the Weaver Lake Member on the Hf-Th-Ta tectonic discrimination diagram of Wood (1980) indicate the suite is of calcalkaline affinity, and was developed within a destructive plate margin (Fig. 4.10). Incompatible trace element spider diagrams and REE plots are also consistent with a medium K calcalkaline magmatic affinity (Fig. 4.11a,b). The incompatible trace element diagram (Fig. 4.11a) displays an overall enrichment of large ion lithophile (LIL) elements relative to HFSE and the strongly spiked pattern characteristic of subduction-related magmatism (Thompson et al., 1984; Wilson, 1988). Volcanic rocks of the Weaver Lake Member are enriched in low field strength elements (LFSE) relative to primordial mantle values. The irregularity among samples in this portion of the diagram may reflect the mobilization of the LFSE elements suggested by the Harker diagrams (Fig. 4.8a). Weaver Lake Member volcanic rocks are depleted in Nb, Sr, and Ti, and enriched in Zr (Fig. 4.11a). Depletion of Nb and Ti, together with low abundances of Ta and high La/Nb ratios of 1.5-2.0 (Table 4.2), is similar to that of modern calcalkaline systems, and may be the result of partial melting and early fractionation of Ti-bearing phases (Pearce, 1982; Thompson et al., 1984). Early fractionation of Ti-bearing phases is supported by a steady decrease in Ti abundances with increasing silica (Table 1, Fig. 4.9a). The marked depletion of Sr is attributed to plagioclase fractionation, which is also suggested by Eu anomalies in REE plots (Fig. 4.11b).

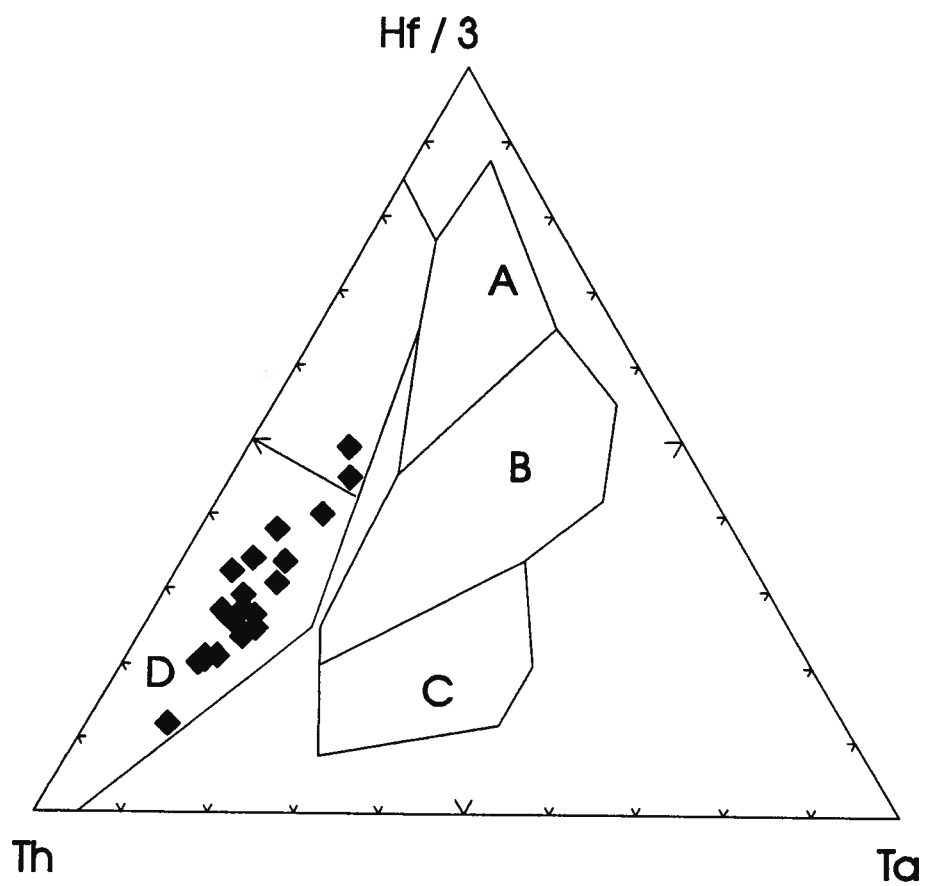


Figure 4.10 - Hf/3-Ta-Th tectonic discrimination diagram for Weaver Lake Member volcanic rocks. Samples plot within destructive plate margin (subduction-related) field (Field D). From Wood (1980). Field A - normal MORB; Field B - enriched MORB; Field C - within plate basalt.

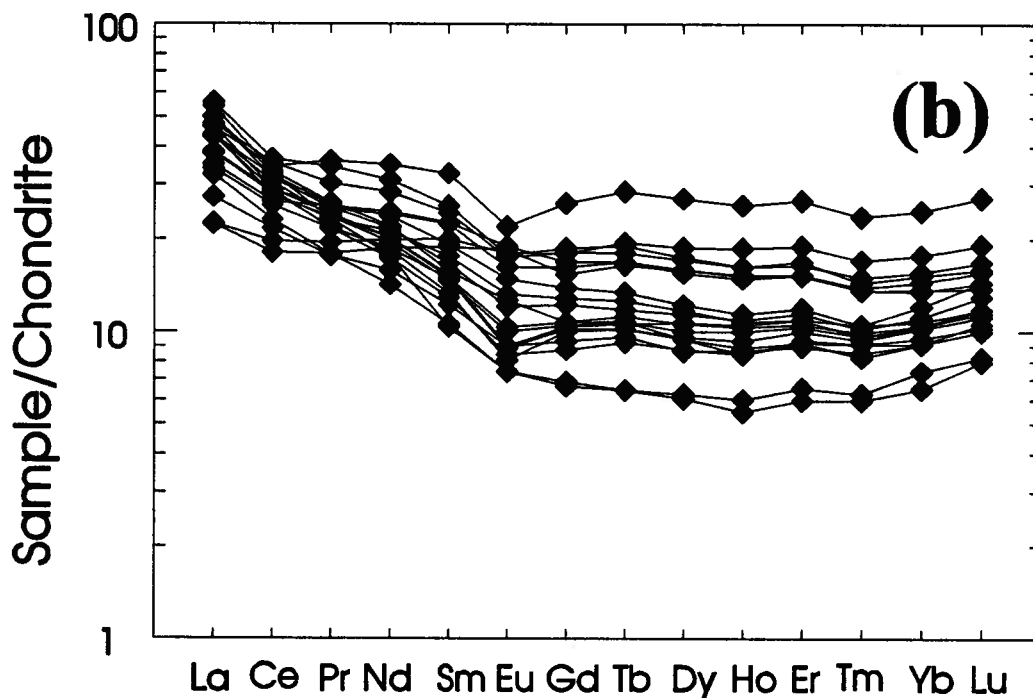
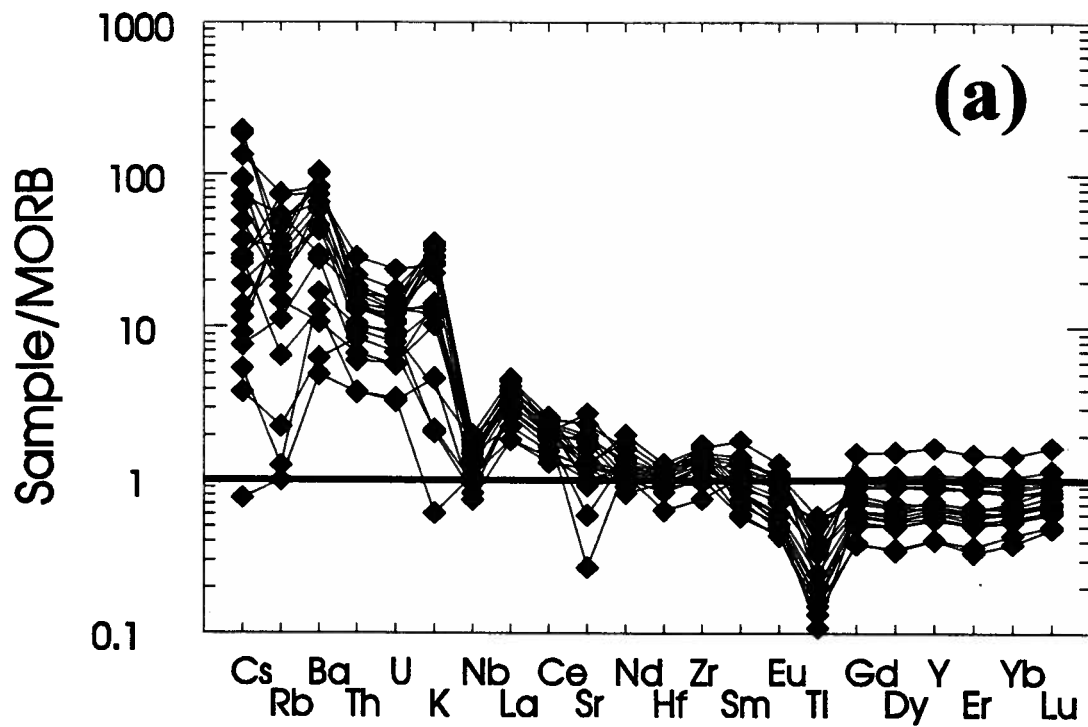


Figure 4.11 - a) extended trace element abundance spider diagram for Weaver Lake Member volcanic rocks. Note scatter in LFSE (Low Field Strength Elements) at left side of diagram, pronounced troughs at Nb, Sr, Ti, and peaks at Zr. Normalized to MORB values, using data from Taylor and McLennan (1985); b) Rare earth element diagram for Weaver Lake Member volcanic rocks. Note LREE enrichment and slight negative Eu anomaly. Normalized to chondritic values, using data from Sun (1982).

Rare earth element plots display LREE enrichment ($\text{La/Yb} = 1.5\text{--}4.25$), characterized by positive La/Sm values ($1.3\text{--}2.25$), slight negative Eu anomalies, and flat to slightly depleted HREE patterns (Fig. 4.11b, Table 1). These patterns are consistent with those of modern medium K calcalkaline suites (Gill, 1981; Wilson, 1988). Total REE values range from 60–115 ppm (Table 4.2), reflecting the slightly enriched character of the suite. One andesitic dike sample (4JBM92) shows an anomalously flat pattern relative to the rest of the suite.

4.8 Nd-Sr ISOTOPIC SYSTEMATICS

Nd and Sr isotopic analyses of a representative suite of Weaver Lake Member volcanic rocks serve to constrain magma source area characteristics, whereas analyses of fine-grained sedimentary rocks from throughout the formation constrain the nature of the sediment provenance (Figs. 4.12, 4.13). Isotopic data are presented in Table 4.3, and isotopic values are plotted on an initial ϵ_{Nd} vs initial $^{87}\text{Sr}/^{86}\text{Sr}$ diagram containing comparative fields and against stratigraphic position (Figs. 4.12, 4.13). Isotopic procedures are detailed in Appendix A.

The Nd and Sr isotopic values of Weaver Lake Member volcanic rocks attest to the juvenile character of the magma source region. The majority of the volcanic rocks have ϵ_{Nd} values of $+4.5\text{--}+6$, and initial $^{87}\text{Sr}/^{86}\text{Sr}$ ratios of 0.7035–0.7050. This restricted range of isotopic values leads to a tight cluster of data points on a ϵ_{Nd} versus $^{87}\text{Sr}/^{86}\text{Sr}$ diagram, and attests to the isotopic homogeneity of an uncontaminated, depleted mantle-derived magma system (Hawkesworth et al, 1993). The ϵ_{Nd} and $^{87}\text{Sr}/^{86}\text{Sr}$ values are only moderately displaced from depleted mantle values (MORB field of figure 4.12), and plot well within the uncontaminated island arc volcanic (IAVu) field. The juvenile isotopic values are consistent with trace element data, particularly the low Ce/Yb (<15) ratios, which have been used to argue for magma derivation from an only slightly enriched mantle wedge (McCulloch and Gamble, 1991; Hawkesworth et al., 1993; Fig. 4.10 and 4.12, Table 4.3). Minor enrichment of the magma source may be attributed to slab-derived elemental flux, subducted sediment, or minor crustal contamination (von Drach et al., 1986). Isotopic values of volcanic

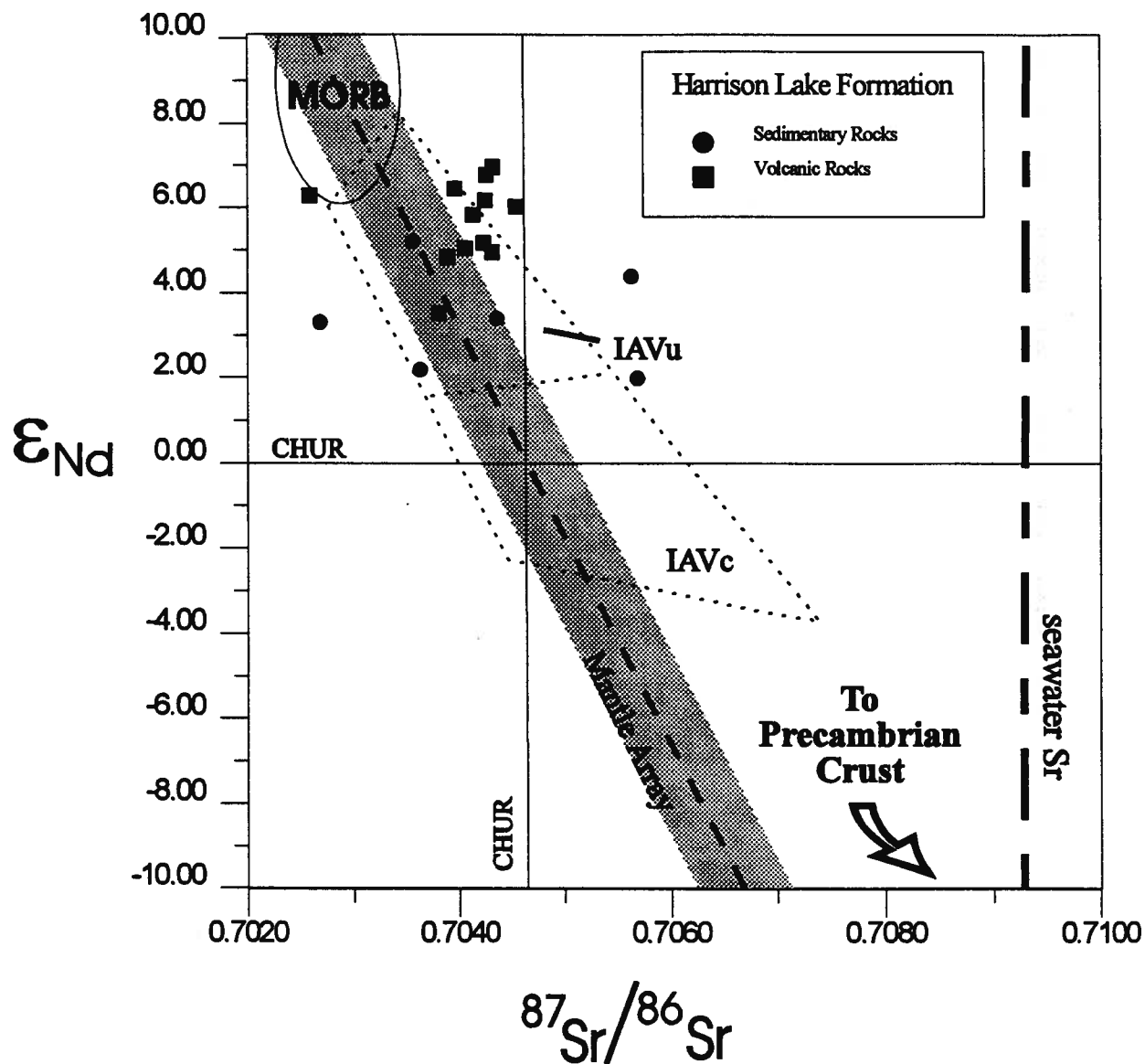


Figure 4.12 - ϵ_{Nd} versus $^{87}\text{Sr}/^{86}\text{Sr}$ for Harrison Lake Formation rocks. Note tight cluster of volcanic rock values (square symbols), and their affinity with uncontaminated volcanic arc field (IAVu). Scatter of sedimentary rock samples (circular symbols) is attributed to detrital mixing of juvenile volcanic detritus and a component of more evolved (continental?) detritus. Samples plotting to left of mantle array suggest local disturbance of Rb/Sr system. IAVc = contaminated island arc volcanic rocks; MORB = mid-ocean ridge basalt; CHUR = Chondritic Uniform Reservoir.

Harrison Lake Formation Isotopic Data Table
Table 4.3

| Map ID | Age | $^{87}\text{Sr}/^{86}\text{Sr}(\text{m})$ | \pm | Rb | Sr | Rb/Sr | $^{87}\text{Rb}/^{86}\text{Sr}$ | $^{87}\text{Sr}/^{86}\text{Sr}(\text{f})$ | Sm | Nd | Sm/Nd | $^{143}\text{Nd}/^{144}\text{Nd}$ | \pm | $\epsilon_{\text{Nd}}(0)$ | $\epsilon_{\text{Nd}}(\text{f})$ | |
|-----------------------------------|-----|---|----------|----|--------|--------|---------------------------------|---|----------|------|-------|-----------------------------------|----------|---------------------------|----------------------------------|------|
| Harrison Lake Formation Sediments | | | | | | | | | | | | | | | | |
| 96JBM92 | 1 | 180 | 0.706820 | 44 | 207.13 | 80.00 | .38 | 1.11 | 0.703975 | 2.66 | 11.51 | 0.1400 | 0.512807 | 0.000008 | 3.30 | 4.60 |
| 102JBM92 | 2 | 180 | 0.706376 | 15 | 231.14 | 23.11 | 0.11 | 0.29 | 0.705636 | 2.37 | 08.96 | 0.1540 | 0.512813 | 0.000011 | 3.41 | 4.40 |
| 124JBM92 | 3 | 175 | 0.707963 | 13 | 135.19 | 82.50 | 0.61 | 1.77 | 0.703569 | 6.35 | 25.86 | 0.1486 | 0.512850 | 0.000007 | 4.14 | 5.21 |
| 129JBM92 | 4 | 180 | 0.706709 | 20 | 456.92 | 54.32 | 0.12 | 0.34 | 0.705829 | 3.64 | 13.17 | 0.1657 | 0.512857 | 0.000004 | 4.27 | 4.99 |
| 131JBM92 | 5 | 180 | 0.706774 | 18 | 319.31 | 46.54 | 0.15 | 0.42 | 0.705695 | 2.78 | 10.54 | 0.1596 | 0.512696 | 0.000018 | 1.13 | 1.98 |
| 136JBM92 | 6 | 180 | 0.706965 | 20 | 174.66 | 78.49 | 0.45 | 1.30 | 0.703637 | 3.25 | 13.64 | 0.1434 | 0.512687 | 0.000007 | 0.96 | 2.18 |
| 143JBM92 | 7 | 180 | 0.719009 | 19 | 39.75 | 100.04 | 2.20 | 6.38 | 0.702689 | 2.51 | 10.57 | 0.1435 | 0.512745 | 0.000007 | 2.09 | 3.31 |
| 288JBM92 | 8 | 175 | 0.706284 | 17 | 228.79 | 61.02 | 0.27 | 0.77 | 0.704364 | 4.25 | 17.92 | 0.1435 | 0.512752 | 0.000005 | 2.22 | 3.41 |
| Harrison Lake Formation Volcanics | | | | | | | | | | | | | | | | |
| 04jbm92 | A | 175 | 0.704426 | 13 | 182.23 | 7.25 | 0.04 | 0.16 | 0.704139 | 3.65 | 12.09 | 0.1849 | 0.512923 | 0.000006 | 5.56 | 5.83 |
| 116jbm92 | B | 175 | 0.705011 | 18 | 268.03 | 25.68 | 0.10 | 0.28 | 0.704321 | 3.81 | 16.22 | 0.1414 | 0.512834 | 0.000004 | 3.82 | 4.96 |
| 142jbm92 | C | 175 | 0.713681 | 26 | 39.75 | 66.77 | 1.68 | 4.86 | 0.701588 | 3.76 | 16.00 | 0.1419 | 0.512824 | 0.000004 | 3.63 | 4.85 |
| 151jbm92 | D | 175 | 0.705164 | 13 | 168.71 | 14.45 | 0.09 | 0.25 | 0.704547 | 6.25 | 23.82 | 0.1590 | 0.512904 | 0.000009 | 5.19 | 6.03 |
| 287jbm92 | E | 175 | 0.705057 | 11 | 317.53 | 35.93 | 0.11 | 0.33 | 0.704241 | 3.46 | 15.03 | 0.1399 | 0.512838 | 0.000009 | 3.90 | 5.17 |
| 291jbm92 | F | 175 | 0.706683 | 10 | 122.09 | 48.62 | 0.40 | 1.15 | 0.703816 | 5.65 | 18.95 | 0.1801 | 0.512800 | 0.000011 | 3.16 | 3.53 |
| 307jbm92 | G | 175 | 0.704190 | 26 | 78.31 | 17.38 | 0.22 | 0.64 | 0.702592 | 4.60 | 16.98 | 0.1626 | 0.512921 | 0.000011 | 5.52 | 6.28 |
| 13jbm93 | H | 175 | 0.704005 | 17 | 218.06 | 1.16 | 0.01 | 0.02 | 0.703967 | 2.98 | 13.03 | 0.1387 | 0.512915 | 0.000005 | 5.40 | 6.70 |
| 14jbm93 | I | 175 | 0.704422 | 16 | 201.19 | 2.68 | 0.01 | 0.04 | 0.704326 | 2.18 | 10.35 | 0.1274 | 0.512916 | 0.000010 | 5.42 | 6.97 |
| 15jbm93 | J | 175 | 0.706820 | 49 | 151.42 | 57.97 | 0.38 | 1.11 | 0.704064 | 5.50 | 20.44 | 0.1627 | 0.512858 | 0.000013 | 4.29 | 5.05 |
| 17jbm93 | K | 175 | 0.704325 | 21 | 115.08 | 0.92 | 0.01 | 0.02 | 0.704268 | 4.12 | 13.95 | 0.1786 | 0.512932 | 0.000006 | 5.74 | 6.14 |
| 21jbm93 | L | 175 | 0.704464 | 17 | 323.94 | 25.32 | 0.08 | 0.23 | 0.703901 | 4.42 | 17.22 | 0.1552 | 0.512839 | 0.000009 | 3.92 | 4.85 |
| 22jbm93 | M | 175 | 0.705464 | 19 | 136.92 | 22.96 | 0.17 | 0.49 | 0.704256 | 3.18 | 14.42 | 0.1332 | 0.512822 | 0.000003 | 4.76 | 6.18 |
| 25jbm93 | N | 175 | 0.705628 | 19 | 153.91 | 38.98 | 0.25 | 0.73 | 0.703805 | 3.13 | 14.94 | 0.1267 | 0.512889 | 0.000008 | 4.90 | 6.46 |

Table 4.3 - Isotopic data for the Harrison Lake Formation.

rocks from the Harrison Lake Formation overlap those reported by Friedman et al. (1994) for Mesozoic plutons in the southern Coast belt. The volcanic rocks have a similar range of ϵ_{Nd} , but display more radiogenic $^{87}\text{Sr}/^{86}\text{Sr}$, which is interpreted to be the result of seawater alteration. One volcanic sample (307JBM92) has a very low initial $^{87}\text{Sr}/^{86}\text{Sr}$ (~ 0.7026), and plots significantly to the right of the mantle array. This sample also has an anomalously low Rb concentration, which may indicate post-depositional disturbance of the Rb/Sr system.

Nd and Sr isotopic values for fine-grained sedimentary rocks of the Harrison Lake Formation are widely distributed, but generally plot within the IAV field (Fig. 4.12). The isotopic values of the sedimentary rocks are displaced from those of volcanic rocks, and are characterized by a broader range of $^{87}\text{Sr}/^{86}\text{Sr}$ and overall lower ϵ_{Nd} values. The shift to more radiogenic $^{87}\text{Sr}/^{86}\text{Sr}$ and lower ϵ_{Nd} may reflect variable degrees of isotopic mixing between volcanic detritus and intrabasinal authigenic sediment or perhaps an extrabasinal evolved component. The lack of identifiable pelagic or carbonate sediment in the Harrison Lake Formation suggests an influx of extrabasinal evolved detritus is most probable. Low values of $^{87}\text{Sr}/^{86}\text{Sr}$ are interpreted to result from disturbance of the Rb/Sr isotopic system.

A plot of isotopic values against stratigraphic position suggests a temporal control on the distribution of isotopic values, particularly ϵ_{Nd} (Fig. 4.13). The most evolved ϵ_{Nd} values occur in fine-grained marine sediments of the Francis Lake Member. There is a significant shift in ϵ_{Nd} values within the member, from approximately $+4.5$ to about $+2$ in the Late Toarcian. This shift occurs during a time of high volcanoclastic influx into the basin (average ϵ_{Nd} values $+4.5$ – $+6$), and thus requires addition of isotopically evolved detritus to account for the lowering of ϵ_{Nd} values. This influx of an evolved component was brief, however, because by the mid-Aalenian, both sedimentary and volcanic rocks again display juvenile values ($\epsilon_{\text{Nd}} = +4.5$ – $+6$) characteristic of the middle Jurassic arc (Fig. 4.13). The upper portion of the formation is isotopically heterogeneous compared to the majority of the formation. This increase in heterogeneity may have been the result increased rhyolitic volcanism coupled with the contamination evident in the U-Pb systematics.

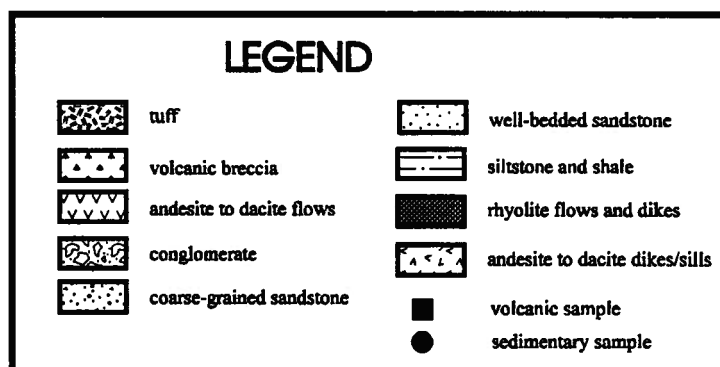
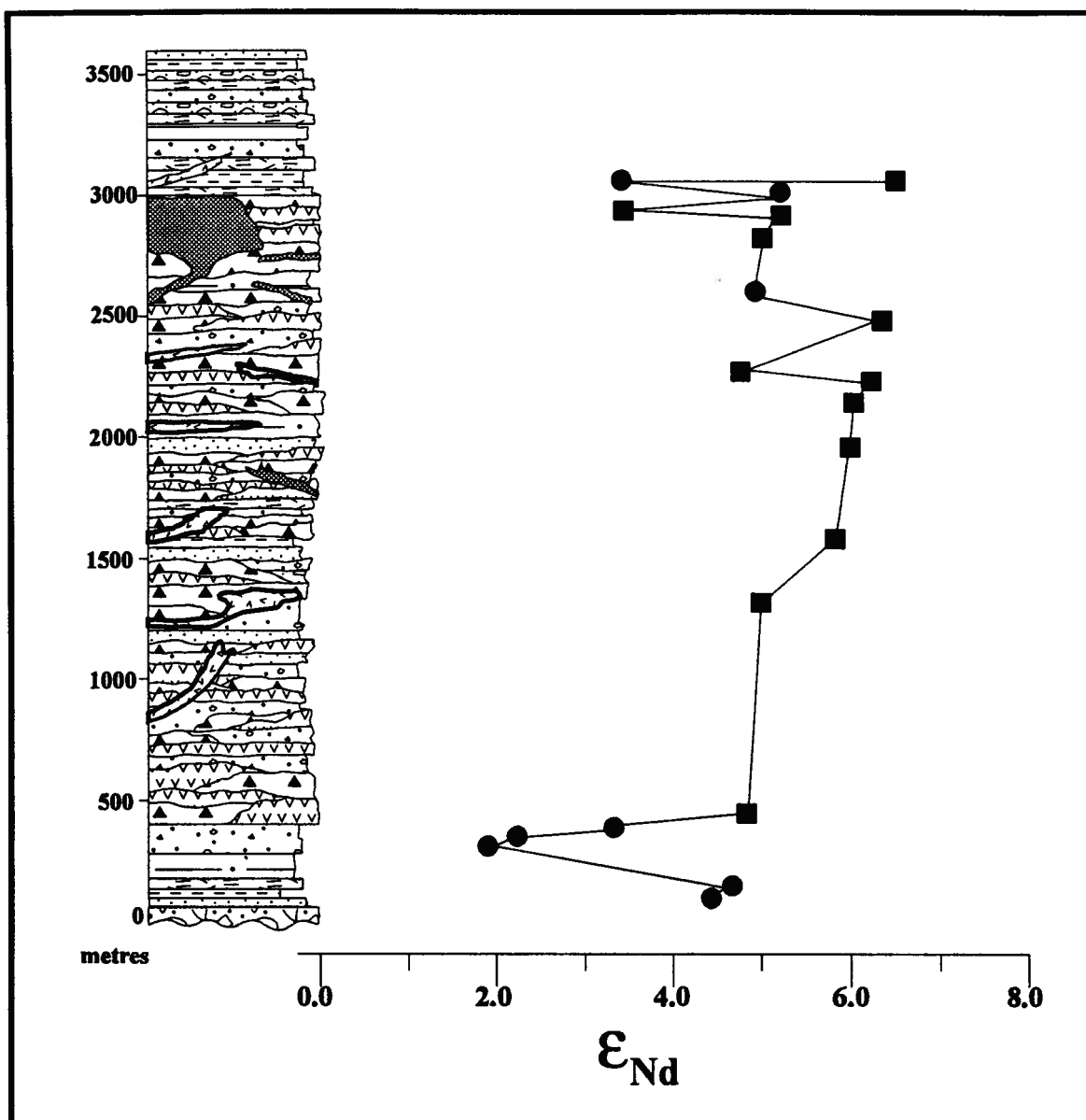


Figure 4.13 - Plot of ϵ_{Nd} values against estimated stratigraphic position for Harrison Lake Formation. Note distinct peak to less juvenile values in Upper Toarcian strata of the Francis Lake Member.

4.9 ALTERATION

The Harrison Lake Formation displays a low-grade alteration assemblage dominated by minerals of the prehnite-pumpellyite facies. Alteration assemblages include, in decreasing order of abundance, calcite, epidote, hematite, zeolites, quartz, and rarely albite. Alteration varies nonsystematically with geographic location and stratigraphic position throughout the outcrop belt. Silicification of volcanic rocks is common. Contact metamorphism adjacent to Middle Jurassic intrusive bodies northwest of Mt. Klaudt and along the western margin of the formation is limited to thin aureoles of hornblende hornfels, silicification and pyritization, suggesting that these intrusions were not responsible for regional alteration. Syndepositional alteration is suggested by the incorporation of silicified lithic clasts in tuff breccia with unaltered lapilli tuff matrix, and by altered lava flows and volcanic breccias cut by unaltered comagmatic dikes. Localized alteration and the presence of relatively unaltered subvolcanic Triassic basement rocks implies the possibility of a structural control focusing the flow of alteration fluids.

4.10 MINERALIZATION

The Harrison Lake Formation hosts Kuroko-style stratiform massive sulfide bodies, as well as stockwork and vein mineralization in the Seneca Zn-Cu-Pb mineralized area in the southwestern portion of the outcrop belt (Urabe, 1983; Fig. 4.2). Host rocks consist of andesite and dacite lava and volcanic breccia, volcanoclastic sedimentary rocks, and abundant synvolcanic dikes and sills of andesitic to rhyolitic composition. Alteration of the host rocks is minor, and generally consists of minor silicification and sericitization; primary volcanic and sedimentologic textures are well preserved. Adjacent to mineralized zones alteration is more intense, and consists of moderate to intense silicification and sericitization and lesser epidote -calcite alteration. McKinley et al. (1994) describe three types of mineralization in the area: 1) semi-massive to massive sulfide bodies, consisting of stratiform lenses of sphalerite, pyrite, and chalcopyrite with lesser galena hosted by fragmental volcanic rocks; 2) semi-massive and disseminated sulfides and barite

associated with altered dacitic epiclastic conglomerate; and 3) stockwork and stringer quartz-sulfide mineralization consisting of veins of sphalerite, pyrite, and chalcopyrite in altered dacite lava.

Stratabound mineralization in the Seneca district is interpreted to be preferentially located near the contact between the Weaver Lake and Echo Island Members of the Harrison Lake Formation. This interpretation is based on: 1) the close spatial relation between stockwork mineralization and rhyolite and quartz feldspar porphyry intrusions; 2) the abundance of sedimentary rocks in the Seneca area; coupled with the presence of the Weaver Lake/Echo Island Member contact to the southeast (Fig. 4.2); and 3) the regional concentration of disseminated sulfide mineralization in the upper portions of the Weaver Lake Member, particularly in the area near Mt. McRae. Dating of the felsic flows and sills in the Seneca area is needed to confirm this interpretation.

4.11 EVOLUTION OF HARRISON LAKE FORMATION

Accumulation of the Harrison Lake Formation is interpreted to have begun in the Early Toarcian with deposition of conglomerate of the Celia Cove Member. The only age control on the Celia Cove Member is its stratigraphic position, unconformably above Middle Triassic rocks of the Camp Cove Formation, and conformably below late Early Toarcian shale of the Francis Lake Member (Arthur, 1987; Arthur et al., 1993). However, the gradational contact between the Celia Cove and Francis Lake members, together with similarities in provenance and style of sedimentation, suggest the Celia Cove Member is roughly coeval with, or only slightly older than, the Early Toarcian Francis Lake Member.

The basal conglomerate of the Celia Cove Member contains angular clasts of chert, argillite, and greenstone derived from immediately subjacent lithologies of the Camp Cove Formation. The sharpness of the contact, angularity of the clasts, local clast derivation, and matrix supported nature of the conglomerate argues for limited transport distance and rapid deposition in a tectonically active environment. The basal conglomerate grades upward into a more polymict conglomerate containing well-rounded clasts of andesite

porphyry, dacite porphyry, chert, volcanic lithic arenite, and rare well-rounded bioclastic limestone clasts. The heterogeneity of the clasts, higher degree of rounding, the better sorting and stratification, and the higher proportion of sandstone interbeds in the upper portion of the Celia Cove Member suggest derivation from a more distal heterolithic source area. The lack of sedimentary structures indicative of traction currents, matrix supported nature of the conglomerate, and the cyclic depositional pattern indicate deposition by a migrating distributary system in a marine environment below effective wave base, probably in the mid- to lower fan region of a submarine fan complex (Walker, 1978).

Coarse clastic rocks of the Celia Cove Member grade upward into sandstone, siltstone and argillite of the Francis Lake Member, culminating in a 15-20 m thick ammonite-bearing argillite succession that caps the fining upward sequence. The fining upward sequence is gradationally overlain by crystal tuff, lapilli tuff, and coarse lithic wacke (Fig. 4.3). The identification of primary pyroclastic deposits in the Francis Lake Member has important implications for the timing and mode of the initiation of volcanism in the Harrison Lake Formation. The transition from fine-grained siltstone and mudstone in the lower portion of the Francis Lake Member to medium to coarse grained lithic wacke, crystal vitric tuff and lapilli tuff interbedded with siltstone and mudstone in the upper portion of the member is critical, as it marks the initiation of volcanism in the Harrison Lake Formation. Age constraints provided by the documentation of the ammonite genera *Dactyloceras* and *Hildaites* in the lower Francis Lake Member indicate that explosive volcanism began in the Harrison Lake Formation by at least the late Early Toarcian (ca. 185 Ma). The increasing proportion of tuffaceous lithic feldspathic wacke, crystal tuff and lapilli tuff in the upper portions of the Francis Lake Member suggest that the frequency and intensity of pyroclastic activity increased throughout the Toarcian and Early Aalenian, perhaps related to an increased proximity to a developing volcanic edifice.

Nd and Sr isotopic analyses of fine-grained sediments and volcanic rocks within the Harrison Lake Formation suggest variation in provenance, from an essentially juvenile ($\epsilon_{Nd} = +4.5$ to $+5$) source in the Celia Cove and lower portions of the Francis Lake Members, to a slightly evolved ($\epsilon_{Nd} = +2$ to $+3.3$) signature in the upper portion of the Francis Lake Member, then back to a distinctly juvenile ($\epsilon_{Nd} = +4.5$ to $+6$)

composition in the majority of the formation (Fig. 4.13). The shift to slightly more evolved Nd values is inferred to record the influx of an evolved component (continental detritus?) into the basin in the Late Toarcian, prior to the main phase of effusive volcanism in the Harrison Lake Formation.

A change in eruptive style is indicated by the transition from pyroclastic and epiclastic rocks of the Francis Lake Member to lava flows and tuff breccias of the Weaver Lake Member in the mid-Aalenian. In the Weaver Lake Member, the cyclic interbedding of epiclastic and resedimented pyroclastic debris with primary flows and volcanic breccias records intermittent volcanic activity alternating with clastic reworking of pyroclastic detritus and older volcanic deposits. The presence of hyaloclastite, mass sediment gravity flows, air fall or waterlain tuffs, peperitic textures and "fire fountain" facies in drill core (McKinley et al., 1994), and the abundance of fine-grained, parallel laminated siltstone and mudstone suggest the Weaver Lake Member was deposited in a subaqueous setting, below effective wave base. However, the presence of well-rounded polymict conglomerate and channels indicates initial subaerial fluvial reworking, and local trough cross-bedding, bioclastic debris (Pearson, 1973), and abundant comminuted wood debris at the base of mass sediment gravity flows suggests shallow water reworking proximal to a landmass. Vent proximity is indicated by volcanic agglomerate, thick volcanic breccias and tuff breccias interpreted as debris flows, and the abundance of sills and dikes.

There is a general compositional trend evident in primary volcanic rocks of the Weaver Lake Member. Flows in the lower portion of the Weaver Lake Member are basaltic andesite and andesite, and there is an overall increase in silica content upward. The majority of the member is dacitic in composition, whereas the upper portion of the member becomes distinctly rhyolitic, typified by the rhyolite dome complex on Echo Island and the abundant felsic flows, dikes, and sills in the Seneca area (McKinley et al., 1994). Kuroko-type massive sulfide deposits in the Seneca area are associated with felsic volcanics, and are therefore interpreted to be stratigraphically located near the Weaver Lake/Echo Island Member contact.

The transition from flows and breccias in the Weaver Lake Member to well-stratified pyroclastic and resedimented pyroclastic debris in the Echo Island Member records the gradual cessation of effusive volcanism and onset of pyroclastic activity. The Echo Island Member is characterized by background sedimentation consisting of thin to medium bedded lithic wacke, tuffaceous siltstone and mudstone that is episodically interrupted by thick-bedded to massive lapilli tuffs, tuffs, and mass sediment gravity flows of resedimented pyroclastic debris. These episodic influxes are interpreted to represent pyroclastic eruptions that flood the depositional basin with fresh juvenile volcanic debris. These periodic clastic inundations lead to rapid aggradation of resedimented pyroclastic debris, which apparently caused dramatic shallowing of the basin, resulting in the reworking of upper portions of mass sediment gravity flows and progradation of conglomeratic channels.

The top of the Echo Island Member is interpreted to be an angular unconformity with the overlying Mysterious Creek Formation. Evidence of post-Early Bathonian, pre-Early Callovian deformation of the Harrison Lake Formation includes variable bedding attitudes, mesoscale folds, and locally overturned strata that are absent in the overlying Mysterious Creek Formation (Fig. 4.2).

4.12 MODEL FOR VOLCANIC ARC DEVELOPMENT

The stratigraphic evolution of the Harrison Lake Formation conforms to a simple model of oceanic arc development as proposed by Larue et al. (1991). The evolution from a basal locally derived conglomerate of the Celia Cove Member into fine-grained, deep water facies and overlying tuffaceous clastic rocks of the Francis Lake Member, and then into the primary volcanic rocks and associated sedimentary rocks of the Weaver Lake and Echo Island Members mimics that of modern arcs in the Caribbean region (Larue et al., 1991). In the early stages of arc growth, subduction processes may have led to thermal expansion of the overriding plate, resulting in minor compressional deformation and uplift of the Middle Triassic ocean floor represented by the Camp Cove Formation. Continued thermal uplift may have led to block faulting, resulting in deposition of coarse clastic deposits of the basal conglomerate by mass sediment gravity flows, and

suspected rapid subsidence and deposition of the basal Harrison Lake Formation (OADS I stage of Larue et al., 1991).

Early explosive volcanic eruptions mark the initiation of the volcanic sequence in early Late Toarcian time, and attest to shallow water depths or subareal volcanic exposure. Early pyroclastic activity is superseded by effusive volcanism as the arc stabilized (OADS II, Early Arc Growth). Epiclastic conglomerate, wood debris, and sedimentary structures indicate that at least a portion of the arc was subaerial during this stage. The earliest stages of effusive volcanism was basaltic andesite to andesite in composition, superseded by the dacitic volcanism that characterizes the majority of the system. Isotopic and geochemical constraints suggest the arc was a medium K calcalkaline system derived from a slightly enriched mantle wedge. The increase in felsic volcanism in the upper portions of the Weaver Lake Formation led to the emplacement of rhyolitic domes, sills, dikes and associated quartz feldspar porphyry intrusions, and resulted in the increase in pyroclastic activity evident in the Echo Island Member (OADS III, Mature Stage). Volcanism waned in the Early Bathonian, and was followed by approximately north-south directed compressional deformation of the formation. The Early Callovian Mysterious Creek Formation may represent an overlap sequence supplied with detritus by the extinct arc (OADS IV of Larue et al., 1991).

4.13 CONCLUSIONS

It has long been recognized that the Harrison Lake Formation constitutes a Middle Jurassic volcanic arc assemblage (Crickmay, 1925; Thompson, 1972; Pearson, 1973; Arthur, 1987; Arthur et al., 1993), but details about the evolution of the arc system have been lacking. New data presented herein serve to constrain the stratigraphy, age, geochemistry, isotopic systematics and depositional history of the Harrison Lake Formation. Important new constraints include:

1. New biostratigraphic data from tuffaceous strata of the Francis Lake Member indicate volcanism in the Harrison Lake Formation began in the late Early Toarcian.

2. New U-Pb geochronology from a rhyolitic dome in the upper portion of the Weaver Lake Member indicate that late, rhyolitic volcanism was active at 166 Ma (earliest Bathonian). Isotopic dates from the upper Weaver Lake Member overlap with the ages of both synvolcanic intrusions within the formation and large batholithic complexes that intrude the formation on the west (Fig. 4.2).

3. Stratigraphic constraints demonstrate the eruptive style of the volcanic arc progressed from explosive (early Late Toarcian to mid-Aalenian) to dominantly effusive (mid-Aalenian to Late Bajocian) and back to explosive (Late Bajocian to Bathonian?).

4. Geochemical data indicate that the volcanic arc is of medium to high K calcalkaline affinity, is LREE enriched ($La/Yb = 1.5-4.25$), and displays overall enrichment of LFSE relative to HFSE, supporting a subduction-related origin. Incompatible-compatible element ratios suggest a simple fractionation trend.

5. Nd and Sr isotopic values for volcanic rocks demonstrate the relatively juvenile nature of the magmatic system, and support magmatic derivation from a slightly enriched mantle wedge.

6. Stratigraphic fluctuations in ϵ_{Nd} values suggest a temporal control on provenance variations, and indicate two component mixing between volcanic arc-derived material and more evolved (continental?) detritus.

7. Mineralization in the Seneca area is associated with felsic volcanism, and is inferred to be stratigraphically associated with the Weaver Lake/Echo Island member contact. This stratigraphic assessment suggests mineralization is probably Bajocian in age.

8. Regional mapping in the Harrison Lake area suggests the Harrison Lake Formation contains mesoscopic folds and overturned strata that are absent in overlying strata. This structural contrast provides

evidence of post-Early Bathonian, pre-Callovian deformation in the southwestern Coast Belt, consistent with the observations of Arthur (1987).

These observations constrain the timing and geologic evolution of a Middle Jurassic volcanic arc in the southern Coast Belt, and provide a basis for comparison with coeval volcanic sequences on adjacent terranes.

CHAPTER 5

EARLY TO MIDDLE JURASSIC VOLCANISM ON WRANGELLIA: EVOLUTION OF THE BONANZA-HARRISON ARC SYSTEM

5. EARLY TO MIDDLE JURASSIC VOLCANISM ON WRANGELLIA: EVOLUTION OF THE BONANZA-HARRISON ARC SYSTEM

5.1 INTRODUCTION

Several terranes in the southern Canadian Cordillera contain Early to Middle Jurassic volcanic arc assemblages or associated volcanoclastic sedimentary sequences overlying Triassic basement. Correlations between the volcanic assemblages are difficult due to complex internal stratigraphies, differences in underlying Triassic basement, and a lack of detail concerning the evolution of individual arc assemblages. Documentation of the geologic evolution of each assemblage, particularly its geochemical and isotopic characteristics, is necessary prior to evaluating potential correlations.

Wrangellia is the westernmost terrane in the southern Canadian Cordillera, and is separated from the nearest terrane to the east, the Harrison terrane, by Jurassic and Cretaceous plutons of the Coast Plutonic Complex (Fig. 5.1). Wrangellia and Harrison terranes both contain Lower to Middle Jurassic volcanic arc assemblages, but differences in the timing of volcanism and the character of Triassic basement led to separate terrane designations (Monger et al., 1982). Lower to Middle Jurassic stratigraphic linkages between the Bonanza Group and the Bowen Island Group of Wrangellia with the Harrison Lake Formation of the Harrison terrane based on overlapping age ranges have been suggested (Roddick, 1965; Friedman et al., 1990). However, supporting stratigraphic, geochemical and isotopic data have been lacking, and the separate terrane designations remain (Monger and Journeay, 1994). The terranes are linked by bridging Middle Jurassic (<167 Ma; Bathonian) plutons (Friedman and Armstrong, 1994).

This chapter describes the stratigraphy, geochemistry, and isotopic signatures of Lower to Middle Jurassic volcanic arc assemblages of the Bonanza Group, Bowen Island Group and Harrison Lake Formation. Evaluation of the geologic, geochemical, and isotopic characteristics of these units is used to constrain source characteristics and the evolution of the Early to Middle Jurassic Bonanza-Harrison volcanic arc. This

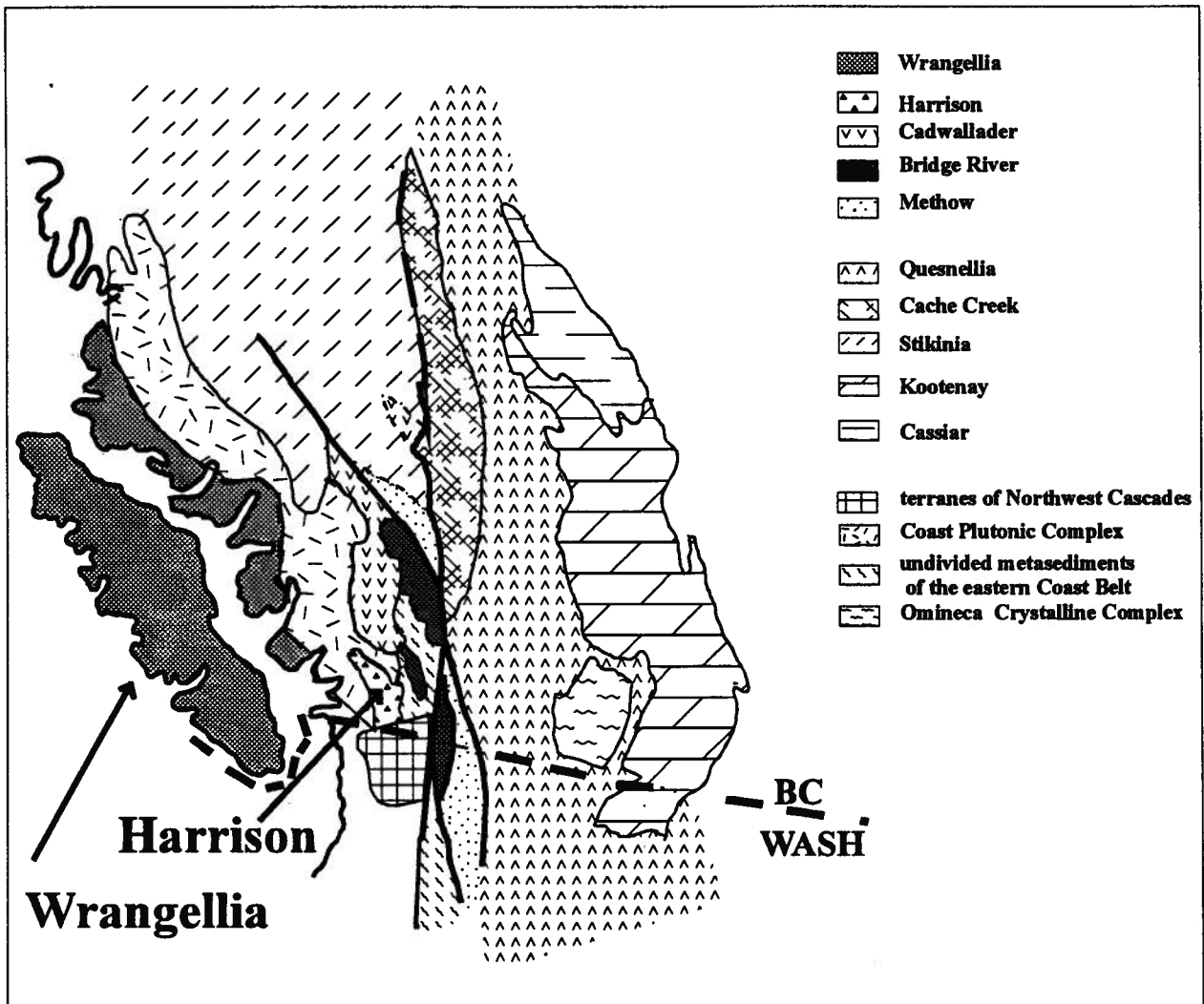


Figure 5.1 - Simplified terrane map of the southern Canadian Cordillera, highlighting Wrangellia and Harrison terranes. Note position of Coast Plutonic Complex.

investigation is the first integrated analysis of the geology, geochemistry, and isotopic characteristics of the Bonanza Group, Bowen Island Group, and the Harrison Lake Formation.

5.2 GEOLOGIC SETTING

Lower to Middle Jurassic strata of the Wrangellia and Harrison terranes form an arcuate band that wraps around the southern end of the Coast Plutonic Complex. The eastern margin of Wrangellia is intruded by Middle to Late Jurassic plutons of the western Coast Plutonic Complex (Nelson, 1979; Monger, 1991a). The southeastern portion of Wrangellia has been imbricated by west vergent compressional deformation associated with both the Late Cretaceous San Juan Thrust System (Brandon et al., 1988) and the Tertiary Cowichan Fold and Thrust system (England and Calon, 1991). Middle Jurassic and, to a lesser extent, Cretaceous plutons incorporate Bowen Island Group strata as roof pendants on the southwestern margin of the Coast Plutonic Complex (Friedman and Armstrong, 1994). Strata of the Bowen Island Group display tight to isoclinal folds and are strongly foliated.

The Harrison terrane is exposed at the southeastern end of the Coast Plutonic Complex (Fig. 5.2). The western margin of the Harrison terrane is intruded by Middle Jurassic plutons (ca. 164-167 Ma); the eastern margin is the Harrison Lake shear zone, a ductile transcurrent fault separating subgreenschist facies rocks of the Harrison terrane from amphibolite facies rocks to the east contained within the imbricate zone of the Coast Belt Thrust System (Journeay and Friedman, 1993). The Coast Belt Thrust System is a west vergent contractional system formed along the eastern edge of the Coast Plutonic Complex in early Late Cretaceous time. Frontal thrust faults at the leading edge of this system displace Jurassic and Early Cretaceous supracrustal rocks and plutonic suites, including Lower to Middle Jurassic volcanic strata of the Harrison terrane (Fig. 5.2). To the east of Harrison Lake and structurally above the Harrison terrane are high-grade metamorphic thrust nappes interleaved within the imbricate zone of the Coast Belt Thrust System (Journeay and Friedman, 1993). These thrust nappes represent metamorphosed supracrustal assemblages derived from the Harrison terrane and terranes to the east. Structurally overlying high grade metamorphic rocks but still

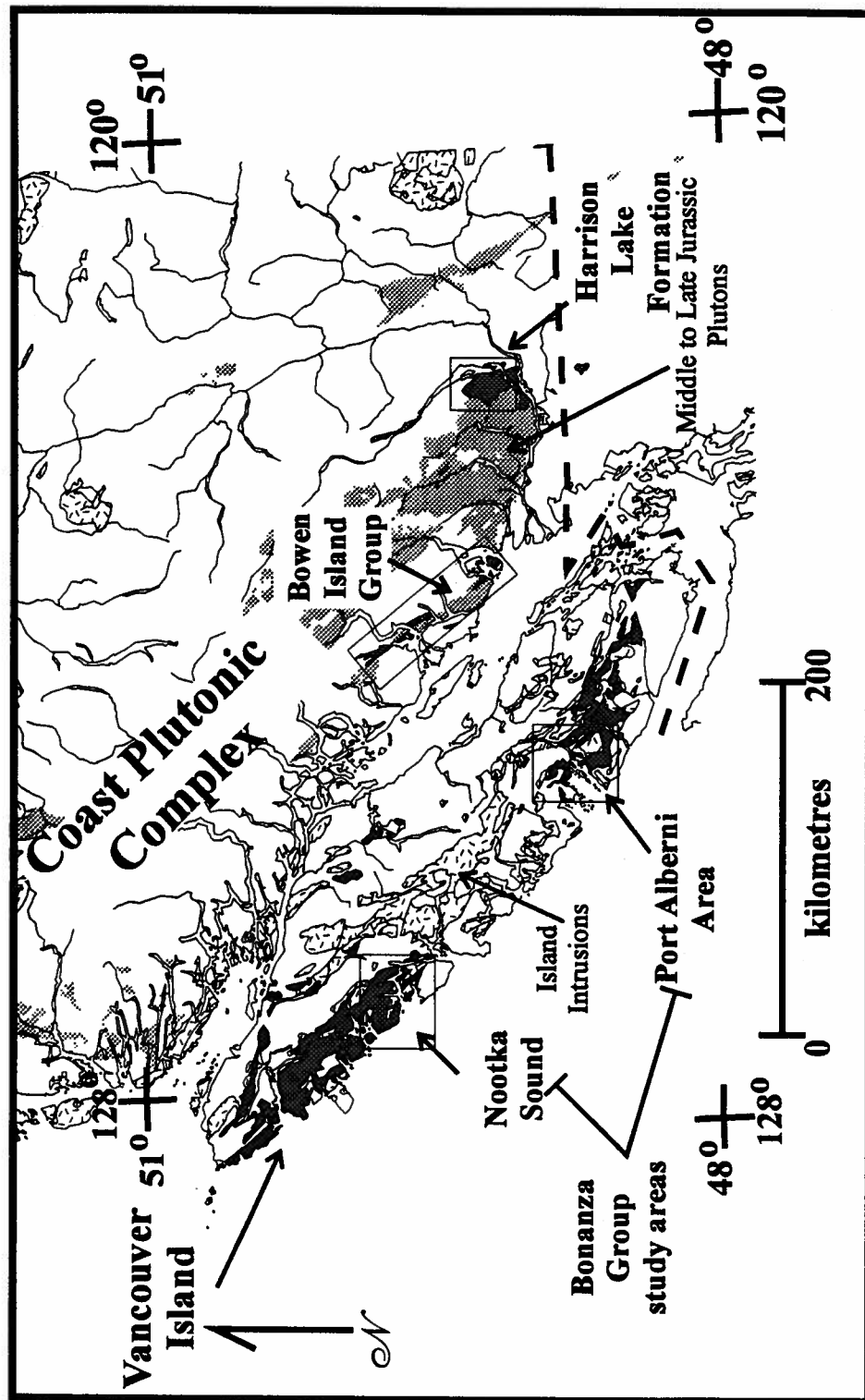


Figure 5.2 - Generalized geologic map of southwestern British Columbia, emphasizing Early to Middle Jurassic volcanic assemblages and Middle to Late Jurassic plutonic assemblages. Study areas are outlined.

within the central Coast Belt Thrust System are Lower and Middle Jurassic volcanic rocks and associated sedimentary rocks correlated with the Harrison terrane (Journey and Mahoney, 1994; Fig. 5.2). These rocks represent the easternmost exposures of the Harrison terrane.

5.3 TERRANE STRATIGRAPHY

Wrangellia is the most distinctive component of the morphogeologic Insular Belt, and extends from the southern end of Vancouver Island north to southeastern Alaska (Fig. 5.1). The terrane is remarkably homogeneous along its length; stratigraphic discussions herein will be limited to rocks exposed on Vancouver Island (Fig. 5.2, 5.3). The terrane consists of arc volcanic rocks and associated sedimentary rocks of the Devonian to Middle Pennsylvanian Sicker Group overlain by crinoidal limestone of the Middle Pennsylvanian to Permian Buttle Lake Group (Muller et al., 1981; Brandon et al., 1986; Monger and Journey, 1992, 1994; Fig. 5.3). Paleozoic rocks are unconformably overlain by the Middle to Upper Triassic Vancouver Group, which contains a basal argillite overlain by the Karmutsen Formation, a thick sequence of tholeiitic basalt that forms the most distinctive component of Wrangellia (Barker et al., 1989). The Karmutsen Formation is gradationally overlain by bioclastic limestone of the Upper Triassic Quatsino Formation, which in turn grades upward into shale, limy mudstone, and tuffaceous wacke and conglomerate of the Upper Triassic Parsons Bay Formation at the top of the Vancouver Group (Muller et al., 1981; Nixon et al., 1993, 1994).

Arc volcanic rocks of the Lower Jurassic Bonanza Group gradationally overlie the Parsons Bay Formation (Muller et al., 1974, 1981; Jeletsky, 1976; Nixon et al., 1993, 1994). The Bonanza Group is interpreted to be cogenetic with Lower to Middle Jurassic plutonic rocks of the Island Intrusions and associated metamorphic and migmatitic rocks of the Westcoast Complex (Debari and Mortensen, 1994). The Bonanza Group is locally unconformably overlain by Middle to Upper Jurassic shallow marine coarse clastic strata of the Kyoquot Group (Muller et al., 1981; Yorath, 1991). Throughout the majority of the outcrop belt, an angular unconformity separates Lower Jurassic strata of the Bonanza Group from coarse sandstone and

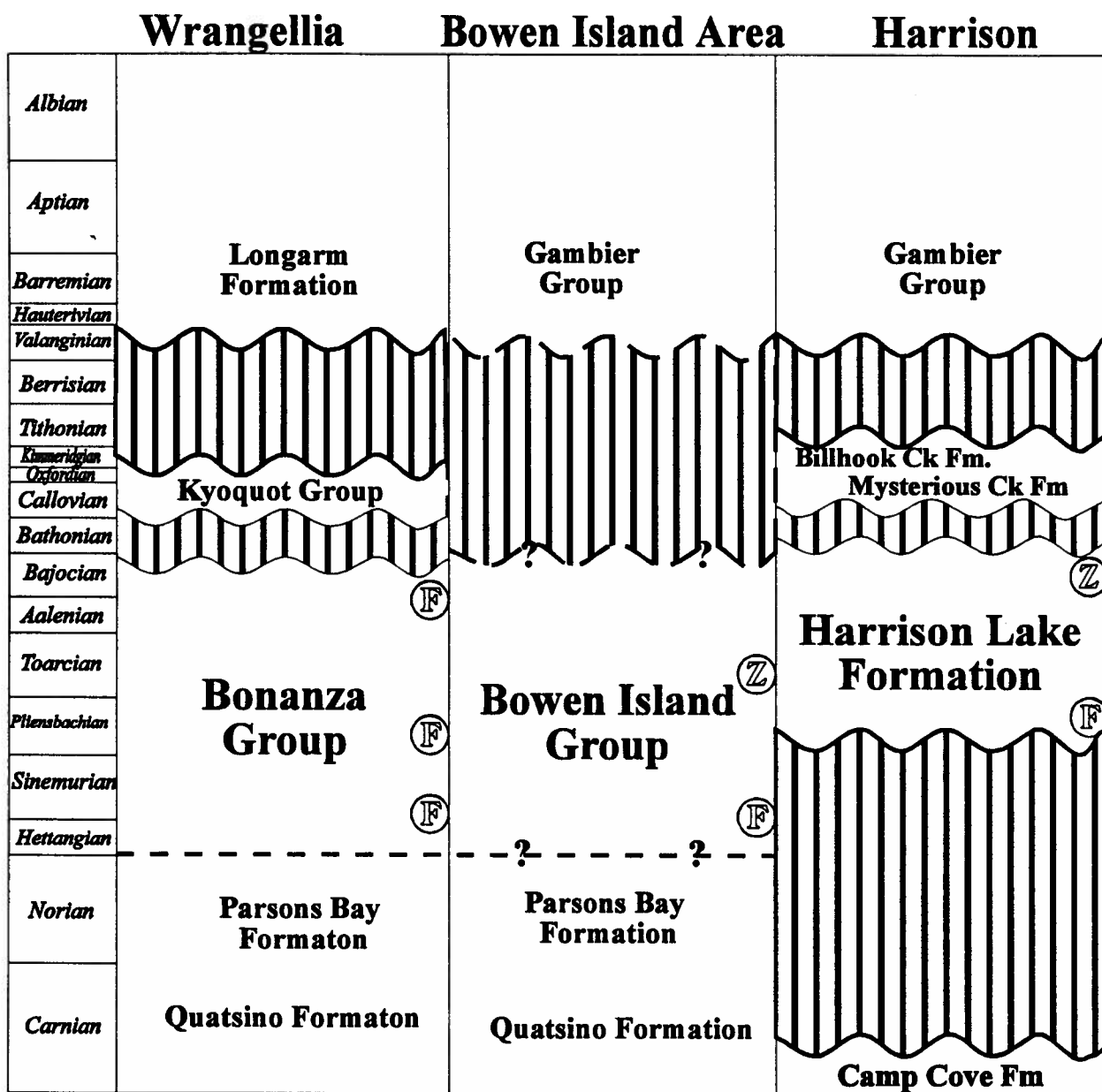


Figure 5.3 - Simplified stratigraphic columns for Wrangellia and Harrison terranes and the Bowen Island area.
 Symbols: F = biostratigraphic control; Z = U-Pb age.

conglomerate of the Lower Cretaceous Longarm Formation and overlying Queen Charlotte Group (Muller et al., 1981; Yorath, 1991; Nixon et al., 1993, 1994).

The Bowen Island Group is exposed in a series of roof pendants within the western margin of the Coast Plutonic Complex along coastal mainland British Columbia (Roddick and Woodsworth, 1979; Journeay and Monger, 1994; Fig. 5.2). The Bowen Island Group was named by Armstrong (1953) for a thick succession of altered volcanic rocks on Bowen Island. Subsequent mapping on the Sechelt Peninsula has documented a stratigraphic contact between the Bowen Island Group and underlying Karmutsen and Quatsino Formation (Monger, 1991, 1993; Journeay and Monger, 1994). Although the name Bowen Island Group remains in the literature (Journeay and Monger, 1994) and will be applied herein to altered volcanic rocks along coastal British Columbia, the stratigraphic relationship between rocks mapped as Bowen Island Group and underlying rocks of the Vancouver Group demonstrates that the Bowen Island Group is directly correlative with the Bonanza Group strata and is therefore part of Wrangellia.

The Bowen Island Group is unconformably overlain by granitoid-bearing conglomerate and volcanic rocks of the Lower Cretaceous Gambier Group (Roddick, 1965; Roddick and Woodsworth, 1979; Lynch, 1991; Journeay and Monger, 1994).

The Harrison terrane consists of oceanic greenstone, chert, and greywacke of the Middle Triassic Camp Cove Formation unconformably overlain by arc volcanic rocks and associated sedimentary rocks of the Lower to Middle Jurassic Harrison Lake Formation (Fig. 5.2; Chapter 4). Shallow marine sandstone and shale of the Middle Jurassic Mysterious Creek Formation unconformably overlie the Harrison Lake Formation, and are in turn overlain by volcanoclastic strata of the Upper Jurassic Billhook Creek Formation (Monger, 1985; Arthur, 1987; Arthur et al., 1993). Granitoid-bearing polymict conglomerate of the Lower Cretaceous Peninsula Formation unconformably overlies Jurassic rocks, and is gradationally overlain by volcanic rocks of the Lower Cretaceous Brokenback Hill Formation (Monger, 1985, Arthur, 1987). These latter two formations are incorporated within the Gambier Group (Journeay and Monger, 1992, 1994)

5.4 LOWER TO MIDDLE JURASSIC VOLCANIC STRATA

The Bonanza Group, Bowen Island Group, and Harrison Lake Formation comprise Lower to Middle Jurassic volcanic arc assemblages and associated volcanoclastic sedimentary rocks. The complicated nature of volcanic facies relationships in arc systems leads to a lack of coherent stratigraphy and an absence of regionally consistent marker beds, making traditional stratigraphic correlations difficult (Cas and Wright, 1987). Middle to Lower Jurassic strata on the Wrangellia and Harrison terranes lack regionally consistent stratigraphy, and are characterized by rapid lateral and vertical facies changes, typical of a volcanic arc origin.

The Bonanza Group comprises basalt, basaltic andesite, andesite, dacite, and rhyolite flows, breccia, tuff breccia and lapilli tuff intercalated with primarily thin to medium bedded tuff, conglomerate, sandstone, siltstone, and argillite (Jeletsky, 1976, Muller et al., 1974, 1981; Nixon et al., 1993, 1994). Fragmental rocks are regionally more abundant than lava flows (Jeletsky, 1976). The base of the Bonanza Group consists of a coarsening upward succession of thin to thick bedded pyroclastic and epiclastic rocks gradationally overlying thin to medium bedded limestone and clastic rocks of the Parsons Bay Formation (Jeletsky, 1976; Muller et al., 1981; Nixon et al., 1993, 1994). Fragmental rocks at the base of the group grade upward into the massive lava flows and breccias that dominate the unit. Nixon et al. (1993) describe a bimodal assemblage of basalt interdigitated with rhyolite on a scale of 100's of metres near the base of the formation on northern Vancouver Island, and suggest flows become intermediate in composition to the east. Descriptions by Muller et al. (1974, 1981) and Jeletsky (1976) indicate extreme lateral and vertical variability in composition and rock type in the Bonanza Group throughout Vancouver Island. Volcanic rocks of the Bonanza Group are locally overlain by up to 600 m of volcanoclastic sedimentary rocks, including conglomerate, tuffaceous sandstone, siltstone, and argillite (Jeletsky, 1976; Muller et al., 1981).

The Bonanza Group includes tuffaceous shale, siltstone, and sandstone of the Lower Jurassic (Sinemurian) Harbledown Formation. The Harbledown Formation is interpreted to be an eastern volcanoclastic

facies distal to the western volcanic edifices represented by the majority of the lower Bonanza Formation (Tipper et al., 1991).

Metamorphic overprint and limited exposure of the Bowen Island Group preclude detailed stratigraphy. The Bowen Island Group is metamorphosed to lower greenschist(?) grade, and consists of massive andesitic flows, tuff breccias and lapilli tuff interbedded with thin bedded tuff, tuffaceous sandstone, siltstone and argillite (Roddick, 1965, Friedman et al., 1990; Monger, 1992). The base of the Bowen Island Group has not been described, but it is mapped in stratigraphic continuity with metabasalt of the Karmutsen Formation and marble of the Quatsino Formation in the northwestern end of the outcrop belt (Monger, 1993; Journeay and Monger, 1994). Thin-bedded tuff and volcanoclastic sedimentary rocks dominate the northwestern end of the outcrop belt, and massive volcanic flows dominate southeastern exposures (Friedman et al., 1990). The Bowen Island Group is apparently unconformably overlain by granitoid bearing conglomerate of the Lower Cretaceous Gambier Group (Roddick and Woodsworth, 1979; Journeay and Monger, 1994), although this contact is commonly faulted (Monger, 1993).

The Harrison Lake Formation consists of basaltic andesite to rhyolite flows, breccias, tuff breccias, lapilli tuff and associated volcanoclastic sedimentary rocks. The formation is subdivided into four members, including, in ascending order, a basal conglomerate (Celia Cove Member), argillaceous interval (Francis Lake Member), primary volcanic rock unit (Weaver Lake Member), and tuffaceous sedimentary rock unit (Echo Island Member; Arthur, 1987, Arthur et al., 1993; Mahoney et al., 1994; Chapter 4). The base of the formation is an unconformity above oceanic rocks of the Middle Triassic Camp Cove Formation. The majority of the formation consists of interdigitated volcanic flows, breccias, tuff breccias, laharic breccias, hyaloclastite, and intermediate dikes and sills. Mahoney et al. (1994; Chapter 4) recognize a compositional transition from andesitic basalt and andesite near the base of the formation to rhyolite near the top of the formation. The upper part of the primary volcanic member is locally characterized by rhyolite domes and associated dikes and sills. The upper tuffaceous unit consists of 400-600 m of thin to thick bedded conglomerate, sandstone, siltstone, and argillite containing abundant resedimented pyroclastic debris.

5.5 AGE CONSTRAINTS

Age constraints in the Bonanza Group, Bowen Island Group, and Harrison Lake Formation is provided by rare marine fossils and radiometric dates in the Bowen Island Group and Harrison Lake Formation.

The Bonanza Group is biostratigraphically constrained to be early Sinemurian to Bajocian in age (Poulton, 1980; Muller et al., 1981). The majority of fossils identified from the Group are ammonites and bivalves of early Sinemurian to late Pliensbachian age recovered from sedimentary beds intercalated with volcanic rocks. However, Trigoniid bivalves, *Myophorella taylori*, of early Bajocian age were recovered in the late 1970's from sedimentary interbeds within volcanic strata of the Bonanza Group exposed in the mine pit at the Island Copper Mine, northern Vancouver Island (Poulton, 1980). This fossil locality and age assignment were largely ignored by subsequent workers (e.g. Muller et al., 1981; Nixon et al., 1993, 1994). The overlap between this biostratigraphic age and the U-Pb ages of the coeval Island Intrusions strongly indicate volcanism in the Bonanza Group was active until at least Early Bajocian time.

The biostratigraphic age determinations agree well with the radiometric ages determined for comagmatic intrusions of the Island Intrusions and Westcoast Complex (DeBari and Mortensen, 1994). Ages for the Island Intrusions and Westcoast Complex overlap, and range from 190 - 176 Ma (Pliensbachian to Aalenian).

The age of the Bowen Island Group is constrained to be Sinemurian to Toarcian by biostratigraphy and one radiometric age determination. Probable Sinemurian ammonites have been recovered from two localities in the northwestern portion of the outcrop belt (Friedman et al., 1990; Monger, 1991a). Zircon recovered from a flow-banded rhyolite yielded a U-Pb age of $185 \pm 8/-3$ Ma (Toarcian; Friedman et al., 1990).

The age of the Harrison Lake Formation is constrained to be Pliensbachian(?) to early Bathonian by biostratigraphy and one radiometric age determination. The lower conglomerate member of the Harrison Lake Formation is undated, but contains Middle Triassic chert clasts derived from the underlying Camp Cove Formation (Arthur, 1987). The conglomerate is gradationally overlain by fine-grained clastic rocks of the Francis Lake Member, which yields ammonites of late Early Toarcian age. The gradational contact with the overlying Francis Lake Member suggests the conglomerate and overlying fine-grained rocks were deposited in the same depositional system, and are therefore nearly age equivalent. The most probable age of the basal conglomerate is late Pliensbachian to Early Toarcian. Tuff beds intercalated with marine argillite constrain the initiation of volcanism in the Harrison Lake Formation to be late Early Toarcian (Chapter 4). Zircon recovered from a rhyolite dome complex near the top of the Weaver Lake Member yielded a U-Pb age of 166 ± 0.4 Ma, suggesting the upper part of the formation is early Bathonian in age. The minimum age of the top of the Harrison Lake Formation is constrained by overlying strata to be early Callovian.

5.6 GEOCHEMISTRY

All volcanic arc assemblages tend to display similar geochemical signatures indicative of their subduction-related tectonic setting, but identification of individual volcanic arc assemblages is inherently difficult. The absence of site-specific geochemical markers in typical island arc suites make it difficult to distinguish between potentially unrelated volcanic assemblages in complex tectonic settings such as the Canadian Cordillera. The most profitable avenue of correlation between tectonically disrupted volcanic suites is identification of consistent, systematic geochemical trends that suggest a genetic relationship between suites. Identification of such geochemical trends coupled with temporal and isotopic constraints are the best methods currently available to relate disrupted suites.

Geochemical analyses are presented from representative suites of the Bonanza Group, Bowen Island Group and Harrison Lake Formation. Samples in the Bonanza Group constitute two subgroups: the first was collected in the Nootka Sound region of northern Vancouver Island ($n=23$), and the second was collected from

Bonanza Group - Alberni area

| Sample | 91-7 | 91-9a | 91-9b | 91-16 | 91-77 | 91-85 | 91-97 | 93-412B | 93-414A | 93-416A |
|--------------------------------|--------|--------|--------|--------|-------|--------|--------|---------|---------|---------|
| SiO ₂ | 70.00 | 52.19 | 58.12 | 55.15 | 51.62 | 49.58 | 53.80 | 47.82 | 55.53 | 55.53 |
| Al ₂ O ₃ | 15.03 | 18.06 | 17.98 | 18.02 | 18.19 | 16.56 | 17.76 | 17.04 | 21.27 | 17.77 |
| TiO ₂ | 0.57 | 0.94 | 1.07 | 1.01 | 0.94 | 0.92 | 0.91 | 1.12 | 0.64 | 0.99 |
| FeO* | 2.91 | 9.00 | 6.99 | 6.68 | 9.32 | 8.40 | 8.22 | 9.90 | 5.79 | 8.65 |
| MnO | 0.09 | 0.16 | 0.15 | 0.16 | 0.21 | 0.16 | 0.19 | 0.20 | 0.19 | 0.18 |
| CaO | 1.46 | 9.25 | 6.77 | 8.01 | 8.52 | 13.69 | 6.64 | 11.65 | 7.15 | 8.62 |
| MgO | 0.83 | 5.24 | 2.23 | 3.73 | 5.78 | 7.80 | 5.06 | 4.95 | 3.13 | 4.02 |
| K ₂ O | 3.30 | 1.51 | 1.43 | 1.47 | 1.52 | 0.23 | 1.16 | 0.37 | 1.09 | 1.26 |
| Na ₂ O | 5.38 | 2.44 | 3.89 | 3.16 | 2.55 | 1.90 | 5.12 | 3.22 | 3.40 | 2.88 |
| P ₂ O ₅ | 0.13 | 0.27 | 0.60 | 0.44 | 0.29 | 0.19 | 0.30 | 0.26 | 0.45 | 0.27 |
| Total | 100.03 | 100.05 | 99.99 | 100.02 | 99.95 | 100.33 | 100.04 | 96.52 | 98.64 | 100.17 |
| LOI | | | | | | | | | | |
| Trace Elements | | | | | | | | | | |
| Ni | 5 | 22 | -3 | 27 | 38 | 75 | 41 | 13 | 1 | 1 |
| Cr | -3 | 50 | 3 | 129 | 81 | 309 | 104 | 44 | 6 | 20 |
| V | 28 | 268 | 106 | 320 | 259 | 305 | 221 | 359 | 91 | 237 |
| Ba | 1069 | 484 | 769 | - | - | 43 | 492 | 241 | 550 | 506 |
| Rb | 66 | 51 | 24 | - | - | 2 | 30 | 4 | 24 | 19 |
| Sr | 303 | 658 | 522 | 407 | 660 | 690 | 520 | 603 | 575 | 347 |
| Zr | 234.00 | 78.76 | 138.10 | 35.73 | 68.59 | 42.73 | 83.46 | 86.00 | 128.00 | 106.00 |
| Y | - | - | - | - | - | 18.01 | - | 20.09 | 25.56 | 29.72 |
| Nb | - | - | - | - | - | 1.54 | - | 5.36 | 10.37 | 6.63 |
| Cu | 10 | 50 | 25 | 55 | 46 | 6 | 21 | 55 | 13 | 71 |
| Zn | 64 | 89 | 76 | 76 | 125 | 41 | 96 | 89 | 101 | 86 |
| Pb | - | - | - | - | - | 1.88 | - | 4.38 | 3.90 | 4.10 |
| La | 22.20 | 11.10 | 16.00 | - | - | 4.73 | 12.80 | 11.73 | 21.29 | 15.25 |
| Ce | 50.20 | 27.50 | 36.20 | - | - | 10.40 | 27.50 | 22.59 | 42.17 | 30.89 |
| Pr | - | - | - | - | - | 1.71 | - | 2.93 | 5.11 | 3.80 |
| Nd | 23.50 | 14.30 | 23.20 | - | - | 8.62 | 17.90 | 13.15 | 21.49 | 16.45 |
| Sm | 6.06 | 3.78 | 5.98 | - | - | 2.57 | 4.29 | 3.73 | 5.13 | 4.70 |
| Eu | 1.39 | 1.24 | 1.71 | - | - | 1.09 | 1.32 | 1.25 | 1.65 | 1.37 |
| Gd | - | - | - | - | - | 2.62 | - | 3.58 | 4.50 | 4.60 |
| Tb | 0.97 | 0.58 | 0.96 | - | - | 0.49 | 0.57 | 0.63 | 0.76 | 0.84 |
| Dy | - | - | - | - | - | 3.16 | - | 3.91 | 4.60 | 5.19 |
| Ho | - | - | - | - | - | 0.65 | - | 0.77 | 0.97 | 1.07 |
| Er | - | - | - | - | - | 1.91 | - | 2.25 | 2.81 | 3.20 |
| Tm | - | - | - | - | - | 0.26 | - | 0.32 | 0.41 | 0.43 |
| Yb | 4.32 | 2.11 | 3.35 | - | - | 1.66 | 2.57 | 1.93 | 2.63 | 2.70 |
| Lu | 0.67 | 0.32 | 0.49 | - | - | 0.26 | 0.33 | 0.32 | 0.42 | 0.44 |
| Hf | 5.93 | 2.18 | 3.62 | - | - | 1.08 | 2.48 | 1.68 | 2.76 | 2.44 |
| Th | 4.60 | 1.90 | 2.00 | - | - | 0.39 | 1.90 | 1.68 | 2.97 | 2.17 |
| U | 2.10 | 0.81 | 0.99 | - | - | 0.27 | <2.8 | 0.56 | 0.81 | 0.60 |
| Ta | 0.69 | 0.26 | 0.52 | - | - | 0.14 | 0.31 | 0.29 | 0.50 | 0.35 |
| Cs | 0.77 | 1.41 | 0.67 | - | - | 0.11 | 0.98 | 0.28 | 1.42 | 0.16 |
| Ce/Yb | 11.6 | 13.0 | 10.8 | | | 6.3 | 10.7 | 11.7 | 16.0 | 11.4 |
| Ba/La | 48.2 | 43.6 | 48.1 | | | 9.1 | 38.4 | 20.5 | 25.8 | 33.2 |
| La/Th | 4.8 | 5.8 | 8.0 | | | 12.1 | 6.7 | 7.0 | 7.2 | 7.0 |
| La/Nb | | | | | | 3.1 | | 2.2 | 2.1 | 2.3 |
| Ba/Nb | | | | | | 27.9 | | 45.0 | 53.0 | 76.3 |
| Zr/Y | | | | | | 2.4 | | 4.3 | 5.0 | 3.6 |
| Normalized values | | | | | | | | | | |
| La/Yb | 3.4 | 3.5 | 3.1 | | | 1.9 | 3.3 | 4.0 | 5.3 | 3.7 |
| La/Sm | 2.2 | 1.8 | 1.6 | | | 1.1 | 1.8 | 1.9 | 2.5 | 2.0 |

Table 5.1a - Geochemical data from the Bonanza Group in the Port Alberni study area.

Bonanza Group - Nootka area

| Sample | 92-145a | 92-153A | 92-169ar | 92-170a | 92-177 | 92-185 | 92-187 | 92-189 | 92-230a | 92-235 | 92-241 |
|--------------------------------|---------|---------|----------|---------|--------|--------|--------|--------|---------|--------|--------|
| SiO ₂ | 48.36 | 47.74 | 48.74 | 49.23 | 52.42 | 56.56 | 55.04 | 53.74 | 57.10 | 62.94 | 57.06 |
| Al ₂ O ₃ | 15.11 | 19.18 | 17.34 | 15.67 | 18.49 | 15.11 | 16.30 | 14.93 | 17.01 | 15.29 | 15.67 |
| TiO ₂ | 0.81 | 0.50 | 1.00 | 2.20 | 1.01 | 1.99 | 1.30 | 1.73 | 1.22 | 1.23 | 1.40 |
| FeO* | 10.37 | 10.64 | 11.13 | 12.42 | 7.99 | 9.77 | 8.70 | 12.01 | 8.66 | 6.77 | 9.09 |
| MnO | 0.20 | 0.19 | 0.17 | 0.21 | 0.32 | 0.33 | 0.26 | 0.22 | 0.15 | 0.21 | 0.23 |
| CaO | 10.75 | 10.72 | 7.10 | 7.42 | 7.49 | 4.91 | 4.38 | 6.74 | 7.03 | 2.78 | 4.60 |
| MgO | 11.36 | 8.08 | 8.02 | 6.46 | 5.96 | 2.76 | 5.05 | 4.46 | 3.28 | 2.00 | 3.05 |
| K ₂ O | 0.46 | 0.14 | 1.16 | 1.37 | 2.34 | 2.93 | 2.87 | 0.73 | 1.13 | 2.79 | 2.19 |
| Na ₂ O | 1.74 | 1.87 | 3.67 | 3.69 | 3.58 | 4.10 | 4.80 | 3.80 | 3.50 | 5.11 | 5.40 |
| P ₂ O ₅ | 0.14 | 0.04 | 0.17 | 0.37 | 0.20 | 0.58 | 0.19 | 0.27 | 0.28 | 0.43 | 0.33 |
| Total | 100.45 | 100.28 | 99.73 | 100.41 | 100.67 | 100.11 | 99.86 | 99.95 | 100.31 | 100.29 | 100.01 |
| LOI | | | | | | | | | | | |
| Trace Elements | | | | | | | | | | | |
| Ni | 190 | 192 | 78 | 61 | 55 | 3 | 48 | 30 | 5 | 9 | 7 |
| Cr | 543 | 81 | 47 | 62 | 159 | 12 | 67 | 18 | 5 | 7 | 9 |
| V | 267 | 201 | 290 | 295 | 247 | 149 | 215 | 437 | 264 | 62 | 270 |
| Ba | 200 | 34 | 443 | 300 | 1591 | 866 | 714 | 163 | 451 | 660 | 507 |
| Rb | 8 | 4 | 20 | 31 | 60 | 69 | 62 | 14 | 28 | 62 | 52 |
| Sr | 169 | 110 | 277 | 229 | 393 | 83 | 136 | 229 | 414 | 163 | 172 |
| Zr | 47.61 | 18.46 | 56.43 | 213.60 | 87.64 | 188.48 | 237.20 | 137.59 | 84.65 | 313.17 | 182.44 |
| Y | 19.91 | 20.98 | 20.13 | 55.21 | 22.91 | 60.81 | 51.08 | 43.80 | 22.64 | 65.46 | 38.77 |
| Nb | 1.96 | 0.23 | 1.96 | 4.91 | 3.01 | 4.96 | 4.84 | 3.05 | 3.35 | 8.06 | 6.15 |
| Cu | 39 | 88 | 80 | 87 | 62 | 5 | 87 | 119 | 32 | 7 | 48 |
| Zn | 106 | 46 | 154 | 135 | 141 | 219 | 200 | 103 | 91 | 94 | 121 |
| Pb | 0.88 | 0.76 | 1.88 | 2.50 | 8.59 | 2.08 | 23.18 | 1.02 | 1.83 | 3.27 | 5.17 |
| La | 4.00 | 0.79 | 3.88 | 11.27 | 7.61 | 12.87 | 10.98 | 8.50 | 8.98 | 18.43 | 13.65 |
| Ce | 9.40 | 1.78 | 8.99 | 26.80 | 16.39 | 31.88 | 26.71 | 20.88 | 19.27 | 41.71 | 28.87 |
| Pr | 1.43 | 0.35 | 1.37 | 3.91 | 2.24 | 4.76 | 3.88 | 3.07 | 2.63 | 5.82 | 3.90 |
| Nd | 7.24 | 2.16 | 7.13 | 20.45 | 10.67 | 25.40 | 19.76 | 15.63 | 12.98 | 28.35 | 18.60 |
| Sm | 2.47 | 1.20 | 2.44 | 6.87 | 3.11 | 8.27 | 6.25 | 5.39 | 3.78 | 8.60 | 5.40 |
| Eu | 0.94 | 0.58 | 0.97 | 2.14 | 1.13 | 3.10 | 1.66 | 1.66 | 1.33 | 2.53 | 1.40 |
| Gd | 2.85 | 2.01 | 2.84 | 7.78 | 3.51 | 9.58 | 6.97 | 6.04 | 3.83 | 9.46 | 5.85 |
| Tb | 0.54 | 0.46 | 0.55 | 1.47 | 0.65 | 1.80 | 1.34 | 1.17 | 0.69 | 1.79 | 1.08 |
| Dy | 3.59 | 3.31 | 3.54 | 9.44 | 4.19 | 11.34 | 8.78 | 7.54 | 4.07 | 11.40 | 7.02 |
| Ho | 0.73 | 0.77 | 0.74 | 1.99 | 0.86 | 2.33 | 1.86 | 1.61 | 0.83 | 2.40 | 1.47 |
| Er | 2.12 | 2.48 | 2.21 | 5.81 | 2.47 | 6.80 | 5.71 | 4.70 | 2.47 | 7.01 | 4.43 |
| Tm | 0.29 | 0.34 | 0.29 | 0.78 | 0.34 | 0.91 | 0.78 | 0.65 | 0.33 | 0.98 | 0.60 |
| Yb | 1.82 | 2.35 | 1.76 | 5.03 | 2.11 | 5.71 | 5.05 | 4.06 | 2.14 | 6.13 | 3.80 |
| Lu | 0.29 | 0.39 | 0.29 | 0.81 | 0.34 | 0.89 | 0.78 | 0.63 | 0.34 | 0.98 | 0.60 |
| Hf | 1.34 | 0.63 | 1.21 | 4.85 | 2.07 | 4.57 | 5.66 | 3.30 | 2.14 | 6.97 | 4.14 |
| Th | 0.46 | 0.08 | 0.27 | 1.10 | 0.68 | 1.53 | 1.51 | 0.79 | 1.03 | 2.70 | 1.72 |
| U | 0.17 | 0.02 | 0.11 | 0.55 | 0.27 | 0.58 | 0.60 | 0.33 | 0.40 | 1.01 | 0.66 |
| Ta | 0.12 | 0.02 | 0.12 | 0.36 | 0.18 | 0.31 | 0.31 | 0.19 | 0.20 | 0.51 | 0.39 |
| Cs | 0.38 | 0.22 | 0.46 | 0.36 | 1.78 | 0.44 | 1.01 | 0.62 | 0.87 | 0.45 | 0.32 |
| Ce/Yb | 5.2 | 0.8 | 5.1 | 5.3 | 7.8 | 5.6 | 5.3 | 5.1 | 9.0 | 6.8 | 7.6 |
| Ba/La | 50.0 | 43.0 | 114.2 | 26.6 | 209.1 | 67.3 | 65.0 | 19.2 | 50.2 | 35.8 | 37.1 |
| La/Th | 8.7 | 9.9 | 14.4 | 10.2 | 11.2 | 8.4 | 7.3 | 10.8 | 8.7 | 6.8 | 7.9 |
| La/Nb | 2.0 | 3.4 | 2.0 | 2.3 | 2.5 | 2.6 | 2.3 | 2.8 | 2.7 | 2.3 | 2.2 |
| Ba/Nb | 102.0 | 147.8 | 226.0 | 61.1 | 528.6 | 174.6 | 147.5 | 53.4 | 134.6 | 81.9 | 82.4 |
| Zr/Y | 2.4 | 0.9 | 2.8 | 3.9 | 3.8 | 3.1 | 4.6 | 3.1 | 3.7 | 4.8 | 4.7 |
| Normalized values | | | | | | | | | | | |
| La/Yb | 1.4 | 0.2 | 1.5 | 1.5 | 2.4 | 1.5 | 1.4 | 1.4 | 2.8 | 2.0 | 2.4 |
| La/Sm | 1.0 | 0.4 | 1.0 | 1.0 | 1.5 | 0.9 | 1.1 | 1.0 | 1.4 | 1.3 | 1.5 |

Table 5.1b - Geochemical data from the Bonanza Group in the Nootka Sound study area.

Bonanza Group - Nootka area

| Sample | 92-244 | 92-249a | 92-252 | 92-253 | 92-256 | 92-258R | 92-259 | 92-261 | 92-265b | 92-270a | 92-272 | 93-329 |
|--------------------------------|--------|---------|--------|--------|--------|---------|--------|--------|---------|---------|--------|--------|
| SiO ₂ | 54.11 | 48.84 | 49.68 | 57.60 | 54.21 | 55.77 | 56.99 | 59.44 | 54.33 | 57.35 | 52.95 | 52.67 |
| Al ₂ O ₃ | 14.74 | 17.25 | 18.19 | 17.43 | 17.48 | 16.48 | 17.45 | 16.34 | 21.24 | 17.75 | 19.08 | 16.86 |
| TiO ₂ | 1.85 | 0.98 | 1.95 | 1.07 | 1.64 | 1.46 | 0.87 | 0.90 | 1.03 | 0.88 | 0.98 | 1.39 |
| FeO* | 12.75 | 9.89 | 11.20 | 8.44 | 9.68 | 9.73 | 6.94 | 7.46 | 7.18 | 7.27 | 8.97 | 9.86 |
| MnO | 0.24 | 0.25 | 0.18 | 0.13 | 0.13 | 0.18 | 0.11 | 0.23 | 0.18 | 0.15 | 0.16 | 0.23 |
| CaO | 6.13 | 11.39 | 8.53 | 2.91 | 4.92 | 4.72 | 6.36 | 3.71 | 3.43 | 7.04 | 8.36 | 5.79 |
| MgO | 4.29 | 7.75 | 4.74 | 3.20 | 3.71 | 4.04 | 4.44 | 3.06 | 3.98 | 3.93 | 4.09 | 5.05 |
| K ₂ O | 0.95 | 1.13 | 1.42 | 1.92 | 0.27 | 1.53 | 2.72 | 2.63 | 0.84 | 2.03 | 1.62 | 1.46 |
| Na ₂ O | 3.46 | 1.83 | 2.63 | 7.18 | 6.65 | 5.61 | 3.40 | 5.56 | 6.60 | 2.62 | 2.81 | 5.50 |
| P ₂ O ₅ | 0.32 | 0.15 | 0.33 | 0.04 | 0.47 | 0.29 | 0.21 | 0.20 | 0.26 | 0.22 | 0.22 | 0.27 |
| Total | 100.23 | 100.54 | 100.07 | 100.86 | 100.22 | 100.90 | 100.24 | 100.35 | 99.85 | 100.03 | 100.23 | 99.08 |
| LOI | | | | | | | | | | | | |
| Trace Elements | | | | | | | | | | | | |
| Ni | 15 | 82 | 39 | 28 | -3 | 18 | 30 | 11 | 28 | 21 | 17 | 31 |
| Cr | 6 | 210 | 54 | 38 | -3 | 21 | 80 | 17 | 62 | 53 | 29 | 74 |
| V | 441 | 306 | 303 | 146 | 216 | 303 | 197 | 212 | 202 | 191 | 246 | 230 |
| Ba | 364 | 215 | 270 | | 74 | 393 | 514 | 510 | 251 | 550 | 453 | 681 |
| Rb | 26 | 29 | 24 | | 8 | 31 | 61 | 51 | 22 | 44 | 34 | 23 |
| Sr | 244 | 265 | 274 | 137 | 113 | 272 | 284 | 92 | 447 | 393 | 395 | 270 |
| Zr | 127.37 | 42.89 | 163.46 | 142.11 | 158.81 | 138.86 | 104.43 | 202.35 | 129.29 | 84.82 | 64.54 | 128.00 |
| Y | 42.34 | 18.16 | 40.47 | | 43.76 | 37.94 | 23.77 | 39.60 | 22.03 | 20.73 | 19.51 | 33.81 |
| Nb | 3.86 | 2.02 | 5.03 | | 5.02 | 3.68 | 4.41 | 4.87 | 4.96 | 3.44 | 2.70 | 4.26 |
| Cu | 18 | 54 | 168 | 3 | 11 | 13 | 9 | 49 | 40 | 56 | 10 | 48 |
| Zn | 130 | 108 | 115 | 61 | 82 | 118 | 62 | 126 | 102 | 72 | 78 | 138 |
| Pb | 2.05 | 0.97 | 2.96 | | 1.64 | 2.10 | 2.59 | 1.78 | 2.57 | 2.17 | 2.54 | 7.82 |
| La | 9.81 | 4.43 | 10.58 | | 8.79 | 9.04 | 16.16 | 12.29 | 8.71 | 10.32 | 8.06 | 9.11 |
| Ce | 22.03 | 9.76 | 24.39 | | 21.58 | 20.38 | 30.73 | 27.51 | 19.68 | 19.09 | 15.51 | 20.35 |
| Pr | 3.19 | 1.41 | 3.50 | | 3.17 | 2.90 | 3.80 | 3.64 | 2.79 | 2.46 | 2.11 | 2.82 |
| Nd | 16.33 | 7.10 | 17.54 | | 16.75 | 14.40 | 16.91 | 16.81 | 13.34 | 11.15 | 9.62 | 13.78 |
| Sm | 5.35 | 2.35 | 5.42 | | 5.61 | 4.67 | 4.36 | 5.08 | 3.82 | 3.00 | 2.78 | 4.30 |
| Eu | 1.78 | 0.97 | 1.82 | | 1.75 | 1.42 | 1.28 | 1.34 | 1.24 | 0.99 | 1.00 | 1.65 |
| Gd | 6.12 | 2.79 | 6.08 | | 6.39 | 5.26 | 4.40 | 5.52 | 3.68 | 3.14 | 3.00 | 5.16 |
| Tb | 1.17 | 0.53 | 1.16 | | 1.19 | 1.04 | 0.72 | 1.03 | 0.68 | 0.56 | 0.57 | 0.96 |
| Dy | 7.44 | 3.32 | 7.25 | | 7.93 | 6.59 | 4.11 | 6.75 | 4.15 | 3.55 | 3.53 | 6.00 |
| Ho | 1.57 | 0.69 | 1.54 | | 1.70 | 1.40 | 0.83 | 1.44 | 0.83 | 0.74 | 0.75 | 1.22 |
| Er | 4.82 | 2.04 | 4.58 | | 5.16 | 4.29 | 2.36 | 4.42 | 2.35 | 2.13 | 2.12 | 3.68 |
| Tm | 0.65 | 0.27 | 0.61 | | 0.71 | 0.59 | 0.30 | 0.61 | 0.31 | 0.30 | 0.29 | 0.51 |
| Yb | 4.08 | 1.73 | 3.87 | | 4.50 | 3.67 | 2.00 | 4.03 | 2.08 | 1.95 | 1.87 | 3.12 |
| Lu | 0.64 | 0.27 | 0.60 | | 0.73 | 0.58 | 0.32 | 0.65 | 0.34 | 0.33 | 0.31 | 0.51 |
| Hf | 3.33 | 1.23 | 3.63 | | 3.88 | 3.20 | 2.68 | 4.75 | 2.98 | 1.90 | 1.59 | 3.02 |
| Th | 1.09 | 0.44 | 1.15 | | 1.62 | 1.19 | 2.34 | 2.04 | 2.86 | 1.86 | 1.19 | 1.07 |
| U | 0.50 | 0.18 | 0.41 | | 0.63 | 0.47 | 0.92 | 0.81 | 1.08 | 0.69 | 0.47 | 0.42 |
| Ta | 0.24 | 0.13 | 0.36 | | 0.32 | 0.23 | 0.32 | 0.33 | 0.41 | 0.33 | 0.24 | 0.25 |
| Cs | 0.35 | 0.77 | 0.55 | | 0.33 | 0.39 | 0.76 | 0.45 | 0.48 | 0.73 | 0.92 | 0.22 |
| Ce/Yb | 5.4 | 5.6 | 6.3 | | 4.8 | 5.6 | 15.4 | 6.8 | 9.5 | 9.8 | 8.3 | 6.5 |
| Ba/La | 37.1 | 48.5 | 25.5 | | 8.4 | 43.5 | 31.8 | 41.5 | 28.8 | 53.3 | 56.2 | 74.8 |
| La/Th | 9.0 | 10.1 | 9.2 | | 5.4 | 7.6 | 6.9 | 6.0 | 3.0 | 5.5 | 6.8 | 8.5 |
| La/Nb | 2.5 | 2.2 | 2.1 | | 1.8 | 2.5 | 3.7 | 2.5 | 1.8 | 3.0 | 3.0 | 2.1 |
| Ba/Nb | 94.3 | 106.4 | 53.7 | | 14.7 | 106.8 | 116.6 | 104.7 | 50.6 | 159.9 | 167.8 | 159.9 |
| Zr/Y | 3.0 | 2.4 | 4.0 | | 3.6 | 3.7 | 4.4 | 5.1 | 5.9 | 4.1 | 3.3 | 3.8 |
| Normalized values | | | | | | | | | | | | |
| La/Yb | 1.6 | 1.7 | 1.8 | | 1.3 | 1.6 | 5.3 | 2.0 | 2.8 | 3.5 | 2.8 | 1.9 |
| La/Sm | 1.1 | 1.1 | 1.2 | | 1.0 | 1.2 | 2.3 | 1.5 | 1.4 | 2.1 | 1.8 | 1.3 |

Table 5.1b (cont.) - Geochemical data from the Bonanza Group in the Nootka Sound study area.

Harrison Lake Formation

| Sample | 04JBM92 | 116JBM92 | 122JBM92 | 123JBM92 | 142JBM92 | 151JBM92 | 287JBM92 | 291JBM92 | 292JBM92 |
|--------------------------------|---------|----------|----------|----------|----------|----------|----------|----------|----------|
| SiO ₂ | 61.68 | 58.12 | 75.29 | 68.40 | 56.32 | 74.74 | 63.00 | 67.51 | 74.68 |
| Al ₂ O ₃ | 16.76 | 19.16 | 12.83 | 15.73 | 19.23 | 13.47 | 0.67 | 15.58 | 14.36 |
| TiO ₂ | 0.87 | 0.77 | 0.29 | 0.51 | 0.83 | 0.32 | 15.90 | 0.51 | 0.25 |
| FeO* | 7.30 | 6.98 | 1.50 | 4.18 | 9.56 | 2.96 | 5.13 | 4.19 | 2.15 |
| MnO | 0.15 | 0.20 | 0.05 | 0.09 | 0.18 | 0.10 | 0.10 | 0.09 | 0.05 |
| CaO | 5.03 | 2.37 | 1.51 | 1.61 | 3.16 | 0.63 | 0.63 | 1.20 | 5.12 |
| MgO | 2.54 | 4.62 | 0.45 | 2.46 | 5.82 | 1.03 | 1.03 | 2.54 | 0.80 |
| K ₂ O | 0.54 | 1.54 | 3.66 | 3.67 | 2.56 | 1.19 | 1.19 | 4.09 | 1.38 |
| Na ₂ O | 4.56 | 5.95 | 3.49 | 3.69 | 1.75 | 5.27 | 5.27 | 4.03 | 0.82 |
| P ₂ O ₅ | 0.25 | 0.21 | 0.07 | 0.17 | 0.22 | 0.07 | 0.07 | 0.15 | 0.05 |
| Total | 100.49 | 100.68 | 99.29 | 100.96 | 100.67 | 100.09 | 96.65 | 100.36 | 99.90 |
| LOI | | | | | | | | | |
| Trace Elements | | | | | | | | | |
| Ni | - | 4 | - | - | 9 | - | - | 5 | - |
| Cr | 10 | 14 | 15 | 13 | 25 | 17 | 16 | 17 | 10 |
| V | 95 | 170 | 14 | 77 | 221 | 4 | 83 | 76 | 11 |
| Ba | 185 | 658 | 1438 | 1189 | 424 | 395 | 838 | 1175 | 616 |
| Rb | 7 | 29 | 37 | 54 | 61 | 13 | 33 | 52 | 30 |
| Sr | 147 | 231 | 147 | 244 | 33 | 153 | 289 | 121 | 219 |
| Zr | 68.12 | 128.34 | 135.92 | 146.53 | 105.54 | 149.39 | 131.10 | 153.98 | 124.63 |
| Y | 30.40 | 23.60 | 19.14 | 23.26 | 21.72 | 56.20 | 33.57 | 24.85 | 19.01 |
| Nb | 2.67 | 4.98 | 5.40 | 6.02 | 4.48 | 5.32 | 6.62 | 6.49 | 5.44 |
| Cu | 19 | 7 | | 8 | 34 | | 9 | 26 | 2 |
| Zn | 88 | 108 | 46 | 53 | 117 | 62 | 68 | 88 | 45 |
| Pb | 2.32 | 3.40 | 1.37 | 4.18 | 1.92 | 1.58 | 3.91 | 17.55 | 7.73 |
| La | 7.37 | 14.33 | 9.03 | 17.85 | 12.60 | 15.32 | 15.66 | 16.47 | 14.16 |
| Ce | 15.73 | 27.75 | 18.72 | 28.71 | 24.31 | 29.73 | 30.56 | 27.24 | 24.98 |
| Pr | 2.34 | 3.36 | 2.30 | 3.40 | 3.02 | 4.66 | 3.95 | 3.28 | 2.80 |
| Nd | 11.81 | 14.92 | 9.99 | 13.86 | 13.34 | 21.95 | 17.82 | 13.66 | 10.93 |
| Sm | 3.83 | 3.90 | 2.49 | 3.20 | 3.59 | 6.63 | 4.91 | 3.38 | 2.63 |
| Eu | 1.43 | 1.15 | 0.69 | 0.98 | 1.02 | 1.69 | 1.35 | 0.93 | 0.65 |
| Gd | 4.26 | 3.85 | 2.57 | 2.98 | 3.56 | 7.21 | 5.01 | 3.38 | 2.41 |
| Tb | 0.82 | 0.67 | 0.48 | 0.56 | 0.63 | 1.42 | 0.90 | 0.59 | 0.46 |
| Dy | 5.45 | 4.21 | 2.96 | 3.64 | 4.04 | 9.27 | 5.87 | 3.92 | 3.01 |
| Ho | 1.18 | 0.88 | 0.67 | 0.80 | 0.83 | 1.98 | 1.25 | 0.84 | 0.65 |
| Er | 3.45 | 2.69 | 2.01 | 2.38 | 2.46 | 5.97 | 3.72 | 2.58 | 2.07 |
| Tm | 0.48 | 0.37 | 0.30 | 0.35 | 0.34 | 0.83 | 0.53 | 0.36 | 0.32 |
| Yb | 2.98 | 2.37 | 2.00 | 2.31 | 2.25 | 5.42 | 3.44 | 2.46 | 2.00 |
| Lu | 0.49 | 0.40 | 0.36 | 0.40 | 0.38 | 0.92 | 0.57 | 0.44 | 0.36 |
| Hf | 1.82 | 2.85 | 3.11 | 3.39 | 2.68 | 3.68 | 3.16 | 3.14 | 3.08 |
| Th | 0.71 | 3.23 | 2.61 | 3.98 | 2.97 | 1.12 | 1.94 | 3.39 | 2.57 |
| U | 0.25 | 0.98 | 0.83 | 1.31 | 0.96 | 0.44 | 0.66 | 1.10 | 1.00 |
| Ta | 0.20 | 0.43 | 0.42 | 0.49 | 0.39 | 0.38 | 0.43 | 0.52 | 0.54 |
| Cs | 0.36 | 0.18 | 0.48 | 0.38 | 0.94 | 0.10 | 1.21 | 0.15 | 2.50 |
| Ce/Yb | 5.3 | 11.7 | 9.4 | 12.4 | 10.8 | 5.5 | 8.9 | 11.1 | 12.5 |
| Ba/La | 25.1 | 45.9 | 159.2 | 66.6 | 33.7 | 25.8 | 53.5 | 71.3 | 43.5 |
| La/Th | 10.4 | 4.4 | 3.5 | 4.5 | 4.2 | 13.7 | 8.1 | 4.9 | 5.5 |
| La/Nb | 2.8 | 2.9 | 1.7 | 3.0 | 2.8 | 2.9 | 2.4 | 2.5 | 2.6 |
| Ba/Nb | 69.3 | 132.1 | 266.3 | 197.5 | 94.6 | 74.2 | 126.6 | 181.0 | 113.2 |
| Zr/Y | 2.2 | 5.4 | 7.1 | 6.3 | 4.9 | 2.7 | 3.9 | 6.2 | 6.6 |
| Normalized values | | | | | | | | | |
| La/Yb | 1.6 | 4.0 | 3.0 | 5.1 | 3.7 | 1.9 | 3.0 | 4.4 | 4.7 |
| La/Sm | 1.2 | 2.2 | 2.2 | 3.4 | 2.1 | 1.4 | 1.9 | 3.0 | 3.3 |

Table 5.1c - Geochemical data from the Harrison Lake Formation.

Harrison Lake Formation

| Sample | 293JBM92 | 306JBM92 | 307JBM92 | 13JBM93 | 14JBM93 | 15JBM93 | 17JBM93 | 21JBM93 | 22JBM93 | 25JBM93 |
|--------------------------------|----------|----------|----------|---------|---------|---------|---------|---------|---------|---------|
| SiO ₂ | 73.44 | 79.57 | 68.11 | 75.52 | 77.39 | 67.44 | 70.40 | 68.11 | 77.88 | 74.53 |
| Al ₂ O ₃ | 15.08 | 11.35 | 15.60 | 13.38 | 13.37 | 15.53 | 14.73 | 14.81 | 12.55 | 13.53 |
| TiO ₂ | 0.25 | 0.20 | 0.61 | 0.25 | 0.23 | 0.59 | 0.51 | 0.54 | 0.16 | 0.30 |
| FeO* | 1.20 | 1.38 | 4.45 | 1.30 | 1.32 | 3.86 | 4.58 | 4.30 | 1.42 | 1.91 |
| MnO | 0.04 | 0.03 | 0.06 | 0.03 | 0.04 | 0.08 | 0.17 | 0.12 | 0.05 | 0.05 |
| CaO | 3.80 | 0.43 | 3.62 | 2.22 | 1.19 | 1.81 | 1.28 | 3.03 | 0.87 | 1.03 |
| MgO | 0.68 | 0.45 | 1.77 | 0.72 | 0.57 | 1.10 | 1.14 | 1.35 | 0.35 | 0.76 |
| K ₂ O | 3.27 | 2.91 | 1.62 | 0.24 | 0.25 | 3.89 | 0.07 | 1.49 | 1.63 | 3.33 |
| Na ₂ O | 1.55 | 3.36 | 4.12 | 5.11 | 6.67 | 5.62 | 7.41 | 4.56 | 5.65 | 4.57 |
| P ₂ O ₅ | 0.05 | 0.06 | 0.21 | 0.05 | 0.05 | 0.22 | 0.15 | 0.16 | 0.03 | 0.07 |
| Total | 99.49 | 99.88 | 100.65 | 98.82 | 101.08 | 100.14 | 100.43 | 98.48 | 100.59 | 100.08 |
| LOI | | | | | | | | | | |
| Trace Elements | | | | | | | | | | |
| Ni | - | - | - | 8 | 9 | 4 | 5 | 7 | 8 | 8 |
| Cr | 13 | 16 | 12 | 3 | 5 | 4 | 0 | 2 | 3 | 4 |
| V | 10 | 11 | 43 | 28 | 13 | 53 | 0 | 45 | 4 | 24 |
| Ba | 1190 | 1060 | 154 | 239 | 91 | 937 | 71 | 667 | 940 | 929 |
| Rb | 84 | 82 | 16 | 1 | 3 | 57 | 1 | 23 | 20 | 38 |
| Sr | 163 | 113 | 72 | 242 | 200 | 161 | 123 | 339 | 147 | 152 |
| Zr | 124.34 | 93.46 | 110.68 | 115.00 | 112.00 | 137.00 | 87.00 | 130.00 | 123.00 | 128.00 |
| Y | 19.40 | 13.98 | 31.08 | 21.01 | 13.94 | 36.08 | 36.85 | 31.61 | 23.22 | 21.24 |
| Nb | 5.44 | 6.31 | 3.38 | 2.95 | 3.47 | 7.22 | 3.87 | 7.00 | 5.36 | 4.77 |
| Cu | | | | 6 | 6 | 13 | 4 | 5 | 8 | 8 |
| Zn | 38 | 35 | 75 | 8 | 11 | 64 | 92 | 69 | 30 | 32 |
| Pb | 8.07 | 1.55 | 2.53 | 0.84 | 0.69 | 6.50 | 1.42 | 4.51 | 2.32 | 2.27 |
| La | 12.65 | 16.50 | 11.55 | 11.10 | 10.66 | 18.38 | 7.38 | 12.46 | 14.24 | 14.42 |
| Ce | 24.62 | 28.13 | 22.86 | 22.24 | 19.99 | 31.50 | 17.06 | 24.93 | 26.51 | 23.89 |
| Pr | 2.84 | 3.01 | 3.31 | 2.81 | 2.32 | 4.45 | 2.53 | 3.25 | 3.07 | 3.07 |
| Nd | 11.59 | 11.15 | 15.41 | 11.77 | 9.01 | 19.59 | 12.52 | 15.16 | 12.74 | 12.27 |
| Sm | 2.72 | 2.11 | 4.59 | 3.02 | 2.16 | 5.19 | 4.06 | 4.53 | 3.11 | 2.99 |
| Eu | 0.62 | 0.57 | 1.46 | 0.68 | 0.57 | 1.37 | 1.39 | 1.25 | 0.69 | 0.77 |
| Gd | 2.76 | 1.89 | 4.67 | 2.82 | 1.83 | 5.16 | 4.96 | 4.50 | 2.88 | 2.90 |
| Tb | 0.51 | 0.32 | 0.84 | 0.51 | 0.32 | 0.95 | 0.97 | 0.84 | 0.53 | 0.54 |
| Dy | 3.25 | 2.07 | 5.48 | 3.30 | 2.14 | 5.98 | 6.43 | 5.35 | 3.68 | 3.25 |
| Ho | 0.68 | 0.42 | 1.17 | 0.72 | 0.46 | 1.25 | 1.44 | 1.15 | 0.81 | 0.65 |
| Er | 2.07 | 1.34 | 3.44 | 2.25 | 1.47 | 3.79 | 4.27 | 3.45 | 2.48 | 2.11 |
| Tm | 0.29 | 0.21 | 0.48 | 0.33 | 0.22 | 0.51 | 0.60 | 0.49 | 0.37 | 0.32 |
| Yb | 2.00 | 1.43 | 3.02 | 2.26 | 1.63 | 3.36 | 3.90 | 3.20 | 2.67 | 2.09 |
| Lu | 0.34 | 0.27 | 0.47 | 0.40 | 0.28 | 0.54 | 0.65 | 0.53 | 0.49 | 0.35 |
| Hf | 3.40 | 2.41 | 2.68 | 2.97 | 2.76 | 3.41 | 2.63 | 3.27 | 3.40 | 3.05 |
| Th | 3.08 | 5.30 | 1.25 | 1.87 | 1.56 | 2.59 | 0.70 | 1.76 | 2.39 | 2.43 |
| U | 1.13 | 1.77 | 0.43 | 0.70 | 0.52 | 0.96 | 0.26 | 0.60 | 0.91 | 0.83 |
| Ta | 0.58 | 0.63 | 0.21 | 0.20 | 0.22 | 0.43 | 0.21 | 0.39 | 0.37 | 0.30 |
| Cs | 1.73 | 0.34 | 1.18 | 0.07 | 0.05 | 0.12 | 0.01 | 0.83 | 0.64 | 0.25 |
| Ce/Yb | 12.3 | 19.7 | 7.6 | 9.8 | 12.3 | 9.4 | 4.4 | 7.8 | 9.9 | 11.4 |
| Ba/La | 94.1 | 64.2 | 13.3 | 21.5 | 8.5 | 51.0 | 9.6 | 53.5 | 66.0 | 64.4 |
| La/Th | 4.1 | 3.1 | 9.2 | 5.9 | 6.8 | 7.1 | 10.5 | 7.1 | 6.0 | 5.9 |
| La/Nb | 2.3 | 2.6 | 3.4 | 3.8 | 3.1 | 2.5 | 1.9 | 1.8 | 2.7 | 3.0 |
| Ba/Nb | 218.8 | 168.0 | 45.6 | 81.0 | 26.2 | 129.8 | 18.3 | 95.3 | 175.4 | 194.8 |
| Zr/Y | 6.4 | 6.7 | 3.6 | 5.5 | 8.0 | 3.8 | 2.4 | 4.1 | 5.3 | 6.0 |
| Normalized values | | | | | | | | | | |
| La/Yb | 4.2 | 7.6 | 2.5 | 3.2 | 4.3 | 3.6 | 1.2 | 2.6 | 3.5 | 4.5 |
| La/Sm | 2.8 | 4.8 | 1.5 | 2.2 | 3.0 | 2.2 | 1.1 | 1.7 | 2.8 | 2.9 |

Table 5.1c (cont.) - Geochemical data from the Harrison Lake Formation.

| Bowen Island Group | | | | Middle Jurassic Plutons | |
|--------------------------------|---------|---------|--------|-------------------------|----------|
| Sample | 90JBM93 | 91JBM93 | Bowen | RMF-89-1 | MV-88-37 |
| SiO ₂ | 50.01 | 52.28 | 79.18 | 71.37 | 69.16 |
| Al ₂ O ₃ | 16.97 | 18.07 | 11.77 | 14.58 | 14.54 |
| TiO ₂ | 0.74 | 0.78 | 0.05 | 0.40 | 0.49 |
| FeO* | 9.06 | 9.18 | 1.68 | 3.48 | 5.13 |
| MnO | 0.19 | 0.14 | 0.02 | 0.05 | 0.10 |
| CaO | 10.79 | 7.58 | 0.36 | 2.71 | 5.67 |
| MgO | 8.98 | 5.86 | 0.31 | 0.86 | 1.51 |
| K ₂ O | 0.49 | 0.73 | 2.43 | 2.15 | 0.54 |
| Na ₂ O | 1.81 | 5.28 | 5.06 | 5.38 | 3.28 |
| P ₂ O ₅ | 0.20 | 0.13 | 0.01 | 0.12 | 0.10 |
| Total | 99.25 | 100.02 | 100.87 | 101.10 | 100.52 |
| LOI | | | | | |
| Trace Elements | | | | | |
| Ni | 129 | 27 | 15 | 11 | 15 |
| Cr | 430 | 38 | 8 | 13 | 18 |
| V | 235 | 253 | 1 | 34 | 85 |
| Ba | 133 | 528 | 584 | 873 | 323 |
| Rb | 12 | 10 | 27 | 23 | 9 |
| Sr | 354 | 640 | 67 | 218 | 307 |
| Zr | 64.00 | 62.00 | 152.00 | 138.00 | 113.00 |
| Y | 17.58 | 19.50 | 80.61 | 23.64 | 32.99 |
| Nb | 2.69 | 1.86 | 29.54 | 6.94 | 3.67 |
| Cu | 66 | 68 | 23 | 30 | 30 |
| Zn | 73 | 78 | 46 | 13 | 42 |
| Pb | 2.00 | 4.15 | 9.60 | 2.61 | 4.61 |
| La | 7.68 | 5.05 | 21.84 | 15.10 | 11.47 |
| Ce | 15.52 | 10.93 | 46.24 | 29.24 | 23.41 |
| Pr | 2.21 | 1.64 | 5.87 | 3.38 | 3.25 |
| Nd | 10.42 | 8.35 | 25.45 | 13.34 | 14.79 |
| Sm | 2.93 | 2.43 | 7.34 | 3.25 | 4.30 |
| Eu | 1.02 | 0.94 | 0.53 | 0.86 | 1.11 |
| Gd | 2.96 | 2.86 | 9.06 | 3.25 | 4.42 |
| Tb | 0.51 | 0.53 | 1.89 | 0.60 | 0.82 |
| Dy | 3.17 | 3.33 | 12.87 | 3.78 | 5.36 |
| Ho | 0.64 | 0.67 | 2.79 | 0.80 | 1.14 |
| Er | 1.92 | 1.97 | 8.39 | 2.55 | 3.48 |
| Tm | 0.26 | 0.27 | 1.25 | 0.38 | 0.51 |
| Yb | 1.61 | 1.73 | 8.12 | 2.53 | 3.29 |
| Lu | 0.26 | 0.27 | 1.25 | 0.45 | 0.53 |
| Hf | 1.24 | 1.08 | 6.21 | 3.19 | 2.89 |
| Th | 0.63 | 0.39 | 8.72 | 2.85 | 1.58 |
| U | 0.22 | 0.16 | 2.15 | 0.95 | 0.61 |
| Ta | 0.15 | 0.11 | 2.28 | 0.47 | 0.20 |
| Cs | 0.23 | 0.55 | 0.09 | 0.08 | 0.15 |
| Ce/Yb | 9.6 | 6.3 | 5.7 | 11.6 | 7.1 |
| Ba/La | 17.3 | 104.6 | 26.7 | 57.8 | 28.2 |
| La/Th | 12.2 | 12.9 | 2.5 | 5.3 | 7.3 |
| La/Nb | 2.9 | 2.7 | 0.7 | 2.2 | 3.1 |
| Ba/Nb | 49.4 | 283.9 | 19.8 | 125.8 | 88.0 |
| Zr/Y | 3.6 | 3.2 | 1.9 | 5.8 | 3.4 |
| Normalized values | | | | | |
| La/Yb | 3.1 | 1.9 | 1.8 | 3.9 | 2.3 |
| La/Sm | 1.6 | 1.3 | 1.8 | 2.8 | 1.6 |

Table 5.1d - Geochemical data from the Bowen Island Group and Middle Jurassic pluton.

the Port Alberni area in southern Vancouver Island (n=10; Fig. 5.2). Bowen Island Group samples were collected from Bowen Island itself and exposures to the north (n=3). Harrison Lake Formation samples represent a uniform coverage of the entire outcrop belt (n=19; Fig. 5.2). Representative samples of Middle Jurassic plutons west of the Harrison terrane are provided for comparative purposes (n=2; Table 5.1). A description of analytical techniques is given in Appendix A.

A. Major and Trace Element Geochemistry

Volcanic rocks from all three units range from basaltic andesite and andesite to rhyolite. The lack of more felsic samples from the Bonanza Group (Fig. 5.4) is probably the result of sampling bias in this investigation, as rhyolitic rocks are reported from throughout the Group (Muller et al., 1974; Jeletsky, 1976; Nixon et al., 1994). Samples from the Bonanza Group were collected in conjunction with a detailed petrologic analysis of the Group, and collection was limited to rocks of basaltic to andesitic composition to facilitate petrologic modeling of the initial source region. Major and trace element values for all three units indicate the rocks are of tholeiitic to calc-alkaline magmatic affinity; the samples define a colinear tholeiitic to calcalkaline trend on an AFM diagram (Fig. 5.4a). There is overlap between samples from all units, and the AFM trend is segmented, with Bonanza Group samples plotting near the tholeiitic/calcalkaline boundary, and Harrison Lake Formation rocks displaying a stronger calcalkaline affinity. Trace element abundances and trace element ratios, such as Ba/La, La/Th, La/Nb, are characteristic of subduction-related volcanic suites (Gill, 1981).

Linear to curvilinear patterns characterize plots of major and trace elements against SiO₂ (Fig. 5.5). The Nootka Sound samples from the Bonanza Group are divisible into two distinct subgroups: 1) incompatible element enriched basaltic andesite-andesite containing abnormally high TiO₂, FeO*, Zr, Y, and HREE (Figs. 5.5, 5.8b); and 2) basalt and basaltic andesite displaying incompatible element values within the range of normal tholeiitic to calcalkaline rocks (Gill, 1981). These two subgroups are well segregated on TiO₂ and Zr Harker diagrams and on REE plots (Figs. 5.5, 5.8b). Colinear Harker diagram patterns characterize samples from all units, disregarding the "enriched basaltic andesite of Nootka Sound". All units display negative

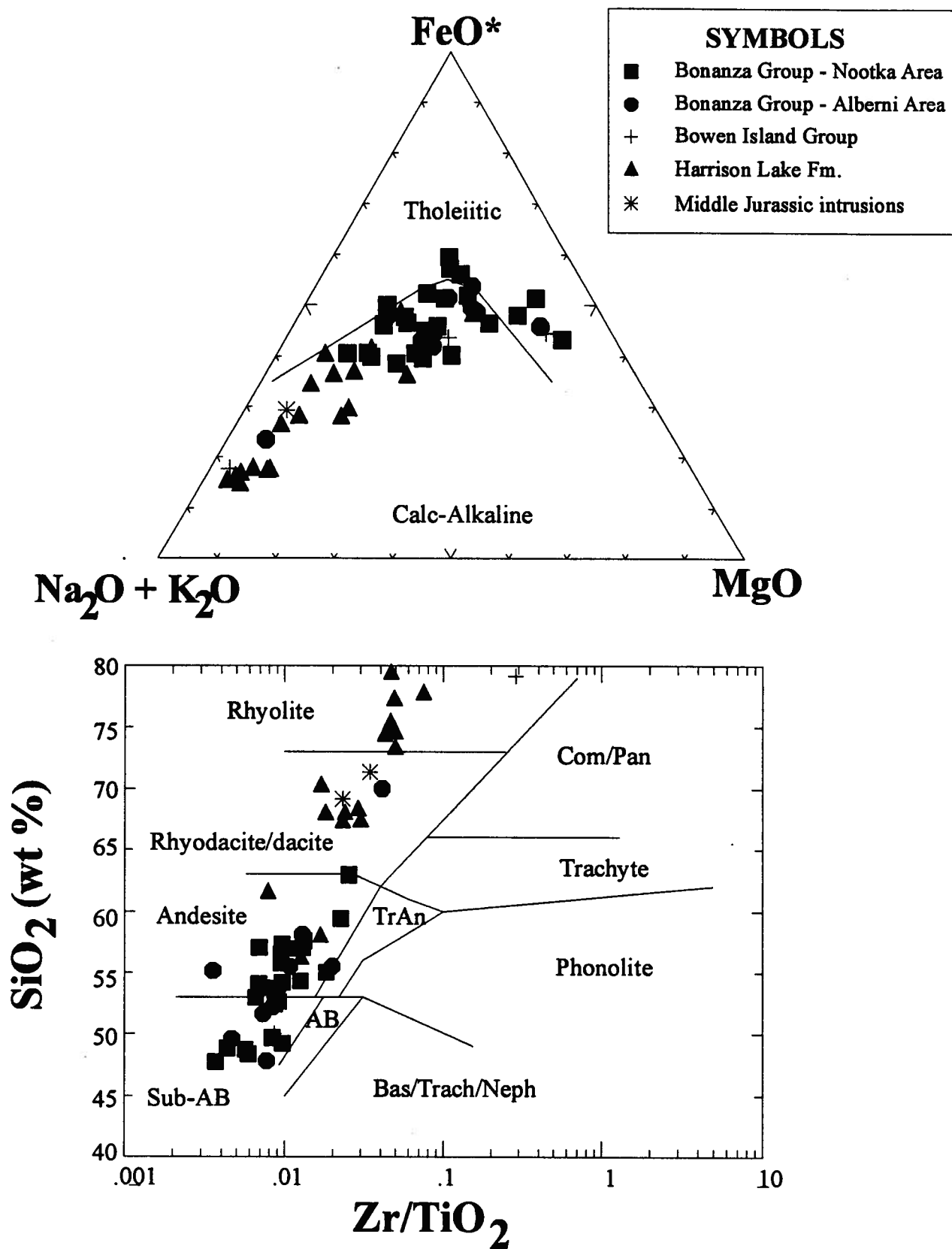


Figure 5.4 - a) AFM diagram for samples of the Bonanza Group, Bowen Island Group, and Harrison Lake Formation. Note sample symbols in legend. b) Zr/TiO_2 vs. SiO_2 compositional discriminate diagram. From Winchester and Floyd (1977).

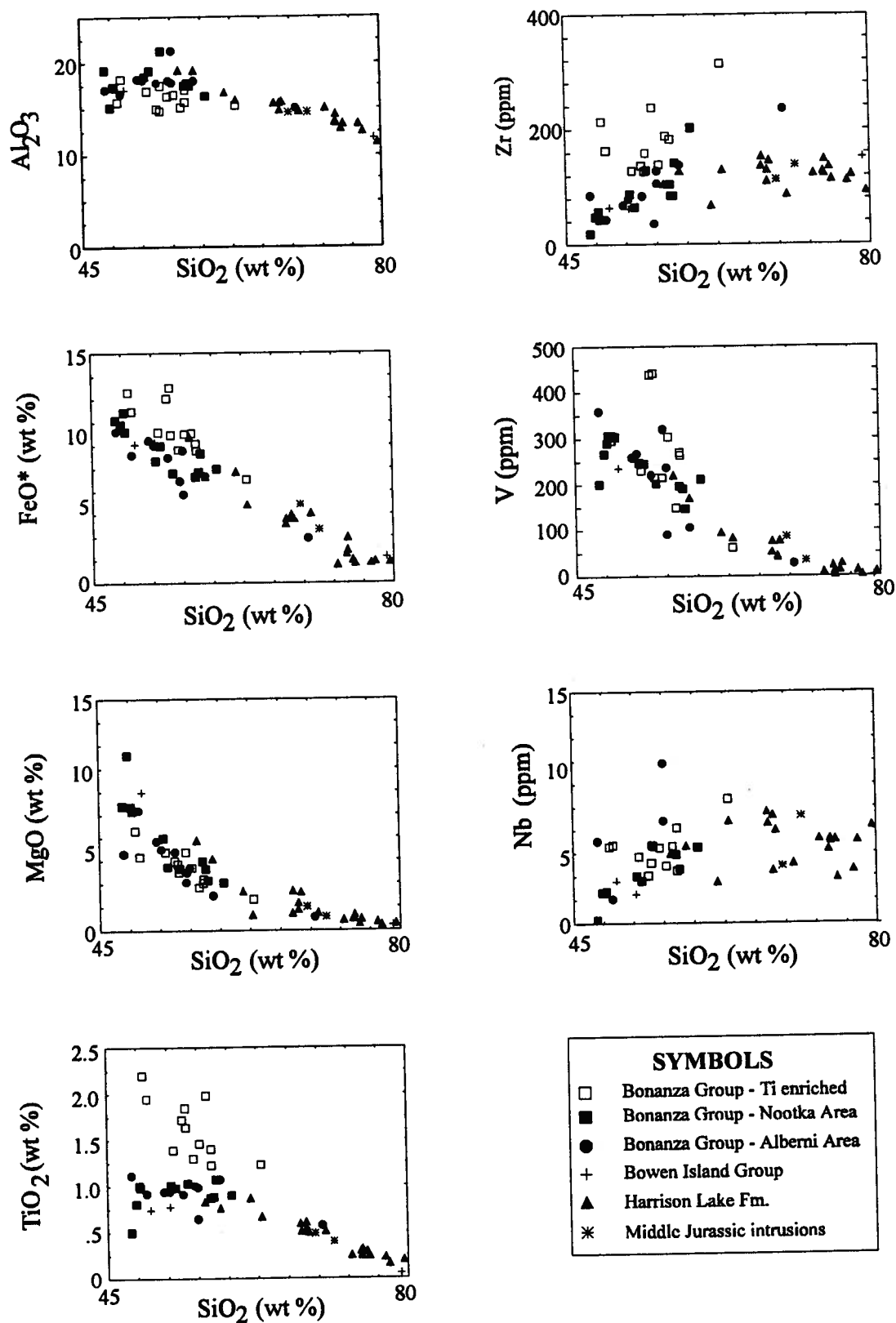


Figure 5.5 - Harker variation diagrams for samples from the Bonanza Group, Bowen Island Group, and Harrison Lake Formation. Note smooth linear to curvilinear trends for most elements, as well as distinct separation of a subset of Nootka Sound samples (open squares).

correlations between Al_2O_3 , FeO^* , MgO , TiO_2 and V and increasing silica content. The trace elements Zr, Nb, and Ta show weak positive correlations with increasing silica content (Fig. 5.5).

Elemental scatter is evident in plots of K, Na, Ba, Ca, and other LIL elements against SiO_2 , indicating partial remobilization of mobile constituents (Gill, 1981). Systematic compositional changes may be evaluated through the use of immobile compatible elements (Al, Ti, V, Cr) as monitors of progressive change within each of the rock suites (MacLean and Barrett, 1993; Fig. 5.6). A plot of Al_2O_3 versus TiO_2 demonstrates a linear relationship between rocks of the Bonanza Group (excluding the enriched basaltic andesite), Bowen Island Group, and Harrison Lake Formation. A similar linear relationship exists between the units on a SiO_2 versus TiO_2 plot, suggesting that the units have not undergone silica mobilization, which would lead to elemental scatter. The unique character of the enriched basalt of Nootka Sound is well illustrated on the plots utilizing the immobile compatible element TiO_2 as a monitor (Fig. 5.6a, b). Note the progressive depletion of TiO_2 at essentially constant levels of SiO_2 and Al_2O_3 for concentrations of TiO_2 greater than 1.2 weight percent. This trend is interpreted to represent progressive crystallization of Ti rich phases, probably Fe-Ti oxides, prior to the crystallization of more silica-rich phases. There is a distinct inflection point evident on the immobile compatible element diagrams between the horizontal linear trends and the sloping trends; this inflection may result from fractional crystallization within a single magma chamber (i.e. a single fractionation sequence), or may indicate multiple magma chambers with distinct sources (i.e. two separate fractionation trends; Gill, 1981).

Mobile-immobile incompatible element ratios monitor variations in magmatic sources (Pearce, 1982). Pairs of incompatible elements from a lava series related by fractional crystallization form a linear trend on a biaxial diagram that passes through the origin (Wood et al., 1979; MacLean and Barrett, 1993). Ta is chosen as an index of fractionation because it is an immobile incompatible element that does not undergo enrichment during the subduction process, thus, assuming an originally homogeneous source, variations in the concentration of Ta are simply the result of fractional crystallization (Wood et al., 1979; Pearce, 1982). The incompatible elements Ce and Th display uniformity in within plate basalt and MORB environments

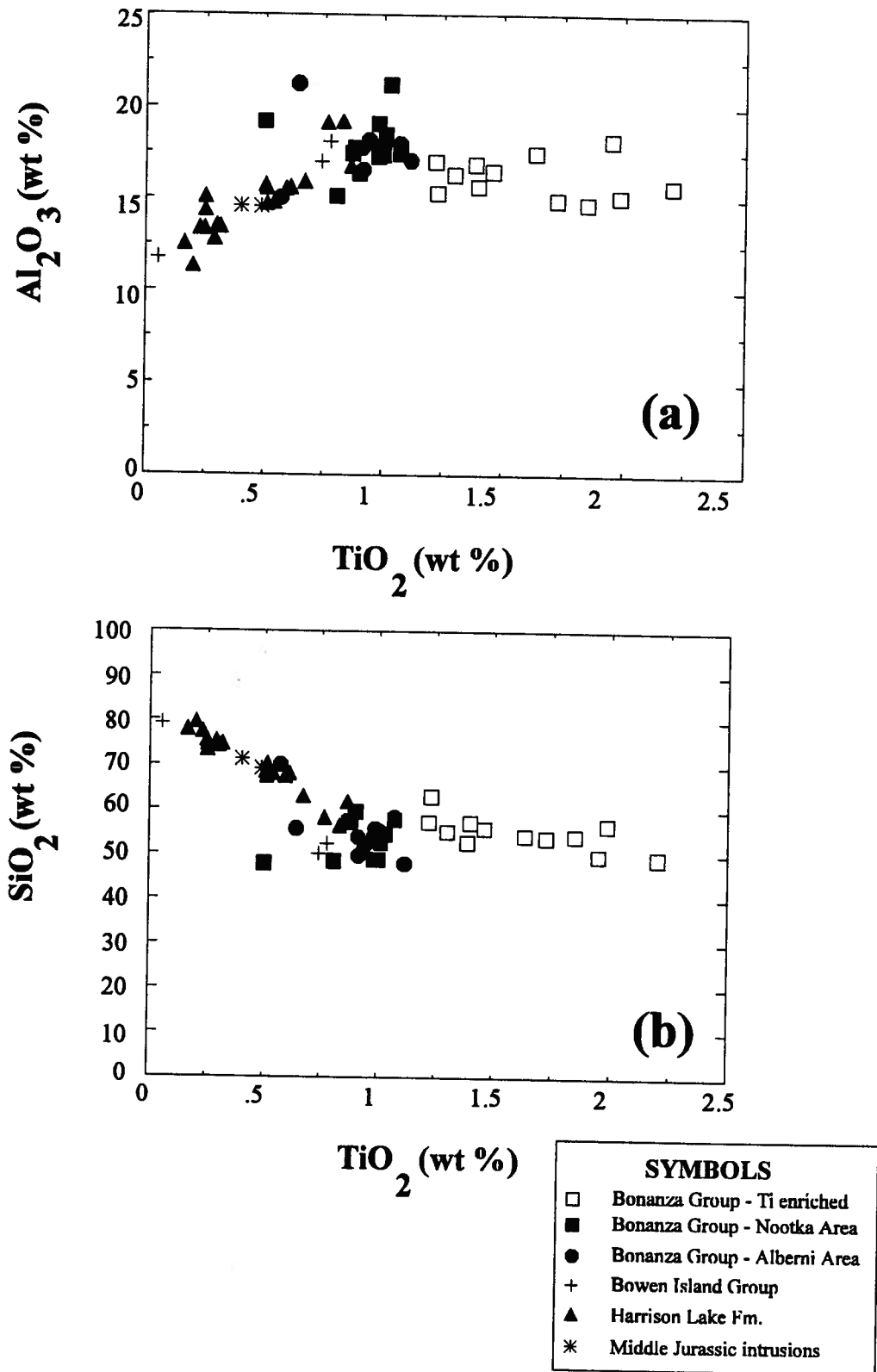
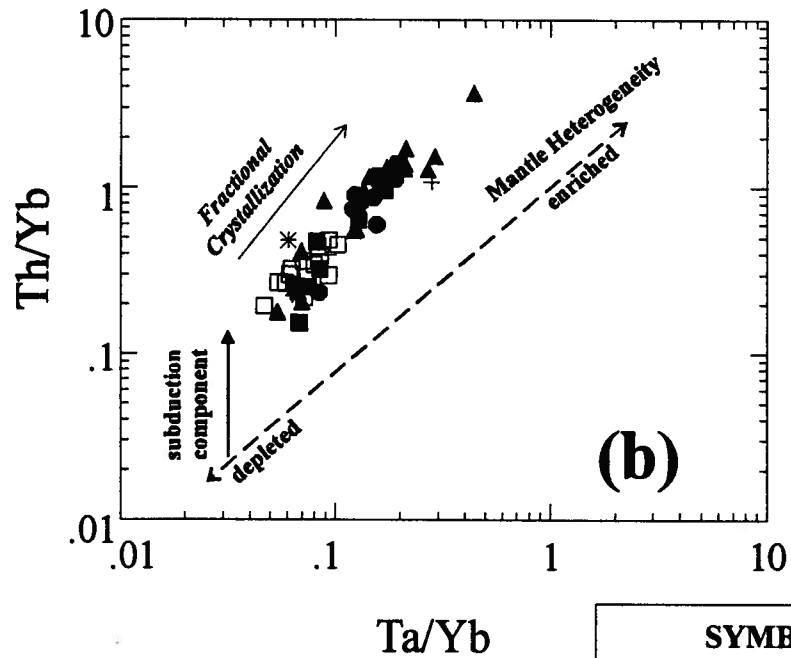
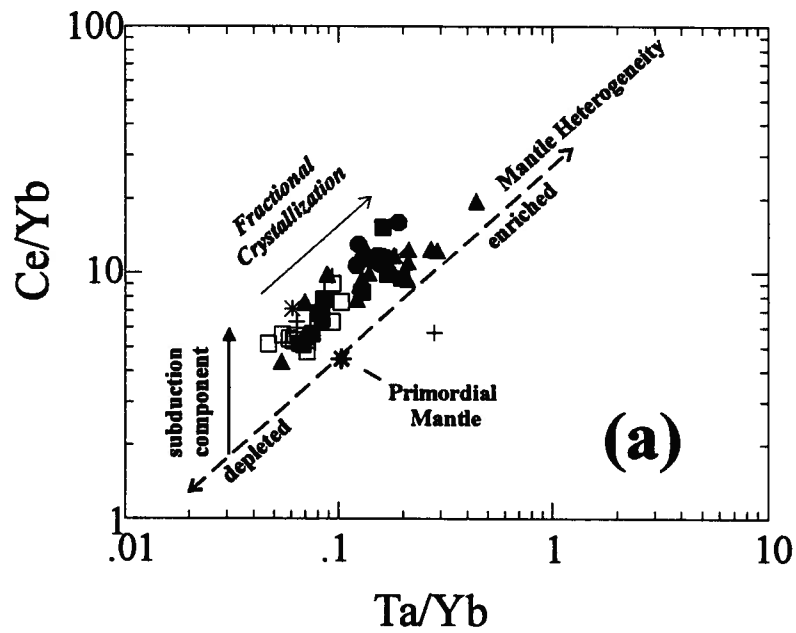


Figure 5.6 - a) TiO_2 vs. Al_2O_3 variation diagram. Note horizontal fractionation pattern at TiO_2 contents of over 1.25 wt %, which corresponds to enriched basaltic andesite of Nootka Sound b) TiO_2 vs. SiO_2 variation diagram. Note similar pattern of TiO_2 fractionation.. Note distinct inflection points between horizontal and sloped fractionation trends.

(i.e. depleted mantle source), but display demonstrable enrichment in arc settings, suggesting enrichment during the subduction process (Wood, 1979; Pearce, 1982). Therefore plots of the incompatible elements Ce or Th against Ta may be used to discriminate enrichment processes in island arc settings (Pearce, 1982). The incompatible elements Ta, Ce, and Th are normalized to Yb because the behavior of an evolving system is more easily evaluated by examining the changes in relationships *between* elements rather than changes in the absolute concentrations of the elements. In addition, use of Yb adds an additional monitor of mantle heterogeneity, as it is not enriched by subduction processes, and variations in its value are related solely to progressive variations in original source composition (Pearce, 1982).

Ce/Yb and Th/Yb are plotted against Ta/Yb on figure 5.7. Note the strong colinear trends evident in both plots, and the transition from Bonanza Group samples close to MORB values toward Harrison Lake Formation samples at the more evolved end of the spectrum. Th, Ce, Ta, and Yb concentrations progressively increase from the Bonanza Group to the Harrison Lake Formation, and reflect either incompatible behavior during fractional crystallization, or the gradual influx of incompatible elements to the system from a crustal source. Deviations away from the mantle array suggest minor enrichment of Ce and more substantial enrichment of Th relative to MORB/depleted mantle values. Differences in the degree of enrichment are probably the result of the higher mobility of Th relative to Ce. The enrichment in Ce is uniform for the compositional range, whereas there is a slight increase in the degree of Th enrichment from the mafic to the felsic end of the range. This shift in Th enrichment may be the result of additional hydrous flux from the descending slab or a minor degree of crustal contamination. Incompatible element ratio diagrams permit estimation of both the initial mantle composition and the degree of enrichment via hydrous flux during subduction (Pearce, 1982). The strong colinear trends between the Bonanza Group, Bowen Island Group, and Harrison Lake Formation are consistent with the evolution of a single magmatic system. If these suites are not derived from a single magmatic system, then each of the individual source regions must have undergone identical degrees of enrichment from the subducting slab, interacted with lower crust to the same degree, and be initially derived from a homogeneous mantle.



| SYMBOLS | |
|---------|------------------------------|
| □ | Bonanza Group - Ti enriched |
| ■ | Bonanza Group - Nootka Area |
| ● | Bonanza Group - Alberni Area |
| + | Bowen Island Group |
| ▲ | Harrison Lake Fm. |
| * | Middle Jurassic intrusions |

Figure 5.7 - a) Ta/Yb vs. Ce/Yb ; b) Ta/Yb vs. Th/Yb, after Gill (1981). Note strong colinear trends and overlap of all units.

B. Rare Earth Elements

Rare earth element patterns from the Bonanza Group, Bowen Island Group, and Harrison Lake Formation vary from flat ($\text{LaN/YbN}=1.0$) to light rare earth element (LREE) enriched ($\text{LaN/YbN}=6.0$; Fig. 5.8). REE patterns from each unit are consistent with range of compositions from low K tholeiite to medium K calcalkaline (Gill, 1981). Each unit displays a mixture of REE patterns that may be subdivided into distinct groups (Fig. 5.8). Figure 5.8 is a series of REE diagrams from each of the sample areas under consideration; the upper diagram displays the entire suite, and the lower diagram displays representative samples characteristic of each REE group. The REE patterns may be subdivided into three distinct groups:

I. Flat REE patterns ($\text{LaN/YbN}=1.2-1.9$). This group is characterized by flat to very slightly LREE enriched REE patterns with abundances 10-12x chondrite, and may contain minor positive Eu anomalies (Figs. 5.8, 5.9a). Group I (Fig. 5.9) represents a small percentage of all samples from the Bonanza ($n=4$) and Bowen Island ($n=1$) groups, and is present in the Harrison Lake Formation ($n=2$) with slightly higher total REE abundances than the rocks to the west. The flat REE patterns and low abundances suggest that a portion of each unit is primitive and has not interacted with the any crustal material or enriched component derived from the subducting slab.

II. LREE enriched REE patterns ($\text{LaN/YbN}=3.0-7.0$). This group is characterized by LREE enriched patterns with LREE abundances 20-70x chondrite (Fig. 5.8, 5.9b). REE pattern generally display a negative slope, and minor HREE enrichment is evident in part. There is an overall increase in LREE enrichment from the Bonanza Group east to the Harrison Lake Formation, but there is no direct correlation between SiO_2 content and LREE enrichment. A second subset occurs within LREE enriched Group II, consisting of LREE enriched patterns ($\text{LaN/YbN}=3.0-4.5$) with a distinct concave upward appearance. This subset is restricted to volcanic rocks from the Harrison Lake Formation and associated plutonic rocks to the west.

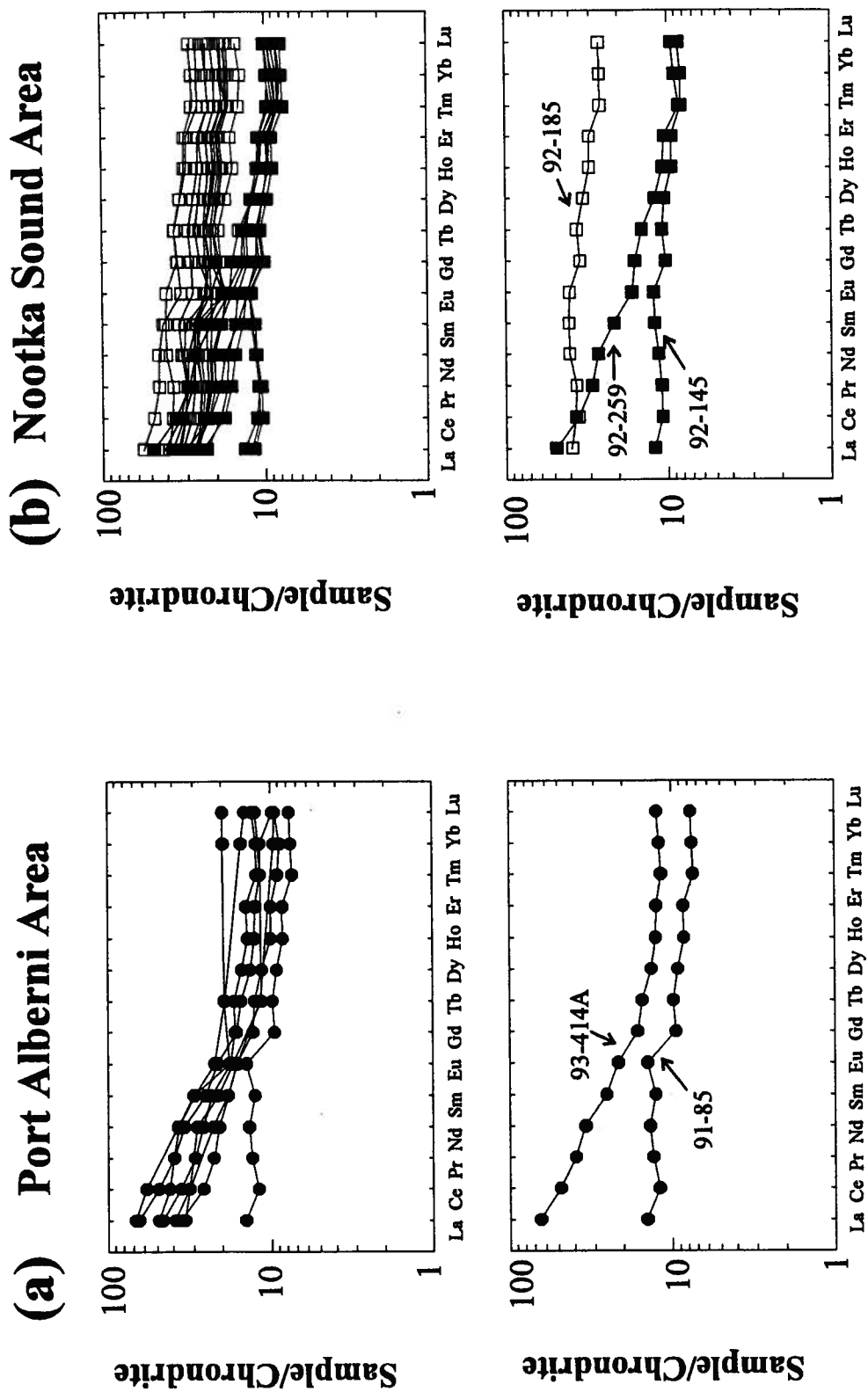


Figure 5.8 - Rare earth element diagrams for all samples, plotted according to sample area. Top diagram in each set is total sample suite, lower diagram is representative sample of each subgrouping of REE patterns. a) Port Alberni area; b) Nootka Sound area. Enriched basaltic andesite shown with open squares.

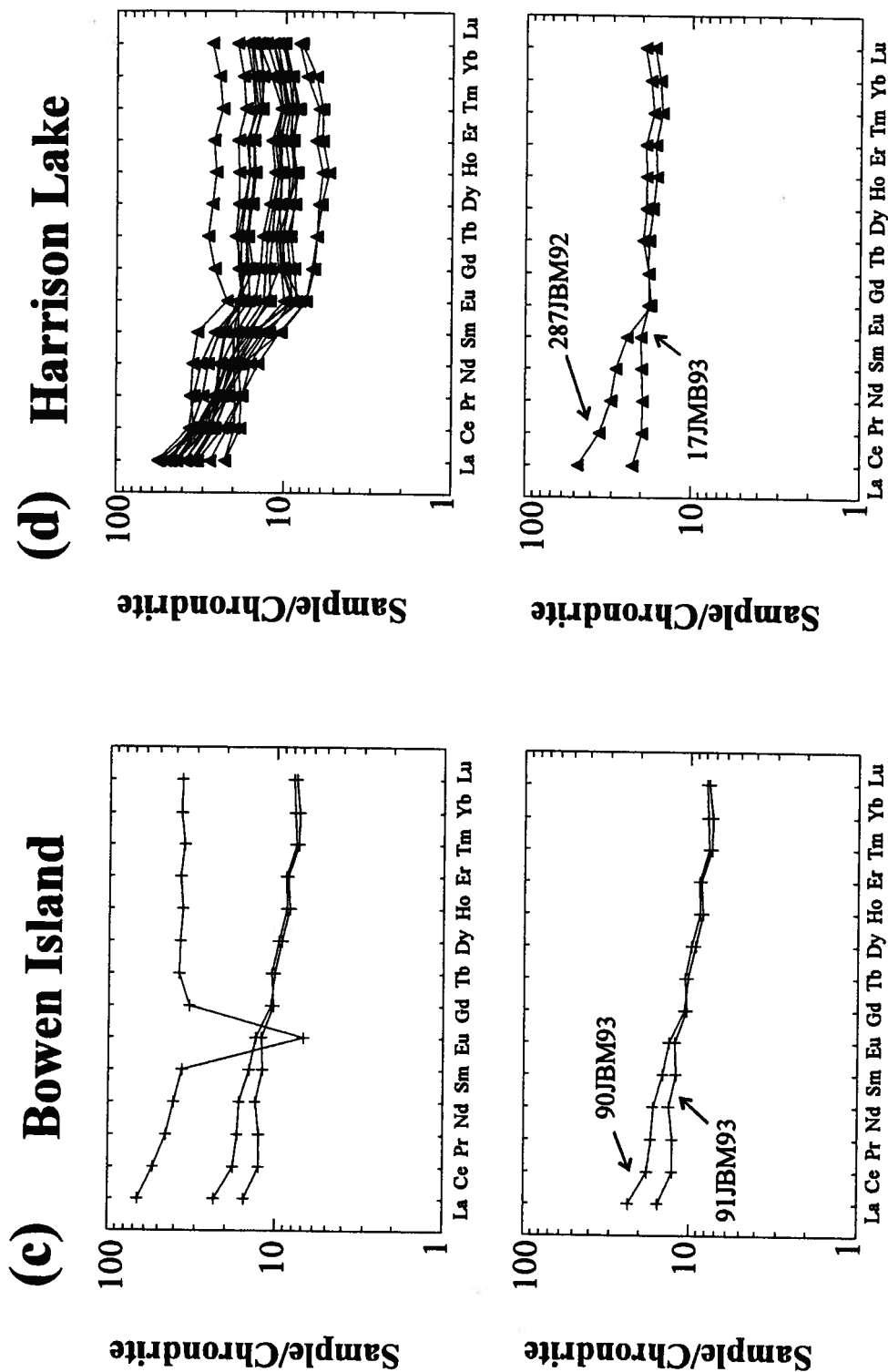


Figure 5.8 - Rare earth element diagrams for all samples, plotted according to sample area. Top diagram in each set is total sample suite, lower diagram is representative sample of each subgrouping of REE patterns. c) Bowen Island Group; d) Harrison Lake Formation. Enriched basaltic andesite shown with open squares.

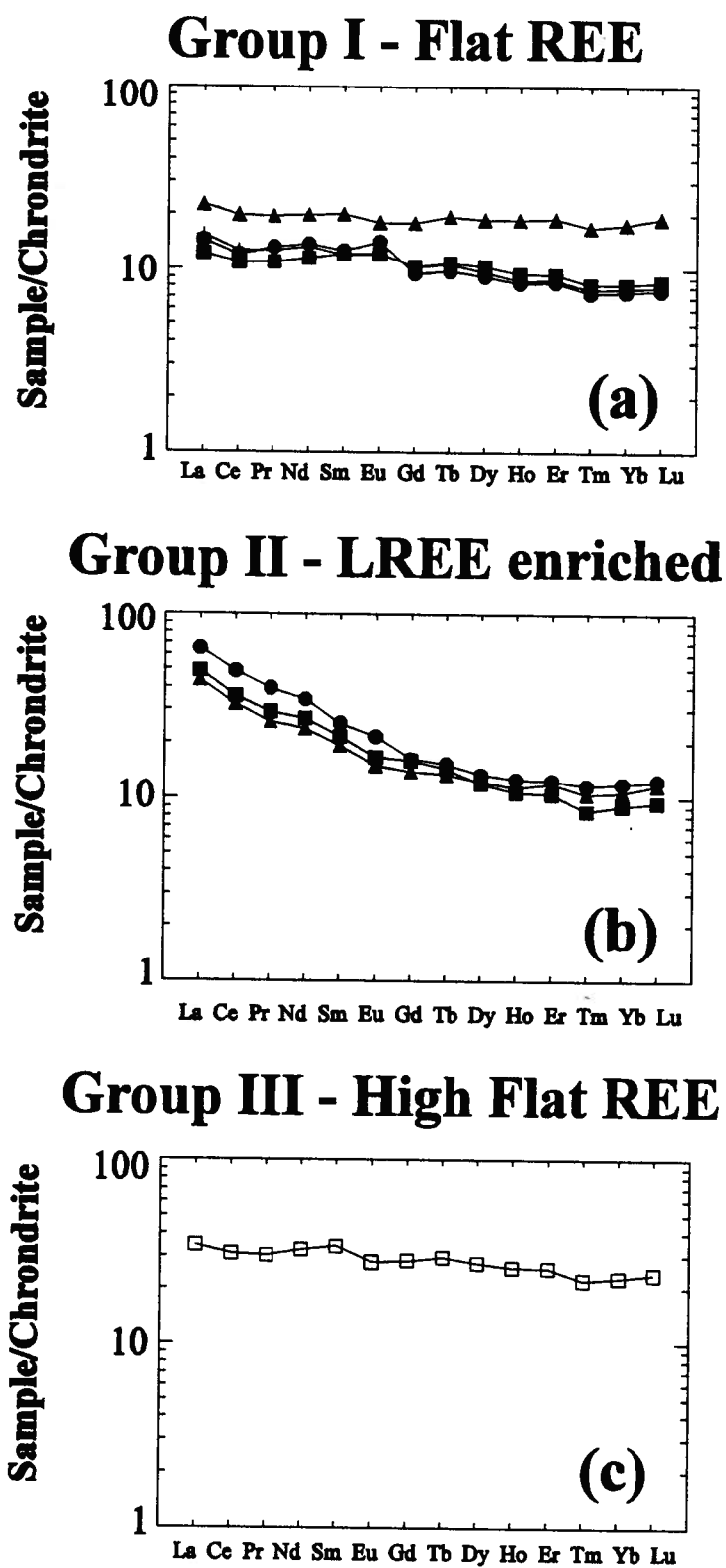


Figure 5.9 - Comparison of REE subgroups from each sample suite. Note strong similarities between patterns from all units in Group I and Group II. Group III corresponds to enriched basaltic andesite from Nootka Sound, and does not occur in other sample suites. Symbols as in figure 5.8.

III. Flat REE patterns with high total REE ($\text{LaN/YbN}=1.0\text{-}2.0$). This group has a flat to slightly LREE enriched REE pattern with relatively high REE concentrations of 20-50x chondrite (Fig. 5.8, 5.9c). This REE pattern is unique to samples from Nootka Sound, and corresponds entirely to the enriched basaltic andesite suite. The flat REE patterns from the Harrison Lake Formation have elevated REE patterns similar to the enriched basaltic andesite of Nootka Sound, but the Harrison Lake samples are placed in Group I instead of Group III due to their low TiO_2 , FeO^* , and Zr values compared to samples from Nootka Sound.

The Bonanza Group, Bowen Island Group and Harrison Lake Formation contain similar groups of REE patterns. Group I and Group II have representatives in each unit, while Group III is constrained to the Nootka Sound area (Fig. 5.9a, b, c). The consistency of REE patterns among the units suggests that each unit contains rocks derived from similar batches of magma. Group I rocks tend to have high MgO values (>6 wt %), and may represent a primitive "parental" magma common to each unit (Wilson, 1988). Group II rocks from each unit display LREE enrichment, with the magnitude of enrichment increasing from the Bonanza Group to the Harrison Lake Formation. This gradual increase in LREE enrichment may reflect an increase in crustal contamination from west to east, or may be the result of progressive differentiation of a magmatic system.

Group III REE patterns are unique to the Nootka Sound area. These samples have anomalously high TiO_2 , FeO^* , Zr, Y, and HREE concentrations compared to other Bonanza Group samples, and must have a different source. Generation of basaltic andesite of this composition require elevating TiO_2 , FeO^* , HFS elements (Zr, Y) and REE element concentrations without fractionating the REE or raising SiO_2 or K_2O contents. Significant assimilation of country rock would elevate SiO_2 and K_2O content and fractionate the REE. Direct derivation from a depleted mantle source (similar to MORB) does not account for the HFS and REE enrichment relative to MORB, and does not explain the spiked incompatible trace element pattern. Addition of a subduction component to a depleted mantle wedge would not elevate the HFSE or REE sufficiently (McCulloch and Gamble, 1991).

Barrie et al. (1991) describe enriched basalts associated with the Kamiskotia Gabbroic Complex, western Abitibi Subprovince, Ontario, Canada, that are remarkably similar to the enriched basaltic andesite suite from Nootka Sound. Barrie et al. (1991) effectively modeled the generation of the enriched basalt through 70-80% fractional crystallization of a partial melt derived from depleted mantle (MORB-like) source. The most plausible explanation for the enriched basaltic andesite of Nootka Sound is derivation from a depleted mantle source coupled with some degree of partial melting of Karmutsen Formation basalt. Karmutsen Formation basalts have SiO_2 contents < 50 weight percent, relatively high FeO^* and TiO_2 , and flat to slightly enriched REE patterns up to 13x chondrite. Interaction of magma derived from a depleted mantle wedge with gabbroic to basaltic crust near the base of the Karmutsen Formation would sufficiently elevate the FeO^* , TiO_2 , HFSE and REE evident in the Nootka Sound samples. Assimilation of small volumes of lower Karmutsen crust, perhaps coupled with periodic recharge from the depleted mantle source, would elevate HFSE and REE without raising SiO_2 content (Barrie et al., 1991).

5.7 ISOTOPIC SIGNATURES

Nd and Sr isotopic analyses were conducted on representative suites from the Bonanza Group, Bowen Island Group, and Harrison Lake Formation, including 18 samples from the Nootka Sound area, 3 samples from Bowen Island and exposures to the north, and 14 samples from the Harrison Lake area (Table 5.2). Analytical techniques are discussed in Appendix A.

Nd and Sr values for the Bonanza Group, Bowen Island Group and Harrison Lake Formation demonstrate the juvenile nature of each of the units. Initial ϵ_{Nd} values generally range from +3.5 to +7.5, and initial $^{87}\text{Sr}/^{86}\text{Sr}$ values cluster between 0.7030 and 0.7045. One sample from the Bonanza Group displays an anomalously high ϵ_{Nd} value ($\epsilon_{\text{Nd}}=11.38$). Two of the Harrison Lake Formation samples have anomalously low strontium concentrations, which lead to initial strontium values that fall below the mantle array, and suggest disturbance of the Rb/Sr isotopic system via Sr loss. Isotopic values partially overlap between units,

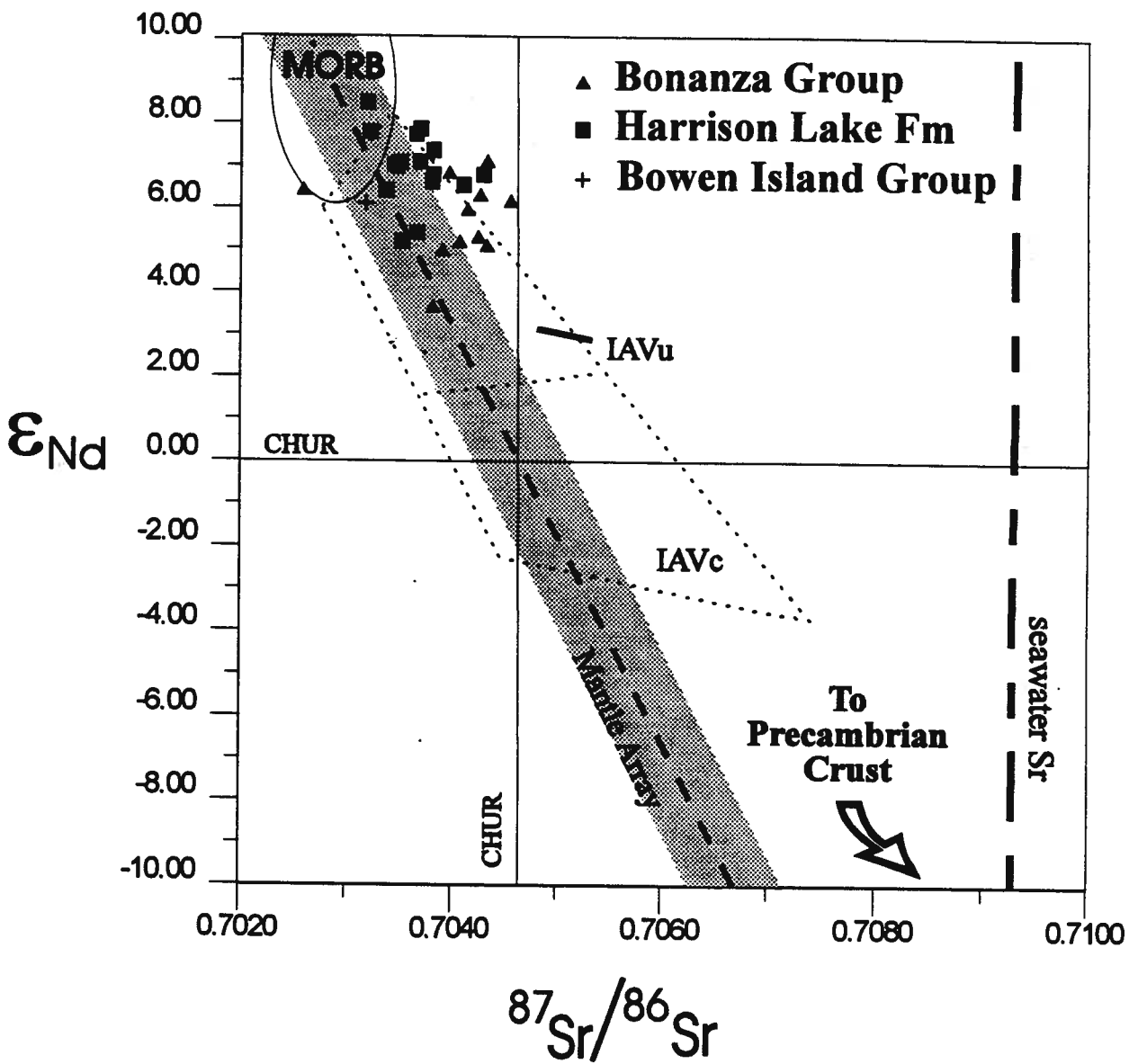


Figure 5.10 - ϵ_{Nd} vs $^{87}Sr/^{86}Sr$ diagram for all samples. Note tight cluster of data points, with distinct shift to lower more evolved values in Harrison Lake Formation. MORB = mid-ocean ridge basalt; IAVu = uncontaminated island arc volcanic rocks; IAVc = contaminated island arc volcanic rocks; CHUR = Chondritic Uniform Reservoir (DePaolo and Wasserburg, 1976).

| Age | 87Sr/86Sr(i) | +/- | Rb | Sr | 7Rb/86S | 87Sr/86Sr(i) | Sm | Nd | Sm/Nd | f | 143/144 | +/- | Epsilon Nd | Ep Nd(i) |
|--|--------------|----------|----|-------|---------|--------------|----------|------|-------|--------|---------|----------|------------|----------|
| Harrison Lake Formation Volcanics | | | | | | | | | | | | | | |
| 04jbm92 | 175 | 0.704426 | 13 | 7.25 | 182.23 | 0.12 | 0.704139 | 3.65 | 12.09 | 0.1849 | -0.060 | 0.512923 | 6 | 5.56 |
| 116jbm92 | 175 | 0.705011 | 18 | 25.68 | 268.03 | 0.28 | 0.704321 | 3.81 | 16.22 | 0.1414 | -0.281 | 0.512834 | 4 | 3.82 |
| 142jbm92 | 175 | 0.713681 | 26 | 66.77 | 39.75 | 4.86 | 0.701588 | 3.76 | 16.00 | 0.1419 | -0.278 | 0.512824 | 4 | 3.63 |
| 151jbm92 | 175 | 0.705164 | 13 | 14.45 | 168.71 | 0.25 | 0.704547 | 6.25 | 23.82 | 0.1590 | -0.192 | 0.512904 | 9 | 5.19 |
| 287jbm92 | 175 | 0.705057 | 11 | 35.93 | 317.53 | 0.33 | 0.704241 | 3.46 | 15.03 | 0.1399 | -0.289 | 0.512838 | 9 | 3.90 |
| 291jbm92 | 175 | 0.706683 | 10 | 48.62 | 122.09 | 1.15 | 0.703816 | 5.65 | 18.95 | 0.1801 | -0.084 | 0.512800 | 11 | 3.16 |
| 307jbm92 | 175 | 0.704190 | 26 | 17.38 | 78.31 | 0.64 | 0.702592 | 4.60 | 16.98 | 0.1626 | -0.173 | 0.512921 | 11 | 5.52 |
| 13jbm93 | 175 | 0.704005 | 17 | 1.16 | 218.06 | 0.02 | 0.703967 | 2.98 | 13.03 | 0.1387 | -0.237 | 0.512915 | 5 | 5.40 |
| 14jbm93 | 175 | 0.704422 | 16 | 2.68 | 201.19 | 0.04 | 0.704326 | 2.18 | 10.35 | 0.1274 | -0.352 | 0.512916 | 10 | 5.42 |
| 15jbm93 | 175 | 0.706820 | 49 | 57.97 | 151.42 | 1.11 | 0.704064 | 5.50 | 20.44 | 0.1627 | -0.173 | 0.512858 | 13 | 4.29 |
| 17jbm93 | 175 | 0.704325 | 21 | 0.92 | 115.08 | 0.02 | 0.704268 | 4.12 | 13.95 | 0.1786 | -0.237 | 0.512932 | 6 | 5.74 |
| 21jbm93 | 175 | 0.704464 | 17 | 25.32 | 323.94 | 0.23 | 0.703901 | 4.42 | 17.22 | 0.1552 | -0.211 | 0.512839 | 9 | 3.92 |
| 22jbm93 | 175 | 0.705464 | 19 | 22.96 | 136.92 | 0.49 | 0.704256 | 3.18 | 14.42 | 0.1332 | -0.323 | 0.512822 | 3 | 4.76 |
| 25jbm93 | 175 | 0.705628 | 13 | 38.98 | 153.91 | 0.73 | 0.703805 | 3.13 | 14.94 | 0.1267 | -0.356 | 0.512889 | 8 | 4.90 |
| Bowen Island Group Volcanics | | | | | | | | | | | | | | |
| 90jbm93 | 185 | 0.703528 | 22 | 16.62 | 359.90 | 0.13 | 0.703176 | 2.86 | 11.31 | 0.1533 | -0.221 | 0.512891 | 10 | 4.94 |
| 91jbm93 | 185 | 0.703808 | 32 | 11.81 | 628.82 | 0.05 | 0.703808 | 2.46 | 09.15 | 0.1631 | -0.171 | 0.51296 | 5 | 6.28 |
| Bonanza Group Volcanics | | | | | | | | | | | | | | |
| 92-145 | 195 | 0.704100 | 16 | 7.50 | 205.34 | 0.11 | 0.703807 | 2.29 | 07.48 | 0.1847 | -0.061 | 0.512957 | 13 | 6.22 |
| 92-153 | 195 | 0.703401 | 18 | 3.32 | 127.90 | 0.08 | 0.703192 | 1.06 | 02.12 | 0.3016 | 0.533 | 0.513198 | 8 | 10.92 |
| 92-169 | 195 | 0.704051 | 15 | 23.02 | 319.97 | 0.21 | 0.703474 | 2.69 | 08.74 | 0.1862 | -0.053 | 0.512975 | 4 | 6.57 |
| 92-170 | 195 | 0.704775 | 19 | 35.69 | 264.42 | 0.39 | 0.703692 | 7.89 | 26.57 | 0.1795 | -0.087 | 0.513011 | 10 | 7.28 |
| 92-177 | 195 | 0.704957 | 15 | 64.59 | 451.60 | 0.41 | 0.703810 | 2.80 | 10.59 | 0.1590 | -0.192 | 0.513173 | 26 | 10.44 |
| 92-185 | 195 | 0.708436 | 12 | 59.61 | 94.38 | 1.83 | 0.703368 | 8.14 | 26.90 | 0.1808 | -0.081 | 0.512939 | 9 | 5.87 |
| 92-187 | 195 | 0.706763 | 20 | 59.63 | 153.80 | 1.12 | 0.703652 | 5.84 | 19.98 | 0.1768 | -0.101 | 0.513001 | 9 | 7.08 |
| 92-235 | 195 | 0.706584 | 19 | 61.71 | 178.85 | 1.00 | 0.703815 | 8.63 | 31.62 | 0.1650 | -0.161 | 0.512967 | 5 | 6.42 |
| 92-241 | 195 | 0.706474 | 13 | 53.41 | 195.97 | 0.79 | 0.704287 | 5.53 | 20.09 | 0.1655 | -0.159 | 0.512939 | 7 | 5.87 |
| 92-244 | 195 | 0.704235 | 18 | 25.52 | 280.89 | 0.26 | 0.703506 | 5.14 | 17.16 | 0.1802 | -0.084 | 0.512972 | 8 | 6.52 |
| 92-249 | 195 | 0.704297 | 87 | 32.60 | 308.61 | 0.31 | 0.703450 | 2.20 | 07.30 | 0.1821 | -0.074 | 0.512972 | 4 | 6.52 |
| 92-252 | 195 | 0.703871 | 15 | 22.98 | 282.44 | 0.24 | 0.703218 | 5.44 | 19.39 | 0.1697 | -0.137 | 0.512957 | 7 | 6.96 |
| 92-256 | 195 | 0.704237 | 17 | 6.71 | 128.00 | 0.15 | 0.703817 | 5.45 | 19.36 | 0.1796 | -0.087 | 0.512957 | 5 | 6.22 |
| 92-258 | 195 | 0.704460 | 19 | 29.75 | 309.80 | 0.28 | 0.703689 | 4.57 | 15.73 | 0.1753 | -0.109 | 0.512967 | 9 | 6.42 |
| 92-259 | 195 | | 20 | 49.78 | 104.68 | 1.38 | 0.704102 | 5.02 | 18.41 | 0.1652 | -0.160 | 0.512926 | 5 | 5.62 |
| 92-261 | 195 | 0.704477 | 12 | 47.50 | 396.83 | 0.35 | 0.703516 | 4.33 | 17.48 | 0.1499 | -0.238 | 0.512837 | 6 | 3.88 |
| 92-270 | 195 | | 15 | 34.65 | 455.55 | 0.22 | 0.703662 | 2.83 | 10.87 | 0.1576 | -0.199 | 0.512858 | 5 | 4.29 |

Table 5.2 - Isotopic data for the Bonanza Group, Bowen Island Group, Harrison Lake Formation, and associated Middle Jurassic plutons.

and are within the range of uncontaminated island arc volcanic rocks (Fig. 5.10). The isotopic values plot very near the MORB field, demonstrating a strong depleted mantle component in the source region (McCulloch and Gamble, 1991). Initial Sr values are displaced to the right of the mantle array, consistent with an influx of evolved Sr from seawater-altered oceanic crust in the descending slab (White and Patchett, 1984; McCulloch and Gamble, 1991).

A comparison of ϵ_{Nd} with $f_{Sm/Nd}$, an expression of the Sm/Nd ratio of the rock relative to chondritic values ($f_{Sm/Nd} = (^{147}Sm/^{144}Nd)_{sample}/^{147}Sm/^{144}Nd_{CHUR} - 1$; Shirey and Hanson, 1986), evaluates the LREE enrichment of a rock suite relative to its isotopic signature (Fig. 5.11). Differences in LREE enrichment between rock suites correspond to differences in $f_{Sm/Nd}$ values, resulting in vertical displacement of points on this diagram. LREE enrichment results in lower values, and LREE depletion results in higher values. The restricted isotopic range of the Bonanza Group, Bowen Island Group, and Harrison Lake Formation contrasts markedly with the range of LREE enrichment evident in them. Note that, while there is significant overlap between the rock units, the Harrison Lake Formation is generally more LREE enriched than the Bonanza Group over the same range of isotopic values. The higher degree of LREE enrichment in the Harrison Lake Formation compared to the other units could be the result of fractional crystallization of a single magmatic system, differences in the type of crust the magmas interacted with, or entirely separate magmatic histories. The gradational nature of the LREE enrichment coupled with the restricted range of isotopic values argues for similar source characteristics of the Bonanza Group, Bowen Island Group, and Harrison Lake Formation.

Bonanza Group, Bowen Island Group, and Harrison Lake Formation isotopic values partially overlap in ϵ_{Nd} - $^{87}Sr/^{86}Sr$ isotopic space, but there is a distinct shift to lower ϵ_{Nd} and higher $^{87}Sr/^{86}Sr$ values from the Bonanza Group to the Harrison Lake Formation. The majority of the Bonanza Group and Bowen Island Group rocks have initial ϵ_{Nd} values within the range of MORB, and that the Harrison Lake Formation values are distinctly shifted to lower ϵ_{Nd} values by up to 3 ϵ_{Nd} units. Island arc volcanic rocks commonly display a downward shift in ϵ_{Nd} values relative to MORB/depleted mantle values; this shift is normally attributed to

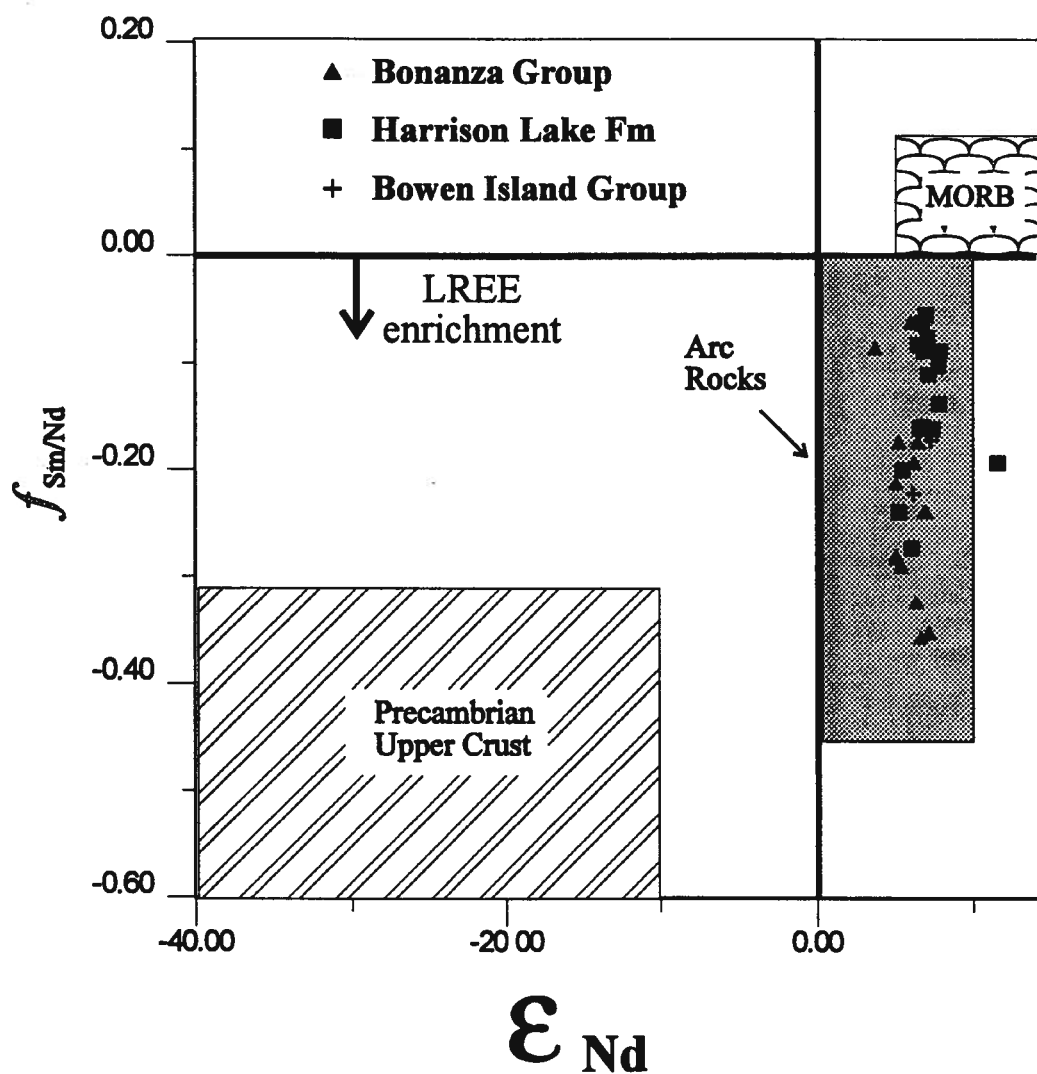


Figure 5.11 - $f_{\text{Sm/Nd}}$ versus ϵ_{Nd} diagram for all samples. Note wide range of LREE enrichment as opposed to tight range of ϵ_{Nd} values.

sediment subduction and consequent enrichment of depleted mantle in the mantle wedge (White and Patchett, 1984; McCulloch and Gamble, 1991). An increase in sediment subduction through time would explain the shift in ϵ_{Nd} values between the Bonanza Group and the generally younger Harrison Lake Formation, or the difference may be the result of magmatic interaction with different types of crust. The latter hypothesis is supported by the presence of an inherited component evident in the U-Pb systematics of zircon derived from rhyolite in the upper portion of the Harrison Lake Formation (Chapter 4). Distinctly concave upward REE patterns evident in a subset of Group II REE patterns also support some level of crustal interaction in the Harrison Lake Formation (Hanson, 1980).

The proposed partial melting of lower crust to explain the isotopic shift between the Bonanza Group and Harrison Lake Formation does not preclude crustal involvement in the generation of Bonanza Group and Bowen Island Group rocks. There is ample evidence of partial melting of lower crust in the Bonanza Group, including abundant amphibolitic inclusions in the comagmatic Westcoast Complex (Debari and Mortensen, 1994), Paleozoic inheritance in zircon from the comagmatic Island Intrusions (Parrish and McNichol, 1993), and the presence of the enriched basaltic andesite of Nootka Sound. The primary difference in the isotopic signature between the different units is probably not the degree of partial melting, but a *difference in the type of crust* that the ascending magma interacted with. The crust beneath the Bonanza Group and Bowen Island Group consists of Paleozoic juvenile arc material and Early Mesozoic Kartmutsen Formation basalt, whereas crust beneath the Harrison Lake Formation is Triassic ocean floor and an unknown quantity of older material (Friedman and Cui, 1994).

5.8 CONSTRAINTS ON ARC CORRELATION

A. Lithostratigraphic Considerations

The Bonanza Group and Harrison Lake Formation both display rapid lateral and vertical facies changes, and consist of interdigitated lava flows, breccias, tuff breccias, lapilli tuff, tuff, and associated

volcaniclastic sedimentary rocks. The four-fold subdivision applied to the Harrison Lake Formation (Arthur, 1987, 1993; Mahoney et al., 1994; Chapter 4) is comparable with local subdivisions evident in the Bonanza Group (Jeletsky, 1976; Nixon et al., 1994); these subdivisions are readily applicable over 10's of square kilometres, but break down over larger areas. Correlations of these successions must therefore be based on contact relations with adjacent strata and permissible age constraints.

The gradational contact at the base of the Bonanza Group represents the initiation of volcanism in Early Jurassic time. Nixon et al. (1994) propose a two-fold stratigraphy on northern Vancouver Island, consisting of a lower, regionally persistent, predominantly subaqueous epiclastic-pyroclastic succession that shoals upward into a subaerial, laterally variable, succession composed of lava flows and associated pyroclastic rocks. The subaerial rocks comprise the vast majority of the section (Nixon et al., 1994). The coarsening upward succession is interpreted by Nixon et al. (1994) to represent the gradual emergence of a volcanic island arc from submarine to subaerial in the Early Jurassic. The predominance of Sinemurian and Pliensbachian marine fauna intercalated with volcanic strata in the Bonanza Group suggests at least part of the arc was intermittently inundated by marine waters until at least the Late Pliensbachian.

The Bowen Island Group contains interbedded black argillite and varicolored tuff intercalated with volcanic flows. The sediment-dominated northwestern portion of the outcrop belt contains probable Sinemurian fossils, and the volcanic dominated southeastern portion contains Toarcian rhyolite flows. Structural complexities and intrusion preclude accurate stratigraphic assessment, but the facies distribution in the Bowen Island sequence is consistent with tuffaceous marine strata overlain by proximal volcanic strata, in a manner similar to the Bonanza Group.

The basal conglomerate of the Harrison Lake Formation records localized uplift and erosion in Early Jurassic time, followed by sub-wave base deposition of marine fine-grained clastic rocks. Tuff intercalated with the marine strata indicate initiation of volcanism in the late Early Toarcian. Thin bedded, fine grained marine strata grade upward into thick bedded coarse grained tuffaceous sandstone and conglomerate, overlain by

volcanic breccia and lava flows. This coarsening upward succession in the Harrison Lake Formation records the gradual emergence of a volcanic island arc in Early to Middle Jurassic time.

It is suggested herein that the initial pyroclastic and epiclastic sedimentation in the Harrison Lake Formation may correspond with active subaerial volcanism in the Bonanza Group. Nixon et al. (1994) document ash flow tuff sheets and caldera collapse features indicating explosive volcanism in the Bonanza Group. Tuffaceous strata in the lower (?) Bowen Island Group and lower Harrison Lake Formation may be distal equivalents to ash flow deposits in the Bonanza Group. Similarly, active submarine and subaerial volcanism in the Harrison Lake Formation may correspond to the pyroclastic and epiclastic succession overlying volcanic rocks of the Bonanza Group (Jeletsky, 1976; Muller et al., 1981).

Strata of the Bonanza Group and Harrison Lake Formation are unconformably overlain by shallow marine clastic strata of Callovian age.

B. Temporal Considerations

Age relations between the Bonanza Group, Bowen Island Group, and Harrison Lake Formation can be used to infer the time transgressive development of a volcanic arc system. Initial development of the arc began in Sinemurian time in the Bonanza Group, and emergence of the Bonanza Group as a subaerial edifice may correspond to the delivery of air fall tuff to Sinemurian strata of the Harbledown Formation and lower (?) Bowen Island Group (Tipper et al., 1991). Continued development of the volcanic edifice may have been responsible for delivery of conglomeratic debris to the base of the Harrison Lake Formation (Celia Cove Member), and perhaps was a causative factor in the subsidence evident in the lower Harrison Lake Formation (Francis Lake Member). Late early Toarcian pyroclastic activity in the Bonanza Group and/or Bowen Island Group may have supplied tuffaceous material to the lower Harrison Lake Formation.

Eastward migration of the main locus of volcanism may have progressed from Sinemurian to Late Pliensbachian (or younger) in the Bonanza Group to Toarcian in the Bowen Island Group, to Aalenian to Late Bajocian in the Harrison Lake Formation. This eastward migration of volcanism encompasses 30-35 Ma, which is a time frame comparable to long-lived Tertiary systems of the western Pacific (Park et al., 1990)

C. Geochemical Considerations

The overall geochemical coherence of the Bonanza Group, Bowen Island Group, and Harrison Lake Formation indicates the units share very similar magmatic histories. Systematic trends on Harker diagrams and immobile compatible element plots may be attributed to progressive differentiation of the magmatic system (Pearce, 1982; Wilson, 1988; MacLean and Barrett, 1994). These systematic trends are not definitive indicators of a cogenetic relationship, but are consistent with derivation of the Bonanza Group, Bowen Island Group, and Harrison Lake Formation volcanic rocks from similar sources, perhaps within a single magmatic system. There is an overall trend from tholeiitic to calcalkaline andesitic basalt and andesite in the Bonanza Group to calcalkaline andesite to rhyolite in the Harrison Lake Formation. Incompatible trace element patterns for all units display enrichment of LIL elements relative to HFS elements, and the LILE/HFSE ratio systematically increases from the Bonanza Group through to the Harrison Lake Formation. Incompatible element ratio diagrams suggest similar degrees of source enrichment for each unit, and are consistent with fractionation of a magmatic system derived from a depleted mantle source (Pearce, 1982). Similar groups of REE patterns are displayed by each unit, suggesting derivation from different batches of magma displaying similar source characteristics.

The primary difference between the units is the existence of enriched basaltic andesite in the Nootka Sound region, which is attributed to partial melting of basaltic lower crust, probably the Karmutsen Formation. The Karmutsen Formation basalt has not been documented beneath the Bowen Island Group or the Harrison Lake Formation, units which do not contain enriched basaltic andesite.

D. Isotopic Considerations

Nd and Sr isotopic data for the Bonanza Group, Bowen Island Group and Harrison Lake Formation demonstrate the juvenile nature of the volcanic rocks, and strongly suggest magma derivation from an uncontaminated depleted mantle source (McCulloch and Gamble, 1991). Displacement of initial Sr values to the right of the mantle array indicates similar levels of Sr enrichment in each of the units (White and Patchett, 1984).

Evaluation of $f_{\text{Sm/Nd}}$ values against ϵ_{Nd} demonstrates progressive LREE enrichment from the Bonanza Group to the Harrison Lake Formation (Shirey and Hanson, 1986). This LREE enrichment may be the result of fractional crystallization, or the result of magma interaction with different crustal sections. Fractional crystallization, however, does not account for the initial difference in ϵ_{Nd} values between the Bonanza Group and the Harrison Lake Formation. The observed isotopic shift is greater than the variation expected from a homogeneous source, and suggests differing degrees of crustal interaction between the Bonanza Group and Harrison Lake Formation. The isotopic and geochemical data are consistent with formation of the Bonanza Group, Bowen Island Group, and Harrison Lake Formation in a single volcanic arc system. Isotopic and geochemical variations across the arc result from the ascent of magma derived from an uncontaminated depleted mantle wedge through different crustal sections.

E. Structural Considerations

Structural evidence for a common history for the Bonanza Group, Bowen Island Group, and Harrison Lake Formation includes evidence for contemporaneous deformation, intrusion by coeval plutons along the margins of the Coast Plutonic Complex, and geophysical constraints.

Each of the units displays evidence of pre-Callovian structural deformation. The Bonanza Group and underlying Vancouver Group are locally overlain with angular unconformity by Callovian strata of the

Kyoquot Group in west-central Vancouver Island (Muller et al., 1974). Elsewhere on the Island, the Bonanza Group is unconformably overlain by Lower Cretaceous strata. East of Vancouver Island, a ductile fault cutting post-Karmutsen strata on Quadra Island is intruded by a 163.8 Ma pluton (Monger and McNichol, 1994), suggesting post-Late Triassic, pre-Callovian ductile deformation. Isoclinally folded Bowen Island Group strata are cut by 155-160 Ma plutons, arguing for post-185, pre-155 Ma deformation (Monger, 1993; Friedman and Armstrong, 1994). Late Bajocian to early Bathonian strata of the Harrison Lake Formation contain mesoscopic tight folds and overturned bedding that are absent in overlying Callovian strata.

Wrangellia and Harrison terranes are separated by Jurassic and Cretaceous plutons of the Coast Plutonic Complex. The eastern edge of Wrangellia is intruded by Middle to Late Jurassic plutons as old as 178 Ma (Webster and Ray, 1990), coeval with the Island Intrusions, which are considered comagmatic to the Bonanza Group. The western edge of the Harrison terrane is intruded by Middle Jurassic plutons and satellite stocks as old as 167 Ma (Friedman and Armstrong, 1994). The age of the plutons intruding the western edge of the Harrison terrane overlap the age of a rhyolite dome in the upper portion of the Harrison Lake Formation. The Bonanza Group and Harrison Lake Formation are both intruded by plutonic rocks that are geochemically and isotopically identical to the coeval volcanics. The plutonic rocks are interpreted herein as the plutonic roots to the Middle Jurassic volcanic system. The Middle Jurassic plutons are apparently restricted to the eastern and western edge of the pre-90 Ma Coast Plutonic Complex (Friedman and Armstrong, 1994), with younger plutons forming margin-parallel belts in the interior of the complex. I propose that the current distribution of the Wrangellia and Harrison terranes is at least in part an artifact of extension induced by the emplacement of younger plutons.

Seismic reflection and refraction data in the southern Coast Belt suggest that Wrangellia and Harrison terranes and intervening plutons form a coherent crustal block (Zelt et al, 1991). Geophysical data demonstrate a distinct change in crustal velocity from rocks of Wrangellia and Harrison terranes to rocks to the east in the vicinity of the Harrison Lake fault, but do not resolve any major crustal structures between the Harrison and Wrangellia terranes (Zelt et al., 1993; O'Leary et al., 1993). The suggestion that Wrangellia and

Harrison terranes form a coherent crustal block agrees with the observations of Journeay and Friedman (1993), who argue these rocks acted as a coherent structural block during Cretaceous compression.

CONCLUSIONS

This investigation represents the first integrated study into the geology, geochemistry, and isotopic characteristics of the Bonanza Group, Bowen Island Group, and Harrison Lake Formation. Stratigraphic, geochemical, isotopic and age considerations suggest that Lower to Middle Jurassic strata of Wrangellia and Harrison terranes originally formed a contiguous arc sequence built upon different Triassic basements. The arc was initiated in the Early Jurassic on Wrangellia, and the locus of volcanism swept eastward from Sinemurian to Bajocian time. Volcanism ceased in the Late Bajocian or earliest Bathonian, and was followed by post-early Bathonian, pre-Calloviaian deformational events of varying intensity. The formation of the Bonanza-Harrison arc requires juxtaposition of Triassic rocks of Wrangellia and Harrison terranes prior to the Early Jurassic. The Bonanza-Harrison arc represents the first stage of magmatism associated with the Coast Plutonic Complex magmatic arc.

CHAPTER 6

REGIONAL TECTONOSTRATIGRAPHIC CORRELATIONS IN THE SOUTHERN CANADIAN CORDILLERA: IMPLICATIONS FOR JURASSIC TERRANE LINKAGES AND BASIN EVOLUTION

6. REGIONAL TECTONOSTRATIGRAPHIC CORRELATIONS IN THE SOUTHERN CANADIAN CORDILLERA: IMPLICATIONS FOR JURASSIC TERRANE LINKAGES AND BASIN EVOLUTION

6.1 INTRODUCTION

The southwestern Canadian Cordillera is a complex mosaic of tectonostratigraphic terranes juxtaposed by regional fault systems and intruded by Jurassic to Tertiary plutons (Fig. 6.1). The terranes have been described as island arc systems, oceanic floor assemblages, accretionary complexes, and other fragments of tectonic flotsam that were accreted to the western margin of North America in the Mesozoic (Coney et al., 1980). The Mesozoic paleogeographic distribution of the terranes is uncertain, as is the timing, sequence, and mechanism of their amalgamation to the continental margin. The pre-accretionary configuration of the terranes that presently comprise the southern Canadian Cordillera has important implications for the tectonic evolution of the region.

A number of models of tectonic evolution have been proposed to explain the amalgamation of terranes in the Canadian Cordillera. These models fall into three general categories:

- 1) early Late Cretaceous accretion of the Insular Superterrane (Terrane II of Monger et al. (1982), comprising amalgamated Wrangellia, Alexander, and Peninsula terranes) with previously accreted terranes of the Intermontane Superterrane (Terrane I of Monger et al. (1982), primarily Cache Creek, Quesnellia, and Stikinia terranes; Monger et al., 1982; Garver, 1992; Garver and Brandon, 1994);

- 2) Middle to Late Jurassic dextral translation and oblique transpression of Insular Superterrane with concomitant development of transtensional rift basins along the western margin of the Intermontane Superterrane (Gehrels and Saleeby, 1985; Saleeby and Busby-Spera, 1992; McClelland et al., 1992);

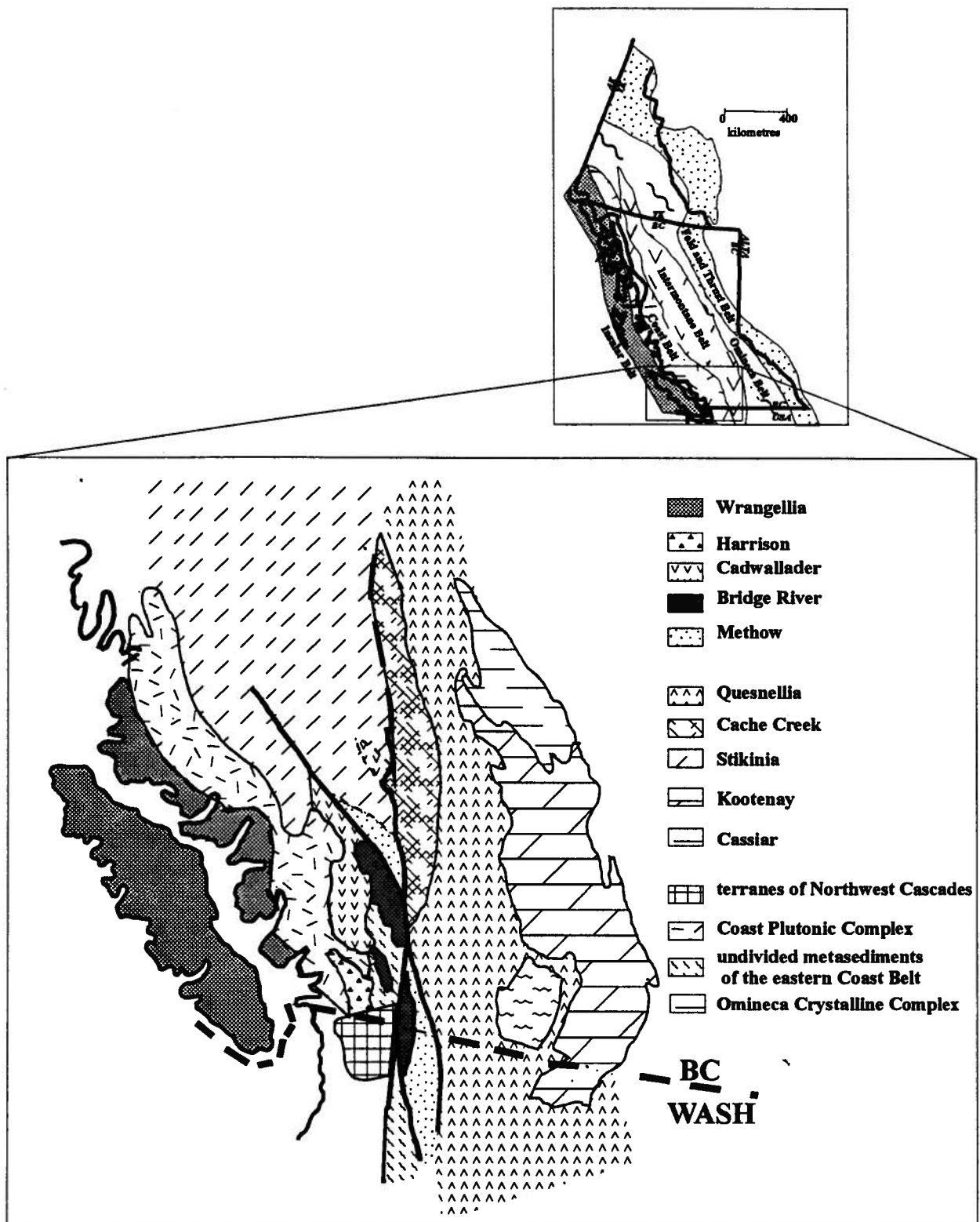


Figure 6.1 - Generalized terrane map of the southern Canadian Cordillera, showing major structures and intrusive complexes. Inset map shows location within morphogeologic belts of the Canadian Cordillera.

3) Middle Jurassic accretion of all terranes and the development of an Andean-Sierran type continental arc, accompanied by Late Jurassic to early Late Cretaceous intra-arc rifting and basin development (van der Heyden, 1992). Critical evaluation of any of these proposed models requires definitive evidence of terrane linkages.

Terranes of the southern Canadian Cordillera include, from west to east, Wrangellia, Harrison, Cadwallader, Bridge River, Methow, and Quesnellia. Each of these terranes contains Lower to Middle Jurassic volcanic arc rocks or volcanoclastic sediments that overlie Triassic and older basement and are overlain by Cretaceous coarse-grained clastic strata (Fig. 6.1). Most workers agree that Lower Cretaceous coarse clastic rocks, particularly polymict, granitoid-bearing conglomerates, provide a stratigraphic link amongst all the terranes. Earlier stratigraphic linkages are more tenuous, and are the subject of this investigation. Links between the Harrison, Cadwallader, Bridge River, and Methow terranes are of particular importance, because these terranes straddle the boundary between rocks traditionally assigned to the Insular and Intermontane Superterranes (Monger et al., 1982; Gehrels and Saleeby, 1985; van der Heyden, 1992).

This investigation examines the lithostratigraphy, biostratigraphy, volcanic geochemistry, Nd and Sr isotopic characteristics, and depositional setting of Middle Jurassic strata in the southern Canadian Cordillera. These data are used to evaluate the stratigraphic evolution of each terrane, document geologic similarities or differences between terranes, propose stratigraphic correlations, and develop a comprehensive basin evolution model for Middle Jurassic strata in the region.

6.2 GEOLOGIC SETTING

Middle Jurassic strata in the southern Canadian Cordillera occur within Wrangellia, Harrison, Cadwallader, Bridge River, Methow, and Quesnellia terranes (Figs. 6.1, 6.2). Late Jurassic to Tertiary structural deformation and magmatic activity have obscured the original structural and stratigraphic relationships between terranes. The current distribution of terranes is controlled primarily by regional

structures of Late Cretaceous to Tertiary age and by Late Jurassic to Tertiary plutons (Monger and Journeay, 1992, 1994; Journeay and Monger, 1994; Figs 6.1, 6.2; Plate 1).

Plutonic rocks locally comprise over 80% of all exposures, particularly in the southwestern Coast Belt (Fig. 3.2, Plate 1). Early Jurassic and older plutons are found primarily in Quesnellia and Wrangellia. Middle to Late Jurassic plutons intrude Wrangellia, Harrison, and Quesnellia terranes, but have not been documented in the Methow, Bridge River, and Cadwallader terranes. Late Early Cretaceous to Early Tertiary plutonic rocks form broad northwest-trending belts that intrude all terranes and cut terrane boundaries throughout the region (Friedman and Armstrong, 1994). Metamorphic grade varies throughout the region, but rarely exceeds lower greenschist grade, with the exception of amphibolite grade rocks in the imbricate zone of the Coast Belt Thrust System (Journeay and Friedman, 1993).

The structural setting of the southern Canadian Cordillera is dominated by post-100 Ma structures; older structures exist, but their timing is difficult to resolve. Pre-100 Ma, terrane specific structures are known only from Quesnellia and Wrangellia, although Late Triassic blueschist occurs in melange of the Bridge River terrane (Monger and Journeay, 1992; Archibald et al., 1990). Late Early Cretaceous to Tertiary west- and east-directed contractional faults, dextral strike-slip faults, and minor sinistral and extensional faults disrupt internal terrane stratigraphies and cut across terrane boundaries (Wheeler and McFeely, 1991; Journeay and Monger, 1994; Plate 1).

A. Terrane Distribution

Wrangellian strata are separated from smaller terranes to the east by Middle Jurassic to Tertiary magmatic suites of the Coast Plutonic Complex. Correlations between Middle Jurassic volcanic arc assemblages of Wrangellia and Harrison terranes were proposed in the preceding chapter. Between the Coast Plutonic Complex and the Yalakom-Hozameen and Fraser fault systems (Fig. 6.2), portions of the Harrison, Cadwallader, Bridge River and Methow terranes are imbricated within the late Early Cretaceous west-directed

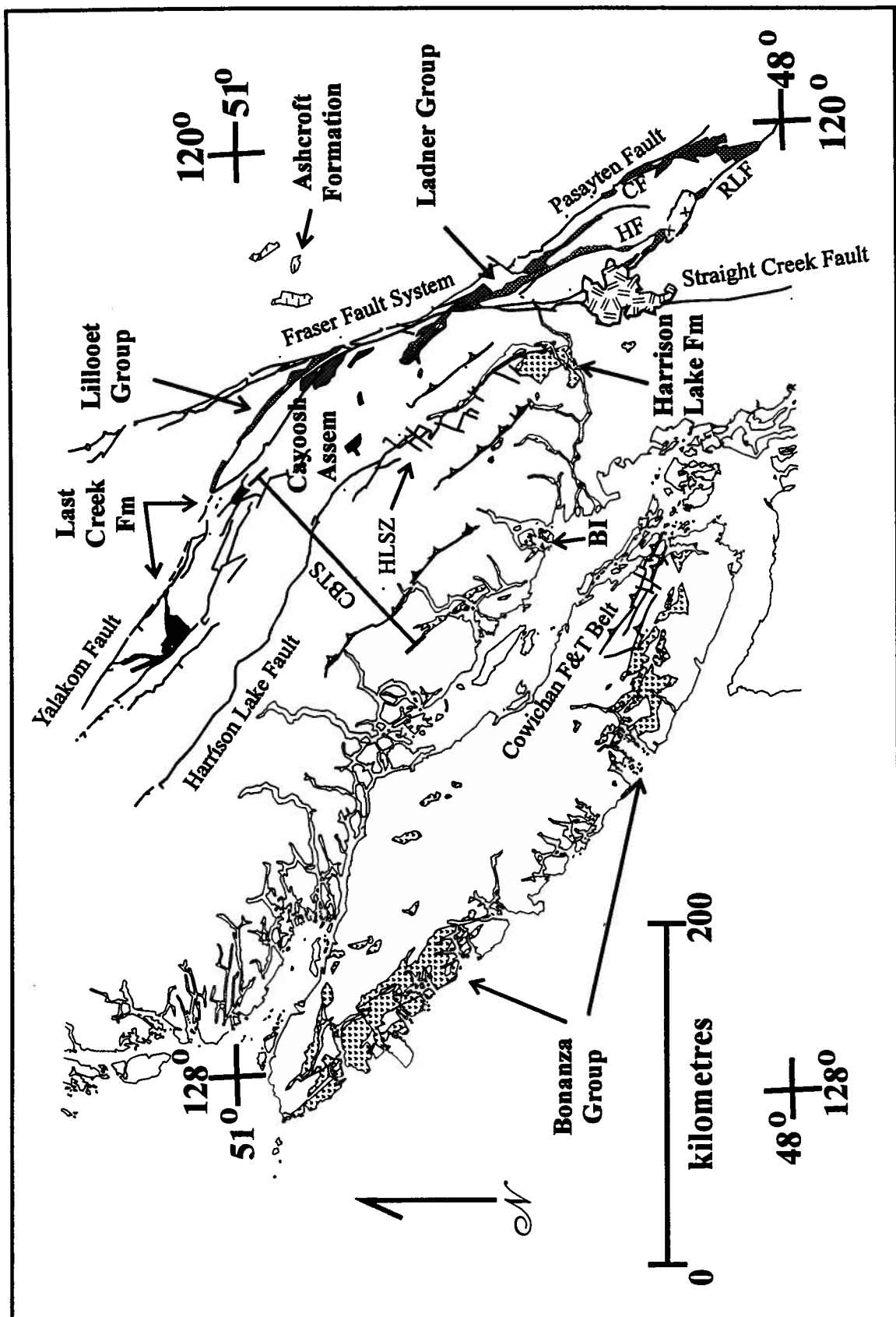


Figure 6.2 - Schematic geologic map of the eastern Coast Belt and western Intermontane Belt, showing distribution of Lower to Middle Jurassic strata. Compare to Fig. 3.2.

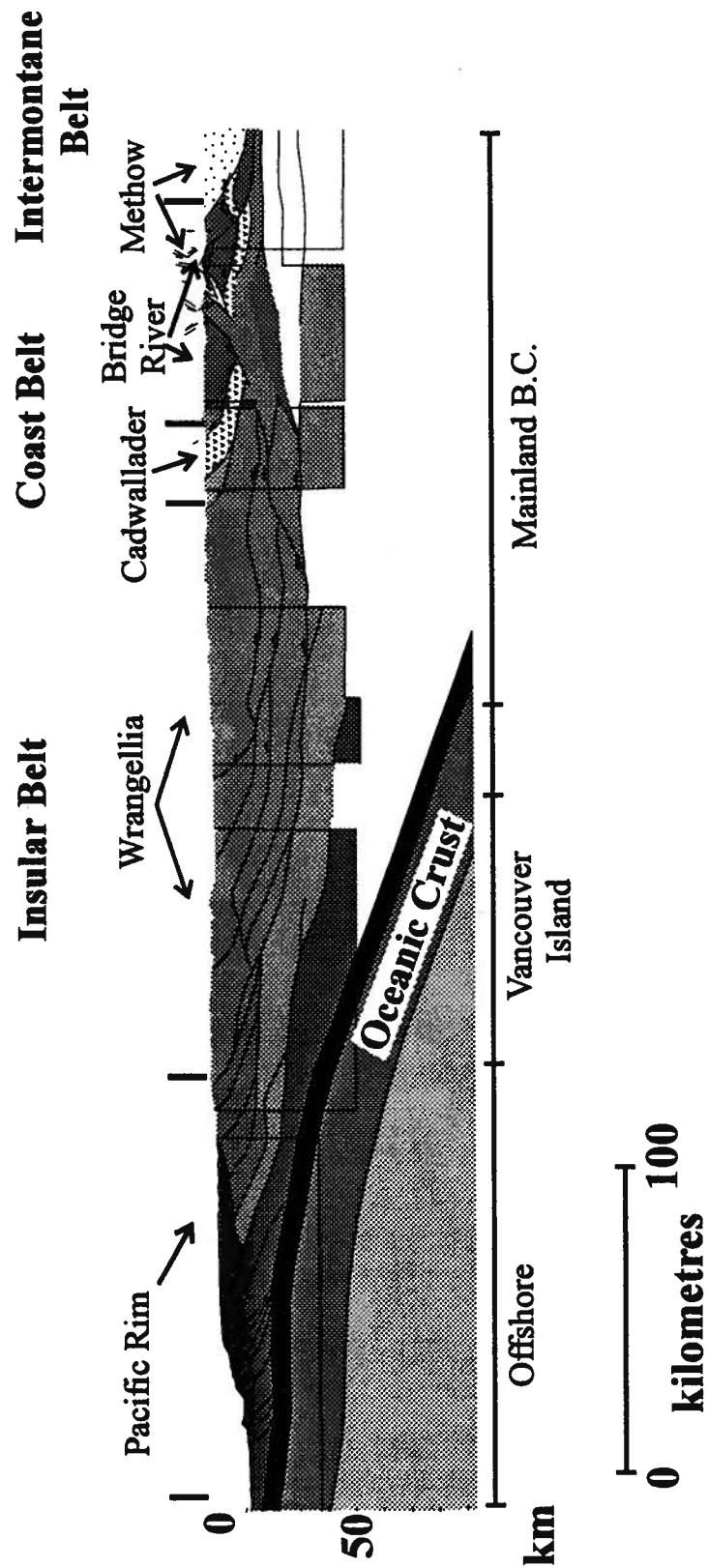


Figure 6.3 - Geologic cross-section of the southern Canadian Cordillera. Data from Journeay and Friedman (1993), and Lithoprobe transect lines. Boxes represent Lithoprobe cross-section lines.

| | Wrangellia | Harrison | Cadwallader | Bridge River | Methow |
|------------|-------------------|-------------------|---------------------------------|----------------------|-----------------|
| Tertiary | | | | | |
| Cretaceous | Nanaimo Group | | Powell Ck Volc. | | |
| | Coal Harbor Fm | | Taylor Ck Gp. | Taylor Ck Gp | Jackass Mtn Gp |
| | Kyuquot Fm | Gambier Group | | | Thunder Lk Seq |
| Jurassic | | Mysterious Ck + | Relay Mtn Group | Cayoosh Assemblage | Ladner Gp. |
| | Bonanza Group | Harrison Lake Fm. | Last Creek Fm. | | |
| | Karmutsen Fm + | | Tyaughton Gp Cadwallader Gp. | Bridge River Complex | |
| Triassic | | Camp Cove Fm. | | | Spider Peak Fm. |
| Permian | | | Bralorne Complex | | |
| Penn. | Buttle Lake Group | | | | |
| Miss. | | | | | |
| Devonian | Sicker Group | | | | |
| | | | | | |

Figure 6.4 - Time-stratigraphic sections of major terranes in the southern Canadian Cordillera.

Coast Belt Thrust System (Journeay and Friedman, 1993). Rocks of the Harrison, Cadwallader and Bridge River terranes are interpreted to be protoliths for imbricate thrust nappes of high-grade metamorphic rocks in the central portion of the Coast Belt Thrust System east of Harrison Lake (Figs. 6.2, 6.3). Cadwallader and Bridge River terranes are complexly interdigitated along transcurrent faults in the eastern Coast belt, west of the Yalakom and Fraser faults (Journeay and Monger, 1994; Schiarizza et al., 1990; Figs. 6.2, 6.3). The Methow terrane occupies a hinterland position to the Coast Belt Thrust System, and is largely separated from the system by the Yalakom-Hozameen and Fraser fault systems. The Pasayten fault separates the Methow terrane from predominantly Triassic and Jurassic arc rocks and plutons of the Quesnellia terrane.

6.3 STRATIGRAPHIC CHARACTERIZATION

A. Harrison Terrane

a. Terrane Description

The Harrison terrane consists of greenstone, chert, limestone, argillite and greywacke of the Triassic Camp Cove Formation unconformably overlain by Lower to Middle Jurassic (Toarcian to Bathonian) volcanic and volcanoclastic strata of the Harrison Lake Formation (Figs. 6.1, 6.2). Fine-grained sandstone, siltstone and shale of the Middle Jurassic (Callovia) Mysterious Creek Formation unconformably overlie the Harrison Lake Formation, and are gradationally overlain by fine-grained volcanoclastic strata of the Upper Jurassic (Oxfordian) Billhook Creek Formation. Capping the sequence is polymict, granitoid-bearing conglomerate of the Lower Cretaceous (Berriasian to Valanginian) Peninsula Formation and overlying volcanic rocks of the Brokenback Hill Formation (Valanginian to Albian). The latter two formations comprise the Gambier Group, a distinctive stratigraphic sequence mapped throughout the southern Coast Mountains (Wheeler and McFeeley, 1992; Journeay and Monger, 1994).

Lower and Middle Jurassic strata of the Harrison Lake Formation comprise the majority of the Harrison terrane, constituting the southern 60% of its area and over 50% of its composite stratigraphic thickness (Figs. 6.2, 6.4). The Harrison Lake Formation has been discussed in detail in Chapter 4, and will only be briefly reviewed here.

b. Lithostratigraphy

The Harrison Lake Formation is subdivided into four members, including the Celia Cove, Francis Lake, Weaver Lake, and Echo Island Members (Arthur, 1987; Arthur et al., 1993; this study; Fig. 6.5). The base of the formation is an angular unconformity with underlying greenstone, chert, graywacke and argillite of the Middle Triassic Camp Cove Formation. The Celia Cove Member consists of a fining upward sequence (50+ m) of polymict conglomerate, sandstone, siltstone, and shale. Subangular conglomerate clasts near the base of the member are primarily derived from the subjacent Camp Cove Formation, although well-rounded Permian limestone clasts in the unit may be derived from the Chilliwack terrane to the south (Monger, 1985; Arthur, 1987; Arthur et al., 1993). Subrounded conglomerate clasts higher up in the sequence are predominantly intermediate volcanic rocks. The Celia Cove Member is gradationally overlain by sandstone and siltstone of the Francis Lake Member (Fig. 6.5).

The lower 15-30 m of the Francis Lake Member fines upward from conglomerate and sandstone of the subjacent Celia Cove Member into a 15-20 m succession of ammonite-bearing shale and siltstone. Above the argillaceous succession, the Francis Lake Member becomes coarser grained and thicker bedded, and comprises tuffaceous lithic wackes, siliceous siltstone, crystal vitric tuff and lapilli tuff. The Francis Lake Member is conformably overlain by andesite flows and breccias of the Weaver Lake Member. The Weaver Lake Member consists of a >2600(+) m thick laterally and vertically variable succession of interdigitated dacite to andesite flows, flow breccias, tuff breccia, lapilli tuff, tuff, and epiclastic conglomerate, sandstone, and siltstone. Andesite to rhyolite dikes and sills are locally abundant, and a prominent rhyolite dome

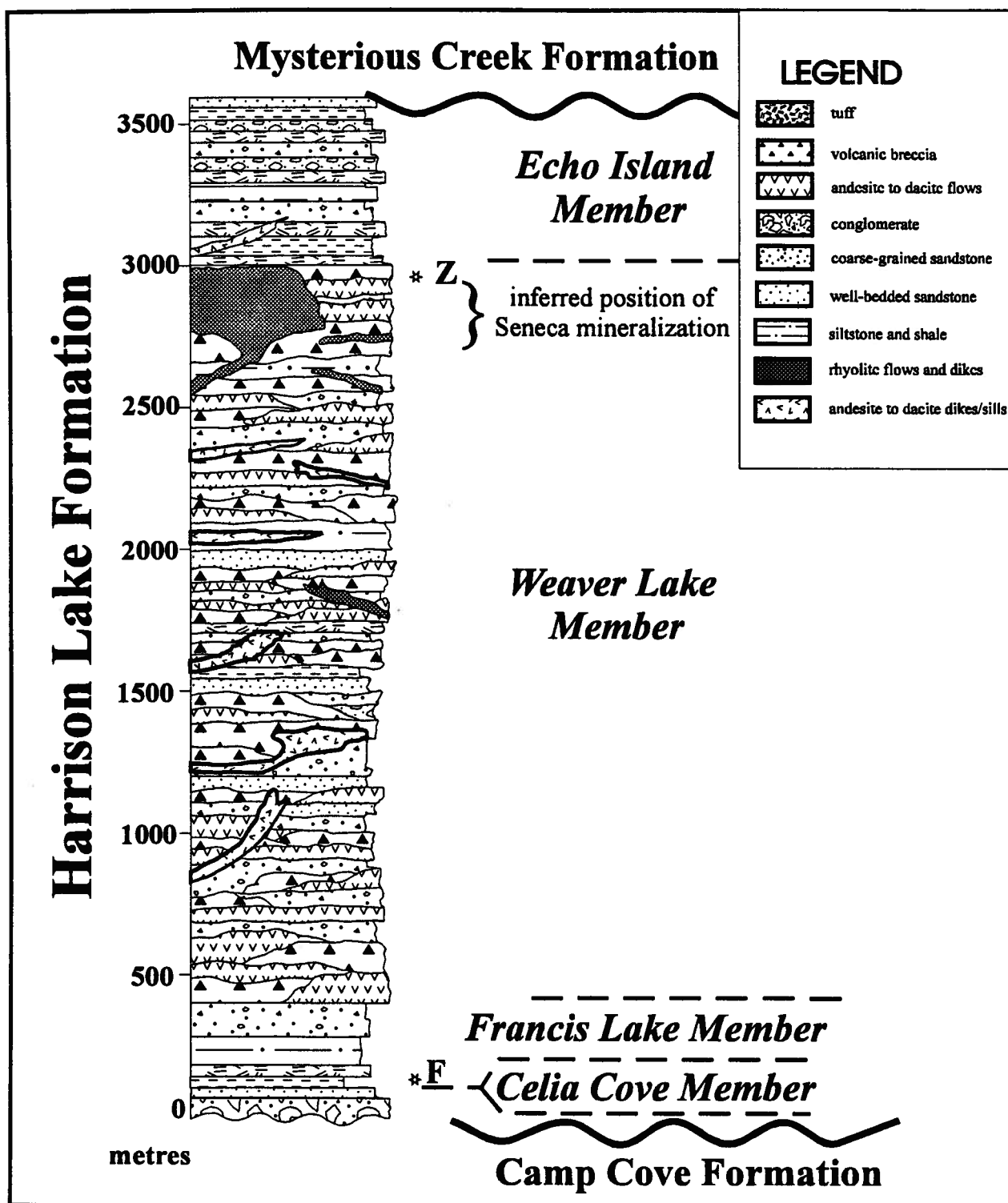


Figure 6.5 - Idealized stratigraphic column of the Harrison Lake Formation. Thicknesses estimated from outcrop patterns and cross-sections. Internal stratigraphic relations, particularly within the Weaver Lake Member, are idealized. Note location of new biostratigraphic data (F), U-Pb geochronology (Z), and inferred location of Seneca mineralization zone.

complex characterizes the upper part of the member on the east side of the outcrop belt (Fig. 6.2). Zircon recovered from the rhyolite dome yields a U-Pb age of 166.0 \pm 0.4 Ma (Early Bathonian).

The Weaver Lake Member is conformably overlain by volcanoclastic sedimentary rocks of the Echo Island Member. The Echo Island Member comprises tuffaceous sandstone, siltstone, mudstone, granule to cobble conglomerate, and lesser tuff breccia, lapilli tuff, and crystal to vitric tuff. The member consists of thin to medium bedded, laterally continuous beds of volcanic sandstone, siltstone, mudstone, and crystal tuff intercalated with thick bedded to massive (2-15 m) tuffaceous sandstone, lapilli tuff, and tuff breccia. The contact between the Echo Island Member and the overlying Mysterious Creek Formation is an angular unconformity.

c. Biostratigraphy

The Harrison Lake Formation consists primarily of volcanic rocks and associated coarse-grained clastic sediments, and is generally unfossiliferous. The Francis Lake Member, and, to a much lesser extent, the Weaver Lake Member, contain the only sparsely fossiliferous strata within the Harrison Lake Formation. Discovery of the ammonite *Dactylloceras* sp. (G.K. Jakobs, personal communication, 1992) in argillaceous strata intercalated with crystal tuff in the Francis Lake Member establishes the time of initiation of volcanism in the Harrison Lake Formation as late Early Toarcian. Age control in the upper part of the formation is provided by U-Pb zircon age from the upper Weaver Lake Member (Chapter 4).

Preservation of the fauna in dark grey argillite intercalated with probable partial turbidites argues for deposition in a low-energy marine environment below effective wave base. Pectinid bivalves and belemnites are associated with ammonites in the Francis Lake Member (Arthur et al., 1993). Pectinid bivalves and belemnites occur in the Weaver Lake Member (Pearson, 1973), and trigoniid bivalves and belemnites are reported from the Echo Island Member (Crickmay, 1925; Arthur et al., 1993). The occurrence of shallow water benthic fauna throughout the formation suggests deposition in a nearshore shallow water environment.

In addition, ammonite and bivalve fragments, together with wood debris, are commonly found at the base of thick, graded sandstone beds, suggesting deposition by mass sediment gravity flows derived from nearshore shallow water environment.

Boreal, Tethyan, and pandemic ammonite genera of Toarcian and Aalenian age have been documented in the Harrison Lake Formation (Table 6.1). The occurrence of this mixed fauna suggests the Harrison Lake Formation may have been deposited at mid-latitude in the Northern Hemisphere (Taylor et al., 1984).

d. Volcanic Geochemistry

Primary volcanic rocks in the Harrison Lake Formation range from basaltic andesite to rhyolite, and are medium- to high-K calcalkaline in composition (Fig. 6.6 a,b). Trace element spidergrams display the strongly spiked pattern indicative of subduction-related calcalkaline suites, and the rare earth element (REE) pattern is light rare earth element (LREE) enriched, which also supports a volcanic arc affinity for the rocks (Gill, 1981; Fig. 6.6c, d). Detailed analysis of the geochemistry of the Harrison Lake Formation is given in Chapter 4, and comparison with arc volcanics of the Bonanza Group on Wrangellia is given in Chapter 5.

e. Isotopic signature

Nd and Sr isotopic analyses of primary volcanic rocks in the Harrison Lake Formation demonstrate the relatively juvenile nature of the arc system. Initial ϵ_{Nd} values range from +3.53 to +6.97, and initial $^{87}\text{Sr}/^{86}\text{Sr}$ range from 0.7026-0.7045. These values plot in the uncontaminated island arc volcanic (IAV) field on a ϵ_{Nd} vs. $^{87}\text{Sr}/^{86}\text{Sr}$ diagram (Fig. 6.7). However, incorporation of a minor amount of subducted sediment or interaction with slightly evolved crust is indicated by more transitional ϵ_{Nd} values ($<+5$; White and Patchett, 1984).

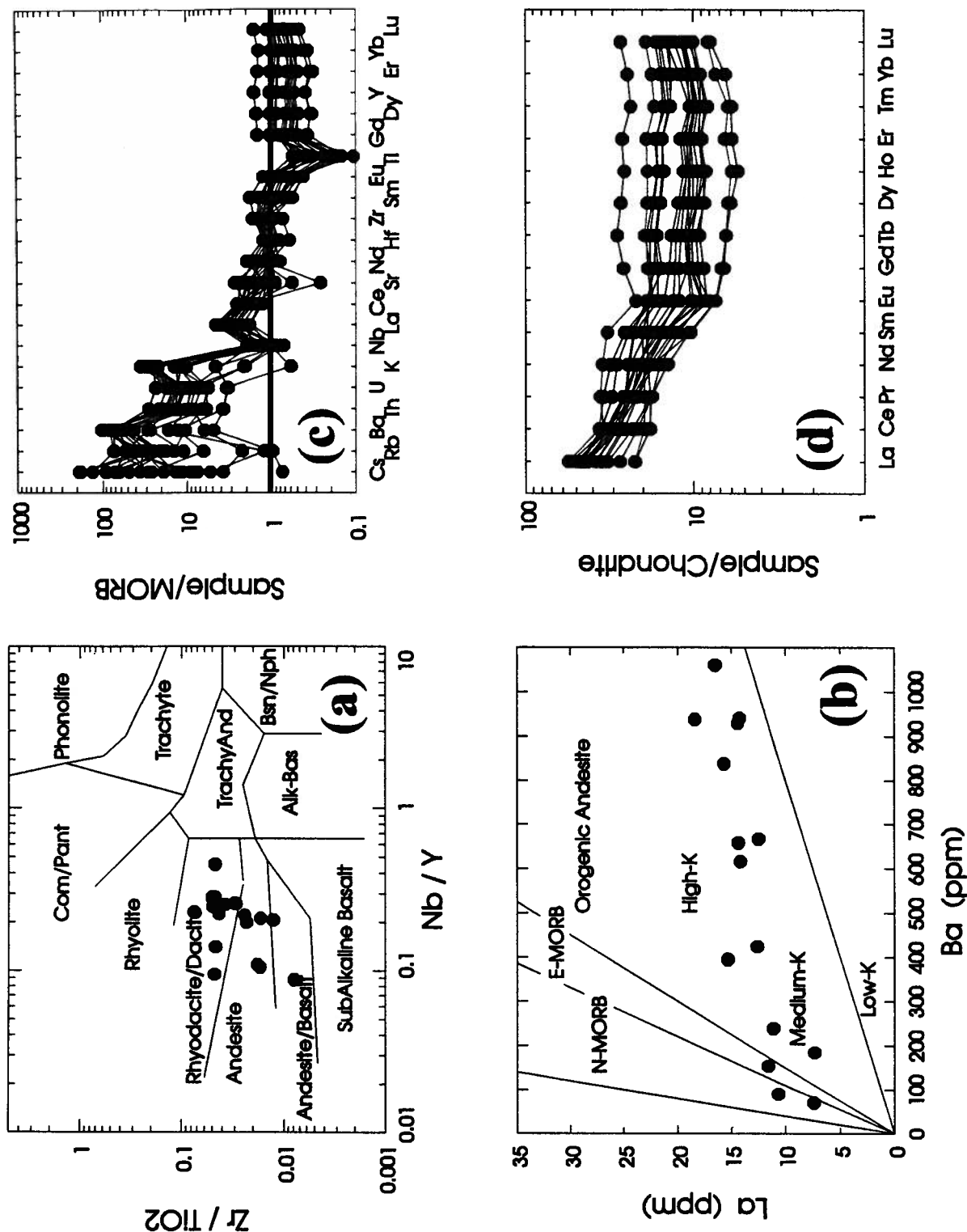


Figure 6.6 - Representative geochemical diagrams for the Weaver Lake Member of the Harrison Lake Formation. a) Nb/Y vs. Zr/TiO₂ plot from Winchester and Floyd (1977); b) Ba vs. La diagram from Gill (1981); c) extended trace element diagram, normalised to MORB (Taylor and McLennan, 1985); d) rare earth element diagram, normalised to chondritic values (Sun, 1982).

Isotopic values of fine-grained clastic sediments within the Harrison Lake Formation display a wider range of initial ϵ_{Nd} and $^{87}\text{Sr}/^{86}\text{Sr}$ than the primary volcanic rocks. Initial ϵ_{Nd} values range from +1.98 to +5.21, and initial $^{87}\text{Sr}/^{86}\text{Sr}$ ratios range from 0.7027-0.7056 (Fig. 6.7). Isotopic analyses of fine-grained clastic sediments reflect the weighted average isotopic composition of the source region(s). Harrison Lake Formation sedimentary rocks have slightly lower ϵ_{Nd} values than associated primary volcanic rocks, indicating that the sedimentary isotopic signature is a mixture of juvenile arc detritus and a more evolved detrital component. The strontium isotopic ratios for the sediments display a significantly wider range than the majority of the volcanic rocks. Higher values of $^{87}\text{Sr}/^{86}\text{Sr}$ can be the result of hydrothermal alteration of volcanic rocks or incorporation of seawater strontium into the sediment (DePaolo and Wasserburg, 1977).

Comparison of ϵ_{Nd} values and stratigraphic position indicates a temporal control on isotopic fluctuations (Fig. 6.8). In the upper portion of the Celia Cove Member and lower portion of the Francis Lake Member, sediment ϵ_{Nd} values are similar to those determined for the underlying Triassic Camp Cove Formation and for volcanic rocks higher in the section (Table 6.3). These values are consistent with derivation of the sediment from either the underlying strata or from laterally adjacent volcanic rocks of the Bonanza-Harrison arc system (Chapter 5). A significant isotopic excursion is evident in Francis Lake Member sediments of Late Toarcian age, as indicated by a drop in ϵ_{Nd} values of up to three epsilon units. These more evolved values could not have been derived from subjacent strata or from laterally adjacent volcanic rocks, and require incorporation of more evolved sediment into the basin in Late Toarcian time. Isotopic values shift back to more juvenile values in the Aalenian, coincident with the main effusive phase of Harrison Lake volcanism, and remain juvenile until the earliest Bathonian. Slightly more evolved values near the top of the section are related to the most silicic period of volcanism, and may reflect partial melting of slightly older crustal materials during the evolution of the magmatic system (DePaolo, 1988; Chapter 4).

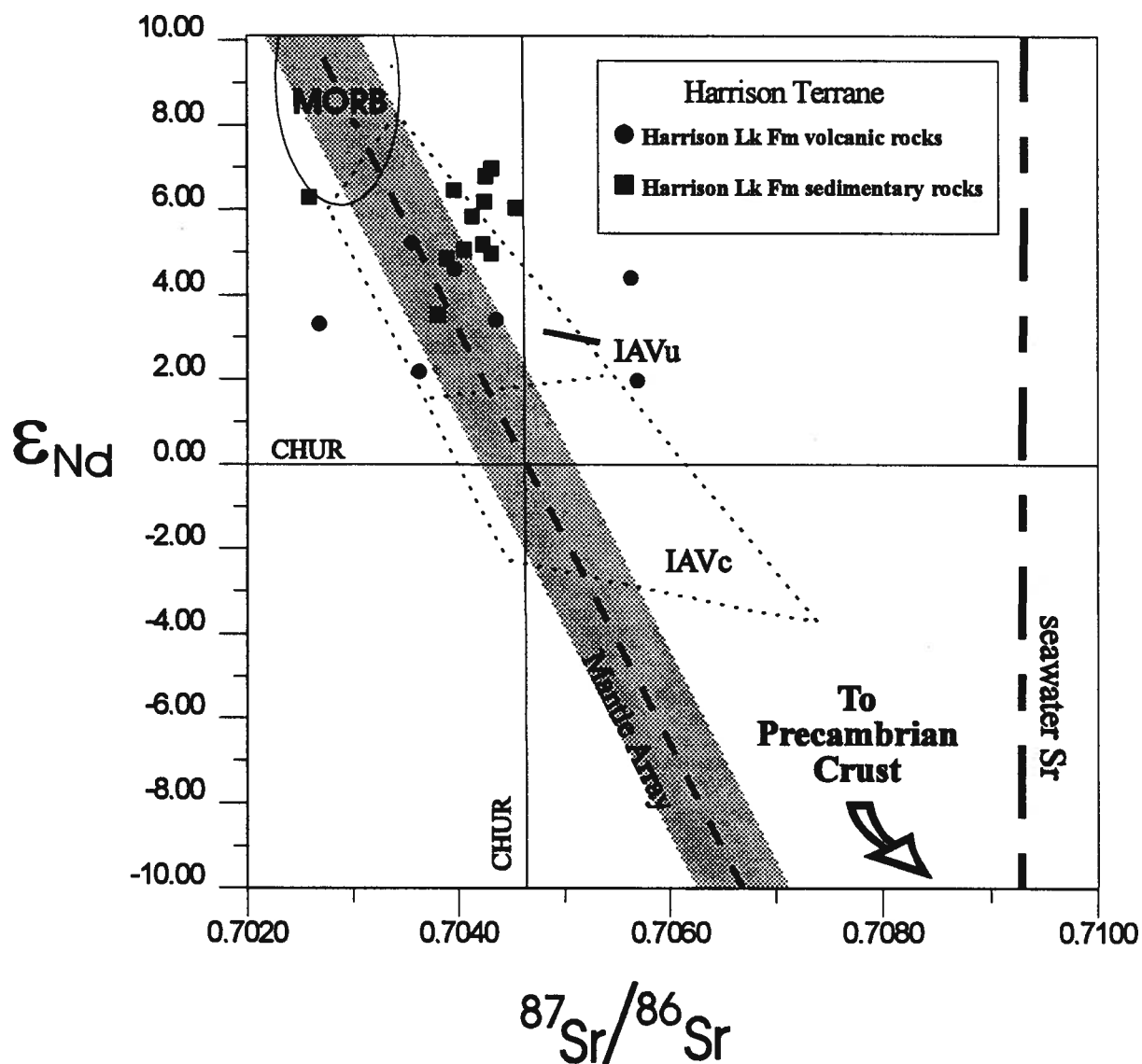


Figure 6.7 - ϵ_{Nd} vs. $^{87}\text{Sr}/^{86}\text{Sr}$ isotopic diagram for Harrison Lake Formation. Note arc fields and position of samples relative to mantle array. Data from DePaolo (1988), Samson et al. (1991), Hawkesworth (1993). IAVc=contaminated island arc; IAVu= uncontaminated island arc; MORB=mid ocean ridge basalt; CHUR=chondritic values.

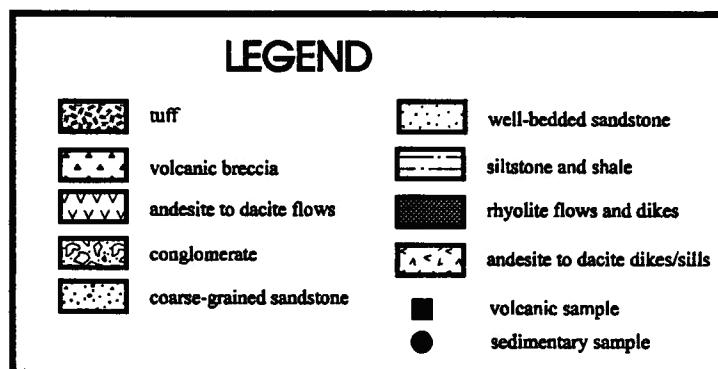
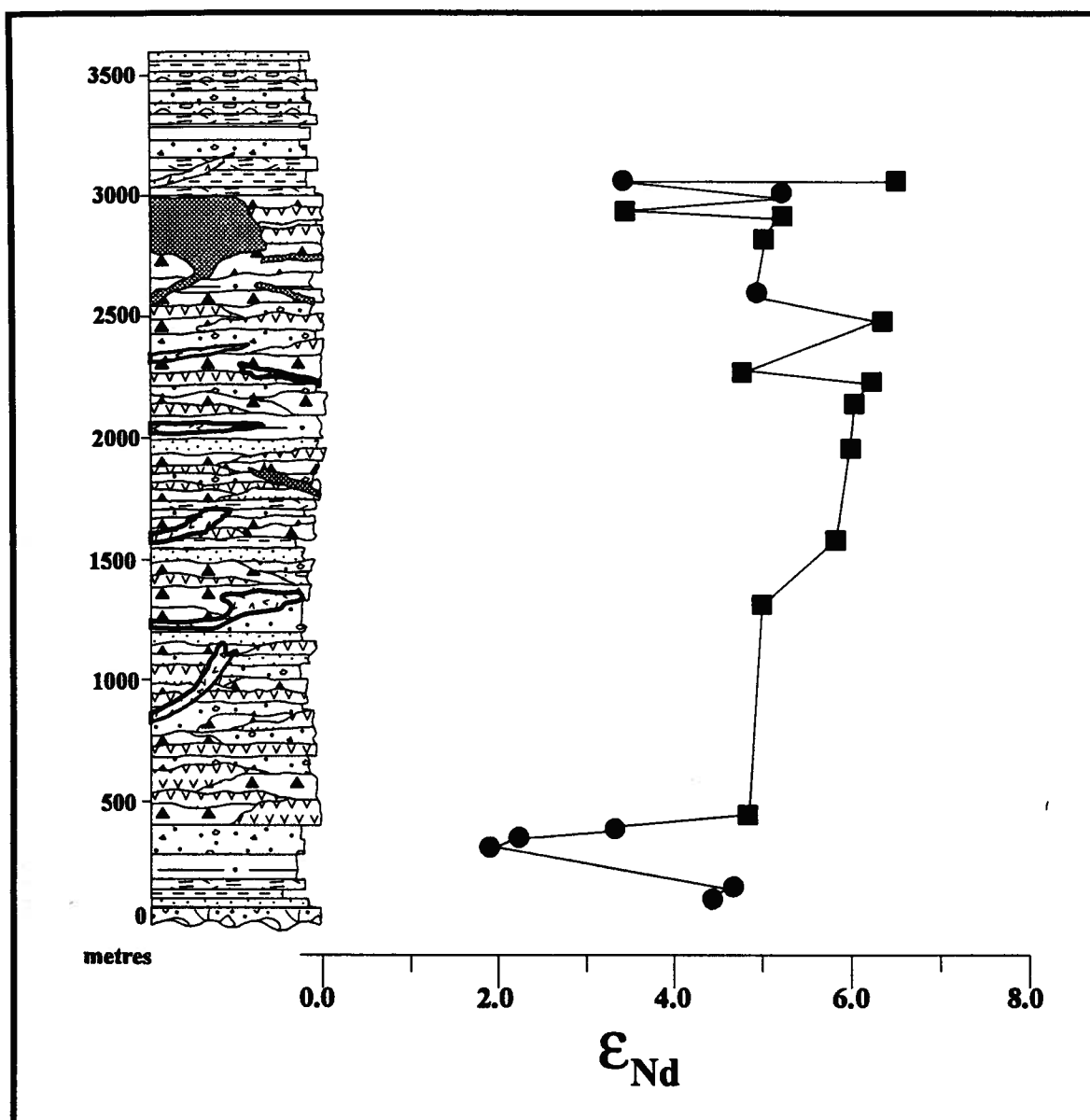


Figure 6.8 - ϵ_{Nd} vs. stratigraphic position for Harrison Lake Formation. Note isotopic shift to more evolved values in Toarcian.

f. Depositional Environment

The Harrison Lake Formation may be described as a classic island arc sequence (Chapter 4), and data presented here reflects the evolution of the island arc sequence through time (Laure et al., 1991). The Celia Cove Member is a basal conglomerate that indicates crustal instability and erosion of Triassic basement, probably due to thermal expansion of the crust induced by subduction of oceanic crust (Laure et al., 1991; Chapter 4). The conglomerate was deposited in a subaqueous environment by mass sediment gravity flows, and is overlain by partial turbidite and hemipelagic deposits. Low-energy hemipelagic deposition was interrupted in the early Late Toarcian by deposition of thick sequences of primary pyroclastic and resedimented pyroclastic sediments, marking the initiation of explosive volcanism in the Harrison Lake Formation.

The transition from tuffaceous sedimentary rocks of the Francis Lake Member to lava flows and volcanic breccias of the Weaver Lake Member indicates submarine deposition of resedimented pyroclastic debris generated by explosive volcanism slowed in the Aalenian, and was superseded by effusive volcanism. Deposition of the Weaver Lake Member was characterised by the accumulation of thick sequences of andesitic to dacitic flows, tuff breccias, agglomerates, hyaloclastites, minor pyroclastic deposits, and epiclastic conglomerates, sandstone, and siltstone. Submarine volcanism is indicated by hyaloclastites and the occurrence of shallow marine fauna, whereas adjacent subaerial deposition is suggested by the abundance of wood debris and well rounded, channelized, epiclastic conglomerate. Composition of the volcanic rocks is apparently controlled by fractional crystallization; flows evolve from basaltic andesite near the base to rhyolitic dikes and domes near the contact with the Echo Island Member (Chapter 4). The transition from flows and breccias of the Weaver Lake Member to the well-stratified pyroclastic debris of the Echo Island Member reflects the change from dominantly effusive volcanism to explosive volcanism in the upper part of the formation.

The Harrison Lake Formation is unconformably overlain by the Callovian Mysterious Creek Formation. Overturned bedding and mesoscale folds in the Echo Island Member indicates the contact is an angular unconformity, and suggests a Bathonian deformational event. The Mysterious Creek Formation contains shale, siltstone, and sandstone deposited in shallow marine to below wavebase environments (Arthur et al., 1993).

B. Cadwallader Terrane

a. Terrane Description

The Cadwallader terrane consists of Triassic volcanic and volcanoclastic rocks sequentially overlain by Upper Triassic, Lower to Middle Jurassic, Middle to Upper Jurassic and Lower Cretaceous clastic successions (Rusmore, 1987; Umhoefer, 1989; Fig. 6.4). The base of the terrane contains volcanic arc rocks and conformably overlying turbidite strata of the Cadwallader Group (Carnian to Norian; Rusmore, 1987). The Cadwallader Group is interpreted to be conformably overlain by fluvial to shallow marine clastic rocks and limestones of the Tyaughton Group (middle to upper Norian; Umhoefer, 1990). The Last Creek Formation (Hettangian to Bajocian) comprises conglomerate, sandstone, siltstone and shale unconformably above the Tyaughton Group (O'Brien, 1985; Umhoefer, 1990). Marine sandstone, siltstone, and shale of the Relay Mountain Group (Callovian to Barremian) is interpreted to unconformably overlie the Last Creek Formation, and these rocks are unconformably overlain by coarse clastic rocks of the Taylor Creek Group (Barremian to Albian; Umhoefer, 1989; Garver, 1989, 1992).

Middle Jurassic strata of the Last Creek Formation form a thin (<400 m), poorly exposed portion of the >5 km thick Cadwallader terrane. The formation has a limited areal extent, and is restricted to the Last Creek drainage and ridges west of Castle Pass (Plate 1). Correlative strata are sporadically exposed to the northwest, in the southwestern portion of the Taseko Lakes map area (Tipper, 1978) and in the southeastern portion of the Mt. Waddington map area to the northwest (Tipper, 1969; Umhoefer and Tipper, 1991;

Schiarizza et al., 1994). Despite limited exposure, the Last Creek Formation has received a great deal of study because of its remarkable ammonite fauna (Frebold, 1967; Frebold et al., 1969; Tipper, 1978; O'Brien, 1985; Poulton and Tipper, 1991; Jakobs, 1992). A detailed analysis of the Last Creek Formation and subjacent strata is the subject of an Geological Survey of Canada bulletin in preparation by H.W. Tipper and P.J. Umhoefer (H.W. Tipper, personal communication, 1994), and their nomenclature is used herein. The following lithologic descriptions are based on reconnaissance stratigraphic studies by the author in 1991 and 1993, supplemented with data from Umhoefer (1989) and Umhoefer and Tipper (1991).

b. Lithostratigraphy

The Last Creek Formation consists of Upper Hettangian to Upper Bajocian clastic strata that have been subdivided into two members (Poulton, 1994; H.W. Tipper, personal communication, 1994; Fig. 6.9). The Castle Pass member comprises Upper Hettangian to Upper Sinemurian conglomerate, sandstone, siltstone, and shale disconformably overlying Upper Norian strata of the Tyaughton Group (Umhoefer, 1989). The basal conglomerate is a distinctive unit that consists of matrix-supported granule to pebble-size clasts of volcanics, chert, and sedimentary lithics set in a coarse lithic wacke matrix. The conglomerate has a bimodal grain size distribution, consisting of granule-size angular chert lithic clasts (45%) and pebble to cobble, subrounded volcanic clasts (51%). Ammonite fragments and wood debris are common, and channels are locally evident (O'Brien, 1985; Umhoefer, 1989). The conglomerate grades upward into thin to medium bedded fine grained, well sorted calcareous sandstone, siltstone, and sandy limestone containing parallel laminae and rare low-angle cross beds. Bioclastic beds are locally evident (O'Brien, 1985; Umhoefer, 1989). The section fines upward into thin to medium bedded, thin laminated shale intercalated with thin bedded dark grey sandy limestone and brown weathering fine grained well sorted sandstone. The Castle Pass Member is gradationally overlain by the Little Paradise Member, and the contact is placed where shale begins to dominate the section (H.W. Tipper, personal communication, 1994).

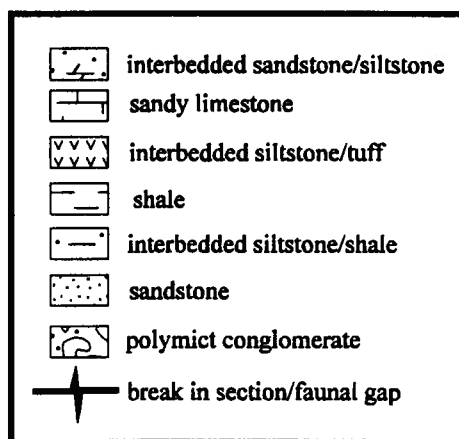
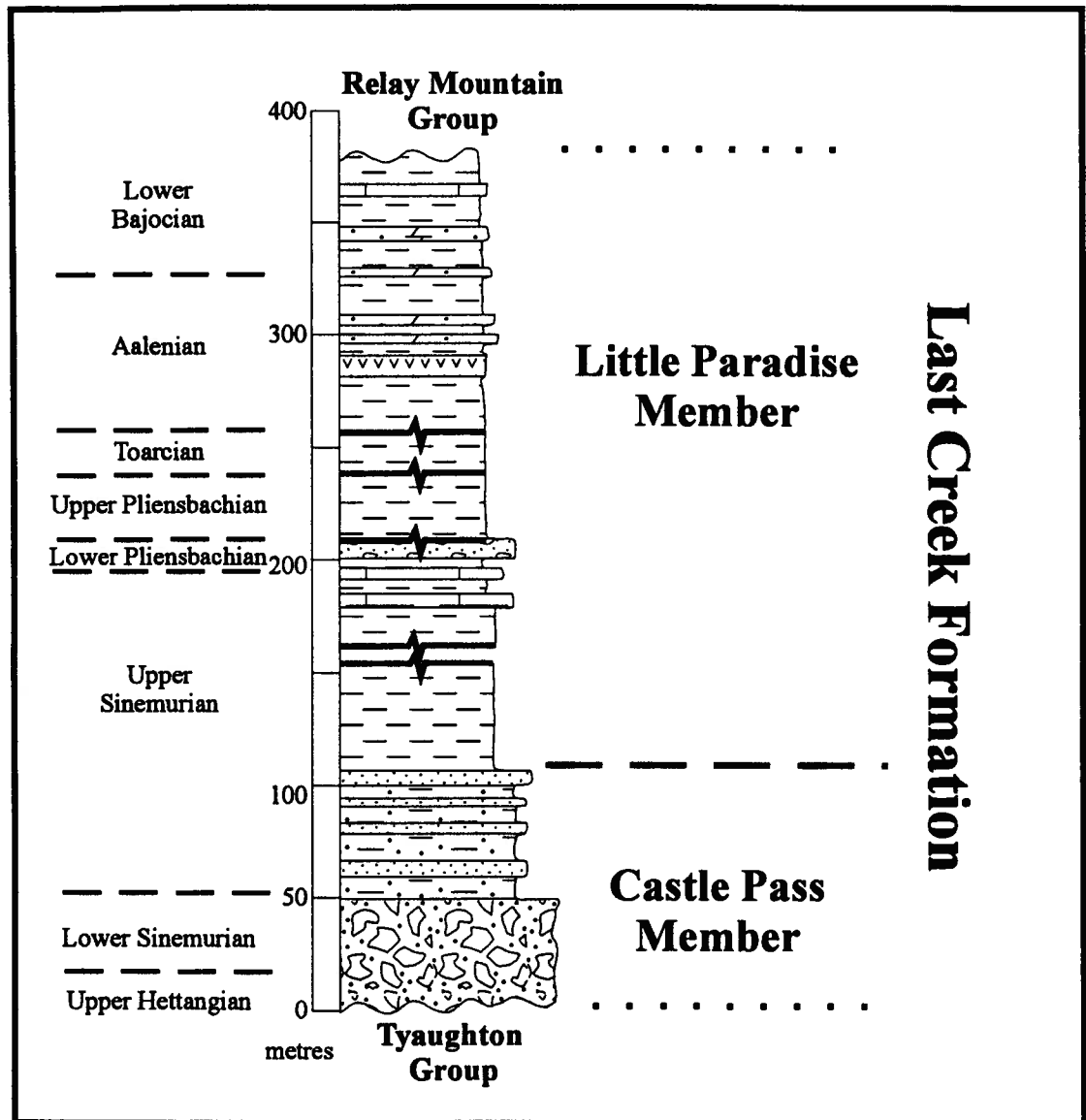


Figure 6.9 - Schematic stratigraphic section of the Last Creek Formation.

The Little Paradise Member is a fine-grained succession of shale, siltstone, limestone, and minor granule conglomerate and sandstone that ranges in age from Late Sinemurian to Late Bajocian (Tipper, 1978; Umhoefer and Tipper, 1991; Poulton, 1994; Fig. 6.9). The lower part of the member is of Late Sinemurian age, and consists of dark grey shale and siltstone locally intercalated with thin bedded fine grained sandstone and limestone (Umhoefer, 1989). These rocks appear to grade upward into dark grey calcareous shale intercalated with 0.25-0.5 m thick dark grey extremely fossiliferous limestone containing abundant ammonites and woody debris of late Early Pliensbachian age (H.W. Tipper, personal communication, 1994). The shale and limestone interval is overlain by medium bedded granule conglomerate and coarse sandstone that may represent an intraformational disconformity (H.W. Tipper, personal communication, 1994). The coarse clastic rocks grade upward into a purple to black shale and siltstone interval containing Late Pliensbachian, Toarcian, and Aalenian ammonites (Poulton and Tipper, 1991; Jakobs, 1992; Umhoefer, 1989).

Aalenian strata consist of thin bedded, thin laminated, locally siliceous argillite, siltstone, and fine sandstone displaying basal scour features, parallel laminae, normal and reverse graded bedding, and minor thin beds of granule conglomerate with shale rip-up clasts. The section is punctuated by distinct thin (1-2 cm) whitish-yellow beds interpreted as air fall(?) tuff. The tuff beds are intercalated with dark-grey to black siltstone and shale and thin bedded, distinctly feldspathic sandstone. This interval grades upward into thin bedded dark grey sandy siltstone, siltstone and shale intercalated with laminated calcareous sandstone and sandy blue-grey limestone of Late Aalenian to Early Bajocian age. Sedimentary structures include parallel laminae, graded bedding, and soft sediment deformation features. Wood debris and bioclastic lag deposits occur locally.

Middle Jurassic strata of the Cadwallader terrane are sporadically exposed to the northwest of the type area; the best exposures are east and north of Chilko Lake (Tipper, 1969, 1978; Umhoefer and Tipper, 1991; Riddell et al., 1993; Schiarizza et al., 1994). Strata in this area comprise Sinemurian to Bajocian shale, siltstone, sandstone and conglomerate, contained in a broadly coarsening upward succession (Umhoefer and Tipper, 1991). Shale and siltstone dominate the lower portion of the succession, and volcanoclastic sandstone

and pebble conglomerate predominate in the upper portion. Umhoefer and Tipper (1991) subdivide the succession into three conformable members: 1) a lower member consisting of Sinemurian to Aalenian shale and siltstone; 2) a middle member consisting of Lower Bajocian siltstone and fine sandstone; and 3) an upper member consisting of upper Lower Bajocian volcanoclastic medium to coarse grained sandstone and pebble conglomerate. These rocks are distinctly coarser grained than coeval strata in the type section (Umhoefer and Tipper, 1991).

Bajocian strata of the Last Creek Formation are overlain by interbedded sandstone and shale of the lower Relay Mountain Group (Callovian to upper Oxfordian) in both the type area and in exposures to the west (Umhoefer, 1989; Umhoefer and Tipper, 1991). The contact is not exposed; however, a faunal gap between the two is inferred to represent an unconformable relationship. Rusmore et al. (1988) suggest that differing structural styles between the Last Creek Formation and Relay Mountain Group indicate the contact is an angular unconformity developed during Late Bajocian to Bathonian deformation. However, the rocks are contained within a belt of transcurrent faults, and the contrasting structural styles may reflect the influence of rheologic differences during Cretaceous and Tertiary deformation (H.W. Tipper, personal communication, 1994)

c. Biostratigraphy

The Last Creek Formation contains a diverse assemblage of ammonite and bivalve fauna ranging in age from Late Hettangian to Late Bajocian (Frebold, 1967; Frebold et al., 1969; Tipper, 1978; O'Brien, 1985; Poulton and Tipper, 1991; Jakobs, 1992; Poulton, 1994; Umhoefer and Tipper, 1991; H.W. Tipper, personal communication, 1994). Faunal gaps do exist, but poor exposures make it difficult to determine if the gaps are due to intraformational disconformities or sampling bias.

The association of neritic ammonite and benthic bivalve fauna, local shelly lag deposits, and the incorporation of shell debris in coarse clastic units suggests the Castle Pass Member was deposited in a high energy environment in or adjacent to a shallow water depositional site. The Little Paradise Member contains a diverse ammonite fauna preserved in thin-bedded shale, siltstone, and limestone, indicating deposition in a low energy environment below effective wavebase. Wood debris is common, and bivalves are rare (O'Brien, 1985; Umhoefer, 1989).

The Hettangian, Sinemurian and Pliensbachian fauna of the Last Creek Formation are of Tethyan, East Pacific, or pandemic biogeographic affinity (Taylor et al., 1984; H.W. Tipper, personal communication, 1994). Boreal fauna are unknown in the North America Cordillera during these stages (Taylor et al., 1984). Toarcian forms include both Boreal and pandemic varieties, and Aalenian and Bajocian ammonites are of Boreal, East Pacific, and Tethyan affinity (Table 6.1). Of particular importance is the occurrence of the genus *Pseudolioceras* in Aalenian and Early Bajocian strata of the Tyaughton Creek area; by the Early Bajocian, *Pseudolioceras* was restricted to the northern margin of the Panthalassic Ocean (Taylor et al., 1984). The association of this genus with the Tethyan forms *Eudmetoceras* and *Asthenoceras* in Lower Bajocian strata limit the paleogeographic setting of the Cadwallader terrane to the northeastern quadrant of the Panthalassic (paleo-Pacific) ocean.

d. Volcanic Geochemistry

Primary volcanic rocks are not found in the Last Creek Formation. Tipper (1969) reports basaltic to andesitic volcanic flows, breccia, and tuff of Bajocian age to the northeast of the aforementioned coarse-grained facies of the Last Creek Formation. These rocks, located northeast of Chilko Lake, on the northeast side of the transcurrent Yalakom Fault, may be correlative with Middle Jurassic strata of either the Cadwallader or Methow terranes.

e. Isotopic Signature

Five isotope samples, encompassing Lower Sinemurian, Lower Pliensbachian, Aalenian, and Lower Bajocian strata, were analysed from the formation. Fine-grained clastic sediments of the Last Creek Formation display relative isotopic homogeneity throughout the sampled interval (Fig. 6.10, 6.11). Initial ϵ_{Nd} values vary from 3.98 to 4.96, and initial $^{87}\text{Sr}/^{86}\text{Sr}$ ratios vary from 0.7039-0.7061. Isotopic values plot within a narrow range of ϵ_{Nd} on an ϵ_{Nd} vs. $^{87}\text{Sr}/^{86}\text{Sr}$ diagram, and display a spread on Sr values, probably due to varying seawater Sr enrichment. Initial ϵ_{Nd} values suggest that, for the time intervals sampled, the Last Creek Formation was supplied with fine-grained detritus from a juvenile source, most likely an oceanic volcanic arc coupled with pelagic or hemipelagic influx.

f. Depositional Environment

The Last Creek Formation was deposited during Early to Middle Jurassic time. Faunal gaps exist in this depositional record, but are difficult to quantify, and previous workers have assumed the formation represents continuous Early to Middle Jurassic deposition (Umhoefer, 1989, 1990; Poulton, 1994). This assumption is followed herein, albeit with the cautionary note that unrecognized intraformational disconformities may mask tectonically significant depositional complexities.

The Last Creek Formation may be subdivided into two depositional facies, one spanning Late Hettangian to Sinemurian time, and the other encompassing Late Sinemurian to Late Bajocian time. The older depositional facies consists of a fining upward succession of polymict conglomerate, sandstone, siltstone and shale. Channelized conglomerate, shelly lag deposits, woody debris, low-angle cross-stratification, shale rip-up clasts, and a shallow water bivalve fauna indicate that the lower part of this facies was deposited in a nearshore, high-energy marine environment. Channelization and the lack of winnowing evident in the basal conglomerate, compositional immaturity of the sandstone (Umhoefer, 1989), preservation of wood and shelly debris, and the abundance of fine-grained detritus suggest rapid deposition and a lack of sediment reworking,

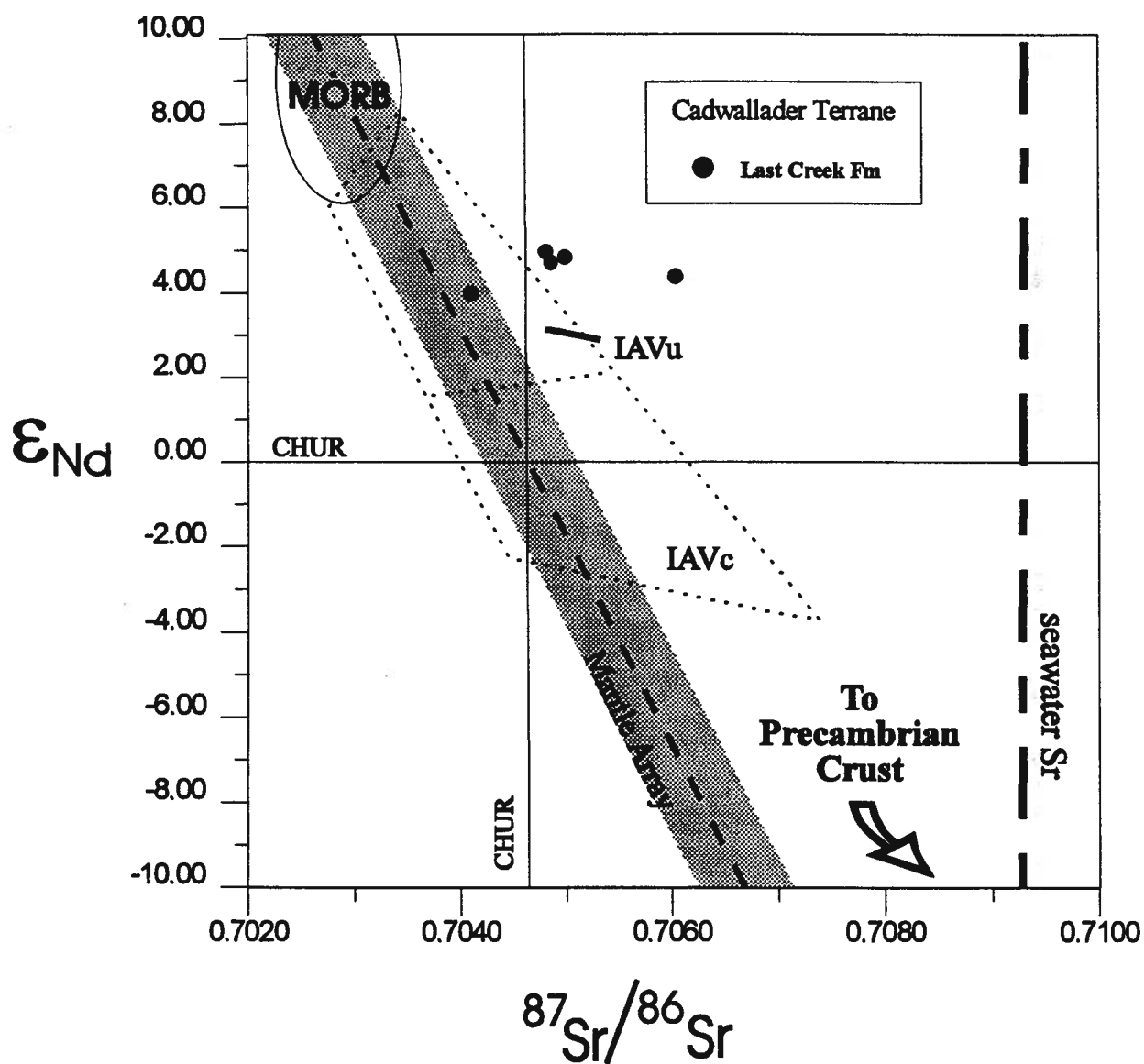


Figure 6.10 - $^{87}Sr/^{86}Sr$ vs. ϵ_{Nd} isotopic diagram for Last Creek Formation. Note arc fields and position of samples relative to mantle array. Data from DePaolo (1988), Samson et al. (1991), Hawkesworth (1993). IAVc=contaminated island arc; IAVu= uncontaminated island arc; MORB=mid ocean ridge basalt; CHUR=chondritic values (DePaolo and Wasserburg, 1976).

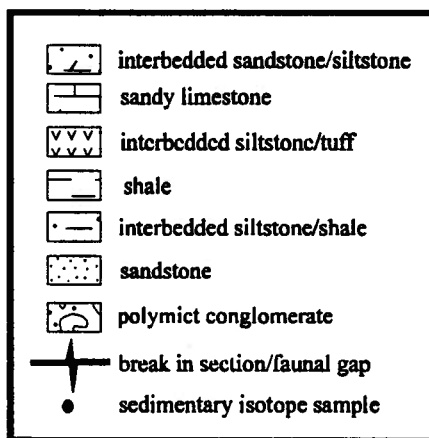
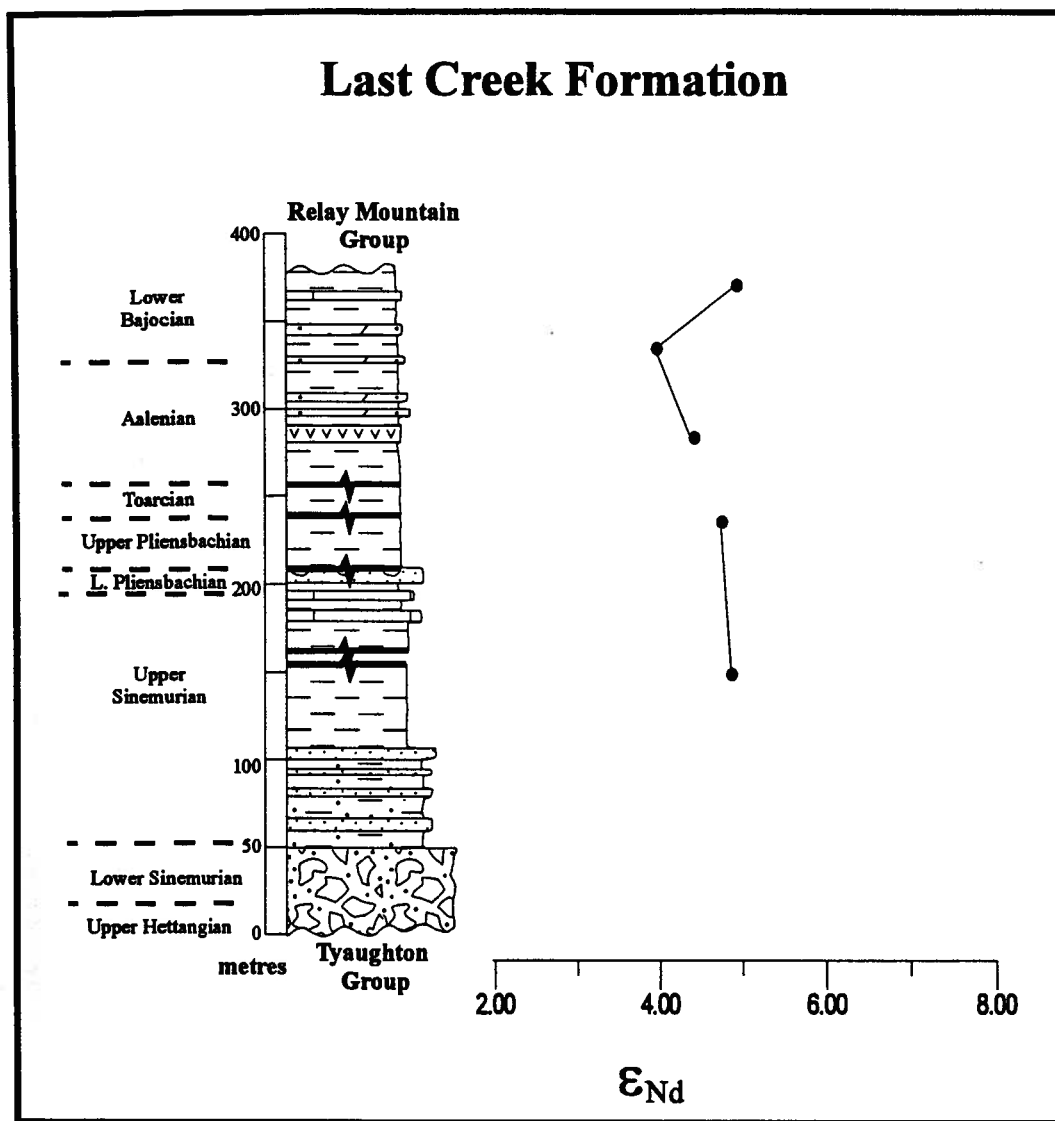


Figure 6.11 - ϵ_{Nd} vs. stratigraphic position for Last Creek Formation. Note homogeneity of isotopic values throughout stratigraphic range, as well as data gap in Toarcian.

such as occurs in a fan-delta environment. The overall fining upward sequence, and the occurrence of laterally continuous, well sorted sandstone beds and turbidite sequences higher in the facies suggests shallow water deposition was superseded by turbidity current deposition in a sub-wavebase environment.

The younger depositional facies in the Last Creek Formation comprises shale and siltstone with subordinate sandstone, conglomerate and limestone. Coarser beds contain sedimentary structures indicative of mass sediment gravity flow deposition, including graded bedding, parallel laminae, soft sediment deformation features, shale rip-up clast horizons, and partial Bouma sequences. Assuming a continuous depositional sequence, the diverse fauna, significant age range (Late Sinemurian to Late Bajocian), and limited stratigraphic thickness (<250 m) suggest this depositional facies may represent a condensed stratigraphic interval characterized by hemipelagic and pelagic deposition punctuated by rare turbidity flows in a sub-wavebase environment. Biostratigraphic correlation of the coarsening upward succession of Sinemurian to Upper Bajocian shale, siltstone, sandstone and granule conglomerate exposed near Chilko Lake with fine-grained siltstone and shale of the type Last Creek Formation suggests the Middle Jurassic strata of the Cadwallader terrane represent an eastward tapering depositional wedge. Umhoefer and Tipper (1991) suggest that the Middle Jurassic succession near Chilko Lake was deposited in a basin adjacent to an active volcanic arc.

C. Bridge River Terrane

a. Terrane Description

The Bridge River terrane comprises Mississippian to Middle Jurassic greenstone, chert, argillite, limestone, and ultramafic rocks of the Bridge River Complex and Hozameen Group (Monger, 1989; Monger and Journeay, 1992; Figs. 6.2, 6.4). These rocks locally form a coherent stratigraphy, but more commonly occur as structurally disrupted tectonic melange, particularly on the east side of the main Bridge River Complex west of the Yalakom River (Fig. 6.2, Plate 1). Late Triassic blueschists are associated with the

melange zone (Archibald et al., 1991). The Hozameen Group consists of Permian and Triassic greenstone, chert, limestone and argillite, together with Middle Jurassic chert and clastic sedimentary rocks, and probably represents a portion of the Bridge River Complex offset along the dextral Fraser River fault system (Fig. 6.2, Plate 1; Haugerud, 1985; Potter, 1983).

Oceanic rocks of the Bridge River Complex are overlain in part by Lower Jurassic to Lower Cretaceous fine-grained clastic rocks of the Cayoosh assemblage (Journeay and Northcote, 1992; Mahoney and Journeay, 1993; Journeay and Mahoney, 1994). The Cayoosh assemblage is locally overlain by an unnamed Lower Cretaceous conglomerate formerly assigned to the Brew Group (Journeay and Mahoney, 1994). Elsewhere, the Cayoosh assemblage is absent and rocks of the Bridge River Complex are unconformably overlain by Lower Cretaceous conglomerate of the Taylor Creek Group (Schiarizza et al., 1994). The Taylor Creek Group is recognized as a Lower Cretaceous stratigraphic overlap assemblage linking the Bridge River and Cadwallader terranes (Garver, 1992).

The Cayoosh assemblage is a coherent package of fine-grained metasedimentary rocks, including phyllitic argillite, phyllite, carbonaceous siltstone, tuffaceous phyllite, lapilli tuff, sandstone, and minor pillow basalt and limestone that conformably overlie the Bridge River Complex. Rocks of the Cayoosh assemblage are complexly imbricated with the Bridge River Complex in a series of thrust nappes that extend from the Fraser River fault system northwest to north of Downton Lake, where the supracrustal rocks are truncated by granodiorite of the Coast Plutonic Complex (Journeay, 1990, Journeay and Northcote, 1992; Journeay and Monger, 1992, 1994; Fig. 6.2). Penetrative deformation and regional greenschist facies metamorphism associated with structural imbrication during Late Cretaceous shortening has led to isoclinal folds, transposition of bedding, clast elongation, and local boudinage of limestone beds. These deformational features preclude accurate estimates of stratigraphic thickness or detailed reconstructions of basin morphology. However, primary sedimentary structures and facies relationships are preserved, and the regional consistency and replication of key stratigraphic relationships within the Cayoosh assemblage allow for a reconstruction of

the assemblage's fundamental stratigraphy (Mahoney and Journeay, 1993; Journeay and Mahoney, 1994; Appendix E).

b. Lithostratigraphy

The Cayoosh assemblage is subdivided into five distinct lithofacies, consisting of, in ascending order: 1) carbonaceous phyllite, siltstone, and fine-grained sandstone (unit 1); 2) phyllite, tuffaceous phyllite, lapilli tuff, tuff breccia, and minor pillow basalt (unit 2); 3) phyllite, siltstone, fine- to medium-grained volcanic sandstone and minor limestone (unit 3); 4) quartz-rich sandstone, quartzite, siltstone and phyllite (unit 4); and, 5) phyllite, siltstone, and volcanic sandstone (unit 5; Fig. 6.12). These rocks are described in detail in Mahoney and Journeay (1993), Journeay and Mahoney (1994), and Appendix E.

The basal unit of the Cayoosh assemblage gradationally overlies greenstone, chert, and argillite of Bridge River Complex, and is characterized by a coarsening upward succession of phyllite, graphitic phyllite, siltstone, thin-bedded fine-grained sandstone and calcareous sandstone. The basal contact is placed at the top of the highest chert bed in the Bridge River Complex, and is best exposed in the headwaters of Melvin Creek (54910 m E, 559540 m N; Fig. 6.2, Appendix E). Locally, the contact is marked by thin lenses of chert pebble conglomerate containing subangular clasts of chert, limestone, siliceous argillite and volcanic rock.

The basal unit of the assemblage is gradationally overlain by tuffaceous phyllite of unit 2, and the contact is placed at a distinct change from black phyllite to thin beds of light green tuffaceous phyllite. Unit 2 is characterized by thick (2-60 m), prominent beds of light to dark green tuff, lapilli tuff, tuff breccia and volcanic sandstone intercalated with black carbonaceous phyllite and siltstone. The volcanic beds are volumetrically subordinate to the fine grained clastic rocks, but form prominent, blocky outcrops. Pillow basalts with well-developed devitrification features occur locally in 2-5 m lenticular beds (Fig. 6.13). Tuffaceous phyllite, siltstone, and sandstone of unit 2 increase in abundance to the east.

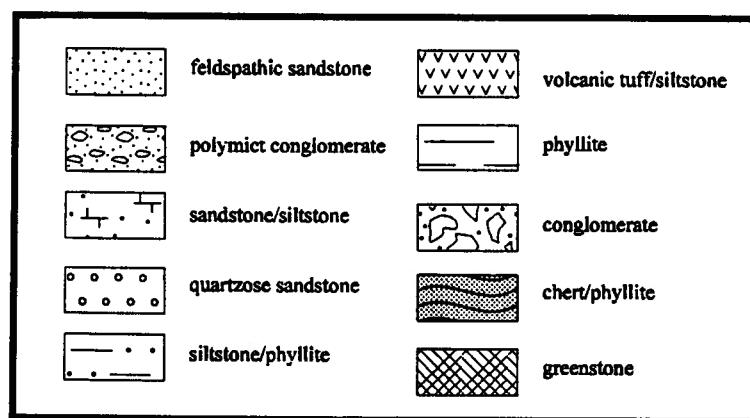
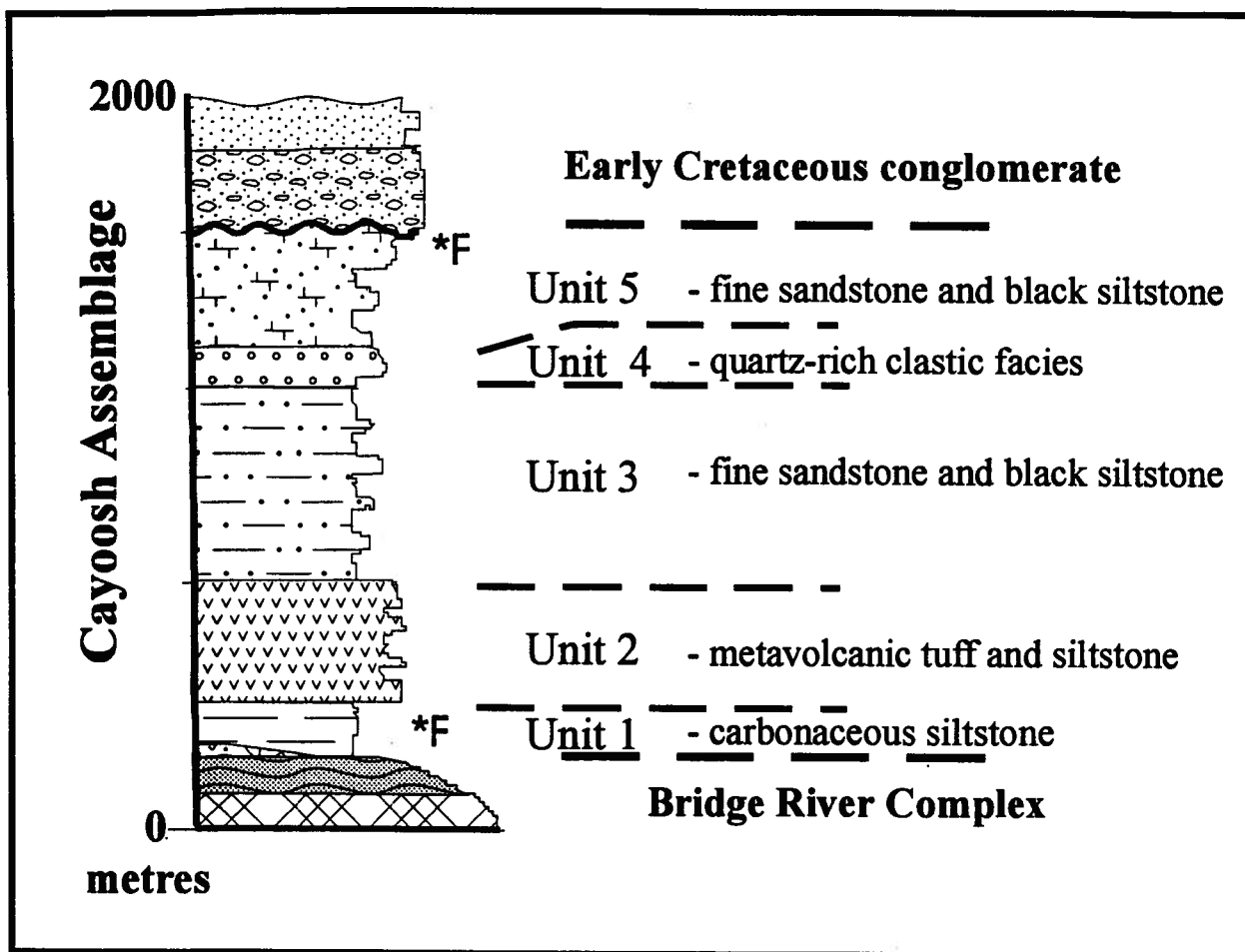


Figure 6.12 - Schematic stratigraphic section of the Cayoosh Assemblage.

Tuffaceous phyllite and lapilli tuff of unit 2 is gradationally overlain by phyllite, siliceous argillite, siltstone, thin to medium bedded fine to medium grained volcanic sandstone, and minor blue-grey sandy limestone of unit 3. Sandstone intervals form cyclic sequences (50-100 m), gradually coarsening- and thickening-upward, then fining- and thinning-upward into the overlying siltstone and phyllite interval. Parallel laminae, graded bedding, basal scour features, shale rip-up clasts, and flame structures are locally well preserved. Sandstone intervals vary in thickness and lateral extent throughout the outcrop belt, and are interpreted to be lenticular in cross-section and lobate in plan view. Petrographically, the sandstone of unit 3 is distinctly more quartz rich than underlying clastic rocks, consisting of volcanic, sedimentary and plutonic lithic fragments, and both mono- and polycrystalline quartz. Sandstone decreases in abundance upward, and the upper portion of unit 3 is dominated by phyllite, siltstone, and thin-bedded fine-grained sandstone.

Unit 4 is a thin (50-100 m) but very distinctive lithofacies consisting of quartz-rich clastic rocks that gradationally overlie phyllite and siltstone of unit 3. The unit comprises phyllitic quartzite, thin to thick bedded fine grained quartz-rich feldspathic arenite and intercalated phyllite, but the most distinctive rock type in the unit is thin bedded, thin laminated fine grained quartz arenite to quartzite that commonly displays chaotic bedding (Fig. 6.14). The disturbed bedding character may represent soft-sediment deformation, perhaps in an accretionary system (J.W.H. Monger, 1994, personal communication). Petrographically, these quartz-rich rocks are commonly recrystallized into a monotonous interlocking mosaic of polycrystalline quartz, but the presence of plagioclase feldspar and zircon confirms the detrital nature of these rocks. The quartz-rich clastic facies is unique among Mesozoic strata in the southwestern Canadian Cordillera, and provides an excellent stratigraphic marker within the Cayoosh assemblage.

Sandstone of unit 4 grades upward into the thick (200-300 m) coarsening-upward succession of thin-bedded carbonaceous phyllite, siltstone, fine grained sandstone and lesser sandy limestone that characterizes unit 5. The unit is dominated by thick intervals of dark grey to black phyllite and dark grey siltstone randomly intercalated with thin bedded fine grained sandstone and sandy limestone. Phyllite is tuffaceous in part.

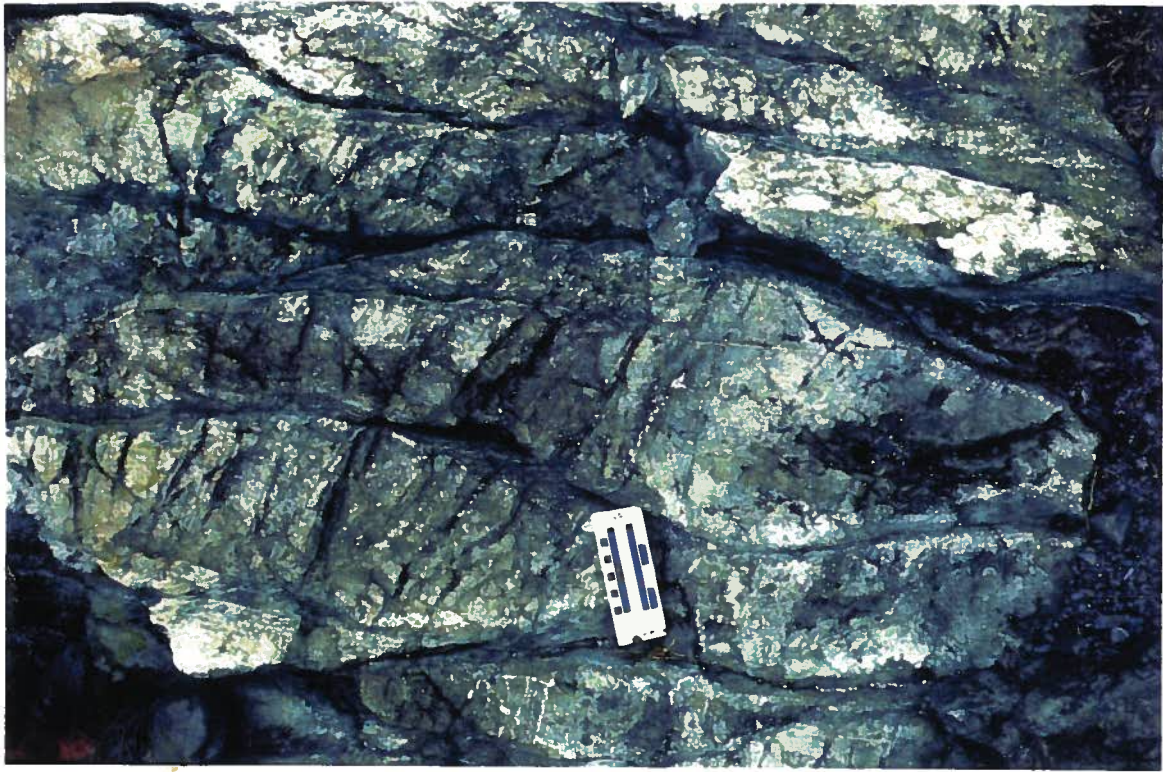


Figure 6.13 - Photograph of pillow basalt from unit 2 of Cayoosh assemblage.

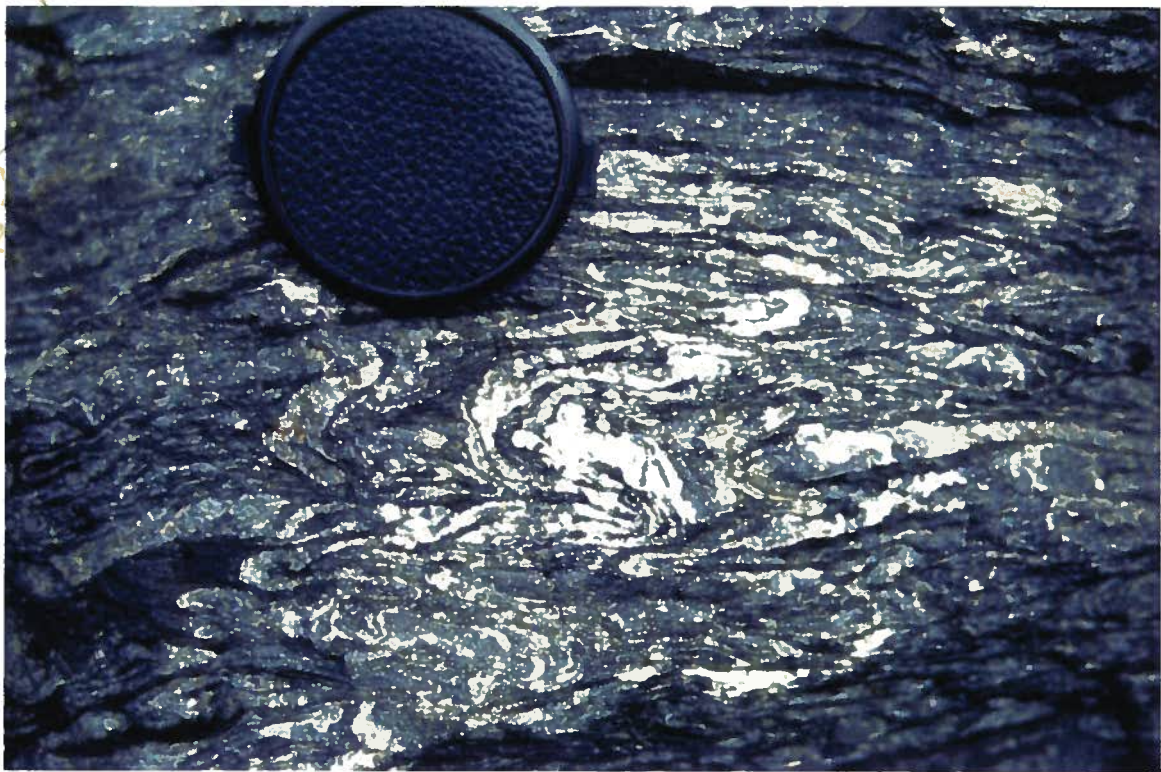


Figure 6.14 - Photograph of thin-bedded quartz-rich clastic facies displaying chaotic bedding character.

Sandstone intervals are locally fine to medium grained and medium bedded. Phyllite and siltstone decrease in abundance upsection, and the upper portion of the unit is dominated by fine to medium grained thin to medium bedded feldspathic sandstone with thin phyllite and siltstone interbeds. Sedimentary structures include parallel laminae, graded bedding, and minor cross-beds. Near Mount Brew, sandstone close to the top of the unit contains a distinctive fossiliferous lag deposit containing Early Cretaceous bivalves (Duffel and McTaggart, 1952; Mustard, 1983).

Fossiliferous sandstone near Mt. Brew grades upward into interbedded polymict conglomerate and medium- to coarse-grained feldspathic sandstone. The pebble to cobble conglomerate forms matrix supported (clast supported in part) lenticular beds up to 1.5 m thick, and contains clasts of plutonic rocks, intermediate to felsic volcanic rock, chert, sandstone, quartzite, siltstone and argillite. Conglomerate occurs as 1-2 m massive beds interbedded with medium to thick bedded sandstone, and in both thin beds and pebbly stringers within thick bedded sandstone. The conglomerate occupies the hinge zone of a kilometre-scale antiformal syncline, and the contact between the conglomerate and unit 5 of the Cayoosh assemblage is structurally disrupted and thus ambiguous. The dramatic change in depositional facies from a well-sorted shallow marine lithic feldspathic arenite to cobble to boulder conglomerate suggests the contact is unconformable (Journeay and Mahoney, 1994; Appendix E).

c. Biostratigraphy

Penetrative deformation and a regional metamorphism precludes macrofossil recovery from the Cayoosh assemblage; consequently, biostratigraphic control is limited. Poorly preserved Late Triassic to Early Jurassic radiolaria have been recovered from the base of the assemblage, and Early Cretaceous bivalves occur near the top of unit 5. Therefore, biostratigraphic data suggests that the Cayoosh assemblage is Late Triassic/Early Jurassic to Early Cretaceous in age. The poor biostratigraphic resolution makes identification of internal disconformities impossible, and the inferred age range must be regarded as a first estimate. Zircon recovered from volcanic rocks in unit 3 may provide additional age control.

Poorly preserved radiolaria recovered from siliceous argillite near the base of the formation in the Boulder Creek section are similar to Late Triassic to Early Jurassic forms documented in cherts of the Bridge River Complex (F. Cordey, personal communication, 1994). This assessment is consistent with biostratigraphic constraints provided by Late Triassic (Norian) conodonts extracted from limestone of the Bridge River Complex underlying the type area on Melvin Creek (Journey and Northcote, 1992; Mahoney and Journey, 1993).

A Late Triassic to Early Jurassic age for the base of the Cayoosh assemblage conflicts with age assessments of chert elsewhere in the Bridge River Complex. North of Carpenter Lake, to the north and east of exposures of the Cayoosh assemblage, Cordey and Schiarizza (1993) report radiolaria as young as late Middle Jurassic (Callovian) from cherts associated with greenstone, limestone, and argillite of the Bridge River Complex. There is no coherent assemblage of clastic rocks such as the Cayoosh assemblage conformably overlying the Bridge River Complex in this area, suggesting that chert deposition in one portion of the basin was synchronous with clastic influx in another part of the basin. Such a time transgressive sediment influx is supported by radiolaria biostratigraphy in the Hozameen Group. Haugerud (1985) documents Middle Jurassic (Aalenian to Bajocian) ribbon chert interbedded with argillite, sandstone, and pebbly mudstone, and suggests these rocks overlie Upper Triassic greenstone, limestone, and chert (Haugerud, 1985, p. 83). This relation demonstrates that chert deposition was at least in part synchronous with substantial clastic influx into the basin. Chert deposition in the Bridge River Complex did not require open ocean pelagic conditions, but was ongoing during basin infilling.

Fossiliferous greywacke near the top of unit 5 contains the Early Cretaceous (Valanginian) bivalve *Buchia crassicolis*, and these provide an upper age constraint on the Cayoosh assemblage (Duffel and McTaggart, 1952). Occurrence of these bivalves in shelly lag deposits in parallel laminated and cross-bedded sandstone suggests a shallow marine depositional environment existed at that time.

d. Volcanic Geochemistry

Primary volcanic rocks in the Cayoosh assemblage occur in Unit 2, and consist of pillow basalts and fragmental rocks. Geochemical analyses are reported for three tuff breccia samples and one pillow basalt sample (Fig. 6.15). Cayoosh assemblage fragmental volcanic rocks are subalkaline basalts, and the pillow basalt is alkaline (Fig. 6.15a). The fragmental rocks are geochemically distinct from the pillow basalt sample, and are discussed separately.

Major and trace element abundances and various elemental ratios (Rb/Sr, K/Ba) of the fragmental rocks display affinities with both arc tholeiite and mid-ocean ridge basalt (MORB; Table 6.2). Affinity to arc tholeiite is evident in Ti-Zr-Sr and Zr/Y space, whereas trace element ratios (Ti/Zr, Ti/Cr, Ta/Yb, Th/Yb) display strong affinity to ocean floor basalt (Pearce and Cann, 1973; Pearce and Norry, 1979). Ba/La ratios (Fig 6.15b), and low K₂O, Rb, and Ba abundances are characteristic of N-MORB, and light rare earth element (LREE) depleted REE patterns are indicative of derivation from a depleted mantle source, similar to that of a normal MORB (Fig 6.15 b,d). However, variations in LIL element abundances form normalised incompatible element patterns more characteristic of E-type MORB, differing only due to Cs and Sr enrichment and a slight depletion in Zr and Nb (Sun and Nesbitt, 1979; Fig. 6.15c). Cs and Sr enrichment and Nb depletion have been documented from back-arc basin basalts (Tarney et al., 1981; Saunders and Tarney, 1984). Element ratios further illustrate the duplicitous nature of the Cayoosh assemblage volcanic rocks, with values that overlap with both average island arc tholeiite (IAT) and MORB values (Table 6.2). Note that values that exceed limits for either IAT (i.e. K/Rb, Zr/Rb, Zr/Y, Ba/La) or MORB (i.e. Hf/Th) consistently overlap back-arc basin basalt values (Shervais, 1982; Volpe et al., 1988; Wilson, 1988).

The pillow basalt sample is relatively enriched in Ti, Nb, Be, La, Ce, Ta, and Th compared to the fragmental rocks, which results in separation between the pillow basalt and fragmental rocks on trace element discrimination diagrams (Fig. 6.15a, b). Enrichment in incompatible elements and LREE relative to the

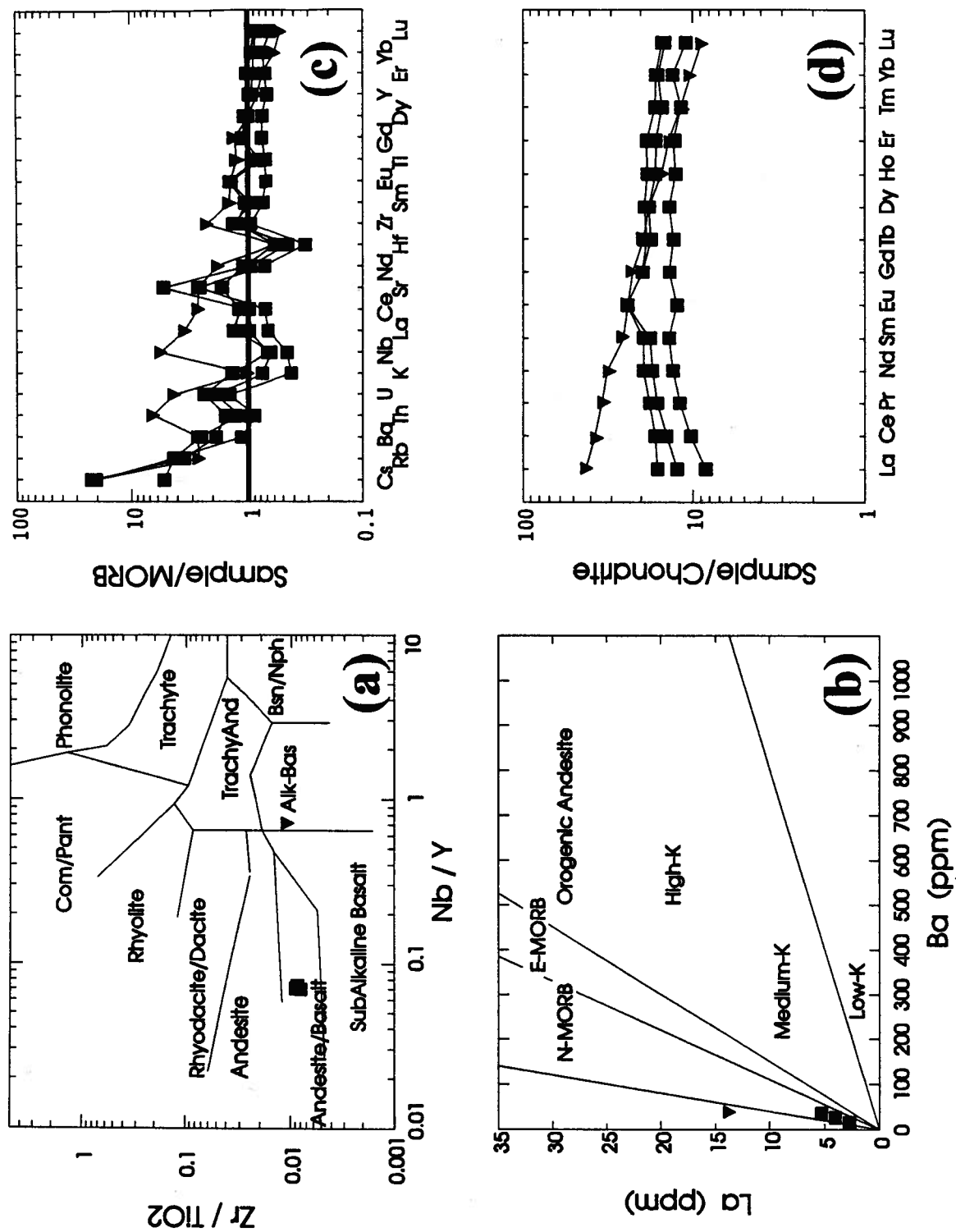


Figure 6.15 - Representative geochemical diagrams for volcanic rocks of Unit 2 of the Cayoosh assemblage. a) Zr/TiO₂ vs. Nb/Y plot from Winchester and Floyd (1977); b) Ba/La diagram, from Gill (1981); c) extended trace element diagram, normalised to MORB (Sun, 1979); d) rare earth element diagram, normalised to chondritic values.

fragmental rocks is pronounced (Fig. 6.15c, d). Incompatible element and rare earth element patterns display strong affinity to both enriched MORB (Sun and Nesbitt, 1979), and back arc basin basalts (Tarney et al. 1981). The combination of K and Rb depletion relative to other LIL elements and enrichment in HFSE elements (Nb, Ta, Ti, Zr) and LREE is unusual, and differs from either E-MORB or arc tholeiite. Similar alkalic high Ti-Nb basalts with high concentrations of incompatible elements and high Zr/Y ratios ($Zr/Y=7.0$) have been reported from the Daito Basin in the Philippine Sea, a trapped marginal basin within the remnant Kyushu-Palau arc (Tarney et al., 1981).

The geochemistry of volcanic rocks from the Cayoosh assemblage strongly indicates a back-arc basin affinity for these rocks. The LREE depletion is similar to MORB signatures, and the LIL element enrichment relative to HFSE is characteristic of island arc tholeiite. The combination of these two features is consistent with magma derivation from a depleted mantle source preferentially enriched in LIL elements. The hybrid nature of the fragmental rocks is common in back arc settings, as basalts from back-arc basins may have geochemical characteristics transitional toward arc magmas, particularly during the early stages of back arc extension (Tarney et al., 1981). The production of subalkalic to alkalic magmas in back arc settings has been attributed to both partial melting of the lower crust and magma generation in a transtensional regime (Saunders and Tarney, 1984; Nakamura et al., 1989). Geochemical complexities are common in back-arc basalts, which tend to display a combination of MORB-like and arc-like characteristics that are a function of the degree of mantle wedge enrichment by devolatilization of the subducted slab (Wilson, 1988). The small volume and limited stratigraphic and areal extent of basaltic material in the Cayoosh assemblage suggests that the inferred back arc extension/transtension in the basin was incipient, and was at best of limited duration and magnitude.

e. Isotopic Signature

Nd and Sr isotopic values for volcanic rocks of the Cayoosh assemblage reflect the juvenile character of the source magma. ϵ_{Nd} values vary from +5.15 to +7.96, and initial $^{87}\text{Sr}/^{86}\text{Sr}$ values are between 0.7045 and 0.7049. These values plot near the uncontaminated island arc field on a Nd/Sr diagram, but are displaced to the right of the mantle array, probably reflecting Sr enrichment via seawater contamination (Fig. 6.16). The fragmental rocks have ϵ_{Nd} values that are very close to N-MORB values; the ϵ_{Nd} value of the pillow basalt sample is distinctly lower, which may reflect a small degree of contamination through partial melting of juvenile lower crust, consistent with the alkalic nature of the sample.

Initial ϵ_{Nd} and $^{87}\text{Sr}/^{86}\text{Sr}$ values of fine-grained clastic rocks from the Cayoosh assemblage are variable and display more evolved signatures than those of the primary volcanic rocks (Fig. 6.16). Initial ϵ_{Nd} values vary from -2.31 to +4.81, and initial $^{87}\text{Sr}/^{86}\text{Sr}$ values vary from 0.7032 to 0.7051. Nd isotopic values vary from values within the uncontaminated island arc field, only slightly lower than the primary volcanic rocks, to slightly negative values indicative of contamination by an evolved detrital component. Initial strontium values display a limited range, although samples plotting below the mantle array may indicate open system behavior of the Rb-Sr system.

A plot of ϵ_{Nd} values against stratigraphic position demonstrates a strong temporal control on isotopic fluctuations (Fig. 6.17). The ϵ_{Nd} values of the primary volcanic rocks may be regarded as the juvenile volcanic component in a multicomponent depositional system, and sedimentary ϵ_{Nd} values substantially different (e.g. $> 2 \epsilon_{\text{Nd}}$ units) than the volcanic rocks indicate influx of an additional, more evolved component. Lithostratigraphic variations within the Cayoosh assemblage are mirrored by isotopic fluctuations; dominantly fine-grained intervals are characterised by low positive to slightly negative ϵ_{Nd} values, and intervals with a high proportion of volcanic debris display juvenile values (Fig. 6.17). Isotopic values of fine-grained clastic sedimentary rocks from unit 1 (+2.2 to +3.8), unit 2 (+.71), and unit 3 ((-2.3 to

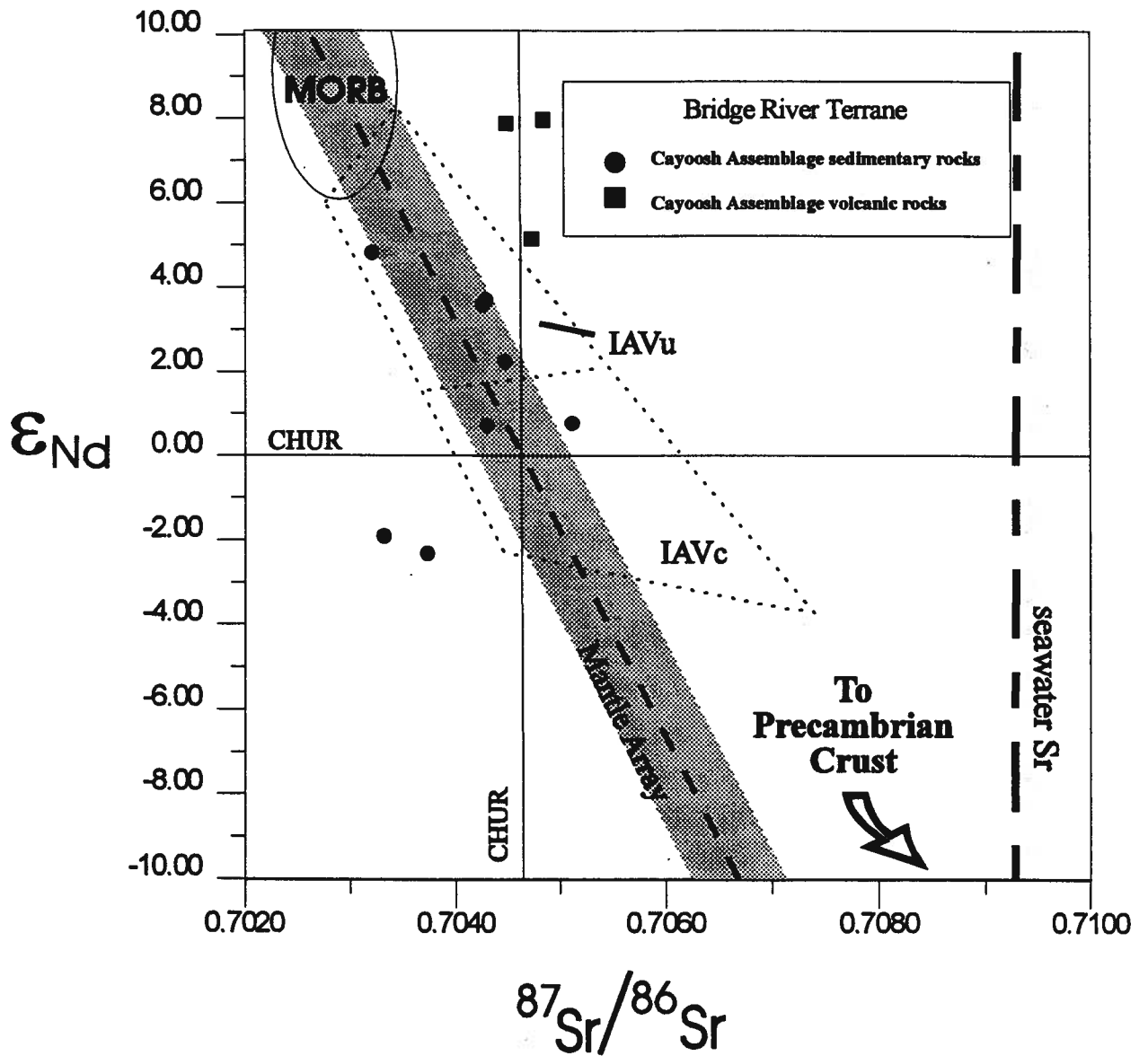


Figure 6.16 - $^{87}\text{Sr}/^{86}\text{Sr}$ vs. ϵ_{Nd} isotopic diagram for Cayoosh assemblage. Note arc fields and position of samples relative to mantle array. Data from DePaolo (1988), Samson et al. (1991), Hawkesworth (1993). IAVc=contaminated island arc; IAVu= uncontaminated island arc; MORB=mid ocean ridge basalt; CHUR=chondritic values (DePaolo and Wasserbure, 1976).

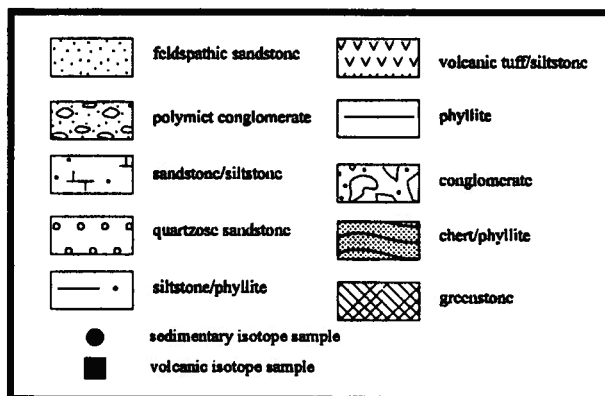
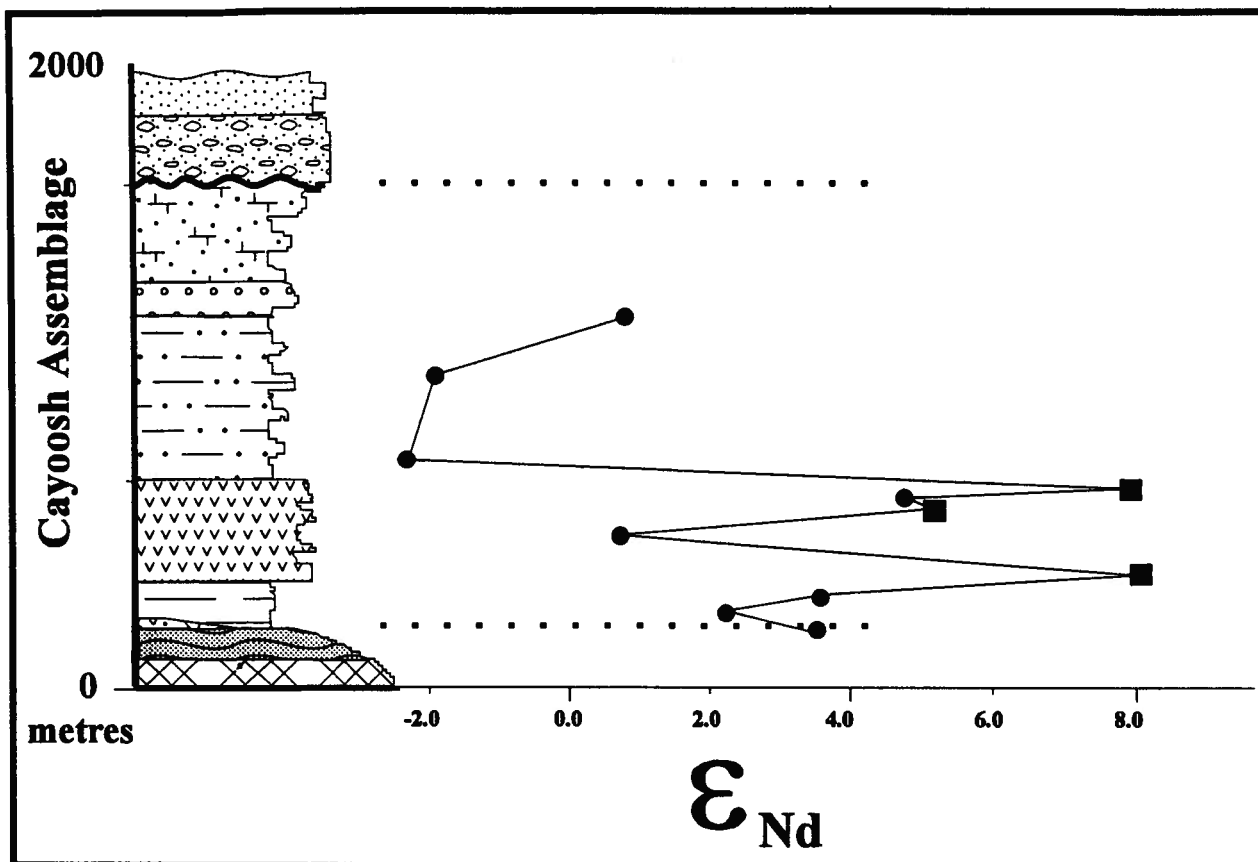


Figure 6.17 - ϵ_{Nd} vs. stratigraphic position for Cayoosh assemblage. Note isotopic shift to more evolved values in Toarcian.

+0.77) are interpreted to reflect ambient "background" sedimentation of mixed provenance detritus in a basin punctuated by influxes of volcanically-derived, juvenile detritus.

f. Depositional Environment

The Cayoosh assemblage is an upward-coarsening clastic succession that records the gradual closure and clastic infilling of the Bridge River "ocean" in Early Jurassic to Early Cretaceous time, concomitant with terrane amalgamation along the western margin of North America. Each of the 5 informal members records an important stage in the evolution of the Bridge River "ocean".

Fine-grained strata of the basal member (unit 1) are pelagic and hemipelagic deposits intercalated with minor partial turbidite deposits unconformably overlying Late Triassic rocks of the Bridge River Complex, and represent the first major detrital influx into the Bridge River "ocean" in Late Triassic/Early Jurassic time. Chert pebble conglomerate locally preserved at the base of the Cayoosh assemblage contains clasts derived from immediately subjacent strata, and may represent localized tectonic uplift within the basin.

Fragmental volcanic rocks, minor pillow lavas, and volcanoclastic sedimentary rocks of unit 2 are important stratigraphic markers representative of distinct pulses of volcanic activity in a sub-wavebase marine basin. The fragmental volcanic rocks are interpreted to be the product of subaqueous mass sediment gravity flows of tuff breccia and lapilli tuff adjacent to intrabasinal volcanic edifices; pillowed lavas represent minor effusive volcanism on the basin floor. Volcanic geochemistry and isotopic data suggest the volcanic rocks are back-arc basin basalts derived from a partially enriched depleted mantle source (Tarney and Saunders, 1984). Volcanoclastic sandstone and siltstone interbedded with the fragmental rocks locally display sharp lower contacts and graded bedding, and are interpreted as turbidite deposits. The abundant black phyllite of unit 2 represents pelagic and hemipelagic rainout during periods of volcanic quiescence.

Interbedded thin bedded sandstone and siltstone of unit 3 locally form rhythmic couplets, and sandstone beds form cyclic coarsening and thickening, then fining and thinning upward sequences indicative of deposition by mass sediment gravity flows in a migrating distributary system, such as a submarine fan complex. Phyllite locally dominates unit 3, and is interpreted to represent hemipelagic deposits laterally adjacent or distal to the coarser clastic intervals. The sandstone of unit 3 is characterised by plagioclase and volcanic lithic grains with subordinate quartz and rare plutonic lithic fragments, indicating a heterogeneous volcanoplutonic provenance. This inference is supported by slightly evolved ϵ_{Nd} signatures of fine-grained clastic rocks from unit 3.

Thin bedded quartzite and sandstone of unit 4 gradationally overlie sandstone and phyllite of unit 3, and represents a very distinctive component of Cayoosh assemblage stratigraphy. The thin bedded quartz-rich clastic facies comprises intercalated thin quartzite and phyllite, and may have been deposited as thin-bedded turbidites, but recrystallization has obliterated any diagnostic sedimentary structures. This facies commonly displays a chaotic bedding character that may be the result of soft sediment deformation. Plagioclase and minor zircon associated with the quartz-rich detritus suggest a plutonic source in part, but the compositional maturity of the unit indicates the detritus may be of second cycle (i.e. continental) origin. The quartz rich facies is unique among Mesozoic strata in the region. There is no local source of mature quartzose detritus, and the quartz-rich clastic facies may represent the first continentally derived detritus in the basin.

The quartz-rich clastic facies is gradationally overlain by a coarsening-upward succession of clastic strata in unit 5. In the lower portion of the unit, black phyllite and siltstone is intercalated with thin-bedded, fine-grained sandstone, locally calcareous, displaying parallel laminae, graded bedding, and partial Bouma sequences. The sandstone beds are thin and laterally continuous, and are interpreted as partial turbidites interbedded with hemipelagic deposits. Sandstone beds increase in abundance, grain size and bedding thickness increase upward, and become texturally and compositionally less mature. Sedimentary structures include graded bedding, parallel laminae, rare cross-bedding, and rip-up clasts. Intercalated sandstone and

siltstone beds are tabular and laterally continuous, and locally form rhythmic couplets, indicative of mass sediment gravity flow deposition. Near the top of the unit, bivalve-shell lag deposits in thick bedded well-sorted feldspathic sandstone are suggestive of shallow water deposition. The coarsening upward succession in Unit 5 is interpreted to record shallowing and progradation associated with incipient basin collapse.

Unit 5 is overlain by polymict granitoid-bearing pebble to cobble conglomerate of inferred Early Cretaceous age. Structural attenuation and clast elongation have eradicated definitive evidence of depositional environment. However, the matrix-supported character of the conglomerate, lack of well developed cross-beds and channels, and interbeds of well-sorted feldspathic sandstone suggest the conglomerate was deposited below wave base in a submarine fan environment (Walker, 1975). Middle Jurassic granitoid boulders (V. Coleman, personal communication, 1992) within the conglomerate indicates that it results from Late Jurassic to Early Cretaceous uplift and erosion.

D. Methow Terrane

a. Terrane Description

The Methow terrane consists of greenstone, chert, limestone and argillite of the Middle Triassic Spider Peak Formation unconformably overlain by argillite, siltstone, volcanic sandstone, conglomerate and minor volcanic rocks of the Lower to Middle Jurassic Ladner Group (Ray, 1986, 1990; O'Brien, 1986, 1987). Locally, the Ladner Group is disconformably overlain by Upper Jurassic siltstone, sandstone and pebble conglomerate of the Thunder Lake sequence (O'Brien, 1987). A thick succession of feldspathic marine sandstone and polymict, granitoid-bearing conglomerate of the Lower Cretaceous Jackass Mountain Group unconformably overlies rocks of the Thunder Lake assemblage near the International Border, and disconformably overlies rocks of the Ladner Group where the Thunder Lake sequence is absent (Figs. 6.2, 6.4).

The Ladner Group is subdivided into the Lower Jurassic Boston Bar Formation and the Lower to Middle Jurassic Dewdney Creek Formation (O'Brien, 1986). The Ladner Group has been offset approximately 80-150 km along the dextral Fraser fault system (Mahoney, 1993; Appendix E); previous workers refer to Middle Jurassic fine-grained clastic rocks northeast of the Yalakom Fault as the Lillooet Group (Duffel and McTaggart, 1952; Trettin, 1961). South of the International Border, Jurassic rocks of the southern Methow terrane correlative with the Ladner Group include the Lower Jurassic(?) Twisp Formation and Middle(?) to Late(?) Jurassic volcanic rocks and associated sediments of the Newby Group.

b. Lithostratigraphy

1. Boston Bar Formation

The Sinemurian(?) to Toarcian Boston Bar Formation comprises argillite, siltstone, thin bedded sandstone, sandy limestone and a thin (<50 m) basal conglomerate unconformably overlying greenstone, limestone, chert, and argillite of the Middle Triassic Spider Peak Formation (Ray, 1986, 1990; Fig. 6.18). The conglomerate is medium to thick bedded, matrix supported and consists of pebble to boulder sized subrounded to rounded clasts of greenstone, chert, limestone, syenite, granodiorite, quartz diorite, polymict conglomerate, sandstone, siltstone and argillite floating in an argillite to siltstone matrix. O'Brien et al. (1992) obtained a 235 +/- 10 Ma U/Pb age on a quartz diorite clast from the basal conglomerate, and suggested it was derived from the Permo-Triassic Mount Lytton Complex to the east. The conglomerate is locally interbedded with fine to medium grained, medium bedded sandstone and siltstone, and commonly occurs as stringers and thin lenticular beds encased in finer grained lithologies.

The basal conglomerate fines upward into a thick succession (>150 m) of thin- to medium-bedded, thinly laminated siltstone, fine grained sandstone, and argillite. Sedimentary structures include graded

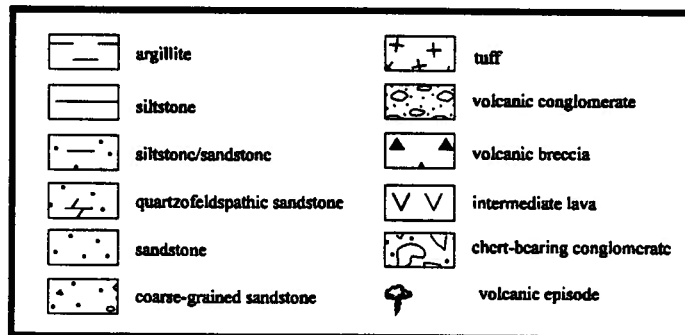
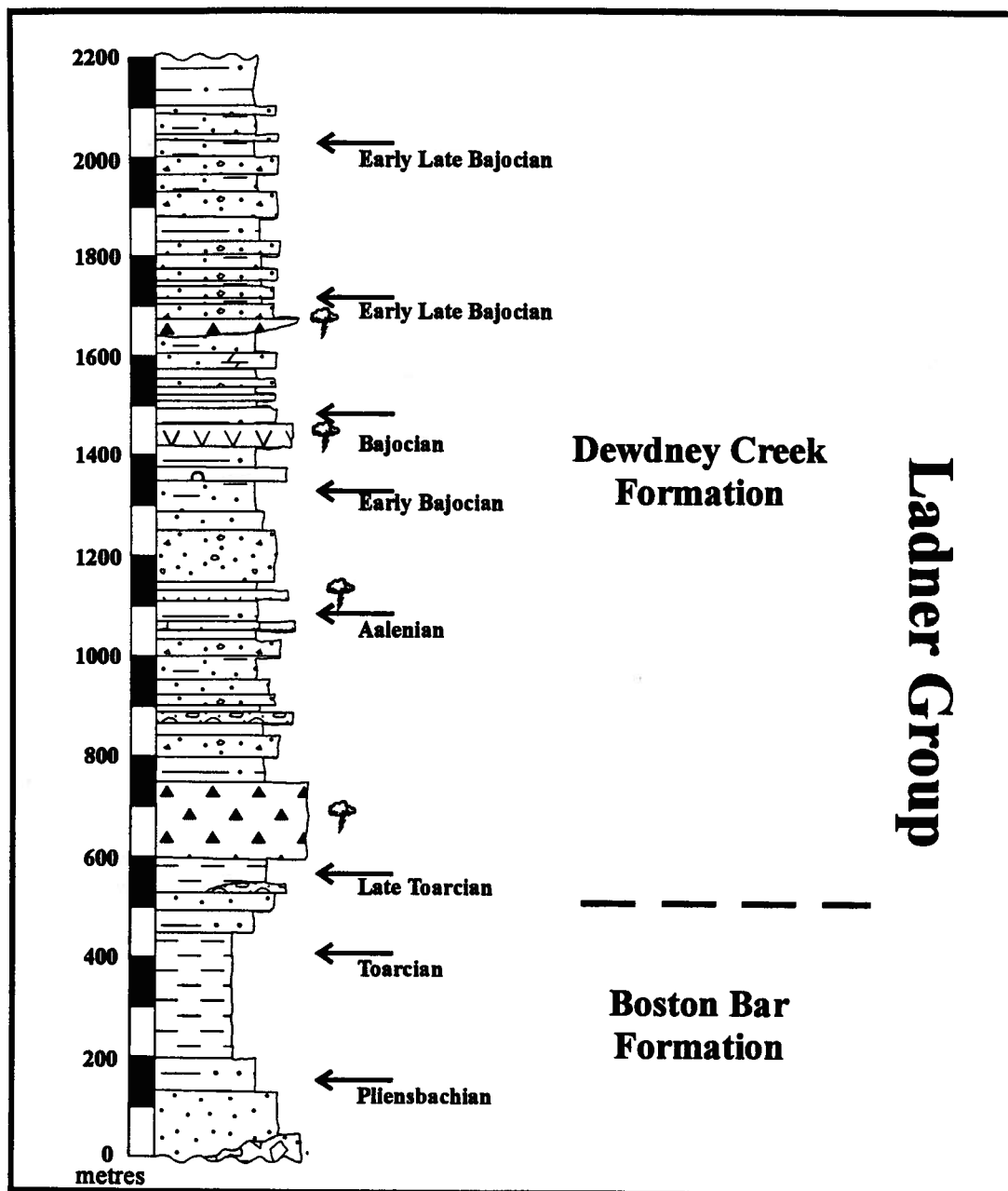


Figure 6.18 - Schematic stratigraphic section of the Ladner Group.

bedding, parallel, convolute, and cross-laminae, and soft sediment deformation features; aligned belemnite(?) fossil casts are locally evident. Ray (1990) reports medium bedded limestone and sandy limestone from this portion of the section. Fine grained sandstone and siltstone are gradationally overlain by the black argillite, siltstone, and lesser fine grained sandstone that dominate the Boston Bar Formation. The majority of the Boston Bar Formation consists of a thick (~500-700 m), monotonous succession of thin bedded, thinly laminated dark grey argillite and siltstone. Sedimentary structures are rare, and consist of parallel laminae and graded bedding in siltstone and fine-grained sandstone interbeds. The argillite has a well-developed spaced cleavage in part, and locally has a well developed phyllitic sheen; the argillite is contact metamorphosed to andalusite schist adjacent to Tertiary intrusions (Fig. 6.2).

Argillite and siltstone of the Boston Bar Formation coarsen upward into a 100-150 m thick succession of thin to thick bedded fine to medium grained sandstone, calcareous sandstone, and siltstone that forms the upper part of the formation. The lithic feldspathic sandstone becomes coarser grained and thicker bedded upward, and is intercalated with thin bedded fine to medium grained sandstone beds containing abundant sedimentary structures, including graded bedding, parallel laminae, wavy to undulose laminae, cross laminae, ripple marks, bioturbation, basal scour features, and shale rip-up clasts. The top of the Boston Bar Formation is a thick bedded, normally graded, matrix supported polymict conglomerate with pebble to cobble sized clasts of limestone, siltstone, felsic volcanic; quartz is locally abundant.

The Boston Bar Formation is gradationally overlain by volcaniclastic strata of the Dewdney Creek Formation. A gradational contact is suggested by the overall coarsening upward succession evident in the upper portion of the Boston Bar Formation, the increase in tractive sedimentary structures indicative of a shallowing trend, and the increase in feldspathic detritus in the Boston Bar Formation below coarse-grained volcaniclastic strata of the Dewdney Creek Formation. The gradational contact is estimated to be Late Toarcian in age based on biostratigraphic data.

2. Dewdney Creek Formation

Dewdney Creek Formation is a heterogeneous succession of coarse-grained volcanic sandstone, conglomerate, siltstone, argillite, and lesser pyroclastic and volcanic rocks (Fig. 6.18). The formation displays considerable lateral and vertical facies variation throughout the outcrop belt (Fig 6.2). The Dewdney Creek Formation comprises two distinct lithofacies belts: an eastern proximal facies and a western distal facies. This distinction was first recognized by Coates (1974) in opposite limbs of a major synclinorium in Manning Park, and is applicable to the entire outcrop belt. Detailed descriptions and schematic stratigraphic sections of each lithofacies are provided in Mahoney (1993; Appendix E); only a brief synopsis is given here.

The eastern proximal facies contains three distinct lithofacies, intercalated in varying proportions throughout the outcrop belt. The lithofacies include, in decreasing order of abundance: 1) coarse grained lithic feldspathic sandstone and volcanic conglomerate; 2) thin to medium bedded fine-grained sandstone, siltstone, and argillite; and 3) primary volcanic rocks, including volcanic breccia, tuff breccia, lapilli tuff, and rare volcanic flows.

The coarse-grained sandstone lithofacies comprises thick bedded to massive, medium to coarse grained, lithic feldspathic sandstone intercalated with thin to medium bedded sandstone and siltstone. Thick sandstone beds range from structureless to crudely laminated, and display basal scour features, rip-up clasts, and normal grading. Sandstone intervals form thick (2-25 m) cyclic coarsening and thickening upward/fining and thinning upward sequences. Pebble to granule volcanic conglomerate stringers occur within the coarsest portions of sandstone intervals and at the base of normally graded sandstone beds. Woody debris is common, particularly at the base of thick sandstone beds, and bioclastic debris is locally evident. The sandstone is compositionally homogeneous, dominated by lithic feldspathic wacke containing abundant plagioclase, sanadine, and trachytic volcanic lithic fragments. Rare quartzofeldspathic sandstone containing detrital illmenite and titanite attest to a plutonic component in the provenance. Matrix to clast-supported, cobble to boulder volcanic conglomerate locally forms lenticular beds with erosive bases interpreted to be channels.

The fine-grained sandstone lithofacies comprises thin to medium bedded, fine to medium grained, moderately well sorted lithic feldspathic wacke intercalated with thin bedded siltstone and argillite. Sedimentary structures include parallel laminae, graded bedding, cross-bedding, undulose to convolute laminae, flame structures, climbing ripples, and scour features. Fossiliferous shelly lag deposits containing pelecypod, echinoderm, ammonite and brachiopod shells intermixed with woody debris were noted in one locale. Thick successions of rhythmic interbeds of thin bedded sandstone and siltstone near the top of the formation are amalgamated partial turbidites. The lithofacies occurs in 10-25 m intervals interbedded with the coarse sandstone lithofacies, but locally amalgamates to 100-200 m successions, particularly near the top of the formation.

The volcanic lithofacies constitutes a small (<20%) but important component of the Dewdney Creek Formation. The volcanic lithofacies is not evenly distributed throughout the formation, but occurs in distinct pulses (Fig. 6.18). Biostratigraphic constraints indicate volcanism was active in Late Toarcian, mid-Aalenian, Early Bajocian, and early Late Bajocian time (Fig. 6.18). Fragmental volcanic rocks predominate, and include andesitic to dacitic breccia, tuff breccia, lapilli tuff, and lesser crystal tuff. Volcanic breccia and tuff breccia form thick bedded to massive, structureless lenticular beds; tuff breccia locally fills conglomeratic channels in the lower portion of the formation. Matrix supported tuff breccia containing sedimentary accidentals and bioclastic debris in the Anderson River area is interpreted as debris flow (Appendix E). Lapilli tuff and crystal tuff form tabular, laterally continuous beds, commonly associated with thick sequences of the coarse grained lithofacies. Volcanic flows are rare and are restricted to the eastern side of the outcrop belt. Flows consist of aphanitic to plagioclase-phyric andesite to dacite, and are commonly associated with volcanic breccia.

The western distal facies is thinner bedded, finer grained, and more homogeneous than the eastern proximal facies (Appendix E). The facies consists of thin bedded fine grained feldspathic sandstone, siltstone, and argillite intercalated with lesser medium to thick bedded medium to coarse grained lithic feldspathic

sandstone and conglomerate. Thin bedded sandstone and siltstone form 3-8 cm graded couplets that give the outcrop a banded appearance. Couplets are amalgamated into cyclic, coarsening and thickening/fining and thinning, upward sequences separated by 0.5 to 1 m argillite intervals. Sedimentary structures in the thin bedded intervals include parallel laminae, graded bedding, convolute laminae, and rare cross-laminae; partial or complete Bouma sequences are common.

Medium to very thick bedded, medium to coarse grained sandstone and granule to pebble conglomerate is intercalated within the thin bedded lithologies, forming prominent ribs that stand out in bold relief against the recessively weathering fine grained rocks. Sandstone and conglomerate are arranged in 50-80 m coarsening and thickening/fining and thinning upward cyclic successions. The sandstone varies from structureless to crudely laminated, and sedimentary structures include parallel laminae, graded bedding, basal scour features, siltstone rip-up clasts, and flame structures.

The western distal facies is truncated against the dextral Fraser fault system south of Boston Bar, and its offset equivalent is exposed northeast of the Yalakom fault in rocks formerly mapped as the Lillooet Group (Fig. 6.2, Appendix E). These rocks are lithologically identical to the western distal facies, but contain a slightly higher proportion of thin, yellowish-white tuffaceous interbeds. Flute casts on the base of coarse sandstone beds indicate northeast or southwest directed paleoflow (n=18).

The Dewdney Creek Formation is locally disconformably overlain by a thin sequence (<300 m) of volcanic sandstone, granule to pebble conglomerate, siltstone and shale of the Upper Oxfordian to Upper Tithonian Thunder Lake sequence (Jeletsky, 1972; Coates, 1970; O'Brien, 1986, 1987). The sequence fines upward from basal granule to pebble conglomerate and pebbly sandstone into thin to medium bedded, fine to medium grained, lithic feldspathic sandstone, thin bedded siltstone, and sandy argillite (Monger, 1970; Coates, 1970; Jeletsky, 1972). The dominantly volcanic conglomerate contains rare granite and argillite clasts, and fine grained beds locally contain abundant pelecypods (Monger, 1970; Coates, 1970). Lateral

facies changes in the Thunder Lake sequence result in variations in the coarse grained to fine grained sediment ratio along the outcrop belt.

c. Biostratigraphy

Faunal preservation in the Ladner Group is uneven; biostratigraphic control is excellent in the Dewdney Creek Formation, and sparse in the Boston Bar Formation. The Boston Bar Formation has a limited areal extent, and where exposed is adjacent to plutons or major regional faults that result in structural and metamorphic overprinting that inhibits fossil preservation (Fig. 6.2). The Boston Bar Formation displays strong near-bedding-parallel cleavage, tight to isoclinal mesoscopic and macroscopic folds, abundant bedding parallel faults, and is locally metamorphosed to hornblende hornfels facies. Deformation more intense in argillaceous intervals, and less pronounced in sandy successions. This strain partitioning may be responsible for the higher degree of deformation apparent in the Boston Bar Formation relative to the overlying Dewdney Creek Formation.

Boston Bar Formation fauna are restricted to rare Pliensbachian ammonites. Sinemurian(?) forms have been reported from the southern portion of the outcrop belt, but are unconfirmed (Coates, 1974). The Pliensbachian *Dubariceras* has been recovered from interbedded argillite and sandstone north of Boston Bar. Toarcian ammonites are reported from lithologically and isotopically identical strata mapped west of the Fraser fault, which are herein correlated with the Boston Bar Formation (Hickson, 1990; Read, 1993). Occurrence of the bivalve *Weyla* in Boston Bar Formation strata is consistent with a Sinemurian to Toarcian age for the formation (O'Brien, 1987)

The Dewdney Creek Formation contains abundant Late Toarcian to Late Early Bajocian ammonites; *Tmetoceras* and *Stephanoceras* (H.W. Tipper, personal communication, 1994), of Aalenian and Early Bajocian age, respectively, are by far the most abundant (Table 6.1). The eastern proximal facies yields contains mixed assemblages of bivalves, including *Myaphorella* sp. (H.W. Tipper, personal communication,

1994), echinoderms, ammonites, and woody debris, indicating shallow water deposition. Fauna in the western proximal facies are restricted to ammonites found in black shale intercalated with turbidite sequences, suggesting subwavebase deposition.

The Aalenian to Early Bajocian fauna in the Ladner Group include forms of Tethyan (*Planamatoceras*, *Eudmetoceras*), East Pacific (*Zemistephanus*), and Boreal (*Pseudolioceras*, *Erycitoides*) affinity (Taylor et al., 1984; Table 6.1). This mixed assemblage limits the paleogeographic setting of the Middle Jurassic basin to the northeastern quadrant of the Panthalassa ocean (Taylor et al., 1984).

d. Volcanic Geochemistry

Primary volcanic rocks in the Ladner Group are restricted to isolated exposures on the east side of the eastern proximal facies of the Dewdney Creek Formation. Geochemical analyses are reported for 3 lava flows and 2 clasts from volcanic breccias. Primary volcanic rocks are more abundant in correlative strata from the Newby Group in the southern Methow terrane, and 7 analyses are reported from these rocks. Geochemical and isotopic similarities between volcanic rocks of the Dewdney Creek Formation and the Newby Group suggest the Newby Group is a southern extension of the Dewdney Creek Formation.

Jurassic volcanic rocks of the Methow terrane are primarily basaltic andesite to dacite, and are compositionally low potassium tholeiite to medium to high potassium calcalkaline in composition (Fig. 6.19 a,b). Trace element abundances and diagnostic elemental ratios (e.g. Zr/Rb, La/Th, La/Nb) are within tholeiitic to calcalkaline volcanic arc values (Gill, 1981; Wilson, 1988). The rocks generally have low Ce/Yb (<15) ratios, consistent with a relatively primitive, uncontaminated volcanic arc setting (Hawkesworth et al., 1993).

Incompatible trace element patterns (Fig. 6.19c) display the strongly spiked patterns characteristic of subduction-related magmatism (Pearce, 1982; Wilson, 1988). The LIL elements are largely enriched relative

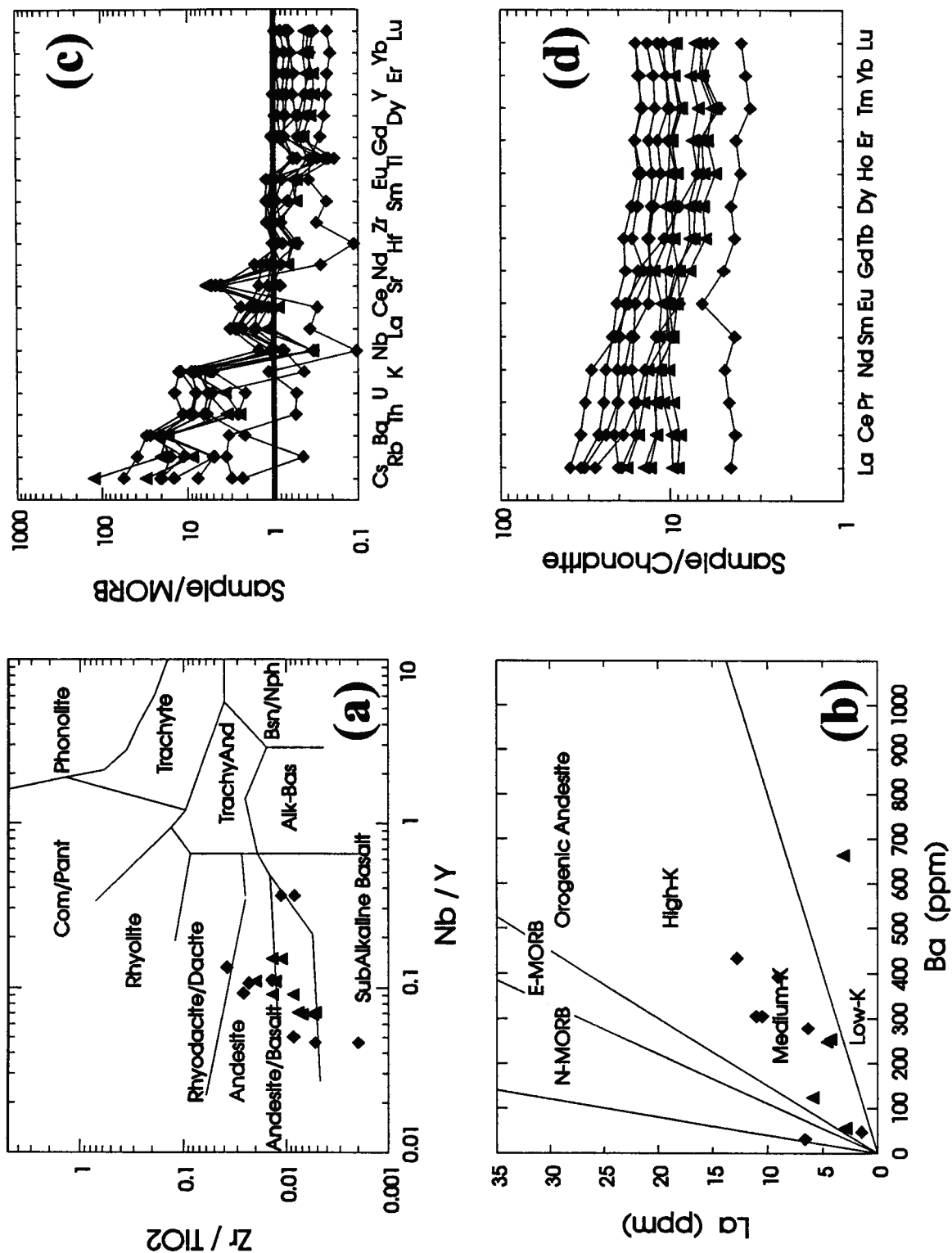


Figure 6.19 - Representative geochemical diagrams for volcanic rocks of the Methow terrane. Triangles are Dewdney Creek Formation; diamonds are Newby Group a) Nb/Y vs. Zr/TiO₂ plot from Winchester and Floyd (1977); b) Ba vs. La diagram from Gill (1981); c) extended trace element diagram, normalised to MORB (Taylor and McLennan, 1985); d) rare earth element diagram, normalised to chondritic values (Sun, 1982).

to MORB, and distinct spikes occur at Ba, K, and Sr. The HFSE are depleted relative to MORB, including a marked depletion of Ti. The REE patterns (Fig. 6.19d) may be subdivided into two subgroups: 1) samples that display a flat to slightly concave down pattern, induced by a slight LREE depletion ($\text{La}_N/\text{Yb}_N = \sim 1.0$); or, 2) samples with a slight concave up pattern, displaying both LREE and very minor HREE enrichment ($\text{La}_N/\text{Yb}_N = \sim 2.0\text{--}2.5$). The first subgroup is characteristic of low-K andesitic volcanic arc suites, and the second subgroup is characteristic of medium-K andesitic suites (Gill, 1981). One sample (369JBM92) displays an anomalously depleted incompatible trace element pattern and a depleted REE pattern.

Geochemistry of Dewdney Creek Formation volcanic rocks and correlative rocks of the Newby Group to the south indicate magma genesis via subduction-related arc volcanism. Minor geochemical differences within the sample suite are ascribed to spatial variations along the evolving arc, or may be a function of the small sample set.

e. Isotopic signature

Nd and Sr isotopic values for primary volcanic rocks in the Dewdney Creek Formation and correlative rocks of the Newby Group reflect the isotopic homogeneity of the magmatic source. Initial ϵ_{Nd} values display a very restricted range from +6.2 to +7.5; initial $^{87}\text{Sr}/^{86}\text{Sr}$ values are equally homogeneous, ranging from 0.7028 to 0.7041. These values are near the upper limit of the uncontaminated volcanic arc field in $\epsilon_{\text{Nd}}\text{--}^{87}\text{Sr}/^{86}\text{Sr}$ space, overlapping with the lower limit of MORB values (Fig. 6.20). The volcanic rocks are isotopically very juvenile, consistent with their incompatible trace element and rare earth element patterns. The isotopic values require magma generation from a depleted mantle source.

Fine-grained clastic rocks from the Ladner Group display a wider range of initial ϵ_{Nd} and $^{87}\text{Sr}/^{86}\text{Sr}$ values than coeval volcanic rocks. Initial ϵ_{Nd} values vary from -0.2 to +6.5, although most of this variation is within the Boston Bar Formation; Dewdney Creek Formation rocks display a much more limited range of ϵ_{Nd} .

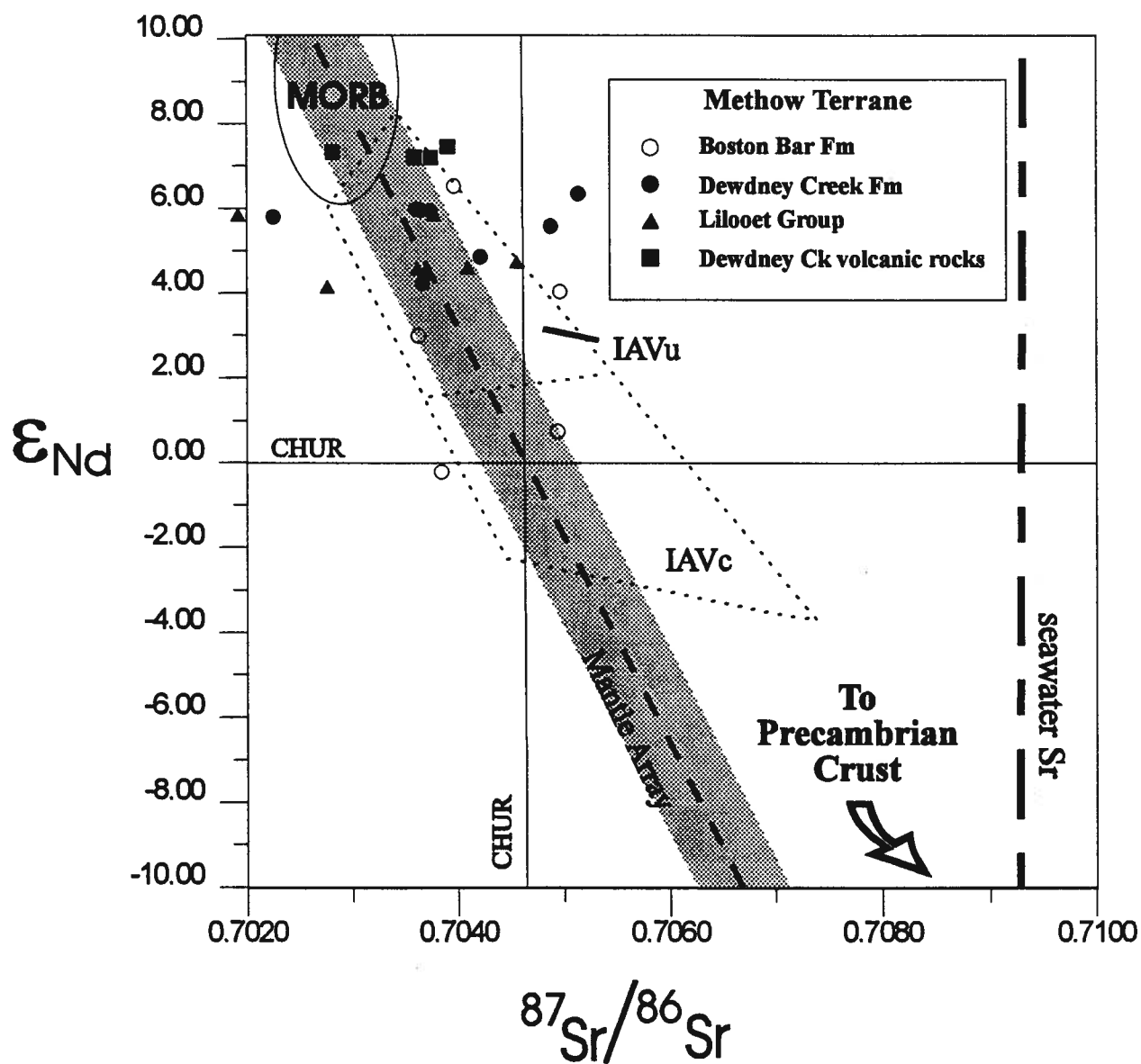


Figure 6.20 - $^{87}\text{Sr}/^{86}\text{Sr}$ vs. ϵ_{Nd} isotopic diagram for Dewdney Creek Formation. Note arc fields and position of samples relative to mantle array. Data from DePaolo (1988), Samson et al. (1991), Hawkesworth (1993). IAVc=contaminated island arc; IAVu= uncontaminated island arc; MORB=mid ocean ridge basalt; CHUR=chondritic values (DePaolo and Wasserburg, 1976).

from +4.1 to +6.2 (Fig. 6.20). Initial strontium values display an anomalously wide range, from 0.7020 to 0.7050. Displacement of initial strontium values to the left of the mantle array suggest post-depositional disturbance of the Rb-Sr isotopic system, most likely reflecting a younger metamorphic event, consistent with low grade metamorphic alteration assemblages documented petrographically (Fig. 6.20; Appendix D).

There is a very strong temporal control on ϵ_{Nd} values in the Ladner Group (Fig. 6.21). A comparison of ϵ_{Nd} values with stratigraphic position illustrates the relatively evolved nature of the Boston Bar Formation compared to the Dewdney Creek Formation. The lower Boston Bar Formation has ϵ_{Nd} values consistent with a relatively juvenile source, such as a volcanic arc. Overlying argillaceous strata display a significant isotopic shift to slightly evolved values ($\epsilon_{Nd} = \sim 0$ to +3), suggesting contamination of the juvenile detritus with an evolved component, probably a small component of continentally-derived hemipelagic debris or oceanic pelagic material. A second major isotopic shift back to juvenile values occurs in the Late Toarcian, coincident with the initiation of volcanism in the Dewdney Creek Formation. Volcanic rocks in the Dewdney Creek Formation have juvenile values ($\epsilon_{Nd} = +6.2$ - +7.4), and are considered to represent one end member in a multicomponent system supplying detritus to coeval sedimentary rocks. Displacement of the ϵ_{Nd} values of associated sedimentary rocks 2 ϵ_{Nd} units below volcanic rock values requires admixture of a small component of more evolved detritus into the depositional system during Late Toarcian to Late Bajocian time.

f. Depositional Environment

Ladner Group records a distinct two-stage depositional sequence encompassing Early to Middle Jurassic time. The first stage involved deposition of fine-grained clastic sedimentary rocks of the Boston Bar Formation, and is followed by a second stage characterized by volcanic and first cycle volcanoclastic deposition evident in the Dewdney Creek Formation.

The majority of the Boston Bar Formation defines a fining upward succession of conglomerate, sandstone, siltstone and argillite, with argillite comprising over 70% of the formation. The timing of initial

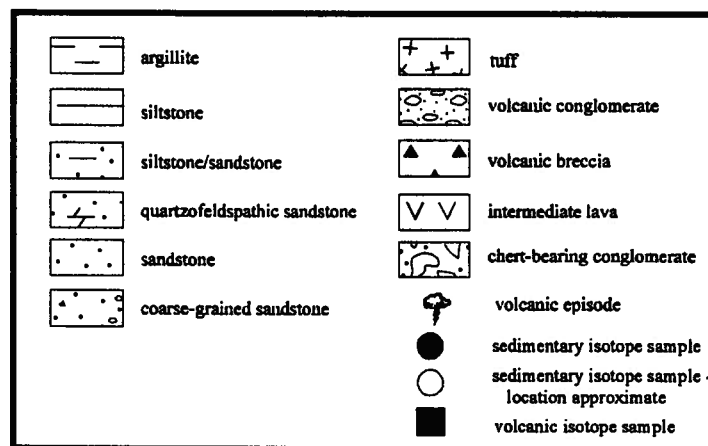
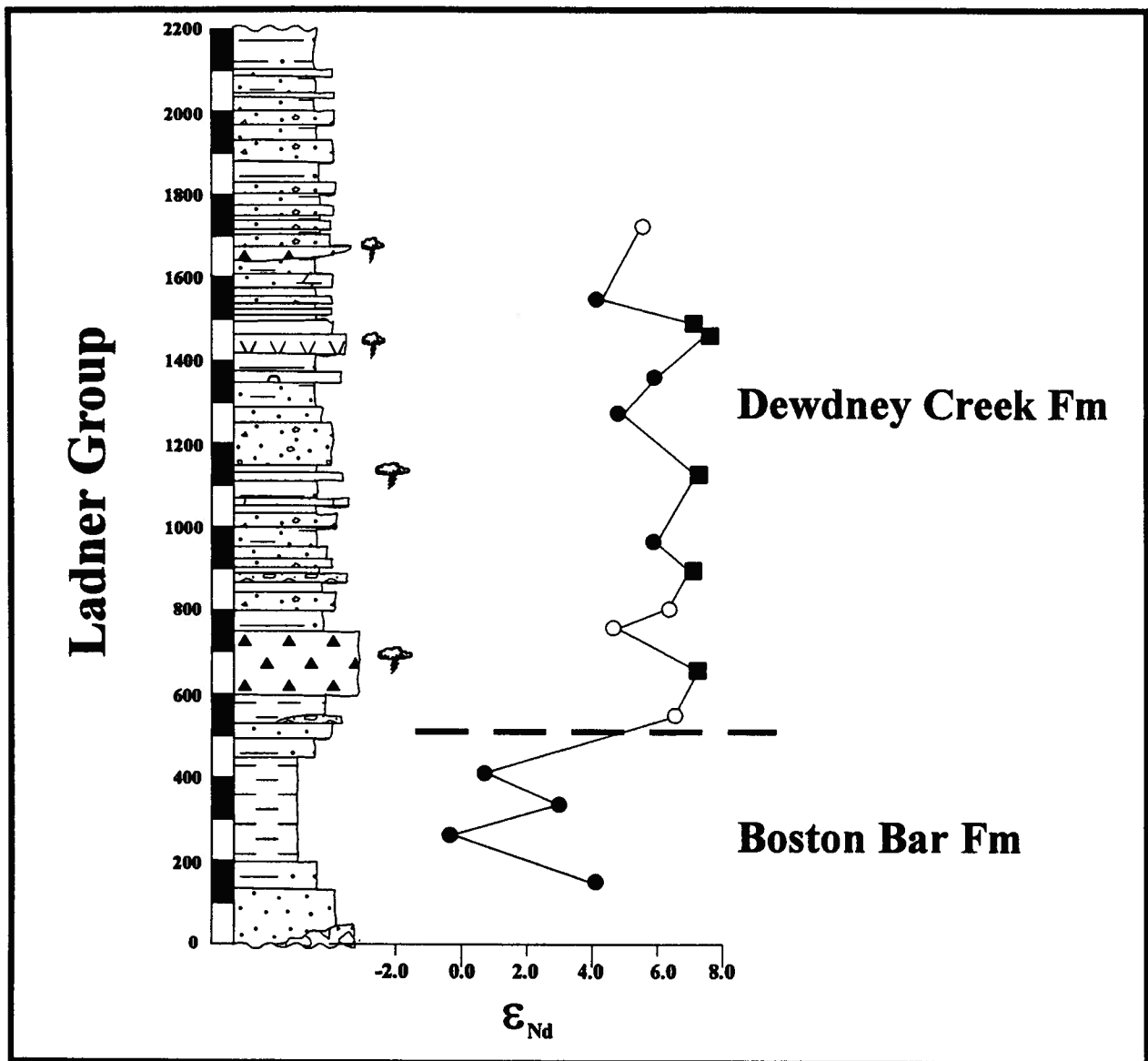


Figure 6.21 - ϵ_{Nd} vs. stratigraphic position for Dewdney Creek Formation. Note isotopic shift to more evolved values in Toarcian.

subsidence in the Boston Bar Formation depocentre is ill-defined due to a lack of biostratigraphic control. Deposition of the basal conglomerate is strictly constrained to only post-Middle Triassic and pre-Pliensbachian in age. However, the occurrence of the bivalve *Weyla* (Late Hettangian to Toarcian; O'Brien, 1987) and possible Sinemurian ammonites in overlying strata suggests the Boston Bar Formation depositional sequence began in the Early Jurassic. Conglomerate clast composition requires a heterogeneous provenance containing oceanic rocks (greenstone, gabbro, chert, limestone), volcanic rocks (intermediate and felsic volcanic rocks), and plutonic rocks (syenite, granodiorite, quartz diorite). The plutonic suite is at least in part Late Triassic in age, based on U-Pb geochronology on a quartz diorite clast (O'Brien et al., 1992). The lenticular nature, matrix supported character, and association with fine grained sediments suggests the conglomerate was deposited in subaqueous channels.

The basal conglomerate is overlain by a thick succession (>150 m) of partial and complete thin to medium bedded turbidite sequences. Partial and complete turbidites grade upward into interbedded siltstone and argillite interpreted as bottom-cut-out partial turbidites. Argillite increases in abundance upward, and hemipelagic and pelagic deposition dominates the majority of the formation. In the upper part of the formation, argillite is gradationally overlain by coarsening upward succession of fine to medium grained sandstone, calcareous sandstone, siltstone, and conglomerate, indicating a renewed clastic influx. This succession is notable for an increase in the abundance and diversity of sedimentary structures relative to underlying strata, suggesting a shallowing of the basin.

Coarse grained sandstone and conglomerate of the eastern proximal facies of the Dewdney Creek Formation were deposited by a combination of channelized and unchannelized subaqueous mass sediment gravity flows, primarily high concentration turbidity currents. Thin bedded sandstone and siltstone intercalated with thick sandstone intervals form both complete and partial Bouma sequences, and represent low concentration turbidity flows. Thin to medium bedded sandstone and siltstone containing abundant sedimentary structures is locally interbedded with coarse grained sandstone and lapilli tuff, and is interpreted to represent shallow water reworking of volcanically-generated mass sediment gravity flows. Channelized

to represent shallow water reworking of volcanically-generated mass sediment gravity flows. Channelized conglomerate and volcanic breccia, bioclasts in volcanic debris flows, lag deposits containing shallow water bivalves and wood debris, and abundant tractive sedimentary structures indicate near shore shallow water deposition.

The eastern proximal facies was deposited in shallow to intermediate depth (below normal wave base) water adjacent to an energetic andesitic to dacitic volcanic arc system. Deposition occurred on a volcanoclastic apron characterised by episodic pyroclastic influx and subaqueous mass sediment gravity flows. The apron shallowed to the east, as suggested by an increase in primary volcanic rocks and shallow water bioclasts at the eastern edge of the outcrop belt. The association of thick, coarse-grained high concentration turbidites and thin bedded shallow water facies indicate periodic inundation of the apron by pyroclastic or resedimented pyroclastic debris mass sediment gravity flows followed by reworking via normal marine processes. Rapid lateral facies changes suggest an uneven bottom topography. The abundance of convolute laminae, ball and pillow structures, overturned flame structures, and a paucity of biogenic structures indicate deposition was rapid. Interbedded quartzo-feldspathic rocks require a heterogeneous provenance including exposed plutonic rocks as well as active volcanic edifices.

The western distal facies is the product of unchannelized turbidity currents and hemipelagic sedimentation below effective wavebase. Episodic coarse clastic influx, perhaps the result of migrating distributary lobes or the progradation of a clastic wedge, produced the intercalated cyclic coarse grained successions. The western distal facies is inferred to have been deposited farther from the volcanic source due to its overall fine grained nature, lack of primary volcanic facies, absence of channelled deposits, abundance of Bouma sequences, and the lack of wood or bioclastic debris. The western distal facies is interpreted to have deposited on the lower, unchannelized, portions of a west-dipping volcanoclastic apron.

The primary source terrane for the Ladner Group was to the east in Early to Middle Jurassic time. Paleocurrents documented in the lower Boston Bar Formation include overturned flame structures indicating westerly paleoflow (Ray, 1990) and aligned belemnite(?) casts indicating a southeast-northwest paleoflow direction (n=12). Paleoflow indicators measured in the Dewdney Creek Formation include slump folds, foreset beds, ripple marks, and groove marks, all of which indicate a north to northwest-striking paleoslope with westerly directed sediment transport. A west-dipping slope is consistent with the interpretation of a westward-thinning volcanoclastic apron, and is in agreement with paleoslope orientations obtained by Coates (1970).

Volcanism in the Ladner Group was episodic from Late Toarcian to Early Bajocian time. The Ladner Group is unconformably overlain by shallow water clastic rocks of the Oxfordian to Tithonian Thunder Lake sequence, indicating a substantial hiatus extending from Late Bajocian to Oxfordian time. There is no evidence of structural deformation during this interval.

6.4 STRATIGRAPHIC CORRELATIONS

Lithostratigraphic, biostratigraphic, and isotopic variations within Middle Jurassic strata on the Harrison, Cadwallader, Bridge River, and Methow terranes are remarkably synchronous, and strongly suggest evolution in a common basin. Volcanic geochemistry, on the other hand, indicates differences among primary volcanic rocks within Middle Jurassic strata, and allows constraints to be placed on basin configuration.

A. Lithostratigraphic Correlations

Lithostratigraphic variations, including pronounced changes in depositional regime (dominant lithology, water depth, transport direction) and provenance, are a function of the crustal dynamics of the basin and its margins, the compositional heterogeneity of source terranes, volcanic episodicity, and climatic fluctuations. Lithostratigraphic variations result in distinctive stratigraphic assemblages that may be used to

correlate strata in tectonically dismembered basinal sequences. Strata examined in this investigation were deposited in volcanogenic marine basins, which are generally restricted to active plate tectonic margins. Profound stratigraphic differences exist between coeval basins along active tectonic margins due to variations in basement character, plate geometry, subduction rate, and subsidence history along the plate margin. The complexities evident in basins along active plate margins indicate that documentation of multiple lithostratigraphic correlation horizons among tectonically separated basinal sequences would strongly support original deposition in a single basin.

Early to Middle Jurassic strata on the Harrison, Cadwallader, Bridge River, and Methow terranes exhibit strikingly similar lithostratigraphic patterns. Available biostratigraphic constraints suggest synchronicity among lithostratigraphic variations on all terranes. Lithostratigraphic correlations among the terranes are proposed based on four regionally consistent stratigraphic relationships:

1) Initiation of basin subsidence in Early Jurassic (post Late Triassic, pre-Toarcian) time. The initiation of subsidence is marked by a thin basal polymict chert pebble conglomerate in all units, regardless of whether or not chert is present in underlying basement rocks (Fig. 6.22). The thickness and lateral extent of the basal conglomerate varies, perhaps due to irregular basement topography and distance from source. Plutonic clasts in the basal conglomerate are restricted to the Ladner Group, and, to a lesser extent, the Last Creek Formation; volcanic, chert, limestone, and clastic sedimentary clasts are ubiquitous. Apparent differences in the timing of conglomerate deposition may be a function of paleontologic resolution, or the result of a time transgressive basal unconformity.

2) Pliensbachian to Toarcian black shale deposition. Each terrane contains a thick succession of Lower Jurassic black shale and thin-bedded siltstone overlying a basal conglomerate and underlying Middle Jurassic volcanic rocks (Fig. 6.22). The black shale interval does not contain primary volcanic detritus. These fine-grained clastic rocks tend to display a slightly evolved isotopic signature, indicating a mixture of juvenile, arc-derived material and a more evolved, possibly continental, component.

3) Initiation of volcanism in Late Toarcian to Aalenian time. Each terrane is interpreted to record the transition from black shale sedimentation to primary volcanic deposition in Late Toarcian to Early Aalenian time (Fig. 6.22). Volcanic deposits vary in thickness and type throughout the region; the coarsest and thickest intervals are exposed in the Harrison Lake Formation on the west and in the Ladner Group to the east. The Cayoosh assemblage contains the only documented pillow basalts, and deposits in the Last Creek Formation are limited to thin Aalenian tuff beds.

4) Cessation of volcanism in Late Bajocian/Early Bathonian time. The Harrison, Cadwallader, and Methow terranes contain significant unconformities between Late Toarcian to Bajocian volcanic deposits and overlying late Callovian to Oxfordian shallow marine deposits (Fig. 6.22). Although age constraints in the Bridge River terrane are lacking, thick volcanic deposits are overlapped by argillaceous rocks intercalated with thick sandy turbidite lobes petrographically distinct from underlying strata. This change in provenance supports the existence of an intraformational disconformity or sequence boundary in the Cayoosh assemblage between units 2 and 3.

Additional contemporaneous lithostratigraphic variations in late Middle Jurassic to Early Cretaceous strata on each terrane lend support to stratigraphic correlation:

5) Shift in provenance and depositional environment in late Middle Jurassic time. The Cadwallader, Bridge River, and Methow terranes display a change in provenance in strata overlying Middle Jurassic volcanic deposits. The Callovian to Tithonian Relay Mountain Formation of the Cadwallader terrane contains plutonic quartz intermixed with volcanogenic debris deposited in a prograding deltaic environment (Umhoefer, 1989). The Cayoosh assemblage records a distinct increase in quartz and associated plutonic

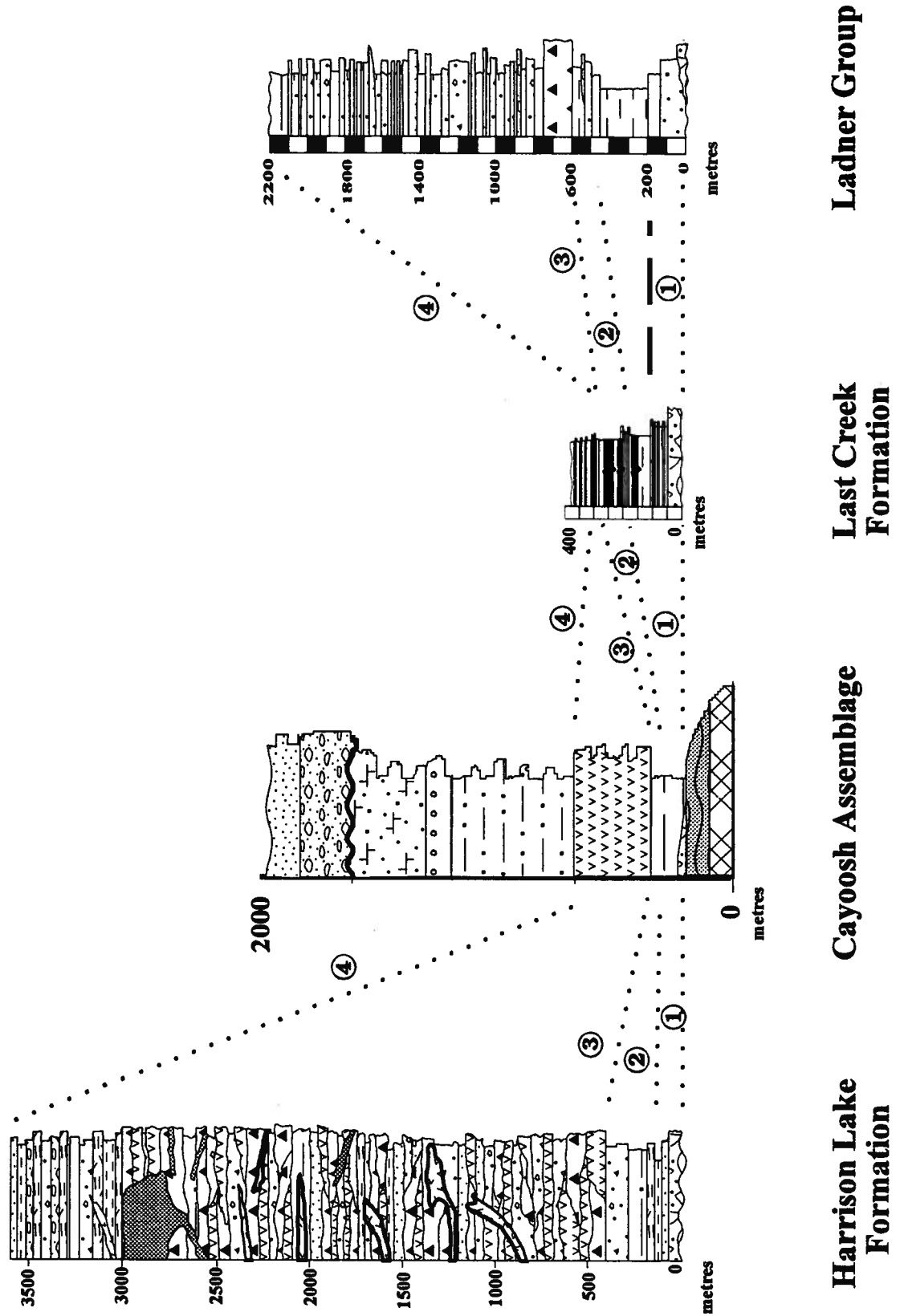


Figure 6.22 - Lithostratigraphic correlation diagram for Lower to Middle Jurassic strata. Numbers refer to synchronous events discussed in text.

detritus in turbidite lobes of unit 3, which overlies volcanogenic rocks of inferred Middle Jurassic age. The Upper Oxfordian to Upper Tithonian Thunder Lake sequence of the Methow terrane contains a subtle increase in quartz content and rare granitic debris in shallow marine strata. Quartz detritus is not reported in upper Middle to lower Upper Jurassic shallow marine strata of the Harrison terrane, although petrographic studies have not been conducted. However, fine grained shallow marine sandstone of the Callovian Mysterious Creek Formation represents a dramatic change in depositional environment from coarse clastic volcanogenic rocks of the underlying Harrison Lake Formation.

6) Deposition of Lower Cretaceous granitoid bearing conglomerate. Polymict granitoid bearing cobble to boulder conglomerate caps Jurassic strata on all terranes. Middle Jurassic granitoid clasts have been recovered from the Jackass Mountain Group on the Methow terrane (O'Brien et al., 1992), from unnamed conglomerate overlying the Cayoosh assemblage on the Bridge River terrane (V. Coleman, personal communication, 1992), and from the Peninsula Formation of the Harrison terrane (O'Brien et al., 1992). West-derived metamorphic and plutonic clasts are intermixed with Upper Jurassic sedimentary clasts in the Paradise Formation of the Cadwallader terrane (Garver, 1992). These Lower Cretaceous conglomerate successions record substantial uplift and erosion of all terranes concomitant with final basin closure.

In summary, there are at least six strikingly similar lithostratigraphic variations common to Jurassic strata of the Harrison, Cadwallader, Bridge River, and Methow terranes. Tertiary and Quaternary sediments deposited in modern marginal basins of the western Pacific record marked differences in provenance, timing and duration of depositional hiatuses, and volcanic episodicity among coeval basins (Leitch, 1984). Contemporaneous lithostratigraphic variations among Jurassic strata of the southern Canadian Cordillera strongly suggest a common basin evolution.

B. Biostratigraphic Correlations

Biostratigraphic control in the Harrison, Cadwallader, and Methow terranes is provided by ammonite zonation (Table 6.1). In addition, biostratigraphic data may be utilized to provide constraints on the paleogeographic position of Middle Jurassic strata. Provinciality in Jurassic ammonites is well-established, and provides a useful tool in paleogeographic reconstructions (Taylor et al., 1984; Smith and Tipper, 1986).

There are three biogeographic provinces important for this analysis: 1) Tethyan fauna, generally restricted to paleolatitudes below 35°N (Smith and Briden, 1977; Smith, 1983; Tipper, 1984); 2) Boreal fauna, restricted to high paleolatitudes north of 45°N (Smith and Briden, 1977; Smith and Tipper, 1986); and 3) East Pacific fauna, restricted to the eastern edge of the paleo-Pacific ocean (Taylor et al., 1984). In cratonal North America, the southern limit of strictly Boreal fauna is approximately 49°N, and the northern limit of strictly Tethyan fauna is about 36°N; a mixing zone separates the two provinces (Taylor et al., 1984; Tipper, 1984; Smith and Tipper, 1986).

A faunal compilation of Lower and Middle Jurassic strata from the terranes under discussion demonstrates the mixed nature of ammonite fauna in all fossiliferous units (Table 6.1). Aalenian and Bajocian strata from the Harrison, Cadwallader, and Methow terranes contain fauna of Tethyan, East Pacific and Boreal affinity. Moreover, each of these terranes contains identical Aalenian fauna related to each faunal province, including *Erycitoides* (Boreal), *Zemistephanus* (East Pacific), and *Planamatoceras* (Tethyan). The distinct faunal overlap among these terranes strongly suggests a close paleogeographic relationship between them. Mixed fauna are also reported from Quesnellia, although the faunal overlap is less pronounced than terranes to the west (Table 6.1). Note that Tethyan fauna are absent from Middle Jurassic strata deposited on the craton north of 49°N (Ferne Formation).

Biogeographic determinations derived from mixed faunal provinciality must be approached cautiously. A faunal assemblage should not be viewed as mixed unless fauna of differing provinciality is found in the same stratigraphic horizon. Provinciality fluctuations within a vertical stratigraphic sequence may not indicate a truly mixed, and therefore geographically restricted, fauna, but may be the result of temporal climatic fluctuations, such as those that characterize the Quaternary microfossil record. However, there is no direct evidence for large climatic fluctuations such as continental glaciations in the Early and Middle Jurassic, that might have caused dramatic variations in biogeography. It is therefore reasonable to assume that the mixed assemblages found within all Early and Middle Jurassic strata in the southern Canadian Cordillera are the result of geographic restriction and not climatic fluctuations.

The mixed Boreal, Tethyan, and East Pacific fauna in the Harrison, Cadwallader, Methow, and Quesnellia terranes are interpreted to indicate a paleogeographic proximity among the terranes during the Middle Jurassic. Biogeographic constraints require that these terranes were in the northeastern portion of the Jurassic Panthalassa ocean, between approximately 36 (northern cratonal limit of Tethyan fauna) and 49 (southern cratonal limit of Boreal fauna) degrees north during the Middle Jurassic. This argument assumes a mixing zone oriented parallel to latitude. North-south ocean circulation could have extended Tethyan and Boreal fauna farther north or south, respectively, but the mixing zone would still be required to be in the northeastern quadrant of the Panthalassa ocean, between latitudinal equatorial and arctic circulation cells.

C. Volcanic Geochemistry Correlations

The geochemical signatures of primary volcanic rocks in the Harrison Lake Formation, Cayoosh assemblage, and Dewdney Creek Formation (Ladner Group) are distinct from one another (Figs. 6.6, 6.15, 6.19). Temporal and lithostratigraphic constraints suggest these formations display contemporaneous Middle Jurassic volcanism. The Harrison Lake Formation and the Dewdney Creek Formation are characterized by volcanic arc signatures, and are very distinct from the MORB-like character of the Cayoosh assemblage (Fig. 6.23).

The Harrison Lake Formation is characterized by medium- to high-K calcalkaline andesitic to rhyolitic volcanism. Incompatible trace element plots are homogeneous, and display strong enrichment of LIL elements relative to HFSE, slight Sr enrichment, and strong Ti depletion (Fig 6.6). Rare earth element patterns show LREE enrichment between 20-60x chondrite and a slight HREE enrichment. Geochemistry of the Harrison Lake Formation is consistent with volcanism in a slightly evolved subduction-related setting. Dewdney Creek Formation volcanic rocks are tholeiitic to calcalkaline andesitic basalt to dacite. Incompatible trace element patterns are heterogeneous, but do display the LIL enrichment relative to HFSE characteristic of arc volcanism. Rare earth element patterns may be subdivided into two subgroups, including a LREE depleted fraction, and a fraction displaying slight LREE enrichment. The geochemical signature of the Dewdney Creek Formation is consistent with arc production in an juvenile arc setting.

Coeval volcanism and similar stratigraphies could be used to argue that the Harrison Lake Formation and the Dewdney Creek Formation were once part of a single, laterally continuous Middle Jurassic arc. It is therefore necessary to compare the geochemical and isotopic signatures of the two formations to evaluate the possibility of previous lateral continuity. Incompatible trace element and rare earth element patterns show a considerable degree of overlap between the Harrison Lake Formation and the Dewdney Creek Formation, although the Harrison Lake Formation is consistently more enriched in LIL, LREE, and HREE. Concave upward REE patterns in the Harrison Lake Formation, along with slightly more evolved ϵ_{Nd} values (compare Figs. 6.7, 6.20), indicate probable lower crustal melts in the Harrison Lake Formation; similar evidence is lacking in the Dewdney Creek Formation. Dewdney Creek Formation volcanics are more heterogeneous, and include a LREE depleted suite that is absent in the Harrison Lake Formation, although flat REE patterns do occur in the correlative Bonanza Formation on Wrangellia to the west (Chapter 5). It is apparent that the Dewdney Creek Formation volcanics are more tholeiitic than the Harrison Lake Formation, differ in elemental abundances and incompatible element ratios, and show less evolved rare earth element patterns and isotopic signatures. These differences in coeval arc assemblages suggest, but do not prove, that the Dewdney Creek

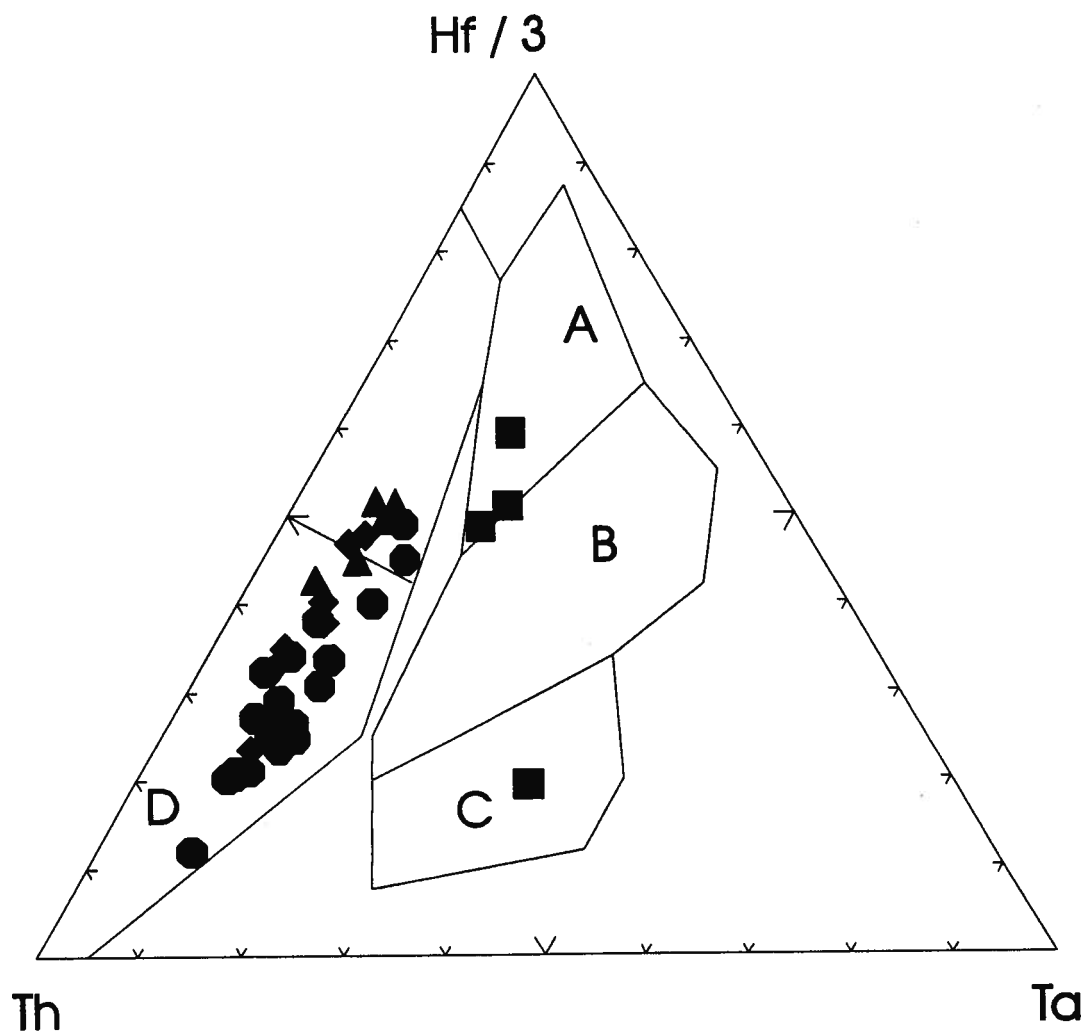


Figure 6.23 - $Hf/3$ - Th - Ta tectonic discrimination diagram from Wood (1980) for Middle Jurassic volcanic samples from Dewdney Creek Formation (circles), Harrison Lake Formation (triangles), and Cayoosh assemblage (squares). Fields are A=N-MORB, B=E-MORB, C=Within Plate Basalt, D=destructive plate margin.

Formation and Harrison Lake Formation were derived from different magmatic systems, and therefore represent different volcanic arcs. However, there is no compelling geochemical or isotopic evidence that prohibit previous lateral continuity, and a single arc model cannot be definitively ruled out.

The Cayoosh assemblage contains subalkaline basalt fragmental rocks and alkaline pillow basalt. The geochemical signature of the volcanic rocks is a hybrid signature that overlaps both arc tholeiite and MORB values, and is most consistent with back arc volcanism. Although the sample set is small, the distinctiveness of the Cayoosh assemblage volcanic rocks from coeval rocks on adjacent terranes is evident on a tectonic discrimination diagram, where Cayoosh assemblage samples are clearly not related to destructive margin volcanism (Wood, 1980; Fig. 6.23). Volcanic rocks of the Cayoosh assemblage are interpreted to represent intrabasin volcanism within a deep marginal basin, perhaps in an extensional or transtensional environment (Tarney et al, 1981).

D. Isotopic Signatures

The isotopic signature of sedimentary and volcanic rocks from Middle Jurassic strata on the Harrison, Cadwallader, Bridge River, and Methow terranes are strongly dominated by unevolved values, illustrating the juvenile character of volcanism and associated sedimentation during this time. Viewed broadly, the ϵ_{Nd} and $^{87}\text{Sr}/^{86}\text{Sr}$ isotopic values for all units plot near the mantle array, and indicate an unevolved volcanic arc affinity for Middle Jurassic strata on each terrane. In this context, the units are virtually indistinguishable. However, there are important isotopic variations, and examination of the fine detail of isotopic fluctuations, particularly variations in ϵ_{Nd} values, provide important insight into differences in the volcanic signatures and similarities in the sedimentary signatures among the terranes.

A fundamental assumption in isotopic geochemistry is the immobility of the isotopic species under investigation. Nd isotopes have been shown to be immobile under a wide range of temperatures and pressures. Sr, on the other hand, is a LIL element that is easily remobilized by relatively low temperature hydrothermal

fluids, and its immobility must be independently assessed. Initial strontium ratios plotted in Figures 6.10, 6.16, 6.20 should therefore be viewed with caution. Note that several of the sediment samples have very low initial $^{87}\text{Sr}/^{86}\text{Sr}$ values (0.7020-0.7035), and plot to the left of the mantle array. These initial strontium values are lower than MORB values, representative of a depleted mantle source (DePaolo, 1988). Initial strontium values of this magnitude have not been reported in modern marine sediments, and are very rare in terrestrial systems, which suggests that some of the initial strontium values reported here are suspect. Calculated initial strontium values are a function of the measured $^{87}\text{Sr}/^{86}\text{Sr}$ ratio, the age of the rock, and its Rb/Sr ratio. Incorrect initial strontium values arise from analytical problems, incorrect age assignments, or altered Rb/Sr ratios. Replicate analyses and the use of international standards eliminate the possibility of analytical problems, and age assignments are generally well constrained by biostratigraphy. Evaluation of Rb and Sr concentrations on the samples in question suggests Sr concentrations are anomalously low, consistent with modification of the Rb/Sr ratio. Post-depositional depletion of Sr would preferentially raise the Rb/Sr value, leading to anomalously low initial strontium values. Each of the samples displaying unusually low initial strontium values have Rb/Sr values >0.5 ($^{87}\text{Rb}/^{86}\text{Sr} > 1.6$; Table 6.2). These values are interpreted to represent alteration of the original Rb/Sr ratio, and suggest that, although the degree of alteration varies regionally, Sr concentrations in Jurassic sedimentary rocks have been modified by post-depositional elemental mobility. Sedimentary rocks more commonly display anomalous Rb/Sr ratios than coeval volcanic rocks, consistent with permeability as a control on alteration. The degree of Rb/Sr alteration for any individual sample is impossible to assess, and therefore isotopic interpretations herein are based primarily on Nd systematics.

Taking into account $^{87}\text{Sr}/^{86}\text{Sr}$ uncertainties, plots of sediment samples in ϵ_{Nd} versus $^{87}\text{Sr}/^{86}\text{Sr}$ space illustrates that in each terrane the isotopic composition of the fine-grained clastic sediment reflects a mixture of juvenile arc-derived material and a more evolved detrital component. Each formation contains fine-grained sediment with low positive or slightly negative ϵ_{Nd} values, consistent with the incorporation of a minor amount of evolved sediment into a basin dominated by deposition of juvenile arc-derived sediment. Incorporation of a few percent of continental detritus would be sufficient to alter the isotopic composition of a

volcanic basin to the observed values (Samson et al., 1991). The source of the more evolved component is unknown; this material may be derived from an adjacent continent, or may be derived from oceanic pelagic input. Modern ocean water has an ϵ_{Nd} value of approximately (-9), reflecting the importance of continental input to the water column (Goldstein et al., 1984). However, the majority of sedimentary rocks in Middle Jurassic strata are clastic rocks deposited by turbidite or hemipelagic processes, and there is little evidence of abundant pelagic sediment that would act as a sink for seawater Nd. It is therefore assumed that the observed shifts to more evolved values are the result of incorporation of an older detrital component, not pelagic deposition. This argument is consistent with trends evident on an ϵ_{Nd} vs. $f^{Sm/Nd}$ diagram, where fine-grained Middle Jurassic sedimentary rocks from all terranes trend toward a mixing line between the juvenile volcanic arc rocks and a Precambrian crustal component (Fig. 6.24).

There is a strong temporal control on ϵ_{Nd} values evident in Lower and Middle Jurassic sedimentary rocks in the Harrison, Bridge River, and Methow terranes. Comparison of ϵ_{Nd} values with stratigraphic position (Figs. 6.8, 6.17, 6.21) demonstrates that each formation is characterised by a relatively juvenile ϵ_{Nd} signature immediately above the basal unconformity, a significant shift to more evolved values in overlying Lower Jurassic argillaceous strata, and a second strong shift at the start of Middle Jurassic volcanism. This pattern is interpreted to represent the influence of arc basement during initial subsidence, followed by deposition of argillaceous strata of mixed juvenile and continental detritus during periods of low clastic influx, followed in turn by deposition of arc-derived detritus associated with the Middle Jurassic volcanic episodes. The influence of the more evolved component is particularly strong in the Cayoosh assemblage, which is interpreted to represent the most distal Middle Jurassic facies. Low volcanoclastic influx into the basin interior led to weaker dilution of the ambient, continentally derived, hemipelagic sediment, thus causing stronger and more frequent shifts away from juvenile values. The Last Creek Formation displays apparent isotopic homogeneity, but this is believed to be an artifact of sampling bias, particularly the lack of samples of Toarcian age.

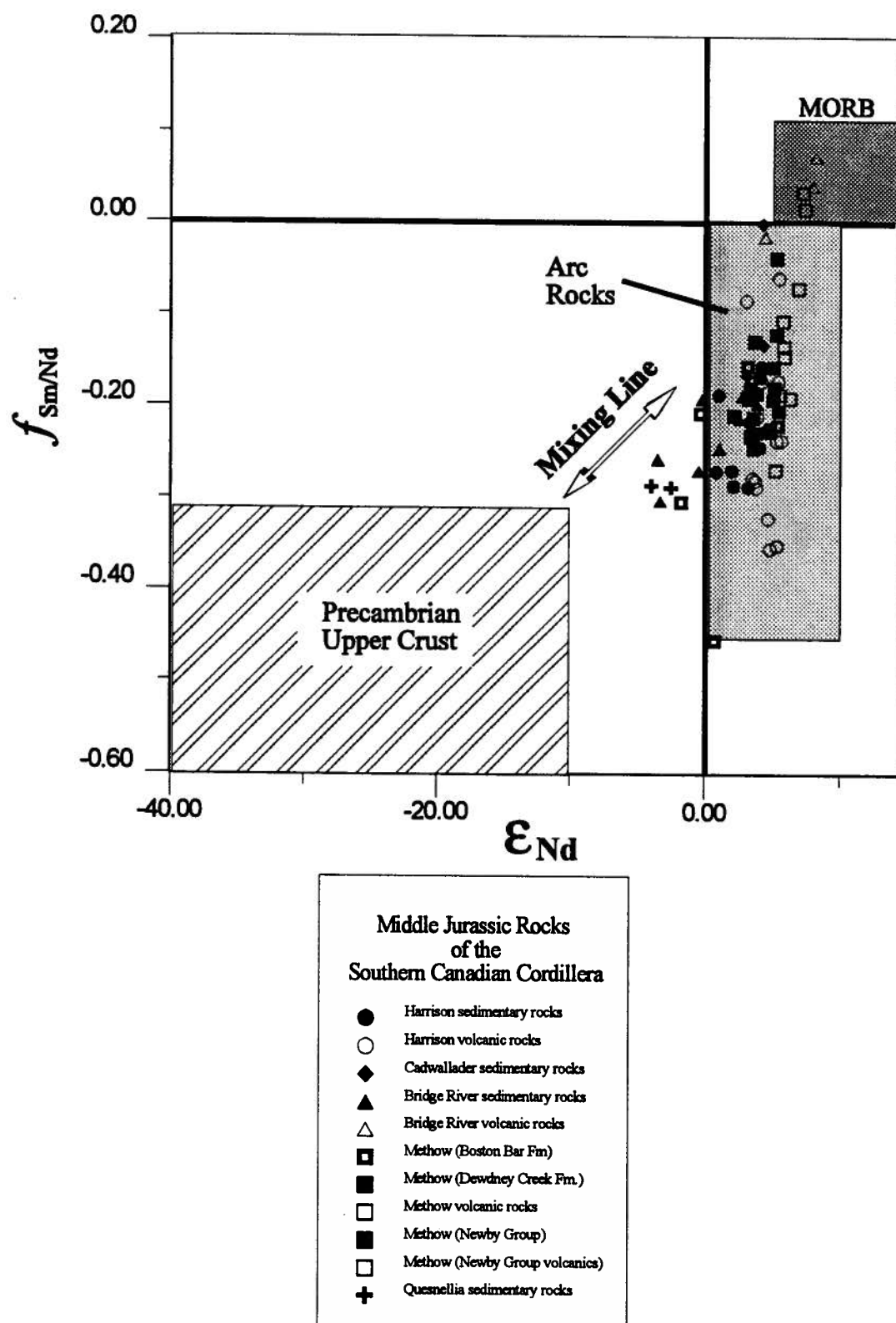


Figure 6.24 - ϵ_{Nd} vs. $f_{Sm/Nd}$ diagram for all Middle Jurassic rocks examined. Note trend toward mixing line for Lower Jurassic samples and samples from Quesnellia, implying admixture of slight continental component.

The apparent synchronicity of isotopic fluctuations in the Harrison, Bridge River, and Methow terranes has important ramifications for basin reconstructions. Studies in western Pacific marginal basins have demonstrated that isotopic fluctuations may be correlated throughout an individual basin (Chapter 2). These isotopic fluctuations would not be expected to be coeval nor of the same magnitude from basin to basin, due to differences in provenance and volcanic episodicity between basins (deVries Klein et al., 1980). Coeval isotopic excursions of similar magnitude documented in Lower and Middle Jurassic strata of the Harrison, Bridge River, and Methow terranes argue for deposition of these sequences in a single basin. This basin was characterized by hemipelagic background sedimentation consisting of mixed juvenile and continental detritus punctuated by massive influxes of juvenile volcanoclastic material generated during volcanic episodes on the basin margins.

6.5 BASIN EVOLUTION MODEL

The fundamental conclusion derived from the correlations presented herein is that Lower and Middle Jurassic strata of the Harrison, Cadwallader, Bridge River, and Methow terranes were deposited in a single marginal basin flanked by volcanic arc assemblages to the west and to the east (Fig. 6.25). The western arc is the composite Bonanza-Harrison arc system, and the Harrison Lake Formation of the Harrison terrane represents the youngest (Late Toarcian to Early Bathonian) deposits of the western arc (Chapter 5). The eastern arc is herein referred to as the Dewdney Creek arc system, and the Ladner Group, particularly the Dewdney Creek Formation, represent fore-arc sediments derived from this arc. The majority of the eastern arc is missing, and the terrane affinity of the arc basement is uncertain.

The Aalenian to Bajocian portion of the Last Creek Formation (Cadwallader terrane) represents the distal edge of an eastward-prograding back arc volcanoclastic wedge derived from the western arc. Coarse grained volcanoclastic rocks to the west of the type area of the Last Creek Formation are interpreted as mass sediment gravity flows associated with this prograding wedge. Tuffaceous beds in this portion of the Last Creek Formation are interpreted as airfall tuffs derived from this arc.

The Cayoosh assemblage contains distal forearc and basin plain sediments deposited on top of the Bridge River Complex. The Bridge River terrane itself represents both oceanic crust and an accretionary wedge trapped behind the Lower to Middle Jurassic western arc. Subduction of oceanic crust of the Bridge River drove magmatism in the Dewdney Creek arc. The presence of back arc basin basalts in the Cayoosh assemblage requires incipient extension or transtension in the basin interior, probably associated with the western arc. Deposition of pelagic chert throughout Middle Jurassic time suggests an irregular bottom topography and uneven clastic sediment distribution in the interior of the basin.

In this model, the Bridge River terrane represents a piece of Late Paleozoic and Early Mesozoic oceanic crust trapped behind the developing Bonanza-Harrison volcanic arc system. The Bridge River ocean thus becomes the Bridge River basin. The first major detrital influx into this basin occurs in early Jurassic time, when conglomerate, sandstone, and siltstone flood the margins of the basin. Much of the coarse material is intrabasinal oceanic detritus, but extrabasinal sources of plutonic and volcanic debris are also indicated, particularly on the eastern side of the basin. Initial basin subsidence is followed by an extensive Pliensbachian to Toarcian hemipelagic and pelagic depositional episode, superseded by a major Middle Jurassic volcanic episode. Cessation of volcanism in the Bathonian was followed by a shallowing of the basin and deposition of mixed volcanic and plutonic debris in shallow marine and turbidite systems. The quartz-rich clastic facies in the Cayoosh assemblage may represent the first coarse clastic continental influx into the basin, probably in late Jurassic time. Basin shallowing and deposition of a coarsening upward clastic sequence, accompanied by minor volcanism on the west, continued through the Late Jurassic, culminating in deposition of polymict granitoid-bearing conglomeratic strata concomitant with basin closure in the Early Cretaceous.

A viable alternative to this two-sided basin model would be a single Jurassic arc system that has been truncated by a sinistral transcurrent fault in Early Cretaceous time. Transcurrent displacement would result in

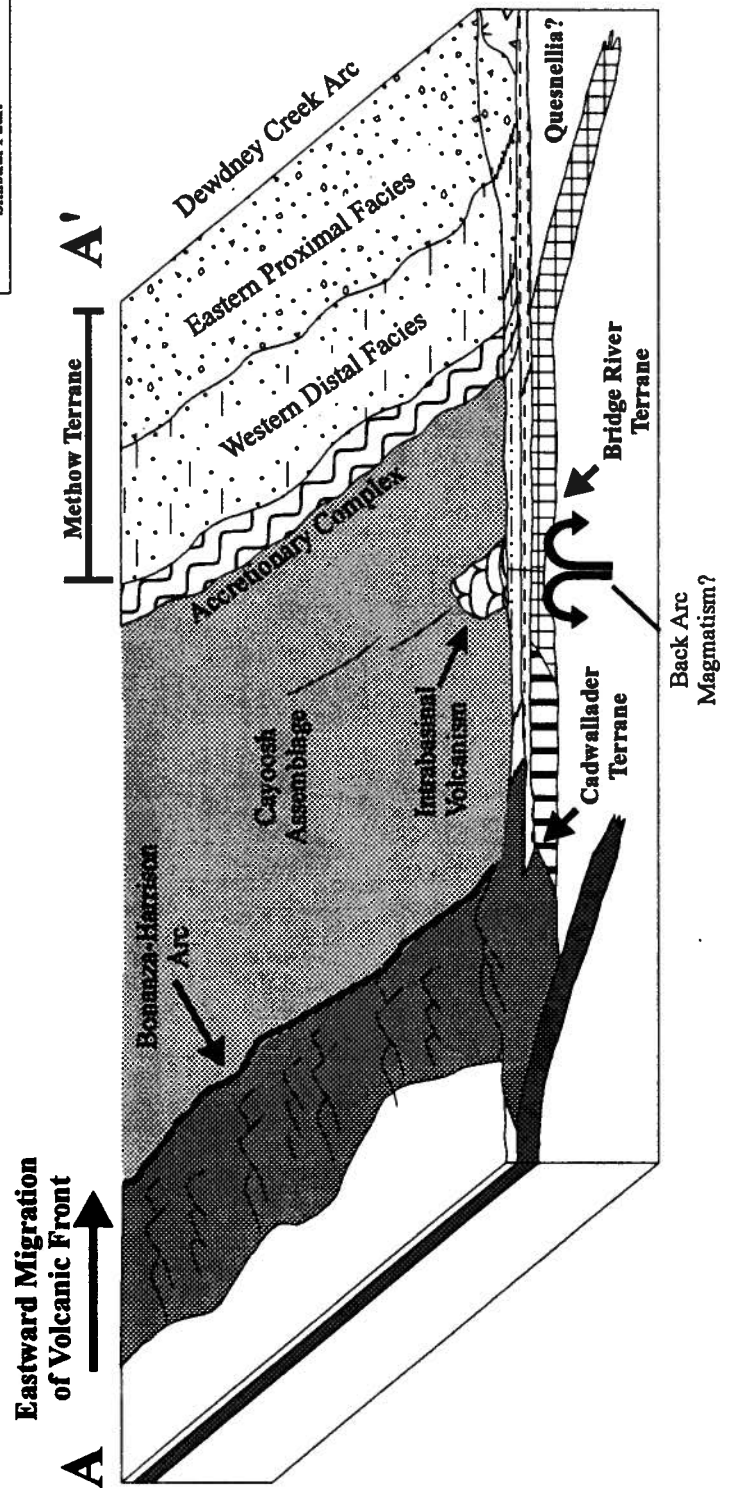
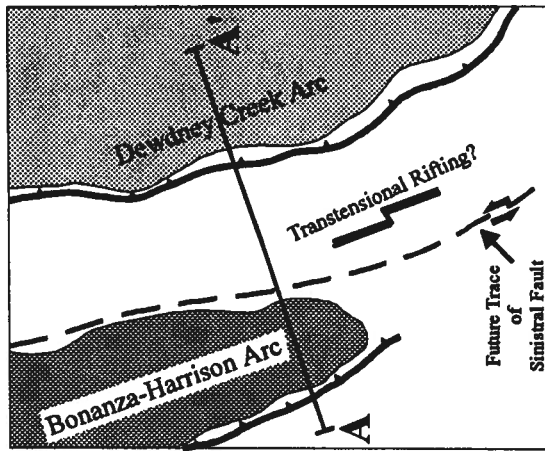


Figure 6.25 - Schematic paleogeographic basin diagram. Details discussed in text. Future trace of sinistral fault from Monger et al., 1994.

entrapment of the Bridge River terrane between the displaced northern portion of the arc on the west (Bonanza-Harrison arc) and the southern portion of the arc on the east (Dewdney Creek arc), in the manner of Monger et al. (1994). A single arc model accounts for the synchronous volcanism in both arc sequences, and a single arc is permissible within the available geochemical data set. However, a single arc model does not account for probable intraplate (i.e. back arc basin) volcanism in the Bridge River terrane.

In either model, Middle Jurassic strata of the southern Canadian Cordillera were deposited in a marginal basin developed on top of the previously amalgamated Harrison, Cadwallader, Bridge River, and Methow terranes. These terranes were amalgamated prior to the initiation of subsidence in the Early Jurassic, and have behaved as a coherent package since that time. Biogeographic evidence suggests these terranes were in the northeastern quadrant of the Panthalassa Ocean in the Middle Jurassic. However, ties between these amalgamated terranes and ancestral North America are tenuous at this time, and no constraints may be placed on post-Middle Jurassic latitudinal translation.

| Terrane | Harrison | Cadwallader | Methow | Quesnellia | Cratonal North America |
|-----------------|---|--|---|---|---|
| Unit | Harrison Lake Formation | Last Creek Formation | Ladner Group | Ashcroft Formation | Fernie Formation |
| Ammonite Genera | | | | | |
| Boreal | <i>Dactyloceras</i> ^{2,3} (Toarcian) <i>Erycitoides</i> ^{2,3} (Aalenian) | <i>Dactyloceras commune</i> ⁴ (Toarcian) <i>Erycitoides</i> ^{2,12} (Aalenian) | <i>Erycitoides</i> ^{6,12} <i>Pseudoliodoceras</i> ^{2,12} (Aalenian) | [<i>Amatheus</i>] ⁷ (L. Pliensbachian) [<i>Erycitoides</i>] ² (Aalenian) | <i>Amatheus</i> ^{9,10} <i>Pleuroceras</i> ¹⁰ (L. Pliensbachian) <i>Dactyloceras commune</i> ¹⁰ (Toarcian) <i>Arkelloceras</i> ^{9,10} (E. Bajocian) <i>Megaspheeroceras</i> ^{9,10} (L. Bajocian) |
| East Pacific | [<i>Zemistephanus</i> - QCI] | | <i>Zemistephanus</i> ^{1,12} (E. Bajocian) | <i>Fanninoceras</i> ⁸ (E. Pliensbachian) | |
| Tethyan | <i>Planamatoceras</i> ² [<i>Planamatoceras</i> ² - QCI] (Aalenian) | <i>Planamatoceras</i> ² (Aalenian) | <i>Dayiceras</i> ⁶ (E. Pliensbachian) <i>Planamatoceras</i> ^{2,6,12} (Aalenian) | <i>Arietoceras</i> ⁸ <i>Fucinoceras</i> ⁸ <i>Leptaleoceras</i> ⁸ <i>Reynosoeloceras</i> ⁸ (L. Pliensbachian) | |
| Pandemic | <i>Harpoceras</i> ⁴ <i>Hildaites</i> ^{1,4} <i>Dactyloceras</i> ^{1,4} (E Toarcian) <i>Dumortieria</i> ^{2,3} (L. Toarcian) <i>Tmetoceras</i> ^{2,3} (Aalenian) | <i>Dumortieria</i> ⁴ <i>Hammatooceras</i> ⁴ <i>Harpoceras</i> ⁴ <i>Lytoceras</i> ⁴ <i>Phymatoceras</i> ⁴ (Toarcian) <i>Tmetoceras</i> ² (Aalenian) <i>Stephanoceras</i> ¹² (E. Bajocian) <i>Chondroceras</i> ¹² <i>Oppelia</i> ¹² (M. Bajocian) | <i>Grammoceras</i> ⁴ <i>Physeogrammoceras</i> ^{2,12} <i>Pleydellia</i> ⁴ (Toarcian) <i>Tmetoceras</i> ^{1,2,12} (Aalenian) <i>Stephanoceras</i> ^{1,6,12} <i>Witchellia</i> ^{2,12} <i>Sonninia</i> ^{2,12} (E. Bajocian) <i>Chondroceras</i> ^{3,12} (M. Bajocian) <i>Poecilomorphus</i> ² (Bajocian) | [<i>Dactyloceras</i>] ⁴ [<i>Harpoceras</i>] ⁴ [<i>Grammoceras</i>] ⁴ (Toarcian) <i>Stephanoceras</i> ⁸ (E. Bajocian) | <i>Brodieia</i> ⁹ <i>Dactyloceras</i> ¹¹ <i>Harpoceras</i> ¹¹ <i>Haugia</i> ^{11/Yakounia} ⁴ <i>Hildaites</i> ¹¹ <i>Peronoceras</i> ^{9,11} <i>Phymatoceras</i> ⁹ (Toarcian) <i>Sonninia</i> ¹¹ <i>Witchellia</i> ¹¹ <i>Stephanoceras</i> ¹¹ <i>Chondroceras</i> ¹¹ <i>Spiroceras</i> ^{9,10} (Bajocian) |

[] - indicates faunas described from the terrane indicated, not from the formation indicated

Table 6.1 - Paleontologic data for the southern Canadian Cordillera.

Table 6.1 (cont.) References for paleontologic data for the southern Canadian Cordillera.

- 1 - this study
- 2 - Poulton and Tipper (1993)
- 3 - Arthur et al. (1993)
- 4 - Jakobs (1992)
- 5 - Arthur (1987)
- 6 - O'Brien (1987)
- 7 - Smith and Tipper (1986)
- 8 - Arthur (1985)
- 9 - Hall (1980)
- 10 - Poulton (1980)
- 11 - Frebold (1976)
- 12 - Frebold et al. (1969)

Biogeographic assignments derived from Taylor et al. (1984) and Jakobs (1992)

| Sample | Cayoosh | | | | | Dewdney Creek | | | | | Methow | | | | |
|------------------------------------|---------|--------|--------|--------|--------|---------------|--------|--------|--------|--------|--------|--------|---------|---------|---------|
| | 171JBM | 176JBM | 319JBM | 321JBM | 213JBM | 215JBM | 329JBM | 349JBM | 350JBM | 363JBM | 369JBM | 7JBM93 | 80JBM93 | 81JBM93 | 84JBM93 |
| SiO ₂ | 48.50 | 46.80 | 47.40 | 50.70 | 58.60 | 50.70 | 48.00 | 43.40 | 58.05 | 54.30 | 47.70 | 73.46 | 56.64 | 78.57 | 65.61 |
| TiO ₂ | 1.56 | 2.33 | 1.32 | 1.65 | 0.58 | 0.75 | 1.02 | 1.01 | 0.73 | 1.05 | 0.66 | 0.29 | 0.86 | 0.34 | 0.79 |
| Al ₂ O ₃ | 14.40 | 15.10 | 15.70 | 15.30 | 16.50 | 19.10 | 17.10 | 14.80 | 16.55 | 16.00 | 18.90 | 14.53 | 19.10 | 13.04 | 15.46 |
| Fe ₂ O ₃ (T) | 11.00 | 13.30 | 10.60 | 11.40 | 7.15 | 7.81 | 12.70 | 10.70 | 6.69 | 8.52 | 10.40 | 2.41 | 8.04 | 1.30 | 5.60 |
| MnO | 0.19 | 0.22 | 0.18 | 0.18 | 0.09 | 0.18 | 0.19 | 0.20 | 0.14 | 0.16 | 0.09 | 0.05 | 0.18 | 0.04 | 0.13 |
| MgO | 6.08 | 6.55 | 7.33 | 5.96 | 2.74 | 4.61 | 6.00 | 3.42 | 3.14 | 4.66 | 4.81 | 1.01 | 2.75 | 0.21 | 1.95 |
| CaO | 7.27 | 7.75 | 9.20 | 8.38 | 6.88 | 6.48 | 8.01 | 13.80 | 6.22 | 5.00 | 8.86 | 1.01 | 8.35 | 0.59 | 3.55 |
| K ₂ O | 0.09 | 0.12 | 0.05 | 0.16 | 1.11 | 0.74 | 1.58 | 0.07 | 0.89 | 1.46 | 0.13 | 1.06 | 0.59 | 0.05 | 0.86 |
| Na ₂ O | 4.57 | 3.50 | 3.53 | 3.25 | 3.49 | 4.65 | 1.42 | 2.25 | 3.67 | 4.55 | 2.97 | 6.71 | 4.03 | 7.60 | 6.06 |
| P ₂ O ₅ | 0.15 | 0.28 | 0.14 | 0.16 | 0.14 | 0.12 | 0.12 | 0.15 | 0.17 | 0.27 | 0.09 | 0.06 | 0.20 | 0.07 | 0.24 |
| Total | 98.31 | 99.20 | 98.55 | 99.74 | 100.12 | 98.34 | 99.64 | 98.40 | 99.79 | 99.12 | 98.01 | 100.59 | 100.74 | 101.81 | 100.25 |
| LOI | 4.50 | 3.25 | 3.10 | 2.60 | 2.85 | 3.20 | 3.50 | 8.60 | 3.55 | 3.15 | 3.40 | | | | |
| Trace Elements | | | | | | | | | | | | | | | |
| Cr | 205 | 300 | 277 | 146 | 130 | 51 | 107 | 63 | 54 | 134 | 118 | 4 | 9 | 4 | 6 |
| Ni | 60 | 201 | 98 | 36 | 24 | 13 | 33 | 14 | 6 | 24 | 17 | 17 | 9 | 10 | 3 |
| Ga | 26 | 31 | 24 | 32 | 28 | 29 | 25 | 23 | 27 | 27 | 26 | 11 | 24 | 10 | 20 |
| Li | 19.51 | 33.54 | 25.38 | 20.40 | 10.28 | 10.78 | 27.33 | 10.35 | 13.96 | 26.69 | 10.16 | - | - | - | - |
| Be | 0.68 | 1.29 | 0.57 | 0.48 | 0.65 | 0.49 | 0.71 | 0.39 | 0.74 | 1.36 | 0.41 | - | - | - | - |
| Sc | 41 | 35 | 41 | 42 | 17 | 26 | 47 | 40 | 18 | 21 | 33 | 7 | 29 | 13 | 23 |
| V | 335 | 293 | 292 | 389 | 166 | 258 | 385 | 357 | 161 | 197 | 288 | 18 | 170 | 64 | 61 |
| Rb | 5 | 3 | 5 | 4 | 23 | 10 | 21 | 6 | 18 | 44 | 4 | 13 | 6 | 1 | 6 |
| Sr | 205 | 327 | 320 | 664 | 577 | 759 | 345 | 255 | 247 | 512 | 499 | 123 | 576 | 101 | 181 |
| Y | 33.26 | 29.44 | 24.26 | 34.27 | 11.33 | 13.85 | 18.60 | 18.30 | 13.38 | 14.66 | 8.23 | 20.22 | 23.99 | 29.45 | 34.44 |
| Zr | 114 | 203 | 89 | 120 | 82 | 79 | 56 | 61 | 74 | 96 | 28 | 108 | 73 | 88 | 107 |
| Nb | 234 | 20.70 | 1.68 | 2.50 | 1.24 | 1.26 | 1.28 | 1.30 | 2.00 | 5.27 | 0.38 | 2.68 | 1.20 | 2.72 | 3.81 |
| Cs | 0.27 | 0.29 | 0.07 | 0.30 | 1.64 | 0.40 | 1.27 | 0.10 | 0.97 | 0.73 | 0.04 | 0.27 | 0.19 | 0.03 | 0.10 |
| Ba | 37 | 39 | 16 | 27 | 254 | 248 | 664 | 56 | 124 | 434 | 48 | 392 | 278 | 31 | 305 |
| La | 5.28 | 13.99 | 2.75 | 4.05 | 4.34 | 4.66 | 3.18 | 2.98 | 5.92 | 12.80 | 1.47 | 9.08 | 6.35 | 6.61 | 11.06 |
| Ce | 14.35 | 32.27 | 8.86 | 12.25 | 10.38 | 10.48 | 8.46 | 7.57 | 13.32 | 29.13 | 3.64 | 16.33 | 13.72 | 18.39 | 22.74 |
| Pr | 2.33 | 4.44 | 1.54 | 2.09 | 1.61 | 1.57 | 1.42 | 1.25 | 1.86 | 4.11 | 0.59 | 2.04 | 2.11 | 2.63 | 3.18 |
| Nd | 12.22 | 19.97 | 8.18 | 10.81 | 7.45 | 7.48 | 7.17 | 6.40 | 8.49 | 18.32 | 3.03 | 8.84 | 10.55 | 12.79 | 15.01 |
| Sm | 3.93 | 5.20 | 2.78 | 3.58 | 1.95 | 1.95 | 2.36 | 2.05 | 2.12 | 4.26 | 0.86 | 2.44 | 3.32 | 4.01 | 4.41 |
| Eu | 1.87 | 1.85 | 0.95 | 1.87 | 0.70 | 0.78 | 0.86 | 0.81 | 0.80 | 1.35 | 0.50 | 0.68 | 1.23 | 1.41 | 1.58 |
| Gd | 5.41 | 6.22 | 3.75 | 5.39 | 2.12 | 2.45 | 3.43 | 2.92 | 2.55 | 4.24 | 1.35 | 2.46 | 3.61 | 3.93 | 5.04 |
| Tb | 0.87 | 0.96 | 0.64 | 0.92 | 0.31 | 0.38 | 0.51 | 0.48 | 0.36 | 0.54 | 0.21 | 0.48 | 0.66 | 0.83 | 0.93 |
| Dy | 6.18 | 6.16 | 4.66 | 6.53 | 2.20 | 2.65 | 3.63 | 3.34 | 2.45 | 3.02 | 1.52 | 3.18 | 4.27 | 5.34 | 4.41 |
| Ho | 1.27 | 1.17 | 0.96 | 1.41 | 0.42 | 0.53 | 0.78 | 0.70 | 0.49 | 0.53 | 0.30 | 0.71 | 0.87 | 1.13 | 1.18 |
| Er | 3.68 | 3.09 | 2.91 | 4.16 | 1.36 | 1.66 | 2.24 | 2.19 | 1.46 | 1.52 | 0.93 | 2.29 | 2.66 | 3.61 | 3.61 |
| Tm | 0.53 | 0.41 | 0.41 | 0.58 | 0.20 | 0.24 | 0.31 | 0.30 | 0.19 | 1.18 | 0.12 | 0.35 | 0.36 | 0.51 | 0.52 |
| Yb | 3.48 | 2.25 | 2.86 | 3.59 | 1.47 | 1.66 | 2.09 | 2.07 | 1.42 | 1.39 | 0.80 | 2.32 | 2.32 | 3.39 | 3.31 |
| Lu | 0.49 | 0.30 | 0.37 | 0.51 | 0.22 | 0.24 | 0.31 | 0.33 | 0.22 | 0.19 | 0.13 | 0.40 | 0.37 | 0.54 | 0.54 |
| Hf | 1.74 | 1.75 | 0.94 | 1.34 | 1.76 | 1.64 | 1.39 | 1.40 | 1.89 | 2.23 | 0.33 | 2.95 | 1.48 | 2.60 | 2.61 |
| Ta | 0.17 | 1.16 | 0.13 | 0.18 | 0.09 | 0.08 | 0.09 | 0.09 | 0.13 | 0.30 | 0.02 | 0.20 | 0.08 | 0.18 | 0.22 |
| Pb | 0.85 | 1.40 | 1.00 | 2.55 | 1.81 | 1.97 | 1.48 | 1.20 | 4.64 | 5.59 | 0.85 | 2.54 | 4.36 | 1.64 | 4.08 |
| Th | 0.23 | 1.25 | 0.17 | 0.29 | 0.46 | 0.65 | 0.38 | 0.35 | 0.64 | 2.12 | 0.10 | 1.63 | 0.48 | 1.11 | 1.75 |
| U | 0.14 | 0.33 | 0.11 | 0.18 | 0.28 | 0.45 | 0.26 | 0.31 | 0.45 | 1.08 | 0.04 | 0.60 | 0.16 | 0.39 | 0.44 |

Table 6.2 - Middle Jurassic geochemical data.

| Age | 87Sr/86Sr(t) | Rb | Sr | Rb/Sr | 7Rb/86S | 87Sr/86Sr(t) | Sm | Nd | Sm/Nd | f | T _{dm} | 143/144 | E Nd(0) | Ep Nd(t) |
|--|--------------|--------|--------|-------|---------|--------------|------|-------|--------|--------|-----------------|----------|---------|----------|
| HARRISON TERRANE | | | | | | | | | | | | | | |
| Harrison Lake Formation | | | | | | | | | | | | | | |
| 96JBM92 | 180 | 79.58 | 207.13 | 0.38 | 1.11 | 0.703975 | 2.66 | 11.51 | 0.1400 | -0.288 | 515 | 0.512807 | 8 | 4.60 |
| 102JBM92 | 180 | 23.11 | 231.14 | 0.10 | 0.29 | 0.705636 | 2.37 | 08.96 | 0.1540 | -0.217 | 613 | 0.512813 | 11 | 4.40 |
| 124JBM92 | 175 | 82.50 | 135.19 | 0.61 | 1.77 | 0.703569 | 6.35 | 25.86 | 0.1486 | -0.245 | 484 | 0.512850 | 7 | 5.21 |
| 129JBM92 | 180 | 54.32 | 456.92 | 0.12 | 0.34 | 0.705829 | 3.64 | 13.17 | 0.1657 | -0.158 | | 0.512857 | 4 | 4.99 |
| 131JBM92 | 180 | 46.54 | 319.31 | 0.15 | 0.42 | 0.705695 | 2.78 | 10.54 | 0.1596 | -0.188 | 985 | 0.512696 | 18 | 1.13 |
| 136JBM92 | 180 | 78.49 | 174.66 | 0.45 | 1.30 | 0.705637 | 3.25 | 13.64 | 0.1434 | -0.271 | 785 | 0.512687 | 7 | 0.96 |
| 143JBM92 | 180 | 100.04 | 39.75 | 2.20 | 6.38 | 0.702689 | 2.51 | 10.57 | 0.1435 | -0.270 | 667 | 0.512745 | 7 | 3.31 |
| 288JBM92 | 175 | 61.02 | 228.79 | 0.27 | 0.77 | 0.704364 | 4.25 | 17.92 | 0.1435 | -0.287 | 652 | 0.512752 | 5 | 2.22 |
| Harrison Lake Formation Volcanics | | | | | | | | | | | | | | |
| 04JBM92 | 175 | 7.25 | 182.23 | 0.04 | 0.12 | 0.704139 | 3.65 | 12.09 | 0.1849 | -0.060 | | 0.512923 | 6 | 5.56 |
| 116JBM92 | 175 | 25.68 | 268.03 | 0.10 | 0.28 | 0.704321 | 3.81 | 16.22 | 0.1414 | -0.281 | 471 | 0.512834 | 4 | 3.82 |
| 142JBM92 | 175 | 66.77 | 39.75 | 1.68 | 4.86 | 0.701588 | 3.76 | 16.00 | 0.1419 | -0.278 | 494 | 0.512824 | 4 | 3.63 |
| 151JBM92 | 175 | 14.45 | 168.71 | 0.09 | 0.25 | 0.704547 | 6.25 | 23.82 | 0.1590 | -0.192 | | 0.512904 | 9 | 5.19 |
| 287JBM92 | 175 | 35.93 | 317.53 | 0.11 | 0.33 | 0.704241 | 3.46 | 15.03 | 0.1399 | -0.289 | 454 | 0.512838 | 9 | 3.90 |
| 291JBM92 | 175 | 48.62 | 122.09 | 0.40 | 1.15 | 0.703816 | 5.65 | 18.95 | 0.1801 | -0.084 | | 0.512800 | 11 | 3.16 |
| 307JBM92 | 175 | 17.38 | 78.31 | 0.22 | 0.64 | 0.702592 | 4.60 | 16.98 | 0.1626 | -0.173 | | 0.512921 | 11 | 5.52 |
| 13JBM93 | 175 | 1.16 | 218.06 | 0.01 | 0.02 | 0.703967 | 2.98 | 13.03 | 0.1387 | -0.237 | 349 | 0.512915 | 5 | 5.40 |
| 14JBM93 | 175 | 2.68 | 201.19 | 0.01 | 0.04 | 0.704326 | 2.18 | 10.35 | 0.1274 | -0.352 | 261 | 0.512916 | 10 | 5.42 |
| 15JBM93 | 175 | 57.97 | 151.42 | 0.38 | 1.11 | 0.704064 | 5.50 | 20.44 | 0.1627 | -0.173 | 585 | 0.512858 | 13 | 4.29 |
| 17JBM93 | 175 | 0.92 | 115.08 | 0.01 | 0.02 | 0.704268 | 4.12 | 13.95 | 0.1786 | -0.237 | 311 | 0.512932 | 6 | 5.74 |
| 21JBM93 | 175 | 25.32 | 323.94 | 0.08 | 0.23 | 0.703901 | 4.42 | 17.22 | 0.1552 | -0.211 | 561 | 0.512839 | 9 | 3.92 |
| 22JBM93 | 175 | 22.96 | 136.92 | 0.17 | 0.49 | 0.704256 | 3.18 | 14.42 | 0.1332 | -0.323 | 340 | 0.512822 | 3 | 4.76 |
| 25JBM93 | 175 | 38.98 | 153.91 | 0.25 | 0.73 | 0.703805 | 3.13 | 14.94 | 0.1267 | -0.356 | 304 | 0.512889 | 8 | 4.90 |
| Camp Cove Formation | | | | | | | | | | | | | | |
| 139JBM92 | 225 | 67.97 | 70.28 | 0.97 | 2.80 | 0.703228 | 2.30 | 09.87 | 0.1412 | -0.282 | 553 | 0.512792 | 12 | 3.00 |
| Mysterious Creek Formation | | | | | | | | | | | | | | |
| 297JBM92 | 160 | 44.69 | 216.25 | 0.21 | 0.60 | 0.704056 | 3.38 | 12.75 | 0.1602 | -0.185 | 784 | 0.512774 | 8 | 2.65 |
| CADWALLADER TERRANE | | | | | | | | | | | | | | |
| Last Creek Formation | | | | | | | | | | | | | | |
| 158JBM91 | 180 | 30.63 | 250.90 | 0.12 | 0.35 | 0.704113 | 4.48 | 16.54 | 0.1638 | -0.167 | 754 | 0.512803 | 14 | 3.22 |
| 9071 | 170 | 25.21 | 147.37 | 0.17 | 0.49 | 0.704820 | 4.07 | 14.45 | 0.1704 | -0.134 | | 0.512863 | 9 | 4.39 |
| 9072 | 175 | 2.24 | 44.38 | 0.05 | 0.15 | 0.706050 | 1.93 | 05.92 | 0.1965 | -0.001 | | 0.512862 | 6 | 4.37 |
| 9073 | 190 | 30.30 | 87.65 | 0.35 | 1.00 | 0.704865 | 3.19 | 12.10 | 0.1593 | -0.190 | 617 | 0.512833 | 10 | 3.80 |
| 9074 | 200 | 33.40 | 179.63 | 0.19 | 0.54 | 0.705000 | 3.28 | 13.28 | 0.1497 | -0.239 | 550 | 0.512824 | 14 | 3.63 |
| Hurley Formation | | | | | | | | | | | | | | |
| 208JBM91 | 220 | 27.95 | 79.18 | 0.35 | 1.02 | 0.703181 | 4.87 | 17.97 | 0.1637 | -0.168 | 638 | 0.512843 | 29 | 4.00 |
| Relay Mountain Group | | | | | | | | | | | | | | |
| 154JBM91 | 160 | 42.26 | 221.52 | 0.19 | 0.55 | 0.703591 | 3.66 | 14.35 | 0.1539 | -0.218 | 773 | 0.512746 | 30 | 2.11 |
| | | | | | | | | | | | | | | 2.98 |

Table 6.3 - Jurassic isotopic data.

| BRIDGE RIVER TERRANE | | | | | | | | | | | | | | | | | |
|------------------------------|------|----------|-----|--------|---------|-------|-------|----------|------|-------|--------|--------|------|----------|----|-------|-------|
| Cayoosh Assemblage | | | | | | | | | | | | | | | | | |
| 160bJBM92 | 170 | 0.705881 | 16 | 44.39 | 198.83 | 0.22 | 0.65 | 0.704319 | 2.03 | 08.55 | 0.1435 | -0.271 | 930 | 0.512618 | 7 | -0.39 | 0.77 |
| 163JBM92 | 170 | 0.707827 | 18 | 34.83 | 68.46 | 0.51 | 1.47 | 0.704269 | 3.98 | 17.95 | 0.1546 | -0.214 | 714 | 0.512774 | 13 | 2.65 | 3.57 |
| 169JBM92 | 170 | 0.705888 | 31 | 43.01 | 189.49 | 0.23 | 0.66 | 0.704300 | 3.75 | 14.22 | 0.1594 | -0.190 | 743 | 0.512785 | 8 | 2.87 | 3.68 |
| 174JBM92 | 170 | 0.709439 | 19 | 59.51 | 105.41 | 0.71 | 2.05 | 0.703739 | 3.17 | 13.24 | 0.1459 | -0.258 | 1302 | 0.512463 | 3 | -3.41 | -2.31 |
| 323JBM92 | 170 | 0.708683 | 16 | 72.79 | 95.01 | 0.77 | 2.22 | 0.703325 | 4.35 | 19.34 | 0.1369 | -0.304 | 1130 | 0.512474 | 8 | -3.20 | -1.90 |
| CAY-A | 170 | 0.709557 | 184 | 91.92 | 101.29 | 0.91 | 2.63 | 0.703211 | 4.17 | 16.02 | 0.1577 | -0.198 | 580 | 0.512841 | 5 | 3.96 | 4.81 |
| CAY-B | 170 | 0.706217 | 21 | 35.06 | 128.74 | 0.27 | 0.79 | 0.704312 | 3.82 | 14.91 | 0.1587 | -0.193 | 1140 | 0.512632 | 6 | -0.12 | 0.71 |
| CAY-C | 170 | 0.706399 | 20 | 50.37 | 183.86 | 0.27 | 0.79 | 0.704483 | 5.82 | 23.79 | 0.1483 | -0.246 | 814 | 0.512699 | 10 | 1.19 | 2.24 |
| Cayoosh Assemblage Volcanics | | | | | | | | | | | | | | | | | |
| 171JBM92 | 170 | 0.704787 | 9 | -1.95 | 215.64 | -0.01 | -0.03 | 0.704851 | 4.06 | 11.64 | 0.2111 | 0.073 | 205 | 0.513062 | 10 | 8.27 | 7.96 |
| 176JBM92 | 170 | 0.704784 | 13 | 2.13 | 322.59 | 0.01 | 0.02 | 0.704738 | 6.57 | 23.69 | 0.1678 | -0.015 | | 0.512870 | 9 | 4.53 | 5.15 |
| 319JBM92 | 170 | 0.7045 | 10 | 0.22 | 342.43 | 0.00 | 0.00 | 0.704496 | 2.61 | 07.72 | 0.2046 | 0.040 | 240 | 0.513050 | 12 | 8.04 | 7.87 |
| 321JBM92 | 170 | 0.704887 | 17 | 3.62 | 705.55 | 0.01 | 0.01 | 0.704851 | 3.79 | 10.79 | 0.2126 | | | | | | |
| Bridge River Group | | | | | | | | | | | | | | | | | |
| 92-JS-5 | 150* | 0.712357 | 12 | 52.07 | 47.28 | 1.10 | 3.19 | 0.703293 | 4.35 | 21.64 | 0.1218 | -0.381 | 1154 | 0.512348 | 28 | -5.66 | -4.23 |
| 92-JS-7 | 150* | 0.708819 | 19 | 76.54 | 193.90 | 0.39 | 1.14 | 0.703571 | 4.85 | 24.50 | 0.1134 | -0.423 | 1157 | 0.512283 | 28 | -6.92 | -5.33 |
| 92-JS-10 | 150* | 0.709805 | 40 | 64.65 | 73.49 | 0.88 | 2.55 | 0.702565 | 6.00 | 26.42 | 0.1375 | -0.301 | 704 | 0.512699 | 8 | 1.19 | 2.30 |
| Lizard Formation | | | | | | | | | | | | | | | | | |
| 92-JS-23 | 100 | 0.708761 | 13 | 72.30 | 111.53 | 0.65 | 1.88 | 0.706096 | 5.12 | 24.03 | 0.1290 | -0.344 | 819 | 0.512594 | 9 | -0.86 | 0.01 |
| 92-JS-25 | 100 | 0.709336 | 27 | 73.25 | 114.75 | 0.64 | 1.85 | 0.706711 | 4.78 | 22.37 | 0.1290 | -0.344 | 881 | 0.512558 | 8 | -1.56 | -0.70 |
| METHOW TERRANE | | | | | | | | | | | | | | | | | |
| Boston Bar Formation | | | | | | | | | | | | | | | | | |
| 20aJBM91 | 190 | 0.708474 | 15 | 73.125 | 118.19 | 0.62 | 1.79 | 0.703638 | 7.56 | 42.55 | 0.1070 | -0.456 | 538 | 0.512679 | 7 | 0.80 | 2.98 |
| 34JBM91 | 190 | 0.706276 | 19 | 29.875 | 176.305 | 0.17 | 0.49 | 0.704951 | 7.64 | 29.71 | 0.1557 | -0.208 | 1100 | 0.512625 | 62 | -0.25 | 0.74 |
| 203JBM91 | 190 | 0.706718 | 14 | 35.94 | 161.14 | 0.22 | 0.65 | 0.704975 | 5.04 | 18.26 | 0.1658 | -0.157 | 774 | 0.512806 | 17 | 3.28 | 4.03 |
| 44JBM92 | 190 | 0.705653 | 20 | 44.33 | 206.85 | 0.21 | 0.62 | 0.703978 | 3.85 | 15.20 | 0.1532 | -0.221 | 359 | 0.512918 | 12 | 5.46 | 6.52 |
| 48JBM92 | 190 | 0.706414 | 16 | 63.32 | 193.45 | 0.33 | 0.95 | 0.703855 | 3.94 | 17.33 | 0.1367 | -0.305 | 977 | 0.512552 | 23 | -1.68 | -0.22 |
| Dewdney Creek Formation | | | | | | | | | | | | | | | | | |
| 232JBM92 | 170 | 0.706612 | 22 | 72.21 | 115.98 | 0.62 | 1.80 | 0.702258 | 2.58 | 10.20 | 0.1520 | -0.228 | 428 | 0.512885 | 5 | 4.82 | 5.79 |
| 234JBM92 | 170 | 0.705418 | 19 | 27.46 | 112.20 | 0.24 | 0.71 | 0.703706 | 2.54 | 10.16 | 0.1510 | -0.232 | 584 | 0.512814 | 3 | 3.43 | 4.43 |
| 235JBM92 | 170 | 0.705629 | 18 | 25.91 | 96.70 | 0.27 | 0.78 | 0.703756 | 3.10 | 10.83 | 0.1728 | -0.122 | | 0.512916 | 9 | 5.42 | 5.94 |
| 233JBM92 | 170 | 0.704458 | 39 | 49.39 | 285.30 | 0.12 | 0.35 | 0.703615 | 4.79 | 17.96 | 0.1613 | -0.180 | | 0.512905 | 6 | 5.21 | 5.98 |
| 261JBM92 | 190 | 0.704951 | 20 | | | | | | 4.80 | 17.91 | 0.1622 | -0.187 | 605 | 0.512840 | 7 | 3.94 | 4.74 |
| 262JBM92 | 170 | 0.705593 | 16 | 22.42 | 352.78 | 0.06 | 0.18 | 0.705149 | 2.63 | 10.18 | 0.1562 | -0.206 | | 0.512922 | 6 | 5.54 | 6.34 |
| 334JBM92 | 170 | 0.705022 | 13 | 30.20 | 265.33 | 0.11 | 0.33 | 0.704226 | 2.55 | 09.28 | 0.1636 | -0.169 | 617 | 0.512850 | 9 | 4.14 | 4.86 |
| 346JBM92 | 170 | 0.70429 | 17 | 41.11 | 455.66 | 0.09 | 0.26 | 0.703659 | 4.78 | 18.24 | 0.1586 | -0.194 | | 0.512901 | 6 | 5.13 | 5.96 |
| 351JBM92 | 170 | 0.704423 | 30 | 36.38 | 341.84 | 0.11 | 0.31 | 0.703679 | 3.87 | 14.63 | 0.1612 | -0.181 | 686 | 0.512815 | 5 | 3.45 | 4.23 |
| 356JBM92 | 170 | 0.708267 | 23 | 53.84 | 111.46 | 0.48 | 1.40 | 0.704889 | 5.44 | 17.14 | 0.1892 | -0.038 | | 0.512910 | 12 | 5.42 | 5.58 |

Table 6.3 (cont.) - Jurassic isotopic data.

| | | | | | | | | | | | | | | | | | |
|-----------------------------------|-----|----------|----|--------|--------|------|------|----------|------|-------|--------|--------|------|----------|----|-------|-------|
| Lillooet Group | | | | | | | | | | | | | | | | | |
| 209JBM91 | 170 | 0.705811 | 14 | 33.79 | 138.69 | 0.24 | 0.70 | 0.704107 | 5.93 | 23.14 | 0.1548 | -0.213 | 587 | 0.512827 | 9 | 3.69 | 4.60 |
| 213JBM91 | 170 | 0.706859 | 18 | 34.22 | 74.13 | 0.46 | 1.34 | 0.703631 | 3.82 | 15.33 | 0.1508 | -0.234 | 563 | 0.512822 | 8 | 3.59 | 4.59 |
| 220JBM91 | 170 | 0.705678 | 25 | 37.34 | 138.13 | 0.27 | 0.78 | 0.703787 | 4.95 | 18.07 | 0.1656 | -0.158 | | 0.512903 | 7 | 5.17 | 5.85 |
| 230JBM91 | 170 | 0.707382 | 30 | 59.02 | 75.67 | 0.78 | 2.26 | 0.701928 | | | 0.1525 | -0.225 | 418 | 0.512891 | 6 | 4.94 | 5.91 |
| 234JBM91 | 170 | 0.706421 | 31 | 42.27 | 80.98 | 0.52 | 1.51 | 0.702771 | 3.93 | 15.65 | 0.1516 | -0.229 | 534 | 0.512838 | 10 | 3.90 | 4.14 |
| 235JBM91 | 170 | 0.705996 | 17 | 39.63 | 194.13 | 0.20 | 0.59 | 0.704569 | 2.34 | 09.55 | 0.1484 | -0.246 | 533 | 0.512827 | 8 | 3.69 | 4.74 |
| Dewdney Creek Formation Volcanics | | | | | | | | | | | | | | | | | |
| 213jmb92 | 170 | 0.70378 | 17 | 22.53 | 639.90 | 0.04 | 0.10 | 0.703780 | 1.96 | 07.35 | 0.1612 | | | | | | |
| 215JBM92 | 170 | 0.703594 | 11 | 7.99 | 760.66 | 0.11 | 0.32 | 0.702825 | 2.08 | 06.88 | 0.1827 | -0.071 | | 0.512997 | 6 | 7.00 | 7.31 |
| 329JBM92 | 170 | 0.704108 | 12 | 17.89 | 359.29 | 0.05 | 0.14 | 0.703760 | 2.35 | 06.99 | 0.2033 | 0.034 | 579 | 0.513014 | 5 | 7.33 | 7.19 |
| 349JBM92 | 170 | 0.703988 | 17 | 2.36 | 242.60 | 0.01 | 0.03 | 0.703920 | 2.11 | 06.40 | 0.1997 | 0.015 | | 0.513023 | 4 | 7.51 | 7.45 |
| 350JBM92 | 170 | 0.704014 | 23 | 14.80 | 252.81 | 0.06 | 0.17 | 0.703605 | 2.17 | 08.27 | 0.1590 | -0.192 | | 0.512965 | 4 | 6.38 | 7.20 |
| Newby Group | | | | | | | | | | | | | | | | | |
| 243JBM91 | 180 | 0.70583 | 18 | 53.59 | 142.17 | 0.38 | 1.09 | 0.703038 | 4.71 | 16.59 | 0.1712 | -0.130 | | 0.512832 | 16 | 3.78 | 4.37 |
| 247JBM91 | 180 | 0.705849 | 15 | 40.45 | 186.55 | 0.22 | 0.63 | 0.704243 | 3.69 | 14.37 | 0.1552 | -0.211 | 770 | 0.512754 | 17 | 2.26 | 3.22 |
| 249JBM91 | 180 | 0.704537 | 17 | 31.98 | 251.58 | 0.13 | 0.37 | 0.703596 | 4.24 | 16.03 | 0.1589 | -0.192 | 953 | 0.512808 | 4 | 3.32 | 4.19 |
| Jurassic Methow Volcanics | | | | | | | | | | | | | | | | | |
| 363JBM92 | 175 | 0.704145 | 14 | 44.45 | 550.55 | 0.08 | 0.23 | 0.703564 | 4.31 | 18.00 | 0.1448 | | | | | | |
| 369JBM92 | 175 | 0.703722 | 20 | 2.29 | 448.64 | 0.01 | 0.01 | 0.703685 | 1.67 | 05.26 | 0.1917 | | | | | | |
| 7JBM93 | 175 | 0.704564 | 18 | 11.98 | 124.76 | 0.10 | 0.28 | 0.703873 | 2.57 | 10.83 | 0.1438 | -0.269 | 328 | 0.512911 | 6 | 5.33 | 6.51 |
| 80JBM93 | 175 | 0.703509 | 18 | 5.82 | 590.94 | 0.01 | 0.03 | 0.703438 | 3.24 | 11.16 | 0.1757 | -0.107 | | 0.512939 | 4 | 5.87 | 6.34 |
| 81JBM93 | 175 | 0.704152 | 17 | 0.67 | 105.44 | 0.01 | 0.02 | 0.704106 | 3.97 | 14.13 | 0.1700 | -0.136 | | 0.512942 | 5 | 5.93 | 6.53 |
| 83JBM93 | 175 | 0.704799 | 13 | 19.36 | 131.69 | 0.15 | 0.43 | 0.703741 | 3.16 | 11.96 | 0.1597 | -0.188 | | 0.512927 | 4 | 5.64 | 6.47 |
| 84JBM93 | 175 | 0.704262 | 18 | 7.39 | 183.82 | 0.04 | 0.12 | 0.703973 | 4.51 | 16.18 | 0.1679 | -0.146 | | 0.512944 | 7 | 5.97 | 7.02* |
| QUESNELLIA | | | | | | | | | | | | | | | | | |
| Ashcroft Formation | | | | | | | | | | | | | | | | | |
| 273JBM92 | 190 | 0.708557 | 11 | 118.07 | 233.05 | 0.51 | 1.47 | 0.704597 | 4.34 | 18.77 | 0.1399 | -0.289 | 1094 | 0.512514 | 6 | -2.42 | -1.04 |
| 279JBM92 | 170 | 0.707617 | 16 | 90.74 | 385.95 | 0.24 | 0.68 | 0.705973 | 4.61 | 19.79 | 0.1403 | -0.287 | 1253 | 0.512439 | 7 | -3.88 | -2.66 |

Table 6.3 (cont.) - Jurassic isotopic data.

7. CONCLUSIONS

This investigation had two primary goals: 1) determination of the applicability of Nd and Sr isotopic analysis of fine grained clastic sediments to stratigraphic correlation and basin analysis; 2) documentation of the stratigraphic characteristics and basinal histories of Lower to Middle Jurassic strata in terranes of the southern Canadian Cordillera in order to evaluate potential terrane linkages.

The applicability of Nd and Sr isotopic analysis of fine grained clastic sediments to stratigraphic correlation and basin analysis was first evaluated through a test study utilizing Neogene sediments from three western Pacific marginal basins (Shikoku Basin, Sea of Japan, Sulu Sea). The test study was designed to determine both the character and uniqueness of an individual basins' isotopic signature and how that isotopic signature varies through time. The Sea of Japan and the Sulu Sea both display distinct isotopic signatures that represent mixing and homogenization of fine grained detritus derived from isotopically heterogeneous source regions. These basinal signatures demonstrate that the isotopic signature of a basin varies within a limited range of values defined by the isotopic character of the source regions, and that each individual basin should have an isotopic signature distinct from neighboring basins resulting from differences in source region geology. However, the isotopic signature of the Sea of Japan and the Shikoku Basin strongly overlap, and the evolved ($\epsilon_{Nd} < (-8)$) signature of the Shikoku Basin contrasts with the juvenile character of the crustal domains on its margins. The evolved signature of the Shikoku Basin requires detrital influx from ancient continental crust, and is interpreted to be the result of aeolian influx of cratonic sediment. Thus, the Sea of Japan and the Shikoku Basin have nearly identical source regions, and can not be readily distinguished isotopically.

The applicability of Nd and Sr isotopic analyses to intrabasinal stratigraphic correlations was tested using Ocean Drilling Program cores from the Shikoku Basin. Analyses demonstrate that the isotopic signature of the Shikoku Basin varies through time, and that isotopic fluctuations are roughly synchronous across the basin. Synchronous isotopic fluctuations result in distinct patterns of isotopic values within sequences of fine grained clastic strata that can be used to correlate strata throughout the basin. Isotopic fluctuations through time result

from temporal variations in the composition of the basins' total sediment budget. The composition of the basins' sediment budget varies in response to the relative contribution of the different crustal domains comprising the source region. The relative contribution of each crustal domain is a function of tectonism, volcanic episodicity, climatic fluctuations and basin hydrology. Isotopic fluctuations in a stratigraphic sequence can therefore be important tools in both stratigraphic correlation and basin analysis.

Isotopic analyses of sediment from modern marginal basins demonstrate the potential of Nd and Sr isotopic analyses in stratigraphic correlation, basin discrimination, and basin evolution studies. Isotopic analyses have been applied to Lower to Middle Jurassic strata from a number of tectonostratigraphic terranes in the southern Canadian Cordillera. Lithostratigraphic, biostratigraphic, volcanic geochemistry and isotopic analyses of Lower to Middle Jurassic strata from the Harrison, Cadwallader, Bridge River, and Methow terranes were conducted to determine the depositional history, provenance, and basin configuration of these strata, and to evaluate potential stratigraphic linkages between the terranes.

The isotopic signatures of Lower to Middle Jurassic strata on the Harrison, Bridge River, and Methow terranes are very similar. Each succession is characterized by juvenile Nd and Sr isotopic values in both fine-grained clastic sedimentary rocks and volcanic rocks, and show no evidence for significant input of evolved (i.e. continental) detritus. The isotopic signature of each succession varies with time, and is characterized by an overall juvenile signature ($\epsilon_{Nd} \sim +6 - +8$; $^{87}Sr/^{86}Sr \sim < 0.7045$) punctuated by isotopic excursions to slightly more evolved values ($\epsilon_{Nd} \sim +2 - -2$; $^{87}Sr/^{86}Sr \sim > 0.7050$). The Harrison, Bridge River and Methow terranes are interpreted to display a synchronous isotopic excursion in the Late Toarcian. The Last Creek Formation of the Cadwallader terrane is isotopically homogeneous ($\epsilon_{Nd} \sim +3.5 - +4.0$), but this homogeneity is interpreted to be the result of a small sample set (n=4) and a lack of Toarcian samples. The greater number of isotopic excursions in the Cayoosh assemblage is consistent with its more distal basinal position relative to coarse volcanoclastic strata of the Harrison and Methow terranes.

Isotopic analyses of Lower to Middle Jurassic strata in the southern Canadian Cordillera suggest, but do not prove, that these strata were deposited in a single basin. Overlap documented between the isotopic signatures of marginal basins of the western Pacific indicates that geographically separated basins can display similar isotopic signatures. However, temporal isotopic fluctuations within a single basin are a result of changes in the composition of the sediment budget due to tectonism, volcanic episodicity, climatic fluctuations, and basin hydrology. Synchronous isotopic fluctuations, in this case, the Late Toarcian excursion common to each succession, are more likely a product of intrabasinal events rather than identical changes in sediment budget in geographically distinct basins.

Lithostratigraphic, biostratigraphic, and volcanic geochemical data, in conjunction with isotopic analyses, support correlation of Lower to Middle Jurassic strata of the Harrison, Cadwallader, Bridge River, and Methow terranes. Lithostratigraphic correlations between the terranes are proposed on the basis of six regionally consistent stratigraphic relationships within Lower Jurassic to Lower Cretaceous strata:

- 1) initiation of basin subsidence in Early Jurassic time (post-Late Triassic, pre-Toarcian);
- 2) Pliensbachian to Toarcian black shale deposition
- 3) Initiation of volcanism in Late Toarcian to Aalenian time
- 4) Cessation of volcanism in Late Bajocian/Early Bathonian time
- 5) Shift in provenance and depositional environment in late Middle Jurassic time
- 6) Deposition of Lower Cretaceous granitoid bearing conglomerate

Available biostratigraphic data provides reasonable constraints on both timing of lithostratigraphic variations and on the paleogeographic affinity of the terranes. Aalenian to Bajocian strata in Harrison, Cadwallader and Methow terranes contain an identical mixed ammonite fauna consisting of *Erycitoides* (Boreal), *Zemistephanus* (East Pacific), and *Planamatoceras* (Tethyan). The occurrence of identical mixed fauna from three overlapping faunal realms strongly suggests each of the terranes was in the northeastern quadrant of the Panthalassic ocean in early Middle Jurassic time.

Geochemical data suggest that Lower to Middle Jurassic volcanic rocks of the Harrison and Methow terranes were deposited in different volcanic arcs, and that volcanic rocks of the Cayoosh assemblage of the Bridge River terrane formed in a back arc basin environment. Volcanic strata of the Harrison terrane are correlated with Lower to Middle Jurassic volcanic rocks of Wrangellia, and represent the youngest, easternmost deposits of the westward migrating Bonanza-Harrison arc system. Dewdney Creek Formation volcanic rocks of the Methow terrane are distinctly less geochemically and isotopically evolved than coeval strata in the Harrison terrane, and are interpreted to represent a separate arc system. Volcanic rocks of the Cayoosh assemblage display hybrid geochemical signatures that overlap both arc tholeiite and enriched MORB values, consistent with deposition in a back arc basin.

Available lithostratigraphic, biostratigraphic, geochemical and isotopic data strongly suggest that Lower to Middle Jurassic strata of Wrangellia, Harrison, Cadwallader, Bridge River, and Methow terranes were deposited in a single marginal basin. Biostratigraphic constraints suggest the basin was developed in the northeastern quadrant of the Panthalassic ocean. This basin was flanked on the west by the composite Bonanza-Harrison volcanic arc system, and on the east by arc volcanic rocks of the Dewdney Creek Formation. The interior of the basin was floored by trapped oceanic crust of the Bridge River terrane. Clastic strata of the Cayoosh Assemblage represent the first clastic influx into the trapped "Bridge River ocean" in Early Jurassic time. Continued chert deposition until late Middle Jurassic time suggests the basin topography was irregular and the clastic influx diachronous. The presence of back arc basin basalts in the Cayoosh assemblage requires incipient extension or transtension in the basin interior. Intrabasinal faults could have accommodated significant (tens to hundreds of kilometres) translational displacement but did not completely dismember the basin.

Stratigraphic correlations presented herein have important implications for the tectonic evolution of the southern Canadian Cordillera. Correlation of Lower to Middle Jurassic strata of the Wrangellia, Harrison, Cadwallader, Bridge River, and Methow terranes requires amalgamation of Triassic and underlying assemblages of each terrane prior to Early Jurassic time. There is no compelling evidence at this time to indicate the basin was adjacent to North American craton. Numerous models of Cordilleran tectonic evolution postulate large-scale

latitudinal displacement of the accreted terranes in Jurassic to Tertiary time (Gehrels and Saleeby, 1985; Saleeby and Busby-Spera, 1992; McClelland et al., 1992; Garver and Brandon, 1994; Cowan, 1994). The stratigraphic correlations proposed here require that any post-Early Jurassic latitudinal displacement of the Wrangellia, Harrison, Cadwallader, Bridge River, and Methow terranes move the terranes en masse as a coherent crustal block. Proposed terrane linkages therefore require that any faults accommodating large scale latitudinal displacement be located east of the Methow terrane.

a. Tectonic Implications

Stratigraphic correlation of Lower to Middle Jurassic strata of the Wrangellia, Harrison, Cadwallader, Bridge River, and Methow terranes requires that these terranes were amalgamated prior to the Early Jurassic, and have behaved as a coherent crustal block since that time. The suggestion that the terranes west of the Pasayten fault were amalgamated prior to the Early Jurassic has implications for the tectonic evolution of the southern Canadian Cordillera.

Current debate in Cordilleran tectonic studies centres on the paleogeographic position of the accreted terranes with respect to North America. Late Cretaceous paleomagnetic data suggest significant paleolatitudinal displacement of all allochthonous terranes west of cratonal North America. Paleomagnetic evidence suggests northward displacements of approximately 1200 km for the Intermontane superterrane (amalgamated Quesnellia and Cache Creek terranes; Monger et al., 1982) and 2900 km for the Insular superterrane (amalgamated Wrangellia, Peninsular, and Alexander terranes; Monger et al., 1982; Marquis and Globberman, 1988; Ague and Brandon, 1992; Maxson et al., 1993; Irving et al., 1993). Harrison, Cadwallader, Bridge River, and Methow terranes are imbricated within a "mid-Cretaceous collisional orogen" associated with the eastern margin of the Insular superterrane, and are therefore assumed to have been translated an equivalent distance (Cowan, 1994). The boundary between the Intermontane and Insular superterrane roughly coincides with the eastern edge of the Methow terrane and the Pasayten fault. Paleomagnetic models suggest that terranes west of the Pasayten fault were unassociated with those east of the Pasayten fault prior to the Early Tertiary (Irving and Wynne, 1990).

Paleomagnetic models conflict with geologic models that suggest that terranes west of the Pasayten fault were in situ by Middle Jurassic (van der Heyden, 1992); Middle to Late Jurassic (McClelland et al., 1992), or mid-Cretaceous time (Monger et al., 1982; Garver, 1992). Resolution of these conflicting data sets requires establishing definitive geologic ties between terranes on either side of the Pasayten fault (Cowan, 1994).

The fundamental conclusion of the present study is that the Wrangellia, Harrison, Cadwallader, Bridge River, and Methow terranes constitute a marginal basin characterized by trapped oceanic crust flanked by two volcanic arcs during Early to Middle Jurassic time. There are no firm ties linking the amalgamated terranes west of the Pasayten fault with either the accreted terranes (e.g. Quesnellia) to the east or cratonal North America prior to Early Tertiary time. Stratigraphic evidence from Lower Jurassic (Ray, 1986), Lower to Middle Jurassic (Mahoney, 1993), and Lower Cretaceous (Klensphen, 1982; Garver, 1992; Hickson and others, 1994) rocks of the Methow terrane suggests these strata received detritus from an eastern source. Quesnellia and associated terranes east of the Methow terrane contain source regions that could have supplied the appropriate mixture of volcanic, plutonic, and metamorphic detritus to westward thinning clastic wedges within the Methow terrane; stratigraphic ties between Quesnellia and terranes to the east have been suggested (Klensphen, 1982; O'Brien et al., 1992; Mahoney, 1993). However, at this time there is no irrefutable evidence tying terranes west of the Pasayten fault with Quesnellia and associated terranes.

I suggest that there is sufficient evidence to correlate Lower to Middle Jurassic strata of Wrangellia, Harrison, Cadwallader, Bridge River, and Methow terranes. Existing data does not allow these amalgamated terranes to be linked with terranes to the east in Lower to Middle Jurassic time. Biostratigraphic data from this study suggest Lower to Middle Jurassic strata of the amalgamated terranes were deposited in the northeast quadrant of the Panthalassa ocean (north of 36°N, present day coordinates), but additional paleolatitudinal constraints are lacking. Post-depositional translation of these amalgamated terranes is permissible, provided the terranes moved as a coherent crustal block.

b. Directions for Future Research

The scientific findings presented in the foregoing dissertation have inevitably highlighted a variety of questions and problems that need to be addressed in future research projects. Suggestions for future research will be presented in two parts: 1) problems related to the isotopic analysis of fine grained clastic rocks; and, 2) questions pertaining to stratigraphic correlation and basin analysis in Middle Jurassic rocks of the southern Canadian Cordillera.

Isotopic analyses of fine grained clastic strata have tremendous potential in stratigraphic investigations and basin evolution studies. However, questions related to isotopic systematics in fine grained clastic sediments remain. Exactly how is Nd partitioned in fine grained clastic detritus? Is the assumption of no diagenetic mobility of Nd valid in all sediment compositions? What is the contribution of sea water Nd to the sediment isotopic signature in basins dominated by terrigenous clastic influx? The isotopic analysis of Western Pacific marginal basins presented herein could be further refined by acquisition of better age control through detailed biostratigraphic analyses or isotopic data. Nd analysis of Miocene and Pliocene sediments in the Shikoku Basin would document the initial influx of aeolian sediment into the basin, and mineralogical studies could be used to verify the existence of aeolian detritus. The utility of Nd isotopic analysis in basin discrimination, stratigraphic correlation and provenance studies could be tested further by analysis of PlioPleistocene sediments in additional marginal basins in the Western Pacific.

Stratigraphic correlations and terrane linkages proposed herein suggest Wrangellia, Harrison, Cadwallader, Bridge River, and Methow terranes have shared a common basin evolution since the Early Jurassic. These correlations will undoubtedly be met with skepticism, and additional lithostratigraphic, biostratigraphic, isotopic, and geochemical data in Middle Jurassic to Lower Cretaceous rocks is required to further strengthen the argument. The most pressing problem is the lack of sufficient age control in the Cayoosh assemblage. Metamorphic and structural overprint in the Cayoosh assemblage makes fossil recovery unlikely, and significant effort should be expended to constrain its age through U-Pb analysis of zircon recovered from volcanic rocks in

member 2. In addition, zircon provenance studies in the quartz rich clastic facies would help to constrain the source of the quartzose detritus and perhaps establish links with source terranes to the east. The geochemical character of volcanogenic strata within the assemblage must be further documented throughout the outcrop belt to verify the back arc nature of volcanism.

The interpretation that the Last Creek Formation is part of an eastward thinning clastic wedge derived from the Harrison-Bonanza arc must be strengthened by geochemical and isotopic analysis of the coarse grained facies of the Last Creek Formation near Chilko Lake. Toarcian strata of the Last Creek Formation must be isotopically analyzed to verify the presence of a Toarcian isotopic excursion in the unit. Facies analysis of western exposures of the Last Creek Formation are necessary to firmly establish stratigraphic ties with the Harrison-Bonanza arc.

The most fruitful avenue of future research will be a detailed analysis of upper Middle Jurassic and Upper Jurassic strata of the Harrison, Cadwallader, Bridge River, and Methow terranes in a manner similar to this investigation. Complete documentation of lithostratigraphic, biostratigraphic, geochemical and isotopic variations in these strata is required to further document or perhaps refute Jurassic stratigraphic correlations and terrane linkages in the southern Canadian Cordillera.

8. REFERENCES

- Ague, J.J., and Brandon, M.T., 1992, Tilt and northward offset of Cordilleran batholiths resolved using igneous barometry: *Nature*, vol. 360, pp. 146-149.
- Allegre, C.J., and Rosseau, D., 1984, The growth of the continent through geological time studied by isotopic analyses of shales: *Earth and Planetary Science Letters*, vol. 67, pp. 19-34.
- Andre, L., Deutsch, S., and Hertogen, J., 1986, Trace element and Nd isotopes in shales as indexes of provenance and crustal growth: the Early Paleozoic from the Brabant Massif (Belgium): *Chemical Geology*, vol. 57, pp. 101-115.
- Andrew, A., and Godwin, C.I., 1989a, Lead and strontium isotope geochemistry of Paleozoic Sicker Group and Jurassic Bonanza Group volcanic rocks and Island Intrusions, Vancouver Island, British Columbia: *Canadian Journal of Earth Sciences*, vol. 26, pp. 894-907.
- Andrew, A., Armstrong, R.L., and Runkle, D., 1991, Neodymium-strontium-lead isotopic study of Vancouver Island igneous rocks: *Canadian Journal of Earth Sciences*, vol. 28, pp. 1744-1752.
- Archibald, D.A., Schiarizza, P., and Garver, J.I., 1990, $^{40}\text{Ar}/^{39}\text{Ar}$ Evidence for the age of igneous and metamorphic events in the Bridge River and Shulaps complexes, southwestern British Columbia: *British Columbia Ministry of Energy, Mines and Petroleum Resources, Geological Fieldwork 1990, Paper 1991-1*.
- Armstrong, J.E., 1953, Preliminary map, Vancouver North, British Columbia: Geological Survey of Canada, Paper 53-28.
- Armstrong, R.L., 1988, Mesozoic and early Cenozoic evolution of the Canadian Cordillera; *in* S.P. Clark Jr., B.C. Burchfiel, and J. Suppe, eds., *Processes in Continental Lithospheric Deformation*; Geological Society of America, Special Paper 218, pp. 55-91.
- Armstrong, R.L., and Parrish, R.R., 1990, A geological excursion across the Canadian Cordillera near 49°N (Highways 1 and 3 from Vancouver to southwestern Alberta and on to Calgary, Alberta): Geological Association of Canada Field Trip Guide, Vancouver, British Columbia, 75 p.
- Arthur, A.J., 1986, Stratigraphy along the west side of Harrison Lake, southwestern British Columbia: Current Research, Part B, Geological Survey of Canada, Paper 86-1B, pp. 715-720.
- Arthur, A.J., 1987, Mesozoic stratigraphy and paleontology of the west side of Harrison Lake, southwestern British Columbia: unpublished M.Sc. thesis, University of British Columbia, 171 p.
- Arthur, A.J., Smith, P.J., Monger, J.W.H., and Tipper, H.W., 1993, Mesozoic stratigraphy and Jurassic paleontology west of Harrison Lake, southwestern British Columbia: *Geological Survey of Canada Bulletin* 441, 62 p.
- Barker, F., Sutherland Brown, A., Budahn, J.R., and Plafker, G., 1989, Back-arc with frontal arc component origin of Triassic Karmutsen Basalt, British Columbia: *Chemical Geology*, vol. 75, pp. 81-102.
- Barrett, T.J., and MacLean, W.H., 1994, Chemostratigraphy and hydrothermal alteration in exploration for VHMS deposits in greenstones and younger volcanic rocks; *in* Lentz, D.R., ed., *Alteration and Alteration Processes associated with Ore-forming Systems*: Geological Association of Canada, Short Course Notes, vol. 11, pp. 433-467.

- Barrie, C.T., Gorton, M.P., Naldrett, A.J., and Hart, T.R., 1991, Geochemical constraints on the petrogenesis of the Kamiskotia gabbroic complex and related basalts, western Abitibi Subprovince, Ontario, Canada: *Precambrian Research*, vol. 50, pp. 173-199.
- Brandon, M.T., Orchard, M.J., Parrish, R.R., Sutherland Brown, A., and Yorath, C.J., 1986, Fossil ages and isotope dates from the Paleozoic Sicker Group and associated intrusive rocks, Vancouver Island, British Columbia: *Geological Survey of Canada Paper 86-1A*, pp. 683-696.
- Brandon, M.T., Cowan, D.S., and Vance, J.A., 1988, The Late Cretaceous San Juan Thrust System, San Juan Islands: *Geological Society of America Special Paper 221*, 81 p.
- Brown, E.H., 1987, Structural geology and accretionary history of the Northwest Cascades System, Washington and British Columbia: *Geological Society of America Bulletin*, vol. 99, pp. 201-214.
- Brown, R.L., Journeay, J.M., Lane, L.S., Murphy, D.C., and Rees, C.J., 1986, Obduction, backfolding, and piggyback thrusting in the metamorphic hinterland of the Canadian Cordillera: *Journal of Structural Geology*, vol. 8, pp. 255-268.
- Calon, T.J., Malpas, J.G., and Macdonald, R., 1990, The anatomy of the Shulaps Ophiolite: British Columbia Ministry of Energy, Mines, and Petroleum Resources, Geological Fieldwork 1989, Paper 1990-1.
- Cas, R.A.F., and Wright, J.V., 1987, Volcanic Successions - modern and ancient: Allen and Unwin, London, 528 p.
- Coates, J.A., 1970, Stratigraphy and structure of Manning Park area, Cascade Mountains, British Columbia: *Geological Association of Canada, Special Paper number 6*.
- Coleman, M.E., and Parrish, R.R., 1991, Eocene dextral strike-slip and extensional faulting in the Bridge River terrane, southwest British Columbia: *Tectonics*, vol. 10, pp. 1222-1238.
- Cordey, F., 1986, Radiolarian ages from the Cache Creek and Bridge River complexes and from chert pebbles in Cretaceous conglomerates, southwestern British Columbia: *Geological Survey of Canada Paper 86-1A*, pp. 595-602.
- Cordey, F., Mortimer, N., DeWever, P., and Monger, J.W.H., 1987, Significance of Jurassic radiolarians from the Cache Creek terrane, British Columbia: *Geology*, vol. 15, pp. 1151-1154.
- Cordey, F., and Read, P.B., 1992, Permian and Triassic radiolarian ages from the Cache Creek Complex, Dog Creek, and Alkali Lake areas, southwestern British Columbia: *Geological Survey of Canada, Current Research, Part E, Paper 92-1E*, pp. 41-51.
- Cordey, F., and Schiarizza, P., 1993, Long-lived Panthalassic remnant: The Bridge River accretionary complex, Canadian Cordillera: *Geology*, vol. 21, p. 263-266.
- Cowan, D.S., 1994, Alternate hypotheses for the mid-Cretaceous paleogeography of the western Cordillera; *GSA Today*, vol. 4, pp. 183-186.
- Crickmay, C.H., 1925, The geology and paleontology of the Harrison Lake District, British Columbia, together with a general review of the Jurassic faunas and stratigraphy of western North America: unpublished Ph.D. thesis, Stanford University, Stanford, California, 140 p.
- Curtis, D.M., and Echols, D.J., 1980, Lithofacies of the Shikoku and Parece Vela Basins; *in* deVries Klein, G., Kobayashi, K., et al., Initial Reports of the Deep Sea Drilling Project, v. 58, Washington (U.S. Government Printing Office), pp. 701-709.

- Cui, Y., and Russell, J.K., Nd-Sr-Pb isotopic studies of the southern Coast Plutonic Complex, southwestern British Columbia; Geological Society of America Bulletin, in press.
- DeBari, S.M. and Mortensen, J.K., 1994, Petrology and field relations of the Jurassic Bonanza island arc, a crustal section from the Wrangellia terrane, Vancouver Island, Canada: Geological Society of America Bulletin, in press.
- deVries Klein, G., Kobayashi, K., et al., 1980, Initial Reports of the Deep Sea Drilling Project, v. 58: Washington (U.S. Government Printing Office)
- deVries Klein, G. and Kobayashi, K., 1980, Geological summary of the North Philippine Sea, based on Deep Sea Drilling Project Leg 58 results; in deVries Klein, G., Kobayashi, K., et al., 1980, Initial Reports of the Deep Sea Drilling Project, v. 58: Washington (U.S. Government Printing Office), pp. 951-963.
- Defant, M.J., Jacques, D., Maury, R.C., De Boer, J., and Joron, J-L, 1989, Geochemistry and tectonic setting of the Luzon arc, Philippines: Geological Society of America Bulletin, vol. 101, pp. 663-672.
- DePaolo, D.J., 1988, Neodymium Isotope Geochemistry: an Introduction: Springer-Verlag, Berlin, xx p.
- DePaolo, D.J. and Wasserburg, G.J., 1977, The Sources of Island Arcs as Indicated by Nd and Sr Isotopic Studies: Geophysical Research Letters, vol. 4, no. 10, pp. 465-468.
- DePaolo, D.J., Linn, A.M., and Schubert, G., 1991, The continental crustal age distribution: Methods of determining mantle separation ages from Sm-Nd isotopic data and application to the southwestern United States: Journal of Geophysical Research, vol. 96, no. B2, pp. 2071-2088.
- Duffell, S., and McTaggart, K.C., 1952, Ashcroft map area, British Columbia: Geological Survey of Canada, Paper 67-10.
- England, T.D.J. and Calon, T.J., 1991, The Cowichan fold and thrust system, Vancouver Island, southwestern British Columbia: Geological Society of America Bulletin, vol. 103, pp. 336-362.
- Faure, G., and Powell, J.L., Strontium Isotope Geology; Springer-Verlag, New York, 188 p.
- Faure, M., Marchadier, Y., and Rangin, C., 1989, Pre-Eocene synmetamorphic structure in the Mindoro-Romblon-Palawan area, West Philippines, and implications for the history of Southeast Asia: Tectonics, vol. 8, no. 5, pp. 963-980.
- Fisher, R.V., and Schmincke, H.-U., 1984, Pyroclastic Rocks: Springer-Verlag, Berlin, 472 p.
- Frebold, H. 1967, Hettangian ammonites of the Taseko Lakes map area, British Columbia; Geological Survey of Canada Bulletin 158, 35 p.
- Frebold, H., Tipper, H.W., and Coates, J.A., 1969, Toarcian and Bajocian rocks and guide ammonites from southwestern British Columbia: Geological Survey of Canada, Paper 67-10.
- Friedman, R.M., Monger, J.W.H., and Tipper, H.W., 1990, Age of the Bowen Island Group, southwestern Coast Mountains, British Columbia: Canadian Journal of Earth Sciences, vol. 27, pp. 1456-1461.
- Friedman, R.M. and Armstrong, R.L., 1994, Jurassic and Cretaceous geochronology of the southern Coast Belt, southern British Columbia, 49-50 degrees N: Geological Society of America Memoir, in press.

- Friedman, R.M., Mahoney, J.B., and Cui, Y., 1994, Juvenile crust in the southern Coast Belt of British Columbia: Evidence from a regional Nd-Sr isotopic study of the southern Coast Plutonic Complex Batholith: *Canadian Journal of Earth Sciences*, in press.
- Frost, C.D., and Coombs, D.S., 1989, Nd isotope character of New Zealand sediments: implications for terrane concepts and crustal evolution: *American Journal of Science*, vol. 289, pp. 744-770.
- Garver, J.I., 1989, Basin evolution and source terranes of Albian-Cenomanian rocks in the Tyaughton basin, southern British Columbia: implications for mid-Cretaceous tectonics in the Canadian Cordillera: unpublished Ph.D. thesis, University of Washington, Seattle, Washington.
- Garver, J.I., 1992, Provenance of Albian-Cenomanian rocks of the Methow and Tyaughton basins, southern British Columbia: a mid-Cretaceous link between North America and Insular terranes: *Canadian Journal of Earth Sciences*, vol. 29, p. 1274-1295.
- Garver, J.I., and Brandon, M.T., 1994, Fission-track ages of detrital zircons from Cretaceous strata, southern British Columbia: Implications for the Baja BC hypothesis: *Tectonics*, vol. 13, no. 2, pp. 401-420.
- Gehrels, G.E., and Saleeby, J.B., 1985, Constraints and speculations on the displacement and accretionary history of the Alexander-Wrangellia-Peninsular superterrane: *Geological Society of America, Abstracts with Programs*, vol. 17, pp. 208-211.
- Ghosh, D.K., 1991, Nd and Sr isotopic constraints on the timing of obduction of Quesnellia onto the western edge of North America; *in*, *Proceedings of the Lithoprobe Southern Cordilleran Transect Workshop*, pp. 113-127.
- Ghosh, D.K., 1991, Nd and Sr isotopic constraints on the timing of obduction of Quesnellia onto the western edge of North America; *Canadian Journal of Earth Sciences*, in press.
- Gill, J.B., 1981, *Orogenic andesites and plate tectonics*: Springer-Verlag, Berlin, 385 p.
- Goldstein, S.L., O'Nions, R.K., and Hamilton, P.J., 1984, A Sm-Nd isotopic study of atmospheric dusts and particulates from major river systems: *Earth and Planetary Science Letters*, vol. 70, pp. 221-236.
- Goldstein, S.J., and Jacobsen, S.B., 1987, The Nd and Sr isotopic systematics of river-water dissolved material: implications for the sources of Nd and Sr in seawater: *Chemical Geology*, vol. 66, pp. 245-272.
- Goldstein, S.J., and Jacobsen, S.B., 1988, Nd and Sr isotopic systematics of river water suspended material: implications for crustal evolution: *Earth and Planetary Science Letters*, vol. 87, pp. 249-265.
- Greig, C.J., 1992, Jurassic and Cretaceous plutonic and structural styles of the Eagle Plutonic Complex, southwestern British Columbia, and their regional significance: *Canadian Journal of Earth Sciences*, vol. 29, pp. 793-811.
- Greig, C.J., Armstrong, R.L., Harakel, J.E., Runkle, D., and van der Heyden, P., 1992, Geochronometry of the Eagle Plutonic Complex and the Coquihalla area, southwestern British Columbia: *Canadian Journal of Earth Sciences*, vol. 29, pp. 812-829.
- Grousset, F.E., Biscaye, P.E., Zindler, A., Prospero, J., and Chester, R., 1988, Neodymium isotopes as tracers in marine sediments and aerosols: North Atlantic: *Earth and Planetary Science Letters*, vol. 87, pp. 367-378.
- Hanson, G.N., 1980, Rare earth elements in petrogenetic studies of igneous systems: *Annual Review of Earth Sciences* 1980, vol. 8, pp. 371-406.

- Haugerud, R.A., 1985, Geology of the Hozameen Group and the Ross Lake shear zone, Maselpalik area, North Cascades, southeast British Columbia: unpublished Ph.D. thesis, University of Washington, Seattle, Washington, 247 p.
- Haugerud, R.A., van der Heyden, P., Tabor, R.W., Stacey, J.S., Zartman, R.E., 1991, Late Cretaceous and Early Tertiary plutonism and deformation in the Skagit Gneiss Complex, North Cascade Range, Washington and British Columbia: *Geological Society of America Bulletin*, vol. 103, pp. 1297-1307.
- Hawkesworth, C.J., 1982, Isotope characteristics of magmas erupted along destructive plate margins: in, *Andesites: Orogenic Andesites and Related Rocks*, Thorpe, R.S., ed., pp. 549-571.
- Hawkesworth, C.J., Gallagher, K., Hergl, J. M., and McDermott, F., 1993, Mantle and slab contributions in arc magmas: *Annual Review of Earth and Planetary Science*, vol. 21, pp. 175-204.
- Hesse, R., 1990, Early diagenetic pore water/sediment interaction: modern offshore basins: in, *Diagenesis*; McIlreath and Morrow, eds., *Geoscience Canada Reprint Series 4*, pp. 277-316.
- Hickson, C.J., 1990, A new Frontier Geoscience Project: Chilcotin-Nechako region, central British Columbia; in, *Current Research, Part F*; Geological Survey of Canada, Paper 90-1F, pp. 115-120.
- Hodell, D.A., Mueller, P.A., and Garrido, J.R., 1991, Variations in the strontium isotopic composition of seawater during the Neogene: *Geology*, vol. 19, pp. 24-27.
- Hurlow, H.A., 1993, Mid-Cretaceous strike-slip and contractional fault zones in the western Intermontane terrane, Washington, and their relation to the North Cascades-Southeastern Coast Belt orogen: *Tectonics*, vol. 12, no. 5, pp. 1240-1257.
- Hurlow, H.A., and Nelson, B.K., 1993, U-Pb zircon and monazite ages for the Okanogan Range batholith, Washington: Implications for the magmatic and tectonic evolution of the southern Canadian and northern United States Cordillera: *Geological Society of America Bulletin*, vol. 105, pp. 231-240.
- Irving, E., Wheadon, P.M., and Thorkelson, D.J., 1993, Paleomagnetic results from the mid-Cretaceous Spences Bridge Group and northward displacement of the eastern Intermontane Belt, British Columbia: *Geological Association of Canada-Mineralogical Association of Canada, Joint Annual Meeting, Program and Abstracts*, p. A47.
- Irvine, T.N., and Barager, W.R.A., 1971, A guide to the chemical classification of the common volcanic rocks, *Canadian Journal of Earth Sciences*, vol.8, pp. 523-548.
- Isozaki, Y., Maruyama, S., and Furuoka, F., 1990, Accreted oceanic materials in Japan; *Tectonophysics*, vol. 181, pp. 179-205.
- Jacobsen, S.B., and Wasserburg, G.J., 1979, Sm-Nd evolution of chondrites: *Earth and Planetary Science Letters*, vol. 50, pp. 139-155.
- Jakobs, G.K., 1992, Toarcian (Lower Jurassic) ammonite biostratigraphy and ammonite fauna of North America: unpublished Ph.D. thesis, University of British Columbia, Vancouver, British Columbia, 381 p.
- Janecek, T.R., and Rea, D.K., 1983, Eolian deposition in the northeast Pacific Ocean: Cenozoic history of atmospheric circulation: *Geological Society of America Bulletin*, vol. 94, p. 730-738.
- Jeletzky, J.A., 1972, Jurassic and Cretaceous rocks along the Hope-Princeton Highway and Lookout Road, Manning Park, British Columbia (suppliment to Section 10 of 24th International Geological Congress Guidebook A03-C03), Geological Survey of Canada, Open File Report 114: 38 p.

- Jeletsky, J.A., 1976, Mesozoic and Tertiary Rocks of Quatsino Sound, Vancouver Island, British Columbia: Geological Survey of Canada Bulletin 242, 243 p.
- Jones, D.L., Silberling, N.J., and Hillhouse, J., 1977, Wrangellia-A displaced terrane in northwestern North America: Canadian Journal of Earth Sciences, vol. 14, pp. 2565-2577.
- Journey, J.M., 1990, Structural and tectonic framework of the southern Coast Belt, British Columbia; in, Current Research, Part A; Geological Survey of Canada, Paper 93-1A, p. 183-197.
- Journey, J.M., 1993, Tectonic assemblages of the Eastern Coast Belt, southwestern British Columbia: implications for the history and mechanisms of terrane accretion: Current Research, Part A; Geological Survey of Canada, Paper 93-1A, p. 221-233.
- Journey, J.M., and Mahoney, J.B., 1994, Cayoosh Assemblage: regional correlations and implications for terrane linkages in the southern Coast Belt, British Columbia: Current Research 1994-A; Geological Survey of Canada, Paper 94-1A, pp. 165-175.
- Journey, J.M. and Monger, J.W.H., 1994, Geology and crustal structure of the southern Coast and Intermontane belts, southern Canadian Cordillera, British Columbia: Geological Survey of Canada Open File XXX.
- Journey, J.M., and Friedman, R.M., 1993, The Coast Belt Thrust System: Evidence of Late Cretaceous shortening in southwest British Columbia: Tectonics, no. 3, pp. 756-775.
- Journey, J.M., and Northcote, B.R., 1992, Tectonic assemblages of the Southern Coast Belt, southwest British Columbia: Current Research, Part A; Geological Survey of Canada Paper 92-1A, pp. 215-224.
- Journey, J.M. and Csontos, L., 1989, Preliminary report on the structural setting along the southeast flank of the Coast Belt, British Columbia: Current Research, Part E; Geological Survey of Canada Paper 89-1E, pp. 177-187.
- Journey, J.M., Sanders, C., Van-Konijnenburg, J.-H., and Jaasma, M., 1992, Fault systems of the Eastern Coast Belt, southwest British Columbia: Current Research, Part A; Geological Survey of Canada, Paper 92-1A, pp. 225-235.
- Kagami, H., Iizumi, S., Tainosho, Y., and Owada, M., 1992, Spatial variations of Sr and Nd isotopic ratios of Cretaceous-Paleogene granitoid rocks, Southwest Japan Arc: Contributions to Mineralogy and Petrology, vol. 112, p. 165-177.
- Karig, D.E., 1975, Basin genesis in the Philippine Sea: in, Karig, D.E., Ingle, J.C., Jr., et al., Initial Reports of the Deep Sea Drilling Project, v. 31, Washington (U.S. Government Printing Office).
- Kleinspehn, K.L., 1982, Cretaceous sedimentation and tectonics, Tyaughton-Methow basin, southwestern British Columbia: unpublished Ph.D. thesis, Princeton University, Princeton, N.J.
- Kleinspehn, K.L., 1985, Cretaceous sedimentation and tectonics, Tyaughton-Methow Basin, southwestern British Columbia: Canadian Journal of Earth Sciences, vol. 22, pp. 154-174.
- Klepacki, D.W., 1985, Stratigraphy and structural geology of the Goat Range area, southeastern British Columbia: unpublished Ph.D. thesis, Massachusetts Institute of Technology, Boston, Massachusetts, 268 p.
- Krogh, T.E., 1973, A low-contamination method for hydrothermal decomposition of zircon and extraction of U and Pb for isotopic age determinations: Geochimica et Cosmochimica Acta, vol. 37, pp. 485-494.

- Larue, D.K., Smith, A.L., and Schellekens, J.H., 1991, Oceanic island arc stratigraphy in the Caribbean region: don't take it for granite: *Sedimentary Geology*, vol. 74, pp. 289-308.
- Leitch, E.C., 1984, Marginal basins of the southwestern Pacific and the preservation and recognition of their ancient analogues: a review: *in*, *Marginal Basin Geology*, B.P. Kokelaar and M.F. Howells, eds., Geological Society Special Publication 16, pp. 97-109.
- Le Maitre, R.W., (ed.), 1989, *A Classification of Igneous Rocks and Glossary of Terms*, Blackwell, Oxford, 193 pp.
- Lynch, J.V.G., 1990, Geology of the Fire Lake Group, southeast Coast Mountains, British Columbia: Current Research, Part E; Geological Survey of Canada Paper 90-1E, pp. 197-204.
- Lynch, J.V.G., 1991, Georgia Basin Project: stratigraphy and structure of Gambier Group rocks in the Howe Sound-Mamquam River area, southwest Coast Belt, British Columbia: *in* Current Research, Part A, Geological Survey of Canada, Paper 91-1A, pp. 49-57.
- Lynch, J.V.G., 1992, Deformation of Early Cretaceous volcanic arc assemblages, southern Coast Belt, British Columbia: *Canadian Journal of Earth Sciences*, vol. 29, pp. 2706-2721.
- MacLean, W.H., and Barrett, T.J., 1993, Lithogeochemical techniques using immobile elements: *Journal of Exploration Geochemistry*, vol. 48, pp. 109-133.
- Mahoney, J.B., 1992, Middle Jurassic stratigraphy of the Lillooet area, south-central British Columbia: Current Research, Part A; Geological Survey of Canada Paper 93-1A, pp. 243-248.
- Mahoney, J.B., 1993, Facies reconstructions in the Lower to Middle Jurassic Ladner Group, southern British Columbia: Current Research, Part A; Geological Survey of Canada Paper 93-1A, pp. 173-182.
- Mahoney, J.B., and Journeay, J.M., 1993, The Cayoosh assemblage, southwestern British Columbia: last vestige of the Bridge River ocean: Current Research, Part A; Geological Survey of Canada Paper 93-1A, pp. 235-244.
- Marquis, G., and Globerman, B.R., 1988, Northward motion of the Whitehorse trough: Paleomagnetic evidence from the Upper Cretaceous Carmacks Group: *Canadian Journal of Earth Sciences*, vol. 25, pp. 2005-2016.
- Marsaglia, K.M., Ingersoll, R.V., and Packer, B.M., 1992, Tectonic evolution of the Japanese Islands as reflected in modal compositions of Cenozoic forearc and backarc sand and sandstone: *Tectonics*, vol. 11, pp. 1028-1044.
- Maxon, J.A., Kleinspehn, K.L., Wynne, P.J., and Irving, E., 1993, Paleomagnetic evidence for northward displacement of western British Columbia from the mid-Cretaceous Silverquick fluvial deposits and Powell Creek volcanics, northern Tyaughton basin; *Geological Society of America Abstracts with Programs*, vol. 25, no. 5, p. 116.
- McClelland, W.C., Gehrels, G.E., and Saleeby, J.B., 1992, Upper Jurassic-Lower Cretaceous basinal strata along the Cordilleran margin: implications for the accretionary history of the Alexander-Wrangelliza-Peninsular terrane: *Tectonics*.
- McCulloch, M.T., and Gamble, J.A., 1991, Geochemical and geodynamical constraints on subduction zone magmatism: *Earth and Planetary Science Letters*, vol. 102, pp. 358-374.
- McGroder, M.F., 1991, Reconciliation of two-sided thrusting, burial metamorphism, and diachronous uplift in the Cascades of Washington and British Columbia: *Geological Society of America Bulletin*, vol. 103, pp. 189-209.

- McKinley, S., Thompson, J.F.H., Barrett, T.J., Sherlock, R.L., Allen, R., and Burge, C., 1994, Geology of the Seneca Property, southwestern British Columbia (92H/5W): British Columbia Ministry of Energy, Mines, and Petroleum Resources Geological Fieldwork 1993, Paper 1994-1
- McLennan, S.M., and Hemming, S., 1992, Samarium/neodymium elemental and isotopic systematics in sedimentary rocks: *Geochimica et Cosmochimica Acta*, vol. 56., pp. 887-898.
- McLennan, S.M., and Taylor, S.R., 1991, Sedimentary rocks and crustal evolution: tectonic setting and secular trends: *The Journal of Geology*, vol. 99, pp. 1-21.
- McLennan, S.M., McCulloch, M.T., Taylor, S.R., and Maynard, J.B., 1989, Effects of sedimentary sorting on neodymium isotopes in deep sea turbidites: *Nature*, vol. 337, pp. 547-549.
- McLennan, S.M., Taylor, S.R., McCulloch, M.T., and Maynard, J.B., 1990, Geochemical and Nd-Sr isotopic composition of deep-sea turbidites: Crustal evolution and plate tectonic associations: *Geochimica et Cosmochimica Acta*, vol. 54, pp. 2015-2050.
- Michard, A., Gurriet, P., Soudant, M., and Albarede, F., 1985, Nd isotopes in French Phanerozoic shales: external vs. internal aspects of crustal evolution: *Geochimica et Cosmochimica Acta*, vol. 49, pp. 601-610.
- McMillan, W.J., 1974, Stratigraphic section from the Jurassic Ashcroft Formation and Triassic Nicola Group contiguous to the Guichon Batholith: British Columbia Department of Mines and Petroleum Resources, Geological Fieldwork 1974, pp. 27-34.
- McMillan, W.J., 1976, Geology and genesis of the Highland Valley ore deposits and the Guichon Batholith: in Porphyry deposits of the Canadian Cordillera, A. Southerland-Brown, ed., Canadian Institute of Mining and Metallurgy Special Volume 15, pp. 85-104.
- Meschede, M., 1986, A method of discriminating between different types of mid-ocean ridge basalts and continental tholeiites with the Nb-Zr-Y diagram: *Chemical Geology*, vol. 56, pp. 207-218.
- Miller, R.B., Whitney, D.L., and Geary, E.E., 1993, Tectono-stratigraphic terranes and the metamorphic history of the northeastern part of the crystalline core of the North Cascades: evidence from the Twisp Valley Schist: *Canadian Journal of Earth Sciences*, vol. 30, pp. 1306-1323.
- Miller, R.G., and O'Nions, R.K., 1984, The provenance and crustal residence ages of British sediments in relation to palaeogeographic reconstructions: *Earth and Planetary Science Letters*, vol. 68, pp. 459-470.
- Miller, R.G., O'Nions, R.K., Hamilton, P.J., and Welin, E., 1986, Crustal residence ages of clastic sediments, orogeny and crustal evolution: *Chemical Geology*, vol. 57, pp. 87-99.
- Misch, P., 1966, Tectonic evolution of the North Cascades of Washington State; Canadian Institute of Mining and Metals, Special Volume 8, pp. 101-148.
- Monger, J.W.H., 1966, A stratigraphy and structure of the type area of the Chilliwack Group, southwestern British Columbia: unpublished Ph.D. thesis, University of British Columbia, Vancouver, British Columbia.
- Monger, J.W.H., 1970, Hope Map-Area, West Half, British Columbia: Geological Survey of Canada, Paper 69-47., 75 p.
- Monger, J.W.H., 1982, Geology of Ashcroft map area, southwestern British Columbia: Current Research, part A, Geological Survey of Canada, vol. Paper 82-1A, pp. 293-297.

- Monger, J.W.H., 1985, Structural evolution of the southwestern Intermontane Belt, Ashcroft and Hope map areas, British Columbia: Current Research, Part A, Geological Survey of Canada, Paper 85-1A, pp. 349-358.
- Monger, J.W.H., 1989, Overview of Cordilleran geology, in Ricketts, B.D., ed., Western Canada Sedimentary Basin: Canadian Society of Petroleum Geologists, pp. 9-32.
- Monger, J.W.H., 1991, Correlation of Settler Schist with Darrington Phyllite and Shuksan Greenschist and its tectonic implications, Coast and Cascade Mountains, British Columbia and Washington: Canadian Journal of Earth Sciences, vol. 28, pp. 447-458.
- Monger, J.W.H., 1991, Georgia Basin Project: structural evolution of parts of southern Insular and southwestern Coast belts, British Columbia: in, Current Research, Part A, Geological Survey of Canada, Paper 91-1A, pp. 219-228.
- Monger, J.W.H., 1993, Georgia Basin Project - geology of Vancouver map area, British Columbia: in, Current Research, Part A, Geological Survey of Canada, Paper 93-1A, pp. 149-157.
- Monger, J.H.W., Price, R.A., and Templeman-Kluit, D.J., 1982, Tectonic accretion and the origin of the two major metamorphic and plutonic belts in the Canadian Cordillera: Geology, vol. 10, pp. 70-75.
- Monger, J.W.H., and McNichol, V., 1993, New U-Pb dates from the southwestern Coast Belt; in Current Research, Geological Survey of Canada.
- Monger, J.W.H., and McMillan, W.J., 1989, Geology, Ashcroft, British Columbia: Geological Survey of Canada Map 42-1989, sheet 1, scale 1:250,000.
- Monger, J.W.H., Wheeler, J.O., Tipper, H.W., Gabrielse, H., Harms, T., Struik, L.C., Campbell, R.B., Dodds, C.J., Gehrels, G.E., and O'Brien, J., 1991, Cordilleran terranes: in Upper Devonian to Middle Jurassic assemblages, Chapter 8 of Geology of the Cordilleran Orogen in Canada, H. Gabrielse and C.J. Yorath, eds.; Geological Survey of Canada, Geology of Canada, no. 4, pp. 281-327.
- Monger, J.W.H., and Journeay, J.M., 1992, Guide to the geology and tectonic evolution of the southern Coast Belt: proceedings to Penrose Conference on the "Tectonic evolution of the Coast Mountains orogen", 97 p.
- Monger, J.W.H., and Journeay, J.M., 1994, Basement geology and tectonic evolution of the Vancouver region, southwestern British Columbia: in prep.
- Morris, P.A., and Kagami, H., 1989, Nd and Sr isotope systematics of Miocene to Holocene volcanic rocks from Southwest Japan: volcanism since the opening of the Japan Sea: Earth and Planetary Science Letters, vol. 92, pp. 335-346.
- Mortimer, N., 1987, The Nicola Group: Late Triassic and Early Jurassic subduction related volcanism in British Columbia: Canadian Journal of Earth Sciences, vol. 24, pp. 2521-2536.
- Mortimer, N., Van der Heyden, P., Armstrong, R.L., and Harkal, J., 1990, U-Pb and K-Ar dates related to the timing of magmatism and deformation in the Cache Creek terrane and Quesnellia, southern British Columbia: Canadian Journal of Earth Sciences, vol. 27, pp. 117-123.
- Muller, J.E., 1977, Evolution of the Pacific margin, Vancouver Island and adjacent regions; Canadian Journal of Earth Sciences, vol. 14, pp. 766-778.
- Muller, J.E., Northcote, K.E., and Carlisle, D., 1974, Geology and mineral deposits of Alert Bay-Cape Scott map area, Vancouver Island, British Columbia: Geological Survey of Canada Paper 74-8, 77 p.

- Muller, J.E., Cameron, B.E.B., and Northcote, K.E., 1981, Geology and mineral deposits of Nootka Sound map area (92E), Vancouver Island, British Columbia: Geological Survey of Canada Paper 80-16, 53 p.
- Murphy, D.C., Gerasimoff, M., van der Heyden, P., Parrish, R.R., Klepacki, D.W., McMillan, W., Struik, L.C., and Gabites, J., 1994, New geochronological constraints on Jurassic deformation of the western edge of North America, southern Canadian Cordillera: Geological Society of America Memoir.
- Mustard, J.F., 1983, The geology of the Mount Brew area, Lillooet, British Columbia: unpublished B.Sc. thesis, University of British Columbia, Vancouver, British Columbia.
- Mustard, P.S., 1994, The Upper Cretaceous Nanaimo Group, Georgia Basin, British Columbia: in Monger, J.W.H., Vancouver Geology, Geological Survey of Canada Bulletin, in press
- Nakamura, E., Campbell, I.H. and McCulloch, M.T., 1989, Chemical geodynamics in a back arc region around the Sea of Japan: Implications for the Genesis of Alkaline Basalts in Japan, Korea, and China: *Journal of Geophysical Research*, vol. 94, no. B4, pp. 4634-4654.
- Nakamura, E., McCulloch, M.T., and Campbell, I.H., 1990, Chemical geodynamics in the back-arc region of Japan based on trace element and Sr-Nd isotopic compositions: *Tectonophysics*, vol. 174, pp. 207-233.
- Nance, W.B., and Taylor, S.R., 1976, Rare earth element patterns and crustal evolution-I. Australian post-Archean sedimentary rocks: *Geochimica et Cosmochimica Acta*, vol. 40, pp. 1539-1551.
- Nelson, J.L., 1979, The western margin of the Coast Plutonic Complex on Hardwicke and West Thurlow Islands: *Canadian Journal of Earth Sciences*, vol. 16, pp. 1166-1175.
- Nelson, B.K., and Depaolo, D.J., 1988, Comparison of isotopic and petrographic provenance indicators in sediments from Tertiary continental basins of New Mexico: *Journal of Sedimentary Petrology*, vol. 58, no. 2, pp. 348-357.
- Nixon, G.T., Hammack, J.L., Hamilton, J.V., and Jennings, H., 1993a, Preliminary geology of the Mahatta Creek map area, northern Vancouver Island (92L/5): *in* Geological Fieldwork 1992, Grant B., and Newell, J.M., eds., B.C. Ministry of Energy, Mines and Petroleum Resources, Paper 1993-1 pp. 17-35.
- Nixon, G.T., Hammack, J.L., Koyanagi, V.M., Payie, G.J., Panteleyev, A., Massey, N.W.D., Hamilton, J.V., and Haggart, J.W., 1994, Preliminary geology of the Quatsino-Port McNeill map areas, northern Vancouver Island (92L/12, 11): *in* Geological Fieldwork 1993, Grant B., and Newell, J.M., eds., B.C. Ministry of Energy, Mines and Petroleum Resources, Paper 1994-1, pp. 63-85.
- Nohda, S., and Wasserburg, G.J., 1981, Nd and Sr isotopic study of volcanic rocks from Japan: *Earth and Planetary Science Letters*, vol. 52, pp. 264-276.
- O'Brien, J.A., 1986, Jurassic stratigraphy of the Methow Trough, southwestern British Columbia, *in* Current Research Part A, Geological Survey of Canada Paper 86-1B, pp. 749-756.
- O'Brien, J.A., 1985, Biostratigraphic studies of Sinemurian (Lower Jurassic) Tyaughton Group strata in Taseko Lakes map area, British Columbia; unpublished B.Sc. thesis, University of British Columbia, Vancouver, British Columbia, 75 p.
- O'Brien, J., 1987, Jurassic biostratigraphy and evolution of the Methow Trough, southwestern British Columbia: unpublished M.Sc. thesis, University of Arizona, Tucson, Arizona, 150 p.

- O'Brien, J.A., Gehrels, G.E., and Monger, J.W.H., 1992, U-Pb geochronology of plutonic clasts from conglomerates in the Ladner and Jackass Mountain groups and the Peninsula Formation, southwestern British Columbia: *Current Research, Part A*; Geological Survey of Canada, Paper 91-1A, pp. 209-214.
- O'Leary, D.M., Clowes, R.M., and Ellis, R.M., 1993, Crustal velocity structure in the southern Coast Belt, British Columbia: *Canadian Journal of Earth Sciences*, vol. 30, no. 12, pp. 2389-2403.
- O'Nions, E.R., Carter, S.R., Evenson, N.M., and Hamilton, P.J., 1979, Geochemical and cosmochemical applications of Nd isotope analysis: *Annual Review of Earth and Planetary Sciences*, vol. 7, pp. 11-38.
- Okada, H., 1980, Calcareous nannofossils from Deep Sea Drilling Project Sites 442 through 446; in deVries Klein, G., Kobayashi, K., et al., 1980, *Initial Reports of the Deep Sea Drilling Project*, v. 58: Washington (U.S. Government Printing Office), pp. 549-566.
- Orchard, M., 1984, Pennsylvanian, Permian, and Triassic conodonts from the Cache Creek Group, Cache Creek, southern British Columbia: *Current Research, Part B*, Geological Survey of Canada Paper 84-1B, pp. 197-206.
- Park, C.-H., Tamaki, K., and Kobayashi, K., 1990, Age-depth correlation of the Philippine Sea back-arc basins and other marginal basins in the world: *Tectonophysics*, vol. 181, pp. 351-371.
- Parrish, R.R., Carr, S.D., and Parkinson, D.L., 1985, Metamorphic complexes and extensional tectonics, southern Shuswap Complex, southeastern British Columbia: *in* *Field Guides to Geology and Mineral Deposits in the Southern Canadian Cordillera*, Geological Society of America, Cordilleran Section Meeting, pp. 12.1-12.15.
- Parrish, R.R., and Carr, S.D., 1986, Extensional tectonics of southeastern British Columbia: new data and interpretations: *Geological Association of Canada, Annual Meeting, Program with Abstracts*, p. 112.
- Parrish, R.R., Carr, S.D., and Parkinson, D.L., 1988, Eocene extensional tectonics and geochronology of the southern Omineca Belt, British Columbia and Washington: *Tectonics*, vol. 7, pp. 181-212.
- Parrish, R.R., and McNicoll, V.J., 1991, U-Pb age determinations from the southern Vancouver Island area, British Columbia: *Geological Survey of Canada Paper 91-2*, pp. 187-191.
- Parrish, R.R., and Monger, J.W.H., 1992, New U-Pb from southwestern British Columbia: *in* *Radiogenic age and isotope studies, Report 5*; Geological Survey of Canada, Paper 91-2, pp. 87-108.
- Pearce, J.A., 1982, Trace element characteristics of lavas from destructive plate margins: *in* *Andesites: Orogenic andesites and related rocks*, Thorpe, R.S., ed., pp. 525-548.
- Pearce, J.A., and Cann, J.R., 1973, Tectonic setting of basic volcanic rocks determined using trace element analysis: *Earth and Planetary Science Letters*, vol. 19, pp. 290-300.
- Pearce, J.A., and Norry, M.J., 1979, Petrogenetic implications of Ti, Zr, Y and Nb variations in volcanic rocks: *Contributions to Mineralogy and Petrology*, vol. 69, pp. 33-47.
- Pearson, D.E., 1973, Harrison, Lucky Jim: *in* *Geology, Exploration, and Mining in British Columbia*, British Columbia Department of Mines and Petroleum Resources, pp. 125-128.
- Piegras, D.J., and Wasserburg, G.J., 1980, Neodymium isotopic variations in seawater: *Earth and Planetary Science Letters*, vol. 50, pp. 128-138.

- Potter, C.J., 1983, Geology of the Bridge River Complex, Southern Shulaps Range, British Columbia: A record of Mesozoic convergent tectonics: unpublished Ph.D. thesis, University of Washington, Seattle, Washington, 192 p.
- Potter, C.J., 1986, Origin, accretion, and postaccretionary evolution of the Bridge River terrane, southwest British Columbia: *Tectonics*, vol. 5, no. 7, pp. 1027-1041.
- Poulton, T.P., 1980, Trigoniid bivalves from the Bajocian (middle Jurassic) rocks of central Oregon: in *Current Research, Part A*, Geological Survey of Canada, Paper 80-1A, pp. 187-196.
- Poulton, T.P., and Tipper, H.W., 1991, Aalenian ammonites and strata of Western Canada: *Geological Survey of Canada Bulletin* 411, 71 p.
- Poulton, T.P., 1994, Middle and Upper Jurassic macrofossil biostratigraphy, Taseko Lakes map area, British Columbia, Geological Survey of Canada Contribution Number ###, in press.
- Project, B.V.S., 1981, Basaltic Volcanism on the Terrestrial Planets: Pergamon, 1286 p.
- Rangin, C., and Silver, E., 1990, Geological setting of the Celebes and Sulu Seas: in, Rangin, C., Silver, E., von Breymann, M.T., et al., *Proceedings of the Ocean Drilling Program, Initial Reports*, vol. 124, pp. 35-42.
- Rangin, C., Silver, E., von Breymann, M.T., et al., 1990, *Proceedings of the Ocean Drilling Program, Initial Reports*, vol. 124: College Station, Texas (Ocean Drilling Program).
- Ray, G.E., 1986, The Hozameen fault system and related Coquihalla Serpentine Belt of southwestern British Columbia: *Canadian Journal of Earth Sciences*, vol. 23, pp. 1022-1041.
- Ray, G.E., 1990, The geology and mineralization of the Coquihalla gold belt and Hozameen fault system, southwestern British Columbia: *Ministry of Energy, Mines, and Petroleum Resources Bulletin* 79, 97 p.
- Rea, D.K., 1993, Geologic records in deep sea muds: *GSA Today*, vol. 3, no. 8, p. 207-210.
- Rea, D.K., Leinen, M., and Janecek, T.R., 1985, Geologic approach to the long-term history of atmospheric circulation: *Science*, vol. 227, pp. 721-725.
- Read, P.B., 1993, Geology of northeast Taseko Lakes map area, southwestern British Columbia: *Current Research, Part A*; Geological Survey of Canada Paper 93-1A, pp. 159-166.
- Riddell, J.M., Schiarizza, P., Gaba, R.G., Caira, N., and Findlay, A., 1993, Geology and mineral occurrences of the Mount Tatlow area (92O/5,6, and 12): *Geological Fieldwork 1992*, British Columbia Ministry of Energy, Mines, and Petroleum Resources Paper 1993-1, pp. 37-52.
- Roddick, J.A., 1965, Vancouver North, Coquitlam, and Pitt Lake map-areas, British Columbia, with special emphasis on the evolution of the plutonic rocks: *Geological Survey of Canada Memoir* 335, 276 p.
- Roddick, J.A., and Woodsworth, G.J., 1979, Geology of the Vancouver west half and mainland part of Alberni map areas: *Geological Survey of Canada Open-File* 611.
- Rusmore, M.E., 1987, Geology of the Cadwallader Group and the Intermontane-Insular superterrane boundary, southwestern British Columbia: *Canadian Journal of Earth Science*, vol. 24, pp. 2279-2291.
- Rusmore, M.E., Potter, C. J., and Umhoefer, P.J., 1988, Middle Jurassic terrane accretion along the western edge of the Intermontane Superterrane, southwestern British Columbia: *Geology*, vol. 16, pp. 891-894.

- Rusmore, M.E., and Woodsworth, G.J., 1990, Distribution and tectonic significance of Upper Triassic terranes in the eastern Coast Mountains and adjacent Intermontane Belt, British Columbia: *Canadian Journal of Earth Science*, vol. 28, pp. 532-541.
- Rusmore, M.E., and Woodsworth, G.J., 1991, Coast plutonic complex: A mid-Cretaceous contractional orogen: *Geology*, vol. 19, pp. 941-944.
- Saleeby, J.B., and Busby-Spera, C., 1992, Early Mesozoic tectonic evolution of the western U.S. Cordillera, in, Buchfiel, B.C., Lipman, P.W., and Zoback, M.L., eds., *The Cordilleran Orogen: Conterminous U.S.*: Geological Society of America, *The Geology of North America*, v. G-3, Boulder, Colorado: pp. 107-203.
- Samson, S.D., Patchett, P.J., Gehrels, G.E., and Anderson, R.G., 1990, Nd and Sr isotopic characterization of the Wrangellia terrane and implications for crustal growth of the Canadian Cordillera: *Journal of Geology*, vol. 98, pp. 749-762.
- Samson, S.D., McClelland, W.C., Patchett, P.J., Gehrels, G.E., and Anderson, R.G., 1991, Evidence from neodymium isotopes for mantle contribution to Phanerozoic crustal genesis in the Canadian Cordillera: *Nature*, vol. 337, pp. 705-709.
- Saunders, A.D., and Tarney, J., 1984, Geochemical characteristics of basaltic volcanism within back-arc basins, in, *Marginal Basin Geology*, B.P. Kokelaar and M.F. Howells, eds., Geological Society Special Publication 16: pp. 59-74.
- Schiarizza, P., Gaba, R.G., Glover, J.K., and Garver, J.I., 1989, Geology and mineral occurrences of the Tyaughton Creek area (92 O/2, 92 J/15): Geological fieldwork 1988. British Columbia Ministry of Energy, Mines and Petroleum Resources, vol. Paper 1989-1, pp. 115-130.
- Schiarizza, P., Gaba, R.G., Coleman, M., Garver, J.I., and Glover, J.K., 1990, Geology and mineral occurrences of the Yalakom River area: Geological Fieldwork 1989 Paper 1990-1, pp. 53-72.
- Shannon, K.R., 1981, The Cache Creek Group and contiguous rocks near Cache Creek, British Columbia: Current Research, Part A, Geological Survey of Canada Paper 81-1A, pp. 217-221.
- Shervais, J.W., 1982, Ti-V plots and the petrogenesis of modern and ophiolitic lavas: *Earth and Planetary Science Letters*, vol. 57, pp. 101-118.
- Shirey, S.B., and Hanson, G.N., 1986, Mantle heterogeneity and crustal recycling in Archean granite-greenstone belts: Evidence for Nd isotopes and trace elements in the Rainy Lake area, Superior Province, Ontario, Canada: *Geochimica et Cosmochimica Acta*, vol. 50, pp. 2631-2651.
- Silberling, N.L., and Jones, D. L., 1987, Lithotectonic terrane maps of the North American Cordillera; United States Geological Survey Miscellaneous Field Studies Maps 1874A, B, C, D, scale 1:2,500,000.
- Singer, A., and Muller, G., 1983, Diagenesis in argillaceous sediments, in, *Diagenesis in Sediments and Sedimentary Rocks*, 2, G.V. Chilingar and Larsen, G., eds., Elsevier Scientific Publishing Company, Amsterdam, 572 p.
- Smith, P.L., 1983, The Pliensbachian ammonite, *Dayiceras dayiceroides* and Early Jurassic paleogeography: *Canadian Journal of Earth Sciences*, vol. 20, pp. 86-91.
- Smith, P.L., and Briden, J.C., 1977, Mesozoic and Cenozoic paleocontinental maps: Cambridge University Press, pp. 1-63.

- Smith, P.L., and Tipper, H.W., 1986, Plate tectonics and Paleobiogeography: Early Jurassic (Pliensbachian) Endemism and diversity: *Palaios*, vol. 1, no. pp. 399-412.
- Steiger, R.H., and Jager, E., 1977, Subcommittee on Geochronology: Convention on the use of decay constants in geo- and cosmo-chronology: *Earth and Planetary Science Letters*, vol. 36, pp. 359-362.
- Stoffel, K.L., Joseph, N.L., Waggoner, S.Z., Gulick, C.W., Korosec, M.A., and Bunning, B.A., 1991, Geologic Map of Washington -Northeast Quadrant: Washington Division of Geology and Earth Resources Geologic Map GM-39, 36 p., scale 1:250,000.
- Sun, S.S., 1982. Chemical composition and origin of the Earth's primitive mantle: *Geochim. Cosmochim. Acta*, vol. 46, pp.179-192.
- Sun, S., and Nesbitt, R.W., 1979, Geochemical characteristics of mid-ocean ridge basalts: *Earth and Planetary Science Letters*, vol. 44, pp. 119-138.
- Tabor, R.W., 1994, Late Mesozoic and possible early Tertiary accretion in western Washington state: the Helena-Haystack melange' and the Darrington-Devils Mountain fault zone: *Geological Survey of America Bulletin*, vol. 106, no. 2, pp. 217-232.
- Tamaki, K, Pisciotto, K, Allan, J, et al., 1990, Proceedings of the Ocean Drilling Program, Initial Reports, Vol. 127, College Station, Texas (Ocean Drilling Program).
- Tarney, J., Saunders, A.D., Mathey, D.P., Wood, D.A., and Marsh, N.G., 1981, Geochemical aspects of back-arc spreading in the Scotia Sea and western Pacific: *Philosophical Transactions of the Royal Society of London*, vol. A300, pp. 263-285.
- Tatsumoto, M., and Nakamura, Y., 1991, DUPAL anomaly in the Sea of Japan: Pb, Nd, and Sr isotopic variations at the eastern Eurasian continental margin: *Geochimica et Cosmochimica Acta*, vol. 55, pp. 3697-3708.
- Taylor, D.G., Callomon, J.H., Hall, R., Smith, P.L., Tipper, H.W., and Westermann, G.E.G., 1984, Jurassic ammonite biogeography of western North America: the tectonic implications; in, Westermann, G.E.G, ed., *Jurassic-Cretaceous Biochronology and Paleogeography of North America*, Geological Association of Canada Special Paper 27: pp. 121-141.
- Taylor, S.R., and McLennan, S.M., 1985, *The Continental crust: its composition and evolution*: Blackwell Scientific Publications, Oxford, England, 312 p.
- Theriault, R.J., 1990, Methods for Rb-Sr and Sm-Nd isotopic analysis at the geochronology laboratory, Geological Survey of Canada, in, *Radiogenic age and isotope studies: Report 3*, Geological Survey of Canada Paper 89-2, p. 3-7.
- Thompson, R.I., 1972, Harrison, Lucky Jim: in, *Geology, Exploration, and Mining in British Columbia*, British Columbia Department of Mines and Petroleum Resources, pp. 102-114.
- Thompson, R.N., Morrison, M.A., Hendry, G.L., and Parry, S.J., 1984, An assessment of the relative roles of crust and mantle in magma genesis: an elemental approach: *Philosophical Transactions of the Royal Society of London*, vol. A310, pp. 549-590.
- Thorkelson, D.J., and Smith, A.D., 1989, Arc and intraplate volcanism in the Spences Bridge Group: implications for Cretaceous tectonics in the Canadian Cordillera: *Geology*, vol. 17, pp. 1093-1096.

- Thorkelson, D.J., and Rouse, G.E., 1989, Revised stratigraphic nomenclature and age determinations for mid-Cretaceous volcanic rocks in southwestern British Columbia: *Canadian Journal of Earth Sciences*, vol. 26, pp. 2016-2031.
- Tipper, H.W., 1969, Mesozoic and Cenozoic geology of the northeast part of the Mount Waddington map area (92 N), Coast District, British Columbia: Geological Survey of Canada, Paper 68-33.
- Tipper, H.W., 1978, Taseko Lakes (92 O) map area: Geological Survey of Canada, Open file 534.
- Tipper, H.W., 1984, The allochthonous Jurassic to Lower Cretaceous terranes of the Canadian Cordillera and their relation to correlative strata on the craton; in Westerman, G.E.G., ed., *Jurassic-Cretaceous biochronology and biogeography of North America*; Geological Association of Canada Special Paper 27, pp. 113-120.
- Tipper, H.W., Smith, P.L., Cameron, B.E.B., Carter, E.S., Jakobs, G.K., and Johns, M.J., 1991, Biostratigraphy of the Lower Jurassic formations of the Queen Charlotte Islands, British Columbia: *in*, *Evolution and Hydrocarbon Potential of the Queen Charlotte Basin, British Columbia*, Geological Survey of Canada, Paper 90-10, pp. 203-235.
- Travers, W.B., 1978, Overturned Nicola and Ashcroft strata and their relation to the Cache Creek Group, Southwestern Intermontane Belt, British Columbia: *Canadian Journal of Earth Science*, vol. 15, pp. 99-116.
- Travers, W.B., 1982, Possible large-scale overthrusting near Ashcroft, British Columbia: Implications for petroleum prospecting: *Bulletin of Canadian Petroleum Geology*, vol. 30, no. 1, pp. 1-8.
- Trettin, H.P., 1961, Geology of the Fraser river valley between Lillooet and Big Bar Creek; Ph.D. thesis, University of British Columbia, Vancouver, British Columbia: 109 p.
- Trettin, H.P., 1980, Permian rocks of the Cache Creek Group in the Marble Range, Clinton area, British Columbia: Geological Survey of Canada Paper 79-17, 17 p.
- Umhoefer, P.J., 1990, Stratigraphy and tectonic setting of the upper part of the Cadwallader terrane, southwestern British Columbia: *Canadian Journal of Earth Sciences*, vol. 27, pp. 702-711.
- Umhoefer, P.J., 1989, Stratigraphy and tectonic setting of the upper Cadwallader terrane and overlying Relay Mountain Group, and the Cretaceous to Eocene structural evolution of the eastern Tyaughton basin, British Columbia: Ph.D. thesis, University of Washington, Seattle.
- Umhoefer, P.J., and Tipper, H.W., 1991, Stratigraphic studies of Lower to Middle Jurassic rocks in the Mt. Waddington and Taseko Lakes map areas, British Columbia; *Current Research, Part A*; Geological Survey of Canada Paper 91-1A, pp. 75-78.
- Urabe, T., Scott, S.D., and Hattori, K., 1983, A comparison of footwall-rocks alteration and geothermal systems beneath some Japanese and Canadian volcanogenic massive sulfide deposits: *Economic Geology*, Monograph 5, pp. 345-364.
- van der Heyden, P., 1992, A Middle Jurassic to Early Tertiary Andean-Sierran arc model for the Coast Belt of British Columbia: *Tectonics*, vol. 11, no. 1, pp. 82-97.
- Varsek, J.L., Cook, F.A., Clowes, R.M., Journeay, J.M., Monger, J.W.H., Parrish, R.R., Kanasevich, E.R., Spencer, C.S., 1993, Lithoprobe crustal reflection structure of the southern Canadian Cordillera 2: Coast Mountain transect: *Tectonics*, vol. 12, no. 2, pp. 334-360.

- Volpe, A.M., Macdougall, J.D., and Hawkins, J.W., 1988, Lau Basin basalts (LBB): trace element and Sr-Nd isotopic evidence for heterogeneity in backarc basin mantle: *Earth and Planetary Science Letters*, vol. 90, pp. 174-186.
- Walker, R.G., 1975, Generalized facies models for resedimented conglomerates of turbidite association: *Geological Society of America Bulletin*, vol. 86, pp. 737-748.
- Walker, R.G., 1978, Deep-water sandstone facies and ancient submarine fans: models for exploration from stratigraphic traps: *American Association of Petroleum Geologists Bulletin*, vol. 62, pp. 932-966.
- Wheeler, J.O., and McFeeley, P., 1992, Tectonic assemblage map of the Canadian Cordillera and adjacent parts of the United States of America: *Geological Survey of Canada, Open File 1565*, scale 1: 2 000 000.
- White, W.M., and Patchett, J., 1984, Hf-Nd-Sr isotopes and incompatible element abundances in island arcs: implications for magma origins and crust-mantle evolution: *Earth and Planetary Science Letters*, vol. 67, pp. 167-185.
- Wilson, M., 1988, *Igneous Petrogenesis: a global tectonic approach*: Unwin and Hyman, London, 466 p.
- Winchester, J.A., and Floyd, P.A., 1977. Geochemical discrimination of different magma series and their differentiation products using immobile elements: *Chemical Geology*, vol. 20, pp. 325-343.
- Wood, D.A., Joron, J-L, Treuil, M., 1979, A re-appraisal of the use of trace elements to classify and discriminate between magma series erupted in different tectonic settings: *Earth and Planetary Science Letters*, vol. 45, pp. 326-336.
- Wood, D.A., 1980, The application of a Th-Hf-Ta diagram to problems of tectonomagmatic classification and to establishing the nature of crustal contamination of basaltic lavas of the British Tertiary volcanic province, *Earth and Planetary Science Letters*, vol. 50, pp.11-30.
- Woodsworth, G.J., Anderson, R.G., and Armstrong, R.L., 1991, Plutonic regimes: Chapter 15 of *Geology of the Cordilleran Orogen in Canada*, H.Gabrielse and C.J. Yorath, eds.; *Geological Survey of Canada, Geology of Canada*, no. 4, pp. 491-531.
- Yorath, C.J., 1991, Upper Jurassic to Paleogene assemblages, Chapter 9 in *Geology of the Cordilleran Orogen in Canada*, H. Gabrielse and C.J. Yorath, eds., *Geological Survey of Canada, Geology of Canada*, no. 4, p. 329-371.
- Zelt, B.C., Ellis, R.M., and Clowes, R.M., 1993, Crustal velocity structure in the eastern Insular and southernmost Coast belts, Canadian Cordillera: *Canadian Journal of Earth Sciences*, vol. 30, pp. 1014-1027.
- Zhang, Z.M., 1985, Tectonostratigraphic terranes of Japan that bear on the tectonics of Mainland Asia: in Howell, D.G., ed., *Tectonostratigraphic Terranes of the Circum-Pacific Region*; *Circum-Pacific Council for Energy and Mineral Resources Earth Science Series*, Number 1, pp. 409-420.
- Zhigang, X., 1990, Mesozoic volcanism and volcanogenic iron-ore deposits in eastern China: *Geological Society of America Special Paper 237*, 46 p.

APPENDIX A

ISOTOPIC PROCEDURES

Sample Selection

This study tests the validity of correlating fine-grained sedimentary sequences via radiogenic isotopic "fingerprinting". Samples were selected from relatively thick sequences (>.5 m) of fine-grained fine siltstone and shale. Thin (< 3 cm) siltstone and shale intervals are commonly associated with individual turbidite deposition, so care was taken to select samples from fine-grained intervals of at least .5-1.5 m in thickness. These thick intervals are assumed to reflect prolonged periods of hemipelagic and pelagic deposition, and to therefore represent a good sampling of the average composition of the source area. Sample selection criteria include: 1) reliability of age determination and stratigraphic position within unit being analyzed; 2) homogeneity of the unit, with thin, coarse grained laminae avoided; 3) freshness of the exposure, with care taken to avoid heavily weathered, iron staining and other evidence of fluid migration. The recessive weathering character of most fine-grained strata made fresh sample acquisition difficult at times, and care was taken to sample only fresh bedrock, devoid of regolith contamination.

Sample Preparation:

Approximately 1-2 kg of sample was collected at each sample locality. The samples were cleaned of surficial alteration by hand picking and chiseling. The samples were crushed to gravel size (< .5 cm) in a Bico Chipmunk jaw crusher, and ground to <80 mesh in a Rocklab chrome steel ring grinder. Approximately 15-20 grams of each sample was powdered to < 200 mesh in a mechanical agate mortar. Separate splits were used for each type (Sr, Nd) of chemical dissolution.

Strontium Chemistry

Strontium isotopic analysis requires separate determination of isotopic composition ($^{87}\text{Sr}/^{86}\text{Sr}$) and rubidium (Rb) and strontium (Sr) concentration. Isotopic composition is determined through mass spectrometry, and isotopic concentration is determined by X-ray fluorescence techniques.

Approximately 0.15-0.20 grams of sample powder are dissolved in 5 ml hydrofluoric acid (HF) in an open beaker on a warm hot plate (100-150°C) in a laminar flow hood to dissolve silicates. The sample is then dried to a crystal mush at 200°C, followed by a second addition of HF. The sample is dried to a crystal mush following the addition of a small amount of perchloric acid, and 3-5 ml of 3.0 N Quartz HCl is added. The

cooled sample is centrifuged to separate insoluble residue from dissolved sample solution. The sample solution is loaded immediately onto cation exchange columns (20 cm long, 1 cm diameter, loaded with 200-400 mesh AG 50W-X8 resin). The sample solution is eluted slowly in with small aliquot of 3.0 N HCl, and approximately 10 ml of Sr solution is collected following calibration values. The Sr solution is dried down, and loaded onto a single tantalum filament on an emission base of tantalum oxide. Strontium isotopic measurements are carried out on a VG Isomass 54R mass spectrometer in single collector mode. Measured ratios have been normalized to a $^{86}\text{Sr}/^{88}\text{Sr}$ ratio of 0.1194. Precision of a single $^{87}\text{Sr}/^{86}\text{Sr}$ ratio was less than 0.00002 (1 sigma). Replicate analyses of National Bureau of Standards standard SrCO_3 (SRM987) during the course of this study give a value 0.000078 below the $^{87}\text{Sr}/^{86}\text{Sr}$ reference value of 0.710190 ± 0.000020 ($n=16$). Regressions are calculated using the technique of York (1967), with decay constants from the International Union of Geological Sciences Subcommission on Geochronology (Steiger and Jager, 1977).

Rubidium and strontium concentrations were determined by X-ray fluorescence. Approximately 4 grams of sample were pressed into a pressed powder pellet with a boric acid backing. Multiple measurements were performed on a Philips PW 1410 X-ray spectroscope, using U.S. Geological Survey rock standards for calibration. Rb/Sr ratios have a precision of < 2%, and concentrations have a precision of < 5%.

Neodymium Chemistry

Neodymium analyses require the separate analysis of neodymium isotopic composition and neodymium and samarium isotopic concentration. Isotopic composition is determined by mass spectrometry on an unspiked sample; isotopic concentration is determined using isotopic dilution techniques.

Isotopic concentration sample preparation consists of a 12 hour warm (150°C) predissolution of approximately 30 milligrams of sample in 5 ml HF in an open Krogh-type dissolution bomb. The dried crystal mush is then reconstituted in 5 ml HF and ~1 ml nitric acid (HNO_3), and placed in a Krogh-type dissolution bomb and a steel pressure jacket, and heated for 5 days at 190°C . This ensures complete dissolution of refractory phases. The sample solution is then dried in a laminar flow hood, and redissolved in 20 ml 6N HCl. The HCl and sample solution is heated covered on a hot plate (100°C) for 2 hours and dried down. The sample precipitate is then reconstituted in ~3 ml 3 N HCl, centrifuged, and immediately loaded onto cation exchange columns. Group rare earth elements (REE) are separated on large cation exchange columns (20 cm long, 1 cm diameter, using 200-400 mesh AG 50W-X8 resin) using 3 N HCl to elute Sr, followed by 6 N HCl to strip Group REE. The REE sample solution is dried down, reconstituted in .125 N HCl, and loaded onto small Teflon columns containing 2 cm Teflon powder treated with HDEHP (DI-2-ethylhexyl orthophosphoric acid) and capped with 0.5 cm anion exchange resin. Nd is separated from Group REE using .25 N HCl as elutant.

The concentrated Nd was loaded onto a double Re filament assembly, and analyzed on a Finnigan MAT 261 multicollector mass spectrometer in static collection mode at the Geochronology Laboratory of the Geological Survey of Canada (Theriault, 1990). Measured ratios are normalized to a $^{146}\text{Nd}/^{144}\text{Nd}$ ratio of 0.7219 (O'Nions, et al., 1979), and corrected to La Jolla Nd standard $^{143}\text{Nd}/^{144}\text{Nd}=0.511850$. Blanks for Sm and Nd are approximately 0.1 and 2 ng, respectively.

Isotopic concentration analyses involves the use of a mixed ^{149}Sm - ^{150}Nd spike, added before dissolution. Dissolution procedure is the same as outlined above, until the final addition of HCl, where 5 N HCl is added in place of the 3 N HCl used in isotopic concentration analyses. The samples are centrifuged, then loaded immediately onto 3 N HCl large cation exchange columns, and eluted with 5 N HCl. The dried REE residue was loaded onto double Re filaments, and run on a modified VG-Isomass 54R mass spectrometer at The University of British Columbia. Replicate analyses of international USGS standards (BCR, BHVO, BIR) and samples from the current study demonstrate a concentration reproducibility of < 5%, and ratio reproducibility of < 2%

WHOLE ROCK GEOCHEMISTRY

Each stratigraphic succession under investigation contains a proportion of primary volcanic lava flows and pyroclastic material. Whole rock geochemistry was performed on volcanic rocks from each succession, to facilitate comparison between successions, and to provide information on the petrogenesis and tectonic setting of each unit.

Sample selection

Sample selection was limited to rocks of intermediate composition (andesite and dacite). Exposures were examined for definitive evidence of flow features (flow banding, basal autoclastic breccia, pillow structures) prior to sampling. Dike rocks were sampled in the Harrison Lake Formation, to allow geochemical comparison with inferred comagmatic lava flows. Primary pyroclastic rocks (lapilli tuffs) were sampled in the Cayoosh assemblage, due to a lack of true flow rocks. In all cases, exposures were examined for evidence of alteration, including silicification, veining, and fractures, and the freshest possible rock was sampled.

Sample preparation:

Approximately 2-3 kg of each sample was collected from each locality. Samples were broken down by

hand, and surficial alteration was removed by hand picking and chiseling. Samples were crushed to gravel size (.5-1 cm) in a Bico Chipmunk jaw crusher, and ground to fine powder (< 100 mesh) in a Rocklab chrome steel ring grinder. Each sample was passed through a sample splitter, and a split was shaken on a mechanical arm to ensure sample heterogeneity.

Geochemical analytical procedure:

Whole rock major and minor element geochemistry was performed on each sample by XRAL Laboratories, Ontario, Canada. Major elements were determined by X-ray fluorescence spectrometry on a fused disc prepared from a 2 gram sample split, with a lower reporting limit of 0.01%. Minor and trace elements were determined by X-ray fluorescence spectrometry using a pressed pellet technique, with the lower detection limit for most elements < 5 ppm.

Rare earth element geochemistry was performed at the University of Saskatchewan at Saskatoon in the laboratory of Dr. Kurt Kyser. Concentrations were measured by an Elan-5000 Induced Coupled Plasma Mass Spectrometer. Analytical precision was < 5% (K. Kyser, personal communication, 1992).

APPENDIX B

ANALYTICAL PRECISION

Precision of isotopic analyses was estimated through replicate analyses of unknown samples throughout this study. The following is a list of duplicate analyses of samples from both the Ocean Drilling Program sample set and the southern Canadian Cordillera sample set.

Analytical accuracy of isotopic analyses was determined through analysis of international standards (U.S. Geological Survey standards BCR, BHVO, BIR). Replicate analyses of international standards are listed following the replicate section.

| Duplicate analyses of 87Sr/86Sr ratios +/- | | Mean | St Dev | %error | | | | | | | | |
|--|-----------|--------------------|---------|--------|---------|--------|--------|---------|--------|---------|--------|--------|
| Sample | 87Sr/86Sr | | | | | | | | | | | |
| 443-11-2 | 0.71140 | | | | | | | | | | | |
| | 0.71125 | | | | | | | | | | | |
| 443-12-2 | 0.71204 | 0.71132 | 0.00011 | 0.015 | | | | | | | | |
| | 0.71201 | 0.71203 | 0.00002 | 0.002 | | | | | | | | |
| 443-15-2 | 0.71293 | | | | | | | | | | | |
| | 0.71381 | | | | | | | | | | | |
| 443-15-2A | 0.71020 | 0.71337 | 0.00062 | 0.087 | | | | | | | | |
| | 0.71490 | acid leech residue | | | | | | | | | | |
| 443-15-4 | 0.71459 | | | | | | | | | | | |
| | 0.71417 | | | | | | | | | | | |
| 444-4-5 | 0.71521 | 0.71465 | 0.00052 | 0.073 | | | | | | | | |
| | 0.70950 | | | | | | | | | | | |
| 444-5-4 | 0.70997 | 0.70973 | 0.00033 | 0.047 | | | | | | | | |
| | 0.71253 | | | | | | | | | | | |
| 444-6-1 | 0.71262 | 0.71258 | 0.00006 | 0.009 | | | | | | | | |
| | 0.71113 | | | | | | | | | | | |
| 444-7-1 | 0.71114 | 0.71114 | 0.00001 | 0.001 | | | | | | | | |
| | 0.71187 | | | | | | | | | | | |
| 444-8-1 | 0.71221 | | | | | | | | | | | |
| | 0.71232 | 0.71213 | 0.00024 | 0.033 | | | | | | | | |
| 444-7-6 | 0.70781 | | | | | | | | | | | |
| | 0.70759 | 0.70770 | 0.00016 | 0.022 | | | | | | | | |
| 444-1-1A | 0.71084 | | | | | | | | | | | |
| | 0.71096 | 0.71090 | 0.00008 | 0.012 | | | | | | | | |
| 795-14-5 | 0.71134 | | | | | | | | | | | |
| | 0.71146 | 0.71140 | 0.00008 | 0.012 | | | | | | | | |
| 795-14-5 | 0.70904 | | | | | | | | | | | |
| | 0.70888 | | | | | | | | | | | |
| 795-14-5 | 0.70901 | | | | | | | | | | | |
| | 0.70903 | 0.70899 | 0.00007 | 0.010 | | | | | | | | |
| Neodymium Concentration Duplicates | | | | | | | | | | | | |
| Sample | Sm | Nd | 147/144 | SmMean | SmStDev | %error | NdMean | NdStDev | %error | 147/144 | StDev | %error |
| 442-12-5 | 5.11 | 25.16 | 0.1227 | | | | | | | | | |
| | 5.13 | 25.79 | 0.1207 | 5.12 | 0.02 | 0.384 | 25.47 | 0.45 | 1.8 | 0.1217 | 0.0014 | 1.2 |
| 442-15-2 | 5.80 | 26.49 | 0.1316 | | | | | | | | | |
| | 5.67 | 28.12 | 0.1225 | 5.74 | 0.09 | 1.611 | 27.30 | 1.15 | 4.2 | 0.1270 | 0.0065 | 5.1 |

259

| | | | | | | | | | | | | |
|-------------------------------------|----------|----------|--------|----------|----------|--------|----------|----------|-------|----------|----------|-------|
| 443-12-2 | 4.71 | 23.70 | 0.1200 | 4.76 | 0.07 | 1.549 | 23.96 | 0.37 | 1.5 | 0.1201 | 0.0000 | 0.0 |
| 443-15-4 | 4.81 | 24.22 | 0.1201 | 0.512183 | 0.000029 | 0.006 | 0.512272 | 0.000013 | 0.002 | 0.512295 | 0.000030 | 0.006 |
| | 6.61 | 33.51 | 0.1187 | | | | | | | | | |
| | 6.28 | 29.09 | 0.1306 | | | | | | | | | |
| | 6.11 | 28.57 | 0.1294 | | | | | | | | | |
| 443-16-2 | 5.69 | 29.39 | 0.1171 | 0.512253 | 0.000033 | 0.006 | 0.512410 | 0.000063 | 0.012 | 0.512525 | 0.000050 | 0.010 |
| | 6.13 | 29.39 | 0.1263 | | | | | | | | | |
| | 5.38 | 27.13 | 0.1199 | | | | | | | | | |
| | 5.60 | 27.69 | 0.1226 | | | | | | | | | |
| 444-7-6 | 6.08 | 28.56 | 0.1286 | 0.512272 | 0.000013 | 0.002 | 0.512295 | 0.000030 | 0.006 | 0.512253 | 0.000015 | -7.06 |
| | 6.37 | 29.68 | 0.1297 | | | | | | | | | |
| 795-7-5 | 4.76 | 20.87 | 0.1376 | 0.512316 | 0.000005 | -6.28 | 0.512273 | 0.000023 | -7.12 | 0.512276 | 0.000010 | -7.96 |
| | 4.56 | 20.87 | 0.1318 | | | | | | | | | |
| 795-9-1 | 5.46 | 25.37 | 0.1302 | 0.512281 | 0.000008 | -6.96 | 0.512263 | 0.000007 | -7.32 | 0.512365 | 0.000014 | -5.23 |
| | 5.88 | 25.34 | 0.1403 | | | | | | | | | |
| Neodymium Isotopic Ratio Duplicates | | | | | | | | | | | | |
| Sample | 143/144 | +/- | eNd | Mean | St Dev | %error | | | | | | |
| 443-15-4 | 0.512176 | 0.000013 | -8.93 | 0.512183 | 0.000029 | 0.006 | 0.512272 | 0.000013 | 0.002 | 0.512295 | 0.000030 | 0.006 |
| | 0.512159 | 0.000014 | -9.34 | | | | | | | | | |
| 444-5-4 | 0.512215 | 0.000003 | -8.25 | 0.512272 | 0.000013 | 0.002 | 0.512272 | 0.000013 | 0.002 | 0.512295 | 0.000030 | 0.006 |
| | 0.512281 | 0.000008 | -6.96 | | | | | | | | | |
| 444-1-1A | 0.512263 | 0.000007 | -7.32 | 0.512316 | 0.000005 | -6.28 | 0.512273 | 0.000023 | -7.12 | 0.512276 | 0.000010 | -7.96 |
| | 0.512316 | 0.000005 | -6.28 | | | | | | | | | |
| 444-7-6 | 0.512273 | 0.000010 | -7.12 | 0.512273 | 0.000007 | -7.32 | 0.512263 | 0.000007 | -7.32 | 0.512365 | 0.000014 | -5.23 |
| | 0.512230 | 0.000010 | -7.12 | | | | | | | | | |
| 795-14-5 | 0.512276 | 0.000015 | -7.06 | 0.512276 | 0.000015 | -7.06 | 0.512276 | 0.000015 | -7.06 | 0.512365 | 0.000014 | -5.23 |
| | 0.512365 | 0.000014 | -5.23 | | | | | | | | | |
| 444-8-1 | 0.512454 | 0.000005 | -3.59 | 0.512454 | 0.000005 | -3.59 | 0.512410 | 0.000063 | 0.012 | 0.512560 | 0.000008 | -1.52 |
| | 0.512560 | 0.000008 | -1.52 | | | | | | | | | |
| | 0.512489 | 0.000027 | -2.91 | 0.512489 | 0.000027 | -2.91 | 0.512525 | 0.000050 | 0.010 | 0.512560 | 0.000008 | -1.52 |
| | | | | | | | | | | | | |

Table B.1 (cont.) - Duplicate Analyses for Ocean Drilling Program sediments.

| Jurassic Isotopic Analyses - Analytical Precision | | | | | | |
|---|---------------------------------|---------|-----------------|------------------|--------|------|
| Sample | $^{87}\text{Sr}/^{86}\text{Sr}$ | +/- | Mean | (n=14) St Dev | %error | |
| 20JBM91 | 0.70877 | 0.00002 | | | | |
| | 0.70847 | 0.00002 | 0.70862 | 0.00021 | | 0.03 |
| 151Jbm92 | 0.70524 | 0.00004 | | | | |
| | 0.70516 | 0.00001 | 0.70520 | 0.00006 | | 0.01 |
| 171Jbm92 | 0.70479 | 0.00001 | | | | |
| | 0.70479 | 0.00002 | 0.70479 | 0.00000 | | 0.00 |
| 176Jbm92 | 0.70492 | 0.00002 | | | | |
| | 0.70468 | 0.00002 | 0.70480 | 0.00017 | | 0.02 |
| 273JBM92 | 0.70863 | 0.00002 | | | | |
| | 0.70849 | 0.00002 | 0.70856 | 0.00010 | | 0.01 |
| 279JBM92 | 0.70765 | 0.00002 | | | | |
| | 0.70757 | 0.00003 | 0.70761 | 0.00006 | | 0.01 |
| 287Jbm92 | 0.70502 | 0.00001 | | | | |
| | 0.70512 | 0.00002 | 0.70507 | 0.00007 | | 0.01 |
| 291Jbm92 | 0.70670 | 0.00001 | | | | |
| | 0.70665 | 0.00002 | 0.70668 | 0.00003 | | 0.00 |
| 319Jbm92 | 0.70460 | 0.00002 | | | | |
| | 0.70446 | 0.00001 | 0.70528 | 0.00163 | | 0.23 |
| 323JBM92 | 0.70869 | 0.00002 | | | | |
| | 0.70868 | 0.00002 | 0.70453 | 0.00010 | | 0.01 |
| 329Jbm92 | 0.70418 | 0.00002 | | | | |
| | 0.70406 | 0.00002 | 0.70412 | 0.00008 | | 0.01 |
| 334JBM92 | 0.70501 | 0.00002 | | | | |
| | 0.70503 | 0.00002 | 0.70502 | 0.00001 | | 0.00 |
| 346JBM92 | 0.70429 | 0.00002 | | | | |
| | 0.70433 | 0.00001 | 0.70431 | 0.00003 | | 0.00 |
| 92-177 | 0.70503 | 0.00002 | | | | |
| | 0.70496 | 0.00002 | 0.70499 | 0.00005 | | 0.01 |
| Neodymium Concentration Duplicate Analyses | | | | | | |
| Sample | Sm | Nd | $^{147}/^{144}$ | (n=5) SmMean | %error | |
| 235JBM91 | 2.21 | 9.47 | 0.1408 | | | |
| | 2.35 | 9.56 | 0.1485 | 2.28 | 0.10 | 3.8 |
| 102JBM92 | 2.27 | 8.93 | 0.1531 | | | |
| | 2.56 | 9.42 | 0.1662 | 2.41 | 0.21 | 5.8 |
| 129JBM92 | 3.78 | 13.16 | 0.1748 | | | |
| | 3.64 | 13.27 | 0.1655 | | | |
| | 3.62 | 13.16 | 0.1664 | 3.68 | 0.09 | 3.1 |
| 356JBM92 | 5.48 | 17.12 | 0.1935 | | | |
| | 5.44 | 17.41 | 0.1887 | 5.46 | 0.03 | 1.8 |

Table B.2 - Duplicate Analyses for Jurassic rocks.

| Sample | Neodymium Isotopic Ratio - Duplicate Analyses | | | | (n=6) StDev | %error |
|----------|---|----------|----------|----------|----------------|--------|
| | ¹⁴³ / ₁₄₄ | +/- | Mean | | | |
| 203JBM91 | 0.512837 | 0.000018 | | | | |
| | 0.512533 | 0.000054 | 0.512685 | 0.000215 | | 0.042 |
| 209JBM91 | 0.512822 | 0.000009 | | | | |
| | 0.512883 | 0.000030 | 0.512828 | 0.000008 | | 0.002 |
| 234JBM91 | 0.512838 | 0.000010 | | | | |
| | 0.512814 | 0.000003 | 0.512826 | 0.000017 | | 0.003 |
| 142jbm92 | 0.512826 | 0.000004 | | | | |
| | 0.512814 | 0.000010 | 0.512820 | 0.000008 | | 0.002 |
| 22jbm93 | 0.512886 | 0.000004 | | | | |
| | 0.512870 | 0.000007 | 0.512878 | 0.000011 | | 0.002 |
| 90jbm93 | 0.512897 | 0.000012 | | | | |
| | 0.512869 | 0.000023 | 0.512883 | 0.000020 | | 0.004 |

Table B.2 (cont.) - Duplicate Analyses for Jurassic rocks.

Isotopic Concentration Lab Standard Runs

BCR

| | | | | | | | |
|-------|--------|------|---------|-------|---------|--------|--------|
| given | | 6.58 | 0.14 | 28.79 | 0.89 | 0.1379 | |
| | Feb-89 | 7.53 | 0.01 | 32.84 | 0.08 | 0.1386 | 0.0005 |
| | Nov-90 | 7.58 | 0.01 | 32.42 | 0.01 | 0.1413 | 0.0002 |
| | Feb-93 | 6.79 | 0.02 | 29.24 | 0.01 | 0.1402 | 0.0004 |
| | Feb-93 | 7.28 | 0.13 | 30.16 | 0.00 | 0.1460 | 0.0026 |
| | %=4.9 | | %=5.5 | | %=2.3 | | |
| | | | 93%=2.1 | | 93%=2.8 | | |

BHVO

| | | | | | | | |
|--|--------|------|-------|-------|--------|--------|--------|
| | Jan-92 | 6.24 | 0.02 | 25.39 | 0.01 | 0.1488 | 0.0063 |
| | Jan-92 | 6.40 | 0.02 | 25.79 | 0.02 | 0.1502 | 0.0005 |
| | Jan-93 | 6.23 | 0.01 | 25.62 | 0.04 | 0.1470 | 0.0002 |
| | %=1.6 | | %=.78 | | %=1.07 | | |

BIR

| | | | | | | | |
|--|--------|------|-------|------|-------|--------|--------|
| | Dec-93 | 1.15 | 0.00 | 2.61 | 0.00 | 0.2654 | 0.0001 |
| | Dec-93 | 1.08 | 0.00 | 2.40 | 0.00 | 0.2731 | 0.0002 |
| | Jan-93 | | | | | | |
| | %=3.9 | | %=5.9 | | %=2.0 | | |

143/144 Standard Runs

BHVO

| | | | |
|--|--------|----------|----------|
| | Jun-93 | 0.513026 | 0.000029 |
| | Jul-93 | 0.513016 | 0.000017 |
| | %=.01 | | |

BIR

| | | | |
|--|--------|----------|----------|
| | | 0.513036 | 0.000019 |
| | Jul-93 | 0.513154 | 0.000039 |
| | May-93 | 0.512703 | 0.000026 |
| | %=.05 | | |

Table B.3 - International Standards.

APPENDIX C

SAMPLE LOCATIONS

KEY TO TABLE ABBREVIATIONS:

HS - Hand sample - all hand samples are stored at the Geological Survey of Canada, Vancouver.

TS - Thin section - all thin sections and rock chips are stored at the Geological Survey of Canada, Vancouver

ISO - Isotopic sample

CHEM - Geochemical Sample

PAL - Paleontology

SAMPLE LOCATION LIST

| SAMPLE # | FORMATION | ROCK TYPE | NORTHING | EASTING | HS | TS | ISO | CHEM | PAL |
|-------------------------|--------------|----------------|----------|---------|----|----|-----|------|-----|
| Harrison Terrane | | | | | | | | | |
| Harrison Lake Formation | | | | | | | | | |
| Celia Cove Member | | | | | | | | | |
| 87JBM92 | Celia Cove | cgl/ss | 585300 | 5466100 | x | x | | | |
| 88JBM92 | Celia Cove | chert cgl | 585600 | 5465600 | x | | | | |
| 89JBM92 | Celia Cove | feld ss | 585700 | 5465600 | x | x | | | |
| 90JBM92 | Celia Cove | med arkose | 585700 | 5465600 | x | x | | | |
| 91JBM92 | Celia Cove | chert cgl | 585700 | 5465600 | x | | | | |
| 92JBM92 | Celia Cove | volc cgl | 585700 | 5465600 | x | | | | |
| 93JBM92 | Celia Cove | bioclasts | 585700 | 5465600 | x | | | | |
| 94JBM92 | Celia Cove | cgl | 585700 | 5465600 | x | | | | |
| 95JBM92 | Celia Cove | chert lith ss | 586000 | 5465500 | x | x | | | |
| 96JBM92 | Celia Cove | siltstone | 586000 | 5465500 | | | x | | |
| 128JBM92 | Celia Cove | crse ss | 584600 | 5466200 | x | x | | | |
| 138JBM92 | Celia Cove | cgl | 583900 | 5468000 | x | x | | | |
| Francis Lake Member | | | | | | | | | |
| 97JBM92 | Francis Lake | fine ss | 586000 | 5465500 | x | x | | | |
| 98JBM92 | Francis Lake | mudstone | 586100 | 5465400 | | | | | x |
| 99JBM92 | Francis Lake | crse lith ss | 586100 | 5465400 | x | x | | | |
| 100JBM92 | Francis Lake | cgl | 586100 | 5465400 | x | x | | | |
| 101JBM92 | Francis Lake | sod breccia | 586100 | 5465400 | x | x | | | |
| 102JBM92 | Francis Lake | mudstone | 586100 | 5465400 | | | x | | |
| 103JBM92 | Francis Lake | frag tuff | 586100 | 5465400 | x | x | | | |
| 104JBM92 | Francis Lake | tuff siltstone | 586300 | 5465300 | x | x | | | |
| 105JBM92 | Francis Lake | xtal tuff | 586500 | 5465100 | x | x | | | |
| 106JBM92 | Francis Lake | lith xtal tuff | 586500 | 5465000 | x | x | | | |
| 107JBM92 | Francis Lake | tuff | 586600 | 5464900 | x | x | | | |
| 108JBM92 | Francis Lake | tuff siltstone | 586600 | 5464800 | x | x | | | |
| 109JBM92 | Francis Lake | crse ss | 586600 | 5464800 | x | x | | | |
| 110JBM92 | Francis Lake | tuff | 586600 | 5464500 | x | x | | | |
| 111JBM92 | Francis Lake | amyg lava | 586600 | 5464500 | x | x | | | |
| 112JBM92 | Francis Lake | ss | 586600 | 5464500 | x | x | | | |
| 129JBM92 | Francis Lake | silt/mudstone | 584900 | 5465900 | | | x | | |
| 130JBM92 | Francis Lake | fine ss | 584900 | 5465950 | x | x | | | |
| 131JBM92 | Francis Lake | shale | 584950 | 5465800 | | | x | | |
| 132JBM92 | Francis Lake | fine ss | 584975 | 5465700 | x | x | | | |
| 133JBM92 | Francis Lake | tuff ss | 584000 | 5465600 | x | x | | x? | |
| 134JBM92 | Francis Lake | tuff ss | 584500 | 5465600 | x | x | | | |
| 135JBM92 | Francis Lake | crse ss | 584400 | 5465400 | x | x | | | |
| 136JBM92 | Francis Lake | mudstone | 584500 | 5464900 | | | x | | |
| 137JBM92 | Francis Lake | tuff | 584200 | 5464900 | x | x | | | |
| 143JBM92 | Francis Lake | mudstone | 584200 | 5464600 | | | x | | |
| Weaver Lake Member | | | | | | | | | |
| 113JBM92 | Weaver Lake | andste lava | 586900 | 5463900 | x | x | | | |
| 114JBM92 | Weaver Lake | rhy | 584700 | 5469500 | x | x | | | |
| 115JBM92 | Weaver Lake | rhy | 584400 | 5470500 | x | x | | x | |
| 117JBM92 | Weaver Lake | bndd rhy tuff | 584100 | 5471300 | x | x | | | |
| 118JBM92 | Weaver Lake | crse ss | 583900 | 5472300 | x | x | | | |
| 120JBM92 | Weaver Lake | ss/silt | 583900 | 5474200 | x | x | | | |
| 122JBM92 | Weaver Lake | columnar rhy | 584100 | 5474800 | x | x | | x? | |
| 123JBM92 | Weaver Lake | dacite lava | 578200 | 5479000 | | | | x? | |
| 124JBM92 | Weaver Lake | siltstone | 578400 | 5478600 | | | x | x | |
| 125JBM92 | Weaver Lake | siltstone | 578400 | 5478600 | | | | | x |
| 126JBM92 | Weaver Lake | ss w/ wood | 578400 | 5478600 | x | x | | | |
| 127JBM92 | Weaver Lake | ss w/ wood | 578400 | 5478600 | x | | | | |
| 140JBM92 | Weaver Lake | lam ss | 583400 | 5464600 | x | x | | | |
| 144JBM92 | Weaver Lake | rhy | 587400 | 5469100 | x | x | | | |
| 145JBM92 | Weaver Lake | rhy | 587400 | 5468800 | x | x | | | |
| 146JBM92 | Weaver Lake | crse ss | 587900 | 5468700 | x | x | | | |
| 147JBM92 | Weaver Lake | dacite | 588100 | 5467600 | x | x | | | |
| 148JBM92 | Weaver Lake | dacite lava | 580200 | 5475900 | x | x | | | |
| 149JBM92 | Weaver Lake | andste dike | 578900 | 5475000 | x | x | | | |

SAMPLE LOCATION LIST

| SAMPLE # | FORMATION | ROCK TYPE | NORTHING | EASTING | HS | TS | ISO | CHEM | PAL |
|-----------------------------------|-------------|------------------|----------|---------|----|----|-----|------|-----|
| 150JBM92 | Weaver Lake | silic dac lava | 578300 | 5478400 | x | x | | x | |
| 288JBM92 | Weaver Lake | sandy silt | 578600 | 5480100 | | | x | | |
| 289JBM92 | Weaver Lake | gran cgl | 578400 | 5480100 | x | x | | | |
| 290JBM92 | Weaver Lake | dacite lava | 578000 | 5480300 | x | x | | | |
| 298JBM92 | Weaver Lake | gran cgl | 577800 | 5479900 | x | x | | | |
| 299JBM92 | Weaver Lake | lith ss | 577800 | 5479900 | x | x | | | |
| 300JBM92 | Weaver Lake | tuff | 574800 | 5478600 | x | x | | | |
| 301JBM92 | Weaver Lake | lam ss | 575100 | 5479500 | x | x | | | |
| 302JBM92 | Weaver Lake | dike | 575100 | 5479500 | x | x | | | |
| 303JBM92 | Weaver Lake | pum ss | 576300 | 5480300 | x | x | | | |
| 304JBM92 | Weaver Lake | lith ss | 576400 | 5480500 | x | x | | | |
| 305JBM92 | Weaver Lake | dike | 575700 | 5479600 | x | x | | | |
| 306JBM92 | Weaver Lake | rhy flow | 584700 | 5469300 | | | | x | |
| Echo Island Member | | | | | | | | | |
| 70JBM92 | Echo Island | tuff/cgl | 582900 | 5461400 | x | x | | | |
| 71JBM92 | Echo Island | tuff | 581200 | 5461000 | x | x | | | |
| 72JBM92 | Echo Island | tuff breccia | 581200 | 5461000 | x | x | | | |
| 73JBM92 | Echo Island | crse ss | 581400 | 5460900 | x | x | | | |
| 74JBM92 | Echo Island | fine ss | 581400 | 5460900 | x | x | | | |
| 75JBM92 | Echo Island | tuff breccia | 581500 | 5460900 | x | x | | | |
| 76JBM92 | Echo Island | weld tuff | 581600 | 5460900 | x | x | | | |
| 152JBM92 | Echo Island | silic. siltstone | 588400 | 5465900 | x | x | | | |
| 153JBM92 | Echo Island | crse ss | 588400 | 5465900 | x | x | | | |
| 154JBM92 | Echo Island | ss | 588500 | 5465800 | x | x | | | |
| 155JBM92 | Echo Island | bio tuff/ ss | 588500 | 5465800 | x | x | | | |
| 156JBM92 | Echo Island | ss | 588600 | 5465800 | x | x | | | |
| 157JBM92 | Echo Island | green ss | 588800 | 5465900 | x | x | | | |
| 281JBM92 | Echo Island | lapilli tuff | 588700 | 5465800 | x | x | | | |
| 282JBM92 | Echo Island | lapilli tuff | 588800 | 5465800 | x | x | | | |
| 283JBM92 | Echo Island | lith ss | 588800 | 5465800 | x | x | | | |
| 284JBM92 | Echo Island | vitric tuff | 588900 | 5465800 | x | x | | | |
| 285JBM92 | Echo Island | lith ss | 589000 | 5465800 | x | x | | | |
| 286JBM92 | Echo Island | tuff | 589100 | 5465800 | x | x | | | |
| 292JBM92 | Echo Island | rhy flow | 586700 | 5467700 | | | | x | |
| 293JBM92 | Echo Island | rhy flow | 587400 | 5466900 | | | | z | |
| 294JBM92 | Echo Island | gran cgl w/clm | 582600 | 5461300 | x | | | | |
| 295JBM92 | Echo Island | lith ss | 582600 | 5461300 | x | x | | | |
| 296JBM92 | Echo Island | welded tuff | 583000 | 5461500 | x | x | | | |
| 26JBM93 | Echo Island | shale | | | | | x | | |
| Harrison Lake Formation Volcanics | | | | | | | | | |
| Weaver Lake Member | | | | | | | | | |
| 4JBM92 | Weaver Lake | andste | | | x | x | x | x | |
| 116JBM92 | Weaver Lake | dacite lava | 584300 | 5470800 | x | x | x | x | |
| 142JBM92 | Weaver Lake | andste | 584500 | 5464300 | x | x | x | x | |
| 151JBM92 | Weaver Lake | dacite lava col. | 578500 | 5473900 | x | x | x | x | |
| 287JBM92 | Weaver Lake | dacite | 578200 | 5479900 | | | x | x | |
| 291JBM92 | Weaver Lake | dacite | 577400 | 5480500 | | | x | x | |
| 307JBM92 | Weaver Lake | dacite flow | 578800 | 5462400 | | | x | x | |
| 12JBM93 | Weaver Lake | lava | 576500 | 5470400 | | | | x | |
| 13JBM93 | Weaver Lake | andste | 576379 | 5471310 | | | x | x | |
| 14JBM93 | Weaver Lake | andste | 573395 | 5472814 | | | x | x | |
| 15JBM93 | Weaver Lake | andste | 576359 | 5477055 | | | x | x | |
| 16JBM93 | Weaver Lake | weld tuff | | | x | | | | |
| 17JBM93 | Weaver Lake | andste | 576215 | 5475849 | | | x | x | |
| 18JBM93 | Weaver Lake | dacite py | | | x | x | | | |
| 19JBM93 | Weaver Lake | tuff breccia | | | x | | | | |
| 20JBM93 | Weaver Lake | xtal tuff | 579700 | 5477300 | x | x | | | |
| 21JBM93 | Weaver Lake | andste | 578366 | 5476126 | | | x | x | |
| 22JBM93 | Weaver Lake | andste | 577439 | 5474754 | | | x | x | |
| 23JBM93 | Weaver Lake | sed | | | x | | | | |
| 24JBM93 | Weaver Lake | ss | | | x | | | | |
| 25JBM93 | Weaver Lake | andste | 575420 | 5483806 | | | x | x | |

SAMPLE LOCATION LIST

| SAMPLE # | FORMATION | ROCK TYPE | NORTHING | EASTING | HS | TS | ISO | CHEM | PAL |
|-----------------------------------|---------------|----------------|----------|---------|----|----|-----|------|-----|
| Camp Cove Formation | | | | | | | | | |
| 77JBM92 | Camp Cove | andste | 585500 | 5465800 | x | | | | |
| 78JBM92 | Camp Cove | lith ss | 585400 | 5465900 | x | | | | |
| 79JBM92 | Camp Cove | dacite breccia | 585300 | 5466100 | x | | | | x |
| 80JBM92 | Camp Cove | chert | 585300 | 5466200 | x | | | | |
| 81JBM92 | Camp Cove | lith ss | 585000 | 5466600 | x | | | | |
| 82JBM92 | Camp Cove | alter volc | 584800 | 5467900 | x | | x | | |
| 83JBM92 | Camp Cove | silic lava | 584600 | 5468600 | x | | | | |
| 84JBM92 | Camp Cove | lava | 584900 | 5467400 | x | | | | |
| 85JBM92 | Camp Cove | thin chert | 585000 | 5467200 | x | | | | |
| 86JBM92 | Camp Cove | chert | 585300 | 5466200 | x | | | | |
| 139JBM92 | Camp Cove | arg | 583600 | 5467300 | | | x | | |
| Mysterious Creek Formation | | | | | | | | | |
| 297JBM92 | Mystery Creek | silt | 584300 | 5461000 | | | x | | |
| CADWALLADER TERRANE | | | | | | | | | |
| Last Creek Formation | | | | | | | | | |
| 145JBM91 | Last Creek | ss | 501200 | 5659100 | x | x | | | |
| 146JBM91 | Last Creek | ss | 501200 | 5659100 | x | x | | | |
| 147JBM91 | Last Creek | fossil | 501200 | 5659100 | x | x | | | |
| 148JBM91 | Last Creek | ss | 501200 | 5659100 | x | x | | | |
| 149JBM91 | Last Creek | cgl | 501200 | 5659100 | x | x | | | |
| 157JBM91 | Last Creek | | | | | | | | |
| 158JBM91 | Last Creek | ls | 502800 | 5659800 | | | x | | x |
| 159JBM91 | Last Creek | shale | 502800 | 5659800 | | | | | |
| 9071 | Last Creek | shale | 498200 | 5662700 | x | x | x | | |
| 9072 | Last Creek | sh/ss/cgl | 498000 | 5662300 | x | x | x | | |
| 9073 | Last Creek | sh/ss/cgl | 498100 | 5661950 | x | x | x | | |
| 9074 | Last Creek | sh/ss/cgl | 499200 | 5659300 | x | x | x | | |
| Hurley Formation | | | | | | | | | |
| 90JBM91 | Hurley | mudstone | 537800 | 5653500 | x | x | | | |
| 108JBM91 | Hurley | ss | 537800 | 5653500 | x | | | | |
| 130JBM91 | Hurley | ss | 587700 | 5599200 | | | | | |
| 134JBM91 | Hurley | silic tuff | 504900 | 5648400 | x | x | | | |
| 135JBM91 | Hurley | tuff breccia | 504900 | 5648400 | x | x | | | |
| 136JBM91 | Hurley | cgl | 504900 | 5648400 | x | x | | | |
| 137JBM91 | Hurley | ss | 505600 | 5648500 | x | x | | | |
| 138JBM91 | Hurley | reef ls | 506000 | 5648300 | x | | | | |
| 139JBM91 | Hurley | micr ss | 504900 | 5645700 | x | x | | | |
| 140JBM91 | Hurley | micr ss | 504900 | 5645700 | x | x | | | |
| 208JBM91 | Hurley | arg | 537800 | 5653400 | | | x | | |
| Tyaughton Group | | | | | | | | | |
| 141JBM91 | Tyaughton | ss/cgl | 500400 | 5659500 | x? | x? | | | |
| 142JBM91 | Tyaughton | ss | 500800 | 5659400 | x | x | | | |
| 143JBM91 | Tyaughton | ss | 500800 | 5659400 | x | x | | | |
| 144JBM91 | Tyaughton | fossil ss | 501000 | 5659400 | x? | | | | |
| Relay Mountain Group | | | | | | | | | |
| 150JBM92 | Relay Mtn. | siltstone | 503200 | 5667200 | x | x | | | |
| 151JBM91 | Relay Mtn. | ss | 503100 | 5667100 | x | x | | | |
| 152JBM91 | Relay Mtn. | ss | 503200 | 5667000 | x | x | | | |
| 153JBM91 | Relay Mtn. | fossil ss | 503000 | 5666900 | x | | | | |
| 154JBM91 | Relay Mtn. | shale | 503000 | 5666800 | | | x | | |
| BRIDGE RIVER TERRANE | | | | | | | | | |
| Cayoosh Assemblage | | | | | | | | | |
| 159JBM92 | Cayoosh | ss | 552200 | 5596700 | x | | x | | |
| 160JBM92 | Cayoosh | phyllite | 552200 | 5596700 | x | x | | | |
| 160bJBM92 | Cayoosh | arg | 552000 | 5596800 | x | x | x | | |
| 161JBM92 | Cayoosh | feld ss | 550700 | 5596400 | x | x | | | |

SAMPLE LOCATION LIST

| SAMPLE # | FORMATION | ROCK TYPE | NORTHING | EASTING | HS | TS | ISO | CHEM | PAL |
|------------------------------|--------------|-----------------|----------|---------|----|----|-----|------|-----|
| 163JBM92 | Bridge River | arg | 548900 | 5595200 | x | x | | x | |
| 166JBM92 | Cayoosh | ss | 549100 | 5595400 | | | x | | |
| 168JBM92 | Cayoosh | ls | 549300 | 5595600 | | | | | |
| 169JBM92 | Cayoosh | arg | 549300 | 5595600 | x | x | x | | |
| 170JBM92 | Cayoosh | thin bed tuff | 549300 | 5595700 | x | x | | | |
| 172JBM92 | Cayoosh | siltstone | 549400 | 5595700 | | | x | | |
| 173JBM92 | Cayoosh | silic siltone | 549400 | 5595800 | x | x | | | |
| 174JBM92 | Cayoosh | arg | 549400 | 5595800 | x | x | x | | |
| 175JBM92 | Cayoosh | pillow lava | 549500 | 5595700 | x | x | | | |
| 177JBM92 | Cayoosh | ss | 549500 | 5595000 | x | x | | | |
| 308JBM92 | Cayoosh | qtz ss | 552200 | 5591800 | x | x | | | |
| 309JBM92 | Cayoosh | ss | 552200 | 5591900 | x | x | | | |
| 310JBM92 | Cayoosh | tuff | 552300 | 5591900 | x | x | | | |
| 311JBM92 | Cayoosh | tuff ss | 552400 | 5592000 | x | x | | | |
| 312JBM92 | Cayoosh | lith ss | 552500 | 5592100 | x | x | | | |
| 313JBM92 | Cayoosh | ss | 552600 | 5592200 | x | x | | | |
| 314JBM92 | Cayoosh | ss | 552600 | 5592300 | | | x | | |
| 315JBM92 | Cayoosh | lith ss | 552700 | 5592300 | x? | x? | | | |
| 316JBM92 | Cayoosh | arg | 552700 | 5592400 | x? | | x | | |
| 317JBM92 | Cayoosh | dike | 552800 | 5592400 | | | x | | |
| 318JBM92 | Cayoosh | qtz ss | 552800 | 5592400 | | | x | | |
| 320JBM92 | Cayoosh | ss | 553000 | 5592800 | | | | | |
| 322JBM92 | Cayoosh | qtz tuff | 553200 | 5592800 | | | | | |
| 323JBM92 | Cayoosh | arg | 553500 | 5592900 | | | x | x | |
| 324JBM92 | Cayoosh | volc arg | 553400 | 5593000 | x | | | x | |
| CAY A | Cayoosh | arg | 552200 | 5591800 | | | x | x? | |
| CAY B | Cayoosh | arg | 552500 | 5592100 | | | x | x | |
| CAY C | Cayoosh | arg | 552700 | 5592400 | | | x | | |
| 44JBM93 | Cayoosh | shale | | | | | x | | |
| 45JBM93 | Cayoosh | ss | | | x | x | | | |
| 49JBM93 | Cayoosh | chert | | | x | | | | |
| 50JBM93 | Cayoosh | volc ss | | | x | x | | | |
| 51JBM93 | Cayoosh | volc ss | | | x | x | | | |
| 53JBM93 | Cayoosh | | | | | | | | |
| 54JBM93 | Cayoosh | | | | | | | | |
| 66JBM93 | Cayoosh | ss | | | x? | x? | | | |
| 67JBM93 | Cayoosh | fossil | | | x | | | | |
| 42JBM93 | Cayoosh 1 | ss | | | x | x | | | |
| 43JBM93 | Cayoosh 1 | ss | | | x | x | | | |
| 46JBM93 | Cayoosh 2 | metatuff | | | x | x | | | |
| 47JBM93 | Cayoosh 2 | | | | | | x? | | |
| 48JBM93 | Cayoosh 2 | siltstone/shale | | | | | x | | |
| 52JBM93 | Cayoosh 2 | shale | | | | | x | | |
| 65JBM93 | Cayoosh 3 | ss | | | x | x | | | |
| 60JBM93 | Cayoosh 4 | ss | | | x | x | | | |
| 61JBM93 | Cayoosh 4 | ss | | | x | | | | z |
| 62JBM93 | Cayoosh 4 | ss | | | x | x | | | |
| 55JBM93 | Cayoosh 5 | shale | | | | | | | |
| 56JBM93 | Cayoosh 5 | tuff | | | x? | x? | | | |
| 57JBM93 | Cayoosh 5 | siltstone/shale | | | ? | | | | |
| 58JBM93 | Cayoosh 5 | shale | | | ? | | | | |
| 59JBM93 | Cayoosh 5 | ss | | | ? | | | | |
| 63JBM93 | Gun Lake | siltstone/shale | | | | | x | x | |
| 68JBM93 | Cayoosh 6 | cgl | | | x | | | | |
| Cayoosh Assemblage Volcanics | | | | | | | | | |
| 171JBM92 | Cayoosh | tuff | 549300 | 5595700 | | | x | x | |
| 176JBM92 | Cayoosh | pillow lava | 549500 | 5595700 | | | x | x | |
| 319JBM92 | Cayoosh | tuff | 552800 | 5592500 | | | x | x | |
| 321JBM92 | Cayoosh | tuff | 553100 | 5592800 | | | x | x | |
| Bridge River Group | | | | | | | | | |
| 92-JS-5 | Bridge River | shale | 522000 | 5639450 | | | x | | |
| 92-JS-7 | Bridge River | shale | 527350 | 5638030 | | | x | | |
| 92-JS-10 | Bridge River | shale | 513400 | 5647430 | | | x | | |

SAMPLE LOCATION LIST

| SAMPLE # | FORMATION | ROCK TYPE | NORTHING | EASTING | HS | TS | ISO | CHEM | PAL |
|------------------------|----------------|----------------|------------|---------|----|----|-----|------|-----|
| 162JBM92 | Bridge River | chert | 548900 | 5595200 | | | | | x |
| 164JBM92 | Bridge River | tuff | 549000 | 5595400 | | | | | |
| 165JBM92 | Bridge River | crse metavolc | 549000 | 5595400 | | | | | |
| Taylor Creek Group | | | | | | | | | |
| Taylor Creek Formation | | | | | | | | | |
| 184JBM91 | Taylor Creek | cgl | 525300 | 5759100 | | | | | |
| 185JBM91 | Taylor Creek | ss | 525300 | 5759100 | | | | | |
| Lizard Formation | | | | | | | | | |
| 181JBM91 | Lizard Fm. | cgl | 491100 | 5658800 | | | | | |
| 182JBM91 | Lizard Fm. | cgl | 491100 | 5658800 | x | | | | |
| 183JBM91 | Lizard Fm. | cgl | 491100 | 5658800 | | | | | |
| 92-JS-23 | Lizard Fm. | shale | 513350 | 5647200 | x | x | x | | |
| 92-JS-25 | Lizard Fm. | shale | 513400 | 5647450 | | | x | | |
| Dash Formation | | | | | | | | | |
| 155JBM91 | Dash Fm. | cgl | 503400 | 5667500 | x | x | | | |
| 156JBM91 | Dash Fm. | ss | 503400 | 5667500 | | | | | |
| Paradise Formation | | | | | | | | | |
| 160JBM91 | Paradise Fm. | cgl | 500100 | 5663100 | x | x | | | |
| 161JBM91 | Paradise Fm. | ss | 500100 | 5663100 | | | | | |
| Elbow Pass Formation | | | | | | | | | |
| 162JBM91 | Elbow Pass | turb ss | 490300 | 5665200 | | | | | |
| 163JBM91 | Elbow Pass | ss | 490300 | 5665200 | | | | | |
| Powell Creek | | | | | | | | | |
| 164JBM91 | Powell Creek | volc | Battlement | Ridge | | | | | |
| 165JBM91 | Powell Creek | volc | Battlement | Ridge | | | | | |
| 166JBM91 | Powell Creek | volc | Battlement | Ridge | | | | | |
| 167JBM91 | Powell Creek | volc | Battlement | Ridge | | | | | |
| 168JBM91 | Powell Creek | volc | Battlement | Ridge | | | | | |
| 169JBM91 | Powell Creek | volc | Battlement | Ridge | | | | | |
| 170JBM91 | Powell Creek | volc | Battlement | Ridge | | | | | |
| 171JBM91 | Powell Creek | volc | Battlement | Ridge | | | | | |
| 172JBM91 | Powell Creek | volc | Battlement | Ridge | | | | | |
| 173JBM91 | Powell Creek | volc | Battlement | Ridge | | | | | |
| 174JBM91 | Powell Creek | volc | Battlement | Ridge | | | | | |
| 175JBM91 | Powell Creek | volc | Battlement | Ridge | | | | | |
| 176JBM91 | Powell Creek | volc | Battlement | Ridge | | | | | |
| 177JBM91 | Powell Creek | volc | Battlement | Ridge | | | | | |
| 177JBM91 | Powell Creek | volc | Battlement | Ridge | | | | | |
| Silverquik Formation | | | | | | | | | |
| 16JBM91 | Silverquik Fm. | pebbi mudstone | 528100 | 5698300 | x | x | | | |
| 19JBM91 | Silverquik Fm. | pebbi mudstone | 528900 | 5698500 | | | | | x |
| 35JBM91 | Silverquik Fm. | volc breccia | 529400 | 5698100 | | | | | x |
| 36JBM91 | Silverquik Fm. | ss | 529100 | 5697900 | x | x | | | |
| 37JBM91 | Silverquik Fm. | siltstone | 529100 | 5697900 | | | | | x |
| 38JBM91 | Silverquik Fm. | ss | 529000 | 5698200 | | | | | x |
| 39JBM91 | Silverquik Fm. | siltstone | 528900 | 5698300 | | | x | | |
| 40JBM91 | Silverquik Fm. | siltstone | 528700 | 5698300 | x | | | | |
| 41JBM91 | Silverquik Fm. | ss | 528600 | 5698500 | x | x | | | |
| 42JBM91 | Silverquik Fm. | siltstone | 528400 | 5698500 | x | x | | | |
| 43JBM91 | Silverquik Fm. | siltstone | 528300 | 5698600 | x | x | | | |
| 44JBM91 | Silverquik Fm. | gran cgl | 528300 | 5698600 | | | | | |
| 45JBM91 | Silverquik Fm. | chert cgl | 532600 | 5700500 | | | | | |
| 178JBM91 | Silverquik Fm. | cgl | 513100 | 5651100 | x | | | | |
| 179JBM91 | Silverquik Fm. | cgl | 513500 | 5651200 | x | | | | |
| 180JBM91 | Emsheeba | gran diorite | 495000 | 5653700 | x | | | | |
| | | | | | | | | | |
| | | | | | | | | | |

SAMPLE LOCATION LIST

| SAMPLE # | FORMATION | ROCK TYPE | NORTHING | EASTING | HS | TS | ISO | CHEM | PAL |
|-----------------------------|---------------|----------------|----------|---------|----|----|-----|------|-----|
| METHOW TERRANE | | | | | | | | | |
| Boston Bar Formation | | | | | | | | | |
| 20JBM91(4) | Jr seds | arg | 541500 | 5608100 | x | | | | |
| 32JBM91 | Jr seds | arg | 529000 | 5734900 | | | x | | |
| 33JBM91 | Jr seds | arg | 529000 | 5734900 | | | | | |
| 34JBM91 | Jr seds | arg | 529000 | 5734900 | | | x | | |
| 106JBM91 | Jr seds | arg | | | | | x | | |
| 107JBM91 | Jr seds | arg | | | x | x | | | |
| 203JBM91 | Toarcian | arg | 529000 | 5734900 | x | x | x | | |
| 35JBM92 | Boston Bar | arg w/ fossil | 628800 | 5483800 | x | x | | | |
| 36JBM92 | Boston Bar | lith wak | 628800 | 5483800 | | | x | | |
| 37JBM92 | Boston Bar | limy mudrock | 628700 | 5883800 | x | x | | | |
| 38JBM92 | Boston Bar | sandy turb | 628700 | 5883800 | ?? | x | | | |
| 39JBM92 | Boston Bar | sandy turb | 628700 | 5883800 | x | x | | | |
| 40JBM92 | Boston Bar | bio siltstone | 628600 | 5483800 | x | x | | | |
| 41JBM92 | Boston Bar | siltstone | 628600 | 5483800 | | | | | x |
| 42JBM92 | Boston Bar | fine ss | 628500 | 5483800 | | | | | |
| 43JBM92 | Boston Bar | arg/ siltstone | 628500 | 5483800 | x | x | | | |
| 44JBM92 | Boston Bar | arg | 628400 | 5483800 | | | x | | |
| 45JBM92 | Boston Bar | ss | 627100 | 5483400 | x | x | | | |
| 46JBM92 | Boston Bar | ss/siltstone | 627000 | 5483300 | x | x | | | |
| 47JBM92 | Boston Bar | ss/siltstone | 626900 | 5483200 | x | x | | | |
| 48JBM92 | Boston Bar | arg | 626900 | 5483100 | x | x | x | | |
| 49JBM92 | Boston Bar | lam ss | 624800 | 5484200 | x | x | | | |
| 50JBM92 | Boston Bar | ss | 624500 | 5484600 | x | x | | | |
| 51JBM92 | Boston Bar | ss/cgl | 624500 | 5484400 | | | | | |
| 52JBM92 | Boston Bar | ss | 628600 | 5480400 | | | | | x |
| 53JBM92 | Boston Bar | organic | 629200 | 5480700 | | | | | |
| 271JBM92 | Boston Bar | lam ss | | | x | | | | |
| 272JBM92 | Boston Bar | ss | | | x | x | | | |
| 352JBM92 | Boston Bar | ss | 619900 | 5502600 | x | x | | | |
| 353JBM92 | Boston Bar | ss | 619700 | 5502600 | x | x | | | |
| 354JBM92 | Boston Bar | ss | 619700 | 5502700 | x | x | | | |
| 357JBM92 | Boston Bar | ss | 619300 | 5502800 | x | x | | | |
| 358JBM92 | Boston Bar | crse ss w/ qtz | 619300 | 5503800 | x | x | | | |
| 360JBM92 | Boston Bar | ss | 620600 | 5503700 | x | x | | | |
| 361JBM92 | Boston Bar | cgl | 620500 | 5503800 | x | x | | | |
| 362JBM92 | Boston Bar | ammonite | 620500 | 5503800 | | | | | |
| Dewdney Creek | | | | | | | | | |
| 240JBM91 | Dewdney Creek | | | | | | | | |
| 241JBM91 | Dewdney Creek | | | | | | | | |
| 242JBM91 | Dewdney Creek | | | | | | | | |
| 54JBM92 | Dewdney Creek | ss | 635600 | 5476100 | x | x | | | |
| 55JBM92 | Dewdney Creek | feld siltstone | 636000 | 5476200 | x | x | | | |
| 56JBM92 | Dewdney Creek | rhy | 633600 | 5470500 | x | x | | | |
| 57JBM92 | Dewdney Creek | arg | 633800 | 5470600 | x | x | | | |
| 58JBM92 | Dewdney Creek | lam ss | 633800 | 5470700 | x | x | | | |
| 59JBM92 | Dewdney Creek | ss | 636200 | 5476500 | x | x | | | |
| 60JBM92 | Dewdney Creek | fine ss | 636200 | 5476500 | x | x | | | |
| 61JBM92 | Dewdney Creek | | 636300 | 5476600 | x | x | | | |
| 62JBM92 | Dewdney Creek | cgl | 636500 | 5476900 | x | x | | | |
| 63JBM92 | Dewdney Creek | ss w/ seds | 636500 | 5476900 | x | x | | | |
| 64JBM92 | Dewdney Creek | ss | 636500 | 5476300 | x | x | | | |
| 65JBM92 | Dewdney Creek | ss | 636600 | 5476500 | x | x | | | |
| 66JBM92 | Dewdney Creek | cgl | 636600 | 5476500 | x | x | | | |
| 67JBM92 | Dewdney Creek | ss | 636600 | 5476500 | x | x | | | |
| 68JBM92 | Dewdney Creek | cgl | 636900 | 5476800 | x | x | | | |
| 69JBM92 | Dewdney Creek | ss | 636900 | 5476400 | x | x | | | |
| 186JBM92 | Dewdney Creek | feld wak | 663300 | 5437600 | x | x | | | |
| 187JBM92 | Dewdney Creek | crse ss | 663300 | 5437600 | x | x | | | |
| 188JBM92 | Dewdney Creek | lithfeld ss | 663300 | 5437600 | x | x | | | |
| 189JBM92 | Dewdney Creek | gran cgl | 663200 | 5437600 | x? | x? | | | |
| 190JBM92 | Dewdney Creek | crse ss | 663200 | 5437600 | x | x | | | |

SAMPLE LOCATION LIST

| SAMPLE # | FORMATION | ROCK TYPE | NORTHING | EASTING | HS | TS | ISO | CHEM | PAL |
|-----------|---------------|-----------------|----------|---------|----|----|-----|------|-----|
| 191JBM92 | Dewdney Creek | lithfeldss | 663200 | 5437700 | | | | | |
| 192JBM92 | Dewdney Creek | lithfeldss | 663200 | 5437800 | x | x | | | |
| 193JBM92 | Dewdney Creek | tuff siltstone | 663200 | 5437800 | x | x | | | |
| 194JBM92 | Dewdney Creek | lithfeldss | 663100 | 5437800 | x | x | | | |
| 195JBM92 | Dewdney Creek | lith wak | 663100 | 5437800 | x | x | | | |
| 196JBM92 | Dewdney Creek | feldlithwak | 662900 | 5437800 | x | x | | | |
| 197JBM92 | Dewdney Creek | gran cgl | 662900 | 5437800 | x | x | | | |
| 198JBM92 | Dewdney Creek | lith wak | 662600 | 5438000 | x | x | | | |
| 199JBM92 | Dewdney Creek | cgl?/ tuff? | 662600 | 5438000 | x | x | | | |
| 200JBM92 | Dewdney Creek | lithfeld wak | 662500 | 5438100 | | | | | |
| 201JBM92 | Dewdney Creek | hblplagpory | 663400 | 5437700 | | | | x? | |
| 202JBM92 | Dewdney Creek | lapilli tuff | 663400 | 5437700 | | | | | |
| 203JBM92 | Dewdney Creek | lithfeld wak | 663200 | 5437800 | | | | | |
| 204JBM92 | Dewdney Creek | pebble cgl | 663200 | 5438100 | | | | | |
| 205JBM92 | Dewdney Creek | xtal tuff | 663200 | 5438100 | | | | | |
| 206JBM92 | Dewdney Creek | qtzfeldss | 663000 | 5438700 | | | | | |
| 207JBM92 | Dewdney Creek | qtzfeldss | 663100 | 5438700 | | | | | |
| 208JBM92 | Dewdney Creek | lithfeldwak | 663300 | 5438400 | x | | | | |
| 209JBM92 | Dewdney Creek | lithfeldwak | 663400 | 5438400 | x | x | | | |
| 210JBM92 | Dewdney Creek | xtal tuff | 663500 | 5438300 | x | x | | | |
| 211JBM92 | Dewdney Creek | lapilli tuff | 663500 | 5438500 | x | x | | | |
| 212JBM92 | Dewdney Creek | lapilli tuff | 663500 | 5438500 | x | x | | | |
| 214JBM92 | Dewdney Creek | tuff breccia | 663400 | 5438700 | x | x | | | |
| 2150JBM92 | Dewdney Creek | qtzfeldss | 663000 | 5438700 | x | x | | | |
| 216JBM92 | Dewdney Creek | feld arenite | 641600 | 5454200 | x | x | | | |
| 217JBM92 | Dewdney Creek | lithfeldwak | 641900 | 5453800 | x | x | | | |
| 218JBM92 | Dewdney Creek | ss | 642200 | 5453900 | x | x | | | |
| 219JBM92 | Dewdney Creek | lam silt | 642300 | 5453900 | x | x | | | |
| 220JBM92 | Dewdney Creek | lithfeldarenite | 642400 | 5453900 | | | x | | |
| 221JBM92 | Dewdney Creek | crse lith ss | 642500 | 5453900 | x | x | | | |
| 222JBM92 | Dewdney Creek | fine ss | 644900 | 5446400 | | | x | | |
| 223JBM92 | Dewdney Creek | calc ss | 645000 | 5446400 | | | x | | |
| 224JBM92 | Dewdney Creek | feld ss | 645500 | 5446500 | x | x | | | |
| 225JBM92 | Dewdney Creek | lith wak | 645600 | 5446500 | x | x | | | |
| 226JBM92 | Dewdney Creek | gran cgl | 645800 | 5446600 | x | x | | | |
| 227JBM92 | Dewdney Creek | gran cgl | 645700 | 5446600 | x | x | | | |
| 228JBM92 | Dewdney Creek | gran cgl | 646000 | 5446700 | x | x | | | |
| 229JBM92 | Dewdney Creek | gran cgl | 646100 | 5446700 | | | | | |
| 230JBM92 | Dewdney Creek | lithwak | 646300 | 5446800 | | | | | |
| 231JBM92 | Dewdney Creek | lithfeldwak | 646200 | 5447400 | x | x | | | |
| 232JBM92 | Dewdney Creek | silty shale | 646400 | 5447400 | x | x | | | |
| 233JBM92 | Dewdney Creek | feld ss | 645300 | 5446500 | x | x | | | |
| 234JBM92 | Dewdney Creek | silty shale | 645300 | 5446500 | x | x | x | | |
| 235JBM92 | Dewdney Creek | silty shale | 663200 | 5440500 | x | x | x | | |
| 240JBM92 | Dewdney Creek | tuff | 634400 | 5474300 | x | x | | | |
| 241JBM92 | Dewdney Creek | tuff | 634300 | 5474400 | x | | x | | |
| 242JBM92 | Dewdney Creek | lam fine ss | 634200 | 5474700 | x | x | | | |
| 243JBM92 | Dewdney Creek | lam ss | 633800 | 5475200 | | | | | |
| 244JBM92 | Dewdney Creek | lith ss | 633300 | 5475600 | | | | | |
| 245JBM92 | Dewdney Creek | airfall tuff | 633300 | 5475600 | x | x | | | |
| 246JBM92 | Dewdney Creek | lam ss | 633300 | 5475600 | x | x | | | |
| 247JBM92 | Dewdney Creek | vitricxtaltuff | 634800 | 5472100 | x | x | | | |
| 248JBM92 | Dewdney Creek | wacke | 635400 | 5471900 | | | | | |
| 249JBM92 | Dewdney Creek | wacke | 635500 | 5471900 | | | | | |
| 250JBM92 | Dewdney Creek | vitric tuff | 635600 | 5471800 | x | x | | | |
| 251JBM92 | Dewdney Creek | black siltstone | 635800 | 5471800 | x? | x | | | |
| 252JBM92 | Dewdney Creek | lapilli tuff | 638300 | 5477400 | x | x | | | |
| 253JBM92 | Dewdney Creek | silty shale | 638200 | 5477300 | x | x | | | |
| 254JBM92 | Dewdney Creek | fine ss | 638200 | 5477300 | x | x | | | |
| 255JBM92 | Dewdney Creek | fine lam ss | 637900 | 5477400 | x | x | | | |
| 256JBM92 | Dewdney Creek | xtal tuff | 637700 | 5477400 | x | x | | | |
| 257JBM92 | Dewdney Creek | lapillixtaltuff | 637400 | 5477600 | x | x | | | |
| 258JBM92 | Dewdney Creek | lapilli tuff | 636900 | 5477600 | x | x | | | |
| 259JBM92 | Dewdney Creek | lith ss | 636800 | 5477700 | x | x | | | |
| 260JBM92 | Dewdney Creek | rip-up ss | 637000 | 5478300 | | | | | |

SAMPLE LOCATION LIST

| SAMPLE # | FORMATION | ROCK TYPE | NORTHING | EASTING | HS | TS | ISO | CHEM | PAL |
|-----------------------|---------------|------------------|----------|---------|----|----|-----|------|-----|
| 261JBM92 | Dewdney Creek | silty shale | | | x | x | x | | |
| 262JBM92 | Dewdney Creek | cleav shale | 635400 | 5467800 | x | x | x | | x |
| 263JBM92 | Dewdney Creek | fossil | 640300 | 5463000 | | | | | x |
| 264JBM92 | Dewdney Creek | lam ss | 640400 | 5463300 | x | x | | | |
| 265JBM92 | Dewdney Creek | lithfeld ss | 640300 | 5463300 | | | x | | |
| 266JBM92 | Dewdney Creek | sandy silt | 640300 | 5463200 | | | | | x |
| 267JBM92 | Dewdney Creek | pebl cgl | 640300 | 5463200 | x | x | | | |
| 268JBM92 | Dewdney Creek | lithfeldss | 640300 | 5463100 | x | x | | | |
| 269JBM92 | Dewdney Creek | feld ss | 640300 | 5463100 | x | x | | | |
| 270JBM92 | Dewdney Creek | feld ss | 640200 | 5463100 | x? | x? | | | |
| 327JBM92 | Dewdney Creek | cgl | | | x | x | | | |
| 328JBM92 | Dewdney Creek | ss | | | x | x | | | |
| 330JBM92 | Dewdney Creek | tuff ss | | | x | x | | | |
| 331JBM92 | Dewdney Creek | ss | 619900 | 55? | | | | | |
| 332JBM92 | Dewdney Creek | fossils | 618900 | 5517800 | | | | | x |
| 333JBM92 | Dewdney Creek | med ss | 618900 | 5517800 | x | x | | | |
| 334JBM92 | Dewdney Creek | siltstone | 618400 | 5517400 | | | x | | |
| 335JBM92 | Dewdney Creek | ammonites | 618900 | 5515700 | x | x | | | |
| 336JBM92 | Dewdney Creek | gran cgl | 618800 | 5515800 | x | x | | | |
| 337JBM92 | Dewdney Creek | crse ss | 618800 | 5515800 | | | x | | |
| 338JBM92 | Dewdney Creek | lith ss | 618800 | 5515800 | x | x | | | |
| 339JBM92 | Dewdney Creek | tuff breccia | 618800 | 5515800 | | | x | | |
| 340JBM92 | Dewdney Creek | lapilli tuff | 618700 | 5515800 | | | x | | |
| 341JBM92 | Dewdney Creek | lam ss | 618600 | 5515800 | x | x | | | |
| 342JBM92 | Dewdney Creek | | 621500 | 5510100 | | | | | |
| 343JBM92 | Dewdney Creek | lam ss/silt | 623000 | 5509300 | | | | | |
| 344JBM92 | Dewdney Creek | ammonite | 623000 | 5509300 | | | | | |
| 345JBM92 | Dewdney Creek | lith ss | 619100 | 5513500 | | | | | |
| 346JBM92 | Dewdney Creek | siltstone/shale | 620700 | 5513200 | | | x | | |
| 347JBM92 | Dewdney Creek | siltstone w/ ash | 620700 | 5513200 | x | x | | | |
| 348JBM92 | Dewdney Creek | lith ss | 620500 | 5513800 | x | x | | | |
| 351JBM92 | Dewdney Creek | siltstone | 615800 | 5527400 | | | x | | |
| 355JBM92 | Dewdney Creek | lapilli tuff | | | | | | | |
| 356JBM92 | Dewdney Creek | siltstone | | | x | x | x | | x |
| 375JBM92 | Dewdney Creek | lam ss | | | x | x | | | |
| Thunder Lake Sequence | | | | | | | | | |
| 376JBM92 | Thunder Lake | cgl | 642700 | 5453900 | | | | | |
| 377JBM92 | Thunder Lake | ss | 642750 | 5453900 | | | x | | |
| 378JBM92 | Thunder Lake | cgl | 642750 | 5453900 | | | | | |
| 379JBM92 | Thunder Lake | cgl | 642800 | 5453900 | x | x | | | |
| 380JBM92 | Thunder Lake | cgl | 642800 | 5453900 | | | | | x |
| | | | 642850 | 5453900 | | | | | |
| Lillooet Group | | | | | | | | | |
| 46JBM91 | Lillooet Fm. | siltstone | 537400 | 5654400 | x | x | | | |
| 47JBM91 | Lillooet Fm. | siltstone | 537300 | 5654600 | x | x | | | x |
| 48JBM91 | Lillooet Fm. | | | | x | x | | | |
| 71JBM91 | Lillooet Fm. | gran cgl | 544100 | 5650200 | x | x | | | |
| 72JBM91 | Lillooet Fm. | lithas | 544100 | 5650300 | x | x | | | |
| 73JBM91 | Lillooet Fm. | lithas | 544000 | 5651200 | x | x | | | |
| 74JBM91 | Lillooet Fm. | woods | 543900 | 5651300 | | | | | x |
| 75JBM91 | Lillooet Fm. | cgl | 543600 | 5651700 | | | | | x |
| 76JBM91 | Lillooet Fm. | tuff | 543600 | 5651700 | x | x | | | |
| 77JBM91 | Lillooet Fm. | ss | 542500 | 5651800 | | | | | |
| 78JBM91 | Lillooet Fm. | gran cgl | 540000 | 5652100 | x | x | | | |
| 79JBM91 | Lillooet Fm. | mudstone | 540100 | 5652200 | | | | | |
| 86JBM91 | Lillooet Fm. | cgl | 537300 | 5654800 | | | | | |
| 87JBM91 | Lillooet Fm. | siltstone | 537400 | 5654800 | | | | | |
| 88JBM91 | Lillooet Fm. | tuff | 537500 | 5654700 | x | x | | | |
| 89JBM91 | Lillooet Fm. | tuff | 537500 | 5654600 | | | | | x |
| 91JBM91 | Lillooet Fm. | siltstone | 537900 | 5653600 | x | x? | | | x |
| 92JBM91 | Lillooet Fm. | cgl | 537900 | 5653600 | | x | | | x |
| 93JBM91 | Lillooet Fm. | mudstone | 538100 | 5653700 | x | x | | | |
| 94JBM91 | Lillooet Fm. | mudstone | 538100 | 5653800 | x | x | | | |
| 95JBM91 | Lillooet Fm. | lithas | 538100 | 5653900 | x | x | | | |

SAMPLE LOCATION LIST

| SAMPLE # | FORMATION | ROCK TYPE | NORTHING | EASTING | HS | TS | ISO | CHEM | PAL |
|-------------------------|---------------|--------------|----------------|---------|----|----|-----|------|-----|
| 96JBM91 | Lillooet Fm. | silty mica | 538100 | 5653900 | x | x | | | |
| 97JBM91 | Lillooet Fm. | ss | 536400 | 5657100 | x | x | | | |
| 100JBM91 | Lillooet Fm. | ss | 539100 | 5654100 | x | x | | | |
| 101JBM91 | Lillooet Fm. | cgl | 539000 | 5653800 | | | | | x |
| 102JBM91 | Lillooet Fm. | cgl | 539000 | 5653800 | x | x | | | |
| 103JBM91 | Lillooet Fm. | cgl | Pavilion sheet | | x | x | | | |
| 104JBM91 | Lillooet Fm. | | | | x | x | | | |
| 105JBM91 | Lillooet Fm. | | | | x | x | | | |
| 109JBM91 | Lillooet Fm. | shale | 537900 | 5635000 | x | x | | | |
| 110JBM91 | Lillooet Fm. | siltstone | 537900 | 5653600 | x | x | | | |
| 111JBM91 | Lillooet Fm. | ss w/Buc | 537900 | 5653600 | x | x | | | |
| 112JBM91 | Lillooet Fm. | sanddike? | Pavilion sheet | | x | x | | | |
| 113JBM91 | Lillooet Fm. | ss | 545800 | 5651000 | | | x | | |
| 116JBM91 | Lillooet Fm. | ss | 555600 | 5643800 | x | x | | | |
| 117JBM91 | Lillooet Fm. | mudstone | 555600 | 5643800 | x | x | | | |
| 118JBM91 | Lillooet Fm. | siltstone | 555800 | 5644000 | | | | | x |
| 119JBM91 | Lillooet Fm. | cgl | 556100 | 5643700 | | | x | | |
| 120JBM91 | Lillooet Fm. | siltstone | 555900 | 5643400 | x | x | | | |
| 121JBM91 | Lillooet Fm. | | | | x | x | | | |
| 122JBM91 | Lillooet Fm. | | | | | | x | | |
| 123JBM91 | Lillooet Fm. | ss | 583800 | 5609700 | x | x | | | |
| 124JBM91 | Lillooet Fm. | siltstone | 584000 | 5607200 | x | x | | | |
| 125JBM91 | Lillooet Fm. | ss | 583900 | 5606800 | x | x | | | |
| 126JBM91 | Lillooet Fm. | micrite | 583800 | 5606500 | x | x | | | |
| 128JBM91 | Lillooet Fm. | crse ss | 583900 | 5606100 | x | x | | | |
| 129JBM91 | Lillooet Fm. | ss | 585200 | 5603800 | x | x | | | |
| 209JBM91 | Lillooet Fm. | arg | 537800 | 5653500 | x | x | x | | |
| 210JBM91 | Lillooet Fm. | cgl | 537800 | 5653500 | x | x | | | |
| 211JBM91 | Lillooet Fm. | ss | 537800 | 5653500 | x | x | | | |
| 212JBM91 | Lillooet Fm. | arg | 537800 | 5653500 | x | x | | | |
| 213JBM91 | Lillooet Fm. | shale | 537800 | 5653600 | x | x | x | | |
| 214JBM91 | Lillooet Fm. | ss | 537900 | 5653700 | x | x | | | |
| 215JBM91 | Lillooet Fm. | ss | 537900 | 5653700 | x | x | | | |
| 216JBM91 | Lillooet Fm. | ss | 537900 | 5653700 | x | x | | | |
| 217JBM91 | Lillooet Fm. | ss | 537900 | 5653800 | x | x | | | |
| 218JBM91 | Lillooet Fm. | | 537900 | 5653800 | | | | | |
| 219JBM91 | Lillooet Fm. | ss | 538000 | 5653900 | x | x | | | |
| 220JBM91 | Lillooet Fm. | sh | 538000 | 5653900 | | | x | | |
| 221JBM91 | Lillooet Fm. | sh | 538000 | 5653900 | | | x | | |
| 222JBM91 | Lillooet Fm. | sh | 538000 | 5653900 | | | x | | x |
| 223JBM91 | Lillooet Fm. | sh | 537600 | 5654500 | | | x | | |
| 224JBM91 | Lillooet Fm. | ss | 537600 | 5654500 | | | | | |
| 225JBM91 | Lillooet Fm. | sh | 537500 | 5654600 | x | | x | | |
| 226JBM91 | Lillooet Fm. | ss | 537300 | 5654600 | x | | | | |
| 228JBM91 | Lillooet Fm. | tuff ss | 537300 | 5654600 | x | | | | |
| 229JBM91 | Lillooet Fm. | ss | 537300 | 5654600 | x | | x | | |
| 230JBM91 | Lillooet Fm. | arg | 537300 | 5654600 | | | | | |
| 231JBM91 | Lillooet Fm. | | 537300 | 5654700 | x | | | | |
| 233JBM91 | Lillooet Fm. | ss | 537300 | 5654800 | x | x | | | |
| 234JBM91 | Lillooet Fm. | shale | 556000 | 5653300 | | | x | | |
| 235JBM91 | Lillooet Fm. | shale | 585000 | 5601300 | | | x | | |
| Dewdney Creek Volcanics | | | | | | | | | |
| 213JBM92 | Dewdney Creek | cgl clast | 663500 | 5438500 | | | x | x | |
| 215JBM92 | Dewdney Creek | tuff breccia | 663000 | 5440500 | x | x | x | x | |
| 329JBM92 | Dewdney Creek | andste lava | | | | | x | x | |
| 349JBM92 | Dewdney Creek | andste | 615800 | 5527400 | | | x | x | |
| 350JBM92 | Dewdney Creek | andste | 615800 | 5527300 | | | x | x | |
| Jackass Mountain Group | | | | | | | | | |
| 80JBM91 | Jackass Mtn. | ss | 540200 | 5652600 | x? | x? | | | |
| 81JBM91 | Jackass Mtn. | wood cgl | 540300 | 5652500 | x | x | | | |
| 82JBM91(3) | Jackass Mtn. | bio ss | 540400 | 5652700 | x | | | | |
| 83JBM91 | Jackass Mtn. | ss | 540500 | 5652800 | x | x | | | |
| 84JBM91 | Jackass Mtn. | ss | 540600 | 5652800 | x | x | | | |

SAMPLE LOCATION LIST

| SAMPLE # | FORMATION | ROCK TYPE | NORTHING | EASTING | HS | TS | ISO | CHEM | PAL |
|-----------------------------|-----------------|--------------|-------------|------------|----|----|-----|------|-----|
| 85JBM91 | Jackass Mtn. | ss | 440900 | 5652700 | x | | | | |
| 98JBM91 | Jackass Mtn. | ss | 549600 | 5649800 | | | | | |
| 99JBM91 | Jackass Mtn. | ss | 539300 | 5654200 | x | x | | | |
| 114JBM91(2) | Jackass Mtn. | cgl | 545800 | 5651100 | | | | | |
| 115JBM91 | Jackass Mtn. | ss | 545900 | 5651200 | x | x | | | |
| 127JBM91 | Jackass Mtn. | ss | 583900 | 5606200 | | | | | |
| 131JBM91 | Jackass Mtn. | ss | 536600 | 5667600 | | | | | |
| 132JBM91 | Jackass Mtn. | cgl | 537800 | 5666700 | x | x | | | |
| 27JBM93 | Jackass Mtn. | drill | | | x | x | | | |
| 30JBM93 | Jackass Mtn. | ss | | | x | x | | | |
| 32JBM93 | Jackass Mtn. | ss | 540400 | 5655800 | | | | | |
| 36JBM93 | Jackass Mtn. | ss/siltstone | 549300 | 5654300 | x | | | | |
| 29JBM93 | Jackass Mtn.1 | ss/siltstone | 535200 | 5660100 | x | x | | | |
| 31JBM93 | Jackass Mtn.1 | ss | 540000 | 5655800 | x | x | | | |
| 33JBM93 | Jackass Mtn.1 | ss | | | x | x | | | |
| 34JBM93 | Jackass Mtn.2 | ss | 548800 | 5655600 | x | x | | | |
| 35JBM93 | Jackass Mtn.2 | cgl | 548800 | 5655600 | x | x | | | |
| 37JBM93 | Jackass Mtn.3 | fine ss | 552200 | 5660600 | x | x | | | |
| 38JBM93 | Jackass Mtn.3 | ss | 549900 | 5661000 | | | | | |
| 41JBM93 | Jackass Mtn.3 | ss | 563100 | 5650900 | | | | | |
| 39JBM93 | Jackass Mtn.4 | siltstone | 549700 | 5661500 | | | | | x |
| 40JBM93 | Jackass Mtn.4 | ss | | | | | | | x |
| 28JBM93 | Chinahead Stock | hbl gran | | | x | | | | |
| Methow Terrane - Washington | | | | | | | | | |
| Twisp Formation | | | | | | | | | |
| 1JBM91 | Twisp Fm. | arg | 48o28'03" | 120o09'57" | x | | | x? | |
| 2JBM91 | Twisp Fm. | ss | 48o28'03" | 120o09'57" | | | | | x |
| 7JBM91 | Twisp Fm. | ss | 48o22' | 120o11'56" | | | x? | | |
| 8JBM91 | Twisp Fm. | siltstone | 48o22' | 120o11'56" | x | | | | |
| 9JBM91 | Twisp Fm. | siltstone | 48o18'54" | 120o16'06" | | | | | |
| 10JBM91 | Twisp Fm. | ss | 48o18'54" | 120o16'06" | x | | | | |
| 2JBM92 | Twisp Fm. | tuff | Lewis Butte | | | | | | x |
| 370JBM92 | Twisp Fm. | arg/tuff | | | | | x | | |
| 371JBM92 | Twisp Fm. | arg | Highway | | x | x | | | |
| 372JBM92 | Twisp Fm. | arg | old highway | | | | | | |
| 21JBM92 | Twisp Fm. | tuff | N Winthrop | | | | | | |
| 22JBM92 | Twisp Fm. | hbl dike | N Winthrop | | | | | | |
| 23JBM92 | Twisp Fm. | arg | fish htcy | | | | | | |
| 24JBM92 | Twisp Fm. | tuff | Pirson Ck | | x | x | | | |
| Newby Group | | | | | | | | | |
| 243JBM91 | Newby Gp. | | | | | | x | | |
| 244JBM91 | Newby Gp. | | | | | | | | |
| 245JBM91 | Newby Gp. | | | | | | x | | |
| 246JBM91 | Newby Gp. | | | | | | | | |
| 247JBM91 | Newby Gp. | | | | | | x | | x |
| 248JBM91 | Newby Gp. | | | | x | x | | | |
| 249JBM91 | Newby Gp. | | | | x | | x | | |
| 1JBM92 | Jr volc | tuff | Lookout Mtn | | x | x | | | |
| 5JBM92 | Jr volc | tuff ss | Lookout Mtn | | x | x | | | |
| 6JBM92 | Jr volc | cgl/breccia | Lookout Mtn | | x | x | | | |
| 7JBM92 | Jr volc | volc w/qtz | Lookout Mtn | | x | x | | | |
| 8JBM92 | Jr volc | siltstone | Lookout Mtn | | | | | | |
| 9JBM92 | Jr volc | ss | Lookout Mtn | | | | | | |
| 10JBM92 | Jr volc | cgl/breccia | Lookout Mtn | | | | | | |
| 11JBM92 | Jr volc | ss | Lookout Mtn | | | | | | |
| 12JBM92 | Jr volc | cgl | Lookout Mtn | | | | | | |
| 13JBM92 | Lookout Mtn | dike | | | | | | | |
| 14JBM92 | unnamed volc | | | | x | x | | | |
| 15JBM92 | unnamed volc | | | | x | x | | | |

SAMPLE LOCATION LIST

| SAMPLE # | FORMATION | ROCK TYPE | NORTHING | EASTING | HS | TS | ISO | CHEM | PAL |
|--------------------|-----------------|--------------|------------|------------|----|----|-----|------|-----|
| 16JBM92 | unnamed volc | | | | | | | | x |
| 26JBM92 | unnamed volc | crse lith ss | Poorman Ck | | x | | | | |
| 27JBM92 | unnamed volc | volc breccia | Poorman Ck | | x | x | | | |
| 28JBM92 | unnamed volc | volc breccia | Poorman Ck | | x | x | | | |
| 29JBM92 | unnamed volc | lithfeld ss | Poorman Ck | | | | | | |
| 30JBM92 | unnamed volc | trace fossil | Poorman Ck | | | | | | |
| 31JBM92 | unnamed volc | cgl | Poorman Ck | | x | | | | |
| 34JBM92?? | unnamed volc | wood frags | | | | | | | |
| 32JBM92 | unnamed volc | ss | Alder Ck | | x | | | | |
| 33JBM92 | unnamed volc | lava | Alder Ck | | | | | | |
| 363JBM92 | unnamed volc | dacite | | | x | | x | x | |
| 365JBM92 | Isabella Ridge | andste | | | x | x | | | |
| 366JBM92 | Patterson Lk | organic | | | x? | x? | x | x | |
| 369JBM92 | Libby Ck | volc | | | x | | | | |
| 1JBM93 | Jr-Methow | tuff | | | | | | x | |
| 2JBM93 | Jr-Methow | dacite | | | | | | | |
| 4JBM93 | Jr-Methow | tuff | | | x | | | | |
| 5JBM93 | Jr-Methow | breccia | | | x | x | | | |
| 6JBM93 | Jr-Methow | breccia | | | | | | | |
| 7JBM93 | Jr-Methow | andste | 707404 | 5359976 | | | x | x | |
| 9JBM93 | Jr-Methow | cgl | | | | | | | |
| 10JBM93 | unnamed volc | | | | | | x | | |
| 11JBM93 | unnamed volc | | | | | | | | |
| 70JBM93 | Jr-Methow | metaqz | | | x | x | | | |
| 71JBM93 | Jr-Methow | | | | | | | | |
| 72JBM93 | Jr-Methow | | | | | | | | |
| 73JBM93 | Jr-Methow | | | | | | x | | |
| 74JBM93 | Jr-Methow | | | | x | x | | | |
| 75JBM93 | Jr-Methow | McClure | | | | | | x | |
| 76JBM93 | Jr-Methow | | | | | | | x | |
| 77JBM93 | Jr-Methow | | | | x | x | | | |
| 78JBM93 | Jr-Methow | shale | | | | | | x | |
| 79JBM93 | Jr-Methow | ss | | | | | | x | |
| 80JBM93 | Jr-Methow | andste | 704671 | 5353478 | | | x | x | |
| 81JBM93 | Jr-Methow | andste | 708008 | 5353600 | | | x | x | |
| 82JBM93 | Jr-Methow | ss | | | | | x | x | |
| 83JBM93 | Jr-Methow | andste | 708159 | 5354533 | | | x | x | |
| 84JBM93 | Jr-Methow | andste | 707593 | 5354790 | x | x | | | |
| Alder Creek Stock | | | | | | | | | |
| 25JBM92 | Alder Ck Stock | granodiorite | | Alder Lk | x | | | | |
| 3JBM93 | Alder Ck Stock | hbl gran | | orient hs | | | | | x |
| Misc. Samples | | | | | | | | | |
| 3JBM91 | Buck Mtn Fm. | volc | 48o26'23" | 120o06'35" | x | x | | | |
| 11JBM91 | Buck Mtn Fm. | andste | 48o18'26" | 120o16'37" | x | | | | |
| 5JBM91 | Virginia Ridge | siltstone | 48o22'49" | 120o13'37" | | | | | x |
| 6bJBM91 | Winthrop SS | coal | 48o22'55" | 120o15'34" | x | x | | | |
| 6JBM91 | Winthrop SS | shale | 48o22'55" | 120o15'34" | | | x | | |
| 12JBM91 | North Creek | grano | 48o26'38" | 120o32'24" | x | | | | |
| 3.3aJBM92 | Virginian Ridge | cgl | Poorman Ck | | | | | | |
| 17JBM92 | K clastic | | | | | | | | |
| 18JBM92 | K clastic | | | | | | | | |
| 19JBM92 | K clastic | | | | x | | | | |
| 20JBM92 | K clastic | | | | | | | | |
| 367JBM92 | Virginian Ridge | organic | | | | | | | |
| 368JBM92 | Winthrop Ridge | organic | | | | | | | |
| QUESNELIA | | | | | | | | | |
| Ashcroft Formation | | | | | | | | | |
| 204JBM91 | Ashcroft Fm. | ss | 619900 | 5617700 | x | | | | |
| 205JBM91 | Ashcroft Fm. | | 620300 | 5617700 | | | | | |
| 206JBM91 | Ashcroft Fm. | ss | 620300 | 5617700 | | | | | |

SAMPLE LOCATION LIST

| 207JBM91 | Ashcroft Fm. | | 620400 | 5617900 | x | | | | |
|------------------------|----------------|----------------|----------|---------|----|----|-----|------|-----|
| 273JBM92 | Ashcroft Fm. | Plen siltstone | | | | | x | | |
| 274JBM92 | Ashcroft Fm. | carb siltstone | | | | | | | |
| 275JBM92 | Ashcroft Fm. | lith ss | | | | | | | |
| 276JBM92 | Ashcroft Fm. | feld wak | | | | | | | |
| 277JBM92 | Ashcroft Fm. | pelycepd / ss | | | | | | | |
| 278JBM92 | Ashcroft Fm. | lith ss | | | x | x | | | |
| 279JBM92 | Ashcroft Fm. | Baj siltstone | | | | | x | | |
| 280JBM92 | Ashcroft Fm. | ss | | | x | x | | | |
| BALD MOUNTAIN | | | | | | | | | |
| SAMPLE # | FORMATION | ROCK TYPE | NORTHING | EASTING | HS | TS | ISO | CHEM | PAL |
| 191JBM91 | Bald Mtn. | ls | 523100 | 5749400 | | | | | x |
| 192JBM91 | Bald Mtn. | ls | 522900 | 5749500 | x | x | | | |
| 193JBM91 | Bald Mtn. | ls | 522300 | 5749700 | x | x | | | |
| 194JBM92 | Bald Mtn. | cgl | 523300 | 5748500 | x | x | | | |
| 195JBM91 | Bald Mtn. | ls | 522500 | 5748300 | x | x | | | |
| 196JBM91 | Bald Mtn. | | 520800 | 5748700 | x | x | | | |
| 197aJBM91 | Bald Mtn. | | 520600 | 5749600 | x | x | | | |
| 197JBM91 | Bald Mtn. | | 520500 | 5749600 | x | x | | | |
| 198JBM91 | Bald Mtn. | red cgl | 520800 | 5748800 | | | | | |
| 199JBM91 | Bald Mtn. | red cgl | 520800 | 5748800 | x | x | | | |
| 200JBM91 | Bald Mtn. | ss | 521600 | 5748400 | x | x | | | |
| 201JBM91 | Bald Mtn. | ss | 521600 | 5748400 | x | x | | | |
| 202JBM91 | Bald Mtn. | siltstone | 521600 | 5748400 | x | x | | | |
| 50F | Bald Mtn. | ls | 523200 | 5748800 | | | | | x |
| 51F | Bald Mtn. | ls | 523100 | 5749000 | | | | | x |
| 52F | Bald Mtn. | ls | 522900 | 5749600 | | | | | x |
| 53F | Bald Mtn. | ls | 522900 | 5748200 | | | | | x |
| 54F | Bald Mtn. | ls | 522300 | 5749100 | | | | | x |
| Farwell Pluton | | | | | | | | | |
| 186JBM91 | Farwell Pluton | gran | 521600 | 5744700 | | | | z | |
| 187JBM91 | Farwell Pluton | gran | 521600 | 5744700 | | | | | |
| 188JBM91 | Farwell Pluton | gran | 521400 | 5744600 | | | | | |
| 189JBM91 | Farwell Pluton | gran | 521400 | 5744600 | x | x | | | |
| 190JBM91 | Farwell Pluton | gran | 521300 | 5744700 | x | x | | | |
| Eocene Rocks | | | | | | | | | |
| 26JBM91 | Edp | dacite phyry | 546600 | 5685700 | x | | | | |
| 27JBM91 | Evolcanics | tuff | 545400 | 5684500 | | | | | |
| 29JBM91 | Evolcanics | dacite | 550900 | 5682900 | | | | | x |
| 70JBM91 | Tdike | hbl dacite | 544200 | 5650100 | | | | | |
| 133JBM91 | Eocene | gran diorite | 542300 | 5668200 | x | x | | | |
| 13JBM91 | Chil. dike | gabbro | 525800 | 56.89.8 | x | x | | | |
| 14JBM91 | dike | | 57. | | x | x | | | |
| 15JBM91 | dike | gphyric | 527900 | 5698200 | x | | | | |
| 17JBM91 | Chil. dike | gabbro | 528100 | 5698300 | x | | | x? | |
| 18JBM91 | dike | gphyric | 528200 | 5698200 | x | x | | | |
| 28JBM91 | Spences Bridge | andste | 530800 | 5683200 | x | | | | |
| 21JBM91 | Spences Bridge | gran cgl | 548200 | 5685500 | | | x | | |
| 22JBM91 | Spences Bridge | ss | 548200 | 5685500 | x | | | | |
| 23JBM91 | Spences Bridge | ss | 548200 | 5685500 | x | | | | |
| 24JBM91 | Spences Bridge | carb ss | 547900 | 5686400 | x | | | | |
| 25JBM91 | Spences Bridge | andste | 548000 | 5685500 | x | | | | |
| Bowen Island Group | | | | | | | | | |
| Bowen Island Formation | | | | | | | | | |
| 90JBM93 | Bowen Island | andste | 469092 | 5466233 | | | | | |
| 91JBM93 | Bowen Island | andste | 476350 | 5469748 | | | | | |
| Bowen | Bowen Island | rhy | 459305 | 5479638 | | | | | |

APPENDIX D - THIN SECTION DESCRIPTIONS

HARRISON LAKE FORMATION

Sample Number:

70JBM92

Formation Name:

Harrison Lake Fm.

Mineral:

Primary

Plagioclase

10%

K-spar

5%

Lithics

<1%

Matrix

85%

Secondary

chlorite

epidote

calcite (minor)

Texture:

Tuffaceous siltstone consisting of fine to very fine grained to microcrystalline(?) interlocking mosaic of plagioclase and k-spar matrix with minor fine grained angular to subangular plagioclase and k-spar crystals floating within; contains thin graded laminae of fine to medium grained angular to subangular partially sericitized plagioclase and angular to subrounded k-spar floating in plag-k-spar matrix; alteration minerals, consisting of clear, amorphous epidote and chlorite, form splotchy "film" across thin section; chlorite is locally aligned in irregular swirls

Rock Name:

Tuffaceous siltstone with minor sandstone laminae

Sample Number:

71JBM92

Formation Name:

Harrison Lake Fm.

Mineral:

Plagioclase

70%

K-spar

15%

Muscovite

15%

Alteration

Chlorite

Texture:

Recrystallized rock consisting of medium grained angular to subangular grains of plagioclase and k-spar, locally heavily sericitized floating in a groundmass of preferentially aligned fine to medium grained plagioclase laths and muscovite, probable sanadine in groundmass as well; unit is interpreted as a metatuff, with original groundmass of fine plagioclase and k-spar recrystallized to observed groundmass

Rock Name:

Dacitic metatuff

Sample Number

72JBM92

Formation Name

Harrison Lake Fm.

Echo Island Member

Mineral

Volcanic lithics

Estimated Volume Percent

65%

Quartz

5%

Plagioclase

10%

Pyroxene

2%

Matrix

15%

Texture:

Coarse-grained volcanoclastic unit consists of poorly sorted coarse-grained to pebble-sized subangular to angular clasts of dacite (plaghyric) and andesite (augite and plaghyric) porphyry, medium to coarse-grained, angular to subrounded quartz and plagioclase feldspar set in a clay? rich matrix. Clasts locally display zeolite rims, and matrix is locally replaced by "dirty" calcite and minor epidote. Lack of welding and absence of readily identifiable glass in matrix suggest rock is first cycle epiclastic

Rock Name:

Volcanic lithic pebble breccia/conglomerate (lapilli tuff)

Sample Number

73JBM92

Formation Name

Harrison Lake Fm.

Echo Island Member

Mineral

Plagioclase

Estimated Volume Percent

20%

| | |
|---------|-----|
| Quartz | 5% |
| Lithics | 30% |
| Matrix | 45% |

Texture:

Medium to coarse grained volcaniclastic sandstone: immature, poorly sorted, with angular to subangular clasts of poikilitic plagioclase (with mafic chloritized inclusions), fine to medium grained angular quartz, and abundant subrounded to subangular lithic clasts, including porphyritic plagioclase porphyry with abundant chlorite (altered mafics); tuffaceous clasts with plagioclase microlites; aphanitic chloritized clasts. Majority of mineral grains appear to be in the process of disaggregating from lithic clasts. Matrix consists of interleaved microcrystalline plagioclase microlites, chlorite and clay. Alteration assemblage includes abundant chlorite, epidote on feldspar, calcite.

Rock Name:

Immature medium to coarse grained feldspathic lithic wacke

| | |
|----------------------|---------------------------------|
| Sample Number | Formation Name |
| 75JBM92 | Harrison Lake Fm. |
| | Echo Island Member |
| Mineral | Estimated Volume Percent |
| Lithics | 75% |
| Plagioclase | 10% |
| Matrix | 15% |

Texture:

Coarse grained sandstone to granule conglomerate: immature, poorly sorted, with subangular to subrounded volcanic lithic clasts (porphyritic clasts with glomerocrysts, crystal tuff clasts, aphanitic chloritized clasts, etc.), lesser angular plagioclase clasts in a recrystallized matrix. Grain boundaries vary from grain to grain to floating. Matrix consists of microcrystalline quartz and feldspar overprinted by abundant epidote, calcite, chlorite

Rock Name:

Immature coarse-grained volcanic lithic wacke to granule conglomerate

| | |
|----------------------|---------------------------------|
| Sample Number | Formation Name |
| 89JBM92 | Harrison Lake Fm. |
| | Celia Cove Member |
| Mineral | Estimated Volume Percent |
| Volcanic lithics | 60% |
| Chert lithics | 5% |
| Plagioclase | 5 |
| Quartz | 1% |
| K-spar | 2% |
| Matrix | 25-30% |

Texture:

Rock is medium to coarse grained volcanic lithic sandstone, with medium to coarse grained clasts of subangular to subrounded, moderately sorted, volcanic lithics (augite porphyry, plagioclase porphyry, aphanitic), subrounded chert, angular clasts of quartz, k-spar, plagioclase. Matrix is highly altered, with abundant secondary calcite and zeolites. Volcanic lithics are strongly altered, with saussurization of groundmass, epidote replacement, chloritic alteration, local zeolitic alteration. Sample is cut by prominent calcite veins

Rock Name:

Green, moderately sorted, subangular to subrounded, medium to coarse-grained volcanic lithic wacke

| | |
|----------------------|---------------------------------|
| Sample Number | Formation Name |
| 90JBM92 | Harrison Lake Fm. |
| | Celia Cove Member |
| Mineral | Estimated Volume Percent |
| Volcanic lithics | 30-40% |
| Plagioclase | 10% |
| Quartz | 2% |
| k-spar | tr |
| Matrix | 50-60% |

Texture:

Matrix supported, moderately well-sorted, fine to medium grained, rounded to angular clasts of volcanic lithics, together with angular clast of plagioclase, k-spar, and quartz. Clasts are floating in very fine grained matrix of presumed altered clay and calcite. Alteration minerals include epidote and chlorite. Pyroxene locally evident, primarily in clasts. Crude grading locally evident

Rock Name:

Moderately well sorted, fine to medium grained volcanic lithic wacke

| | |
|----------------------|-----------------------|
| Sample Number | Formation Name |
|----------------------|-----------------------|

95JBM92 **Harrison Lake Fm.**
Celia Cove Member

| Mineral | Estimated Volume Percent |
|------------------|--------------------------|
| Volcanic lithics | 75% |
| k-spar | 5% |
| plagioclase | 5% |
| apatite | tr |
| Matrix | 15% |

Texture: Matrix to clast supported, poorly sorted, medium to coarse grained, subangular to subrounded clasts of volcanic lithics (aphanitic, plagioclase phyrlic, microcrystalline pilotaxitic, etc.) in an altered presumed clay rich matrix. Lesser angular to subangular medium grained apatite, k-spar, and plagioclase interspersed. Alteration of feldspars includes calcite, saussuritization; matrix alteration produces epidote, chlorite

Rock Name:
 Reddish brown, poorly sorted medium to coarse grained volcanic lithic wacke

Sample Number **97JBM92** **Formation Name**
Harrison Lake Fm.
Francis Lake Member

| Mineral | Estimated Volume Percent |
|-------------|--------------------------|
| Plagioclase | 30-40% |
| Augite | 15-20% |
| k-spar | 1% |
| quartz | 1% |
| titanite | tr |
| matrix | 40% |

Texture: Pilotaxitic fine-grained plagioclase laths and euhedral augite; augite is euhedral, occurs as elongate blades, locally as long axis cross sections; plagioclase occurs as euhedral to subhedral blades. Minor K-spar and quartz occur as coarse grains floating in finer grained pilotaxitic matrix; grains commonly embayed, locally appear broken. Calcite replacement common; locally concentrates around margins of larger phenocrysts of quartz, k-spar

Rock Name:
 Crystal tuff (possibly air fall tuff)

Sample Number **99JBM92** **Formation Name**
Harrison Lake Fm.
Francis Lake Member

| Mineral: | Estimated volume percent |
|--------------------------|--------------------------|
| Volcanic lithics | 50% |
| Plagioclase | 25% |
| Chlorite after augite(?) | 2% |
| k-spar | tr |
| Matrix | 25% |

Texture Graded coarse lithic sandstone to granule (fine pebble conglomerate. Clasts are subrounded to angular, moderately well sorted, coarse sand to fine pebble-sized; consist of crystal lithic tuff (70%), very fine siltstone (5%); coarse-grained euhedral plagioclase, chlorite after mafics (augite?), k-spar, quartz (25%). Matrix is aphanitic, presumed to be fine clay. Calcite replacement common; chloritization of mafics, both in single grains and in clasts is common; locally epidote is prominent alteration mineral.

Rock Name:
 Graded coarse-grained to fine pebble volcanic lithic wacke

Sample Number **100JBM92** **Formation Name**
Harrison Lake Fm.
Francis Lake Member

| Mineral | Estimated Volume Percent |
|--|--------------------------|
| volcanic lithic clasts (crystal tuff clasts) | 90% |
| matrix clay + calcite | 10% |

Texture: Monolithic, moderately sorted, very coarse grained to granule-sized (very fine pebbles) subangular to subrounded volcanic lithic wacke/granule conglomerate. Clasts consist entirely of trachytic to subtrachytic plagioclase crystal tuff, commonly in grain to grain contact, locally encased in amorphous brown "grungy" matrix interpreted to be clay and secondary calcite. Calcite replacement of matrix and clast matrix common. Unit is crudely laminated on 5 mm scale, clasts appear imbricated in part

Rock Name:
volcanic lithic (crystal tuff) granule conglomerate

| | |
|------------------------------|--------------------------|
| Sample Number | Formation Name |
| 101JBM92 | Harrison Lake Fm. |
| | Francis Lake Member |
| Mineral | Estimated volume percent |
| volcanic lithics | 10% |
| plagioclase | 25% |
| (large xtals and microlites) | |
| groundmass | 65% |

Texture: Matrix supported volcanic breccia consists of subtrachytic plagioclase microlites (strongly trachytic around lithic and crystal/matrix grain boundaries) in a black aphanitic groundmass encasing angular pebble-sized clasts of volcanic lithics/tuffs and coarse grained euhedral plagioclase crystals. Sorting not recognizable in thin section, but apparent on outcrop scale. Calcite replacement of lithics and crystals is common.

Rock Name
Lithic crystal vitric tuff/lapilli tuff

| | |
|--|--------------------------|
| Sample Number | Formation Name |
| 105JBM92 | Harrison Lake Fm. |
| | Francis Lake Member |
| Mineral | Estimated Volume Percent |
| Plagioclase | 1-3% |
| K-spar(?) | 1-3% |
| Vugs | 5-10% |
| Groundmass: trachytic plagioclase microlites | |

Texture Dominant texture is flattened, oriented arrangement of vugs within microcrystalline plagioclase-phyric trachytic groundmass. Vugs are elongate, lenticular, with angular terminations, filled with radial habit zeolites. Strong calcitic alteration of groundmass and rare euhedral plagioclase and k-spar

Rock Name
Crystal vitric tuff

| | |
|---------------|--------------------------|
| Sample Number | Formation Name |
| 106JBM92 | Harrison Lake Fm. |
| | Francis Lake Member |
| Mineral | Estimated Volume Percent |
| Plagioclase | 50% |
| vugs | 5-10% |
| groundmass | 40% |

Texture: Trachytic fine-grained plagioclase microlites with aphanitic groundmass, commonly replaced by calcite; includes elongate lenticular vugs with angular terminations, vugs filled/replaced by quartz then chlorite then calcite

Rock Name:
Crystal tuff

| | |
|-----------------------|--------------------------|
| Sample Number | Formation Name |
| 110JBM92 | Harrison Lake Fm. |
| | Francis Lake Member |
| Mineral | Estimated Volume Percent |
| Plagioclase | 60% |
| Chlorite after augite | 15% |
| Groundmass | 25% |

Texture: Trachytic assemblage of euhedral medium-grained plagioclase and altered augite. Plagioclase is strongly saussuritized; augite is completely replaced by chlorite; silicification is locally evident. Calcite is replacing matrix in part

Rock Name:
Crystal tuff

| | |
|---------------|-------------------|
| Sample Number | Formation Name |
| 112JBM92 | Harrison Lake Fm. |

| | | |
|---------|--------------------------|-----|
| Mineral | Francis Lake Member | |
| | Estimated Volume Percent | |
| | Plagioclase | 50% |
| | Chlorite after mafics | 10% |
| | Matrix | 40% |

Texture:

Sample is poorly sorted, very immature, medium to coarse grained, feldspathic wacke with large, angular (euhedral) grains of plagioclase floating in a highly altered matrix of plagioclase laths, pyroxene?, and clay. Matrix is altered to chlorite, calcite, and lesser epidote. Matrix is more highly altered than clasts

Rock Name

Very immature coarse-grained feldspathic wacke

| | | | |
|---------------|--------------------------|-------------------|--|
| Sample Number | | Formation Name | |
| 113JBM92 | | Harrison Lake Fm. | |
| Mineral | Estimated Volume Percent | | |
| | Plagioclase | 40% | |
| | Pyroxene | 10% | |
| | Matrix | 50% | |

Texture:

Rock is bizarre. Phenocrysts consist of medium to coarse grained euhedral to subhedral plagioclase, locally forming glomerocrysts, and medium grained subhedral pyroxene set in an unidentifiable matrix. Matrix is strongly altered to chlorite, calcite. Plagioclase is sausseritized, with abundant epidote and calcite concentrating along twin planes; pyroxene is almost totally replaced by chlorite, zeolites, and an opaque iron oxide attacking the rims. Sample appears to be cut by calcite(?) -filled fracture, which brecciates country rock

Rock Name

Greenish grey medium to coarse grained andesite tuff breccia

| | | | |
|---------------|--------------------------|--------------------|--|
| Sample Number | | Formation Name | |
| 114JBM92 | | Harrison Lake Fm. | |
| | | Weaver Lake Member | |
| Mineral | Estimated Volume Percent | | |
| | Plagioclase | 15% | |
| | K-spar | 1% | |
| | Quartz | 2% | |
| | Hornblende | 3% | |
| | Groundmass | 80%+ | |

Texture:

Banded/foliated porphyritic rhyolite. Contains coarse grained euhedral plagioclase, with minor, medium grained euhedral hornblende, alkali feldspar and quartz. Groundmass consists of distinctly laminated quartz and k-spar?, forming alternating coarser and finer grained laminae; coarse laminae are recrystallized quartz, finer laminae are microcrystalline intergrowths of quartz and feldspar. Local wispy laminae and concentric laminae are evident. Alteration includes chloritization of hornblende

Rock Name:

Flow-banded rhyolite

| | | | |
|---|--------------------------|-------------------|--|
| Sample Number | | Formation Name | |
| 116JBM92 | | Harrison Lake Fm. | |
| Mineral | Estimated Volume Percent | | |
| | Plagioclase | 20-25% | |
| | Pyroxene | <5% | |
| | Opagues | 5% | |
| | Matrix | 70-75% | |
| intergrown plagioclase and cryptocrystalline matrix | | | |

Texture:

Dark greenish grey porphyritic rock with medium to coarse grained euhedral plagioclase, fine to medium grained pyroxene, and sub- to anhedral opaques set in a subtrachytic, felted matrix. Approximately 73 degree extinction angle. Microcrystalline plagioclase laths locally "flow" around phenocrysts. Plagioclase commonly forms large (1-2 mm) glomerocrysts, locally with Carlsbad twinning. Plagioclase is sausseritized, with incipient replacement by epidote and minor calcite. Pyroxene replaced by chlorite and epidote. Matrix strongly chloritized. Matrix is locally replaced by "spitchy" calcite

Texture:

Fine to very fine grained; angular to subangular plagioclase, locally sericitized; angular to subangular k-spar, very minor undulose extinction quartz; subrounded to rounded fine-grained volcanic lithics; moderately sorted; matrix supported, with clay matrix; sample contains abundant very fine grained plagioclase laths, locally oriented parallel to laminae, locally chaotically mixed within matrix; sample is interpreted as medium to fine grained lithic feldspathic siltstone with locally abundant tuffaceous content (plag laths are assumed to be primary pyroclastics)

Rock Name:

Greenish grey medium to coarse grained dacite porphyry

Sample Number

122JBM92

Formation Name

Harrison Lake Fm.

Mineral

Estimated Volume Percent

Plagioclase

5-10%

Quartz

2%

Sanadine

2%

Zircon

tr

Matrix

85-90%

Texture:

Sample is light greenish grey, and appears siliceous. Plagioclase is medium grained, euhedral, locally forms glomerocrysts; quartz is fine to medium grained, anhedral. Matrix consists of microcrystalline intergrowths of plagioclase laths, k-spar(?) and quartz. Slight epidote and calcite replacement of plagioclase. Matrix contains abundant small, evenly spaced, roughly concentric light green concretions believed to be chlorite?, as well as randomly spaced microcrystalline calcite

Rock Name:

Light greenish grey rhyolite

Sample Number

128JBM92

Formation Name

Harrison Lake Fm.

Celia Cove Member

(lowest sandstone sample)

Mineral

Estimated Volume Percent

Volcanic lithics

65%

Plagioclase

10%

K-spar

5%

chert

2%

matrix

20%

Texture:

Sample contains moderately sorted, medium to coarse grained, angular to rounded clasts of volcanic lithics (aphanitic, plagioclase porphyry), with angular (euhedral and broken) grains of k-spar, quartz, plagioclase, and subrounded chert. Volcanic lithics are strongly saussuritized, altered to calcite, epidote, chlorite, within indistinct grain boundaries and uncertain original composition. Chert appears as rare polycrystalline quartz clasts. These lithic grains are much more altered and seem to be more well-rounded than most grains contained in overlying units, suggesting derivation from older source.

Rock Name:

Brownish green medium to coarse-grained volcanic lithic wacke

Sample Number

130JBM92

Formation Name

Harrison Lake Fm.

Celia Cove Member

Mineral

Estimated volume percent

calcite

60%

silt grains (qtz, k-spar)

15%

opaque organic matter

25%

Texture:

Wispy laminated well sorted fine to medium grained calcareous feldspathic(?) siltstone. Silt grains are angular grains of k-spar, quartz floating in a matrix of predominantly calcite and clay(?). Rare rounded calcite clasts may be replaced bioclasts. Organic material is concentrated in discrete laminae, separated by more silt and calcite rich laminae. Wispy character most likely traction current induced, indicated by regularity of laminae

Rock Name:

Calcareous siltstone

Sample Number

132JBM92

Formation Name

Harrison Lake Fm.

Francis Lake Member

Mineral

Estimated Volume Percent

calcite

90%

quartz, k-spar, plag

10%

Texture:

Sample consists of silt-sized subrounded to subangular calcite grains with minor component of silt-sized quartz, feldspar, plagioclase randomly distributed throughout. Large (1-2 mm) angular grains of recrystallized calcite float in crude lamination; believed to be recrystallized bioclastic debris. Amount of calcite in sample suggests this siltstone is composed primarily of comminuted carbonate detritus with a minor terrigenous influx

Rock Name:

Calcareous siltstone/Silty micrite(?)

Sample Number**142JBM92****Formation Name****Harrison Lake Fm.****Mineral**

Plagioclase
Chlorite after Augite
Opaques
Matrix

Estimated Volume Percent

25%
15%
3%
55+0%

Texture:

Dark greenish grey porphyritic rock consists of coarse grained subhedral to euhedral plagioclase crystals and medium to coarse grained pale green euhedral augite crystals set in a microcrystalline matrix of plagioclase laths and possibly heavily chloritized clinopyroxene. Plagioclase locally displays Carlsbad twinning, and augite locally forms distinct groups of small crystals. Sample is strongly altered, with strong chloritization and calcite replacement of plagioclase grains. Plagioclase locally has albitized rims. Microcrystalline quartz invades matrix adjacent to quartz, calcite, and zeolite filled vugs.

Rock Name:

Augite andesite porphyry

Sample Number**148JBM92****Formation Name****Harrison Lake Fm.****Mineral**

Plagioclase
Pyroxene?
Matrix

Estimate Volume Percent

15%
2%
85%

Texture:

Sample is greenish grey with distinct pinkish white phenocrysts. Phenocrysts are plagioclase (andesine), locally forming glomerocrysts and displaying pericline and Carlsbad twinning; plagioclase is altered to sericite? in part. Pyroxene is rare and completely chloritized. Microcrystalline matrix consists of randomly oriented intergrowths of plagioclase laths and chloritized mafic?. Sample is strongly chloritized, with patches of chlorite uniformly distributed across thin section. Microcrystalline epidote and hematitic alteration are common.

Rock Name:

Andesite Porphyry

Sample Number:**149JBM92****Formation Name:****Harrison Lake Fm.****Mineral:****Primary**

plagioclase
hornblende
apatite
groundmass

Estimated volume percent:

15%
5%
5%
75%

Secondary

chlorite
k-spar
zeolite
calcite

Texture:

Euhedral, randomly oriented, fine to medium crystalline, partially sericitized plagioclase and minor hornblende, with euhedral finely crystalline apatite in a fine to microcrystalline plagioclase-rich, matrix; plagioclase locally forms glomerocrysts; sample contains abundant chloritic alteration; three stage vug filling characterized by sequential addition of k-spar, zeolite, and calcite

Rock Name:

Fine to medium grained andesite porphyry

Sample Number:**150JBM92****Formation Name:****Harrison Lake Fm.****Mineral:****Primary**

Plagioclase
K-spar
Hornblende
groundmass

Estimated volume percent:

15%
10%
<1%
75%

Secondary

Zeolite
Calcite
Chlorite

Texture:

Fine to medium grained subhedral to euhedral partially sericitized plagioclase and lesser k-spar, locally forming large (>30 mm) glomerocrysts; set in finely crystalline to microcrystalline plagioclase and k-spar matrix; locally contains altered hornblende, chloritized in part; secondary alteration consists of zeolite reaction rims around k-spar, calcite vug filling and replacement; sericitization of feldspars

Rock Name:

fine to medium grained dacite porphyry

Sample Number:

151JBM92

Formation Name:

Harrison Lake Fm.

Mineral:

Primary

Plagioclase
K-spar
groundmass

15%
5-10%
70-75%

Secondary

Calcite
Chlorite
Zeolite
Hematite
Epidote

Estimated volume percent:

Texture:

Medium grained subhedral to euhedral plagioclase and anhedral (round) to euhedral k-spar set in a finely crystalline to microcrystalline plagioclase lath and k-spar groundmass; glomerocrysts are locally evident; platy chlorite comprises 5-10% of rock, possible replacement of Fe mineral (hornblende?); calcite preferentially replaces plagioclase; zeolite occurs as radial reaction rims and as chlorite replacement; hematite(?) forms opaque rims; epidote locally replaces hornblende(?)

Rock Name:

Medium grained dacite porphyry (may be close to trachyte)

Sample Number

152JBM92

Formation Name

Harrison Lake Fm.
Echo Island Member

Mineral

Plagioclase
Quartz
Sanadine
Pyrite(secondary)

Estimated Volume Percent

5-10%
10-15%
5-10%
5%

Matrix

70%

Texture:

Fine siltstone, consisting of angular, broken fragments of plagioclase, quartz, sanadine set in an microcrystalline/aphanitic clay rich matrix. Texturally immature. Grains are fine-sand to medium silt, angular, locally acicular, moderately sorted, weakly laminated. Grains are broken. Segregation in section consists of curvilinear tracts of clay and organic rich material separating more silt rich zones; interpreted to be bioturbated. Matrix consists of altered feldspathic material, clay, and aphanitic organic material. Pyrite forms euhedral crystals of fine to medium sand size, obviously secondary. Subhedral epidote common, minor calcite.

Rock Name:

Bioturbated tuffaceous feldspathic quartz-bearing siltstone

Sample Number:

153JBM92

Formation Name:

Harrison Lake Fm.

Mineral:

Volcanic lithics
Plagioclase
K-spar
Cement
calcite

Estimated volume percent:

25-30%
35%
15%
20-25%

Texture:

Angular to subrounded medium to coarse grained volcanic lithics (andesite to dacite porphyry and minor tuff), angular to subangular fine to medium grained, partially sericitized, locally zoned plagioclase; subangular k-spar; matrix supported, set in calcite matrix with minor clay; poorly sorted

Rock Name:

Medium to coarse grained, subangular to subrounded, poorly sorted lithic feldspathic arenite

| | | | |
|----------------|-------------------------------|---------------------------|-------------------|
| Sample Number: | 154JBM92 | Formation Name: | Harrison Lake Fm. |
| Mineral: | | Estimated volume percent: | |
| | Plagioclase | | 35% |
| | Volcanic lithics | | 20% |
| | K-spar | | 15% |
| | Quartz | | <2% |
| | Matrix/Cement clay/calcite | | 30% |

Texture: Angular to subangular fine to medium grained plagioclase (sericitized in part) and lesser k-spar (oscillatory zoned in part), with minor quartz(?), and subrounded to rounded, medium grained volcanic lithics (altered dacite to andesite porphyry); volcanic lithics and matrix chloritized; matrix supported, with a matrix of clay and secondary? calcite; exhibits fine to medium laminations; moderately well sorted, plagioclase grains oriented parallel to laminae; finer laminae preferentially iron stained

Rock Name:
Fine to medium grained, moderately well sorted lithic feldspathic wacke

| | | | |
|----------------|-------------|---------------------------|-------------------|
| Sample Number: | 155JBM92 | Formation Name: | Harrison Lake Fm. |
| Mineral: | | Estimated volume percent: | |
| | K-spar | | ~10% |
| | Plagioclase | | ~10% |
| | Quartz | | 5% |
| | Matrix | | |

Texture: Matrix supported, angular to subangular matrix is locally replaced by "splotchy" calcite

Texture: Fine to very fine grained; angular to subangular plagioclase, locally sericitized; angular to subangular k-spar, very minor undulose extinction quartz; subrounded to rounded fine-grained volcanic lithics; moderately sorted; matrix supported, with clay matrix; sample contains abundant very fine grained plagioclase laths, locally oriented parallel to laminae, locally chaotically mixed within matrix; sample is interpreted as medium to fine grained lithic feldspathic siltstone with locally abundant tuffaceous content (plag laths are assumed to be primary pyroclastics)

Rock Name:
fine to medium grained lithic feldspathic tuffaceous siltstone

| | | | |
|----------------|-------------------------|---------------------------|-------------------|
| Sample Number: | 155JBM92 | Formation Name: | Harrison Lake Fm. |
| Mineral: | | Estimated volume percent: | |
| | K-spar | | ~10% |
| | Plagioclase | | ~10% |
| | Quartz | | 5% |
| | Matrix | | |
| | clay with minor calcite | | 75% |

Texture: Matrix supported, angular to subangular fine to very fine grained clasts of k-spar, plagioclase, and quartz set in a clay-rich matrix; locally contains bioturbation features, which consist of lenticular 'blebs' of dark, carbon rich?, silt, irregularly surrounded by silty matrix, appears ripped up

Rock Name:
Bioturbated feldspathic siltstone

| | | | |
|----------------|-------------------------|---------------------------|-------------------|
| Sample Number: | 156JBM92 | Formation Name: | Harrison Lake Fm. |
| Mineral: | | Estimated volume percent: | |
| | Volcanic lithics | | 30-35% |
| | Plagioclase | | 25% |
| | K-spar | | 20% |
| | Quartz | | <2% |
| | Matrix | | |
| | clay, sericite, calcite | | 20-25% |

Texture:

Altered sandstone; medium to coarse grained, subangular to subrounded, locally highly sericitized plagioclase and medium grained k-spar, medium to coarse grained, finely crystalline volcanic lithics, locally highly seritized; minor fine to medium grained, undulose extinction quartz; difficult to distinguish altered plagioclase vs. altered fine-grained volcanic matrix; matrix to clast supported, matrix consists of clay, sericite, and calcite; chloritization is locally heavy; poorly sorted; alteration products consist of chlorite, zeolite, calcite (replaces both clasts and matrix); clasts locally flattened

Rock Name:

Medium to coarse grained, poorly sorted feldspathic lithic wacke

Sample Number:

157JBM92

Formation Name:

Harrison Lake Fm.

Mineral:

Estimated volume percent:

Plagioclase (detrital)

10%

K-spar

10%

Volcanic lithics

20%

Quartz

<3%

Matrix

clay + locally abundant plag laths

~60%

Note: matrix is locally replaced by "splotchy" calcite

Texture:

Fine to very fine grained; angular to subangular plagioclase, locally sericitized; angular to subangular k-spar, very minor undulose extinction quartz; subrounded to rounded fine-grained volcanic lithics; moderately sorted; matrix supported, with clay matrix; sample contains abundant very fine grained plagioclase laths, locally oriented parallel to laminae, locally chaotically mixed within matrix; sample is interpreted as medium to fine grained lithic feldspathic siltstone with locally abundant tuffaceous content (plag laths are assumed to be primary pyroclastics)

Rock Name:

fine to medium grained lithic feldspathic tuffaceous siltstone

Sample Number

284JBM92

Formation Name

Harrison Lake Fm.

Echo Island Member

Mineral

Estimated Volume Percent

Plagioclase

35%

Quartz

5%

Lithics

2%

Chloritoid filled voids

5-10%

Groundmass

~50%

Texture:

Fine-grained subtrachytic plagioclase microlites floating in a dark brown cryptocrystalline groundmass, with subhedral/broken? grains of quartz, k-spar, plagioclase. Abundant chloritoid-filled vesicles/voids, roughly elongate with subtrachytic textures, angular terminations. Minor coarse-grained subrounded altered porphyritic lithic fragments. Prominent dark brown, semi-translucent alteration mineral????

Rock Name:

Fine-grained lithic vitric crystal tuff

Sample Number

290JBM92

Formation Name

Harrison Lake Fm.

Weaver Lake Member

Mineral

Estimated Volume Percent

Plagioclase

30%

Chlorite after Px?

5%

brown grungy mineral

5%

Matrix

60%

Texture:

Rock is equigranular porphyritic, with coarse grained euhedral to subhedral plagioclase crystals and subhedral pyroxene? crystals set in a pilotaxitic groundmass comprised of plagioclase microlites and possible k-spar. Plagioclase is locally glomerocrystic with mafic crystals. Large 1-2 mm rounded vesicles(?) are filled with chlorite and locally replaced by polycrystalline quartz. Plagioclase contains abundant chloritized mafic inclusions, and is locally altered to epidote. Matrix is strongly chloritized, and contains evenly dispersed epidote blebs

Rock Name:

Dacite Porphyry

Sample Number

293JBM92

Formation Name

Harrison Lake Fm.

| Mineral | Weaver Lake Member |
|-------------|--------------------------|
| | Estimated Volume Percent |
| Quartz | 10% |
| Sanadine | 5% |
| Plagioclase | 10% |
| Zircon | tr |
| Groundmass | 75% |

Texture:

Sanadine, plagioclase, quartz porphyry consisting of sub to euhedral coarse grained sanadine, subhedral plagioclase, and anhedral quartz. Plagioclase is altered, sausseritized, with calcite and locally albite? replacement. Sanadine displays clear square cross sections in part. Quartz is broken up, and embayed in part. Groundmass is microcrystalline to cryptocrystalline, consisting of intergrown potassium feldspar and quartz. Calcite alteration common

Rock Name:

CAYOOSH ASSEMBLAGE

| Sample Number | Formation Name |
|----------------|--------------------------|
| 165JBM92 | Cayoosh Assemblage |
| Mineral | Estimated Volume Percent |
| Muscovite | 40% |
| Sillimanite | 5% |
| Zoicite | 25% |
| drusy mineral? | 30%? |

Texture:

Granoblastic; fine to medium grained randomly oriented assemblage of muscovite, sillimanite?, zoicite. Muscovite occurs as radiating fibrous bundles with minor intergrown sillimanite; zoicite occurs as distinctly bluish pleochroic, euhedral, fine grained crystals. Muscovite bundles occur in "swirl pattern", and zoicite and muscovite are not randomly distributed, but occur in distinct circular zones

Rock Name:

zoicite muscovite schist????

| Sample Number | Formation Name |
|---------------------|------------------------------|
| 181JBM92 | Cayoosh Assemblage Unit 3 |
| Mineral | Estimated Volume Percent |
| quartz | 25% |
| k-spar | 15% |
| plagioclase | 15 |
| volcanic lithics | 10-30% |
| sedimentary lithics | 10-20% |
| matrix | 20% |

Texture:

Fine to medium grained sandstone: moderately well sorted, subangular to subrounded lithic quartz-rich feldspathic wacke, consisting of fine to medium grained monocrystalline quartz with undulose extinction, polycrystalline quartz, medium grained k-spar (sanadine in part?), fine-grained plagioclase, medium grained porphyritic volcanic lithic fragments, rare plutonic fragments, altered fine grained sedimentary lithic fragments. Much of the fine grained polycrystalline fragments may be recrystallized chert. Strong sericitic to muscovite alteration assemblage, particularly in matrix and on plagioclase grains; matrix locally contains fine-grained polycrystalline quartz; rock has moderately foliated texture

Rock Name:

quartz-bearing lithic feldspathic wacke

BOSTON BAR FORMATION

| | |
|----------------------|---------------------------------|
| Sample Number | Formation Name |
| 41JBM92 | Boston Bar Fm. |
| Mineral | Estimated Volume Percent |
| Andalusite | |
| Texture: | |
| Rock Name | |
| Andalusite schist | |

DEWDNEY CREEK FORMATION

| | |
|----------------------|---------------------------------|
| Sample Number | Formation Name |
| 186JBM92 | Dewdney Creek Fm. |
| Mineral | Estimated Volume Percent |
| volcanic lithics | 60% |
| plagioclase | 25% |
| pyroxene | 5% |
| plutonic rock frags? | tr |
| quartz - polyxln | tr |
| matrix | 10% |

Texture:

Fine to medium grained, poorly to moderately sorted, volcanic sandstone, consisting of fine to medium grained, subrounded volcanic lithics (primarily fine grained to aphanitic tuff clasts, locally containing plagioclase microlites; rare porphyritic clasts), fine to medium grained plagioclase grains, fine grained angular pyroxene grains in a clay/chlorite rich matrix. Low grade alteration assemblage of chlorite, calcite, minor epidote. Grain to grain contacts. Dark brown (hematitic?) alteration rinds around many lithics

Rock Name:

fine to medium grained lithic wacke

| | |
|----------------------|---------------------------------|
| Sample Number | Formation Name |
| 187JBM92 | Dewdney Creek Fm. |
| Mineral | Estimated Volume Percent |
| plagioclase | 50-60% |
| volcanic lithics | 20-25% |
| pyroxene | tr |
| matrix | 15-25% |

Texture:

Fine grained moderately sorted feldspathic sandstone with a bimodal grain size distribution consisting of fine to medium grained rounded to subrounded volcanic lithics and rare angular plagioclase grains floating in a fine grained matrix composed of angular to subangular plagioclase grains, minor rounded volcanic lithics and rare angular to subangular pyroxene. Strong alteration includes saussuritization of plagioclase - most feldspar has strong epidote alteration, chloritization of volcanic lithics, and local calcite replacement

Rock Name

fine-grained volcanic lithic feldspathic wacke

| | |
|----------------------|---------------------------------|
| Sample Number | Formation Name |
| 202JBM92 | Dewdney Creek Fm. |
| | Lookout Mtn |
| Mineral | Estimated Volume Percent |
| volcanic lithics | 75-80% |
| plagioclase | 10-15% |

| | |
|----------|------|
| sanadine | 5% |
| matrix | <10% |

Texture

Submature very coarse sand to fine pebble conglomerate: moderately well sorted volcanic conglomerate consisting of well rounded to subrounded clasts of volcanic lithics (porphyritic andesite to dacite, crystal tuff with trachytic plagioclase microlites, very fine grained to aphanitic clasts), angular to subangular medium to coarse grained plagioclase, subangular to subrounded (partially resorbed), commonly fractured very clear sanadine. Clasts are in grain to grain contact, with locally "bent" contacts (i.e.) modified by compaction; clasts locally float in a hematitic clay-rich matrix. Hematitic staining/cement is evident around grains. Minor epidote replaces feldspar; chlorite preferentially replaces mafics within clasts and fine-grained to aphanitic clasts

Rock Name:

submature volcanic fine to very fine pebble conglomerate

| | |
|------------------------|---------------------------------|
| Sample Number | Formation Name |
| 206JBM92 | Dewdney Creek Fm. |
| Mineral | Estimated Volume Percent |
| plagioclase | 50% |
| sanadine | 25% |
| volcanic lithics | 10-15% |
| matrix (chlorite/clay) | 10-15% |

Texture:

Moderately well sorted submature feldspathic sandstone, consisting of coarse to very coarse grained angular to subangular plagioclase grains, coarse grained subangular to subrounded very clear, fractured sanadine grains, and subrounded volcanic lithics (primarily crystal tuff, locally porphyritic). Matrix is presumed to be clay altered primarily to chlorite; minor hematitic alteration. Plagioclase varies from incipiently altered to partially replaced by epidote

Rock Name:

Submature coarse grained sanadine-bearing feldspathic arenite

| | |
|----------------------|---------------------------------|
| Sample Number | Formation Name |
| 207JBM92 | Dewdney Creek Fm. |
| | Lookout Mtn section |
| Mineral | Estimated Volume Percent |
| sanadine | 35% |
| plagioclase | 30% |
| volcanic lithics | 25% |
| pyroxene | tr |
| matrix | <10% |

Texture:

Submature, moderately sorted coarse to very coarse grained sandstone, consists of angular to subangular, fractured, very clear sanadine, angular to subangular, altered plagioclase, subrounded to rounded volcanic lithics (crystal tuffs, porphyritic andesite to dacite). Alteration is strong, consisting of biotite replacement of pyroxene, chloritization of volcanic lithics and matrix, and epidotization of feldspars.

Rock Name:

sanadine-bearing lithic feldspathic arenite

| | |
|----------------------|---------------------------------|
| Sample Number | Formation Name |
| 216JBM92 | Dewdney Creek Fm. |
| Mineral | Estimated Volume Percent |
| volcanic lithics | 40% |

| | |
|-------------|--------|
| plagioclase | 20% |
| quartz | 15-20% |
| k-spar | 10% |
| tourmaline | 5 |
| matrix | 15-20% |

Texture:

Crudely laminated, fine to medium grained volcanic sandstone; consists of rounded to subrounded medium grained volcanic lithics (primarily tuff clasts, with plagioclase microlites, or fine-grained to aphanitic, altered; rarely porphyritic); angular, fine to medium grained, clear, conchoidal fractured quartz; angular to subangular, medium to fine grained, sausseritized k-spar, angular fine to medium grained plagioclase; angular (euhedral), blue pleochroic, fine grained tourmaline, locally displaying well developed zonation and radiating bundles of euhedral crystals. Matrix is fine-grained/aphanitic, believed to be comprised of volcanic clay. Alteration assemblage includes chlorite (esp. of volcanic lithics), calcite

Rock Name:

quartz, tourmaline-bearing feldspathic lithic wacke

| Sample Number | Formation Name |
|------------------|--------------------------------------|
| 257JBM92 | Dewdney Creek Fm. Dewdney Ck area |
| Mineral | Estimated Volume Percent |
| volcanic lithics | 50% |
| plagioclase | 30% |
| matrix | 20% |

Texture:

Submature, moderately sorted volcanic sandstone: medium to coarse grained, consisting of subangular to rounded volcanic lithics (crystal tuff, feldspar porphyry/dacite) and medium to coarse grained plagioclase feldspar, with rare relict glomerocrysts. Matrix is dark, aphanitic, with minor fine grained plagioclase. Alteration assemblage consists of chlorite replacement of plagioclase and matrix.

Rock Name:

Medium to coarse grained feldspathic lithic wacke

| Sample Number | Formation Name |
|------------------|--------------------------|
| 268JBM92 | Dewdney Creek Fm. |
| Mineral | Estimated Volume Percent |
| volcanic lithics | 60% |
| plagioclase | 20 |
| sanadine | 5 |
| pyroxene | tr |
| matrix | 15+ |

Texture:

Coarse to very coarse grained immature poorly sorted volcanic sandstone, containing subangular to subrounded coarse to very coarse grained volcanic lithics (primarily crystal tuff with trachytic plagioclase microlites, lesser porphyritic volcanics), clast supported; plagioclase is coarse grained, angular; sanadine is rounded (probably partially resorbed) to subrounded, clear. Matrix is dark, aphanitic, with minor fine-grained plagioclase. Alteration assemblage includes minor chloritization, calcite replacement. This rock appears to be a reworked pyroclastic sediment

Rock Name

Coarse to very coarse grained feldspathic lithic wacke

APPENDIX E
CURRENT RESEARCH PUBLICATIONS

- E1 - Mahoney, J.B., 1992, Middle Jurassic stratigraphy of the Lillooet area, south-central British Columbia; in Current Research. Part A; Geological Survey of Canada, Paper 92-1A, p. 243-248.
- E2 - Mahoney, J. Brian, 1993, Facies reconstructions in the Lower to Middle Jurassic Ladner Group, southern British Columbia; in Current Research. Part A; Geological Survey of Canada, Paper 93-1A, p. 173-182.
- E3 - Mahoney, J.B., and Journeay, J.M, 1993, The Cayoosh Assemblage, southwestern British Columbia: last vestige of the Bridge River Ocean; in Current Research. Part A; Geological Survey of Canada, Paper 93-1A, p. 235-244.
- E4 - Journeay, J.M. and Mahoney, J.B., 1994, Cayoosh Assemblage: regional correlations and implications for terrane linkages in the southern Coast Belt, British Columbia; in Current Research. Part A; Geological Survey of Canada, Paper 93-1A, p. 165-175.

Middle Jurassic stratigraphy of the Lillooet area, south-central British Columbia

J. Brian Mahoney¹
Cordilleran Division, Vancouver

Mahoney, J.B., 1992: Middle Jurassic stratigraphy of the Lillooet area, south-central British Columbia; in *Current Research, Part A*; Geological Survey of Canada, Paper 92-1A, p. 243-248.

Abstract

An elongate outcrop belt (~75 km long) of Middle Jurassic volcanic sandstone occurs on the northeast side of the Yalakom Fault from south of Lillooet to the headwaters of the Yalakom River. This unnamed unit comprises granule to pebble volcanic conglomerate, arkosic litharenite, laminated siltstone, and carbonaceous shale lithofacies. The stratigraphic base of the unit is not exposed, and the lower contact is everywhere the Yalakom Fault. The upper contact is a disconformity(?) with the overlying Cretaceous Jackass Mountain Group. Ammonite biostratigraphy indicates an Aalenian to Bajocian age. Paleocurrent indicators suggest transport to the northeast during deposition. The Middle Jurassic volcanic sandstone unit records mass sediment gravity flow deposition in a marine basin proximal to a volcanic source during Aalenian to Bajocian time.

Résumé

Un affleurement de grès volcanique du Jurassique moyen (~75 km de longueur) s'allonge sur le compartiment nord-est de la faille Yalakom, du sud de Lillooet jusqu'au cour supérieur de la rivière Yalakom. Cette unité non désignée comprend un conglomérat volcanique caillouteux, une arénite lithique arkosique, un siltstone laminé et un lithofaciès de shale carboné. La base stratigraphique de l'unité n'est pas exposée, et le contact inférieur est partout constitué de la faille Yalakom. Le contact supérieur est une discordance (?) avec le groupe de Jackass Mountain du Crétacé sus-jacent. La biostratigraphie des ammonites indique un âge de l'Aalénien au Bajocien. Les indicateurs de paléocourants révèlent un transport vers le nord-est durant la sédimentation. L'unité de grès volcanique du Jurassique moyen révèle une sédimentation par coulée de gravité dans un bassin marin à proximité d'une source volcanique durant la période allant de l'Aalénien au Bajocien.

¹ University of British Columbia, Department of Geological Sciences, 6339 Stores Road, Vancouver, B.C. V6T 2B4

INTRODUCTION

A Middle Jurassic volcanic sandstone exposed along the Yalakom River, northwest of Lillooet, was examined during the 1991 field season. Detailed mapping and stratigraphic analysis document lateral and vertical facies changes, clarify regional stratigraphic relations, and define the depositional environment. The strata record submarine mass sediment gravity flow deposition adjacent to a volcanic source during Aalenian-Bajocian time.

This investigation is part of a regional study of mid-Jurassic stratigraphy in south-central British Columbia concentrating on stratigraphic analysis and regional correlation. The purpose of the study is to constrain the timing of orogenic events during the middle to late Jurassic. Documentation of the stratigraphy, age range, and depositional environment of the middle Jurassic volcanic sandstone will aid in regional stratigraphic correlation and Jurassic basin reconstruction. The study is part of a doctoral thesis jointly sponsored by Geological Survey of Canada and The University of British Columbia, Department of Geological Sciences. Field work during the 1991 field season concentrated on the area northeast of the Yalakom Fault (Fig. 1), in conjunction with regional 1:50 000 scale mapping of the Taseko Lakes (920) map area.

REGIONAL GEOLOGY

Middle Jurassic volcanic sandstone is exposed on the west side of the Fraser fault in an approximately 75 km long, northwest-trending outcrop belt that extends from the junction of the Fraser and Yalakom faults near Lillooet to the headwaters of the Yalakom River on the northeast side of the Yalakom Fault (Fig. 1). Northeast of the Yalakom Fault the unit is steeply southwest dipping, overturned, and youngs to the northeast. The Yalakom Fault separates the unit from structurally complex imbricate fault slices of the Bridge River complex and the structurally higher Triassic Hurley Formation (Fig. 1).

In the study area, the Yalakom Fault is a high angle, vertical to east dipping structure that parallels bedding in the volcanic sandstone unit. The Yalakom Fault forms the base of the volcanic sandstone unit, and, near this contact, the unit contains west vergent mesoscopic folds with northwest-trending fold axes that parallel the trace of the fault.

The Yalakom Fault is interpreted as a dextral strike-slip fault with offset of 80 to 190 km, based on stratigraphic displacements and kinematic indicators within the fault zone (Tipper, 1978; Monger, 1985; Glover et al., 1988; Schiarizza et al., 1990). The presence of fault-parallel west vergent mesoscopic folds adjacent to the fault, the bedding-parallel attitude of the fault, and the apparent lack of strike-slip shear features in the volcanic sandstone unit near the fault suggest reverse movement along the Yalakom Fault has been significant in the study area.

The volcanic sandstone unit is overlain by lithic sandstone and conglomerate of the mid-Cretaceous (Barremian to Albian) Jackass Mountain Group with no apparent structural discordance. Both the volcanic sandstone and the overlying Jackass Mountain Group strata are deformed into simple, northwest-trending megascopic folds. The lack of structural discordance and similarity in structural style between the formations suggest the contact may be a disconformity.

PREVIOUS INVESTIGATIONS

Duffell and McTaggart (1952) mapped a sequence of argillite, greywacke, volcanic conglomerate and tuffaceous sandstone near Lillooet as the Lower Cretaceous Lillooet Group. Leech (1953) mapped middle Jurassic volcanic sandstone along the Yalakom River, north of the area described by Duffell and McTaggart (1952). Trettin (1961) described the Lillooet Group between the Bridge River and Lillooet, measured stratigraphic sections, and subdivided the unit into 3 divisions. Frebold et al. (1969) briefly described the lithology and paleontology of the unit at the northern end of the outcrop belt.

Woodsworth (1977) mapped the volcanic sandstone unit described by Trettin (1961) as the upper Jurassic-lower Cretaceous Relay Mountain Group. Tipper (1978) correlated the rocks east of the Yalakom River with the lower Jurassic Tyaughton Group. Monger (1989) abandoned the name Lillooet Group for the rocks near Lillooet, and correlated the strata with the upper Jurassic-lower Cretaceous Relay Mountain Group. They remapped a small area near the confluence of the Bridge and Fraser rivers as the Lower Jurassic Ladner Group (Fig. 2). Schiarizza et al. (1990) mapped the volcanic sandstone described by Leech (1953) and Woodsworth (1977) along the Yalakom River as an unnamed mid-Jurassic volcanic sandstone (mJvs), and suggested a tentative correlation between the rocks along the Yalakom River and those near Lillooet.

The stratigraphic nomenclature in the literature is confusing due to discontinuous exposure, a lack of fossils, and the wide age range of the fossils that have been recovered (Table 1). Geological mapping, stratigraphy, and paleontology completed during this study document the lateral continuity of the unit throughout its outcrop belt, and indicate that the rocks near Lillooet are continuous with those to the northwest along the Yalakom River.

STRATIGRAPHY

Lithofacies

The middle Jurassic volcanic sandstone unit comprises granule to pebble volcanic conglomerate, arkosic litharenite, laminated siltstone and carbonaceous shale lithofacies. Whereas the recessive weathering fine-grained lithofacies are volumetrically more abundant, the resistant arkosic litharenite and conglomerate lithofacies form prominent ribs throughout the outcrop belt and locally dominate the stratigraphy. A 585 m thick partial section was measured along the Yalakom River northeast of its confluence with

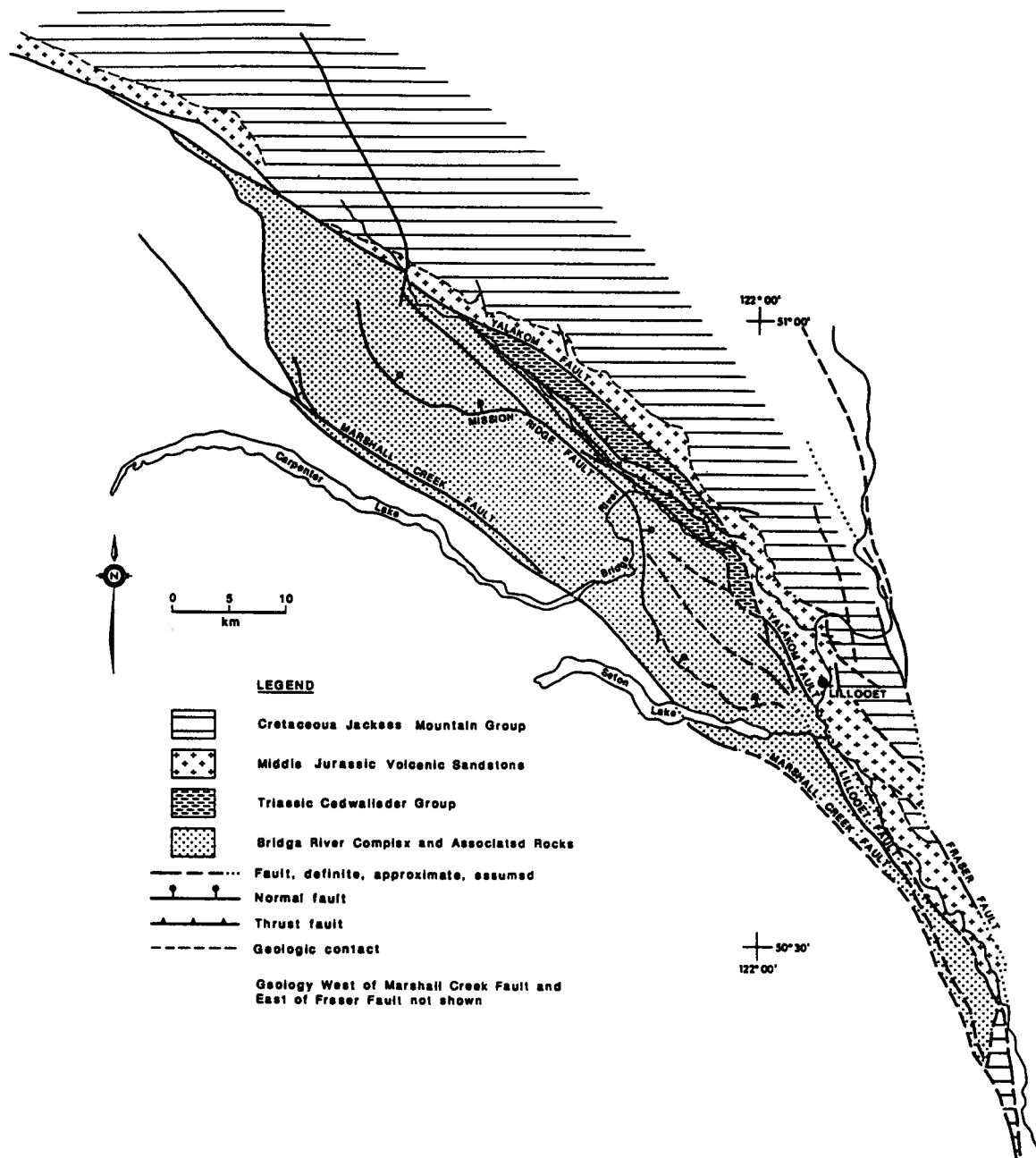


Figure 1. Simplified geologic map of the Lillooet area, showing major faults and the distribution of the middle Jurassic volcanic sandstone unit and associated units. Modified from Woodsworth (1977), Coleman (1989), Monger (1989), Schiarizza, et al. (1990).

Blue Creek (Fig. 2). The maximum thickness of the unit is estimated to be approximately 800 m. The stratigraphic base of the unit is not exposed; the basal contact of the unit is everywhere the Yalakom Fault. An unknown amount of section has been structurally removed. The upper contact of the unit is an unconformity with the overlying Jackass Mountain Group.

The granule to pebble conglomerate lithofacies is medium to thick bedded, and contains angular to subangular clasts of chert, volcanic, and minor sandstone clasts in a medium- to coarse-grained, poorly sorted arkosic litharenite matrix. Angular plagioclase feldspar crystals are locally abundant in the matrix. Abundant platy, angular to subangular mudstone clasts (2-8 cm) commonly occur near the base of beds, and display a preferential alignment parallel to bedding. Bedding appears tabular and laterally continuous, although lenticular beds 25 to 30 m wide and 1 to 2 m deep occur locally. Beds have sharp, scoured basal contacts and are commonly graded. The conglomerate lithofacies displays well-developed fining and thinning upward sequences (1-2 m thick). Thick-bedded, structureless conglomerate grades upward into thin- to medium-bedded, medium- to coarse-grained arkosic litharenite, which is gradationally overlain by thin-bedded, parallel laminated fine- to coarse-grained siltstone. Individual 1 to 2 m thick conglomerate to siltstone sequences aggregate into 5 to 15 m thick fining and thinning upward intervals; each successive conglomerate/siltstone sequence is more fine-grained and thinly bedded than the one below.

The arkosic litharenite lithofacies consists of medium to thick bedded (0.25-1 m), medium to coarse grained, moderately sorted, arkosic volcanic lithic sandstone characterized by an abundance of angular (euhedral) plagioclase grains. Beds are commonly graded, have sharp bases, and become finer grained and parallel laminated near the upper contact. Pebble to granule conglomerate stringers are locally abundant, particularly near the base of beds. Angular mudstone clasts occur locally at the base of beds. Fining and thinning upward sequences are common. Medium- to thick-bedded, medium- to coarse-grained

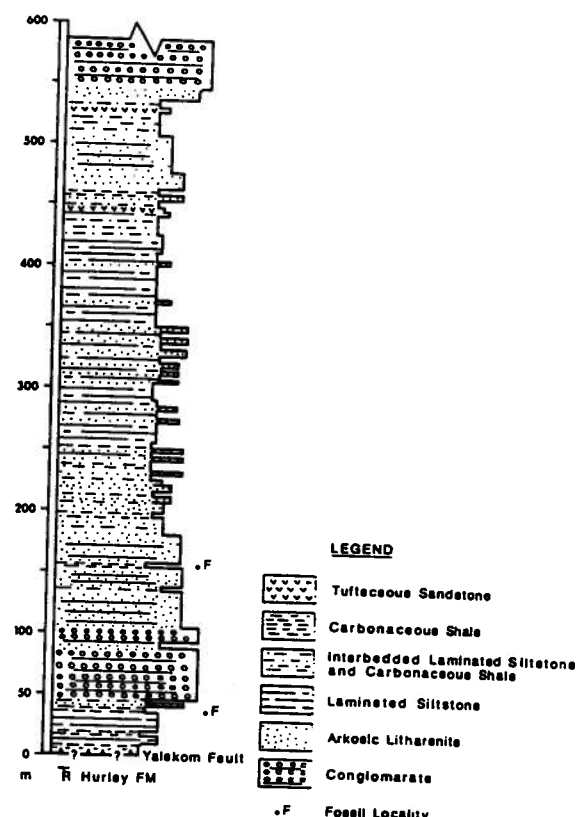


Figure 2. Measured stratigraphic section of the middle Jurassic volcanic sandstone unit. Section measured upstream from the confluence of Blue Creek and the Yalakom River (10U EN, 537800mE, 565370mN)

Table 1. Review of Jurassic stratigraphic nomenclature near Lillooet, B.C.

| Formation name | age | location | author |
|------------------------------------|------------------------------|---|----------------------------|
| Lillooet Group | Neocomian* | Lillooet | Duffel and McTaggart, 1952 |
| unnamed | Aalenian* | Blue Creek | Leech, 1953 |
| Lillooet Group | Neocomian | Bridge River | Trettin, 1961 |
| unnamed | Bajocian* | Blue Creek | Frebold, et al., 1969 |
| Relay Mountain Group | U. Jurassic to L. Cretaceous | east of Yalakom R. | Woodsworth, 1977 |
| Tyughton Group | Sinemurian to Bajocian | east of Yalakom R. | Tipper, 1978 |
| Relay Mountain Group | Neocomian | Lillooet | Monger, 1989 |
| middle Jurassic volcanic sandstone | Aalenian to Bajocian | east of Yalakom R. | Schriazza et al., 1990 |
| middle Jurassic volcanic sandstone | Aalenian to Bajocian* | east of Yalakom R. to south of Lillooet | this study |

* Indicates new data presented

sandstone grades upward into thin- to medium-bedded, fine-grained sandstone to coarse siltstone that is capped by dark grey fine- to medium-grained siltstone. The arkosic litharenite lithofacies locally aggregates to 10 to 25 m, but commonly occurs as medium- to thick-bedded interbeds within the conglomerate lithofacies, or as thin beds intercalated within the fine-grained lithofacies.

The laminated siltstone lithofacies is composed of thin-bedded fine- to coarse-grained siltstone and very fine grained sandstone. The lithofacies commonly consists of rhythmic interbeds of thin bedded, parallel to crosslaminated, fine sandstone to coarse siltstone gradationally overlain by thin-bedded, parallel laminated fine siltstone to mudstone. Tuffaceous intervals occur locally. The laminated siltstone lithofacies commonly occurs near the top of coarse-grained intervals, where it may be intercalated with the conglomerate or arkosic litharenite lithofacies, or may form homogeneous sequences up to 50 to 60 m thick. Wood fragments are common on bedding planes.

The carbonaceous shale lithofacies consists of thin bedded, thinly laminated, fissile dark grey shale with locally abundant ammonite and *Buchia* pelecypod impressions. The lithofacies occurs as thin beds intercalated with all other lithofacies, and does not aggregate to greater than 1 m. Faunal impressions are most abundant in the 0.25 to 1 m thick carbonaceous shale intervals. The lithofacies comprises less than 20% of the entire unit.

Minor amounts of thin-bedded, silty micrite and micritic siltstone occur throughout the unit as thin ribs within the laminated siltstone or carbonaceous shale lithofacies. The calcium carbonate content apparently fluctuates throughout the unit, but is highest in the fine-grained lithofacies that are devoid of coarse clastic detritus.

Age

Duffell and McTaggart (1952) assigned an Early Cretaceous age to the Lillooet Group based on pelecypods (??) (*Aucella*) collected south of Lillooet (Table 1). Trettin (1961) supported the Neocomian age determination. Monger (1989) correlated the rocks north of Lillooet with the Upper Jurassic Relay Mountain Group based on lithological similarities and the pre-existing fossil collections of Duffell and McTaggart (1952). However, Monger (1989) mapped a small area at the confluence of the Bridge and Fraser rivers as Ladner Group, based on a probable early Jurassic ammonite.

Leech (1953) and Frebold et al. (1969) collected Aalenian to Bajocian ammonites from the northern end of the outcrop belt. In the same area, two new fossil collections from the measured section (from 46 and 155 m) yielded specimens of *Tmetoceras scissum*, an Aalenian ammonite (P.L. Smith, written comm., 1991). A new fossil collection above the confluence of the Bridge and Fraser rivers, near the southern end of the outcrop belt, yielded the Bajocian ammonite *Stephanoceras* (P.L. Smith, written comm., 1991). This collection is believed to be from the upper one-third of the volcanic sandstone unit, suggesting the entire unit may be Aalenian to Bajocian.

Detailed mapping demonstrates that the Aalenian to Bajocian strata described by Leech (1953), Frebold et al. (1969) and in this report is laterally continuous with the Lillooet Group of Duffell and McTaggart (1952). This correlation suggests the age of the Lillooet Group is Aalenian to Bajocian. The Neocomian age reported by Duffell and McTaggart (1952) is problematic, as the stratigraphic position the Neocomian fauna is unknown. This fauna may indicate a disconformity within the volcanic sandstone unit, or may have been recovered from a lithologically similar but unrelated unit. Detailed mapping and stratigraphic analysis south of Lillooet is needed to resolve this question.

Paleocurrents

The majority of the mid-Jurassic volcanic sandstone unit is structureless or parallel laminated, and paleocurrent indicators are rare. Flute casts measured at the base of arkosic litharenite beds in two stratigraphic levels (at 75 m and 420 m) indicate a northeast (020-040°) paleocurrent during deposition (n=18).

DEPOSITIONAL ENVIRONMENT

The lithofacies in the middle Jurassic volcanic sandstone are interpreted as the product of mass sediment gravity flow in a subwave base marine environment. The conglomerate lithofacies and interbedded arkosic litharenite represent top-cut-out (TAB) coarse-grained turbidites, with minor complete (TABCDE) turbidites. The apparently tabular and laterally continuous conglomerate beds locally contain shallow channel features, and are lenticular on a kilometre scale. Abundant fining and thinning upward stratigraphic intervals suggest deposition by a migrating distributary system. Angular mudstone clasts are interpreted as rip-up clasts due to basal scour by mass sediment gravity flows.

The arkosic litharenite lithofacies consists primarily of top-cut-out turbidites (TAB). Granule to pebble stringers within massive, thick-bedded arkosic litharenite are interpreted as lag deposits within amalgamated TAAA sequences. Beds are tabular and laterally continuous, have sharp bases and graded bedding, and display no evidence of channelling, suggesting deposition by unchanneled turbidity currents.

The laminated siltstone lithofacies comprises base-cut-out partial turbidites (TCDE,DE), as indicated by the sharp basal contacts, graded bedding, parallel and crosslaminations, and the tabular, laterally continuous character of the lithofacies. The carbonaceous shale lithofacies represents hemipelagic deposition during periods of reduced clastic influx. A hemipelagic interpretation is supported by the significant amount of faunal preservation in this lithofacies.

The lithofacies present in the middle Jurassic sandstone unit are contained in fining and thinning upward sequences that represent deposition by both channelized and unchanneled turbidity currents in a migrating distributary system. The conglomerate lithofacies is interpreted to be

deposited in shallow anastomosing channels in the mid-fan region of a submarine fan. The arkosic litharenite and laminated siltstone lithofacies were deposited by unchanneled turbidity currents in the mid- to outer fan region. The carbonaceous shale lithofacies represents hemipelagic deposition between channels in the mid-fan and during periods of low clastic influx on the outer fan.

Proximity to a volcanic source is required by the abundance of volcanic debris in the middle Jurassic volcanic sandstone unit, particularly the amount of unaltered plagioclase. The angularity of the lithic clasts and preservation of coarse plagioclase grains suggest limited transport distance. The locally abundant wood debris suggests proximity to a land mass, and the minor tuffaceous interbeds indicate contemporaneous volcanism. Paleocurrent data suggest the source terrane lay to the southwest of the depositional site. The middle Jurassic volcanic sandstone unit is interpreted to represent submarine fan deposits in a marine basin near a volcanic highland, perhaps in an actively subsiding marginal basin during Aalenian to Bajocian time.

REFERENCES

- Coleman, M.
1989: Geology of Mission Ridge, near Lillooet, British Columbia (92I, J); in Geological Fieldwork 1988; British Columbia Ministry of Energy, Mines and Petroleum Resources, Paper 89-1, p. 99-104.
- Duffell, S. and McTaggart, K.C.
1952: Ashcroft map area, British Columbia; Geological Survey of Canada, Memoir 262, 122 p.
- Frebold, H., Tipper, H.W., and Coates, J.A.
1969: Toarcian and Bajocian rocks and guide ammonites from southwestern British Columbia; Geological Survey of Canada, Paper 67-10, 55 p.
- Glover, J.K., Schiarizza, P., and Garver, J.I.
1988: Geology of the Noaxe Creek map area (92O/2); in Geological Fieldwork 1987, British Columbia Ministry of Energy, Mines and Petroleum Resources, Paper 1988-1, p. 105-123.
- Leech, G.B.
1953: Geology and mineral deposits of the Shulaps Range, southwestern British Columbia; British Columbia Department of Mines, Bulletin 32, 54 p.
- Monger, J.W.H.
1985: Structural evolution of the southwestern Intermontane Belt, Ashcroft and Hope map areas, British Columbia; in Current Research, Part A; Geological Survey of Canada, Paper 85-1A, p. 349-358.
- 1989: Geology, Ashcroft, British Columbia; Geological Survey of Canada, Map 41-1989, sheet 1, scale 1:250 000.
- Schiarizza, R., Gaba, R.G., Coleman, M., Garver, J.I., and Glover, J.K.
1990: Geology and mineral occurrences of the Yalakom River area, in Geological Fieldwork 1989, British Columbia Ministry of Energy, Mines and Petroleum Resources, Paper 1990-1, p. 53-72.
- Tipper, H.W.
1978: Taseko Lakes (92O) map area; Geological Survey of Canada, Open File 534.
- Trettin, H.P.
1961: Geology of the Fraser river valley between Lillooet and Big Bar Creek; Ph.D. thesis, University of British Columbia, Vancouver, 109 p.
- Woodsworth, G.J.
1977: Pemberton (92J) map area; Geological Survey of Canada, Open File 482.

Geological Survey of Canada Project 890039

Facies reconstructions in the Lower to Middle Jurassic Ladner Group, southern British Columbia

J. Brian Mahoney¹

Cordilleran Division, Vancouver

Mahoney, J.B., 1993: Facies reconstructions in the Lower to Middle Jurassic Ladner Group, southern British Columbia; in Current Research, Part A; Geological Survey of Canada, Paper 93-1A, p. 173-182.

Abstract: The Lower to Middle Jurassic Ladner Group comprises the argillaceous Boston Bar Formation and the overlying volcanoclastic Dewdney Creek Formation. The latter is subdivided into a proximal, eastern facies and a distal, western facies. The proximal facies comprises pyroclastic rocks and lava flows, coarse grained lithic sandstone and conglomerate, and fine grained sandstone, siltstone, and argillite. This facies was deposited in a subaerial to subwave-base environment on a steep, west-dipping volcanoclastic apron by subaqueous pyroclastic flows and mass sediment gravity flows. The distal facies comprises two lithofacies: coarse grained sandstone and conglomerate and thin-bedded sandstone, siltstone and argillite. The distal facies is the product of subwave-base mass sediment flows and hemipelagic deposition on the distal portions of a volcanoclastic apron. The Middle Jurassic Lillooet Group is correlated with the western distal facies, and represents a slice of the Ladner Group offset along the dextral Fraser Fault.

Résumé : Le Groupe de Ladner, qui couvre l'intervalle du Jurassique inférieur à moyen, englobe la Formation de Boston Bar, composée de strates argileuses, et la Formation de Dewdney Creek sus-jacente, composée de roches volcanoclastiques. Cette dernière est subdivisée en un faciès est de type proximal et un faciès ouest de type distal. Le faciès proximal englobe des roches pyroclastiques et des coulées de laves, un grès lithique grossier et un conglomérat, et un grès, un siltstone et une argilite à grain fin. Ce faciès sédimentaire s'est accumulé dans un milieu subaérien passant à un milieu situé au-dessous de la base des vagues, sur une plaine d'épandage volcanoclastique de fort pendage ouest, par des coulées pyroclastiques subaquatiques et des glissements gravitaires des sédiments. Le faciès distal englobe deux lithofaciès: un grès et un conglomérat grossiers, et un grès, un siltstone et une argilite finement lités. Ce faciès distal est le produit des glissements gravitaires des sédiments au-dessous de la base des vagues et de la sédimentation hémipélagique sur les portions distales d'une plaine d'épandage volcanoclastique. Le Groupe de Lillooet du Jurassique moyen peut être corrélié avec le faciès ouest de type distal, et représente une tranche des couches décalées le long d'une faille dextre, à savoir la faille de Fraser.

¹ Department of Geological Sciences, University of British Columbia, 6339 Stores Road, Vancouver, B.C. V6T 1Z4

INTRODUCTION

The Ladner Group is a Lower to Middle Jurassic clastic succession exposed in southwestern British Columbia east of the Fraser fault system. The succession was deposited on the eastern margin of the Intermontane Belt in the Jurassic-Cretaceous Methow basin (Fig. 1). The group is subdivided into: 1) Sinemurian? to Upper Toarcian(?) Boston Bar Formation, a thick section of thin bedded argillite; and 2) Upper Toarcian to Upper Bajocian Dewdney Creek Formation, a sequence of coarse grained volcanoclastic rocks and lava flows (O'Brien, 1986, 1987).

Two distinct facies belts may be mapped within the Dewdney Creek Formation throughout its outcrop belt (Fig. 1). Delineation of these facies belts allow direct correlations to be made between the Ladner Group and Middle Jurassic Lillooet Group, exposed to the north near Lillooet on the opposite side of Fraser fault. This correlation adds additional constraints on the magnitude of transcurrent offset along the Fraser fault system (Fig. 1), and permits restoration of the original facies configuration of the Ladner Group.

This investigation is part of a regional analysis of Jurassic stratigraphy and basin configuration undertaken as a doctoral research project under the joint sponsorship of the Geological Survey of Canada and the University of British Columbia. Fieldwork in 1992 was completed under the auspices of the Chilcotin-Nechako Project, a regional mapping program in the south-central Intermontane Belt (Hickson, 1992). Field work in 1992 concentrated on a narrow outcrop belt of Jurassic strata situated between the Coast and Intermontane belts, in the Hope (92H), Pemberton (92J), and Taseko Lakes (92O) map areas.

GEOLOGICAL SETTING

The Boston Bar Formation of Ladner Group lies unconformably on oceanic greenstone and chert of the Triassic Spider Peak Formation, interpreted to be the basement of the Methow basin (Cairnes, 1924; Ray et al., 1985; Ray, 1986, 1990). Boston Bar Formation is overlain by volcanogenic sedimentary rocks of the Dewdney Creek Formation of Ladner Group. Dewdney Creek Formation is in turn locally overlain unconformably by sandstone and conglomerate of the Upper Jurassic Thunder Lake sequence and the Lower Cretaceous Jackass Mountain Group (Monger, 1970; Coates, 1974; O'Brien, 1986).

Methow basin strata comprise Lower Jurassic to Upper Cretaceous rocks exposed east of the Yalakom and Hozameen fault systems (Garver, 1992), and west of the Pasayten Fault. The Pasayten Fault separates Jurassic and Cretaceous basinal sediments from gneisses and plutonic rocks of the Late Permian-Triassic Mount Lytton Complex and the Late Jurassic Eagle Plutonic complex (Greig, 1989; Friedman and van der Heyden, 1992) (Fig. 1). The eastern limit of Jurassic strata is the Chuwanten fault, an east-vergent thrust fault that places Jurassic strata over Cretaceous rocks

(Monger, 1989) (Fig. 1). The western limit of Methow basin strata south of Boston Bar is the Hozameen fault system, which separates Methow strata from Permian to Jurassic oceanic greenstones and chert of Hozameen Group (Monger, 1970, 1989; Ray, 1986, 1990).

North of Lytton, black siltstone, argillite, sandstone and conglomerate of the Aalenian to Bajocian Lillooet Group are exposed west of the Fraser fault system. Lillooet Group is unconformably overlain by strata of the Cretaceous Jackass Mountain Group (Kleinspehn, 1982; Schiarizza et al., 1989, 1990; Mahoney, 1992); the base of the Lillooet Group is not exposed. The western limit of the Lillooet Group is the Yalakom Fault, which separates an imbricate stack of Triassic, Jurassic, and Cretaceous clastic rocks on the northeast from the oceanic greenstone and chert of the Mississippian to Jurassic Bridge River Group (Schiarizza et al., 1989, 1990).

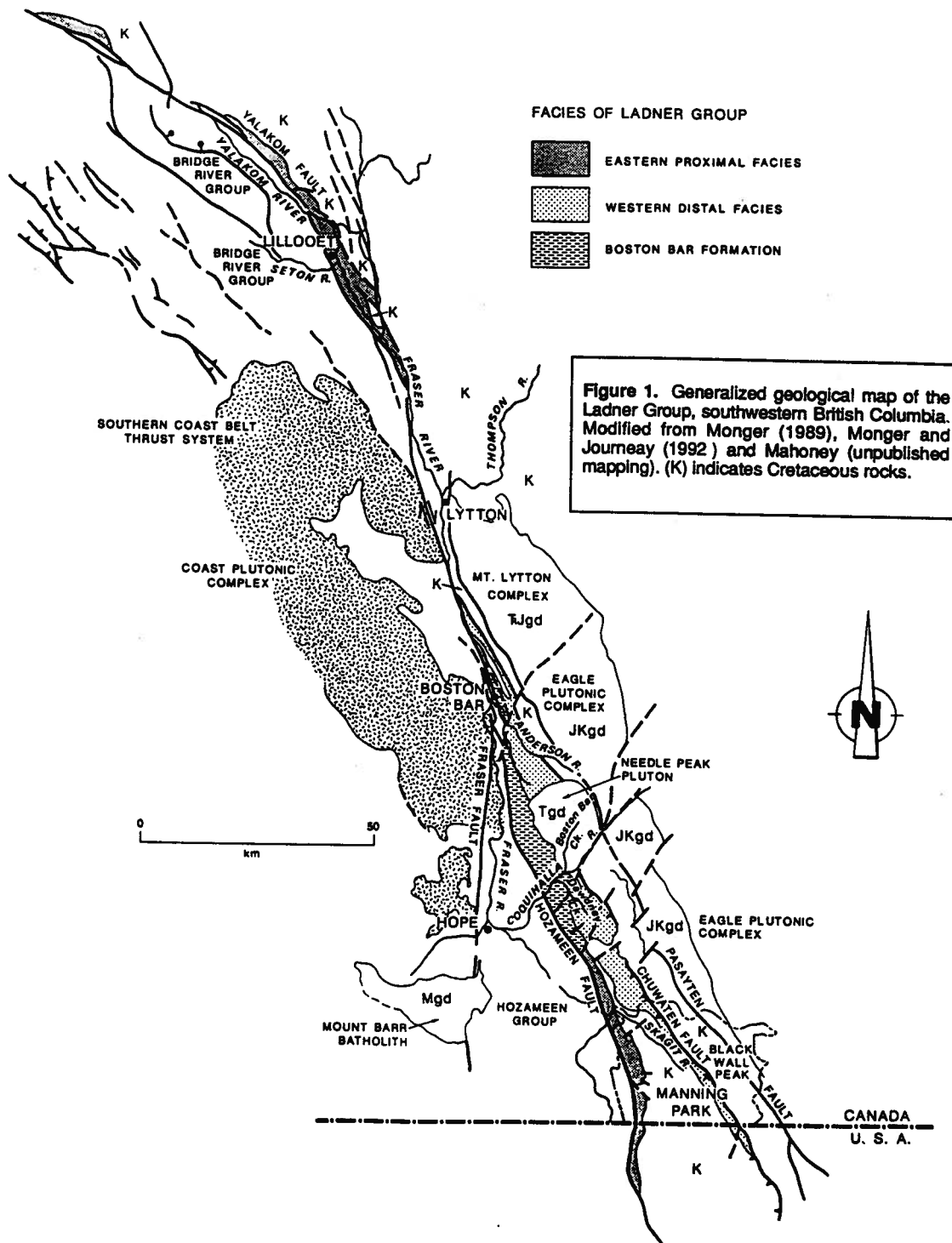
PREVIOUS WORK

Nomenclature of Jurassic rocks of the Methow basin has a long and complex history, primarily due to the lack of well exposed sections, poor age control, and complex structural relations. Significant strides in biostratigraphy, particularly by Coates (1974) and O'Brien (1986, 1987) have delineated the range and distribution of units, although disagreements still exist (Ray, 1990).

Cairnes (1924, 1944) named the Ladner Group for a thick sequence of slate and tuffaceous greywacke exposed along Ladner Creek northeast of Hope. Dewdney Creek Group was named for a sequence of coarse grained volcanogenic strata exposed in the Dewdney Creek area, and tentatively assigned a Late Jurassic to Early Cretaceous age (Cairnes, 1924, 1944).

Coates (1974) applied the name Ladner Group to rocks of Sinemurian(?), Toarcian, and Bajocian age that lie disconformably or with slight angular unconformity beneath rocks of Late Jurassic age in the Manning Park area. He subdivided the Ladner Group into an eastern and western outcrop belt, and established two reference sections for the group (Lookout section in the eastern belt; Divide section in the western belt). Coates (1974) correlated Upper Jurassic (Oxfordian to Portlandian) volcanogenic siltstone, sandstone, and rounded pebble conglomerate overlying Ladner Group with the Dewdney Creek Group of Cairnes (1924, 1944).

O'Brien (1986, 1987) significantly revised the nomenclature of Jurassic strata in the region based on new paleontological control in the Coquihalla and Anderson River areas (Fig. 1). O'Brien (1986) found that the type area of the "Upper Jurassic to Lower Cretaceous" Dewdney Creek Group of Cairnes (1924, 1944) consisted of Middle Jurassic strata, which she interpreted to lie conformably above Jurassic strata of Ladner Group. Consequently, O'Brien (1986, 1987) incorporated all Lower and Middle Jurassic rocks of the region into the Ladner Group, and subdivided the group into Lower Jurassic Boston Bar Formation and the overlying Middle Jurassic Dewdney Creek Formation. Upper Jurassic and Lower Cretaceous clastic strata disconformably



above Ladner Group, including the Dewdney Creek Group as defined in Manning Park (Coates, 1974), were renamed the Thunder Lake assemblage.

Ray (1986) mapped and described the stratigraphy of Ladner Group in Coquihalla River area in detail, documented the basal unconformity between the group and the underlying Spider Peak Formation, and analyzed the deformation of the group. Ray (1990) found Late Jurassic *Buchia* bivalves in fine grained siltstone lithologically indistinguishable and apparently conformable with argillaceous strata of the lower Ladner Group. On this basis, Ray (1990) disagreed with the subdivisions of O'Brien (1987), and mapped both Lower and Upper Jurassic siltstone and argillite as Ladner Group.

Ray (1990) mapped coarse grained volcanogenic strata overlying argillaceous rocks of Ladner Group as Jura-Cretaceous Dewdney Creek Group. The presence of Middle Jurassic ammonites in these overlying rocks suggests this assignment is incorrect. However, the applicability of the stratigraphy defined by O'Brien (1987) and described in this paper to the area mapped by Ray (1990) north of the Coquihalla River remains in dispute.

Mahoney (1992) reviewed the previous work and described the stratigraphy and depositional setting of Middle Jurassic volcanogenic strata of Lillooet Group near Lillooet (Fig. 1).

LADNER GROUP STRATIGRAPHY

Boston Bar Formation

Boston Bar Formation comprises strongly deformed and metamorphosed argillite, siltstone, lithic sandstone and minor conglomerate exposed in the west-central part of the Ladner Group outcrop belt, from south of the Coquihalla River northward to north of Boston Bar, where it is truncated by the Fraser fault system. The western limit of exposure is the Hozameen Fault, and the eastern boundary is the contact with the Dewdney Creek Formation or the Tertiary Needle Peak pluton (Monger, 1989) (Fig. 1).

O'Brien (1986) and Monger (1989) showed the Boston Bar Formation extending along the western edge of the Jurassic outcrop belt as far south as the International Border. Mapping during 1992 indicates that the unit does not extend south of Mt. Dewdney, and that all Lower and Middle Jurassic strata in Manning Park should be included in Dewdney Creek Formation. Fine grained strata mapped as Boston Bar Formation in Manning Park contains abundant coarse grained volcanic detritus and Late Toarcian to Middle Bajocian fossils, characteristics of the distal facies of Dewdney Creek Formation. Undated strata of Twisp Formation in Methow Valley, in Washington State, are lithologically similar to the Boston Bar Formation, but definitive correlation awaits age control.

Argillaceous strata characterize the Boston Bar Formation, although siltstone is equally abundant. The formation grades upward over a few hundreds of metres from a basal conglomerate and sandstone section into the siltstone

and argillite that dominate the section (Ray, 1990). New mapping in the Anderson River area demonstrates that the formation coarsens upward into medium- to coarse-grained sandstone and limestone-bearing volcanic conglomerate in the upper 200 m of section, near the contact with the overlying Dewdney Creek Formation.

The Boston Bar Formation unconformably overlies Triassic Spider Peak Formation (Ray, 1990). Matrix supported, polymict pebble to boulder conglomerate at the base of the formation contains subangular to rounded clasts of greenstone, quartz diorite, syenite, limestone, sandstone, and siltstone in a matrix of fine grained sand and silt. O'Brien et al. (1992) reported a 235 ± 10 Ma quartz diorite clast from this basal conglomerate and suggested it was derived from the Late Permian Mount Lytton Complex to the east. This correlation, if correct, indicates that the Methow basin has been adjacent to Quesnellia since its inception (O'Brien et al., 1992).

The upper contact of Boston Bar Formation is not exposed, but is believed to be gradational with the overlying Dewdney Creek Formation (O'Brien, 1986, 1987). The age of Boston Bar Formation is poorly constrained by sparse fossils as Sinemurian(?) to Toarcian(?) (Monger, 1989). The stratigraphic position of the Late Jurassic *Buchia* bivalves reported by Ray (1990) remains unclear.

Structural features in Boston Bar Formation consists of strong near-bedding-parallel cleavage, tight to isoclinal mesoscopic and macroscopic scale folds, and abundant bedding-parallel faults. Deformation increases significantly adjacent to both the Needle Peak pluton and to major faults, particularly the Fraser fault system (Fig. 1). The rocks are locally metamorphosed to hornblende hornfels facies. Structural and metamorphic alteration in the Boston Bar Formation is locally much higher than in the overlying Dewdney Creek Formation. These differences may be the result of pre-Toarcian deformation or may be apparent features created by competency differences in units adjacent to major faults and intrusions.

Dewdney Creek Formation

The Upper Toarcian to Upper Bajocian Dewdney Creek Formation is a heterogeneous package of coarse grained sandstone, conglomerate, siltstone, pyroclastic rocks, and volcanic flows with considerable lateral and vertical variation throughout the outcrop belt. It is exposed in a 200 km-long northwest trending outcrop belt extending from south of the International Border to north of Boston Bar (Fig. 1). The formation is exposed in two distinct outcrop belts contained in the limbs of a broad synclinalorium situated between Hozameen and Chuwanten faults (Coates, 1974) (Fig. 1).

Dewdney Creek Formation comprises an eastern proximal facies assemblage and a western distal facies assemblage (Fig. 2, 3a). This distinction, first recognized by Coates (1974) in the Manning Park area, is herein extended throughout the entire Middle Jurassic part of the Methow basin.

Eastern proximal facies

This assemblage comprises three distinct lithofacies: 1) fine- to coarse-grained pyroclastic rocks and lava flows; 2) coarse grained lithic sandstone and conglomerate lithofacies; and 3) fine grained sandstone, siltstone, and minor argillite. These lithofacies are interbedded with one another in varying proportions throughout the area, but a very general fining upward sequence in the order of thousands of metres is generally recognized along the length of the outcrop belt (Fig. 2).

The volcanic lithofacies consists of coarse grained andesitic to dacitic breccia, tuff-breccia, lapilli tuff, lithic crystal tuff, crystal tuff, vitric tuff, and rare andesitic lava flows. Coarse pyroclastic rocks are typified by andesitic breccia exposed at Blackwall Peak in the Lookout section in Manning Park, where the breccia consists of matrix-supported pebble to boulder sized angular to subangular clasts of green hornblende crystal tuff in a fine grained plagioclase-bearing matrix. The most voluminous pyroclastic lithology in the formation is medium to very thick bedded (0.3 to 2 m) andesitic tuff-breccia and lapilli tuff.

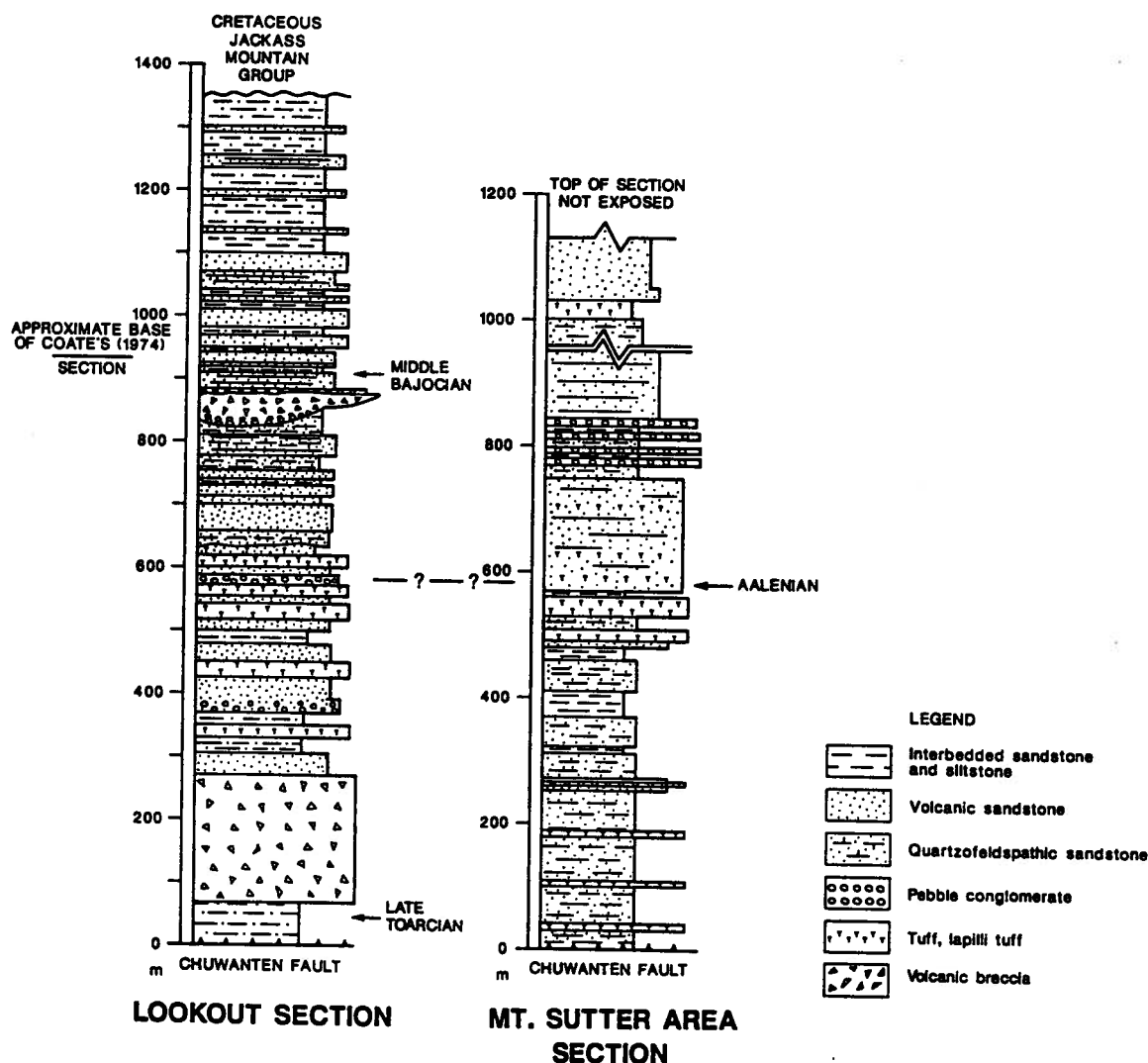


Figure 2. Partial stratigraphic sections of the eastern proximal facies of Dewdney Creek Formation. The Lookout section is in Manning Park, south of Blackwall Peak, with the base of the section at co-ordinates (10U, 663200mE, 5440600mN). The upper portion of the section is a revision of the Lookout section of Coates (1974). The Mt. Sutter section is a composite section measured on the east and west flanks of Mt. Sutter, and on the ridge above Mt. Tulameen. The base of the section is at (10U, 638700mE, 5477300mN).

These beds commonly show crude normal and reverse grading, parallel laminae, and locally contain siltstone rip-up clasts and other accidentals, including rare bioclasts. Many of the coarser pyroclastic beds are lenticular and, in the Lookout section, tuff-breccia fills submarine channels. Fine grained lithic crystal tuff, crystal tuff and vitric tuff is common in the upper third of the formation, and tends to be thin to medium bedded (3-30 cm), parallel laminated, and laterally continuous. These tuffs locally aggregate to 10-25 m.

Rare andesitic lava flows occur along the eastern margin of the outcrop belt in the Anderson River area (Fig. 1). The flows are generally green, aphanitic to porphyritic, with hornblende phenocrysts in an aphanitic matrix. Calcite and zeolite amygdulites are common near the base and tops of flows, and the flows are commonly highly altered.

The coarse grained sandstone and conglomerate lithofacies consists of medium to thick bedded (0.1 to 0.8 m), medium to coarse grained lithic feldspathic wacke and arenite interbedded with minor fine to medium grained arenite and siltstone. Sandstone beds amalgamate to 2-25 m. The sandstone commonly contains siltstone rip-up clasts in the basal few centimetres, and generally exhibit normal grading and crude parallel laminae. Scour features, channel cuts, soft-sediment deformation and granule conglomerate stringers are locally abundant. Woody debris is common, and a medium bedded shelly lag deposit was noted at one locality. Coarsening and thickening and fining and thinning upward sequences (1-10 m thick) are common. The majority of the sandstone is volcanic, with plagioclase the most abundant clastic component, and lesser volcanic lithics, chloritized mafic grains, and quartz, all indicating a first-cycle volcanic source. One 40+ m thick section within the Lookout section of Manning Park contains abundant quartzofeldspathic arenite of unknown derivation. Pebble to boulder, matrix and clast-supported conglomerate with angular to subrounded volcanic clasts form lenticular horizons throughout the section, but are more common in the lower portions of the formation.

Fine grained sandstone, siltstone, and argillite lithofacies is characterized by thin bedded, thin laminated, fine to very fine grained, well sorted, lithic feldspathic arenite, medium to coarse grained laminated siltstone, and minor argillite. The unit contains abundant sedimentary structures, including parallel laminae, cross laminae, graded bedding (normal and reverse), flaser bedding, scour features, load casts, pinch and swell features, ripple marks, climbing ripples, and convolute laminae. Partial Bouma sequences are locally evident. This lithofacies commonly gradationally overlies thick sandstone sequences, but also forms thick (10-100 m) sequences, particularly near the upper portion of the section.

Depositional environment

The volcanic lithofacies was deposited by a combination of pyroclastic flows, debris flows, and air fall. Thick bedded (0.75-2 m) lapilli tuff that fine upwards from a basal rip-up horizon into lithic crystal tuff with inversely graded pumice

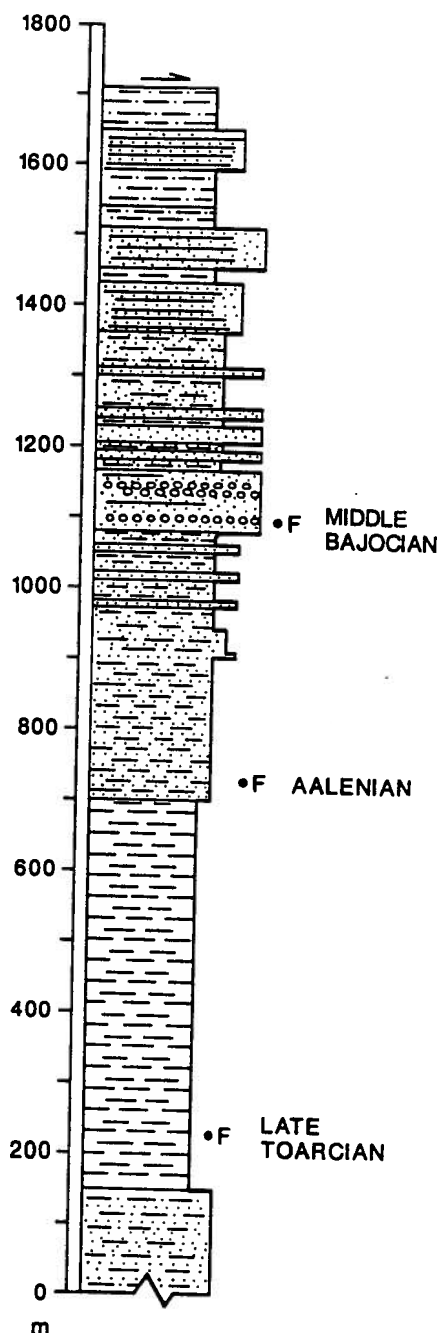
clasts near the upper contact are interpreted as subaqueous pyroclastic flows (Fisher and Schmincke, 1984). Thick bedded tuff-breccia and lapilli tuff with inversely graded bases overlain by normally graded crudely laminated medium bedded lapilli tuff and lithic crystal tuff may also indicate subaqueous pyroclastic flows. Thin, normally graded crystal tuffs with irregular lower contacts, randomly oriented plagioclase crystals and reworked tops are believed to be air fall deposits. Thick, lenticular, and locally channel-filling breccia and tuff-breccia with rare clast alteration rinds represent lahars. Non-pillowed lava flows in the Anderson River drainage indicate a nearby subaerial vent region.

The coarse grained sandstone and conglomerate lithofacies was primarily deposited by subaqueous mass flow mechanisms. Thick (0.6-2 m), structureless to crudely laminated sandstone and granule conglomerate with abundant basal rip-up clasts dominates the facies, and is the product of high-concentration turbidity currents. Inter-calated thin-bedded siltstone represent low-concentration partial turbidites. Lenticular pebble to boulder conglomerate within fine grained facies indicates subaqueous channelized flow in the eastern part of the outcrop belt.

Fine grained sandstone and siltstone lithofacies is the product of low concentration turbidity currents, hemipelagic suspension sedimentation, and tractional sediment transport. Thin bedded, bottom-cut-out partial Bouma sequences (TCDE, TDE) are normally associated with thick bedded sandstone successions, and represent deposition in the waning stages of high concentration mass sediment flows. However, parallel laminated sandstone, siltstone and argillite locally aggregate to 10-25 m, and are believed to be the result of both low concentration turbidity currents and tractive sedimentation. Tractive sedimentation is indicated by locally abundant sedimentary structures, and by parallel and crosslaminated fossil-rich lag deposits near the eastern boundary of the outcrop belt. Thick sequences (5-15 m) of black argillite are the product of hemipelagic sedimentation.

The eastern proximal facies was deposited rapidly in shallow to intermediate depth (below normal wave base) water adjacent to an energetic andesitic to dacitic volcanic system. Deposition occurred on a volcanoclastic apron characterized by episodic pyroclastic influx and subaqueous mass sediment gravity flows. The apron shallowed to the east, as evidenced by an increase in bioclastic debris, woody debris, coarse volcanic breccia and lava flows toward the eastern edge of the outcrop belt. A steep gradient is implied by the proximity of high concentration turbidites and subaerial(?) lava flows, and by the overall coarse grain size of the sediment. Sediment transport was dominantly to the west, as indicated by the east-to-west proximal-distal transition, and by rare paleocurrent indicators. Rapid lateral facies changes suggest an uneven bottom topography, and the presence of quartzofeldspathic rocks in Manning Park suggest multiple source areas. The abundance of convolute laminae, ball and pillow structures, overturned flame structures, and lack of biogenic structures suggest deposition was rapid.

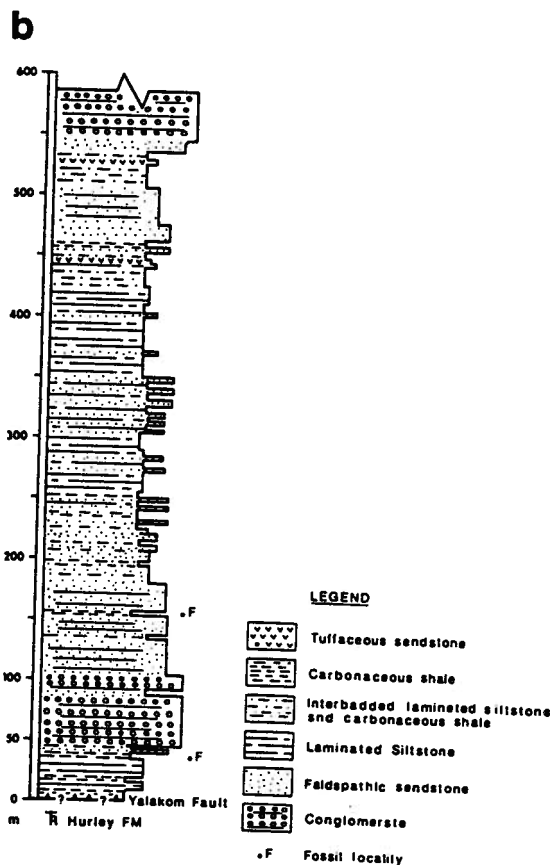
a UPPER JURASSIC
THUNDER LAKE SEQUENCE



DIVIDE SECTION

Figure 3.

a) Partial stratigraphic section of the western distal facies of the Dewdney Creek Formation. The Divide section is in Manning Park, on the ridge between Skagit River and Twenty-six Mile Creek. The base of the section is at (10U 647700mE, 5447200mN). The section is an expansion and revision of the section of Frebold et al. (1969). b) Stratigraphic section of the Lillooet Group, measured upstream from the confluence of Blue Creek and Yalakom River north of Lillooet. The base of the section is at (10U, 537800mE, 565370mN). This section is from Mahoney (1992). Note difference in scale between the two sections. F=lower and upper fossil localities are Vaalenian and Bajocian, respectively.



LILLOOET GROUP

Western distal facies

The western distal facies may be subdivided into two lithofacies: 1) a coarse grained sandstone and conglomerate lithofacies and 2) a fine grained facies of thin bedded sandstone, siltstone and argillite. The thin bedded lithofacies is volumetrically dominant, but it weathers recessively, creating prominent ribs of sandstone and conglomerate that appear to dominate the section. Figure 3a contains a partial stratigraphic section of the western distal facies.

The thin bedded lithofacies consists of rhythmically interbedded 2-5 cm thick fine- to very fine-grained sandstone, siltstone, and argillite. Thin-bedded, fine grained sandstone and gradationally overlying siltstone form thin (3-8 cm) couplets that give the outcrop a banded appearance. Sedimentary structures consist of parallel lamination, with subordinate crosslaminae, convolute laminae, and graded bedding, organized into partial and complete Bouma sequences. Bioturbation is locally evident. Cyclicity is common, with fine sandstone beds alternately coarsening and thickening, then fining and thinning upward on a 10-50 m scale. Thin bedded carbonaceous argillite is intercalated throughout the section, and locally forms 0.5 to 1 m beds.

Coarse grained sandstone and conglomerate lithofacies consists of medium to very coarse grained lithic feldspathic arenite and wacke and granule to pebble volcanic conglomerate. The sandstone and conglomerate is medium to very thickly bedded, structureless to crudely laminated, and commonly contains fine grained rip-up clasts at the base. Sandstone and conglomerate beds are gradationally overlain by, and intercalated with, the fine grained lithofacies. Granule to pebble conglomerate is generally matrix-supported, crudely graded, and commonly forms thin "stringers" within sandstone-dominated sections. Medium and thick bedded sandstone and conglomerate beds occur in 50-80 m thick sequences, which commonly display coarsening and thickening upward and fining and thinning upward cyclicity.

Depositional environment

The western distal facies is the product of subaqueous mass sediment flow and hemipelagic deposition in a subwave-base marine environment. The thin bedded lithofacies was deposited by low concentration turbidity currents. This interpretation is based on the abundance of both complete and bottom-cut-out partial (TBCDE, TCDE, TDE) Bouma sequences and the uniform, laterally continuous bedding. Homogeneous argillite sequences are the product of hemipelagic sedimentation, as shown by minor normal grading, lack of tractive sedimentary features, and the preservation of ammonite fauna. Episodic increases in clastic influx, perhaps due to migrating distributary lobes or the progradation of a clastic wedge, introduced coarse clastic debris into the basin. The coarse grained lithofacies is the product of unchannelized, high concentration turbidity current deposition during these periods of high clastic influx. This interpretation is supported by the abundance of thick to

very thick bedded, structureless to crudely graded sandstone beds, inferred to be amalgamated mass sediment gravity flows, enveloped in fine grained hemipelagic sediments.

The western distal facies is thought to have been deposited farther from the volcanic highland than the eastern proximal facies due to its overall finer grained nature, lack of primary pyroclastic debris and lava flows, lack of channels, abundance of organized turbidite features, and the absence of wood and shallow water shelly debris. The western distal facies is believed to have been deposited at the base of a volcanoclastic apron which received sediment from the east.

Age

The age of Dewdney Creek Formation is constrained as Late Toarcian to Late Bajocian (O'Brien, 1986; this study), although the age of the upper and lower contacts is unknown. Five new fossil localities were discovered during 1992, including the oldest and youngest fossils yet found in the eastern outcrop belt. A well-preserved ammonite, *Zemistephanus richardsoni*, of late Early Bajocian to early Late Bajocian age from the Anderson River area extends the known age range of the formation (H.W. Tipper, pers. comm., 1992). The association of *Tmetoceras* with Trigonid pelecypods and brachiopods in volcanic strata suggests sediments east of the Anderson River are Early Aalenian or older, indicating that volcanism was active from at least Early Aalenian to Late Bajocian time. A Toarcian(?) to Aalenian initiation of volcanism is indicated by a thick sequence of lapilli tuffs and tuff stratigraphically below an Aalenian(?) ammonite discovered by O'Brien (1986), on the east flank of Mt. Sutter.

The Early Bajocian ammonite identified by O'Brien (1987) from below the breccia of Blackwall Peak is problematic. Frebold et al. (1969) noted a Late Toarcian ammonite from the same section, and the fine grained nature of the sediments preclude reworking to account for this contradiction. The discovery of Aalenian ammonites stratigraphically above the breccia of Blackwall Peak supports a Late Toarcian age for the breccia (Coates, 1974), suggesting volcanism was active as early as Late Toarcian. The ammonite discovered by O'Brien (1987) may indicate structural duplication along a strand of the Chuwanten Fault.

Lillooet Group

The Aalenian to Bajocian Lillooet Group consists of 800+ m of fine grained sandstone, siltstone, argillite, and lesser conglomerate exposed west of the Fraser fault system (Mahoney, 1992, and references therein) (Fig. 1). The age, lithology, sediment transport direction, faunal types, inferred depositional environment, and stratigraphic and structural position of the Lillooet Group (Fig. 3b) is similar to that of the western distal facies of Dewdney Creek Formation (Mahoney, 1992).

Examination of facies distribution on a regional scale shows that the western distal facies of Dewdney Creek Formation does not extend north of the Eocene Needle Peak

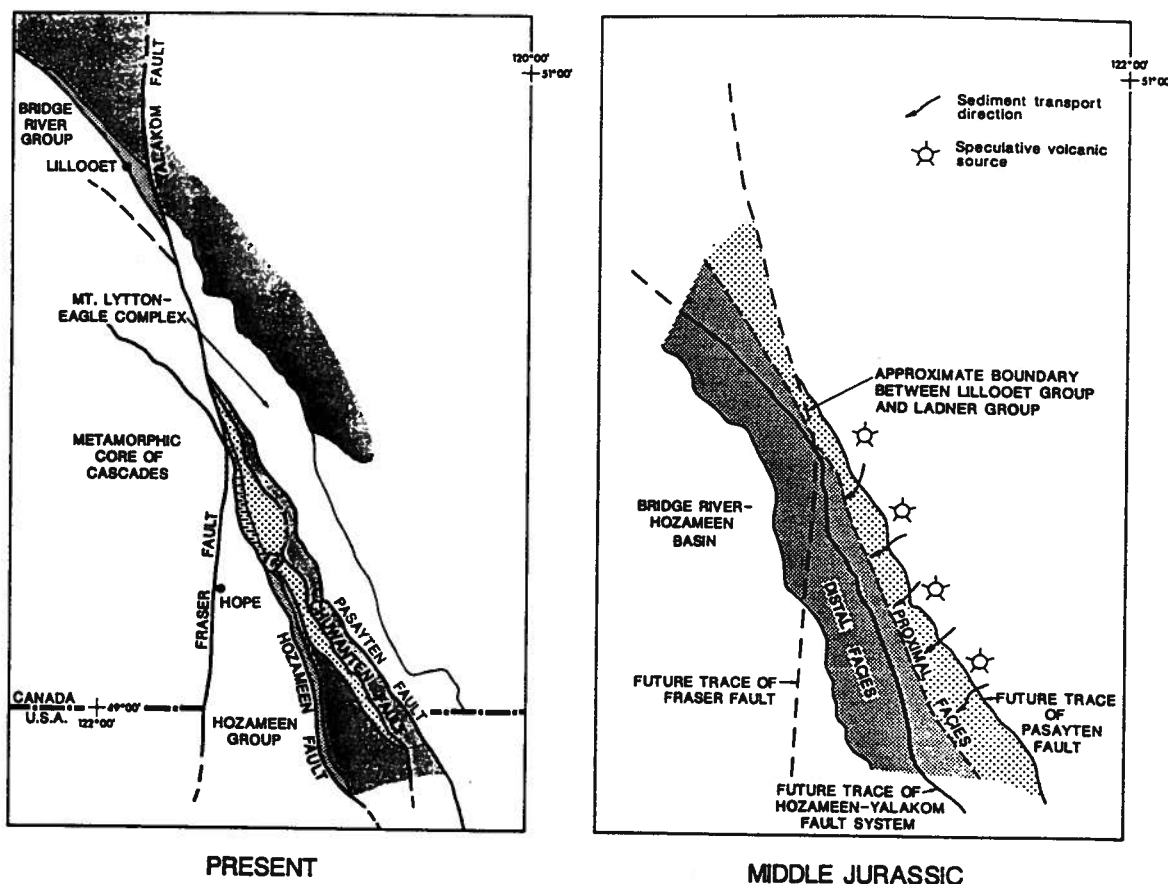


Figure 4. Diagrammatic reconstruction of the facies assemblages of the Dewdney Creek Formation, with offset on the Fraser Fault System restored. See Figure 1 for legend; light grey = Cretaceous rocks.

Pluton. The entire formation north of the pluton consists of the eastern proximal facies, with the distal facies missing. However, the western margin of Dewdney Creek Formation is truncated north of Boston Bar by the Fraser fault system. Displacement estimates on the Tertiary Fraser fault system range from 80-150 km, based on the offset of the Hozameen/Yalakom fault system, displacement of the Jackass Mountain Group, and correlation of the Permian Farwell Pluton and the Mount Lytton Complex (Kleinspehn, 1982; Monger, 1985; Friedman and van der Heyden, 1992; Monger and Journeay, 1992). Restoration of this magnitude places the Lillooet Group adjacent and west of the proximal facies of Dewdney Creek Formation (Fig. 4). I suggest that the Lillooet Group may be directly correlated with the western distal facies of Dewdney Creek Formation based on sedimentologic, stratigraphic, and structural grounds, and that Lillooet Group therefore represents a slice of the Ladner Group offset along the dextral Fraser Fault System. It is

further suggested that the name Lillooet Group be abandoned, and those rocks be assigned to Dewdney Creek Formation of Ladner Group.

ACKNOWLEDGMENTS

Darcy McDonald provided excellent assistance in the field, and is gratefully acknowledged for his motivation and good cheer. Time spent in the field with P.K. Link in the Dewdney Creek area proved invaluable, as always. I thank C.J. Hickson for her support and interest in the project. Reviews by R.M. Bustin, J.V. Ross, J.W.H. Monger, P.S. Mustard and G.J. Woodsworth were extremely helpful, as were numerous conversations with J.W.H. Monger concerning the stratigraphy and tectonics of the region. Bev Vanlier's help with the manuscript is much appreciated. This study was partially supported by EMR Research Agreement 111-4-92.

REFERENCES

- Cairnes, C.E.
1924: Coquihalla area, British Columbia; Geological Survey of Canada, Memoir 139.
1944: Hope, British Columbia; Geological Survey of Canada, Map 737A.
Coates, J.A.
1974: Geology of the Manning Park area, British Columbia; Geological Survey of Canada, Bulletin 238, 177 p.
Fisher, R.V. and Schmincke, H.-U.
1984: Pyroclastic Rocks; Springer-Verlag, Berlin, 472 p.
Frebold, H., Tipper, H.W., and Coates, J.A.
1969: Toarcian and Bajocian rocks and guide ammonites from southwestern British Columbia; Geological Survey of Canada, Paper 67-10, 55 p.
Friedman, R.M. and van der Heyden, P.
1992: Late Permian U-Pb dates for the Farwell and Northern Mt. Lytton plutonic bodies, Intermontane Belt, British Columbia; in Current Research, Part A; Geological Survey of Canada, Paper 92-1A, p. 137-144.
Garver, J.I.
1992: Provenance of Albian-Cenomanian rocks of the Methow and Tyaughton basins, southern British Columbia: a mid-Cretaceous link between North America and the Insular terrane; Canadian Journal of Earth Sciences, v. 29, no. 6, p. 1274-1295.
Greig, C.J.
1989: Geology and geochronometry of the Eagle Plutonic Complex, Coquihalla area, southwestern British Columbia; M.Sc. thesis, University of British Columbia, Vancouver, 423 p.
Hickson, C.J.
1992: An update on the Chilcotin-Nechako project and mapping in the Taseko Lakes area, west-central British Columbia; in Current Research, Part A; Geological Survey of Canada, Paper 92-1A, p. 129-135.
Kleinspehn, K.L.
1982: Cretaceous sedimentation and tectonics, Tyaughton-Methow Basin, southwestern British Columbia; Ph.D. thesis, Princeton University, New Jersey, 184 p.
Mahoney, J.B.
1992: Middle Jurassic stratigraphy of the Lillooet area, south-central British Columbia; in Current Research, Part A; Geological Survey of Canada, Paper 92-1A, p. 243-248.
Monger, J.W.H.
1970: Hope map-area, west half, British Columbia; Geological Survey of Canada, Paper 69-47, 75 p.
1985: Structural evolution of the southwestern Intermontane Belt, Ashcroft and Hope map areas, British Columbia; in Current Research, Part A; Geological Survey of Canada, Paper 85-1A, p. 349-358.
Monger, J.W.H. (cont.)
1989: Geology, Hope, British Columbia; Geological Survey of Canada, Map 41-1989, sheet 1, scale 1:250 000.
Monger, J.W.H. and Journeay, J.M.
1992: Guide to the geology and tectonic evolution of the southern Coast Belt; field guide to accompany Penrose Conference on "Tectonic Evolution of the Coast Mountains Orogen", 92 p.
O'Brien, J.
1986: Jurassic stratigraphy of the Methow Trough, southwestern British Columbia; in Current Research, Part B; Geological Survey of Canada, Paper 86-1B, p. 749-756.
1987: Jurassic biostratigraphy and evolution of the Methow trough, southwestern British Columbia; M.Sc. thesis, University of Arizona, Tucson, 150 p.
O'Brien, J.A., Gehrels, G.E., and Monger, J.W.H.
1992: U-Pb geochronology of plutonic clasts from conglomerates in the Ladner and Jackass Mountain groups and the Peninsula Formation, southwestern British Columbia; in Current Research, Part A; Geological Survey of Canada, Paper 92-1A, p. 209-214.
Ray, G.E.
1986: Geology of the Hozomeen Fault between Boston Bar and the Coquihalla River; British Columbia Ministry of Energy, Mines and Petroleum Resources, Open File 1986-1, scales 1:20 000 and 1:6 000.
1990: The geology and mineralization of the Coquihalla gold belt and Hozomeen fault system, southwestern British Columbia; British Columbia Ministry of Energy, Mines and Petroleum Resources, Bulletin 79, 97 p.
Ray, G.E., Coombes, S., MacQuarrie, D.R., Niels, R.J.E., Shearer, J.T., and Cardinal, D.G.
1985: Precious metal mineralization in southwestern British Columbia; in Field Guides to Geology and Mineral Deposits in the Southern Canadian Cordillera, (ed.) D.J. Tempelman-Kluit; Geological Society of America Cordilleran Section Field Guide, Vancouver, B.C., p. 9.1 - 9.31.
Schiarizza, R., Gaba, R.G., Coleman, M., Garver, J.I., and Glover, J.K.
1990: Geology and mineral occurrences of the Yalakom River area; in Geological Fieldwork 1989, British Columbia Ministry of Energy, Mines and Petroleum Resources, Paper 1990-1, p. 53-72.
Schiarizza, R., Gaba, R.G., Glover, J.K., and Garver, J.I.
1989: Geology and mineral occurrences of the Tyaughton Creek area; in Geological Fieldwork 1988, British Columbia Ministry of Energy, Mines and Petroleum Resources, Paper 1989-1, p. 115-143.

Geological Survey of Canada Project 890039-02

The Cayoosh Assemblage, southwestern British Columbia: last vestige of the Bridge River Ocean

J.B. Mahoney¹ and J.M. Journeay
Cordilleran Division, Vancouver

Mahoney, J.B. and Journeay, J.M., 1993: The Cayoosh Assemblage, southwestern British Columbia: last vestige of the Bridge River Ocean; in Current Research, Part A; Geological Survey of Canada, Paper 93-1A, p. 235-244.

Abstract: The Cayoosh Assemblage is a coherent succession of fine grained clastic metasedimentary rocks that conformably overlies oceanic assemblages of the Bridge River Terrane in southwestern British Columbia. Thin-bedded phyllitic siltstones near the base of the Cayoosh Assemblage are intercalated with sandy and tuffaceous siltstones, thin-bedded greywacke and limestone. These rocks grade upwards into a succession of siltstones, fragmental metavolcanic rocks and associated volcanoclastic sandstones. Phyllitic siltstones and pyritiferous shales of the upper Cayoosh Assemblage grade upwards into a succession of interlayered thin- and thick-bedded feldspathic arenites, quartz-rich feldspathic arenites and phyllitic sandstones. This upper siltstone/sandstone lithofacies is correlated on the basis of rock type with Lower Cretaceous fossiliferous rocks of the Brew Group. These rocks provide a record of Jura-Cretaceous sedimentation in the Eastern Coast Belt and offer a means of reconstructing the evolution of the Bridge River 'ocean,' and the history of terrane interactions along the boundary between the Intermontane and Insular superterranes.

Résumé : L'assemblage de Cayoosh est une succession cohérente de roches métasédimentaires clastiques à grain fin qui recouvrent en concordance les assemblages océaniques du terrane de Bridge River dans le sud-ouest de la Colombie-Britannique. Des siltstones graphiteux finement lités, proches de la base de l'assemblage de Cayoosh, sont interstratifiés avec des siltstones sableux et tufacés, et avec une grauwwacke et un calcaire finement lités. Ces roches passent vers le haut à une succession de siltstones, de roches métavolcaniques détritiques et de grès volcanoclastiques associés. Les siltstones phylliteux et les shales pyriteux de la partie supérieure de l'assemblage de Cayoosh passent vers le haut à une succession d'arénites feldspathiques à lits fins et à lits épais, d'arénites feldspathiques riches en quartz et de grès phylliteux. Ce lithofaciès supérieur à siltstone et grès peut être mis en corrélation, en fonction du type lithologique, avec les roches fossilifères du Crétacé inférieur qui font partie du Groupe de Brew. Ces roches constituent une colonne stratigraphique jurassique-crétacée de la zone de la côte orientale dont l'étude permettra aux chercheurs de reconstituer l'évolution de l'«océan» de Bridge River et d'établir les interactions successives des terranes qui se sont produites sur la limite entre le superterrane intermontagneux et le superterrane insulaire.

¹ Department of Geological Sciences, University of British Columbia, 6339 Stores Road, Vancouver, B.C. V6T 1Z4

INTRODUCTION

The Bridge River Complex is a Mississippian to Middle Jurassic assemblage of greenstone, chert and fine-grained clastic rocks that occurs along the boundary between the Insular and Intermontane superterrane of the southern Coast Belt. It is conformably overlain by Jura-Cretaceous clastic rocks of the Cayoosh Assemblage and is structurally interleaved with other terranes of the southern Coast Belt along an array of contractional and strike-slip faults that range in age from Late Cretaceous to Early Tertiary (Fig. 1, 2).

Evolution of the Bridge River 'ocean' and its linkage to adjacent terranes of the Insular and Intermontane belts prior to the onset of crustal imbrication, are fundamental to an understanding of the Coast Belt orogen, and to the history of superterrane accretion in the southern Canadian Cordillera (Monger and Journeay, 1992). Estimates for the timing of terrane accretion in the southern Coast Belt range from Middle Jurassic (Rusmore et al., 1988; van der Heyden, 1992) to Early Cretaceous (Monger et al., 1982). There is no direct evidence for the timing or mechanism of terrane accretion in

the Bridge River Complex. However, conformably overlying fine-grained clastic successions of the Cayoosh Assemblage are gradational upwards into Lower Cretaceous quartz-rich sandstones and conglomerates of the Eastern Coast Belt (Journeay and Northcote, 1992). These rocks record Jura-Cretaceous sedimentation in the region, and may provide a means of reconstructing the terminal history of the Bridge River 'ocean' and the history of terrane accretion in the Eastern Coast Belt.

This study focuses on the stratigraphy of the Cayoosh Assemblage in its type locality (Fig. 1, 3), and explores potential linkages with clastic successions in adjacent parts of the southern Coast Belt. Stratigraphic studies by Mahoney are part of a PhD dissertation jointly sponsored by the Geological Survey of Canada and the University of British Columbia.

GEOLOGICAL SETTING

The Bridge River Complex is an oceanic assemblage of greenstone, chert, siliceous siltstone and serpentinite, locally interleaved with lesser greywacke, limestone, and ultramafic

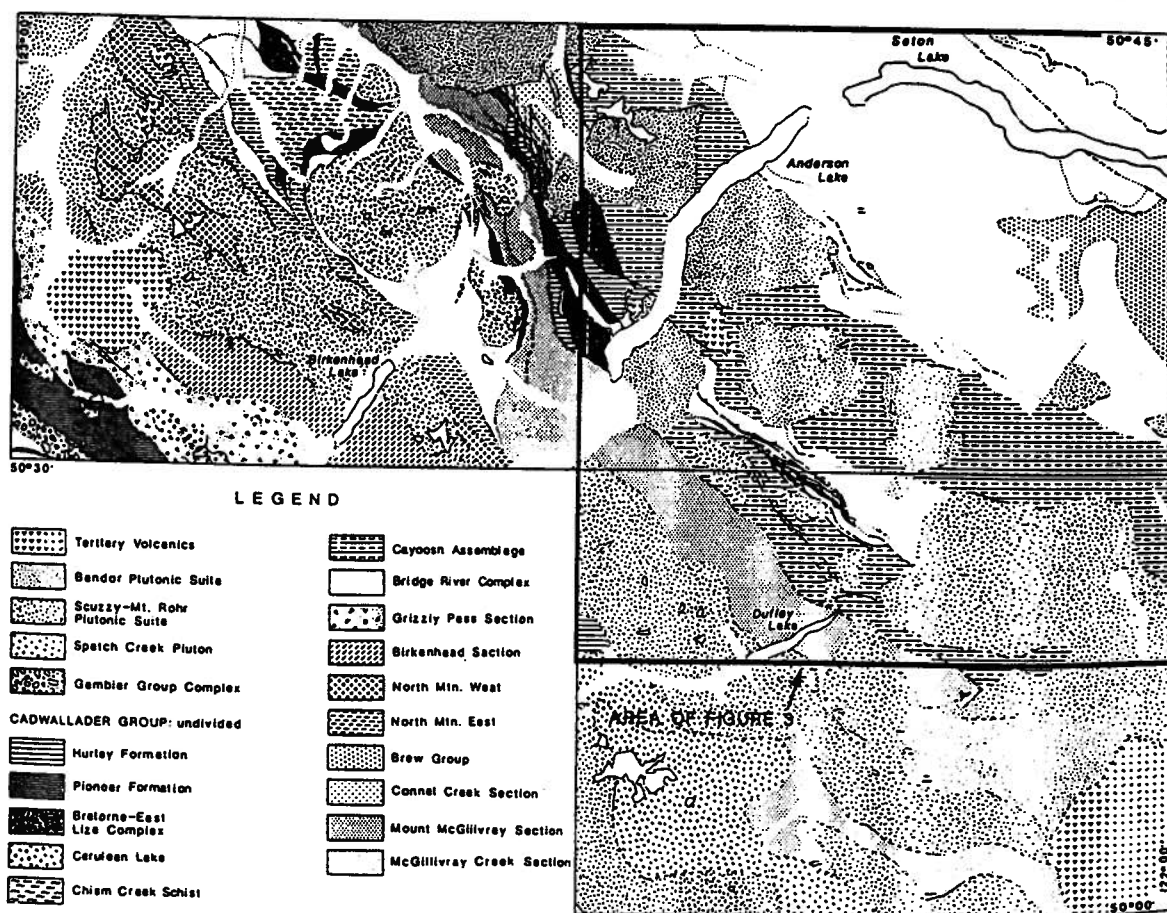


Figure 1. Regional Geology of the Eastern Coast Belt. See Journeay (1993) for map credits.

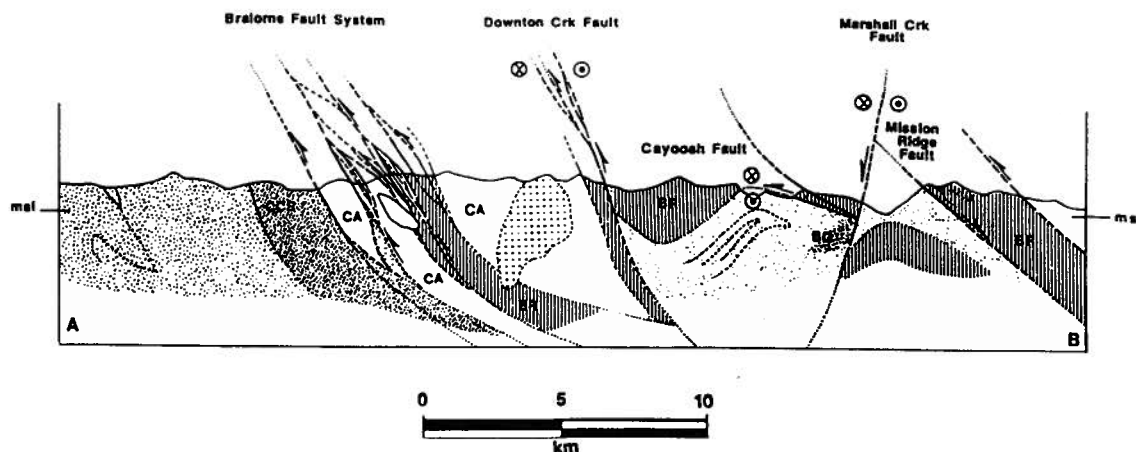


Figure 2. Geological cross-section of the Eastern Coast Belt. See Figure 3 for location of section line.

rock (Schiarizza et al., 1989, 1990; Journeay et al., 1992; Journeay, 1993). Two distinct zones of structural imbrication (tectonic *mélange*) are recognized in the Bridge River Complex (see Journeay, 1993). The eastern *mélange* zone is well-exposed in the eastern Cayoosh and Chilcotin ranges. It is flanked by the Downton Creek and Fraser Fault systems, and contains dismembered cherts and greenstones that range in age from Mississippian to late Middle Jurassic (Cordey, 1988, 1990). The western *mélange* belt, well-exposed in the eastern Cadwallader Range, is similar in composition to its eastern counterpart, and is cut by high angle imbricate faults of the Bralorne Fault Zone. Situated between these two *mélange* belts, in the upper plate of the Bralorne Fault and in the lower plate of the Downton Creek Fault, is a deformed but coherent succession of Bridge River greenstone, thin-bedded ribbon chert, calcareous greenschist, graphitic siltstone and fine grained volcanoclastic sandstone (Fig. 1, 2; Journeay and Northcote, 1992).

The Cayoosh Assemblage is a Jura-Cretaceous succession of fine grained clastic metasedimentary rocks that conformably overlies interbedded greenstone, chert and siliceous siltstone of the Bridge River Complex (Journeay and Northcote, 1992). The type section is characterized by thin-bedded siltstone and sandstone, quartz-rich feldspathic arenite, laminated phyllitic arenite and volcanoclastic sandstone, and is well exposed in alpine ridges of the western Cayoosh Range. It is flanked to the west by the Bralorne Fault and to the east by the Downton Creek Fault (Fig. 3).

The Brew Group (Duffell and McTaggart, 1952) is a fault-bounded sequence of argillite, siltstone, greywacke, quartz-rich sandstone and conglomerate, locally containing fossiliferous sandstone of Early Cretaceous (Early Neocomian) age. It is flanked by the Cayoosh Creek Fault and, as presently mapped, includes a sequence of interlayered greenstone, greenschist and associated fine grained volcanoclastic sandstone and siltstone of uncertain age and correlation.

CAYOOSH ASSEMBLAGE STRATIGRAPHY

The Cayoosh Assemblage, previously mapped as part of the Bridge River Group (Roddick and Hutchison, 1973; Woodsworth, 1977), comprises a thick succession of fine grained metasedimentary rocks. At its type locality, the Cayoosh Assemblage conformably overlies interlayered greenstone, chert and fine grained siltstone/sandstone couplets of the Bridge River Complex. It occupies the core of a southwest-verging syncline, the limbs of which are cut by southwest-directed thrusts of the Bralorne and Downton Creek fault zones (Fig. 2). Primary sedimentary structures and stratigraphic relationships are preserved, but have been modified by the effects of penetrative deformation and regional metamorphism.

Rocks of the Bridge River Complex and overlying Cayoosh Assemblage share the same history of penetrative deformation and metamorphism. Compositional layering is isoclinally folded (locally transposed and disrupted) and is cut by a penetrative slaty cleavage containing lower greenschist grade metamorphic assemblages. In contact aureoles adjacent to crosscutting plutons, these rocks are recrystallized and contain lower amphibolite grade assemblages of garnet, hornblende, biotite, staurolite \pm andalusite. Structural styles vary with rock type and record a history of inhomogeneous strain. Competent sandstone and greywacke beds are only weakly deformed, whereas thin-bedded siltstone/shale and argillite successions are isoclinally folded and locally transposed. Bedding parallel shear zones are common, particularly along the boundaries between competent and incompetent horizons. However, they do not significantly disrupt the stratigraphic succession, and are interpreted to have accommodated relatively small amounts of displacement.

These structural and metamorphic complexities negate any attempt to estimate primary stratigraphic thicknesses or to reconstruct detailed patterns of sedimentation in the

Cayoosh Assemblage. However, continuity of individual map units and preservation of regional facies relationships lead us to conclude that the Cayoosh Assemblage, although deformed and metamorphosed, is stratigraphically coherent and preserves a record of Jura-Cretaceous sedimentation in the Eastern Coast Belt. For the purposes of discussion, we use sedimentary terminology and vertical rock columns (Fig. 4, 5) to describe stratigraphic relationships in the Cayoosh Assemblage. These columns were compiled from measured structural sections and should not be used to infer primary stratigraphic thickness.

Sections that were examined during the 1992 field season (Fig. 4) include the upper transitional facies of the Bridge River Complex and the lower fine grained clastic succession of the Cayoosh Assemblage. Both sections occur on the

upright lower limb of the Cayoosh syncline and are well-exposed along ridge crests adjacent to Melvin Creek (Fig. 3). The upper part of the Cayoosh Assemblage is exposed in the core of the syncline, along strike to the southeast in the Lillooet Range (Joumeay and Northcote, 1992).

The Cayoosh Assemblage comprises five lithofacies, including: 1) an argillite/siltstone succession; 2) volcanic tuff/tuff-breccia; 3) volcanic sandstone; 4) a siltstone/quartz-rich sandstone succession; and 5) granitoid-bearing conglomerate.

Argillite/siltstone succession

The base of the Cayoosh Assemblage is well-exposed along steep ridges flanking the northern headwaters of Melvin Creek (54910mE, 559540mN; Fig. 3). At this locale,

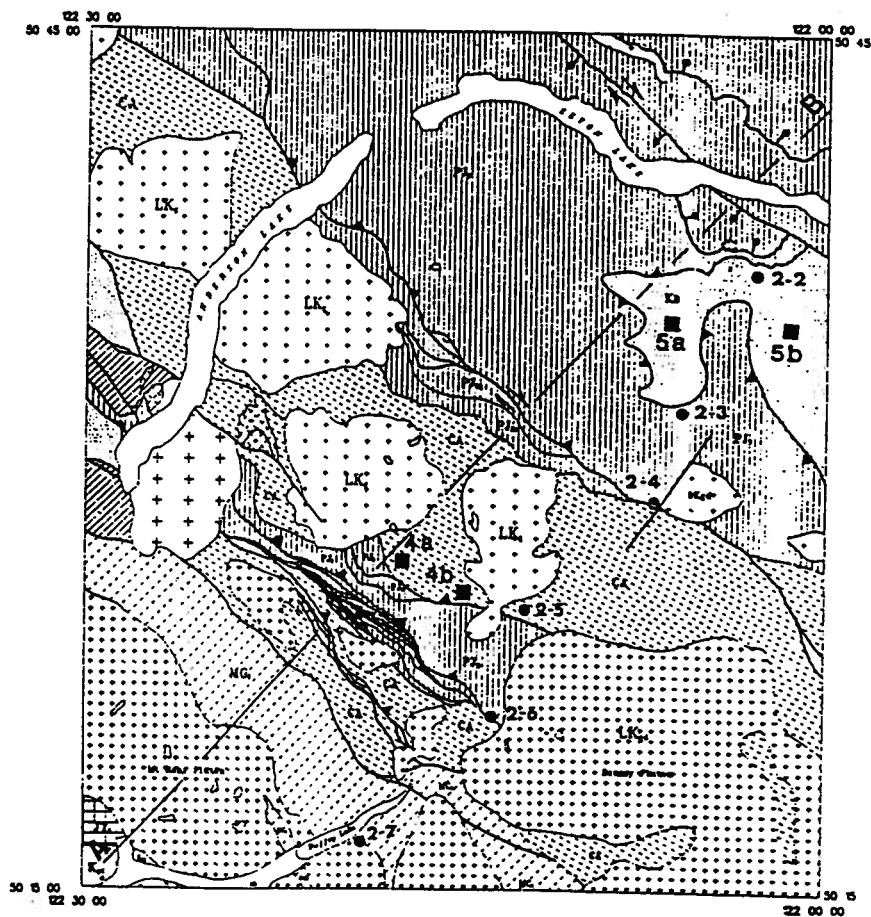


Figure 3. Geological map of the Cayoosh Range (92J/9 map area) showing the distribution and regional structural setting of the Cayoosh Assemblage and the location of measured structural sections. Field trip stops from Monger and Joumeay (1992). Section locations include: 4a=Melvin Creek section; 4b=Cayoosh Creek section; 5a=lower Brew Group section; 5b=upper Brew Group section. Map symbols include: CA= Cayoosh Assemblage; KB=Brew Group; MCs=Chism Creek Schist; PJB=Bridge River Complex; cross pattern= intrusive rock.

interbedded greenstones, ribbon cherts, and black siliceous argillites of the Bridge River Complex are conformably overlain by a thick sequence of dark grey to black, thin bedded argillite and siltstone of the Cayoosh Assemblage. The contact is sharp, and is placed at the top of the stratigraphically highest chert horizon in the Bridge River Complex (Fig. 4).

The basal portion of the Cayoosh Assemblage is approximately 350 m thick and comprises a monotonous succession of dark grey to black, thin-bedded and laminated phyllitic argillite, argillaceous siltstone, siltstone, and sandy siltstone, locally interlayered with discontinuous horizons of thin and medium bedded greywacke and limestone. Thin (2-5 cm) sandy siltstone beds form resistant horizons within

more recessive argillite, and have the appearance of thin-bedded turbidites. Greywacke beds are light grey, thin to medium bedded (5-25 cm), fine grained feldspathic wackes with sharp upper and lower contacts, parallel laminae and locally developed graded bedding. Limestone beds are thin to medium bedded, blue grey, locally sandy and everywhere recrystallized. Greywacke and limestone beds comprise less than 10% of the section near its base, but become increasingly more abundant upsection. A distinctive unit in the argillite/siltstone succession is a mottled, phyllitic argillite characterized by irregular, light grey elongate lenses. When viewed down-plunge, these lenses appear as discontinuous thin (<0.5 cm) light grey to white laminae in a matrix of folded

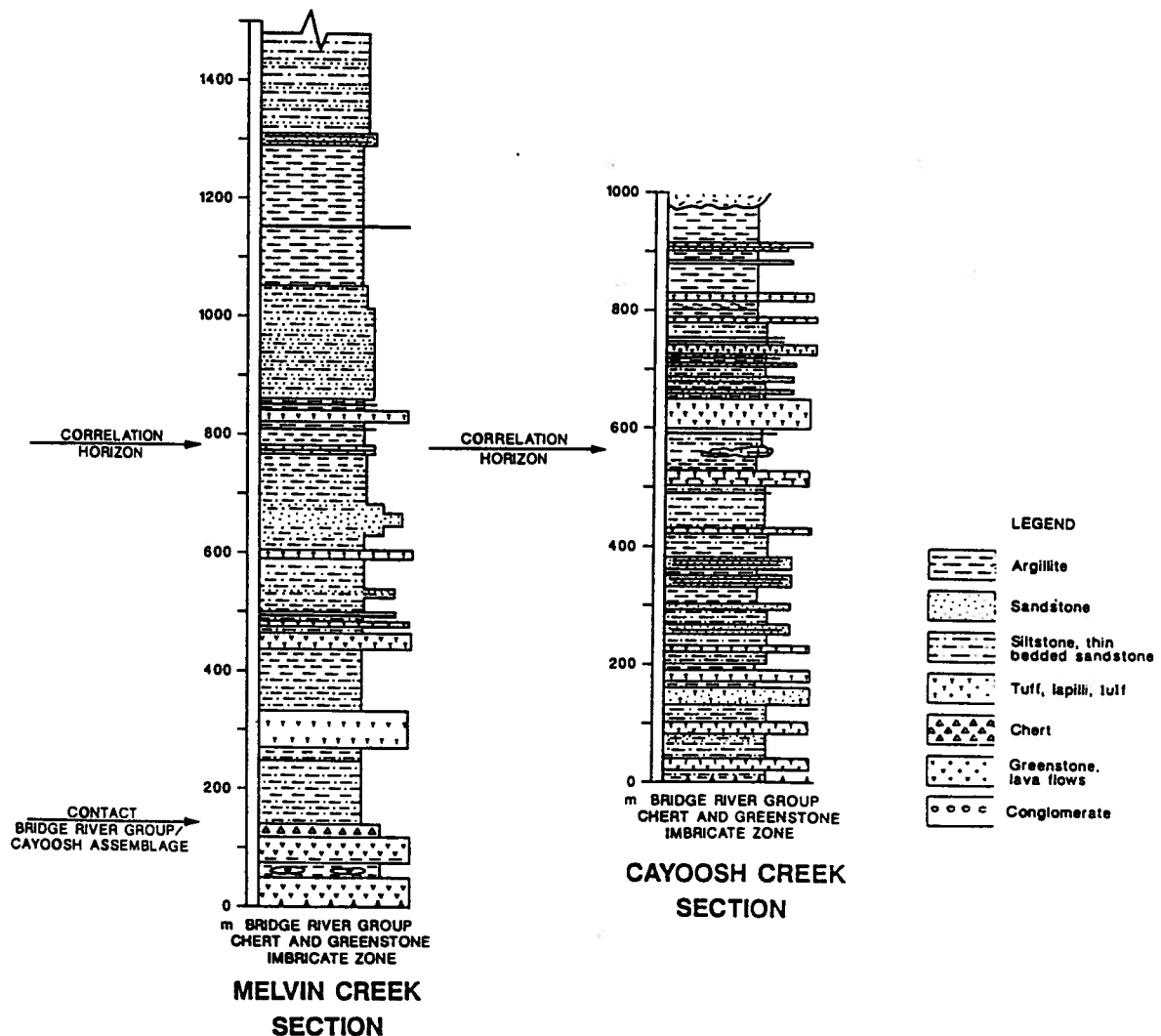


Figure 4. Structural sections of the Cayoosh Assemblage in its type locality of the western Cayoosh Range. See Figure 3 for location of sections.

dark grey argillite. They are interpreted to be thin ash horizons that have been isoclinally folded and transposed parallel to the dominant schistosity.

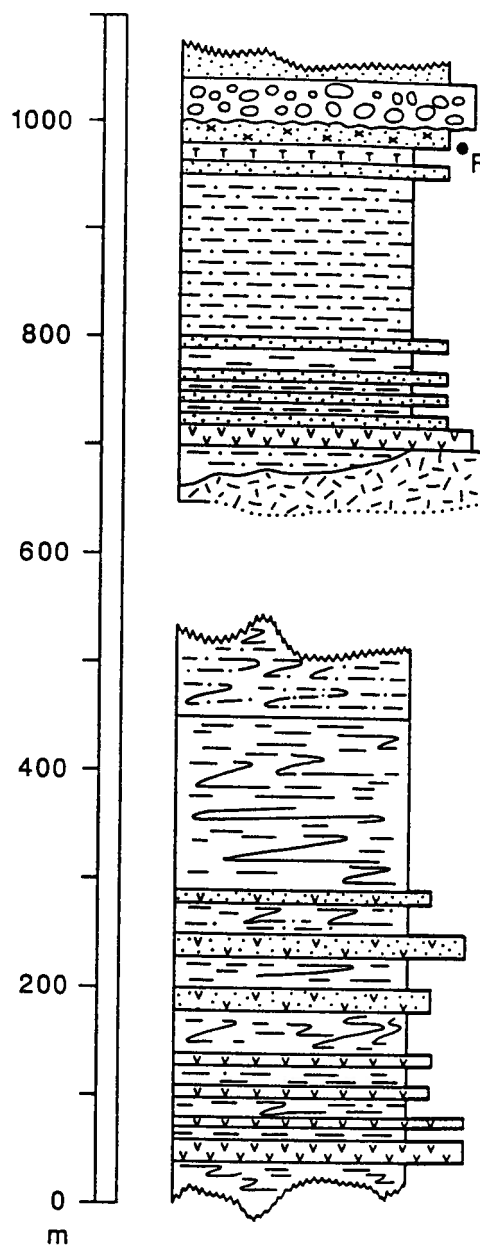
Volcanic tuff/tuff-breccia succession

Thin-bedded argillites and siltstones of the basal Cayoosh Assemblage are locally interlayered with thick (2-60 m) horizons of light to dark green, medium and thick bedded tuff, lapilli tuff, and tuff-breccia (Fig. 4). These horizons are characterized by sharp upper and lower contacts and form laterally continuous and resistant blocky outcrops. The majority of the tuffaceous units are medium bedded, fine grained tuffs and lapilli tuffs consisting of plagioclase grains set in a green, aphanitic matrix. Parallel and wavy lamination and thin (2-5 cm) lenses of dark grey argillite occur locally. Lithic clasts are stretched and consist primarily of fine grained tuff. Coarsening upward sequences are locally evident, with fine grained vitric and crystal tuff coarsening upward into lapilli tuff and tuff-breccia. Rare andesitic(?) flows, locally containing stretched pillows and remnant devitrification structures (spherulites) are also present. These volcanic rocks represent a minor (10-25%) but stratigraphically important component of the lower Cayoosh Assemblage. They represent distinct pulses of volcanic activity in a basin characterized by thick accumulations of fine grained sediments.

Volcanic sandstone succession

Fine grained siltstone, greywacke and associated tuffaceous volcanic rocks grade upwards into a thick (approximately 500-600 m) sequence of fine to coarse grained volcanic sandstone and siltstone (Fig. 4). This volcanoclastic succession consists primarily of interlayered lithic feldspathic arenite and greywacke with thin laminated siltstone. The ratio of sandstone to siltstone varies from 4/1 to 1/2. Sandstone is light grey to light brown on weathered surfaces, thin to medium bedded, fine to coarse grained, and generally well sorted. Parallel laminations, graded bedding, scour features, rip-up clasts, and flame structures are locally well preserved. Sandstone beds commonly have sharp basal contacts, and gradational upper contacts into overlying siltstone beds. Sandstone and siltstone beds are arranged in both coarsening and thickening upward, and fining and thinning upward sequences that range from 5 to 50 m thick (Fig. 4). Sandstone intervals vary in thickness and lateral extent on a scale of 1-2 km. They are interpreted to be lenticular in cross-section and lobate in plan view.

Sandstone units are composed primarily of subangular plagioclase grains and subrounded volcanic lithic fragments, with variable amounts of quartz (5-15%). The quartz content



COMPOSITE STRUCTURAL SECTION OF BREW GROUP

Figure 5. Composite structural section of the Brew Group. The lower part of the section is compiled from exposures along the Cayoosh River, in the footwall of the Cayoosh Creek Fault. The upper part of the section represents the lower upright limb of an antiformal syncline exposed along the south flank of Mount Brew and includes rocks initially defined as part of the Brew Group by Duffell and McTaggart (1952). See Figure 4 for legend. F = Lower Neocomian fossil locality.

increases upwards, with the sandstones in the upper portion of the Cayoosh Assemblage distinctly more quartz-rich than those in the lower portion. Rare thin-bedded, reddish weathering quartz-rich feldspathic arenite occurs throughout the section, and suggests the Cayoosh Assemblage received detritus from multiple source regions.

Siltstone/quartz-rich sandstone succession

The volcanic sandstone succession is gradationally overlain by a thick (200-300 m) sequence of argillite, siltstone and sandstone (Fig. 4). Tuffaceous volcanic horizons occur locally near the base of the sequence, but decrease in abundance upwards. Thin light grey to white laminae, interpreted as tuffaceous ash layers, are locally abundant and attest to continued volcanic activity. Pyritiferous shales and siltstones grade upwards into feldspathic sandstones, similar in appearance to those of the lower argillite/siltstone succession, but containing much higher proportions of detrital quartz. These sandstones consist primarily of thin to thick bedded, fine to coarse grained quartz-rich feldspathic arenite and thin-bedded phyllitic quartzite. Feldspathic arenite beds are 5-8 m thick, locally graded and contain basal shale rip-up clast horizons.

This clastic succession is stratigraphically and compositionally similar to interbedded sandstone, siltstone and shale of the lower portion of the Brew Group (Journeay and Northcote, 1992). Similarities in sandstone composition, interbedded volcanic units, and coarsening upwards stratigraphy suggest a correlation between the Cayoosh Assemblage and the Brew Group. We interpret the Cayoosh Assemblage to be laterally equivalent to and gradationally overlain by rocks of the Brew Group, which suggests that the Cayoosh Assemblage and Brew Group formed a coherent, widespread stratigraphic succession that was dismembered by large-scale crustal imbrication in the Late Cretaceous and early Tertiary.

The lower portion of the Brew Group consists of interbedded dark grey argillite and siltstone, thin-bedded greywacke, thin and thick bedded quartz-rich sandstone, and minor tuffaceous intervals (Fig. 5). Amphibolite lenses near the bottom of the sequence are interpreted to be metavolcanic flows (Journeay and Northcote, 1992). These rocks grade upwards into a distinctive clastic facies of interlayered siltstones, quartz-rich feldspathic arenites and thin laminated phyllitic quartzites. Sandstones become thicker bedded and compositionally and texturally less mature upwards, and are interlayered with tuffaceous siltstones and calcarenites. Calcareous sandstones at the top of this succession contain bivalves of Early Neocomian age (Duffell and McTaggart, 1952).

Conglomerate

Overlying the quartz-rich clastic facies of the Brew Group is a 100-150 m thick section of boulder conglomerate (Fig. 5). The conglomerate cores a southwest-verging antiformal syncline (Mustard, 1983), and represents an important marker horizon in the Brew Group. Well-rounded cobbles and boulders consist primarily of granite and granodiorite, argillite, felsic and intermediate volcanic rock, chert, quartzite, and foliated gneissic rock. One of these granodiorite boulders yielded Middle Jurassic zircons (V. Coleman, pers. comm., 1992).

AGE OF THE CAYOOSH ASSEMBLAGE

The age of the Cayoosh Assemblage is poorly constrained. No macrofossils have been recovered, and due to the structural and metamorphic overprint, it is unlikely that any will be. Microfossil (radiolaria and conodonts) recovery has been unsuccessful. Felsic volcanics from the middle portion of the assemblage are being processed for zircon.

Age constraints for the Cayoosh Assemblage are provided by its relationship with other units in the region. The assemblage must be younger than greenstones and cherts of the Bridge River Complex, which it conformably overlies. Radiolaria as young as Callovian have been recovered from several localities in the eastern imbricate zone, although the majority of dates are Late Triassic (Anisian to Late Norian) and Early to Middle Jurassic (Pliensbachian to Bajocian) (Cordey, 1988, 1990; P. Schiarizza, pers. comm., 1992). No radiolaria have yet been recovered from the western imbricate zone or the central coherent section of the Bridge River Complex. The structural complexity and uncertainty about original basin configuration make it entirely possible that chert deposition in the west either ended before or continued after the cessation of chert deposition in the eastern Bridge River Complex. The age of the transition zone between the Bridge River Complex and overlying Cayoosh Assemblage is therefore unknown.

Fossiliferous greywacke underlying the granite-bearing boulder conglomerate that caps the Brew Group succession yield the bivalve *Buchia crassicollis* of Early Neocomian (Berriasian?) age. Assuming the correlation between the upper Cayoosh Assemblage and the Brew Group is valid, it follows that the majority of the Cayoosh Assemblage/Brew Group stratigraphy must be older than Early Neocomian. As a working hypothesis, we postulate that rocks of the Cayoosh Assemblage and correlative rocks of the Brew Group are part of a widespread clastic succession that ranges in age from Middle(?) Jurassic to Early Cretaceous, with the majority of the unit being Middle(?) to Late Jurassic.

EQUIVALENT ROCKS OF THE SOUTHERN COAST BELT

Structural complexities and the absence of timing constraints from the Cayoosh Assemblage preclude a direct correlation with other clastic successions of the southern Coast Belt. However, the assemblage overlies the Bridge River Complex, which is locally as young as Middle Jurassic, and contains Early Neocomian fossils near the top of the succession, arguing against correlation with pre-Middle Jurassic strata, such as the Triassic Cadwallader and Tyughton groups (Rusmore et al., 1988; Umhoefer, 1989). Jura-Cretaceous clastic and volcanic successions of the southern Coast Belt that may be in part correlative with the Cayoosh Assemblage include the Harrison Lake Formation, the Gambier Assemblage, the Relay Mountain Group, and the Ladner Group (Fig. 6). Metamorphosed clastic rocks of the Cayoosh Assemblage are recognized in the Settler and Chism Creek schist units of the Coast Belt Thrust System (Journeay, 1990; Monger, 1991).

Harrison Lake Formation/Gambier Assemblage

The Harrison Lake Formation, exposed on the west side of Harrison Lake and in fault slivers of the Coast Belt Thrust System, comprises a thick succession of rhyolitic to andesitic volcanic flows and pyroclastic rocks of probable Toarcian to Bajocian age (Fig. 6). The Harrison Lake Formation is overlain by a sequence of Lower Callovian shale and thin bedded sandstone (Mysterious Creek Formation), which are, in turn, overlain by volcanoclastic rocks of the Oxfordian Billhook Creek Formation. These units are unconformably overlain by coarse sandstone and granitoid-bearing conglomerate of the Berriasian Peninsula Formation (Arthur, 1986) and volcanic arc sequences of the Brokenback Hill Formation of the Gambier Assemblage.

Relay Mountain Group

The Middle Jurassic to Lower Cretaceous (Callovian to Hauterivian) Relay Mountain Group is well-exposed in the Chilcotin Range, west of the Yalakom Fault and east of the Downton Creek Fault. It lies unconformably above fine grained volcanoclastic sandstone, siltstone, and minor conglomerate of the Lower to Middle Jurassic (Hettangian to Bajocian) Last Creek Formation (Fig. 6; Umhoefer, 1989). The Relay Mountain Group consists predominantly of volcanoclastic thin bedded siltstone and medium to thick bedded sandstone. Primary volcanic rocks are absent in both the Last Creek Formation and Relay Mountain Group, with the exception of probable thin ash beds in the Last Creek Formation. The Relay Mountain Group is unconformably overlain by conglomerate of the Taylor Creek Group (Garver, 1989).

Ladner Group

Ladner Group is exposed on the east side of the Fraser Fault System, and in tectonic slivers along the west side of the fault (Monger, 1986; Mahoney, 1993). Lower Jurassic argillite and thin-bedded siltstone of the Boston Bar Formation is gradationally overlain by the Toarcian to Bajocian Dewdney Creek Formation, which is a thick volcanoclastic unit that consists of an eastern proximal facies and a western distal facies (O'Brien, 1986; Mahoney, 1993). Ladner Group is disconformably overlain by the Thunder Lake sequence, a thin feldspatholithic sandstone of Oxfordian to Tithonian age (O'Brien, 1986), and by quartz-bearing lithic feldspathic sandstone and granitoid-bearing conglomerate of the Hauterivian(?) to Albian Jackass Mountain Group (Kleinspehn, 1985).

TENTATIVE CORRELATIONS

We interpret the Cayoosh Assemblage to be both laterally equivalent to and gradationally overlain by rocks of the Brew Group. Together, these rocks represent a coherent Jura-Cretaceous clastic succession that conformably overlies oceanic rocks of the Bridge River Complex and is capped by Early Cretaceous and younger conglomerates. Three lithofacies in the Cayoosh Assemblage/Brew Group succession are considered distinct enough to be useful in regional correlation, including: 1) volcanic tuff and tuff-breccia; 2) quartz-rich clastic rocks, and 3) granitoid-bearing conglomerates. Although undated, these distinctive lithofacies provide the basis for lithostratigraphic correlation with other clastic successions of the southern Coast Belt.

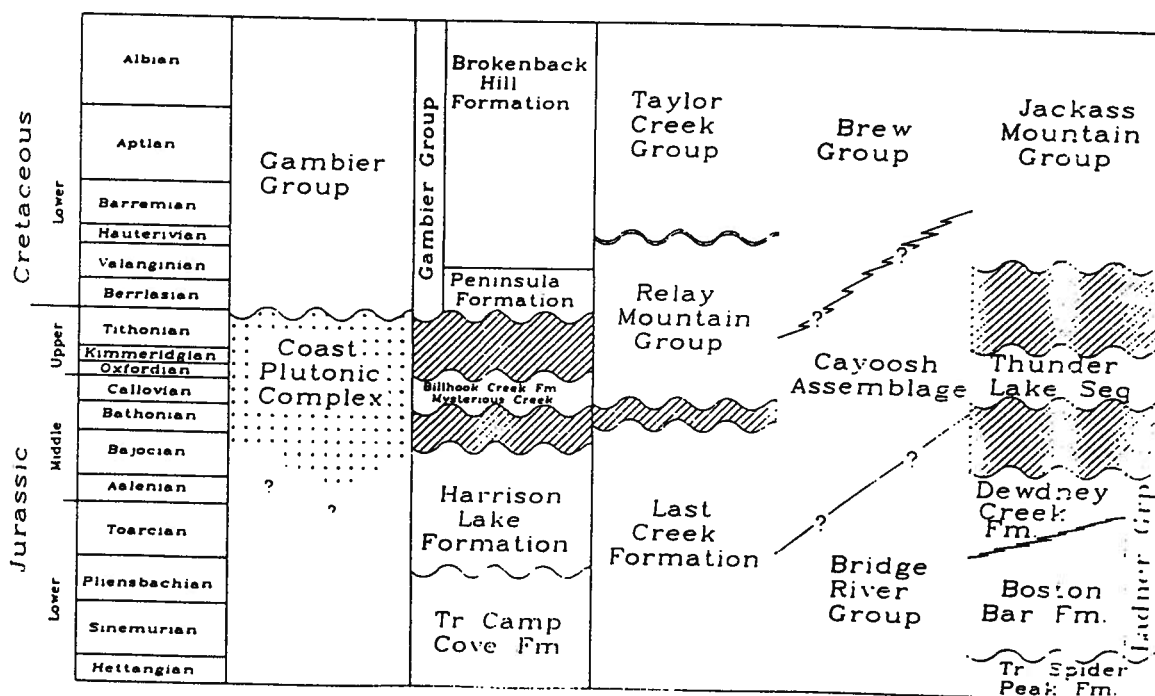


Figure 6. Correlation chart of Jura-Cretaceous units in the southern Coast Belt. Data from Arthur (1986; O'Brien (1986); Umhoefer (1989); Lynch (1991); Mahoney (1993).

Volcanic/volcaniclastic facies

Volcanic and volcanoclastic rocks of the Cayoosh Assemblage are interlayered with thick accumulations of siltstone/greywacke turbidite, graphitic siltstone and shale. The presence of fragmental volcanic flows and abundant tuffaceous detritus suggest a proximal source. These volcanics could be westerly derived, from Middle and Upper Jurassic volcanic flows and pyroclastic rocks of the Harrison Lake Formation and overlying Billhook Creek Formation, or easterly derived, from Middle Jurassic volcanic and volcanoclastic rocks of the Dewdney Creek Formation (Ladner Group) (Fig. 6). The Relay Mountain Group lacks primary volcanic rocks. Harrison Lake Formation and overlying units provide a source for volcanic material, but are lacking in quartz-rich detritus. The association of volcanoclastic rocks and overlying quartz-rich feldspathic sandstone in the Middle Jurassic Ladner Group and younger rocks is similar to that of the Cayoosh Assemblage, and suggests a possible correlation between the two.

Quartz-rich clastic facies

The quartz-rich clastic facies of the Cayoosh Assemblage conformably overlies the volcanic lithofacies and is overlain by the Lower Cretaceous conglomerate lithofacies.

In the Harrison Lake area, volcanic and volcanoclastic rocks of the Harrison Lake Formation are overlain by sandstone and siltstone of the Mysterious Creek Formation and volcanoclastic sediments of the Billhook Creek Formation, which are in turn overlain by granitoid-bearing conglomerate of the Peninsula Formation. Harrison Lake Formation contains abundant quartz-bearing rhyolitic volcanic rocks, but quartz-rich detritus is absent. The detrital component of both the Mysterious Creek and Billhook Creek formations are distinctly quartz poor.

Quartz detritus is minimal in the Relay Mountain Group, although Upper Jurassic (lower Oxfordian) sandstone in the lower Relay Mountain Group contains up to 17% detrital quartz of inferred plutonic origin (Umhoefer, 1989). However, these quartzofeldspathic sandstones are overlain by a thick sequence of quartz-poor volcanoclastic rocks of the middle and upper Relay Mountain Group.

The Dewdney Creek Formation of Ladner Group contains an anomalous sequence of quartzofeldspathic sandstone of inferred Aalenian age that interrupts the predominantly volcanoclastic succession (Mahoney, 1993). The source of this sandstone is unknown. The formation also contains quartz-bearing tuffs and lapilli tuffs. The Thunder Lake assemblage and lower Jackass Mountain Group lie above the volcanoclastic Dewdney Creek Formation, and below granitoid bearing conglomerate of the Jackass Mountain Group. These strata display an increase in plutonic debris over the underlying units, but do not constitute a "quartz-rich" facies. The transition from volcanoclastic rocks with minor quartz-rich detritus in the Dewdney Creek Formation to feldspathic sandstones and conglomerates of the Thunder Lake Sequence and lower Jackass Mountain Group is similar to that observed in the upper Cayoosh Assemblage, and may be correlative.

Lower Cretaceous granitoid-bearing conglomerate

Lower Cretaceous granitoid-bearing conglomerates form an important marker horizon in the southern Canadian Cordillera. They represent the first definitive tie between the Insular and Intermontane superterrane. Granitoid-bearing conglomerates containing granitic clasts of Middle to Late Jurassic age are known from the Lower Cretaceous Gambier Group of the Insular Terrane (Lynch, 1991), from the Berriasian Peninsula Formation of the Harrison Lake Terrane (Arthur, 1986; O'Brien et al., 1992), from the Lower Cretaceous(?) Brew Group of the Bridge River Terrane (Duffell and McTaggart, 1952; Journeay and Northcote, 1992), and from the Hauterivian to Albian Jackass Mountain Group of the Methow Terrane (Kleinspehn, 1985). These conglomerates probably represent a clastic pulse related to uplift and erosion of arc assemblages either during or after terrane amalgamation.

The top of the Cayoosh Assemblage/Brew Group succession is marked by a granitoid-bearing conglomerate containing Middle Jurassic plutonic clasts that overlies Lower Neocomian fossiliferous sandstone. We interpret this conglomerate to be part of a Lower Cretaceous overlap assemblage that includes coarse clastic rocks of the Gambier Assemblage and the Jackass Mountain Group.

The correlation of the granitoid-bearing conglomerate in the upper Cayoosh Assemblage/Brew Group with a regional Lower Cretaceous overlap assemblage is important. The stratigraphy of the Cayoosh Assemblage/Brew Group consists of pelagic sediments overlain by volcanoclastic to quartz-rich clastic sediments, capped by granitoid-bearing conglomerate. We suggest that this stratigraphy records the cessation of pelagic sedimentation in the Bridge River "ocean", the initiation of Middle(?) to Late(?) Jurassic arc volcanism associated with basin closure, and the eventual uplift and erosion of this arc in Early Cretaceous time.

ONGOING INVESTIGATIONS

Our geological understanding of the Cayoosh Assemblage and its tectonic implications is in its infancy. Critical questions currently under investigation:

1. What is the age of the Cayoosh Assemblage? How does the age of this clastic assemblage fit into the established Mesozoic basin framework (Garver, 1989; Umhoefer, 1989; Mahoney, 1992, 1993)?
2. What is the affinity/derivation/source of the volcanic rocks in the Cayoosh Assemblage? The isotopic and geochemical signatures of these rocks may allow for correlations with other Mesozoic volcanic arcs in southern British Columbia.
3. What is the source of the granitic clasts found in the conglomerate, and how does this conglomerate relate to similar units in the region?
4. Finally, can the Cayoosh Assemblage be definitively correlated with other units in the region, thus providing a stratigraphic framework that places constraints on the tectonic evolution of the region?

ACKNOWLEDGMENTS

Fieldwork was carried out in collaboration with Bill McClelland, who has undertaken a pilot U-Pb study of detrital zircons and felsic flows to help constrain the age and provenance of the Cayoosh Assemblage. We thank him for his astute observations and contributions in the field and for many stimulating and entertaining discussions of Coast Belt and cosmic geology. Our understanding of Jura-Cretaceous stratigraphy in the southern Coast Belt has evolved through discussions with Jim Monger, Glenn Woodsworth and Paul Schiarizza. We thank them for sharing their ideas and experience. Helicopter and logistical support were provided by John and Patricia Goats of Pemberton Helicopters.

REFERENCES

- Arthur, A.J.
1986: Stratigraphy along the west side of Harrison Lake, southwestern British Columbia; in *Current Research, Part A: Geological Survey of Canada, Paper 86-1B*, p. 715-720.
- Corday, F.
1988: Etude des radiolaires Permians, Triassiques et Jurassiques des complexes ophiolitiques de Cache Creek, Bridge River et Hozomeen (Columbic Britannique, Canada): implications paleogeographiques et structurales; Ph.D. thesis, Université Pierre et Marie Curie, Paris, France.
- 1990: Radiolarian age determinations from the Canadian Cordillera; in *Current Research, Part E: Geological Survey of Canada, Paper 90-1E*, p. 121-126.
- Duffell, S. and McTaggart, K.C.
1952: Ashcroft map area, British Columbia; Geological Survey of Canada, Paper 67-10, 55 p.
- Garver, J.I.
1989: Basin evolution and source terranes of Albian-Cenomanian rocks in the Tyaughton Basin, southern British Columbia: implications for mid-Cretaceous tectonics in the Canadian Cordillera; Ph.D. thesis, University of Washington, Seattle.
- Journey, J.M.
1990: A progress report on the structural and tectonic framework of the southern Coast Belt, British Columbia; in *Current Research, Part E: Geological Survey of Canada, Paper 90-1E*, p. 183-195.
- 1993: Tectonic assemblages of the eastern Coast Belt, British Columbia: Implications for the history and mechanisms of terrane accretion; in *Current Research, Part A: Geological Survey of Canada, Paper 93-1A*.
- Journey, J.M. and Northcote, B.R.
1992: Tectonic assemblages of the Eastern Coast Belt, southwest British Columbia; in *Current Research, Part A: Geological Survey of Canada, Paper 92-1A*, p. 215-224.
- Journey, J.M., Sanders, C., van-Konijnburg, J.-H., and Jaasma, M.
1992: Fault systems of the Eastern Coast Belt, southwest British Columbia; in *Current Research, Part A: Geological Survey of Canada, Paper 92-1A*, p. 225-235.
- Kleinspehn, K.L.
1985: Cretaceous sedimentation and tectonics, Tyaughton-Methow Basin, southwestern British Columbia; *Canadian Journal of Earth Sciences*, v. 22, p. 229-233.
- Lynch, J.V.G.
1991: Georgia Basin Project: stratigraphy and structure of Gambier Group rocks in the Howe Sound-Mamquam River area, southwest Coast Belt, British Columbia; in *Current Research, Part A: Geological Survey of Canada, Paper 91-1A*, p. 49-57.
- Mahoney, J.B.
1992: Middle Jurassic stratigraphy of the Lillooet area, south-central British Columbia; in *Current Research, Part A: Geological Survey of Canada, Paper 92-1A*, p. 243-248.
- 1993: Facies reconstructions in the Lower to Middle Jurassic Ladner Group, southern British Columbia; in *Current Research, Part A: Geological Survey of Canada, Paper 93-1A*.
- Monger, J.W.H.
1986: Geology between Harrison Lake and Fraser River, Hope map area, southwestern British Columbia; in *Current Research, Part B: Geological Survey of Canada, Paper 86-1B*, p. 699-706.
- 1991: Correlation of Settler schist with Darrington Phyllite and Shuksan Greenschist and its tectonic implications, Coast and Cascade Mountains, British Columbia and Washington; *Canadian Journal of Earth Sciences*, v. 28, p. 447-458.
- Monger, J.W.H., Price, R.A., and Tempelman-Kluit, D.J.
1982: Tectonic accretion and the origin of two major metamorphic and plutonic belts in the Canadian Cordillera; *Geology*, v. 10, p. 70-75.
- Monger, J.W.H. and Journeay, J.M.
1992: Guide to the geology and tectonic evolution of the southern Coast Belt: field guide to accompany Penrose Conference on "Tectonic Evolution of the Coast Mountains Orogen", 92 p.
- Mustard, J.F.
1983: The geology of the Mount Brew area, Lillooet, British Columbia; M.Sc. thesis, University of British Columbia, Vancouver, 74 p.
- O'Brien, J.A.
1986: Jurassic stratigraphy of the Methow Trough, southwestern British Columbia; in *Current Research, Part B: Geological Survey of Canada, Paper 86-1B*, p. 749-756.
- O'Brien, J.A., Gehrels, G.E., and Monger, J.W.H.
1992: U-Pb geochronology of plutonic clasts from conglomerates in the Ladner and Jackass Mountain groups and the Peninsula Formation, southwestern British Columbia; in *Current Research, Part A: Geological Survey of Canada, Paper 92-1A*, p. 209-214.
- Roddick, J.A. and Hutchison, W.W.
1973: Pemberton (east half) map-area, British Columbia; Geological Survey of Canada, Paper 73-17, 21 p.
- Rusmore, M.E., Potter, C.J., and Umhoefer, P.J.
1988: Middle Jurassic terrane accretion along the western edge of the Intermontane superterrane, southwestern British Columbia; *Geology*, v. 16, p. 891-894.
- Schiarizza, P., Gaba, R.G., Glover, J.K., and Garver, J.I.
1989: Geology and mineral occurrences of the Tyaughton Creek area (92O/2, 92J/15,16); in *Geological Fieldwork 1988*, British Columbia Ministry of Energy, Mines and Petroleum Resources, Paper 1989-1, p. 115-130.
- Schiarizza, P., Gaba, R.G., Coleman, M., Glover, J.K., and Garver, J.I.
1990: Geology and mineral occurrences of the Yakom River area (92I/1,2, 92J/15,16); in *Geological Fieldwork 1989*, British Columbia Ministry of Energy, Mines and Petroleum Resources, Paper 1990-1, p. 53-73.
- Umhoefer, P.J.
1989: Stratigraphy and tectonic setting of the Upper Cadwallader Terrane and overlying Relay Mountain Group, and the Cretaceous to Eocene structural evolution of the eastern Tyaughton Basin, British Columbia; Ph.D. thesis, University of Washington, Seattle, 186 p.
- van der Heyden, P.
1992: A Middle Jurassic to early Tertiary Andean-Sierran arc model for the Coast Belt of British Columbia; *Tectonics*, v. 11, p. 82-97.
- Woodsworth, G.J.
1977: Pemberton (92J) map area, British Columbia; Geological Survey of Canada, Open File 482.

Geological Survey of Canada Project 890036

Cayoosh Assemblage: regional correlations and implications for terrane linkages in the southern Coast Belt, British Columbia

J.M. Journeay and J.B. Mahoney¹
Cordilleran Division, Vancouver

Journeay, J.M. and Mahoney, J.B., 1994: Cayoosh Assemblage: regional correlations and implications for terrane linkages in the southern Coast Belt, British Columbia; in Current Research 1994-A; Geological Survey of Canada, p. 165-175.

Abstract: The Cayoosh Assemblage is an upward-coarsening succession of metamorphosed phyllitic argillite, siltstone, and sandstone that conformably overlies oceanic rocks of the Bridge River Complex. The age and regional distribution of these rocks suggest that the Bridge River ocean was long-lived, and remained open to marine sedimentation until Late Jurassic or Early Cretaceous time. New stratigraphic and paleontological data suggest that outboard terranes, including the Cadwallader and Harrison island arc complexes, may have been linked prior to accretion along the continental margin. Coarsening-upward clastic successions near the top of the Cayoosh Assemblage overlap these outboard terranes and record the final stages of terrane accretion along the ancestral continental margin.

Résumé : L'Assemblage de Cayoosh est une succession à cycle négatif d'argilite, de siltstone et de grès métamorphisés, qui surmonte en concordance les roches océaniques du complexe de Bridge River. L'âge et la distribution régionale de ces roches indiquent que l'océan de Bridge River a eu une existence de longue durée et est demeuré ouvert à la sédimentation marine jusqu'à la fin du Jurassique ou au début du Crétacé. De nouvelles données stratigraphiques et paléontologiques indiquent que des terranes situés au large, dont les complexes d'arc insulaire de Cadwallader et de Harrison, auraient pu être reliés avant leur accrétion à la marge continentale. Les successions détritiques à cycle négatif, près du sommet de l'Assemblage de Cayoosh, recouvrent ces terranes extracôtiers et témoignent des derniers stades de l'accrétion des terranes à la protomarge continentale.

¹ Department of Geological Sciences, University of British Columbia, 6339 Stores Road, Vancouver, British Columbia V6T 2B4

INTRODUCTION

Conceptual tectonic models of the western Canadian Cordillera, as it may have appeared in early to middle Jurassic time, portray ancestral terranes of the Coast and Insular belts as an array of island arc festoons and oceanic plateaus situated outboard of an accretionary/fore-arc complex (Monger et al., 1982; van der Heyden, 1992), a setting similar to that of the present southwest Pacific plate margin.

Outboard terranes of the northern Coast Belt (54° - 60° N), which include Wrangellia and Alexander island arc complexes (Fig. 1), appear to have been amalgamated into a single superterrane in the Late Paleozoic and accreted onto the western margin of ancestral North America (Intermontane

Belt) by Middle to Late Jurassic time. During the final stages of accretion, the zone of active subduction shifted westward from the Cache Creek suture to the outboard margin of the Insular superterrane, leading to the development of a post-Middle Jurassic accretionary/fore-arc complex (Chugach terrane) and an Andean-style magmatic arc (van der Heyden, 1992).

Terranes of the southern Coast Belt (49° - 54° N), which include island arc assemblages of Wrangellia, Cadwallader, and Harrison terranes and oceanic rocks of the Bridge River terrane (Fig. 1), appear to have remained outboard of the ancestral continental margin throughout much of the Jurassic. Mississippian to Callovian (ca. 330-160 Ma) pelagic cherts of the Bridge River Complex and overlying Early Jurassic(?)

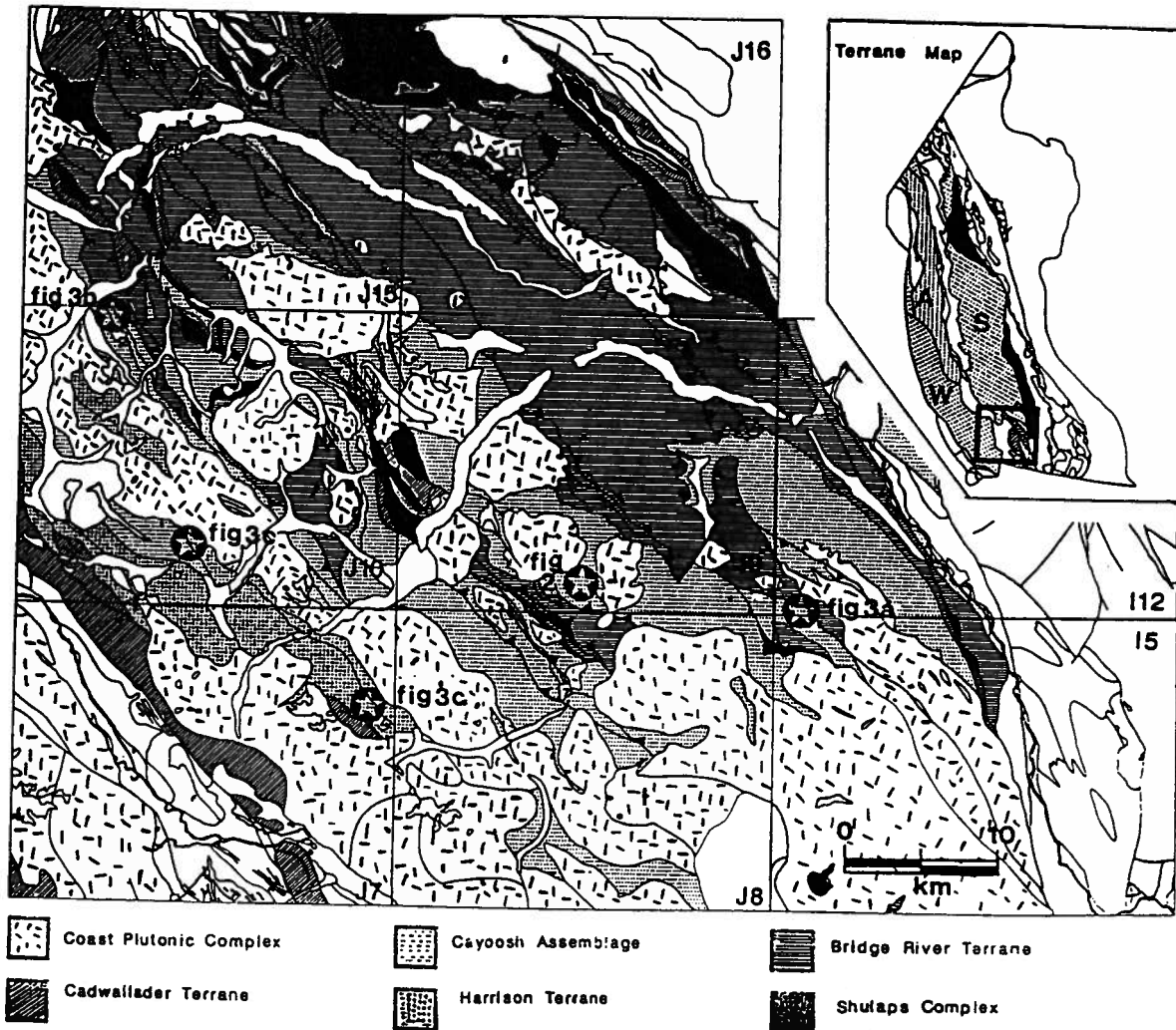


Figure 1. Tectonic setting (inset) and regional geology of the eastern Coast Belt. W: Wrangellia terrane; A: Alexander terrane; S: Siikinia terrane.

to Early Cretaceous(?) fine grained, clastic rocks of the Cayoosh Assemblage suggest that the Bridge River ocean remained open to marine sedimentation until Early Cretaceous time (Journeay and Northcote, 1992; Cordey and Schiarizza, 1993; Mahoney and Journeay, 1993). Early to mid-Cretaceous fluvial conglomerates and shallow marine clastic rocks (Gambier, Taylor Creek, and Jackass Mountain groups) form the oldest demonstrable overlap assemblage among terranes in the southern Coast Belt, and indicate that outboard terranes were stratigraphically linked prior to the onset of crustal shortening and large-scale crustal imbrication (Journeay and Friedman, 1993). However, it is not clear whether these outboard terranes were amalgamated prior to the Early Cretaceous and situated near the ancestral continental margin in a marginal basin setting, or whether they may have been added incrementally as part an accretionary/forearc complex in response to ongoing post-middle Jurassic subduction of the Bridge River ocean.

To address this question, we have focused our investigations on the internal stratigraphy and regional distribution of Jurassic and Cretaceous clastic successions that overlie oceanic rocks of the Bridge River Complex and associated island arc assemblages of the Cadwallader and Harrison terranes. These include turbidites and upward-coarsening clastic successions of the Cayoosh Assemblage, coarse clastic and shallow marine successions of the Tyaughton and Relay Mountain groups, and fine grained marine and volcanoclastic successions of the Mysterious and Billhook Creek formations, respectively. Fieldwork during the 1993 season involved 1:50 000 scale mapping in the Cadwallader and Cayoosh ranges of the eastern Coast Belt (92J/7, 92J/8, 92J/9, 92J/10, 92J/5, and 92J/12; Fig. 1), and detailed stratigraphic and sedimentological studies of the Cayoosh Assemblage.

CAYOOSH ASSEMBLAGE

The Cayoosh Assemblage is an upward-coarsening succession of metamorphosed phyllitic argillite, siltstone, and sandstone that conformably overlies interbedded greenstone, chert, and phyllitic argillite of the Bridge River Complex (Fig. 1; Journeay and Northcote, 1992; Journeay, 1993; Mahoney and Journeay, 1993). Primary sedimentary structures and stratigraphic relationships are preserved, but have been modified by the effects of penetrative deformation and regional metamorphism associated with Alpine-style folding and large-scale imbrication of the eastern Coast Belt (Journeay and Friedman, 1993). These structural and metamorphic complexities preclude accurate estimates of primary stratigraphic thicknesses or detailed reconstructions of sedimentation patterns and basin configuration. However, the integrity and lateral continuity of regional lithofacies lead us to conclude that the Cayoosh Assemblage is a stratigraphically coherent succession that preserves a record of Jurassic and Early Cretaceous sedimentation during the final stages in the evolution of the Bridge River ocean.

Stratigraphy

We have subdivided the Cayoosh Assemblage into five distinct lithofacies (Fig. 2). In ascending stratigraphic order, these include: graphitic phyllite, siltstone, and sandstone (unit 1), tuffaceous phyllite, graphitic phyllite, minor lapilli tuff, and tuff breccia (unit 2), graphitic phyllite, siltstone, limestone, and volcanoclastic sandstone (unit 3), graphitic siltstone, shale, phyllite, arkosic sandstone, and quartzite (unit 4), and thin-bedded graphitic phyllite, siltstone, and volcanoclastic sandstone (unit 5). For the purposes of discussion, we have used a standard rock column format to summarize and to describe the internal stratigraphy of the Cayoosh Assemblage (Fig. 2). This column is compiled from measured structural sections in reference localities of the Cayoosh Assemblage and does not indicate primary stratigraphic thickness.

This stratigraphy represents a more detailed subdivision of the Cayoosh Assemblage than that initially proposed by Mahoney and Journeay (1993). Neocomian sandstones and siltstones of unit 5, initially included in the upper siltstone/quartz-rich sandstone succession of the Cayoosh Assemblage, are here recognized as a distinct lithofacies. Fluvial conglomerate, initially included as the uppermost member of the Cayoosh Assemblage, is interpreted to unconformably overlie fossiliferous sandstones of unit 5 in the vicinity of Mount Brew. This conglomerate represents a fundamental change in depositional environment, and has been split out as a separate stratigraphic unit. Clast compositions and the occurrence of Late Jurassic granitoid boulders (ca. 151 Ma; V. McNicoll, pers. comm., 1992) suggest correlation with Early Cretaceous conglomerate of the Jackass Mountain Group. Detailed descriptions of the Cayoosh Assemblage in its type locality are reported by Mahoney and Journeay (1993). The following is a brief synopsis.

Interlayered greenstone, ribbon chert, limestone, calcareous greenschist, and graphitic phyllite of the Bridge River Complex grade upward with apparent conformity into a succession of graphitic siltstone, phyllite, greywacke and thin-bedded turbidites of the Cayoosh Assemblage (unit 1). The basal contact of the Cayoosh Assemblage is defined at the top of the stratigraphically highest chert horizon, and is locally marked by a thin, intra-formational pebble conglomerate containing clasts of limestone, siliceous argillite, and chert. Thinly laminated tuffaceous siltstone occurs near the top of this succession and signals an important change in provenance.

Unit 2 is characterized by thick (2-60 m) horizons of metamorphosed light to dark green, medium- and thick-bedded tuff, lapilli tuff, and tuff breccia, which occur as distinct layers in a succession of graphitic phyllite and siltstone. These pyroclastic rocks represent a minor (10-25%) but stratigraphically important component of the section. They record distinct pulses of volcanic activity in a basin characterized by thick accumulations of fine grained sediments. Both lower and upper boundaries of this succession are gradational.

Unit 3 comprises a thick (500-600 m) succession of fine- to coarse-grained volcanic sandstone and siltstone (30-35%) interlayered with graphitic phyllite (55-65%) and thin bands

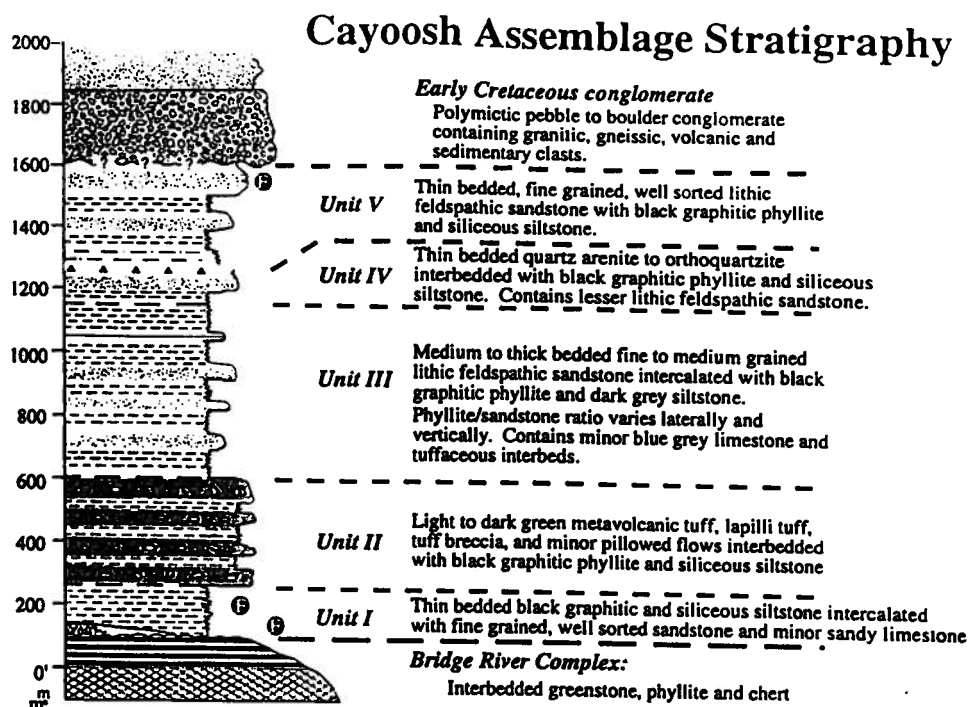


Figure 2. Schematic stratigraphic section of the Cayoosh Assemblage, as compiled from measured structural sections in the Melvin Creek and Mount Brew regions.

of limestone (5%). Sandstone horizons consist primarily of interlayered feldspathic arenite and greywacke with intercalations of thinly laminated siltstone. Horizons of quartz-rich feldspathic arenite occur near the top of the unit, suggesting that the Cayoosh Assemblage may have received detritus from multiple source regions. Sandstone intervals vary in thickness (50-100 m) and lateral extent throughout the unit, and are interpreted to be lenticular in cross-section and lobate in plan view. They define a cyclic coarsening- and thickening-upward/fining- and thinning-upward succession, with the highest proportion of sandstone occurring near the middle of the unit. Pyritiferous shale and siltstone near the top of unit 3 grade upward into feldspathic sandstone, similar in appearance to those of unit 1, but containing a higher proportion of detrital quartz.

Unit 4 is characterized by the presence of a quartz-rich clastic facies in, what is otherwise, a thick and monotonous succession of graphitic siltstone, shale, and phyllite. Thin, light grey and white laminae, interpreted as tuffaceous ash layers, are locally abundant and attest to continued volcanic activity. Sandstone horizons consist primarily of thin- and thick-bedded, fine- to coarse-grained, quartz-rich feldspathic arenite, orthoquartzite, and thinly laminated phyllitic quartzite. Feldspathic arenite beds are 5-8 m thick, locally graded and contain basal shale rip-up clasts. Quartzite horizons, which represent an unusual but very distinctive component of the upper Cayoosh Assemblage, consist primarily of quartz

with lesser amounts of detrital feldspar and hornblende (Fig. 4). The appearance of compositionally mature quartz-rich detritus in this part of the section suggests a continental influence. Provenance studies, including systematic petrography and U-Pb analysis of detrital zircon, are underway.

Quartz-rich clastic rocks of unit 4 grade upward into a thick (200-300 m) sequence of thin-bedded graphitic phyllite, siltstone, and fine- and medium-grained volcanoclastic sandstone (unit 5). Near Mount Brew, this section coarsens upward into a sequence of interlayered calcareous sandstone, phyllite, and green lithic feldspathic arenite. This upper clastic section is interpreted to be unconformably overlain by fluvial conglomerate, tentatively correlated with Early Cretaceous conglomerates of the Jackass Mountain Group. The upward coarsening trend and the occurrence of fossiliferous shallow marine sandstone near the top of unit 5 signal an important change in depositional environment, and may reflect the end of marine sedimentation in the Cayoosh Assemblage.

Age and regional distribution

Available age constraints indicate that the Cayoosh Assemblage probably ranges from Early Jurassic(?) to Early Cretaceous (Journeay and Northcote, 1992; Mahoney and Journeay, 1993). Basal turbidites in the type locality of

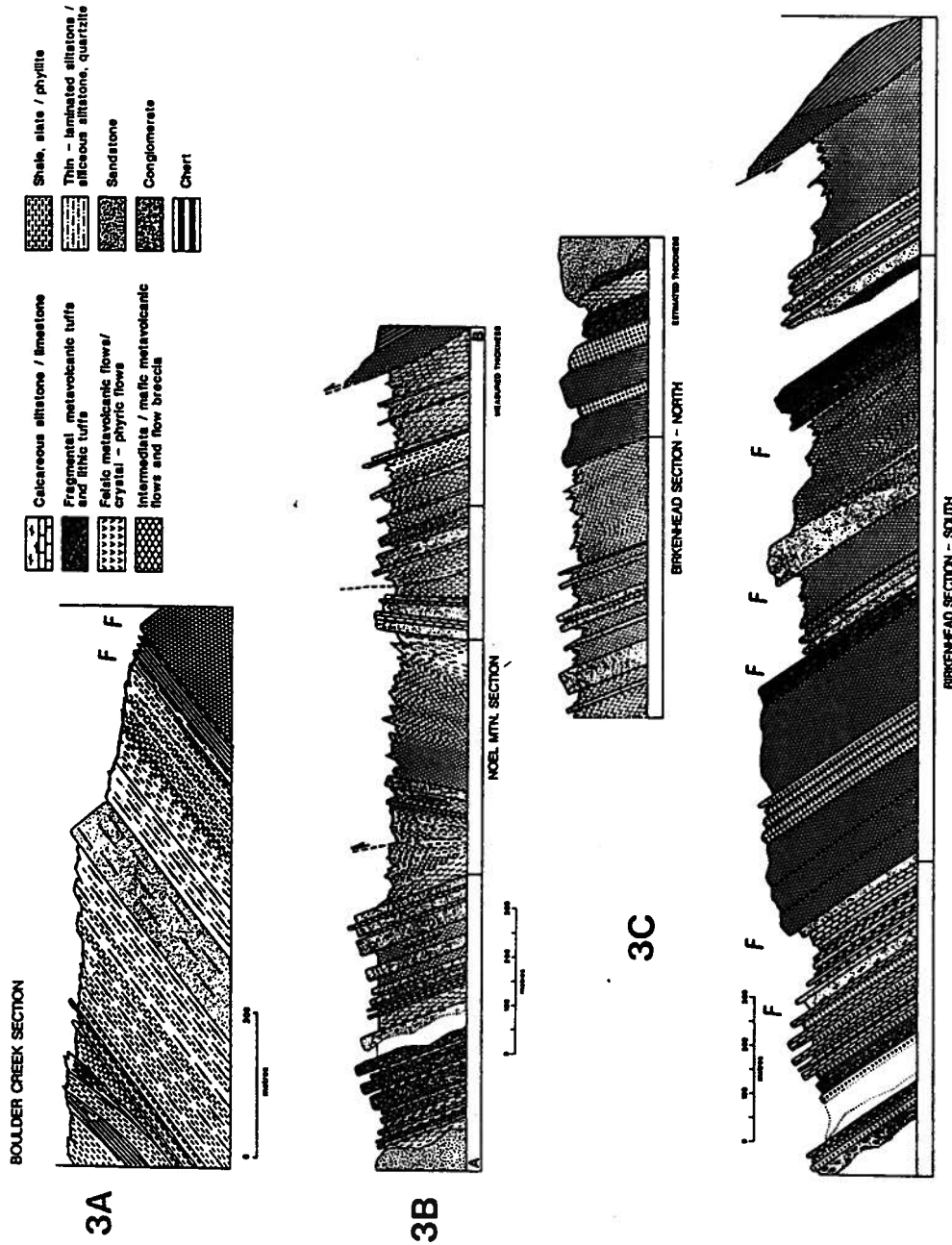


Figure 3. (A) Geological setting and stratigraphy of the Boulder Creek section. (B) Geological setting and stratigraphy of the Noel Mountain section. (C) Geological setting and stratigraphy of the Birkenhead section.

Melvin Creek overlies Upper Triassic (Norian) limestone-bearing oceanic rocks of the Bridge River Complex with apparent conformity. The uppermost clastic facies of the Cayoosh Assemblage (unit 5) contains shallow marine volcanic sandstones that yield bivalves (*Buchia*) of Early Neocomian age (Duffell and McTaggart, 1952).

In its type locality, the Cayoosh Assemblage occupies the core of a regional southwest-verging syncline, the limbs of which are cut by southwest-directed thrusts of the Bralorne and Downton Creek fault zones (Fig. 1). The axis of this syncline extends more than 100 km along strike to the southeast from the mining district of Bralorne, across the Cayoosh and Lillooet ranges into the Fraser Canyon, where it is cut by dextral transcurrent faults of the Fraser River fault system. In the course of systematic 1:50 000 scale mapping of stratified rocks in the eastern Coast Belt (Fig. 1; Journeay and Northcote, 1992; Journeay, 1993), we have expanded the outcrop belt of the Cayoosh Assemblage to include imbricated panels of fine grained metasedimentary rocks in both upper and lower plates of the Bralorne Fault (previously mapped as Noel Formation and Chism Creek Schist, respectively). Reconnaissance work in the region north of Carpenter Lake, and mapping by Schiarizza et al. (1989), suggest that clastic rocks of the Cayoosh Assemblage may also extend northward into the Chilcotin Mountains to include graphitic phyllite, siltstone, and sandstone successions presently mapped as part of the Bridge River Complex.

NEW DATA AND INTERPRETATIONS

Stratigraphic relations, the apparent age range, and regional distribution of the Cayoosh Assemblage in the eastern Coast Belt suggest that clastic sedimentation, derived in part from volcanic source terranes, was active in parts of the Bridge River ocean throughout much of the Jurassic. However, stratigraphic linkages between fine grained clastic successions of the Cayoosh Assemblage and outboard island arc assemblages (Wrangellia, Cadwallader and Harrison terranes) remain tenuous. Contact relationships are obscured by an array of postaccretionary thrust and strike-slip faults, which have imbricated and shuffled the eastern Coast Belt since Early Cretaceous time (Schiarizza et al., 1989; Journeay et al., 1992; Journeay and Friedman, 1993), and by eastward-younging batholithic suites of the Coast Plutonic Complex (Friedman and Armstrong, in press). Although isolated by faults and surrounded by plutons, the stratigraphic components of this geological puzzle continue to yield surprising and important new bits of information.

Boulder Creek Section

The Boulder Creek section (Fig. 3A) is well exposed at the southeast end of the Bridge River mélange belt (Journeay et al., 1992; Monger and Journeay, 1992). It is flanked to the west by the Downton Creek Fault, and to the east by

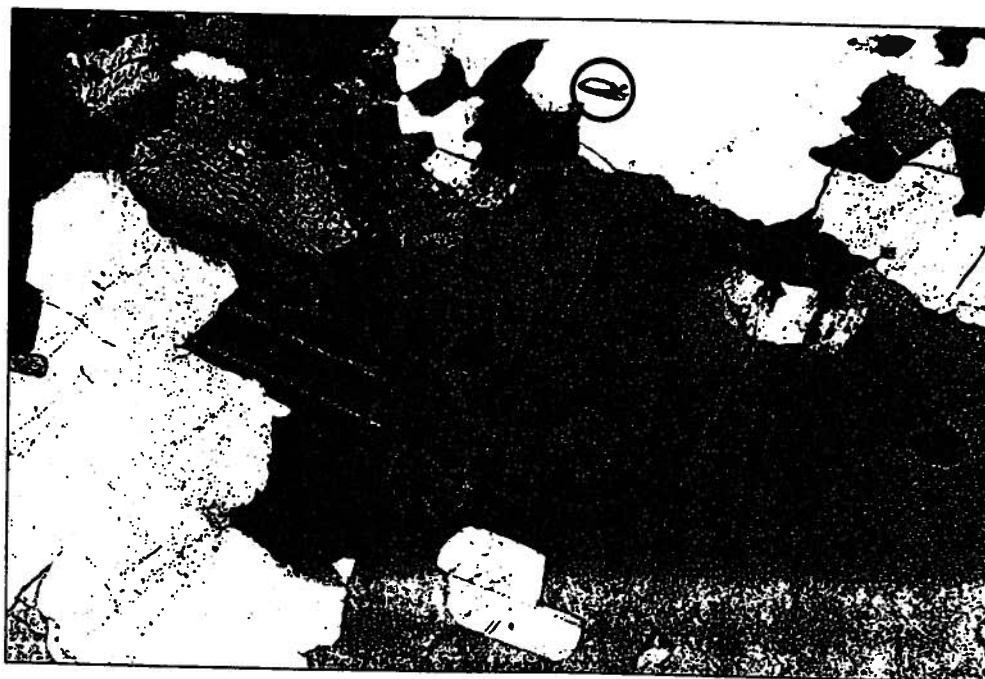


Figure 4. Photomicrograph of quartz-rich clastic facies. Note recrystallized quartz surrounding plagioclase feldspar. Subhedral zircon grain is circled.

low-angle mylonites of the Cayoosh Creek Fault. Imbricated fault slivers of greenstone, chert, limestone, and siltstone, locally containing pods of Upper Triassic (Norian) limestone, characterize the lower part of this section. The highest of these fault slivers contains a stratigraphically coherent panel of interlayered greenstone and chert which grades upward into a thick succession of siltstone, shale, and phyllite of the Cayoosh Assemblage. The contact, defined at the top of the highest chert horizon of the Bridge River Complex, is concordant and locally marked by thin lenses of chert pebble conglomerate. Siliceous argillite and thin bedded turbidites (125 m) at the base of the clastic succession grade upwards into a 75 m thick sequence of interbedded graphitic siltstone and phyllite containing 0.5 to 1.0 m thick horizons of chloritic (metatuffaceous) siltstone. This sequence coarsens upwards into a thick succession (90 m) of immature, medium- to thick-bedded volcanoclastic sandstone, dark grey siltstone, and metatuffaceous phyllite. Sandstones at the top of this clastic succession are, in turn, overlain by an upward-fining succession (200 m) of monotonous dark grey and black graphitic siltstone and phyllite, locally containing thin horizons of metatuffaceous siltstone and limestone. Imbricate fault slivers of greenstone, chert, and siltstone mark the southeast end of this section.

Stratigraphic similarities and lithological associations suggest to us a direct correlation of the Boulder Creek section with both the lower members of the Cayoosh Assemblage (units 1-3; compare Fig. 2 and 3A), and with the Lower to Middle Jurassic Ladner Group (Boston Bar and Dewdney Creek formations), which occurs along strike to the southeast (Fig. 1). Radiolaria extracted from siliceous argillite and siltstone at base of the Boulder Creek section are recrystallized, but include forms that are found in Upper Triassic and Lower Jurassic cherts of the Bridge River Complex (F. Cordey, pers. comm., 1993). Elsewhere in the Bridge River Complex, Cordey and Schiarizza (1993) have documented radiolarian cherts and associated siltstones that are as young as late Middle Jurassic (Callovian). These data suggest to us a complex and protracted history of basin evolution in which parts of the Bridge River ocean began to receive clastic detritus in the Late Triassic/Early Jurassic while other parts of the basin, presumably more distal, remained open to deep water sedimentation until late Middle Jurassic time. The implication is that the Cayoosh Assemblage may represent a time transgressive basin margin succession.

Noel Mountain section

The Noel Mountain section comprises a western assemblage of interlayered siltstone, sandstone and conglomerate, and an eastern assemblage of fine grained volcanoclastic sandstone, siltstone, and phyllite (Journeay, 1993; Fig. 3B).

The western assemblage is an upright panel of siltstone, thin- and thick-bedded greywacke, quartz-rich feldspathic arenite, and heterolithic conglomerate. Thick lenses of conglomerate in the middle of the section mark the transition from a lower coarsening-upward succession of fine grained volcanic sandstone and siltstone into an overlying, fining-upward succession of sandstone, siltstone, and phyllite.

Conglomerate horizons include both pebble- and boulder-sized clasts of quartz-rich sandstone, volcanic wacke, limestone, chert, and both fine grained volcanic and coarse grained plutonic rock. Conglomerates and the overlying, fining-upward clastic succession are interpreted to be part of the Early Cretaceous Taylor Creek Group (Rusmore, 1985; Woodsworth, 1977), which is well-exposed along strike to the northwest. The coarsening-upward succession of quartz-rich sandstones and siltstones that underlie these conglomerates is interpreted to be part of the upper Cayoosh Assemblage (units 4 and/or 5).

The eastern assemblage is a thick (400-450 m) succession of thin bedded, dark grey graphitic shale, siltstone, phyllite, and fine grained volcanic sandstone, locally interlayered with feldspathic and calcareous wacke and thin, but distinctive lenses of dark grey limestone, limestone pebble conglomerate, and calcareous siltstone. Graded turbidites at the base of the section, locally containing thin horizons of light grey tuffaceous siltstone, calcareous wacke, and pebble conglomerate, grade upward into monotonous dark grey phyllite and siltstone (220 m). Fine grained volcanic sandstone at the top of this siltstone succession coarsens upward into 140 m of thick bedded, fine grained volcanic sandstone and siltstone. Stratigraphic repetition of this sandstone/siltstone facies, together with dip reversals of the dominant bedding-parallel foliation (S₁) and stratigraphic reversals of thin limestone pebble conglomerate horizons to the east, are interpreted to be the result of tight and isoclinal (F₂) folding (Fig. 3B). These folds are overturned to the southwest and appear to be localized in the footwall of the Bralorne Fault, a regional southwest-directed thrust system of Late Cretaceous age (Rusmore, 1985; Journeay et al., 1992; Journeay, 1993). Stratigraphic facing directions along the limbs of these second generation folds imply that the entire eastern Noel Mountain section must have been structurally overturned prior to F₂ folding and fault imbrication. We have traced this overturned panel of siltstone and volcanic sandstone northwestward across Green Mountain into the Downton Lake region. It appears to be the overturned limb of an alpine-scale, southwest-verging recumbent nappe structure.

The age of the eastern Noel Mountain section is unknown. The association of volcanic sandstone, calcareous siltstone, and thin horizons of limestone pebble conglomerate suggests a possible correlation with fine grained Late Triassic volcanoclastic rocks of the Hurley Formation (Cadwallader Group; Rusmore, 1985; Woodsworth, 1977; Journeay, 1993). However, the overall thickness of this succession, the abundance of thick volcanic sandstone and graphitic siltstone/phyllite successions, local occurrences of stretched pelecypods (*Buchia*?) and gastropods, and the notable absence of conodonts or thick limestone horizons anywhere in the section, suggest that a correlation with lower and middle members (units 2/3) of the Cayoosh Assemblage is more likely. This interpretation is corroborated by the investigations of Cairnes (1937), who documented a conformable relationship between thin bedded siltstones exposed along Noel Creek (Eastern Noel Mountain section) and underlying cherts of the Bridge River Group (Fergusson Series), a relationship similar to that documented in the type section of the Cayoosh Assemblage

(Journey and Northcote, 1992; Mahoney and Journey, 1993). Cairnes assigned these siltstones and shales to what he defined as the Noel Formation and proposed correlations with other siltstone/sandstone successions in the region, including those exposed along Cadwallader Creek and in the vicinity of Bralorne and Gun Lake. We support these correlations and propose that other siltstone/sandstone successions mapped by Cairnes (1937) as Noel Formation be included as part of the Cayoosh Assemblage. These correlations, coupled with regional stratigraphic and structural continuity, suggest a potential tie between the Cayoosh Assemblage and fine grained clastic rocks of the Last Creek formation and lower Relay Mountain Group, which overlie Triassic arc assemblages of the Cadwallader Group along strike to the north (Schiarrizza et al., 1989).

Birkenhead section

The Birkenhead section is a northeast-dipping panel of interlayered massive and fragmental volcanic flows and associated volcanoclastic rocks that grade upward into a succession of volcanic sandstone, siltstone, and phyllite (Fig. 3C; Journey, 1993). The section locally contains ammonite and bivalve forms of probable Late Triassic and Early Jurassic age, and has been included as part of the Cadwallader terrane (Cadwallader and Tyaughton groups; Woodsworth, 1977). Fieldwork during the 1993 season involved 1:50 000 scale mapping and detailed stratigraphic studies in a region extending northward from Cayoosh Mountain to the Birkenhead River (Fig. 1). These studies, initially aimed at investigating a stratigraphic tie between basal turbidites of the Cayoosh Assemblage (unit 1) and Lower Jurassic siltstones of the Last Creek formation, have uncovered exciting new evidence, including new fossil data and a previously undescribed volcanic succession, that require significant revision of existing correlations.

Fragmental volcanic rocks at the base of this section occupy the core of a regional southwest-verging anticlinal nappe (Birkenhead Anticline), the axial surface of which extends northwestward from Cayoosh Mountain to the west end of Birkenhead Lake (Fig. 1). The lowest portion of this section comprises a thick (220 m) sequence of dark green and maroon feldsparphyric flows, flow breccias, and associated fragmental lithic tuffs. Overlying these massive volcanics is a thick (150 m) succession of interlayered felsic metavolcanic flows, calcareous sandstone, and recrystallized limestone. This transitional facies grades upward into a thick (150 m) sequence of dark grey volcanoclastic sandstone, sandy limestone, and dark grey siltstone, locally containing corals and bivalves of probable Late Triassic age (Fig. 3C). Stratigraphic similarities and available age constraints suggest that these volcanic and sedimentary successions represent the Upper Triassic Pioneer and Hurley formations of the Cadwallader Group (Woodsworth, 1977).

Overlying this Upper Triassic arc assemblage with apparent conformity is a thick (450 m) succession of green and dark green metavolcanic flows, porphyritic flows and tuffs, locally containing light grey, fine grained felsic metavolcanic flows (50-80 m) and lesser amounts of fine grained volcanoclastic

sandstone and siltstone (Fig. 3C). Pyroclastic rocks at the top of this section are gradational upward into a 400-450 m thick succession of volcanoclastic sandstone, siltstone, shale, and phyllite, locally containing tuffaceous interbeds and intermediate volcanic flows. The contact between this volcanic succession and overlying volcanoclastic sequence is well exposed along the north and east flanks of Cayoosh Mountain, and can be traced northwestward to Gates Lake and into ridges west of Birkenhead Peak. This same section is overturned along the east flank of the Birkenhead River valley (Journey, 1993) and may correlate with volcanic and volcanoclastic successions that overlie Upper Triassic arc assemblages of the Cadwallader Group in the Tenquille Lake region (Grizzly Pass section of Journey, 1993).

Ammonite forms at the base of the volcanic section (Fig. 5) are characterized by distinctive ornamentation that suggest a probable lower to middle Toarcian age (H.W. Tipper and G. Jakobs, pers. comm., 1993). Bivalves that occur within sandstone of the overlying volcanoclastic succession (Fig. 6) resemble pelecypods collected by G.J. Woodsworth and interpreted by T.P. Poulton as trigoniid forms of probable Middle Toarcian to Bajocian age. The internal stratigraphy and age range of this arc assemblage is similar to that of the Middle Jurassic Harrison Lake Formation (Arthur et al., 1993), and suggests to us a probable correlation. This interpretation extends the known limits of the Harrison terrane northward and eastward into the imbricate zone of the Coast Belt Thrust System (Journey and Friedman, 1993), and implies a potential link between Harrison and Cadwallader terranes.

Intermediate and felsic metavolcanic flows mark the boundary between this Middle Jurassic arc sequence and overlying volcanoclastic sandstones, siltstones, and phyllites of the upper Birkenhead section (Fig. 3C). The contact between these two units is exposed along the margin of the Mt. Rohr pluton, near Birkenhead Peak, and appears to be conformable. The lower 80 to 100 m of this succession are characterized by interlayered volcanic sandstone, tuffaceous siltstone, and thinly laminated calcareous and graphitic siltstone. Sandstone horizons are fine- to medium-grained, thin- and thick-bedded (0.5-2 m), and include both immature feldspathic wacke and moderately well-sorted feldspathic arenite. This sandstone/siltstone facies fines upwards into a thick (250 m) succession of graphitic siltstone and phyllite. This upward-fining clastic succession is flanked to the east by imbricate fault slivers of the Bridge River Complex, and is repeated on the overturned limb of the Birkenhead Anticline, where it is apparently truncated by the Birkenhead River Fault. Stratigraphic relations suggest that this upper clastic succession is younger than Middle Jurassic, and may be correlative with either fine grained sedimentary rocks of the Callovian Mysterious Creek Formation (Harrison Terrane) or with undated volcanic sandstone/siltstone successions (units 3-5) of the Cayoosh Assemblage. Associations with quartz-rich meta-sandstones and conglomerates, which occur along strike to the northwest in roof pendants of the Mt. Rohr pluton, support the latter of these two interpretations. This correlation provides a potential link between outboard terranes (Cadwallader and Harrison arc assemblages) and clastic



Figure 5. Lower to Middle Toarcian ammonite collected from the middle unit of the Birkenhead section. Sample found by Jan Daly and identified by Howard Tipper and Giselle Jakobs. See Figure 5 for location.

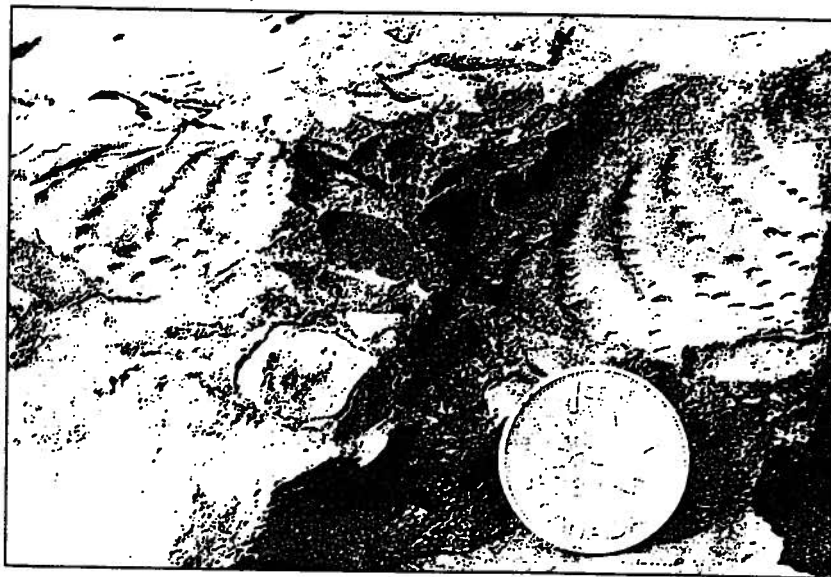


Figure 6. Late Toarcian to Bajocian bivalves collected from the middle unit of the Birkenhead section.

Regional Correlations and Terrane Linkages

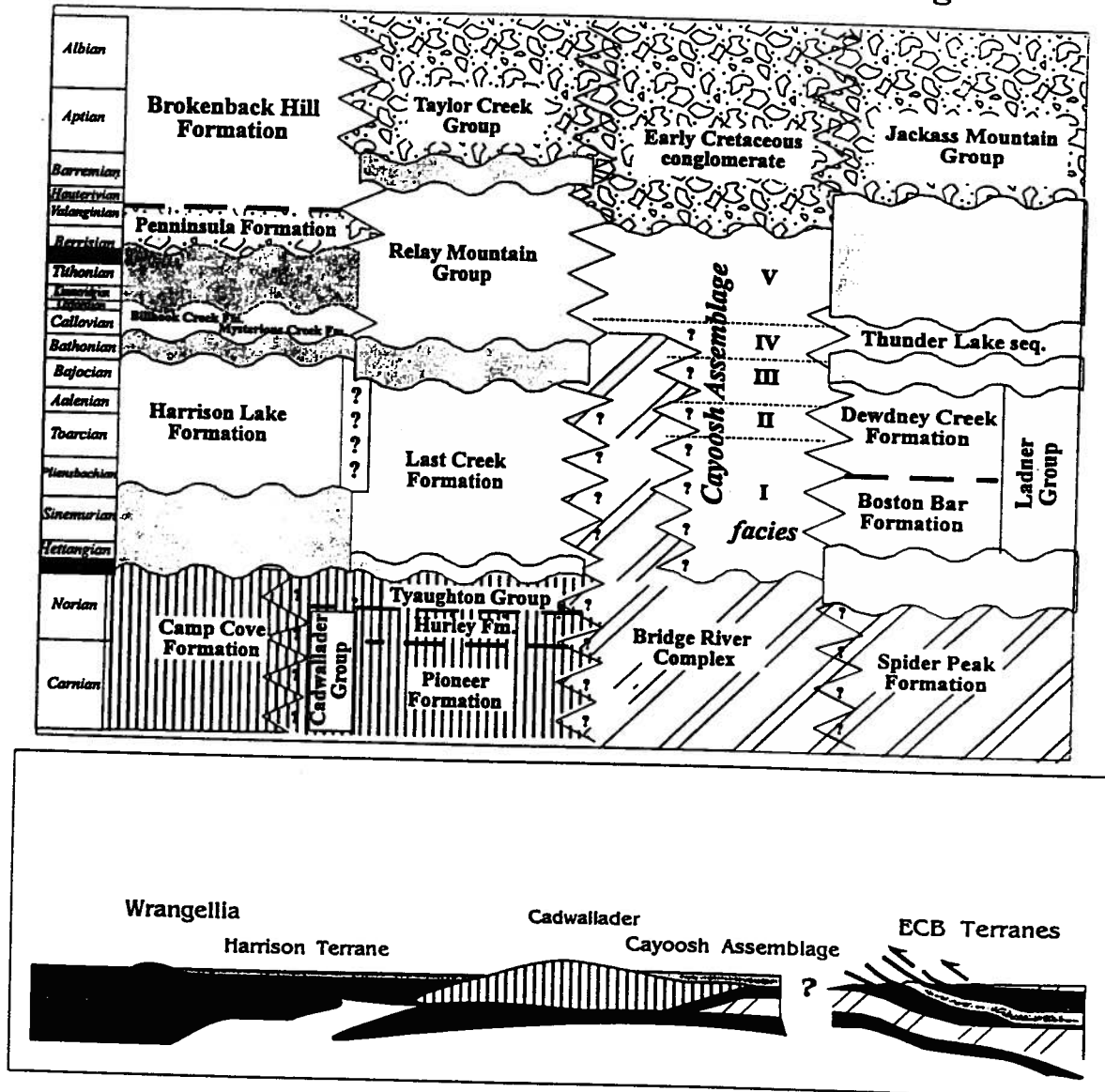


Figure 7. Proposed regional stratigraphic correlation of Jurassic basin successions in the eastern Coast Belt.

successions that overlie oceanic rocks of the Bridge River terrane, and may represent a stratigraphic bridge that predates final accretion along the continental margin and subsequent onlap of Early Cretaceous conglomerate.

SUMMARY AND CONCLUSIONS

Stratigraphic relationships documented in this and previous reports (Journeay and Northcote, 1992; Journeay, 1993; Mahoney and Journeay, 1993) have established the Cayoosh Assemblage as a coherent stratigraphic succession that conformably overlies oceanic rocks of the Bridge River Complex. Stratigraphic associations and available age constraints support a correlation with Lower and Middle Jurassic rocks of the Ladner Group (Methow basin) and with clastic successions that overlie Triassic and Middle Jurassic island arc assemblages of the Cadwallader and Harrison terranes (see Fig. 7). Stratigraphic ties with Jurassic clastic successions of the Last Creek formation and Relay Mountain Group are probable, but have not yet been established.

These correlations suggest to us a complex basin evolution in which parts of the Bridge River ocean began to receive clastic detritus in the Late Triassic/Early Jurassic, while other parts of the basin, presumably more distal, remained open to pelagic sedimentation until late Middle Jurassic time. Quartz-rich sandstone and upward-coarsening clastic successions of the Cayoosh Assemblage (units 4 and 5), the youngest of which are Early Cretaceous, reflect the arrival and/or emergence of both crystalline and volcanic source terranes and the closure of the Bridge River ocean.

Stratigraphic relationships and new paleontological data in the Birkenhead section suggest a disconformable relationship between the Upper Triassic Cadwallader arc and overlying Middle Jurassic rocks of the Harrison Lake Formation. Along strike to the south, this Middle Jurassic arc overlaps Triassic rocks of the Camp Cove Formation (Arthur et al., 1993). This implies the Cadwallader Group and Camp Cove Formation are either part of the same Triassic arc complex, or fragments of separate terranes that were amalgamated prior to the development of the Harrison Lake arc in Middle Jurassic time. Linkages between clastic successions at the top of the Birkenhead section and the upper Cayoosh Assemblage suggest that this Middle Jurassic arc most likely formed along the outboard margin of the ancestral Bridge River ocean.

ACKNOWLEDGMENTS

Our ideas have evolved through many stimulating discussions with Jim Monger, Howard Tipper, Glenn Woodsworth, Peter van der Heyden, Paul Schiarizza, Bill McClelland and Fabrice Cordey. Fieldwork was carried out with volunteer assistance from Jan Daly. Her mountaineering skills and keen eyes led the way through the Birkenhead section and to important new fossil localities. We are grateful to Howard Tipper, Giselle Jakobs, and Fabrice Cordey for sharing the

preliminary results of their biostratigraphic investigations. Will Husby provided valuable photographic documentation of fossil collections from the Birkenhead section.

REFERENCES

- Arthur, A.J., Smith, P.L., Monger, J.W.H., and Tipper, H.W.
1993: Mesozoic stratigraphy and Jurassic paleontology west of Harrison Lake, southwestern British Columbia; Geological Survey of Canada, Bulletin 441, 62 p.
- Cairnes, C.E.
1937: Geology and mineral deposits of the Bridge River mining camp, British Columbia; Geological Survey of Canada, Memoir 213, 140 p.
- Cordey, F. and Schiarizza, P.
1993: Long-lived Panthalassic remnant: The Bridge River accretionary complex, Canadian Cordillera; *Geology*, v. 21, p. 263-266.
- Duffell, S. and McTaggart, K.C.
1952: Ashcroft map area, British Columbia; Geological Survey of Canada, Paper 67-10, 55 p.
- Friedman, R.M. and Armstrong, R.L.
in press: Jurassic and Cretaceous geochronology of the southern Coast Belt, southern British Columbia, 49-50 degrees N; Geological Society of America in Jurassic magmatism in the western North American Cordillera, (ed.) D. Miller; Memoir.
- Journeay, J.M.
1993: Tectonic assemblages of the Eastern Coast Belt, southwestern British Columbia: Implications for the history and mechanisms of terrane accretion; in *Current Research, Part A: Geological Survey of Canada, Paper 93-1A*, p. 221-233.
- Journeay, J.M. and Friedman, R.M.
1993: The Coast Belt Thrust System: evidence of Late Cretaceous shortening in the Coast Belt of SW British Columbia; *Tectonics*, v. 12, no. 3, p. 756-775.
- Journeay, J.M. and Northcote, B.R.
1992: Tectonic assemblages of the Southern Coast Belt, SW British Columbia; in *Current Research, Part A: Geological Survey of Canada, Paper 92-1A*, p. 215-224.
- Journeay, J.M., Sanders, C., Van-Konijnburg, J.-H., and Jasma, M.
1992: Fault systems of the eastern Coast Belt, southwest British Columbia; in *Current Research, Part A: Geological Survey of Canada, Paper 92-1A*, p. 225-235.
- Mahoney, J.B. and Journeay, J.M.
1993: The Cayoosh Assemblage, southwestern British Columbia: last vestige of the Bridge River ocean; in *Current Research, Part A: Geological Survey of Canada, Paper 93-1A*, p. 235-244.
- Monger, J.W.H. and Journeay, J.M.
1992: Guide to the geology and tectonic evolution of the southern Coast Belt: A field guide to accompany the Penrose Conference on the "Tectonic Evolution of the Coast Mountain Orogen", May 1992, 97 p.
- Monger, J.W.H., Price, R.A., and Tempelman-Kluit, D.J.
1982: Tectonic accretion and the origin of two major metamorphic and plutonic belts in the Canadian Cordillera; *Geology*, v. 10, p. 70-75.
- Rusmore, M.E.
1985: Geology and tectonic significance of the Upper Triassic Cadwallader Group and its surrounding faults, southwestern British Columbia; Ph.D. thesis, University of Washington, Seattle, 170 p.
- Schiarizza, P., Gaba, R.G., Glover, J.K., and Garver, J.I.
1989: Geology and mineral occurrences of the Tyaughton Creek area (92 O/2, 92 J/15); in *Geological Fieldwork 1988*; British Columbia Ministry of Energy, Mines and Petroleum Resources, Paper 1989-1, p. 15-130.
- van der Heyden, P.
1992: A Middle Jurassic to Early Tertiary Andean-Sierran Arc Model for the Coast Belt of British Columbia; *Tectonics*, v. 11, no. 1, p. 82-97.
- Woodsworth, G.J.
1977: Pemberton (92J) map area, British Columbia; Geological Survey of Canada, Open File 482.

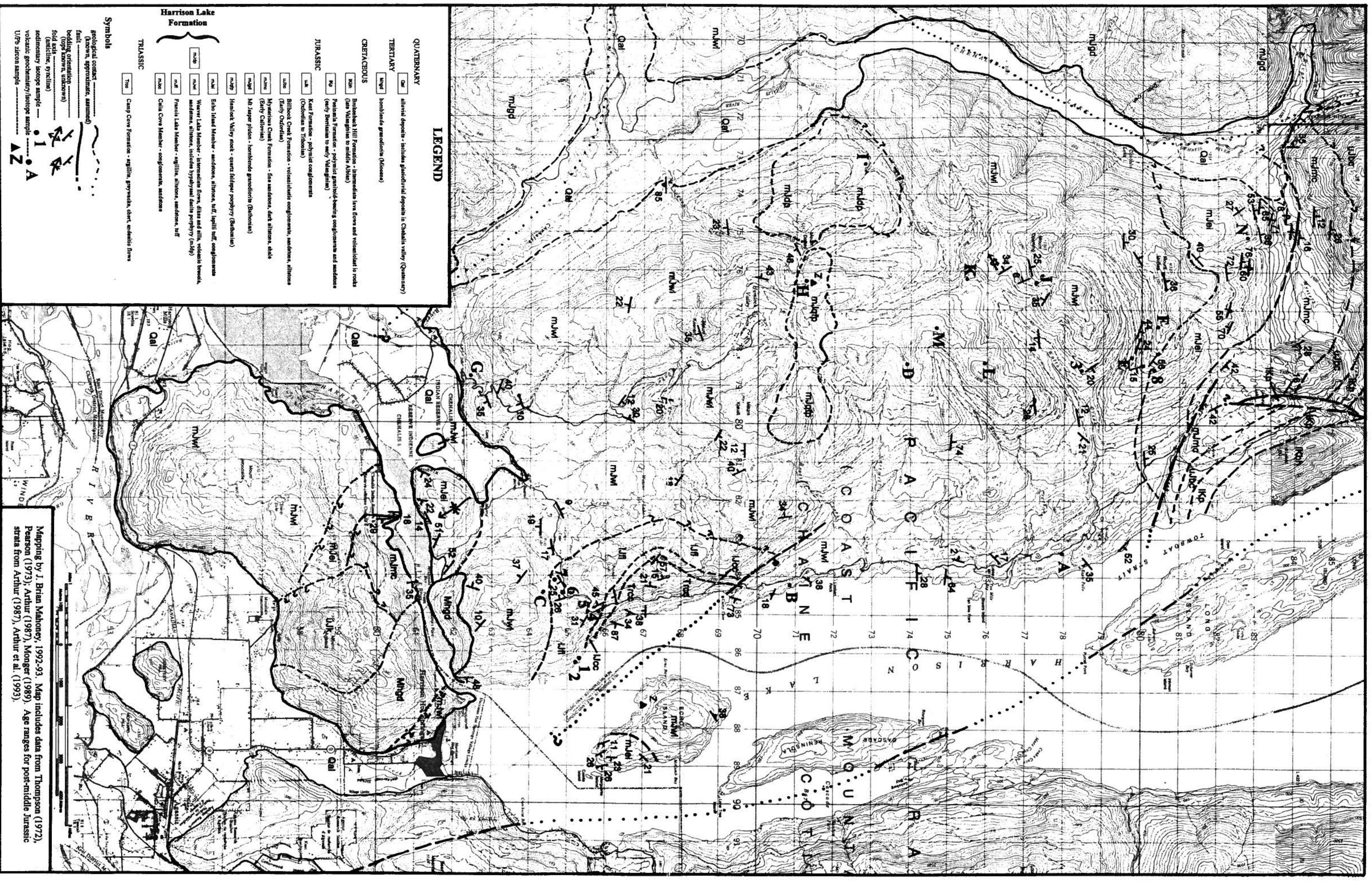


Figure 4.2